Ecosystem Status Report 2024

EASTERN BERING SEA

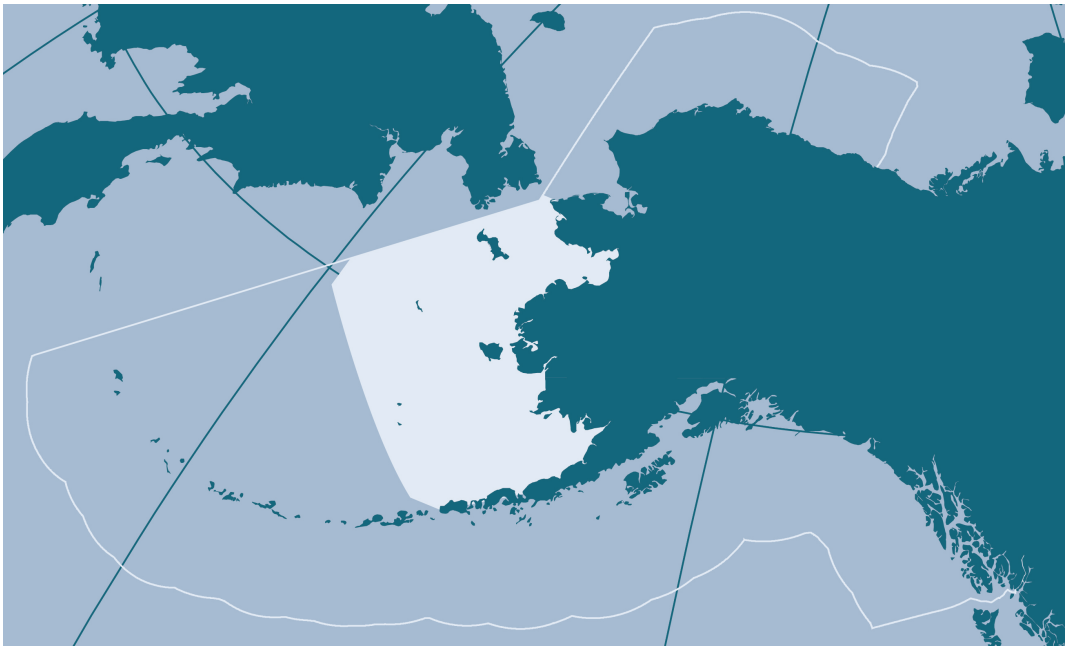

Edited by:

Elizabeth Siddon

Auke Bay Laboratories, Alaska Fisheries Science Center, NOAA Fisheries

With contributions from:

Grant Adams, Donald M. Anderson, Alex Andrews, Kelia Axler, Kerim Aydin, Diana Baetscher, Sunny Bak-Hospital, Steve Barbeaux, Cheryl Barnes, Lewis Barnett, Sonia Batten, Jessica Beck, Shaun Bell, Emily Bowers, Caroline Brown, Thaddaeus Buser, Matt Callahan, Patrick Charapata, Dan Cooper, Bryan Cormack, Jessica Cross, Deana Crouser, Curry J. Cunningham, Lukas DeFilippo, Andrew Dimond, Lauren Divine, Sherri Dressel, Lisa B. Eisner, Jack Erickson, Evangeline Fachon, Thomas Farrugia, Erin Fedewa, H. William Fennie, Emily Fergusson, Sarah Gaichas, Jeanette C. Gann, Sabrina Garcia, Alicia Godersky, Benjamin Gray, Shannon Hennessey, Tyler Hennon, Kirstin K. Holsman, Kathrine Howard, Rebecca Howard, Jim Ianelli, Kelly Kearney, Esther Kennedy, Mandy Keogh, David Kimmel, Jesse Lamb, Geoffrey M. Lang, Ben Laurel, Kimberly Ledger, Elizabeth Lee, Kathi Lefebvre, Emily Lemagie, Aaron Lestenkof, Mike Levine, Jackie Lindsey, Mike Litzow, W. Christopher Long, Jacek Maselko, Annie Masterman, Cathy Mattson, Sara Miller, Todd Miller, Natalie Monacci, James Murphy, Laurel Nave-Powers, Jens Nielsen, Clare Ostle, Jim Overland, Johanna Page, Robert Pickart, Darren Pilcher, Cody Pinger, Drew Porter, Steven Porter, Bianca Prohaska, Patrick Ressler, Jonathan Reum, Jon Richar, Nancy Roberson, Lauren Rogers, Sean Rohan, Matthew Rustand, Emily Ryznar, Gay Sheffield, Kalei Shotwell, Elizabeth Siddon, Margaret Siple, Brooke Snyder, Adam Spear, Phyllis Stabeno, Raphaela Stimmelmayr, Anna Sulc, Rob Suryan, Jasmine Terry-Shindelman, Rick Thoman, James T. Thorson, Cathy Tide, Stacy Vega, Muyin Wang, Sophia Wassermann, George A. Whitehouse, Ellen Yasumiishi, Stephani Zador, and Adam Zaleski

Reviewed by:
The Bering Sea and Aleutian Islands Groundfish Plan Team
November 15, 2024
North Pacific Fishery Management Council
1007 West 3rd Ave., Suite 400
Anchorage, AK 99501

Support for the assembly and editing of this document was provided jointly by NOAA Fisheries and the NOAA Integrated Ecosystem Assessment (IEA) program. This document is NOAA IEA program contribution #2024_5.

Citing the complete report:
Siddon, E. 2024. Ecosystem Status Report 2024: Eastern Bering Sea, Stock Assessment and Fishery Evaluation Report, North Pacific Fishery Management Council, 1007 West 3rd Ave., Suite 400, Anchorage, Alaska 99501.

Citing the Ecosystem Assessment:
Siddon, E. 2024. Ecosystem Assessment. In: Siddon, E. 2024. Ecosystem Status Report 2024: Eastern Bering Sea, Stock Assessment and Fishery Evaluation Report, North Pacific Fishery Management Council, 1007 West 3rd Ave., Suite 400, Anchorage, Alaska 99501.

Citing an individual contribution:
Contributor name(s), 2024. Contribution title. In: Siddon, E. 2024. Ecosystem Status Report 2024: Eastern Bering Sea, Stock Assessment and Fishery Evaluation Report, North Pacific Fishery Management Council, 1007 West 3rd Ave., Suite 400, Anchorage, Alaska 99501.

Citing information within a Synthesis section:
Contributor name(s), 2024. Sub-section heading. In: Synthesis section. In: Siddon, E. 2024. Ecosystem Status Report 2024: Eastern Bering Sea, Stock Assessment and Fishery Evaluation Report, North Pacific Fishery Management Council, 1007 West 3rd Ave., Suite 400, Anchorage, Alaska 99501.

QR code for NOAA Alaska Fisheries Science Center's Ecosystem Status Reports webpage[1]. Time series from the report cards are also available[2].

[1] https://www.fisheries.noaa.gov/alaska/ecosystems/ecosystem-status-reports-gulf-alaska-bering-sea-and-aleutian-islands

[2] https://alaskaesr.psmfc.org

2024 Contributing Partners

Purpose of the Ecosystem Status Reports

This document is intended to provide the North Pacific Fishery Management Council, including its Scientific and Statistical Committee (SSC) and Advisory Panel (AP), with information on ecosystem status and trends. This information provides context for the SSC's acceptable biological catch (ABC) and overfishing limit (OFL) recommendations, as well as for the Council's final total allowable catch (TAC) determination for groundfish and crab. It follows the same annual schedule and review process as groundfish stock assessments, and is made available to the Council at the annual December meeting when Alaska's federal groundfish harvest recommendations are finalized.

Ecosystem Status Reports (ESRs) include assessments based on ecosystem indicators that reflect the current status and trends of ecosystem components, which range from physical oceanography to biology and human dimensions. Many indicators are based on data collected from NOAA's Alaska Fishery Science Center surveys. All are developed by, and include contributions from, scientists and fishery managers at NOAA, other U.S. federal and state agencies, academic institutions, tribes, nonprofits, and other sources. The ecosystem information in this report will be integrated into the annual harvest recommendations through inclusion in stock assessment-specific risk tables (Dorn and Zador, 2020), presentations to the Groundfish and Crab plan teams in annual September and November meetings, presentations to the Council in their annual October and December meetings, and submission of the final report to the Council in December (see Figure 1).

The SSC is the primary audience for this report, as the final ABCs are determined by the SSC, based on biological and environmental scientific information through the stock assessment and Tier process[3],[4]. TACs may be set lower than the ABCs due to biological and socioeconomic information. Thus, the ESRs are also presented to the AP and Council to provide ecosystem context to inform TAC as well as other Council decisions. Additional background can be found in the Appendix (p. 251).

[3] https://www.npfmc.org/wp-content/PDFdocuments/fmp/GOA/GOAfmp.pdf
[4] https://www.npfmc.org/wp-content/PDFdocuments/fmp/BSAI/BSAIfmp.pdf

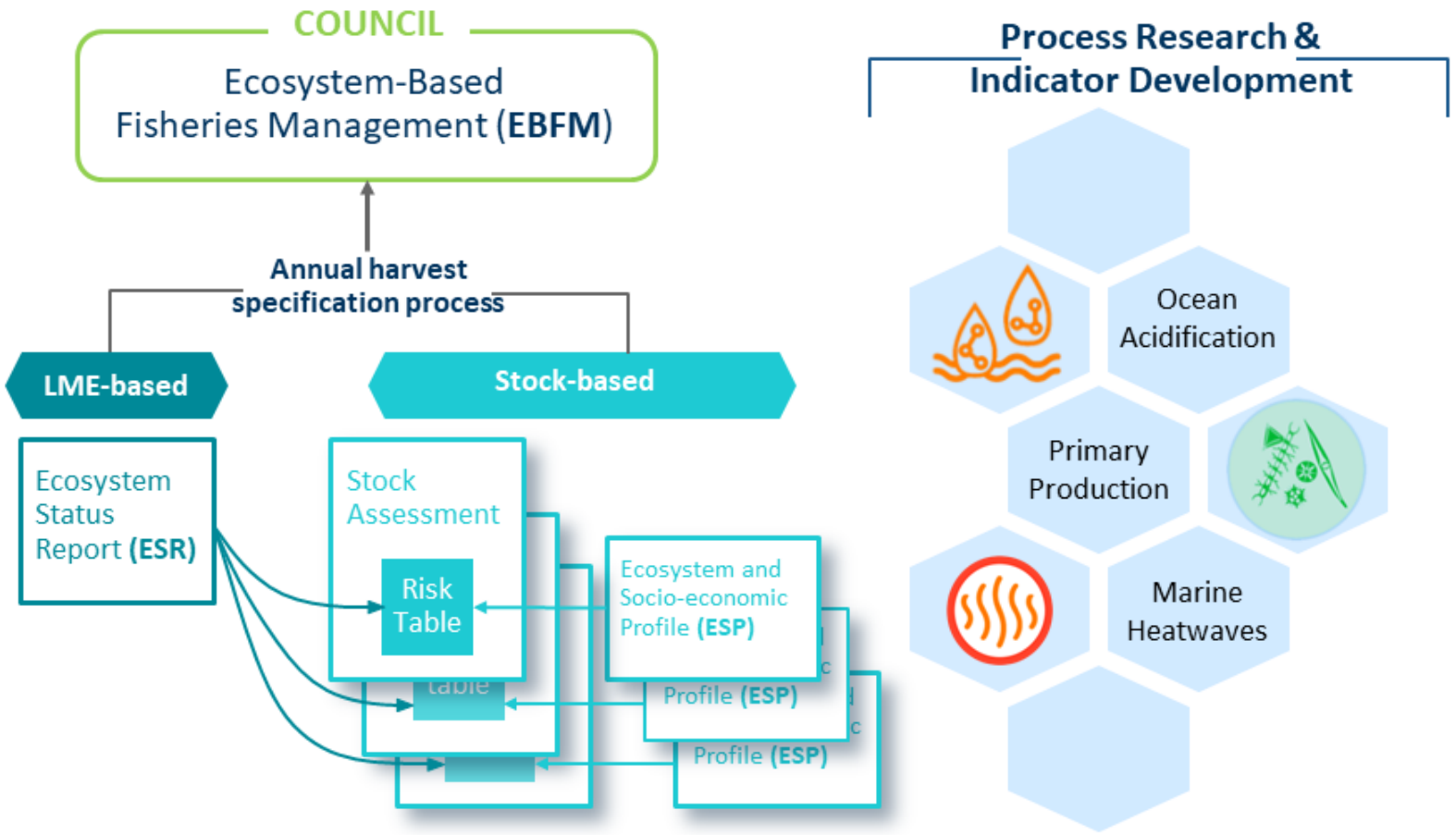

Figure 1: Ecosystem information mapping to support Ecosystem-Based Fisheries Management through Alaska's annual harvest specification process. The 'honeycomb' on the right shows examples of ecosystem indicators that are provided to Ecosystem Status Reports (ESRs) at the Large Marine Ecosystem (LME) scale and/or to Ecosystem and Socioeconomic Profiles (ESPs) at the stock-based level.

Southeastern Bering Sea 2024 Report Card

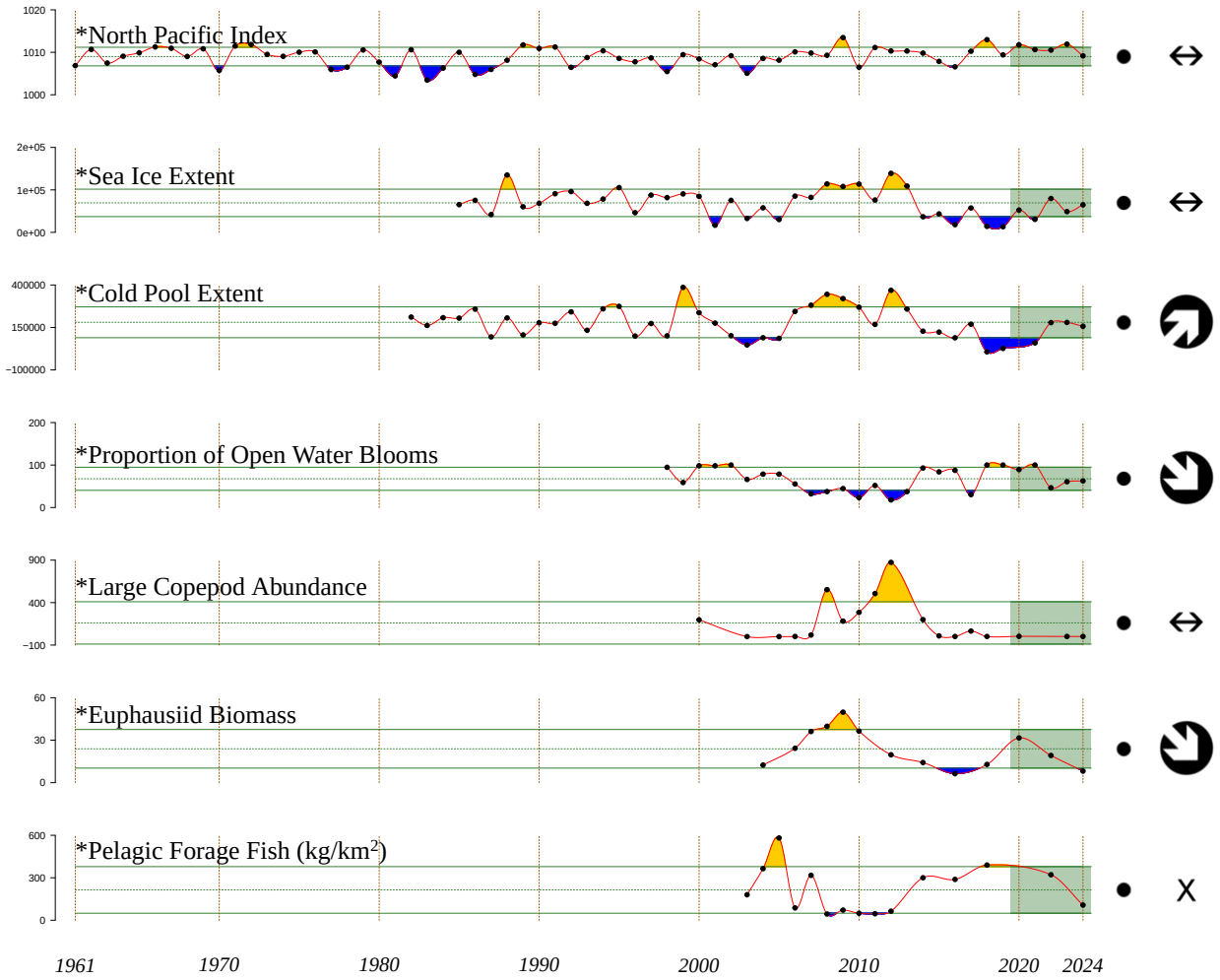

2020–2024 Mean

- 1 s.d. above mean
- 1 s.d. below mean
- within 1 s.d. of mean
- X fewer than 2 data points

2020–2024 Trend

- increase by 1 s.d. over time window
- decrease by 1 s.d. over time window
- ↔ change <1 s.d. over window
- X fewer than 3 data points

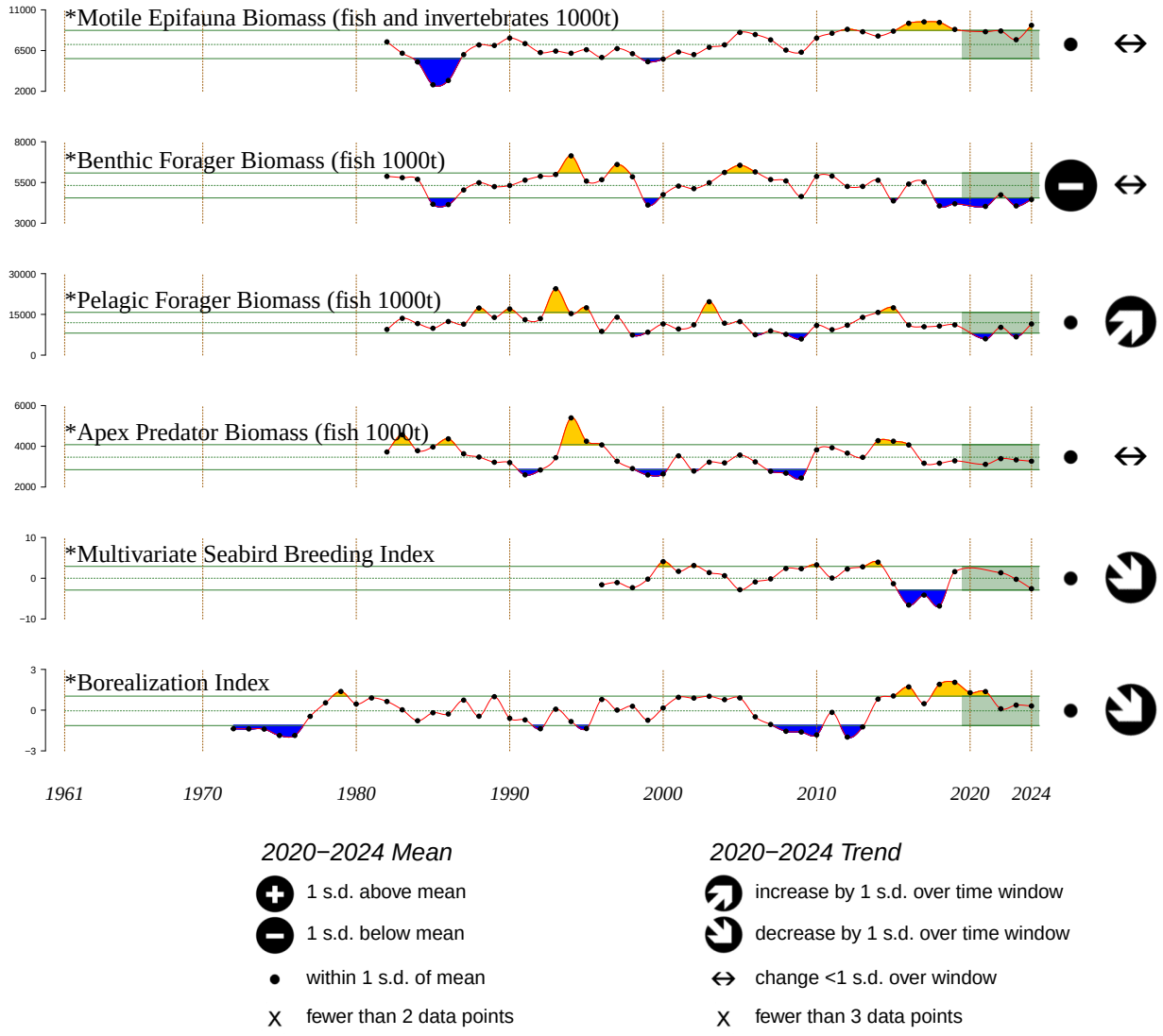

Figure 2: 2024 Southeastern Bering Sea report card; see text for indicator descriptions.
*indicates time series updated with 2024 data.

For more information on individual Report Card indicators, please see 'Description of the Report Card indicators' (p. 261 and p. 266). For more information on the methods for plotting the Report Card indicators, please see 'Methods Description for the Report Card Indicators' (p. 268).
* indicates Report Card information updated with 2024 data.

- *The **North Pacific Index (NPI)** effectively represents the state of the Aleutian Low Pressure System. Above average (below average) winter (Nov-Mar) NPI values imply a weak (strong) Aleutian Low and generally calmer (stormier) conditions. The **NPI was average** during winter 2023–2024 (Figure 12) that may partially explain the near-normal sea ice extent.

- *The mean **sea-ice extent** over the southeastern Bering Sea shelf (south of 60°N) was **at the long-term mean** (1985–2024) in 2024 (ice year defined as 1 Sept to Aug 31). Seasonal sea-ice extent has implications for the cold pool, spring bloom strength and timing, and bottom-up productivity.

- *The areal **extent of the cold pool** in the eastern Bering Sea (EBS), as measured during the bottom trawl survey (Jun-Aug; including strata 82 and 90; 1982–2024), **was just below the time series average in 2024**. The 2024 extent (156,800 km^2) was 12.7% smaller than 2023.

- *The **proportion of open water blooms** in the southeastern Bering Sea (south of 60°N) was 62.5% during 2024, similar to 2023,and **just below the time series average** (1998–2024). 2024 had fewer open water blooms than during the warmer period 2014–2021, but higher than during the cold period 2007–2012. A higher proportion of ice-associated blooms is correlated with higher abundances of large zooplankton (Hunt et al., 2011).

- *The **abundance of large copepods** (predominantly *Calanus* spp.) as measured during August/September along the 70 m isobath over the southeastern shelf, peaked in 2008 and 2012 during cold years, but has remained **below the time series mean** (2000–2024) since 2015.

- *An acoustic estimate of euphausiid density increased from 2018 through 2022, but declined to the **second-lowest value in the time series in 2024**.

- *The density of **pelagic forage fish** (i.e., age-0 pollock, age-0 Pacific cod, herring, capelin, rainbow smelt, saffron cod, and all species of juvenile salmonids) sampled by surface trawl over the southeastern Bering Sea shelf in late-summer (Aug-Sep; 2003–2024) peaked in 2005, was below the time series average in 2008–2012, was above average in 2014, 2016, and 2018, but **dropped to below the long-term mean in 2024**. The trends are dominated by age-0 pollock and juvenile sockeye salmon; in 2024 the densities of both were low.

- *The biomass of **motile epifauna** measured during the standard bottom trawl survey (Jun-Aug; 1982–2024) increased from 2023 to 2024 and **remains above the long term mean**. Collectively, brittle stars, sea stars, and other echinoderms have accounted for more than 50% of the biomass in this guild. Brittle stars alone have accounted for more than 30% of motile epifauna biomass since 1997. Brittle stars have trended downward since their peak biomass in 2016 but remain above their long-term mean. The biomass index sharply increased for tanner crabs and snow crabs, while king crabs remain below their long term mean.

- *The biomass of **benthic foragers** measured during the standard bottom trawl survey (Jun-Aug; 1982–2024) increased 10% from 2023 to 2024 but **remain below the time series mean**. The biomass of flathead sole, northern rock sole, and yellowfin sole all contributed to the increasing

guild index. However, both northern rock sole and yellowfin sole remain below their long term means.

- *The biomass of **pelagic foragers** measured during the standard bottom trawl survey (Jun-Aug; 1982–2024) increased 71% from 2023 to 2024 to **just above their long-term mean**. The biomass of the pelagic forager guild was generally stable from 2016 to 2019, but dropped to their third lowest value in 2021. The trend in the pelagic forager guild is largely driven by walleye pollock who on average account for 68% of the biomass in this guild. In 2024, the index for **pollock increased 78% from 2023**. Among species of secondary importance, Pacific herring have decreased 5% from 2023, but remain above their long-term mean.

- *The biomass of **apex predators** measured during the standard bottom trawl survey (Jun-Aug; 1982–2024) in 2024 is nearly equal to their value in 2023 and is **below their long term mean**. The trend in the apex predator guild is largely driven by Pacific cod, which decreased 5.5% from 2023, and is also influenced by arrowtooth flounder, which increased 26% from 2023.

- *The **multivariate seabird breeding index** indicated that seabird reproductive timing and success at the Pribilof Islands **was slightly below average in 2024**, although there were differences between islands and species that may reflect local-scale processes and/or diversity in foraging strategies. Reproductive success and/or hatch timing can be influenced by their food supply, therefore below-average values may indicate lower than average recruitment of year classes that seabirds feed on (e.g., age-0 pollock), or lower than average supply of forage fish that commercially fished species feed on (e.g., capelin eaten by both seabirds and Pacific cod).

- *The **borealization index** (1972–2024) describes the transition from an Arctic physical state supporting a cold-adapted species assemblage to a subarctic (boreal) physical state supporting a warm-adapted assemblage. Arctic-like conditions occurred in the 1970s and 2007–2013. Boreal conditions occurred during the warm, lower-ice years of 2014–2021. The borealization index has **returned to values similar to the time series mean during 2022–2024**.

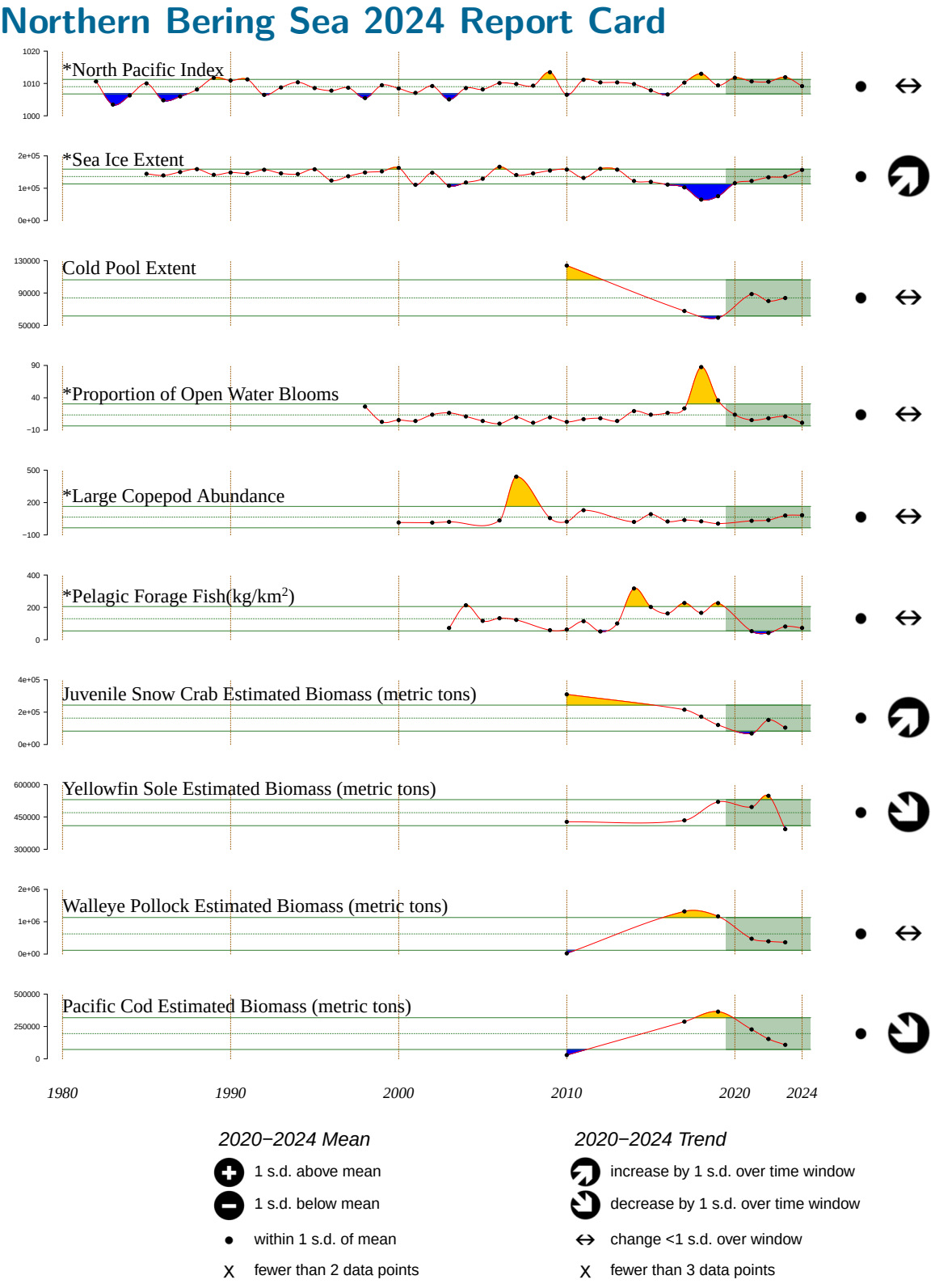

Figure 3: 2024 Northern Bering Sea report card; see text for indicator descriptions.
*indicates time series updated with 2024 data.

- *The **North Pacific Index (NPI)** effectively represents the state of the Aleutian Low Pressure System. Above average (below average) winter (Nov-Mar) NPI values imply a weak (strong) Aleutian Low and generally calmer (stormier) conditions. The **NPI was average** during winter 2023–2024 (Figure 12) that may partially explain the near-normal sea ice extent.

- *The mean **sea-ice extent** over the northern Bering Sea shelf (north of 60°N) has been increasing since the time series (1985–2024) low ice extent in 2018 (ice year defined as Sept 1 to Aug 31). Sea ice extent **was above average in 2024**. Seasonal sea-ice extent has implications for the cold pool, spring bloom strength and timing, and bottom-up productivity.

- The areal **extent of the cold pool** in the northern Bering Sea (NBS), as measured during the bottom trawl survey (Jun-Aug; strata 70, 71, and 81; 2010, 2017, 2019, 2021–2023), decreased between 2010 and 2019, but returned to the time series average in 2023. The 2023 extent (83,797 km^2) was similar to 2022.

- *The **proportion of open water blooms** in the northern Bering Sea (north of 60°N) was about 1.4% during 2024, which is the lowest value since 2008. A higher proportion of ice-associated blooms is correlated with higher abundances of large zooplankton (Hunt et al., 2011).

- *The **abundance of large copepods** (predominantly *Calanus* spp.) as measured during August/September over the northern shelf, peaked in 2011 during a cold year, and has remained **near the time series mean** (2000–2024) since 2021.

- *The density of **pelagic forage fish** (i.e., age-0 pollock, age-0 Pacific cod, herring, capelin, rainbow smelt, saffron cod, and all species of juvenile salmonids) sampled by surface trawl in late-summer (Aug-Sep; 2003–2024) peaked in 2004 and 2014 and remained above average through 2019, then **dropped to below the long-term mean in 2021–2024**. The trends are dominated by age-0 pollock and herring; in 2024 the densities of both were low.

- The biomass of **juvenile snow crab** measured during the northern Bering Sea bottom trawl survey (2010, 2017–2019, 2021–2023) peaked in 2010 and decreased through 2023, with a smaller peak in biomass in 2022. The trend in juvenile snow crab biomass (combination of small male and immature female crab) reflects **benthic production of the ecosystem and is a signal for future crab recruitment into the eastern Bering Sea**.

- The biomass of **yellowfin sole** observed during the northern Bering Sea bottom trawl survey (2010, 2017, 2019, 2021–2023) plateaued from 2019–2022 and then decreased in 2023. Trends in yellowfin sole biomass reflect **relative predation pressure on small infaunal prey (e.g., polychaete worms, bivalves, small crustaceans)**.

- The biomass of **walleye pollock** observed during the northern Bering Sea bottom trawl survey (2010, 2017, 2019, 2021–2023) peaked from 2017–2019 and decreased through 2023. Trends in walleye pollock biomass reflect **relative predation pressure on zooplankton and forage fish**.

- The biomass of **Pacific cod** observed during the northern Bering Sea bottom trawl survey (2010, 2017, 2019, 2021–2023) peaked in 2019 and then decreased through 2023. Trends in Pacific cod biomass reflect **relative predation pressure on forage fish and crab**.

Ecosystem Assessment

Elizabeth Siddon
Auke Bay Laboratories, Alaska Fisheries Science Center, NOAA Fisheries
Contact: elizabeth.siddon@noaa.gov

Last updated: November 2024

Introduction

In recent decades, the eastern Bering Sea (EBS) transitioned from an ecosystem governed by inter-annual variability (1982–2000) into one that experienced multi-year stanzas of warm (2000–2005) and cold (2007–2013) conditions (Baker et al., 2020). In 2014, the EBS entered a warm period that was unprecedented in terms of magnitude and duration (Figure 20) and that persisted until 2021. This recent warm period included the near-absence of sea ice in the winters of 2017/2018 and 2018/2019 (Figure 36) and subsequent lack of cold pool in summers 2018 and 2019 (Figures 41 and 42) that had distinct impacts to the ecosystems of the southeastern (SEBS) and northern (NBS) Bering Sea shelves.

Since ∼2021, oceanographic metrics (e.g., sea ice extent, sea surface temperatures, and bottom temperatures) over the EBS shelf have cooled to near average based on respective time series. Currently, the broader North Pacific is predicted to transition from El Niño to La Niña conditions by spring 2025, which is expected to bring continued cooler temperatures to the EBS shelf. This Assessment aims to synthesize recent biological metrics (e.g., zooplankton and fish dynamics) to characterize the current status of the SEBS and NBS ecosystems in response to the cooler oceanographic conditions.

Seasonal sea ice and the resulting cold pool extent are defining features over the Bering Sea shelf. Combined, sea ice and the cold pool create thermal barriers, both horizontally (i.e., north/south) and vertically in the water column. Such thermal barriers affect the spatial distributions of crab and groundfish (e.g., Thorson et al., 2019; DeFilippo et al., 2023) that have subsequent direct (e.g., habitat expansion) and indirect (e.g., changes in predator/prey dynamics) impacts to managed stocks.

The delineation between the SEBS and NBS is often considered to be at 60°N latitude on the basis of the physical and biological distinctions between these ecological systems, existing research and analyses in these areas, and available data and survey designs. This delineation is supported by broad-scale analyses of the physical oceanography and hydrography (Stabeno et al., 2012*a*; Baker et al., 2020) and zoogeography of the region (Sigler et al., 2017). For an in-depth review of distinguishing characteristics

between these ecoregions, see Baker (2023).

This assessment documents the ecosystem response to the average oceanographic conditions experienced since ∼2021, in contrast with the prolonged warm period (2014–2021) and pulse events of 2017/2018 and 2018/2019.

Southeastern Bering Sea

Since 2021, the SEBS has experienced a more neutral thermal state. Over the past year (August 2023–August 2024) many metrics, including sea surface temperature (Figure 23, Figure 30, Figure 34), wintertime sea ice areal extent (Figure 36) and thickness (Figure 39, Figure 40), and cool pool extent (Figure 41, Figure 42) have continued to be near historical averages. While the spatial extent of waters <2°C in 2024 was only slightly (12.7%) smaller than in 2022 and 2023, the extent of ≤-1°C and ≤0°C isotherms decreased by 54.4% and 75.0%, respectively, and was similar to warm years (see p. 75).

Seasonally, winter atmospheric conditions contribute to determining summer oceanographic conditions over the EBS shelf. Both the North Pacific Index (NPI) and Aleutian Low Index (ALI) provide complementary views of the atmospheric pressure system in the North Pacific. During winter 2023–2024, the NPI was average (Figure 2) and the strength (Figure 14) and location (Figure 15) of the Aleutian Low Pressure System were both near climatological averages. Thus, despite delayed formation of sea ice in fall 2023 (Figure 35), cold winds from the Arctic helped advance sea ice to near-normal extent by mid-winter.

Winds can impact transport and surface (upper ∼30-40 m) drift of early life stages of crab and groundfish. December 2023 had significant along-shelf winds to the southeast, and weaker but more sustained winds to the southeast from March to May 2024 (Figure 19; *note*: winds to the southeast also occurred in March and May of 2023). Such winds favor offshore transport, which has been correlated with below-average recruitment for some winter-spawning flatfish (e.g., northern rock sole, arrowtooth flounder) because larvae are transported away from suitable nursery habitat (Wilderbuer et al., 2002, 2013). Beginning in May and continuing through summer 2024, persistent storms resulted in a deeper mixed layer, which brought up deeper, cooler water from depth, such that SSTs remained cooler through at least August 2024 (Figure 27). Sea surface temperatures (SSTs) and bottom temperatures were near the long-term averages in all regions by summer 2024. Notable deviations include (i) warm SSTs in the outer domain from fall 2023 through spring 2024 and (ii) unusually warm bottom temperatures in the northern outer domain since spring 2024 that may indicate an intrusion of shelf water (Figure 34).

Measures of benthic productivity showed mixed signs over the SEBS in 2024. Increases were observed for sedentary sea anemones and sea pens (Figure 43), as well as motile eelpouts and poachers (Figure 116). The biomass of the motile epifauna guild (e.g., echinoderms, crabs) remains above the long term mean, buoyed by above-average biomass of echinoderms (Figure 2). Crab populations in the EBS remain low, though relative increases were observed for tanner crab and snow crab in 2024 (Figure 118). Decreases were observed for sedentary sponges (Figure 43), as well as motile sea stars (Figure 116). The biomass of the benthic forager guild (e.g., small-mouthed flatfishes) remains below the time series mean (Figure 2). The condition of small-mouthed flatfish was also mixed in 2024 (Figure 95), potentially reflecting species-level differences in metabolic demand and/or spatial overlap with prey resources.

The community of St. Paul Island has been collecting regular (∼weekly) CTD observations for nearly

the past decade, including chlorophyll a concentrations (Figure 45). June–August 2024 had some of the highest chlorophyll a concentrations on record with values $\sim$10 μg/L in June and July, which was considerably higher than 2023. At mooring M2, the peak of the 2024 spring bloom was slightly later than average, but the fall bloom occurred unusually early (Figure 46). The fall bloom started in early September, $\sim$ 1 month earlier than usual (Sigler et al., 2014). Frequent storm events during summer 2024 resulted in weaker water-column stratification (P. Stabeno, pers comm). A large storm in late August likely caused water column mixing, which introduced nutrients to the surface, and initiated the early fall bloom. Weak stratification and the early fall bloom likely contributed to a lesser coccolithophore bloom (J. Nielsen, pers comm). The fall bloom may provide a sustained prey resource for zooplankton through the fall.

The Rapid Zooplankton Assessment in spring 2024 noted moderate abundance of small copepods, but low abundance of large copepods and near-zero abundance of euphausiids, which is typical for the spring. In summer, small copepods remained abundant throughout the region. Large copepods remained in low abundance while euphausiids increased, especially towards the northern portion of the SEBS (see p. 89). Euphausiid density during the summer acoustic survey declined in 2024 to the second-lowest value in the time series (Figure 61). In fall, both small and large copepods as well as euphausiids were in low abundance, but increased towards the north (Figure 53). Euphausiids had significantly higher lipid content in 2024 relative to 2022 (Figure 59). The biomass of jellyfish remained low to average in 2024 (Figures 62, 63), representing no significant change in competitive pressure for planktivorous predators like pollock.

As the numerically dominant forage fish in the EBS, age-0 pollock are an important component of available forage over the SEBS shelf to piscivorous predators such as Pacific cod, pollock, seabirds, and marine mammals. In spring 2024, larval pollock abundance was the highest of years sampled (2012, 2014, 2016, 2018, 2024; Figure 66), with larval condition highest in the southeast and lowest to the northwest (Figure 67). By late summer, age-0 pollock CPUE estimates were low in the middle domain (Figure 71), but at the same time in the inner domain, age-0 pollock were the most numerous non-salmonid species collected in the ADF&G nearshore survey (Figure 7). In the middle domain, age-0 pollock were distributed shallower (Figure 73), similar to a warm year, even though the mixed layer depth was deeper (Figure 27) and SSTs were cooler. Since 2022, with the cooler SSTs, pollock weights and energy density have been low while % lipid has been average (see p. 126). Juvenile and adult Pacific herring and capelin are predominantly caught in the NBS (Andrews et al., 2015). As such, both species were in low abundance in the SEBS (Figures 78 and 79). Conversely, the 2024 forecast for Togiak herring was the fifth highest on record, but was 32% lower than the 2023 forecast (see p. 134). Quantitative linkages among ecosystem drivers and forage fish biomass were explored (see p. 115) using dynamic structural equation modeling (DSEM) to illustrate how environmental changes might affect the availability of different forage fish species.

Salmon have unique, species-specific life histories that can extend throughout the Bering Sea ecosystem and into the Gulf of Alaska. Species have shown contrasting responses to the recent return to cooler average temperatures following persistent warm conditions from 2014–2021. Western Alaska chum salmon, for example, occupy the EBS in summer as juveniles before overwintering in the Gulf of Alaska, therefore their dynamics as juveniles are reflective of the pelagic environment in the EBS. These stocks collapsed during the warm period, driven by changes in prey and subsequent energetic condition (Figure 54, Figure 86, Farley Jr et al., 2024). In the SEBS, juvenile chum salmon fish condition has remained below average in 2022 and 2024 (Figure 86). Conversely, juvenile chum salmon condition has improved in the NBS since 2021 (Figure 87) and the 2024 juvenile abundance estimate from the NBS surface

trawl survey was the highest on record (Figure 89). These divergent trends indicate better pelagic foraging conditions for juvenile chum salmon in the NBS than the SEBS. Bristol Bay sockeye salmon life history strategies and population dynamics reflect their freshwater rearing (i.e., lakes) and marine migratory pathways that favor warm conditions. In cooler years, Bristol Bay sockeye delay offshore migration to remain in warmer nearshore waters (Farley et al., 2007) while in warmer years they migrate offshore more rapidly, avoiding extreme marine heatwave conditions over the shelf. Thus, in the recent cooler (i.e., average) conditions, sockeye salmon may have remained nearshore and reflect nearshore foraging conditions. Adult run sizes in Bristol Bay in 2023 and 2024 have been closer to long-term averages (Figure 90). In 2024, juvenile sockeye salmon abundance and fish condition was low in the SEBS. Chinook salmon population dynamics are not as straightforwardly linked to marine conditions; populations have been declining more broadly since the early 2000s, indicating a more complex set of stressors that may be constraining production of these stocks (see p. 139).

Groundfish condition (i.e., length-weight residuals) can provide insights into the foraging conditions for both benthic (e.g., small-mouthed flatfishes) and pelagic (e.g., pollock) foragers. The condition of benthic foragers has been mixed since 2021, showing no clear trends of increasing or decreasing (Figure 95), with estimates of biomass also being mixed (yellowfin sole +8%, northern rock sole +4%, and Alaska plaice -3%) in 2024. Trends in benthic infaunal prey are indirectly assessed via the motile epifauna guild which has remained above the time-series mean since 2010 (Figure 2). The condition of pelagic foragers has decreased and/or remained below the time-series average since ∼2021 (Figure 95), yet estimates of biomass from the bottom trawl survey increased (pollock +74%, arrowtooth flounder +26%) or showed a slight decline (Pacific cod -4%) in 2024[5]. The revised Oscillating Control Hypothesis (Hunt et al., 2011) would predict a return of large, lipid-rich copepods under cooler conditions. It is important to note that thermal conditions over the EBS shelf have largely cooled to average, not cold, conditions (e.g., Figure 30). This may partially explain why the thermal conditions over the SEBS shelf since 2021 have not yet prompted a return of large, lipid-rich copepods or euphausiids over the shelf.

Individual groundfish species may be more or less able to shift their distribution to find preferred thermal conditions or more abundant and/or energetically favorable forage. For example, based on Food Habits Lab stomach content analysis, pollock consumption of copepods increased from 2023 to 2024, replacing euphausiids as the greatest percent by weight in the diets (K. Aydin, pers comm). This may be explained by the spatial distribution of the pollock population in 2024, which was concentrated over the northwest outer domain (L. Barnett, pers comm), where large 'oceanic' copepods occur (euphausiids mainly occur over the middle domain). Additionally, rates of cannibalism have been low between 2021–2024; the lowest year for cannibalism on record was 2018 (K. Aydin, pers comm). More generally, from 2010–2024 adult and juvenile pollock and P. cod growth potential across the EBS (SEBS and NEBS) remains below the long-term average (1982–2010), likely due to metabolic demands that have increased faster than consumption rates or changes in energetic density (see p. 168).

Metrics of stability in the fish community (for species regularly caught in the SEBS bottom trawl survey) indicate overall stability and resilience, although there are anomalous peaks in individual species (e.g., capelin, sablefish). Trends in mean lifespan (Figure 123) show little year-to-year variability and give no indication of shifts between short-lived and longer-lived species. The mean length and the stability of the groundfish community remained above average in 2024 (1982–2024; Figures 124, 125).

Seabirds are indicators of secondary productivity and shifts in prey availability that may similarly affect commercial fish populations. Species that experienced recent population losses (e.g., least auklets) have

[5] https://meetings.npfmc.org/CommentReview/DownloadFile?p=f2da5d6f-17ae-4af0-961a-112377153dc6.pdf&fileName=2024%20EBS%20Bottom%20Trawl%20Survey%20Presentation.pdf

not rebounded. Overall, reproductive success was mixed for both fish-eating and plankton-eating species, but generally higher for species on St. George Island, similar to 2023 (Figures 119 and 120). This may indicate differences in local availability of small schooling forage fish and zooplankton, respectively, in feeding areas utilized by seabirds of each island. High rates of colony disturbance by bald eagles at St. Paul Island also contributed to the reduced reproductive success there (M. Rustand and H. Renner, pers comm). No major seabird die-off events were observed in 2024 (Figure 121).

We track emerging stressors like ocean acidification (OA), as well as emerging science tools and quantitative applications to better understand dynamics and potential impacts to the EBS ecosystem. Metrics of OA (pH and Ω_{arag}) continued a multi-decadal decline, indicating more corrosive bottom-water conditions for marine calcifiers, though values have improved slightly since 2022. At this time, there is no evidence that OA can be linked to recent declines in crab populations. It is worth noting that Ω_{arag} is approaching the threshold value ($<$1.0) for pteropod shell dissolution that could have subsequent biological significance through the food web (Figure 128). Environmental DNA (eDNA) can provide single-species and community level information that could be used in fisheries assessments and management (see p. 29). While eDNA cannot replace some of the biological data collected from traditional survey methods, there are numerous opportunities to expand eDNA collections and leverage eDNA data for fisheries research and management. Several current and on-going collaborations are addressing gadid populations in the Arctic, groundfish communities in the EBS, northern fur seal and Steller sea lion diet studies in the Aleutian Islands, and ice seal surveys along the ice edge during spring break-up. Borealization, or the broad reorganization of Arctic ecosystems to a more temperate physical and biological state, is included as a new index for the SEBS (Figure 2). The index includes nine time series, from physical to biological, and may be useful for summarizing climatic and ecological changes in the SEBS. The borealization index has reverted to values similar to the time series mean during 2022–2024 (Figure 8b).

Northern Bering Sea

Similar to the SEBS, the NBS has returned to more neutral thermal conditions since ~2021. While the extent of sea ice has been steadily increasing in the NBS since 2018 (Figure 3), ice thickness increased dramatically in the Bering Strait region (i.e., a step-change increase) since 2021 (Figure 39b) and has been above average through 2024. Ice thickness may also be a proxy for ice residency over the shelf, which may be related to the abundance of ice algae that contributes to the productivity of the NBS ecosystem. Additionally, the proportion of open-water phytoplankton blooms has been low since 2021 (2024 was the lowest since 2008) (Figure 3), therefore the proportion of ice-associated blooms has been higher. Previous research indicates that a higher proportion of ice-associated blooms is thought to result in a higher abundance of pelagic secondary producers in the summer and fall (Coyle et al., 2008; Kimmel et al., 2018). In fact, the abundance of large copepods measured in fall over the NBS shelf has increased to the time series mean (2000–2024) since 2021 (Figure 3). In 2024, large copepods were patchy with the highest values north and south of St. Lawrence Island (Figure 55) and their lipid content was significantly higher in 2024 compared to 2023 (Figure 58). Jellyfish biomass increased in 2023 and remained high in 2024 (Figure 62). Taken together, these indicators show that pelagic forage has increased in the NBS since 2021.

Measures of pelagic productivity in the NBS include age-0 pollock, herring, capelin, and juvenile salmonids CPUE. Age-0 pollock CPUE estimates have remained low compared to those in the SEBS

(Figure 71). Age-0 pollock weight has been below average in 2022–2024 and while % lipid increased from below average in 2021 to above average in 2024. Age-0 pollock energy density has decreased from above average in 2021 to below average in 2024 as fish are smaller overall (see p. 126). Herring also remained low in the NBS, but capelin increased dramatically from 2023 to 2024 (Figure 79). Juvenile salmonid condition, measured as energy density anomalies, varied among species in the NBS in 2024 (Figure 87). For juvenile pink, chum, and coho salmon condition decreased from positive in 2023 to average in 2024. Juvenile Chinook salmon condition increased from average to positive in 2024. The abundance of juvenile Chinook salmon was at record low in 2024 (Figure 88) while fall juvenile chum salmon was at a record high in 2024 (Figure 89). Trends in pelagic productivity have been mixed since 2021, indicating a potential lagged response to the average thermal conditions.

In the NBS, we track harmful algal blooms (HABs) as an emerging stressor to the ecosystem as well as people's nutritional, cultural, and economic needs. Recent oceanographic changes in the EBS has made conditions more favorable for HAB species, particularly the dinoflagellate *Alexandrium catenella* and diatoms in the genus *Pseudo-nitzschia* (Anderson et al., 2012). In October of 2023, no harvested bowhead whales contained domoic acid, but 90% contained low levels of saxitoxin (Figure 131). This confirms a consistent trend of higher prevalence of saxitoxin than domoic acid in Arctic food webs observed in all regions including the Bering Strait (see p. 215).

Looking ahead through spring 2025, the expected transition to La Niña is projected to bring continued cooler conditions to the EBS shelf with SST anomalies within 0.25°C of normal (Figure 16). Relatively cool SSTs during the early ice season (Oct 15 - Dec 15) may contribute to earlier formation of sea ice than has been observed over the last several years. However, recent storms (e.g., October 20–22, 2024) in the NBS and Bering Strait region, which caused extreme flooding in Shishmaref, may now entrain relatively warmer water into the surface layer and delay sea ice formation. The NBS has shown some indications of 'recovery' from the prolonged warm period (2014–2021). Some trends remain mixed since the return to neutral thermal conditions in 2021. If continued neutral or cool conditions persist, it will be informative to observe how benthic and pelagic indicators of crab and groundfish populations respond to those conditions in the NBS in 2025.

Contents

† indicates new Ecosystem Status Indicator contribution
* indicates Ecosystem Status Indicator contribution updated with 2024 data

List of Tables

List of Figures

Ecosystem Indicators

Noteworthy Topics

Here we present items that are new or noteworthy and of potential interest to fisheries managers.

Environmental DNA: Poised to Transform How We Track Fish Populations

Background
Environmental DNA (eDNA) consists of skin, scales, cells, and DNA from organisms released into the environment. In marine ecosystems, researchers collect and filter water to concentrate biological and genetic material. DNA is then extracted, and DNA sequencing provides information about species near the sampling location. This technology can yield presence and relative abundance data for individual species-of-interest or community composition and biodiversity (Thomsen et al., 2012). Each water sample can be analyzed for multiple taxonomic groups: for example, DNA primers can be selected to target fishes, zooplankton, bacteria, or marine mammals.

The two primary approaches for analyzing eDNA samples are: 1) single-species quantitative PCR (qPCR) and 2) multi-species metabarcoding. Single-species qPCR data provide quantification, whereas metabarcoding results in compositional data that can be analyzed for relative abundance of the species present (Figure 4).

eDNA can reliably generate presence/absence data with appropriate DNA primers and reference DNA libraries. eDNA concentration is correlated with abundance or biomass (Spear and Andrews III, 2021), but multiple factors influence this relationship, most notably body size (Rourke et al., 2022; Yates et al., 2023) and distance between the organism and sampling location (Baetscher et al., 2024). Both presence/absence data and eDNA concentration could be paired with other survey approaches to identify species, for example, in acoustic trawl surveys, particularly in the absence of catch data. Similarly, eDNA could be collected alongside camera images and used to verify species identities or potentially increase the detection distance beyond the camera field-of-view.

Applications
The relative ease of collecting eDNA from water compared to more resource-intensive methods makes eDNA an efficient way to add biological observations that could be used for species distribution models (Riaz et al., 2020), generating indices of abundance (Shelton et al., 2022), filling in spatial data gaps

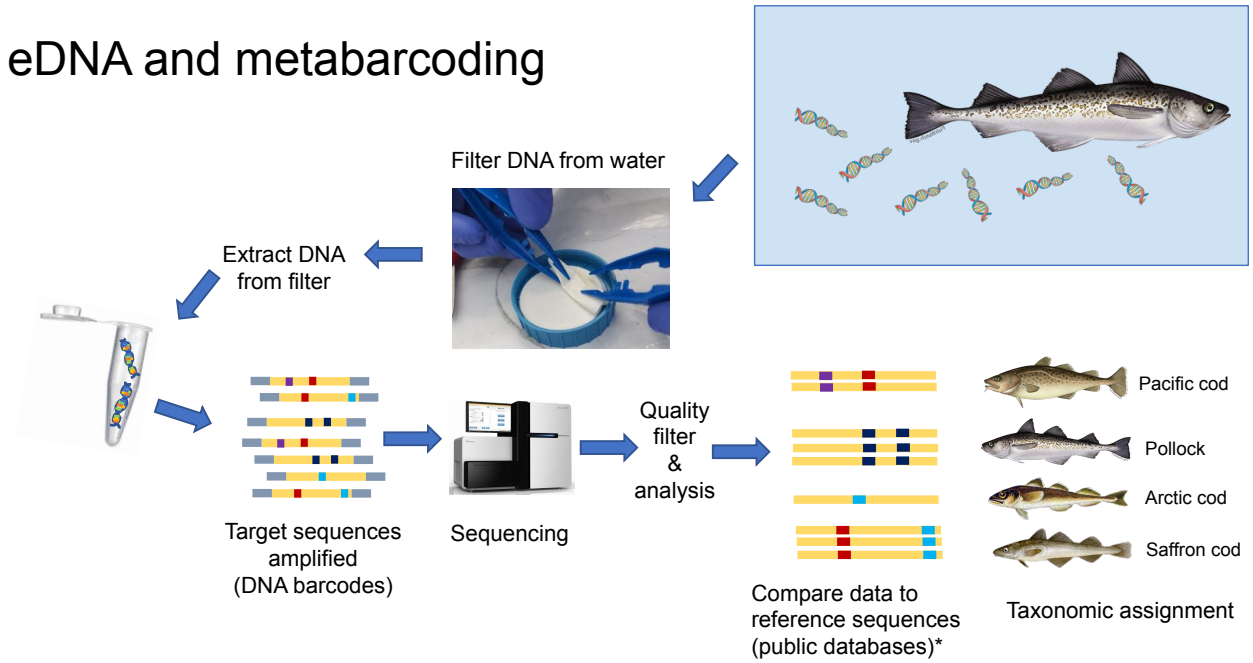

Figure 4: Schematic of the process from water filtration to taxonomic assignment used in eDNA metabarcoding.

between trawl stations, or extending a survey footprint into habitats poorly suited to other collection methods. Further, because sampling is non-lethal, eDNA is a viable sampling option within protected areas (Gold et al., 2021). Water samples for eDNA may be collected from fisheries survey vessels at stations using cast rosettes of Niskin bottles or using passive collectors deployed alongside or independent of nets (i.e., Maiello et al., 2022). Samples may also be collected autonomously from moorings and uncrewed vessels, including Saildrone using flow-through systems while underway (Preston et al., 2024).

Although in the early stages of its field applications, eRNA may provide information about life-history stages (juveniles vs. adults) and physiology (Parsley and Goldberg, 2024; Yates et al., 2023), expanding the potential utility of environmental genetic data for contributing to survey data products.

The potential for eDNA to provide data for fisheries assessments and management is recognized by both eDNA researchers and assessment scientists (Kasmi et al., 2023; Ramírez-Amaro et al., 2022; Rourke et al., 2022; Stoeckle et al., 2020). However, discrepancies between eDNA and more traditional survey methods are perceived as limitations that undermine the utility of eDNA (Jerde, 2021). Some of these limitations include information about abundance or biomass; size/age class; or questions about the spatial and temporal area sampled by eDNA (Jerde, 2021). Furthermore, eDNA typically detects more species than surveys, which could be an asset (e.g., detecting species that can avoid nets), but also complicates comparisons between data sources. While outstanding questions remain, the field of eDNA has done considerable work to better characterize the dynamics of eDNA, including understanding shedding and degradation rates (Collins et al., 2018), dilution and transport (Baetscher et al., 2024; Shea et al., 2022), and the relationship between eDNA concentration and biomass (Figure 5,

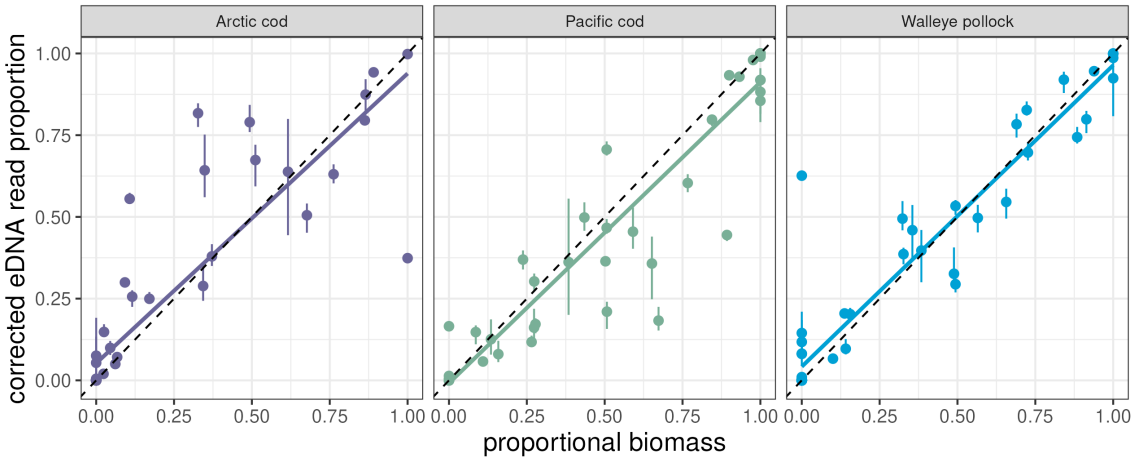

Figure 5: Results from an eDNA aquarium study with Pacific and Arctic cods and walleye pollock that shows a strong correlation between proportional biomass and eDNA sequencing reads. Aquarium tanks included fish from one or more species and each point in the figure corresponds to the biomass in a given trial. Solid lines represent linear models for each species. eDNA data were transformed using a quantitative metabarcoding model that accounts for amplification bias across the three species. Aquarium experiments were performed by the AFSC Fisheries Behavioral Ecology Program at the Hatfield Marine Science Center.

In order to validate the data generated from eDNA, species composition has been compared to other survey methods, including trawl catches (Kasmi et al., 2023; Maes et al., 2024; Salter et al., 2019), acoustic data (Shelton et al., 2022), beach seines (Shelton et al., 2019), and angling catches (Ogonowski et al., 2023).

Generally there is agreement that in its present form, eDNA cannot replace some of the biological data collected from traditional survey methods (i.e., size, fecundity, body condition, etc.). Despite these limitations, there are numerous opportunities to expand eDNA collections and leverage eDNA data for fisheries research and management. eDNA collected from moorings and autonomous platforms can expand spatial and temporal sampling, particularly in hard-to-access environments, including the Arctic.

Collaborations

Through a collaboration between PMEL and the NOAA AFSC, eDNA sampling is being performed throughout the Chukchi Sea to identify changes in distributions of arctic cod and walleye pollock. The AFSC Genetics Program has also sampled eDNA alongside bottom trawl surveys, the BASIS surface trawl ecosystem survey in the northern and southeastern Bering Sea, Marine Mammal Lab (MML) northern fur seal and Steller sea lion diet studies in the Aleutian Islands, and ice seal surveys along the ice edge during spring break-up.

Specifically, in collaboration with AFSC's NBS surface trawl survey, the Genetics Program is using paired trawls/eDNA to analyze concordance between the fish communities identified by each method. This research will be used to compare species distribution models from eDNA and trawls and provide insight into future applications for eDNA alongside surveys.

Contributed by
Diana Baetscher and Kimberly Ledger
Auke Bay Laboratories, Alaska Fisheries Science Center, NOAA Fisheries

Alaska Department of Fish & Game Nearshore Survey

In September 2024, the Alaska Department of Fish & Game surveyed nearshore marine waters of the southeastern Bering Sea (SEBS). The aim of this survey is to study the early marine life stage, known as the juvenile stage, of salmon originating from southwestern Alaska systems (primarily Kuskokwim River and Bristol Bay). The juvenile life stage (i.e., the first summer in the ocean) is a critical period within the salmon life cycle. Juvenile salmon surveys provide valuable insights on the early marine ecology (e.g., abundance, distribution, size, diet, and condition) of juvenile salmon, which are needed to understand which parts of the salmon life cycle are most critical for survival. This project used trawl gear fished at the surface to sample the shallow juvenile salmon habitat on the SEBS shelf. The goals of this project are to estimate the juvenile abundance of SEBS stocks of salmon and to evaluate their life history and health characteristics, such as size at capture, diet, and energetic status.

Survey operations were conducted onboard a chartered commercial fishing vessel between August 25 and September 22 at stations spread across the SEBS shelf between Nunivak Island and Bristol Bay. At each of 55 stations successfully sampled in 2024, a Conductivity-Temperature-Depth instrument was deployed to measure oceanographic characteristics of the water column, like salinity and temperature; a Calvet net (vertical tow) and bongo net array (oblique tow) were deployed to assess the distribution and abundance of various zooplankton species; and a surface trawl net (Nordic 264, NET Systems, Bainbridge, WA, USA) was towed for one hour to collect epipelagic species. The average vertical and horizontal dimensions of the net were 15.6 m and 21.5 m, respectively. Following each tow, juvenile salmon were counted, measured for length and weight, and sampled for various biological analyses (e.g., genetics, diet, and energetic density). Other pelagic species caught in the trawl were also enumerated, measured, and retained for various analyses.

Juvenile salmon were captured at all but two stations in the survey grid. Chum salmon (*Oncorhynchus keta*) were the predominant salmon species captured (n=1,302) followed by sockeye salmon (*O. nerka*; n=471), Chinook salmon (*O. tshawytscha*; n=310), coho salmon (*O. kisutch*; n=215), and pink salmon (*O. gorbuscha*; n=95). Juvenile pink salmon catches were expected to be relatively low given that pink salmon runs in western Alaska are predominantly even-year dominant and thus juveniles would be expected to be present in higher abundances in odd years. Juvenile Chinook and coho salmon catches were higher in nearshore stations, especially around Cape Newenham. Juvenile chum salmon catches were spread across the survey grid but absent in the furthest offshore stations. Juvenile pink salmon were concentrated in the western portion of the grid while sockeye salmon were concentrated in the middle of the grid (Figure 6).

Catches of non-salmonid fish species were variable (Figure 7). Capelin (*Mallotus villosus*; all age-0 individuals) were only found at four stations throughout the survey (n=35). Pacific cod (*Gadus macrocephalus*; predominantly age-0) were present at the most offshore stations (n=527). Pacific herring (*Clupea pallasii*; predominantly age-1+) were caught in relatively low numbers at both nearshore and offshore stations (n=324). Pacific sand lance (*Ammodytes hexapterus*; various ages) were primarily caught at the nearshore most stations (n=2,255). Walleye pollock (*Gadus chalcogrammus*; predominantly age-0) were the most numerous and commonly encountered non-salmonid fish species in the survey grid (n=66,087). In total, 23 fish species were caught during survey operations.

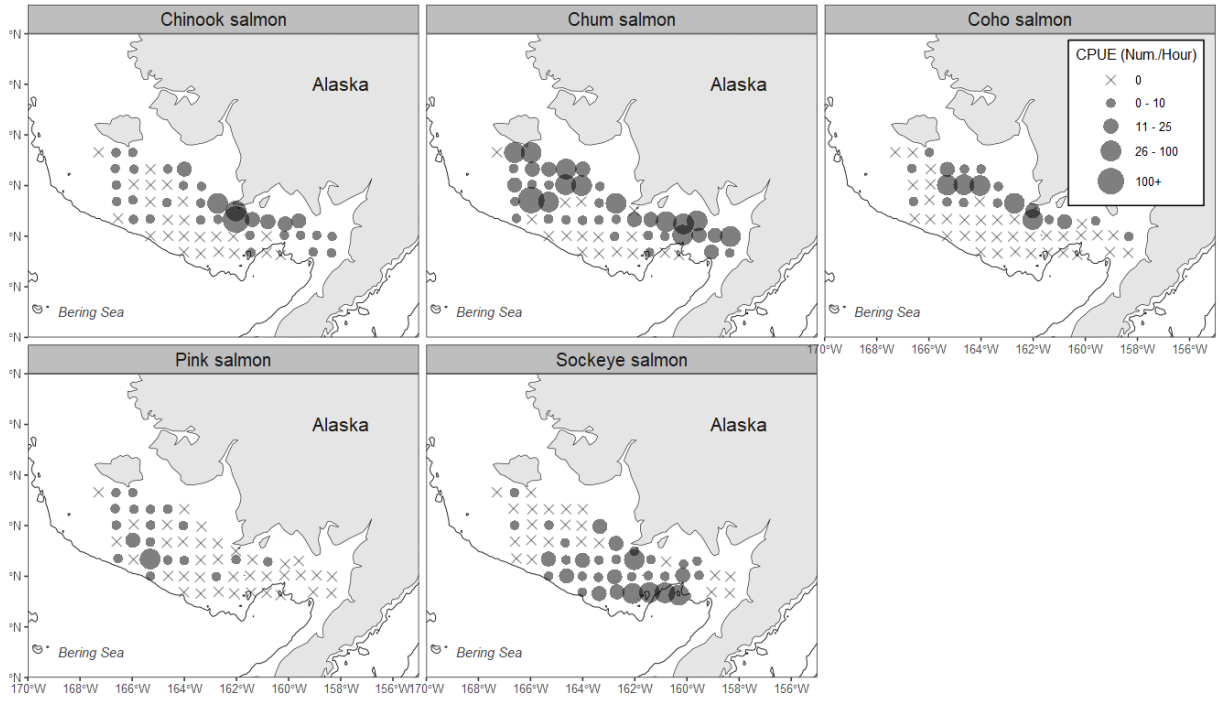

Figure 6: Juvenile salmon (*Oncorhynchus* spp.) catch-per-unit-effort (number/hour) at 55 stations sampled during the ADF&G nearshore southeastern Bering Sea salmon survey. Solid line on the map denotes the 50 m isobath.

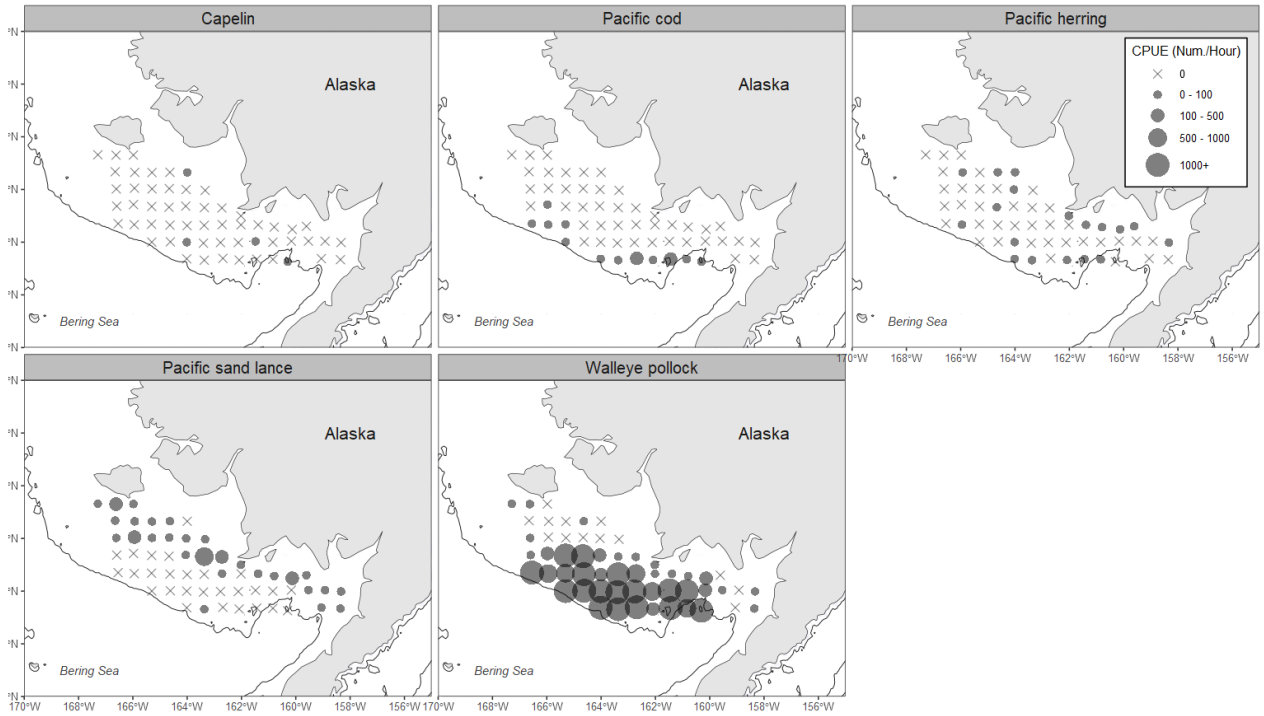

Figure 7: Non-salmonid fish catch-per-unit-effort (number/hour) at 55 stations sampled during the ADF&G nearshore southeastern Bering Sea salmon survey. Solid line on the map denotes the 50 m isobath.

This survey is intended to be the start of a long-term project to assess the early marine ecology of southwestern Alaska stocks, understand factors that influence population dynamics, and make progress towards the long-term goal to develop a forecasting tool for Kuskokwim River salmon. Funding has been secured to continue survey operations into 2027. Zooplankton abundance and distribution, juvenile salmon genetic stock compositions, and juvenile salmon diet and energetic density results should be available in Spring 2025.

Contributed by
Sabrina Garcia, Dr. Kathrine Howard, and Benjamin Gray
Alaska Department of Fish & Game
Division of Commercial Fisheries

A Borealization Index for the Southeastern Bering Sea

Borealization – the transition from an Arctic physical state supporting a cold-adapted species assemblage to a subarctic (boreal) physical state supporting a warm-adapted assemblage – is one of the most consequential impacts of climate change for the Bering Sea and Arctic marine ecosystems generally. While "borealization" sometimes references only changes in species composition, we use the term to refer to the broad reorganization of Arctic ecosystems to a more temperate physical and biological state.

Here, we present an index of borealization for the southeastern Bering Sea. This index was developed to help understand, attribute, and project the causes of the snow crab collapse in 2019–2021, and the index outperforms bottom temperature as a predictor of snow crab abundance. Because the physical and ecological changes associated with borealization involve nearly every component of the ecosystem, the index may be useful for summarizing climatic and ecological changes to a wide range of species of management interest beyond snow crab.

To measure the progression of borealization, we analyzed nine time series that reflect the difference between Arctic and boreal conditions in the southeastern Bering Sea between 1972 and 2024, covering changes in ice cover, bottom temperature, primary production, and community composition for phytoplankton, zooplankton, and groundfish. To create an overall index of borealization from the individual time series we used Dynamic Factor Analysis (DFA), a state-space approach for identifying shared variability across multiple time series. The DFA model identified a single shared trend that combines negative loadings for time series associated with Arctic conditions, and positive loadings for time series associated with boreal conditions (Figure 8a). The DFA trend provides a clear index of borealization with transition from the most Arctic-like conditions in the 1970s and 2007–2013 to the most boreal conditions during the warm, low-ice years of 2018–2019 (Figure 8b). The borealization index has reverted to values similar to the time series mean during 2022–2024.

Contributed by
Mike Litzow[1], Erin Fedewa[1], David Kimmel[2], Jens Nielsen[2,3], and Emily Ryznar[1]
[1]NOAA Alaska Fisheries Science Center, Kodiak, AK
[2]NOAA Alaska Fisheries Science Center, Seattle, WA
[3]Cooperative Institute for Climate, Ocean, and Ecosystem Studies, University of Washington, Seattle, WA

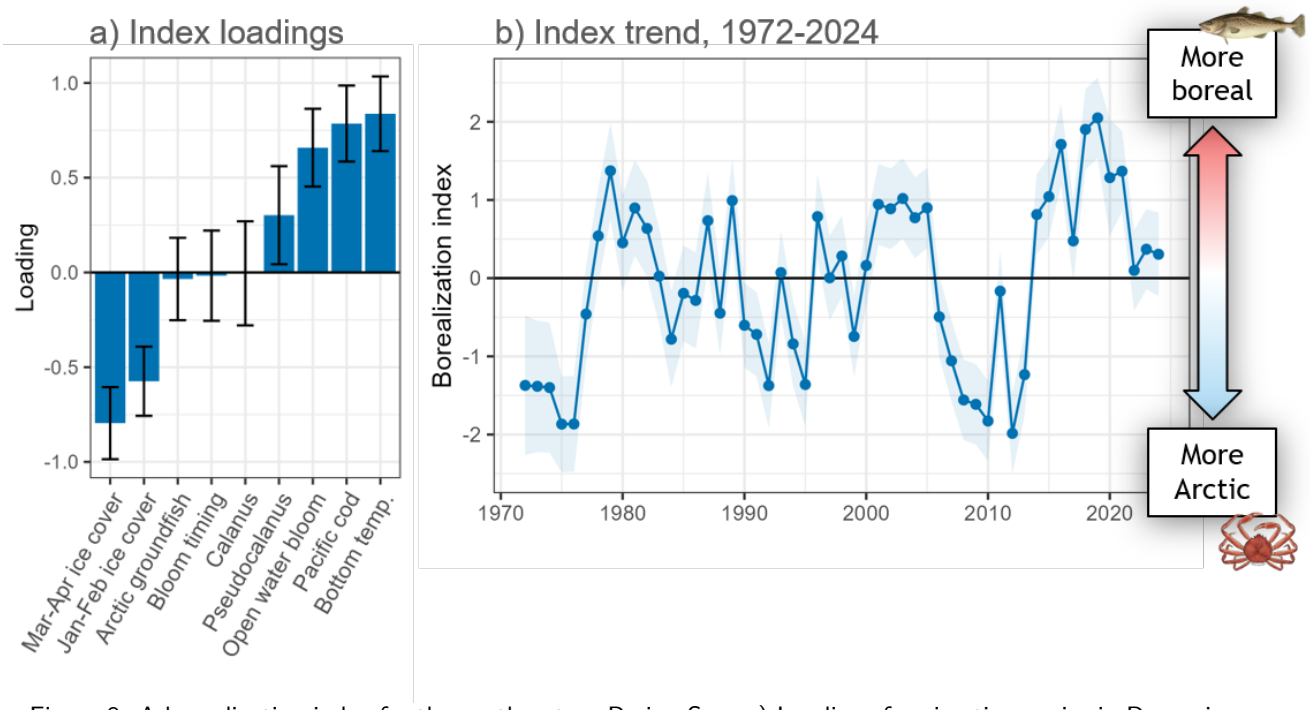

Figure 8: A borealization index for the southeastern Bering Sea. a) Loadings for nine time series in Dynamic Factor Analysis (DFA) model. Negative (positive) loadings indicate time series associated with Arctic (boreal) conditions. b) The borealization index, defined as the shared trend from the DFA model. Negative (positive) values indicate more Arctic (boreal) conditions in the southeastern Bering Sea. Error bars and ribbon indicate 95% confidence interval. For information on methods for individual time series and their relationship with borealization, see Litzow et al. (2024).

Ecosystem Status Indicators

Physical Environment Synthesis

This synthesis section provides an overview of physical oceanographic variables and contains contributions from (in alphabetical order):

Kelia Axler - NOAA Fisheries, Alaska Fisheries Science Center, Resource Assessment and Conservation Engineering Division, EcoFOCI Program
Lewis Barnett - NOAA Fisheries, Alaska Fisheries Science Center, Resource Assessment and Conservation Engineering Division
Shaun Bell - NOAA Pacific Marine Environmental Lab [PMEL]
Matt Callahan - Pacific States Marine Fisheries Commission
Lauren Divine - Ecosystem Conservation Office at Aleut Community of St. Paul Island
Tyler Hennon - University of Alaska Fairbanks, College of Fisheries and Ocean Sciences
Kelly Kearney - University of Washington, Cooperative Institute for Climate, Ocean, and Ecosystem Studies [CICOES] and NOAA Fisheries, Alaska Fisheries Science Center, Seattle WA
Emily Lemagie - NOAA Pacific Marine Environmental Lab [PMEL]
Aaron Lestenkof - Ecosystem Conservation Office at Aleut Community of St. Paul Island
Jim Overland - NOAA Pacific Marine Environmental Lab [PMEL]
Lauren Rogers - NOAA Fisheries, Alaska Fisheries Science Center, Resource Assessment and Conservation Engineering Division, EcoFOCI Program
Sean Rohan - NOAA Fisheries, Alaska Fisheries Science Center, Seattle, WA
Phyllis Stabeno - NOAA Pacific Marine Environmental Lab [PMEL]
Rick Thoman - University of Alaska Fairbanks, International Arctic Research Center, Alaska Center for Climate Assessment and Policy
Muyin Wang - University of Washington, Cooperative Institute for Climate, Ocean, and Ecosystem Studies [CICOES] and NOAA Pacific Marine Environmental Lab [PMEL]

Last updated: October 2024

Introduction

In this section, we provide an overview of the physical oceanographic conditions impacting the eastern Bering Sea (EBS), describe conditions observed from fall 2023 through summer 2024, and place 2024 in historical context. The physical environment impacts ecosystem dynamics and productivity important to fisheries and their management. We merge across information sources, from broad-scale to local-scale, as follows:

1. Alaska-wide Trends
    (a) Climate Overview
    (b) Regional Highlights
2. Eastern Bering Sea Trends
    (a) Bering Sea Climate Overview
    (b) Surface Winds and Air Temperatures
    (c) Water Temperature
    (d) Sea Ice
    (e) Cold Pool

Executive Statement

Contributed by Tyler Hennon, *tdhennon@alaska.edu*

Observations over the last year (August 2023–August 2024) show that the thermal state of the eastern Bering Sea (EBS) is close to the historical baseline of many metrics. There have been no sustained sea surface temperature (SST) marine heatwaves since January 2021 over either the northern or southeastern Bering Sea (delineated at 60°N; Figure 9), and modeled EBS bottom temperatures were mostly near-normal over the past year. Beginning in May and continuing through summer 2024, persistent storms resulted in a deeper mixed layer, which entrained deeper, cooler water, such that SSTs remained below seasonal means into fall of 2024. However, observations suggest the vertically integrated heat content was still slightly above average (Figure 28).

Atmospheric conditions are one of the primary drivers that impact the oceanographic setting in the EBS. The strength and location of the Aleutian Low Pressure System during winter 2023–2024 were near climatological averages. Thus, despite delayed formation of sea ice in fall 2023, winds from the U.S. Arctic helped advance sea ice to near-normal extent by mid-winter. While near-normal sea ice extent and thickness may have contributed to an average cold pool ($<$2°C water) extent similar to the two prior years, the footprint of the coldest waters ($<$0°C) was diminished in 2024.

For projections into 2025, the aggregate estimate from the National Multi-Model Ensemble (NMME) predicts that SSTs over the EBS are expected to be near normal (anomalies within $<$0.5°C of the 1982–2010 baseline). With the expected transition to La Niña, cooler conditions in the EBS may follow.

Synthesis Summary

Contributed by Tyler Hennon, *tdhennon@alaska.edu*

Beginning in about 2021, the eastern Bering Sea (EBS) exited the prolonged warm stanza and has entered a more neutral thermal state. Over the past year (August 2023–August 2024) many metrics, including sea surface temperature (Figure 23, Figure 30, Figure 34), wintertime sea ice areal extent (Figure 36) and thickness (Figure 39, Figure 40), and cool pool extent (Figure 41, Figure 42) have continued to be near historical averages.

The NINO3.4 index, which tracks the state of El Niño/Southern Oscillation (ENSO) was positive for much of the last year (Figure 12), though it did not correspond to warmer conditions as it did in 2016. However, unlike 2016, the Pacific Decadal Oscillation (PDO) index was now in a negative state, countering the effect of the El Niño. For the EBS, atmospheric drivers like the Beaufort High and Aleutian Low pressure systems (Figure 13) are stronger determinants of oceanic conditions. NCEP/NCAR Reanalysis winds show that the strength of the Aleutian Low was very near the historical (1991–2020) average (Figure 14), and that the Low's center during winter 2024 was also near the historical average (Figure 15).

Satellite observations of sea surface temperature (SST) have recorded no sustained marine heatwaves in the southeastern or northern Bering Sea (delineated at 60°N; Figure 9, Figure 18) since January 2021 (Figure 29). Similarly, ROMS-based bottom temperatures were fairly consistent with seasonal averages (1985–2014 baseline) from August 2023 to August 2024 over much of the Bering Sea (Figure 34). Of note, however, unusually warm bottom waters were modelled in the outer domain (between 100-200 m isobaths) of the Northern Bering Sea (NBS) beginning in early spring 2024. Also beginning in spring 2024, SSTs cooled to average conditions (Figure 34). Both of these observations may be due to increased storminess and wind intensity, which (i) drew warmer slope water onto the outer shelf and (ii) deepened the mixed layer over the middle shelf, mixing cooler bottom water into the surface layer. Although a deeper mixed layer (Figure 27) contributed to cooler SSTs, observations at mooring M2 show that integrated heat content has remained slightly above average (1995–2010) from late spring to summer (Figure 28).

The temporal evolution of sea ice extent in the Bering Sea (Figure 37) generally resembled the 2022–2023 season, where sea ice formation was again delayed due to residual warmth in the system in fall 2023 (Figure 35). Despite warmer fall conditions, cold southward winds from the Arctic helped sea ice advance quickly after mid-December. Ice extent then oscillated below the historical average for much of the winter due to short-term shifts (periods of 2-4 weeks) in the prevailing weather patterns (Figure 37). The average sea ice extent for the 2023–2024 winter was greater than extents seen during the most recent warm stanza (2014–2021), but would have been considered a 'low ice' year prior to 2010 (Figure 36).

Sea-ice thickness across the EBS was close to, or moderately above, the median (2011–2024), except in the Norton Sound region that was slightly below the median (Figure 39, Figure 40). Sea-ice thickness generally declined through the 2010s, reaching lows between 2018–2020 corresponding to years of record-low sea ice extent (Figure 36). The return of sea ice and ice thickness has coincided with a freshening of waters near St. Paul Island (Figure 26), which, prior to about 2021, had seen a general salinization trend that was likely due to the absence of sea ice (a fresh water source) (Figure 25).

In 2024, the cold pool exhibited trends of both average and warm years. Observations during the standard bottom trawl survey show that, though the spatial extent of the cold pool (<2°C waters) was only slightly below that of 2023 (12.7% reduction; Figure 2), the extent of the coldest waters was greatly reduced (Figure 41, lower panel). The observed spatial extent of the <-1°C and <0°C isotherms were down 54.4% and 75.0%, respectively, similar to extents observed during warm years (e.g., 2005, 2014, and 2016). Both observations (Figure 24) and model output (Figure 42) show the presence of a weak cold tongue extending into the southeastern middle domain, with the coldest water remaining over the northern middle shelf.

The National Multi-Model Ensemble (NMME) projections last year (August 2023) predicted a near-normal (compared to the 1982–2010 baseline) SST environment in the Bering Sea for the period of November 2023 to April 2024. This was largely borne out by observations. For the coming year (winter 2024 through spring 2025), with the expected transition to La Niña cooler conditions, NMME model projections for SST anomalies are within 0.5°C of normal, with most of the EBS falling within 0.25°C of normal (Figure 16).

1. Alaska-Wide Trends

(a) Climate Overview

Monthly Sea Surface Temperature (SST) and Surface Winds

Contributed by Emily Lemagie, *emily.lemagie@noaa.gov*, and Shaun Bell

Sea surface temperatures (SST) and sea ice data from the NOAA High-resolution Blended Analysis of Daily SST and Ice (OI SST V2), along with 10 m wind data from the NCEP/NCAR Reanalysis II[6] from September 2023–August 2024 are described across regions of the North Pacific Ocean and U.S. Arctic (Figure 9). SSTs were anomalously warm throughout most of the Alaskan marine waters in November 2023. Prevailing wind anomalies and storminess in the winter through spring 2024 associated with the Aleutian Low Pressure System contributed to cooling the surface waters until, by the summer, SSTs were similar to or cooler than climatological mean temperatures. While the decreasing tendency of the SST anomaly was consistent across most of the geographic area (Figure 10), the mechanisms and details of this evolution varied by region.

Southward winds associated with the near normal location of the Aleutian Low (Figure 15) advected seasonal sea ice southward in winter 2023–2024. Through spring 2024, southward winds from the U.S. Arctic, along with low heat transport from the south, contributed to a maximum sea-ice extent over the Bering Sea shelf that reached near historical norms despite the warm fall 2023 conditions. Eastward wind anomalies around 45–50°N in winter through early spring, associated with southward Ekman transport, may have reduced northward heat transport through the Aleutian Island passes and along the eastern coastal Gulf of Alaska, leading to a cooling trend across the shelf and coastal regions. The cooling trend over the Gulf of Alaska basin in spring may have been associated with counterclockwise wind anomalies driving Ekman pumping of subsurface waters towards the surface. Storminess and strong winds also contributed to vertical mixing across the regions, which is associated with cooler surface temperatures.

[6] `https://psl.noaa.gov/data`

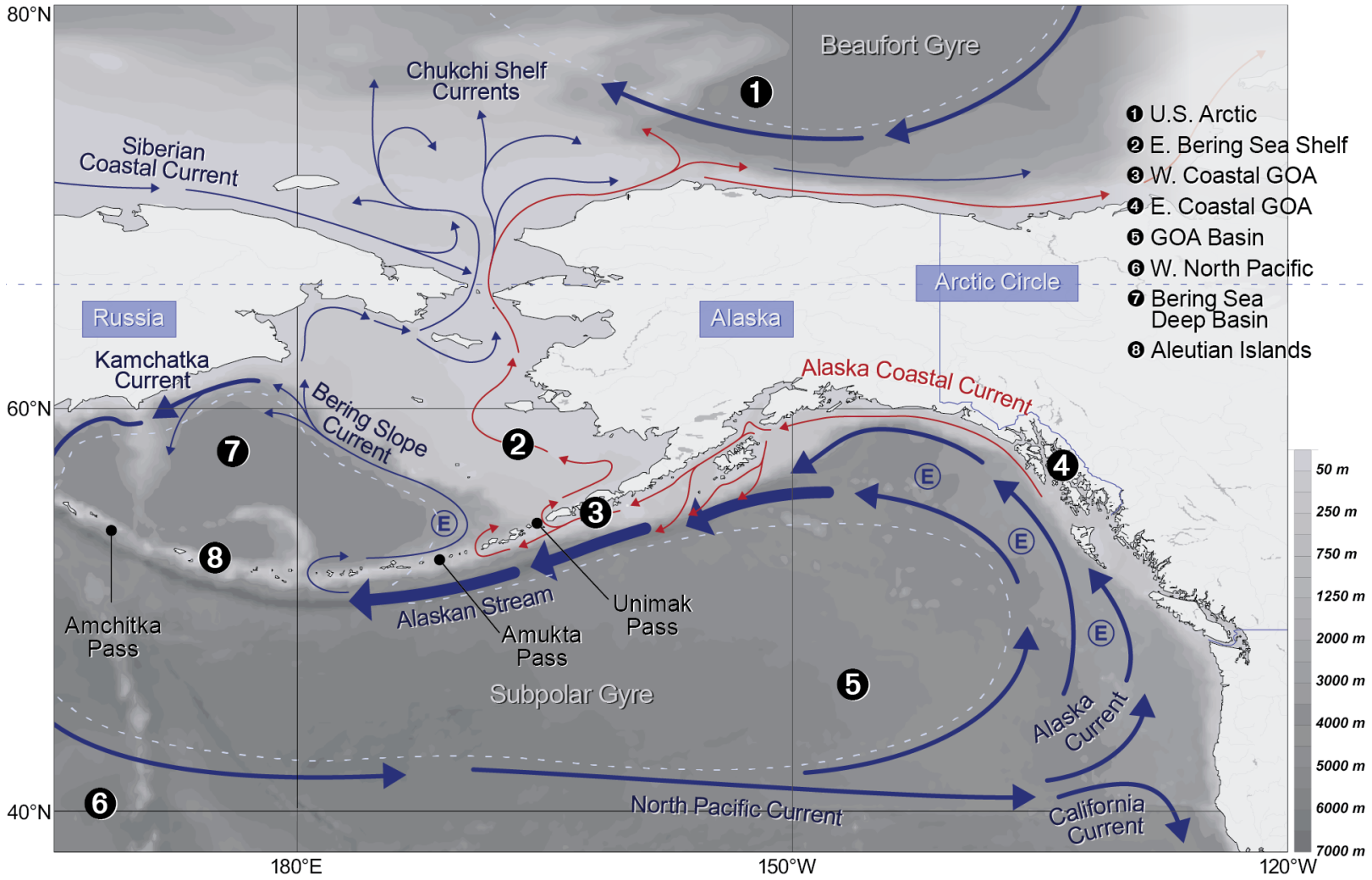

Figure 9: Geographic regions of interest, ocean bathymetry, and mean currents across the North Pacific and U.S. Arctic. Circled "E" denote eddies. Figure courtesy of Sarah Battle, PMEL.

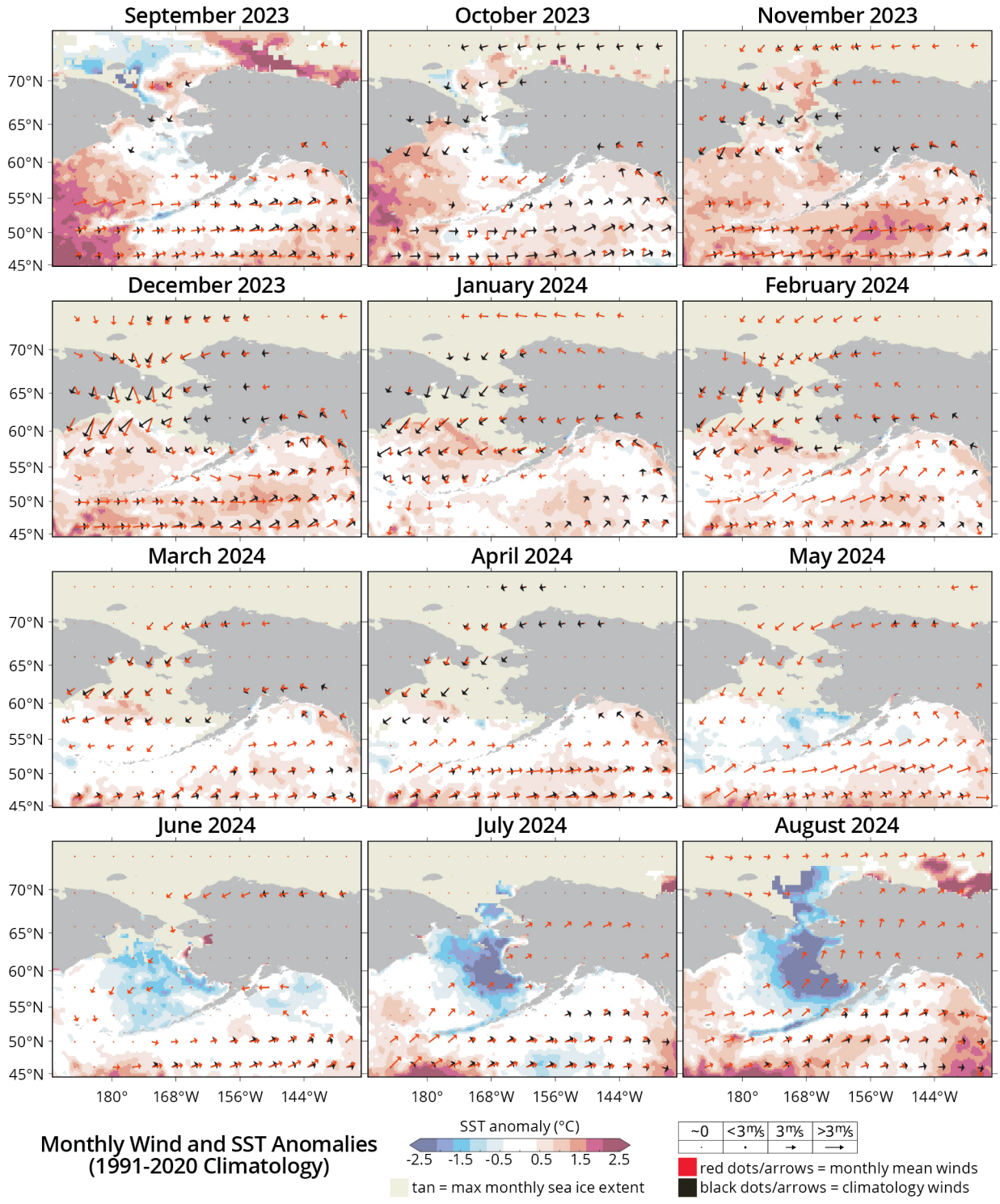

Figure 10: Monthly mean maps of sea surface temperature (SST) anomalies and surface winds. Monthly climatological winds (black) are compared to monthly mean winds (red). The climatological period is 1991–2020. SST data are from the NOAA High-resolution Blended Analysis of Daily SST and Ice (OISST), and 10 m wind data are from the NCEP/NCAR Reanalysis II; both are available from NOAA's Physical Sciences Laboratory. Figure courtesy of Sarah Battle, PMEL.

Seasonal SST and Sea Level Pressure (SLP)

Contributed by Emily Lemagie, *emily.lemagie@noaa.gov*, and Shaun Bell

The sea surface temperatures over the North Pacific were anomalously warm from fall 2023 through winter 2024 (Figure 10). The warmth was greatest between 30°N–45°N, where SST anomaly peaks over the western Pacific remained above 2.5°C into spring 2024. Warm seasonal SST anomalies extending over most of the mid-latitude Western Pacific with peak magnitudes above 2°C have persisted since the winter of 2019–2020, a pattern that is represented by the negative PDO index over the last 5 years (Figure 12). Over the most recent fall and winter, strong warm anomalies were also measured along the Equator (captured by the El Niño index, Figure 12). Warm fall SST along the eastern Pacific coast are also consistent with El Niño conditions. Equatorial anomalies have weakened, but remained positive, in spring 2024. North of 45°N, and throughout much of the Alaska marine waters, the winter warmth abated and SST were near historical mean temperatures in spring 2024. Seasonal average summer temperatures were near normal over most of the Alaska marine waters, except over the Bering Sea shelf where the mixed layer depth was deeper than average resulting in cooler SSTs.

The fall (Sept-Nov 2023) SLP was near the climatological mean (Figure 11), a result of shifting atmospheric conditions, and was associated with fall storms and variable wind speed and direction throughout the season. Jan-Feb 2024 winter mean sea level pressure was also similar to the mean winter pattern. The center of the Aleutian Low Pressure System was shifted to the southwest from the historical mean (Figure 15), and with westward wind anomalies >2 m/s along the Aleutian Islands. The seasonal mean SLP in spring (Mar-May 2024) resulted in a clockwise wind anomaly of $\sim$2-3 m/s eastward between 45-50°N, westward focused between 20-30°N, and southward off the U.S. west coast, enhancing coastal upwelling (not shown). In summer, near-normal surface pressure and wind patterns were associated with near-normal surface temperatures over much of the region, except through the Aleutian Island passes and eastern Bering Sea shelf where surface temperatures were below average due to the deep surface mixed layer.

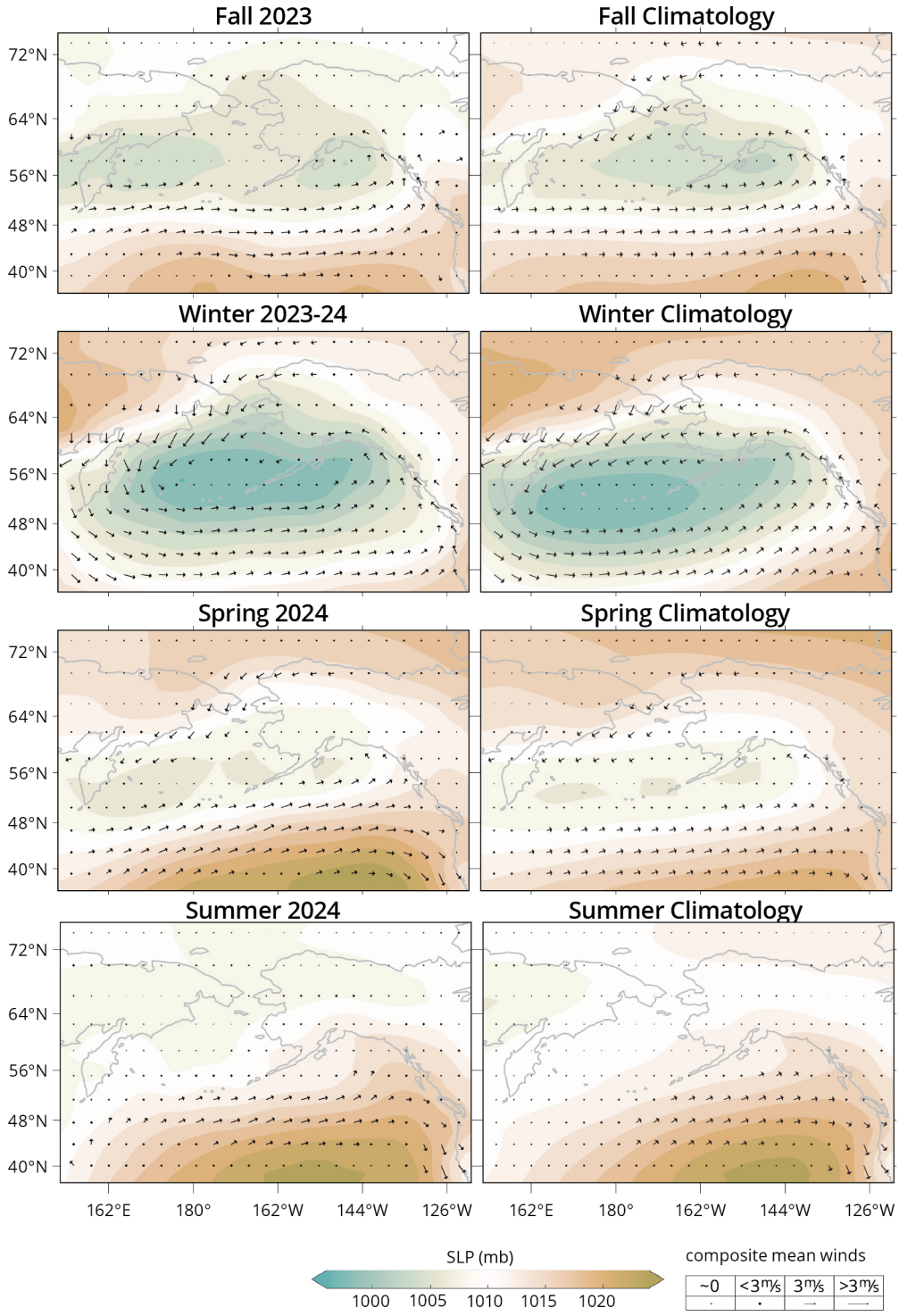

Figure 11: Seasonal (left hand column) sea level pressure (SLP) for fall (Sep-Nov 2023), winter (Dec 2023-Feb 2024), spring (Mar-May 2024), and summer (Jun-Aug 2024), as well as seasonal mean winds. SLP and wind climatologies (right hand column) for the same four time periods. Climatologies are calculated from 1991–2020.

State of the North Pacific Ocean

Contributed by Emily Lemagie, *emily.lemagie@noaa.gov*, and Shaun Bell

Commonly used climate indices for relating patterns across the Alaska marine ecosystem include the NINO3.4 index for the state of the El Niño/Southern Oscillation, the Pacific Decadal Oscillation (PDO), North Pacific Index (NPI), North Pacific Gyre Oscillation (NPGO), and the Arctic Oscillation (AO) (Figure 12).

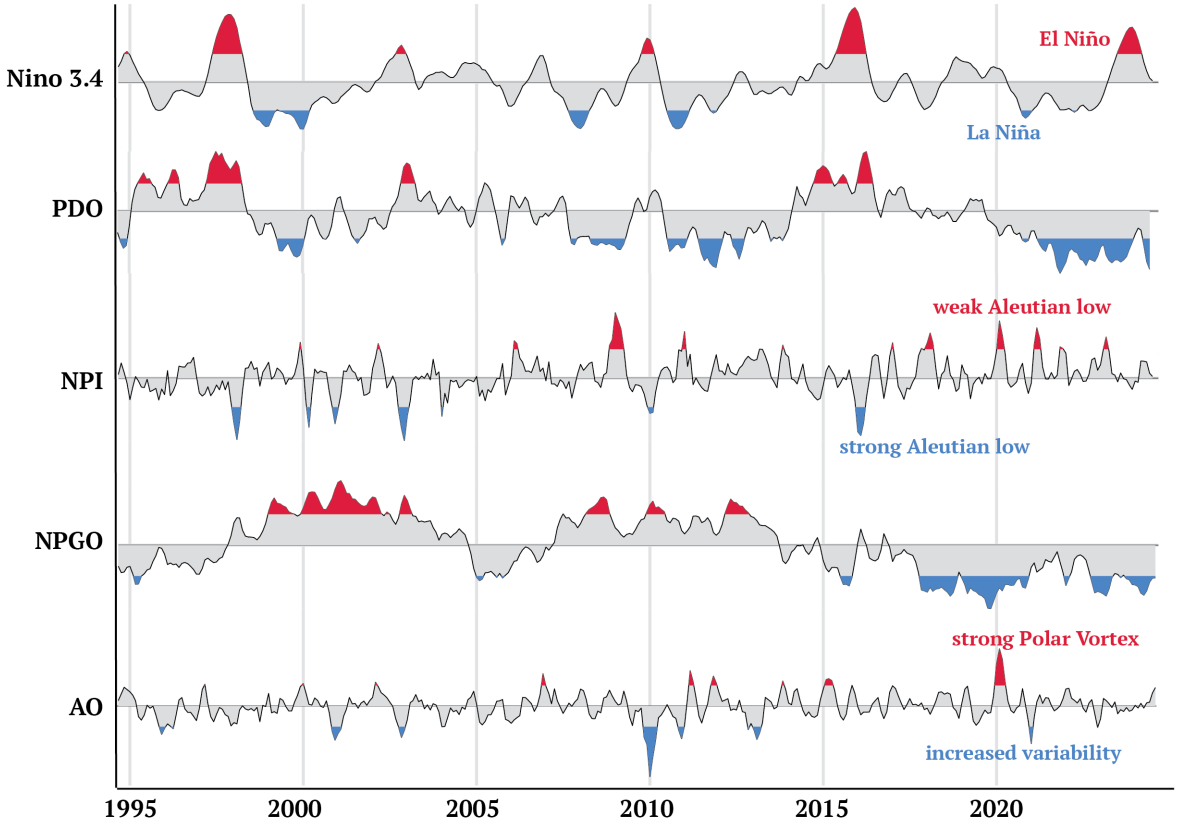

Figure 12: Time series of five commonly used indices for relating patterns across the Alaska marine ecosystem, including the NINO3.4 index for the state of the El Niño/Southern Oscillation, the Pacific Decadal Oscillation (PDO), North Pacific Index (NPI), North Pacific Gyre Oscillation (NPGO), and the Arctic Oscillation (AO) indices for 1995–2024. Each monthly index is normalized using a 30-year climatology from 1991–2020 and smoothed using a 3-month running mean. Lighter shaded areas are within one standard deviation of the 30-year climatology, while red (positive) and blue (negative) shading indicates values exceeding one standard deviation from the 30-year climatology. Additional information on these indices can be found on the NOAA Physical Sciences Laboratory website (`https://psl.noaa.gov/data/climateindices/`).

Winter atmospheric conditions over Alaska are heavily dominated by the Aleutian Low Pressure System (ALPS), which develops and strengthens seasonally between the Beaufort High and North Pacific high pressure regions. The strength and location of the ALPS in January-February 2024 were similar to historical means (Figure 13).

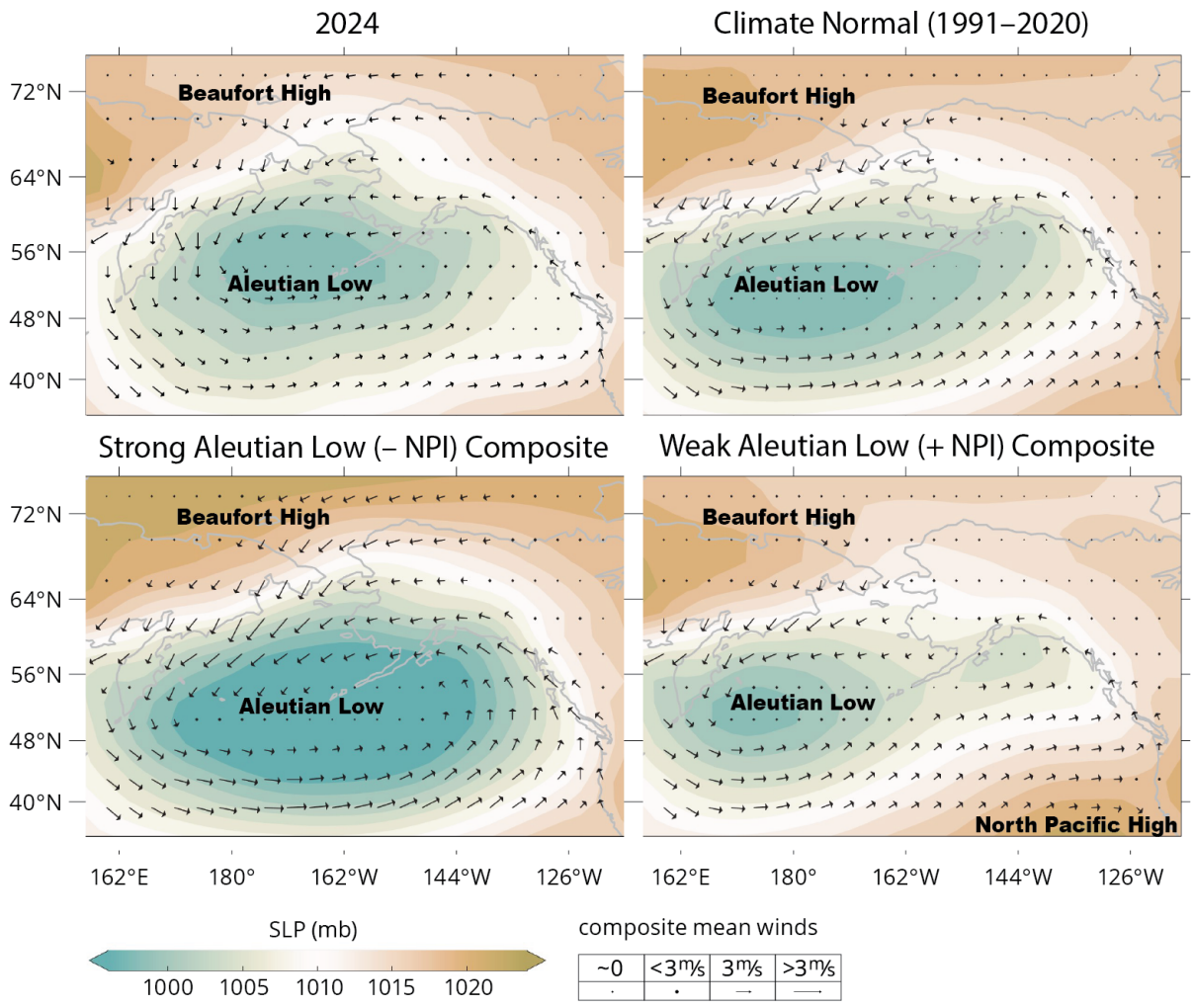

Figure 13: Top row: Mean January-February sea level pressure (SLP) and surface wind patterns in 2024, from the climatological mean (1991–2020). For reference, January-February SLP composite mean patterns for negative (strong Aleutian Low Pressure System) and positive NPI (weak Aleutian Low Pressure System) conditions are also shown.

Wintertime Aleutian Low Index

Contributed by James Overland, *james.e.overland@noaa.gov*, and Muyin Wang

Both the North Pacific Index (NPI) and Aleutian Low Index (ALI) provide complementary views of the atmospheric pressure system in the North Pacific, with the NPI offering a broader perspective of the atmospheric pressure over a larger area of the North Pacific, while the ALI focuses on the Aleutian Low Pressure System itself. The two indices have an inverse relationship: when the NPI is strong, the ALI tends to be low.

The Aleutian Low is the dominant feature of the atmospheric pressure system in the northern North Pacific during winter (Dec-Mar). Variability in the strength and the position of the Low is important to the Alaska marine ecosystem through its impact on circulation, surface heat fluxes, mixed layer depth, and the extent of sea ice cover over the Bering Sea, all of which influence the rich biological resources of the sea (Rodionov and Overland, 2005; Wooster and Hollowed, 1995). In general, the intensity and position of the Aleutian Low can significantly influence storm tracks, ocean circulation, and weather patterns across the North Pacific, impacting North America.

Motivated by work from Rodionov and Overland (2005), we defined the Aleutian Low Index (ALI) as the areas where sea level pressure (SLP) is less than or equals to 1000 hPa in the North Pacific region (40-60°N, and 160E-160°W). The Aleutian Low is a statistical low, which exists in winter only (Figure 11). We computed the monthly Aleutian Low Index, and then averaged for the winter mean (Jan-Feb). A 30-yr climatology (1991–2020) mean is removed from the index. Figure 14 shows the anomalies of the ALI from the 30-yr mean for each winter since 1980.

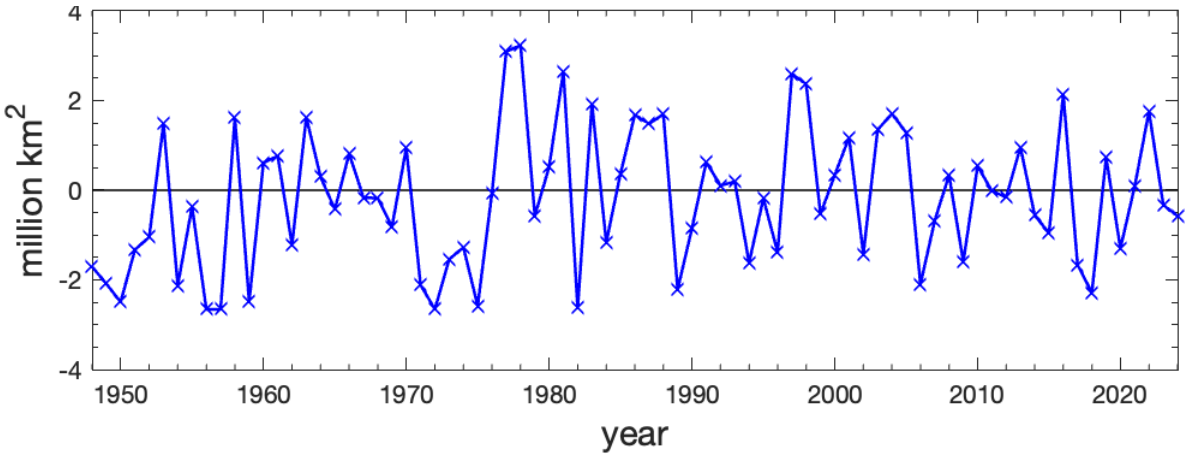

Figure 14: Winter (Jan-Feb) Aleutian Low index which is defined as the area occupied by sea level pressure less than or equal to 1000 hPa in the North Pacific region (40-60°N, and 160E-160°W). Time series shows the anomalies relative to 1991–2020 period mean.

When there is a strong Aleutian Low Pressure System present, the ALI is positive, i.e. the low center occupies a larger area. However, the other factors that matter are how strong the Aleutian Low center is and where the Low center is located, with the latter playing a more important role. The east-west position of the Aleutian Low center is captured relative to longitude 180°: when the Aleutian Low center is located to the west of 180°, it is associated with warm ocean temperatures and low winter sea-ice extents over the Bering Sea shelf. Following Rodionov and Overland (2005), cases with the Aleutian Low central pressure south of 51°N are removed, and these years are left blank in Figure 15, as those

tend to have a more zonal pattern. Based on Figure 14 and Figure 15 together, we can see that the Aleutian Low Pressure System in 2024 was relatively weak (negative anomaly in Figure 14) and the center is more toward the eastern part of the Bering Sea (near 170°W in Figure 15). Both the strength and location of the Aleutian Low resemble its climatological condition, i.e. it is a normal year. This may partially explain the near-normal sea ice extent observed in winter 2023–2024 in the Bering Sea, as a weaker Low allows for colder conditions and potentially greater sea ice coverage.

The Aleutian Low is a key driver of the Pacific storm track and cyclones that form in the North Pacific tend to follow the path of the Aleutian Low. The strength and position of the Low determine whether these cyclones move northward into the Bering Sea or remain in the mid-latitudes. A strong Aleutian Low brings more storms - stronger winds - to the Bering Sea, leading to increased precipitation. This is not the case for 2024. It can also be seen from Figure 13.

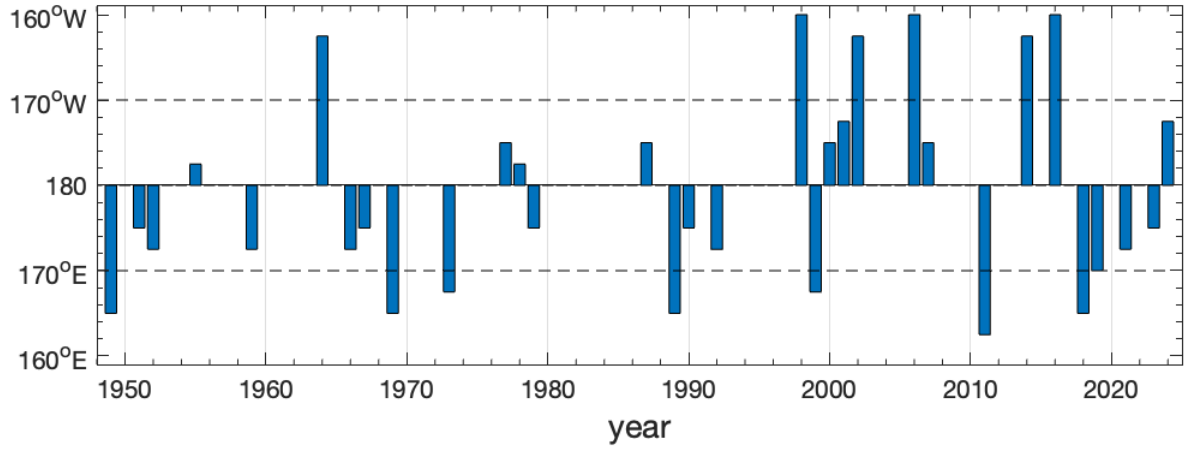

Figure 15: Longitude of the winter (Jan-Feb) Aleutian Low central pressure location when the center is located north of 51°N for 1948–2024. Dashed line indicates 170°W/E. For center locations south of 51°N, or the low center above 1000 hPa, the plot has a blank year. Sea level pressure data are based on NCEP/NCAR Reanalysis.

Seasonal Projections of SST from the National Multi-Model Ensemble (NMME)

Contributed by Emily Lemagie, *emily.lemagie@noaa.gov*

Seasonal predictions of SST anomalies from the National Multi-Model Ensemble (NMME) are shown in Figure 16. An ensemble approach incorporating different models is particularly appropriate for seasonal and interannual predictions. The NMME represents the average of eight climate models. The uncertainties and errors in the predictions from any single climate model can be substantial. More detail on the NMME, and predictions of other variables, are available at the NCEP website[7].

The NMME SST forecast projects warm anomalies in the approaching winter and spring over the western North Pacific between 30°N and 50°N, with a decreasing anomaly towards the Eastern Pacific, where temperatures along the U.S. West Coast are forecast to be near the historical mean (Figure 16). Further north, in the Gulf of Alaska, SST anomalies are forecast to drop to cool anomalies 0.25–0.5°C below the historical mean by spring 2024. Cool ocean temperature anomalies along the U.S. and Canadian west coasts and eastern Gulf of Alaska are consistent with the La Niña conditions that are predicted

[7] `http://www.cpc.ncep.noaa.gov/products/NMME`

by the NOAA Climate Prediction Center. While SSTs over the eastern Bering Sea shelf are forecast to remain near the historical mean for each time period, warm anomalies of 0.25–0.5°C magnitude are forecast in the Arctic Ocean and cool anomalies as low as -2°C are forecast in the vicinity of the Bering Strait in winter 2024–2025. Cool SST anomalies over the Chukchi Sea and near the Bering Strait may be positive indicators of seasonal sea ice advance.

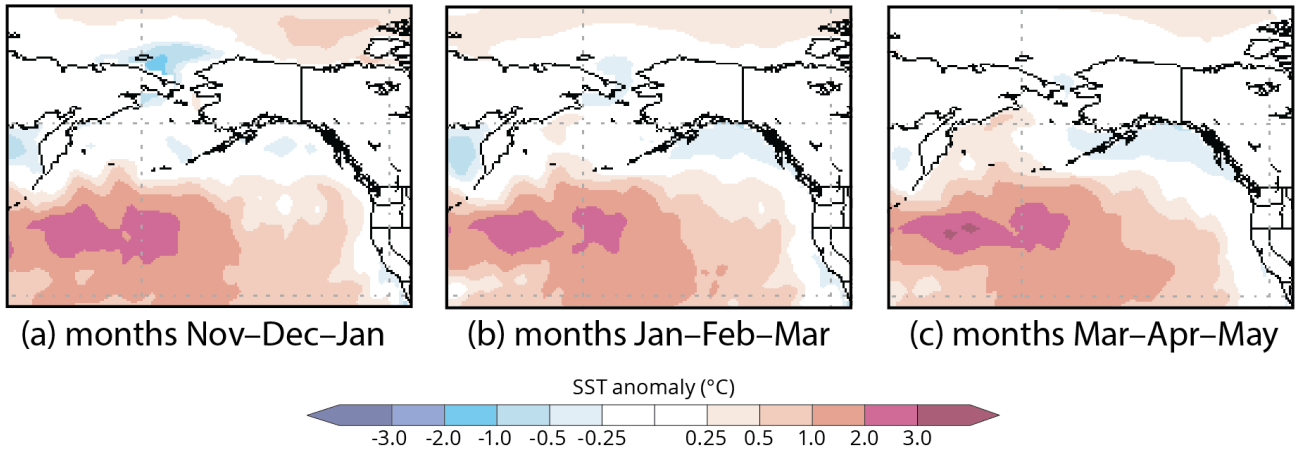

Figure 16: Predicted SST anomalies from the National Multi-Model Ensemble for Nov-Dec-Jan (1-month lead) 2024–2025, Jan-Feb-Mar (3-month lead) 2025, and Mar-Apr-May (5-month lead) 2025.

(b) Regional Summaries

Contributed by Emily Lemagie, *emily.lemagie@noaa.gov*

U.S. Arctic

Fall 2023 through spring 2024 was generally characterized by above average wind variability and late winter seasonal ice advance through the Bering Strait (Dec vs. Nov). Positive air temperature anomalies were present over the U.S. Arctic in fall, coincident with high variability in the mean sea level pressure and anomalously weak and variable winds in the Chukchi Sea, Bering Strait, and northern Bering Sea regions (Figure 10). In November, SST was anomalously warm in the ice-free regions of the Chukchi Sea and northern Bering Sea shelf. The Aleutian Low Pressure System developed in January and was located eastwards from its mean location (Figure 15). This was associated with the anomalously strong and southward winds over the northern Bering Sea region (Figure 10). Winter seasonal mean winds were near the climatological average (Figure 17), but strong winds in early winter and late spring contributed to advecting sea ice southwards. The spring transition was also characterized by above-average wind variability, with southward winds through the Bering Strait region in the late spring stronger than the climatological mean. Cool surface temperature anomalies were present in summer over the open-water parts of the Chukchi Sea following the seasonal sea ice retreat.

Bering Sea Deep Basin

Warm SST anomalies, up to 1°C, were present over much of the Bering Sea deep basin in the fall of 2023, but a decreasing tendency throughout the winter and spring culminated with cool or near-climatological mean SST by June 2024 (Figure 10). Stormy weather was prevalent in fall through spring which can act to stir the water column, deepen the mixed layer, and decrease SST anomalies. Wind anomalies over the northern basin were towards the south, advecting cooler continental air masses over the basin, but the southern basin wind anomalies were towards the east much of the winter through summer. Eastward wind anomalies result in equatorward Ekman transport anomalies and reduce northward advection of relatively warmer waters.

Eastern Bering Sea Shelf

Despite warm SST anomalies over the eastern Bering Sea in the fall through winter, and late winter sea-ice advance relative to historical norms, the maximum sea-ice extent was near historical norms including timing of sea-ice retreat. Strong off-shelf winds in October 2023, resulting in northward Ekman transport along the shelf, followed by weaker-than-mean westward winds from the Alaska mainland in November were accompanied by an increase in the SST anomaly over the Bering Sea shelf in the fall (Figure 10). Historical mean winds along the southern Bering Sea shelf are westward in fall and winter, with mean ocean currents flowing from the Gulf of Alaska northwards. In February, wind anomalies over the southern Bering Sea shelf were strong and towards the east, such that the local wind-driven Ekman transport opposed the mean current and reduced heat transport of warmer waters from the south. Stormy weather also increases vertical ocean mixing that can entrain cooler water from depth into the surface layer. Spring 2024 observations from the ecosystem observatory mooring M2 on the eastern Bering Sea shelf reported that throughout the summer the mixed layer depth was substantially deeper than the historical mean (Figure 27). Surface temperature anomalies were cool in spring and summer, following seasonal sea-ice retreat, but the heat content distributed over the deeper-than-average surface layer was similar to the climatological mean.

Aleutian Islands

Anomalously strong and eastward winds from fall 2023 through summer 2024 corresponded with a negative trend in the SST anomalies and a decline from warm SST anomalies in fall to cool SST anomalies by summer (Figure 10). Along the Aleutian Islands, winds towards the east and northeast were stronger than the historic mean conditions throughout most of the last fall through the summer. Winds in this sense increase southward Ekman transport, which opposes the mean ocean currents over the eastern Aleutian Islands that typically transport warmer water from the North Pacific onto the Bering Sea shelf. Strong winds also mix the water column, deepening the mixed layer and entraining colder water from below. Over the western Aleutian Islands, spring SSTs were near normal conditions, but warm anomalies returned in summer. Warm SST anomalies over the western Aleutian Islands have been the dominant trend for the last decade, which may be due to weaker wind-driven mixing, warmer air temperature, or advection of warm water from the North Pacific Ocean.

2. Eastern Bering Sea Trends

(a) Bering Sea Climate Overview

Introduction

Contributed by James Overland, *james.e.overland@noaa.gov*

The largest recent Bering Sea climate/ecosystem events were associated with unprecedentedly low sea ice extent in winters 2017–2018 and 2018–2019. There were connections from jet stream meanders and warm sea temperatures, through northward pollock/cod movements and ecosystem reorganization, to societal impacts. Since then, the Bering Sea has returned to more typical sea-ice extent conditions, although slightly below long term normals from 2020–2024. North of the Bering Sea in the Chukchi and Beaufort Seas, winter air temperatures continue to be above normal (+3-7°C) near the center of the Beaufort High pressure region (77.5°N, 170°W) beginning around 2015, as part of the continuing Arctic Amplification (AA). Before 2015, cold and high pressures dominated the southern Chukchi and northern Bering Seas with cold northeast winds and sea-ice advance in almost every winter. The unprecedented low sea ice in 2017–2019 related to both the warmer Arctic conditions plus a western location of the Aleutian Low that brought southerly wind and warmer temperatures to the eastern and northern Bering Sea. Since 2020, the Aleutian Low has had a more southern location track, allowing cold air to accumulate over the northern Bering Sea. In summary, the Beaufort High was dominant in almost every year before 2015, giving near normal long term northern Bering Sea conditions. Because of AA, future warm/low sea ice Bering Sea years, and resulting impacts on the ecosystem, will depend on when the Aleutian Low center is located to the far west. Based on data back to 1950, historically, that may happen one to three times a decade. Thus, one can expect to repeat extreme low sea ice/ecosystem years multiple times over the next decades, but they will not occur every year as noted in the last few years and for 2024.

(b) Surface Winds and Air Temperatures

Winter Wind Speed and Direction

Contributed by Rick Thoman, *rthoman@alaska.edu*

The average winter (Nov-Mar) wind speed categorizes years as having prevailing north winds or south winds. No long-term trend is exhibited, although winters ending in 2018 and 2019 were among 5 years with the strongest south winds, which contributed to low sea ice extent in those years. The north-south component of the low level wind for the 2023–2024 winter was almost exactly at the long term average (Figure 17). This is the outcome of frequent changes in storm track pattern and subsequent prevailing wind direction that characterized the second half of the winter.

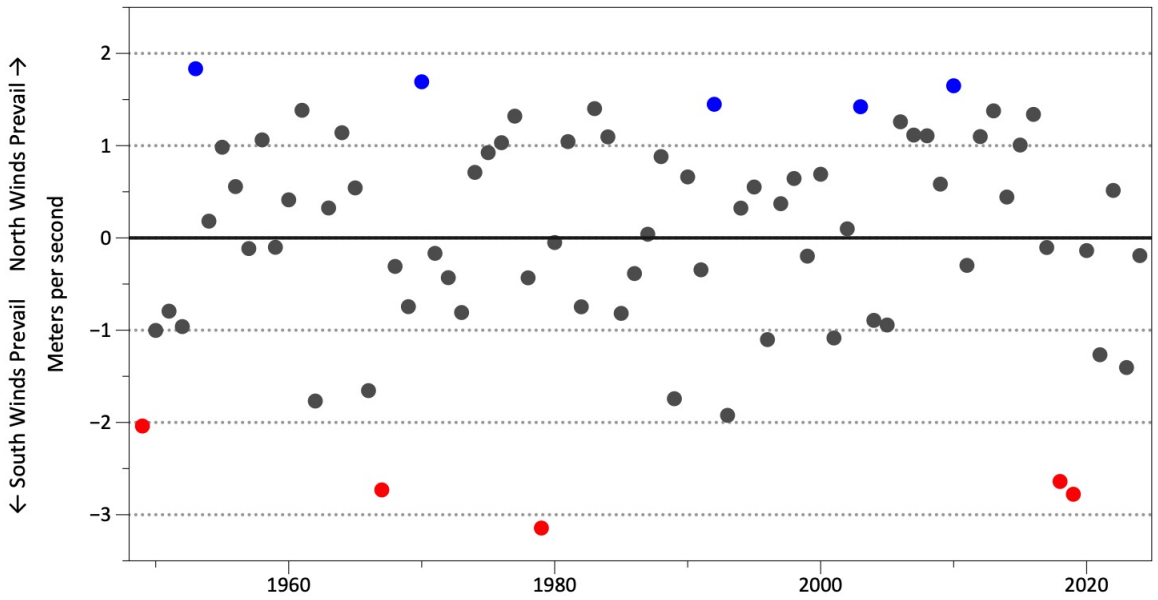

Figure 17: Winter (Nov-Mar) average north-south wind speed anomaly in the Bering Sea, 1949–2024. Red dots denote five years with strongest south winds, blue dots the five strongest north winds. **Note:** the north-south (meridional) component of the wind is plotted inverse to meteorological convention with south to north as negative values and north to south as positive values. Source: NCEP/NCAR reanalysis.

Winds at the Shelf Break

Contributed by Tyler Hennon, *tdhennon@alaska.edu*

NCEP/NCAR wind reanalysis is used to look at the along- and cross-slope wind components along the Bering shelf break. Four-times daily wind data dating back to January 2000 are interpolated to a transect approximating the shelf break (Figure 18), and the zonal and meridional components are rotated into along- and cross-shelf components. These components of wind are then averaged across the whole transect for each month through 2024.

The average annual cycle (2000 to 2022) is stronger for the cross-shelf component than along-shelf, and wind speeds are generally higher for the cross-shelf component as well (Figure 19). Generally, the Ekman transport associated with cross-shelf winds will be parallel to the shelf break, and could either inhibit or enhance near surface transport associated with the current along the shelf break. Winds oriented along the shelf break will either favor on- or off-shelf transport. Measurements taken at the M2 mooring show that the Ekman layer is no deeper than 30-40 meters from May-October (Noel Pelland, pers comm). This suggests the cross-shelf transport driven by winds is unlikely to drive upwelling or downwelling at the shelf break, as the water is substantially deeper there (∼200 m). However, the Ekman transport associated with surface wind stress may still be informative to understanding egg and larval dispersal of crab or groundfish in the upper ocean.

From August 2023 to August 2024, there were several notable departures from climatology (2000–2022). Whereas there are normally not substantial winds in the alongshore direction during winters, December 2023 had significant along-shelf winds (to the southeast) that could drive offshore Ekman transport. There were also weaker, but more sustained winds that favor offshore transport from March to May 2024.

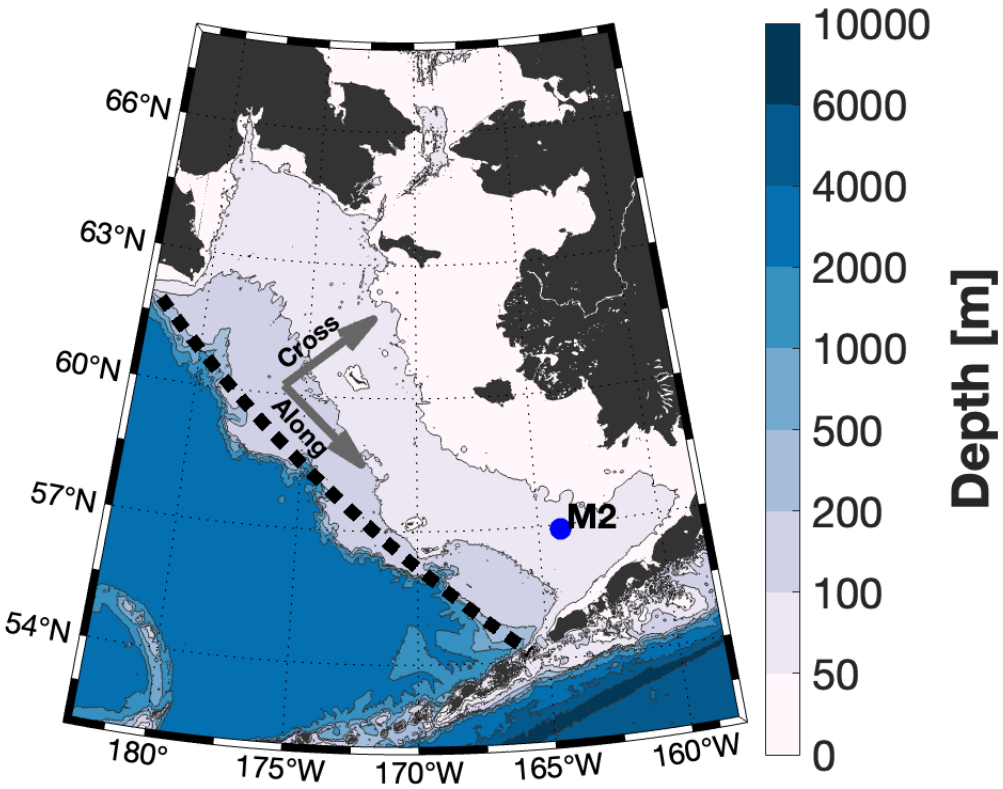

Figure 18: The dashed black line shows the section chosen to evaluate along-shelf and cross-shelf wind components in the Bering Sea. Annotation arrows show the direction used to define positive cross- and along-shelf components of wind. The blue dot shows the location of the M2 mooring.

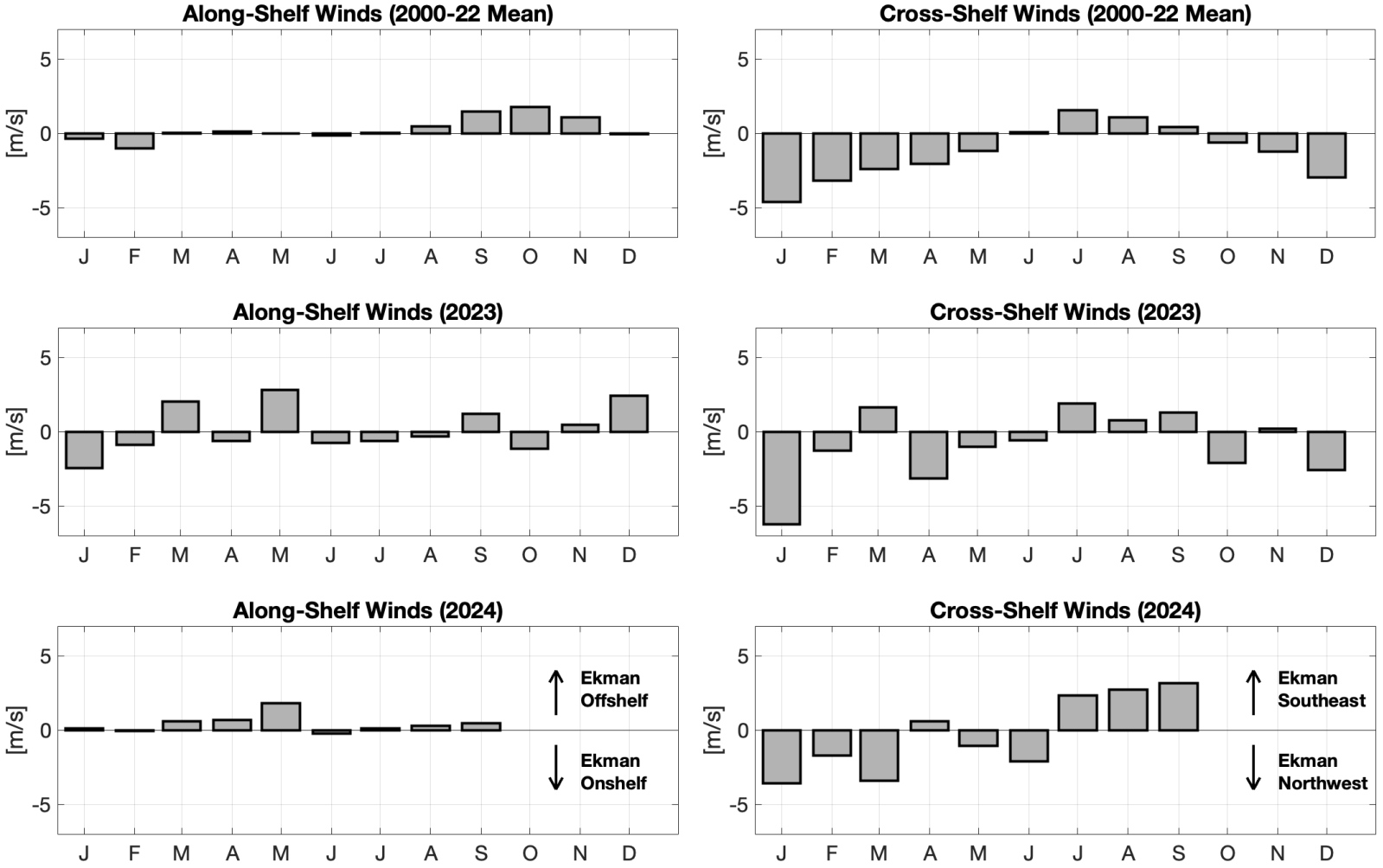

Figure 19: Along shelf (left set of panels) and cross shelf (right set of panels) wind components averaged along the dashed line in Figure 18. Top panels show the monthly averages across the period of record. Middle panels show the monthly averages for 2023, and bottom panels show the monthly averages for 2024 through September. Positive along-shelf winds are defined as blowing to the southeast, and positive cross-shelf winds are defined as blowing to the northeast. Expected directions of Ekman transport is denoted in the 2024 figures for along- and cross-shelf break winds.

St. Paul Air Temperature Anomalies

Contributed by James Overland, *james.e.overland@noaa.gov*, and Muyin Wang

Monthly surface air temperature anomalies at St. Paul Island (WMO ID 25713) are shown in Figure 20[8]. The anomaly is computed relative to the 1981–2010 period mean.

A linear trend of 0.60°C/decade has been observed since 1980. Although the temperature anomalies have been on the positive side for almost the entirety of 2023 and the first half of 2024, the magnitudes of positive anomalies are smaller than previous years (2016–2021). Since the beginning of 2020, there are only 3 months when the temperature at St. Paul Island is below its historical mean (defined as the average of 1981–2010), they are: Nov 2021 (-1.57°C), Jan 2022 (-0.33°C), and Dec 2023 (-0.16°C).

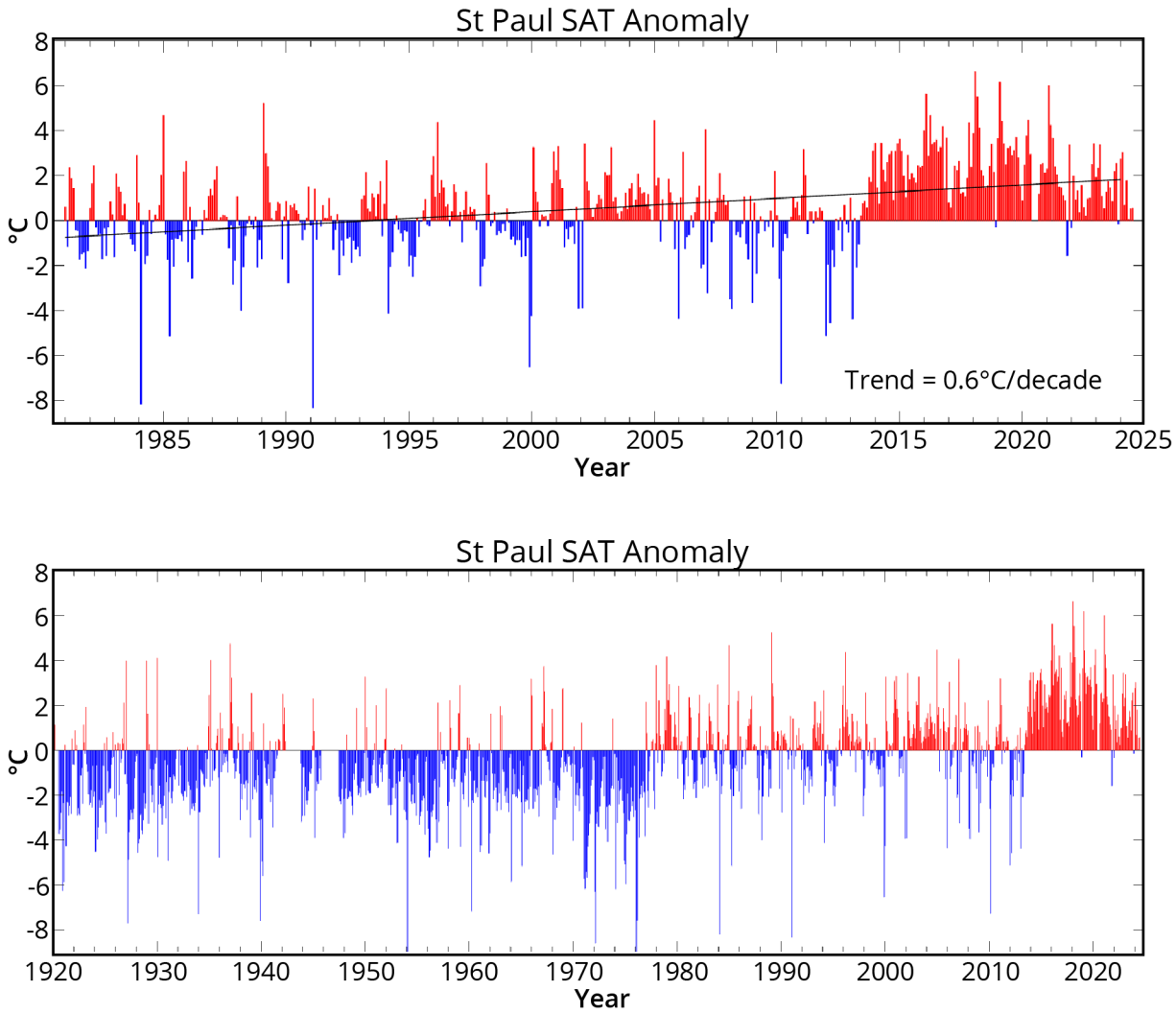

Figure 20: St. Paul air temperature anomalies updated to July 2024.

[8]Data are obtained from `https://data.giss.nasa.gov/gistemp/station_data_v4_globe`

(c) Water Temperature

Spring Temperatures

Contributed by Kelia Axler, *kelia.axler@noaa.gov*, and Lauren Rogers

NOAA-Alaska Fisheries Science Center's EcoFOCI program conducts biennial surveys in spring (May-June) in the eastern Bering Sea, targeting early life stages of fishes and their zooplankton prey. At each sampling station, a bongo net array is towed obliquely from surface to 300 meters or to 10 meters off-bottom in shallower waters. Attached to the wire above the bongo frame is a Seabird FastCAT profiler which measures temperature, salinity, and depth. Up casts were processed and used to generate maps and time-series of temperatures at the surface and at depth using the custom R package FastrCAT[9]. While surveys have been ongoing for multiple decades, time-series are provided here for the five most recent surveys with similar survey extent and timing (2012, 2014, 2016, 2018, and 2024). Surveys did not take place in 2020 and 2022.

Springtime temperatures in the eastern Bering Sea averaged 2.77 $\pm$ 1.18°C at the surface (top 5 m) and 2.49 $\pm$ 1.27°C at depth (300 m or 10 m off-bottom if shallower) in 2024. Mean sea surface temperatures were average to cool across the study region compared to 2014–2018, which were nearly 2-4°C warmer than in 2024 (Figure 21). The warmest bottom temperatures in spring 2024 were found near Unimak Pass and along the Alaskan peninsula, while the coolest temperatures were north of the Pribilof Islands, a typical pattern observed in the springtime (Figure 22). Additionally, temperatures <2°C were observed at 41 of 122 stations, providing evidence of cold pool conditions across the shallow shelf waters north of the Pribilof Islands (~56.5-58.5°N).

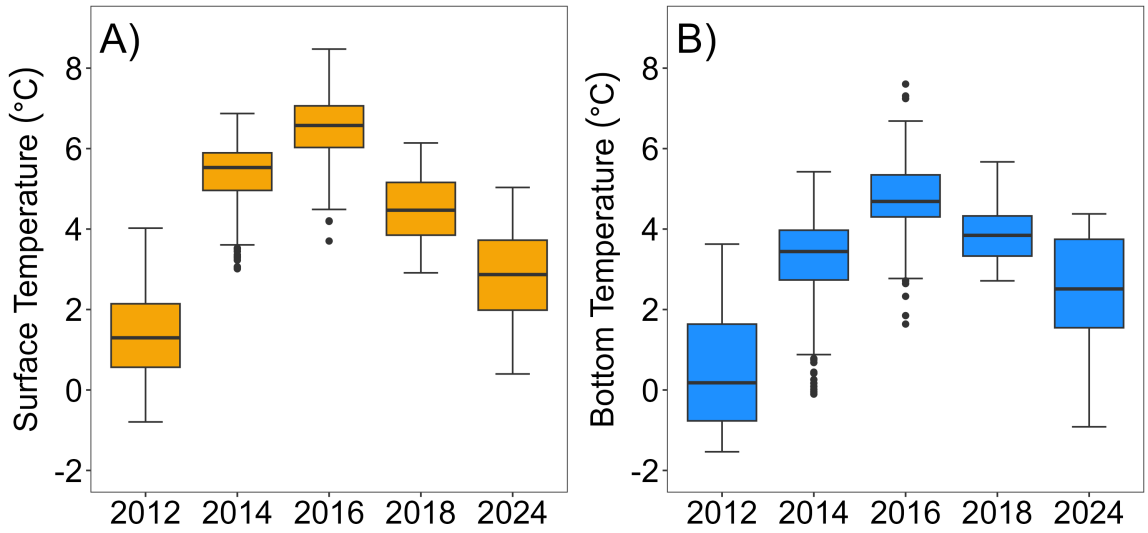

Figure 21: Distributions of observed A) surface (1-5 m) and B) bottom (300 m or 10 m off-bottom if shallower) temperatures (°C) across all stations sampled during spring eastern Bering Sea surveys (2012–2024). Boxes show the median, 25th, and 75th percentiles, whiskers show the full range, and dots denote outliers.

[9] https://github.com/Copepoda/FastrCAT

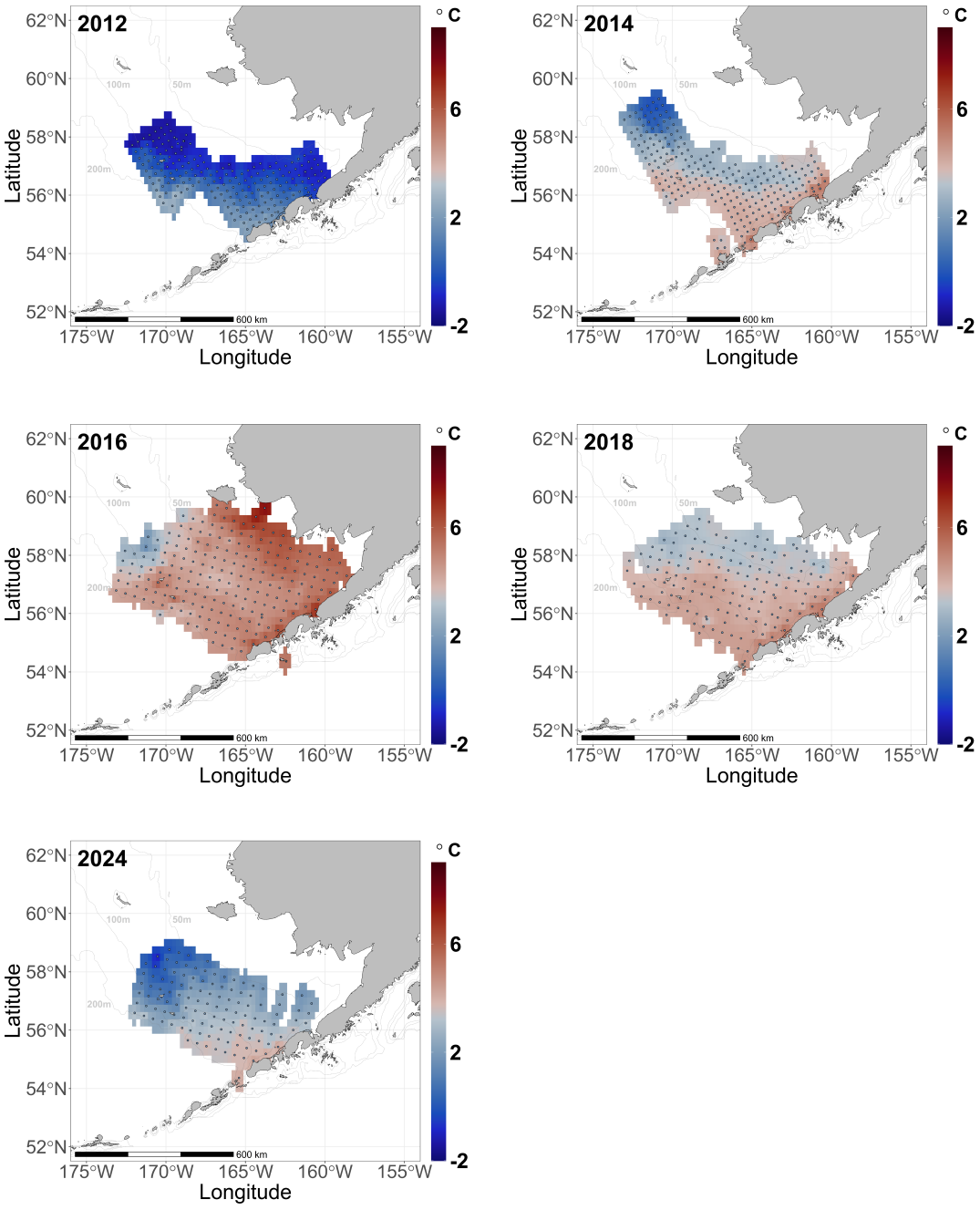

Figure 22: Observed bottom temperatures (°C) measured during the eastern Bering Sea EcoFOCI spring larval survey in 2012 (May 17-June 1), 2014 (May 21-June 6), 2016 (May 19-June 8), 2018 (May 14-June 1), and 2024 (May 17-31).

Summer Temperatures

Contributed by Sean Rohan, *sean.rohan@noaa.gov*, and Lewis Barnett

Annual mean surface and bottom temperatures were calculated from spatially interpolated measurements collected during NOAA-AFSC's summer bottom trawl surveys of the EBS shelf (1982–2024, except 2020) and NBS (2010, 2017, 2019, 2021–2023). Temperature interpolation was conducted using ordinary kriging with Stein's parameterization of the Matérn semivariogram model (Rohan et al., 2022). Code, figures, and data products presented in this contribution are provided in the *coldpool* R package version 3.3-1.

In the EBS, the mean surface temperature (5.83°C) was 0.90°C cooler than the time series average and 0.51°C cooler than in 2023 (Figure 23). The 2024 mean bottom temperature in the EBS (2.49°C) was approximately equal to the time series average (2.48°C) and 0.20°C warmer than in 2023. Overall, the cooler than average surface temperature and near-average bottom temperature in 2024 represent a continuation of near-average temperature conditions observed in 2022 and 2023. The three consecutive near-average years are a departure from the extremely warm conditions observed from 2016–2021 that included four of the five warmest years in the time series. **Note:** There are no NBS temperature updates in this year's contribution because the NBS bottom trawl survey was not conducted in 2024.

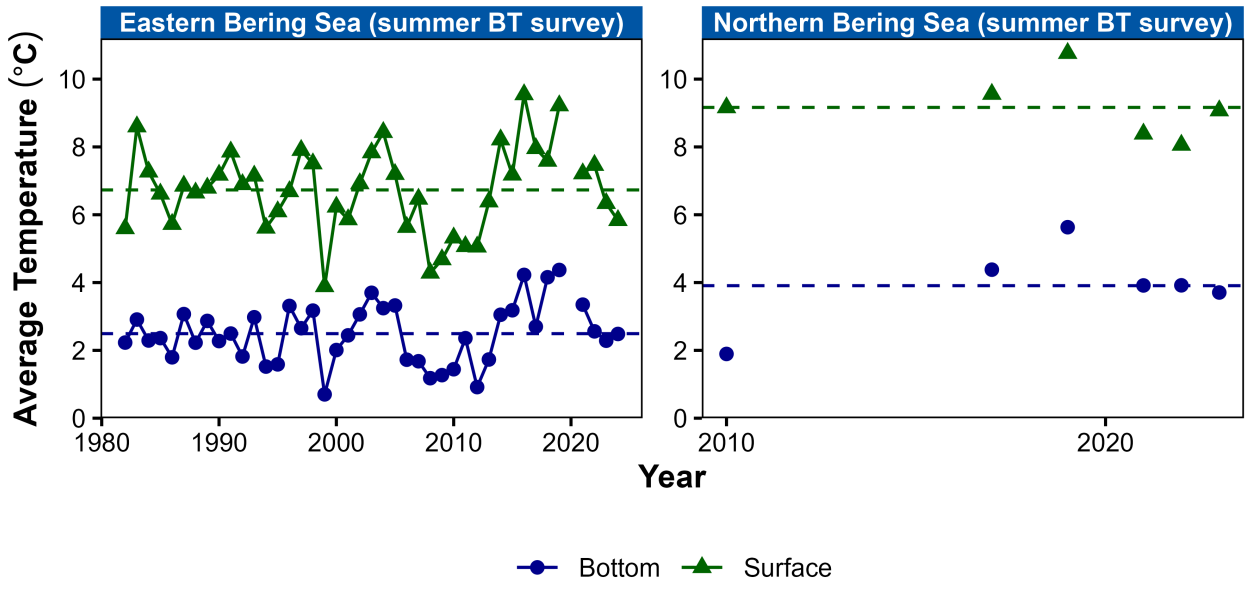

Figure 23: Average summer surface (green triangles) and bottom (blue circles) temperatures (°C) on the eastern Bering Sea shelf based on data collected during standardized summer bottom trawl surveys from 1982–2024. Dashed lines represent the time series mean.

In 2024, bottom temperatures <2°C occurred north of 57°N over the middle (50-100 m) and outer (100-200 m) domain (Figure 24). The coldest bottom temperatures (<-1°C) were restricted to the northern portion of the EBS shelf survey area to the north and east of St. Matthew Island. Unlike in 2023, bottom temperatures <-1°C did not extend south of St. Matthew Island. In contrast to 2022 and 2023, there was no tongue of bottom temperature <2°C along the 50 m isobath. The warmest bottom temperatures (5–6°C) occurred along the coast of the Alaska mainland near Nunivak Island.

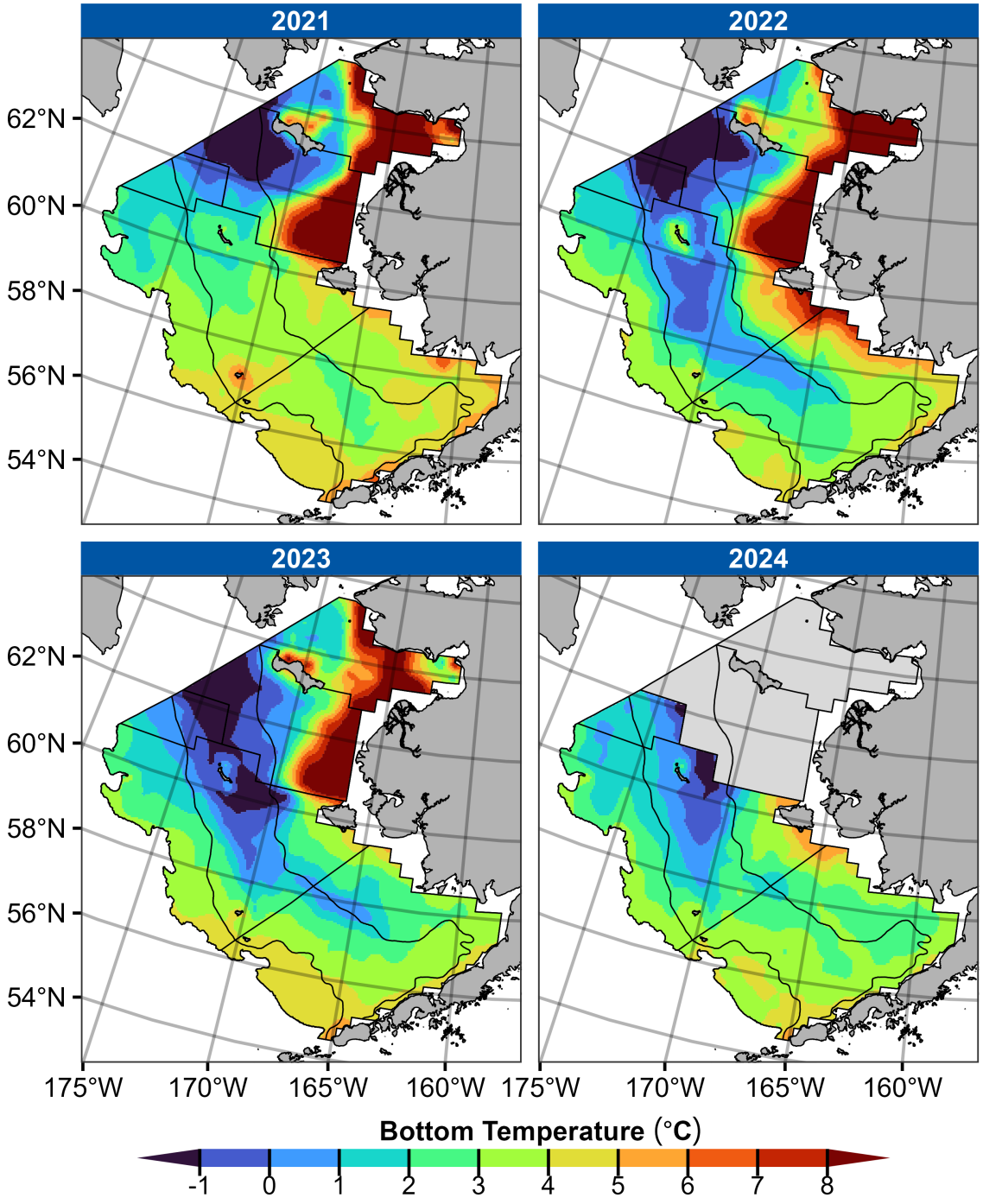

Figure 24: Contour maps of bottom temperatures from the 2021–2024 eastern Bering Sea shelf and northern Bering Sea bottom trawl surveys.

St. Paul Island Temperature and Salinity

Contributed by Lauren Divine, Aaron Lestenkof, and Tyler Hennon, *tdhennon@alaska.edu*

Community-led monitoring of temperature and salinity from North Dock on the St. Paul Island breakwater have been made since 2014 using CTD data loggers. Water depth at the sample site is approximately 8 m. Water column profiles are collected nominally weekly (Figure 25) and have been averaged into monthly means with annual signal removed (Figure 26).

Following the trends exhibited elsewhere, temperature anomalies over the 2024 spring/summer months show cool conditions compared to the preceding years. Temperature anomalies from May to August 2024 have been >2°C cooler than the seasonal average (Figure 26). It is important to note, however, that across the North Pacific as a whole, 2014 through 2023 were appreciably warmer than the long-term average, such that the baseline temperature in this record is significantly warmer than other time series with a longer period-of-record (e.g., Danielson et al., 2020).

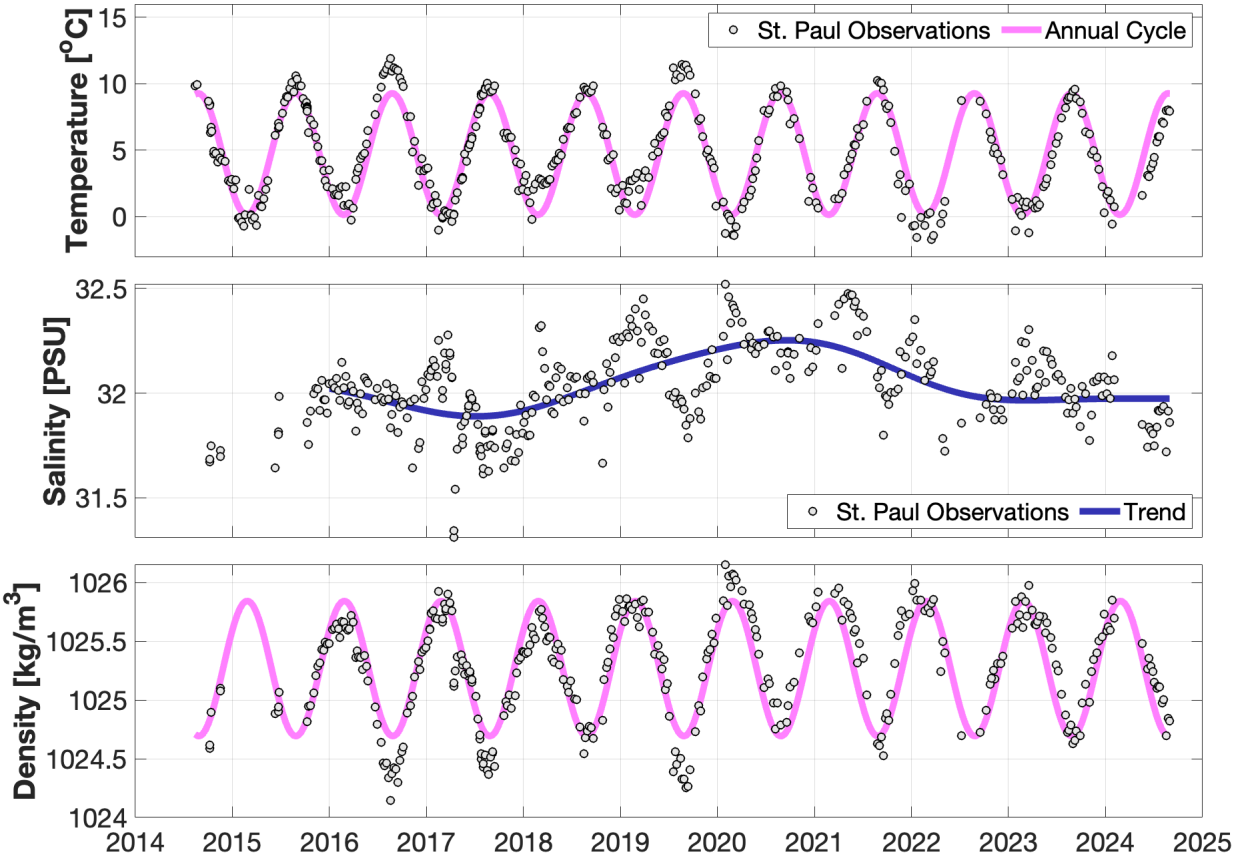

Figure 25: Observations of temperature (top), salinity (middle), and density (bottom) collected at St. Paul Island since 2014 (grey dots). Fitted annual cycles are in magenta, and the 3-year low-passed trend is represented by the blue line.

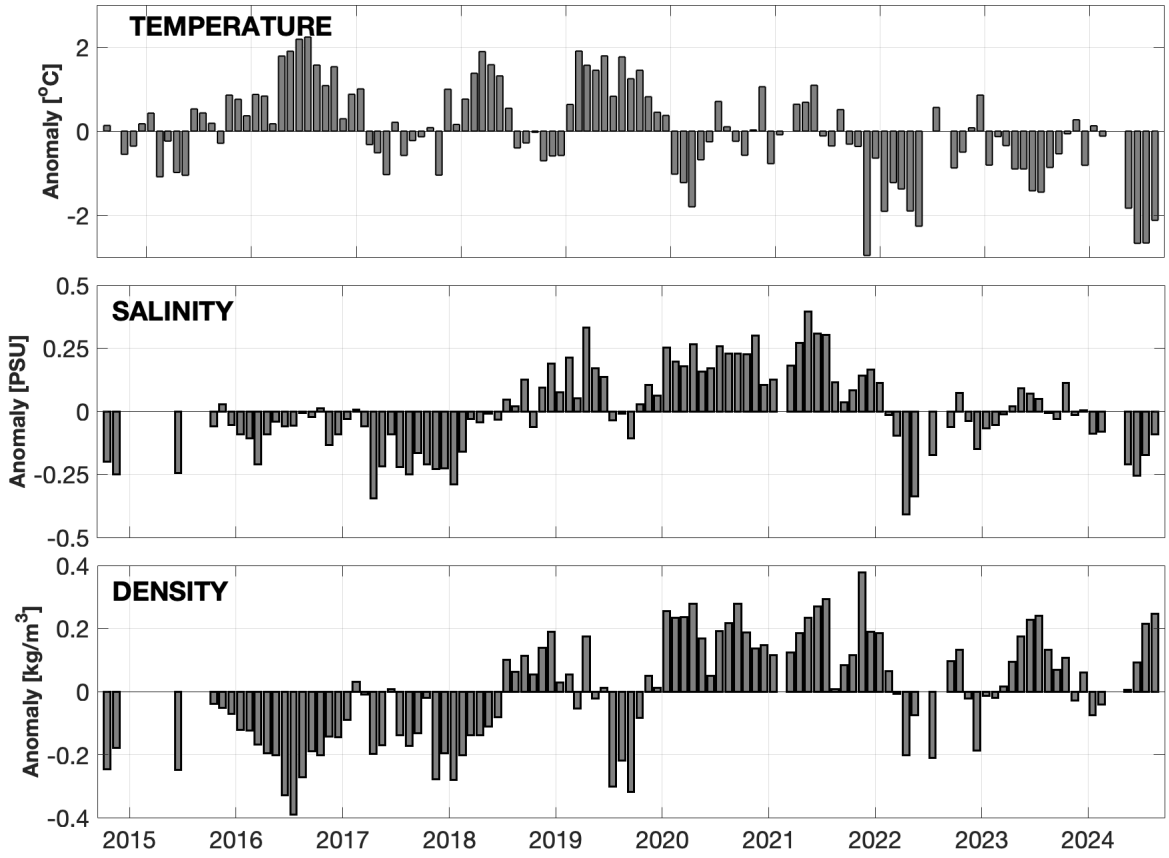

Figure 26: Monthly averages with the seasonal cycle removed for temperature (top), salinity (middle), and density (bottom).

Until about 2021, salinity had been generally increasing over the period-of-record. As noted in the 2022 Eastern Bering Sea Ecosystem Status Report (Siddon, 2022), this trend appeared to undergo reversal from August 2021 to August 2022. Similarly, during the span of August 2023 to August 2024, salinity anomalies remained significantly below the highs reached in ∼2019–2021 (Figure 26). Contributing factors to salinity variability on the EBS shelf include river discharge, precipitation, evaporation, ice advection, inflows from the Gulf of Alaska, and cross-slope exchanges with the basin (Aagaard et al., 2006). It is not completely clear what is responsible for the reversal in the salinity trend, but it is likely that the increased presence of sea ice over the prior three years is a factor (see Figure 36).

Water Column Temperature at Mooring M2

Contributed by Phyllis Stabeno, *phyllis.stabeno@noaa.gov*

In 2024, sea surface temperatures in the Bering Sea during late spring and summer were below average. Temperature data from mooring M2, which has been occupied nearly continuously since 1995, provides an indication of the cause of these cool temperatures. Historically (1995–2020), the average summer mixed layer depth at M2 has been ∼20 m deep. In 2024, it was deeper (Figure 27). Storms during May supported a deeper mixed layer than usual. In June 2024 winds had mixed the water column to a depth 40 m, introducing cold water upward. Another substantial storm occurred in late June supporting a mixed layer of ∼25 m. The mixed layer deepened from August into September, reaching a depth of >30 m. These events resulted in cooler sea surface temperatures through the summer months.

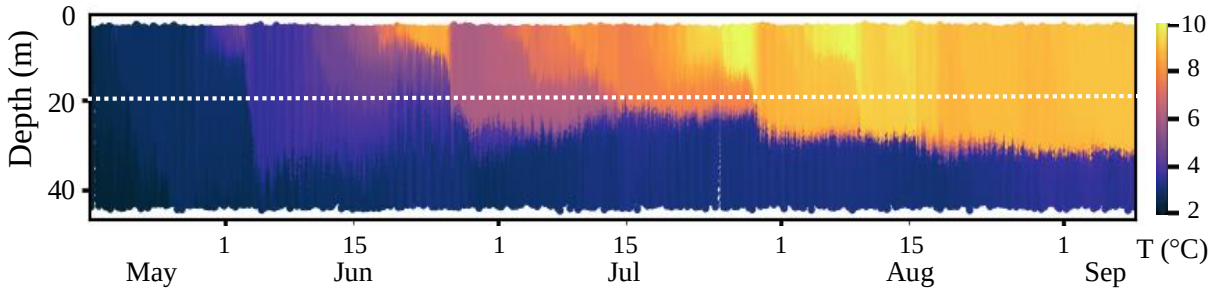

Figure 27: Temperature measured at M2 during 2024 summer season. The dashed white line indicates 20 m, which is the long-term mean summer mixed layer depth.

M2 measures temperature throughout the water column (0–72 m). Using these data the depth-averaged temperature can be calculated (Figure 28). Average temperature in 2019 was among the warmest in the 30-year timeseries and 2012 was among the coldest. The blue line indicates the average over 1995–2010. In contrast to cooler sea-surface temperatures, the depth-averaged temperatures in summer 2024 were slightly above this long-term average. Thus, 2024 showed cooling compared to 2014–2022, but was still above the long-term mean.

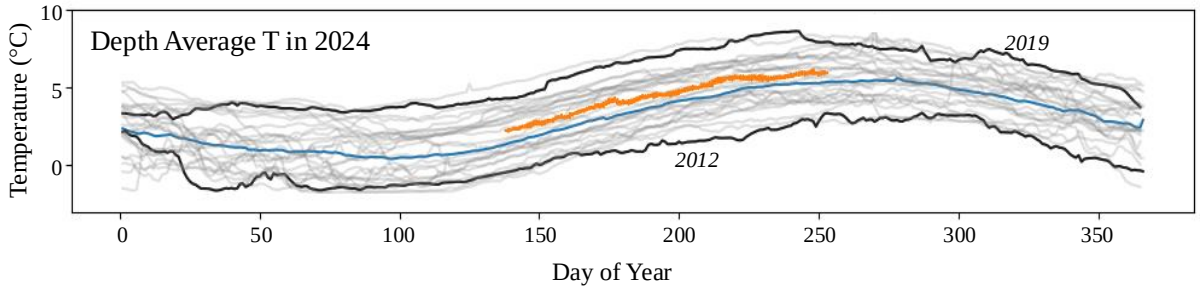

Figure 28: Depth-averaged temperature at M2. The blue line is the average from 1995–2010 and the orange line is the 2024 summer time series.

Bering Sea SST anomalies

Contributed by Matt Callahan, *matt.callahan@noaa.gov*, and Emily Lemagie

Satellite SST data (source: NOAA Coral Reef Watch Program) were accessed via the Alaska Fisheries Information Network (AKFIN). Daily data were averaged within the southeastern (south of 60°N) and northern (60–65.75°N) Bering Sea shelf (10–200 m depth). Detailed methods are available online[10].

Marine Heatwaves (MHWs)

MHWs in 2024 have been infrequent and generally minor relative to recent years prior to 2021, with only a few brief and predominantly moderate events (Figure 29). **Note:** this MHW information is based on SST, which is strongly influenced by sea ice and stratification in the Bering Sea, particularly over the middle shelf where surface and bottom temperature dynamics can be decoupled much of the year (Ladd and Stabeno, 2012). Bottom temperature in the Bering Sea is an important ecosystem indicator (Stabeno and Bell, 2019).

SST Anomaly Trends

Trend analysis removed seasonality and variability from the SST time series (Edullantes, 2019) to better illustrate the long term trends in the SST data (Figure 30). Trends are compared to the mean (± 1 standard deviation) from a 30-yr baseline (1985–2014). While there were local and periodic warm and cold anomalies, surface temperatures over the northern and southern Bering Sea shelves have largely remained within a standard deviation of the historical mean for the last two years, a break from the recent warm stanza $\sim$2014–2022.

Annual and Seasonal SST Trends

The cumulative SSTs for 2024 were within a standard deviation of average for the third consecutive year (Figure 31). At the seasonal level, mean SST patterns were within one standard deviation of the long-term mean in both 2022 and 2023 (Figure 32). Seasonal mean SSTs have generally shown a decreasing trend since peaks around 2019, except fall 2024 was slightly warmer than 2022 or 2023.

[10] `https://github.com/MattCallahan-NOAA/ESR/tree/main/SST/EBS`

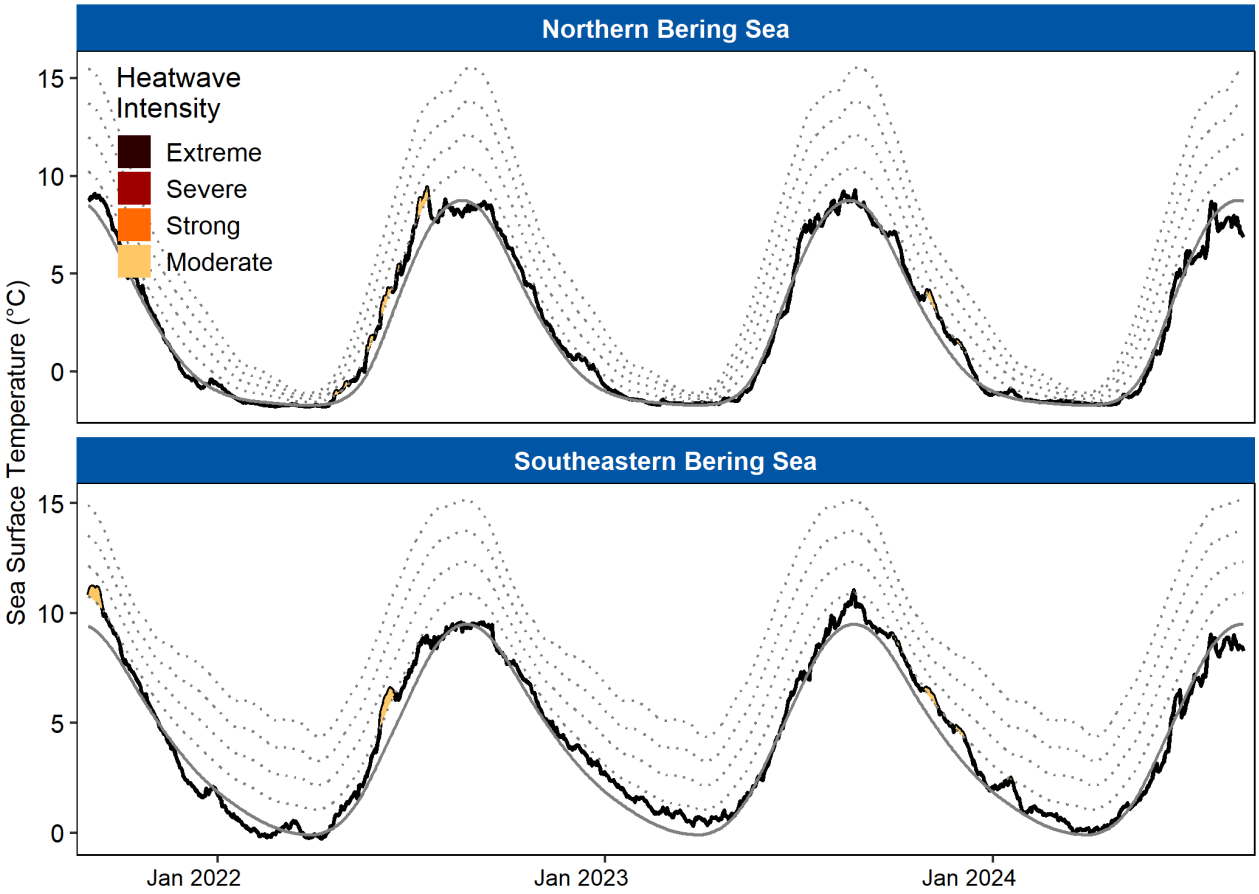

Figure 29: MHWs in the northern and southeastern Bering Sea since September 2021. The smoothed solid black line represents the baseline average temperature (i.e., climatology) for each day during the 30-yr baseline period (1985–2014). The jagged solid black line is the observed (satellite-derived) SST for each day. Dotted lines illustrate thresholds for increasing MHW intensity categories (moderate, strong, severe, extreme). Colored portions indicate periods during which MHW occurred, with intensity increasing as colors darken.

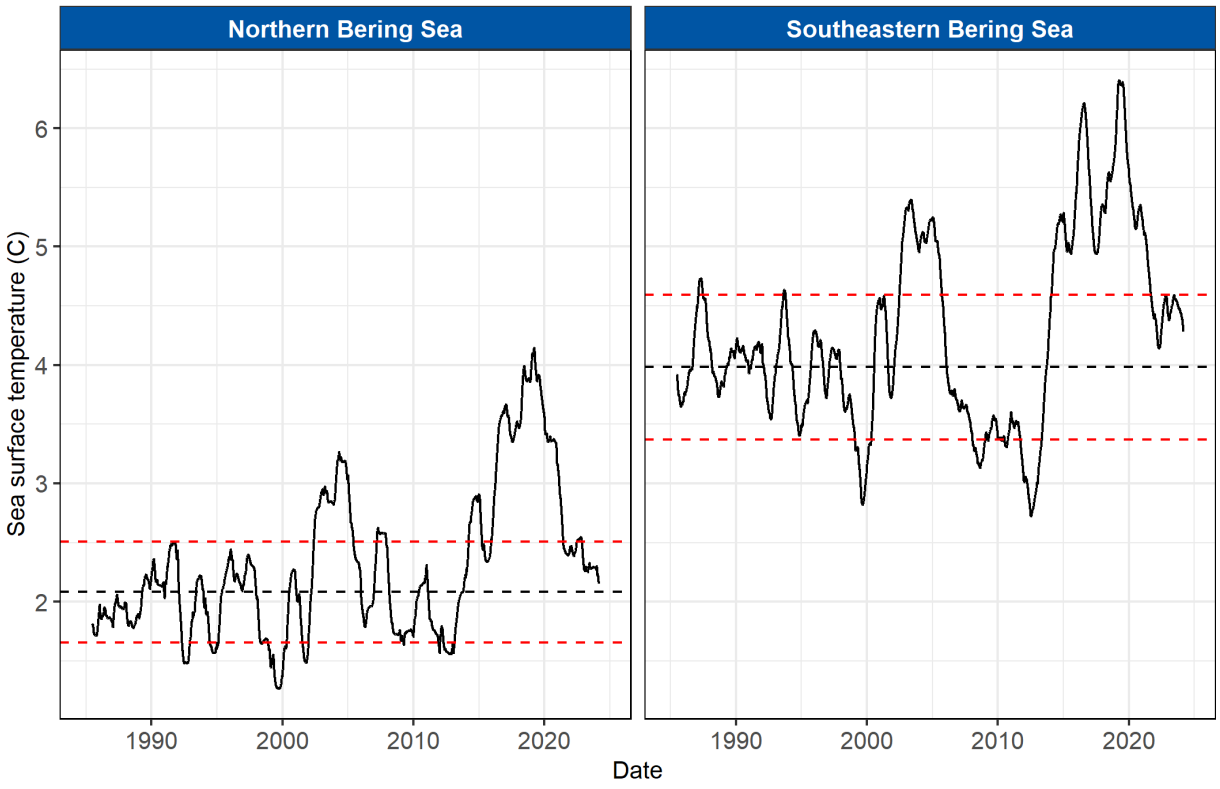

Figure 30: Time series trend of SST (seasonality and noise removed) for the northern (left) and southeastern (right) Bering Sea shelves. The black horizontal dotted line is the 30-year mean (1985–2014) of the trend and the red lines are ± 1 standard deviation. **Note:** The time series trend analysis requires truncation of the ends of the time series (due to differencing) so the trend line extends only to March 1, 2024.

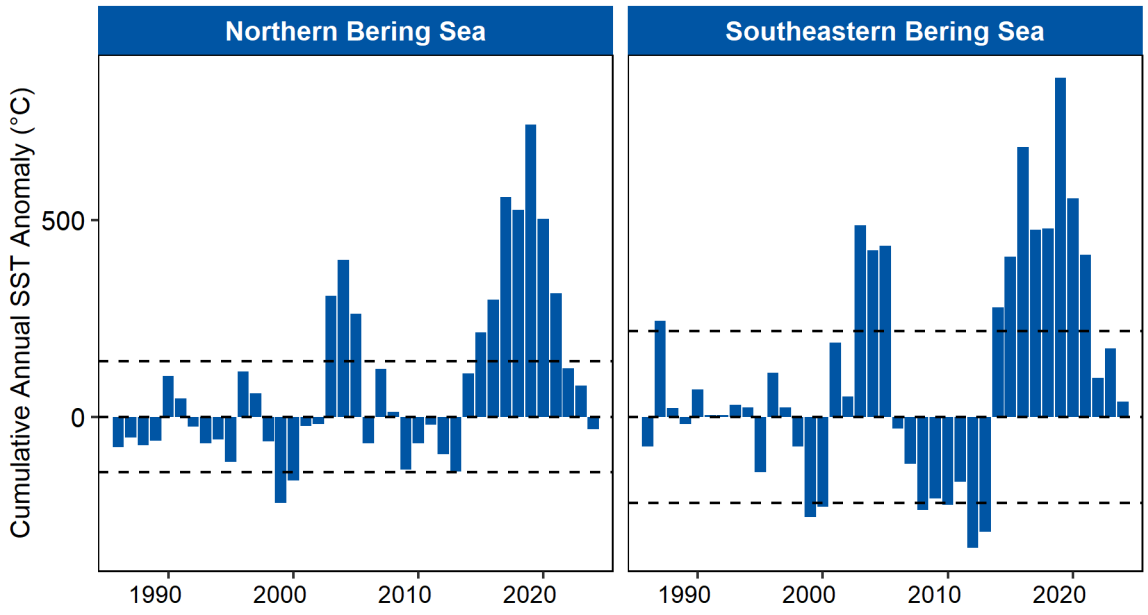

Figure 31: Cumulative annual SST anomalies (sum of daily temperatures). Horizontal lines are ±1 standard deviation from the mean during the 30-yr baseline period (1985–2014).

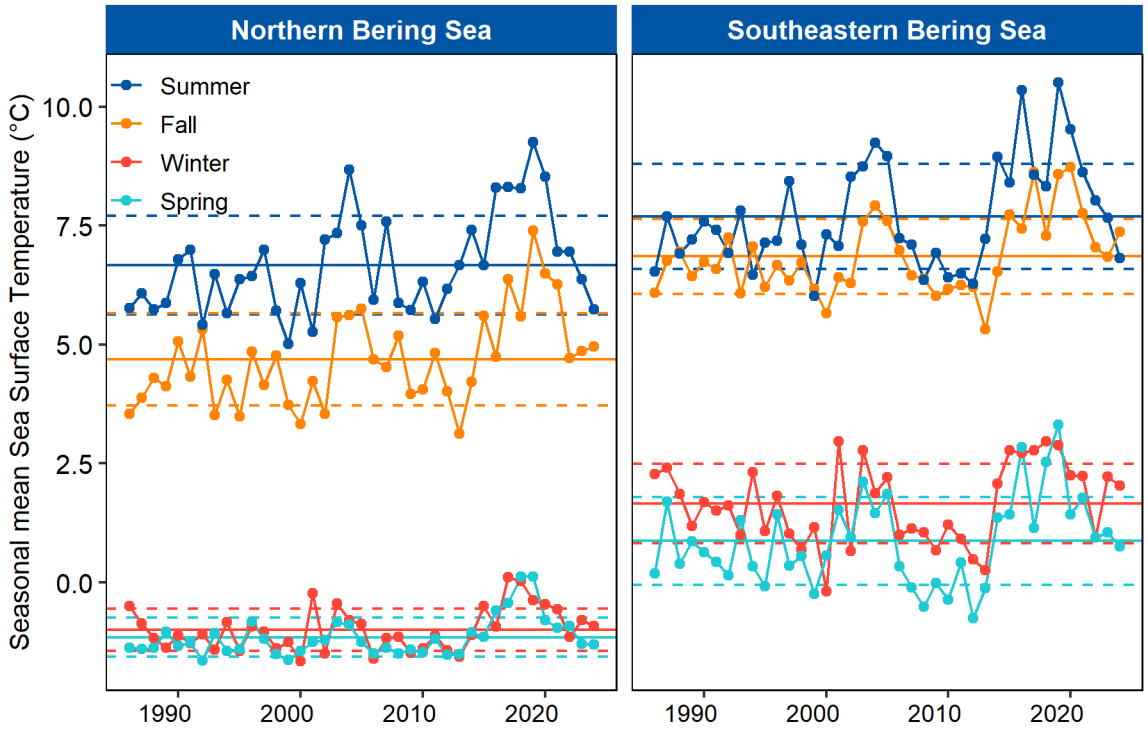

Figure 32: Seasonal mean SSTs for each year, apportioned by season: summer (Jun–Aug), fall (Sept–Nov), winter (Dec–Feb), and spring (Mar–May). Horizontal dashed lines are ±1 standard deviation from the seasonal mean for all years (horizontal solid line) during the 30-yr baseline period (1985–2014).

Bering Sea SST and Bottom Temperature Trends

Contributed by Matt Callahan, *matt.callahan@noaa.gov*, Kelly Kearney, and Emily Lemagie

Estimates of bottom temperature are derived from the Bering 10K Regional Ocean Modeling System (ROMS) hindcast simulation, which was extended to the near-present, using reanalysis-based input forcing. This hindcast simulation now extends from Jan 15, 1970 to Aug 24, 2024.

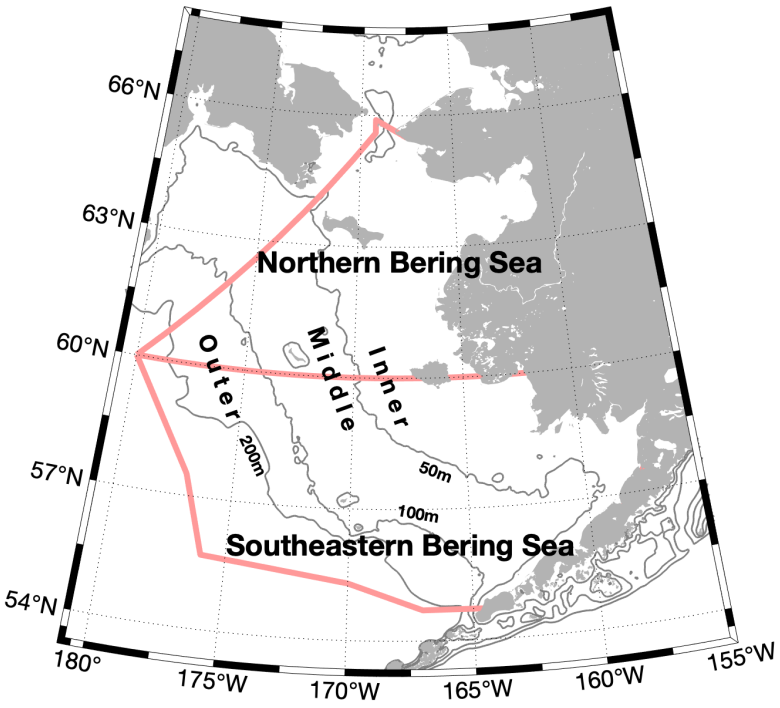

Figure 33: Map of the eastern Bering Sea domains. The inner (<50 m isobaths), middle (50–100 m isobaths), and outer (100–200 m isoboaths) domains are shown. The southeastern and northern Bering Sea are delineated at 60°N.

After an eight year warm stanza (2014–2022), SST over the past year (September 2023-August 2024) in the northern Bering Sea (NBS) and southeastern Bering Sea (SEBS) (see Figure 33 for domains) broadly returned to within 1 standard deviation of the 30-year baseline (1985–2014) (Figure 34, top two rows). Sea surface temperatures over the eastern Bering Sea were average to warmer than average in fall through winter, especially evident in the outer domain where SSTs remained warm through spring 2024. By summer 2024, SSTs across the eastern Bering Sea were near the long-tem mean (Figure 34, top two rows).

ROMS-estimated bottom temperatures were also near the historical averages across the entire shelf domain with the exception of the small northern outer domain. This region was influenced by warmer water arriving from the southern slope, which led to waters approximately 1°C higher than average during the summer, near the warmest on record. This intrusion may be due to persistent storminess during the spring.

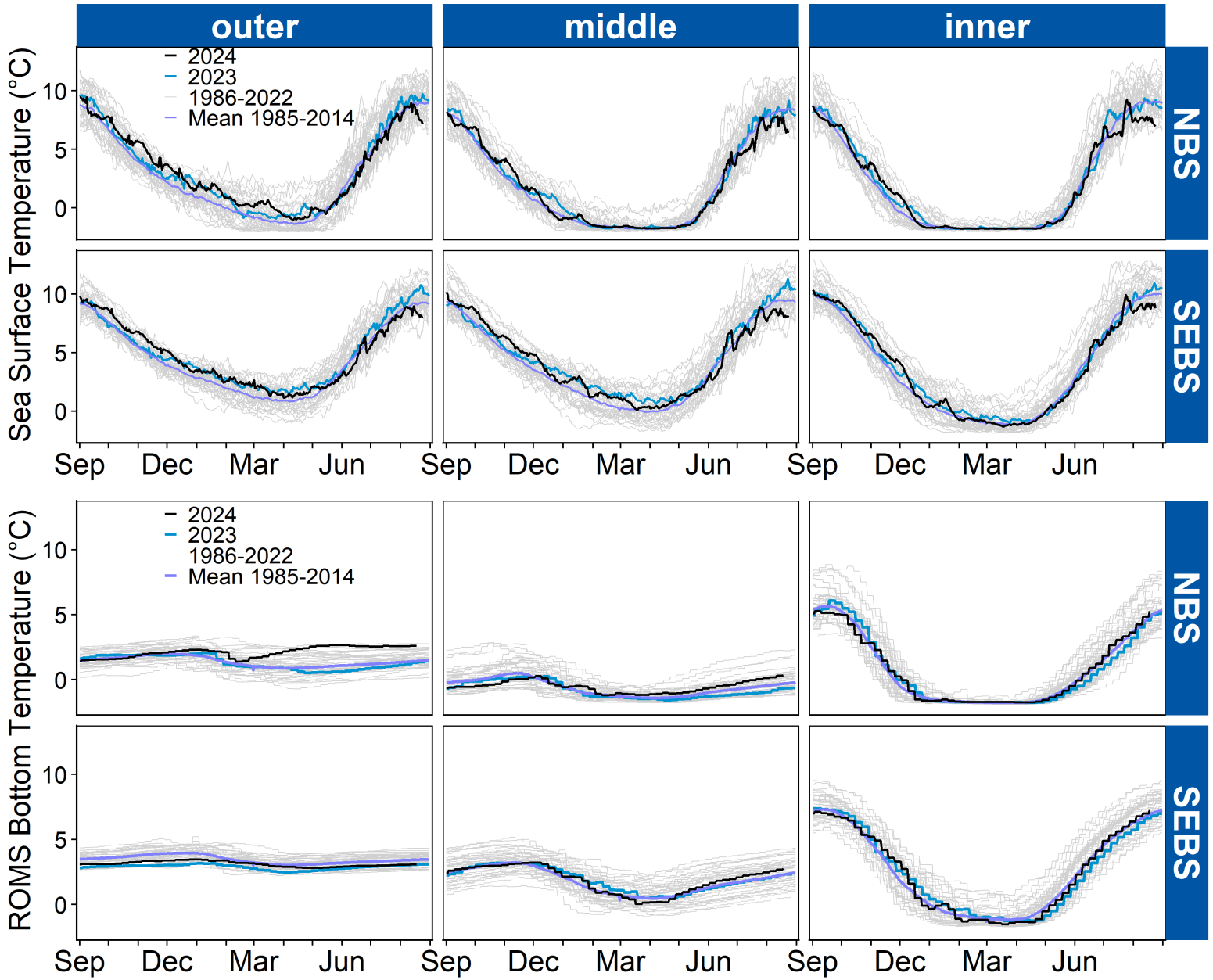

Figure 34: Top: Mean daily SST for the NBS and SEBS outer, middle, and inner shelf domains. Bottom: Mean weekly bottom temperature for the NBS and SEBS outer, middle, and inner shelf domains.The most recent year (2023–2024; through August 24) is shown in black, 2022–2023 is shown in blue, and the historical mean is shown in purple. Individual years in the time series are shown in light gray.

(d) Sea Ice

Early Season Ice Extent

Contributed by Rick Thoman, *rthoman@alaska.edu*

The presence or absence of early sea ice in the Bering Sea is important because, at least during the passive microwave era, nearly all ice in the Bering Sea is first year ice, therefore Bering Sea ice thickness is related to both the air temperature and the age of the ice.

Early season (Oct 15 - Dec 15) ice extent in 2023 was similar to most years since 2013, except for 2021's very high values, and lower than any year prior to 2007. Over the 46 year period of record, early season mean sea ice extent has decreased by 63% (Figure 35).

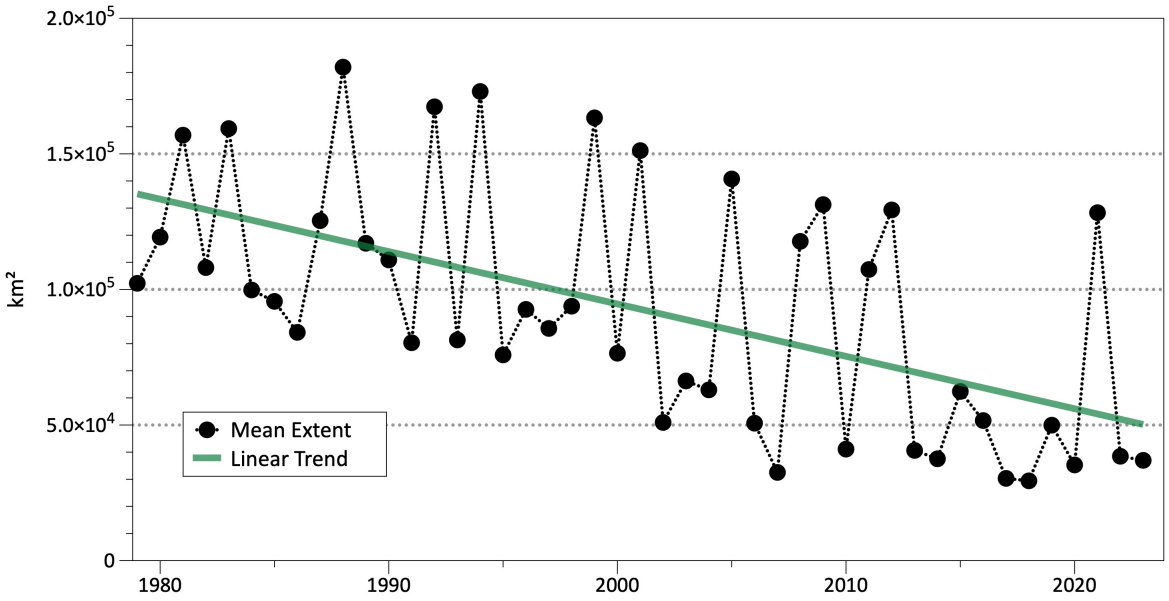

Figure 35: Early (15 Oct-15 Dec) mean sea-ice extent in the Bering Sea, 1979–2023.

Annual Bering Sea Ice Extent

Contributed by Rick Thoman, *rthoman@alaska.edu*

The Bering Sea has historically been ice-free in the middle and late summer, with ice developing during the second half of October. To account for this seasonal cycle, the Bering Sea ice year is defined as 1 August to 31 July. Bering Sea ice extent data are from the National Snow and Ice Center's Sea Ice Index, version 3 (Fetterer et al., 2017), and use the Sea Ice Index definition of the Bering Sea (effectively south of the line from Cape Prince of Wales to East Cape, Russia).

Annual mean daily sea ice extent in the Bering Sea has declined overall and interannual variability has increased significantly since the mid-1990s (Figure 36). The 2023–2024 average ice extent was slightly

higher than 2022–2023. While a significant recovery from the extreme 2017–2018 and 2018–2019 seasons, the 12-month average extent was similar to what were considered "low ice" years prior to 2010. **Note:** The current season is based on preliminary data and slight changes usually occur in extent values after final processing.

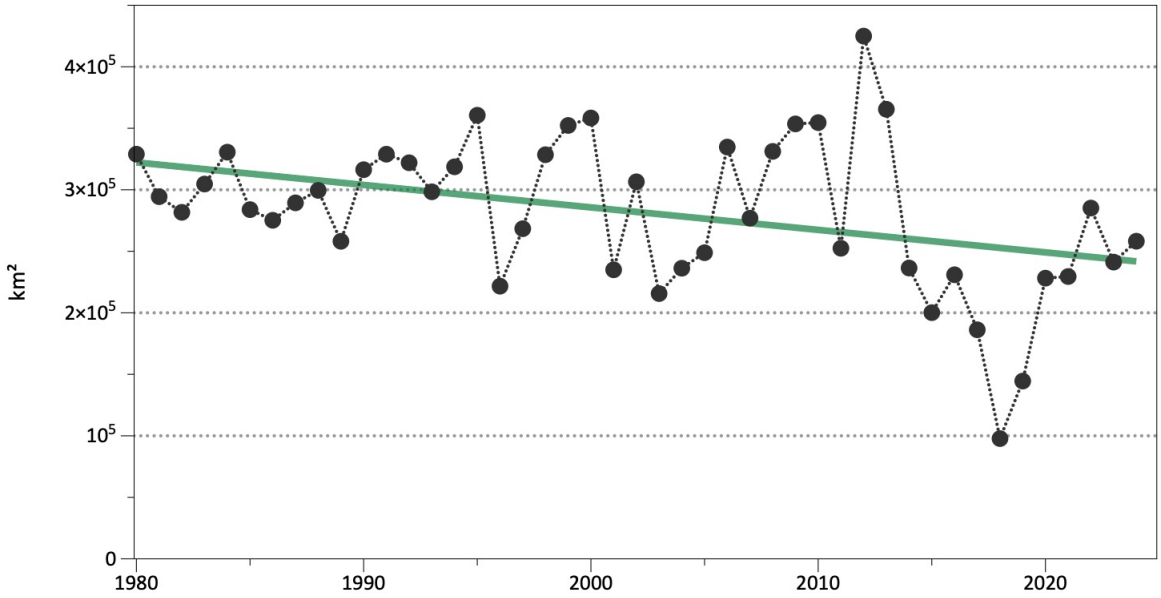

Figure 36: Mean sea ice extent in the Bering Sea from 1 August to 31 July, 1979/1980 – 2023/2024.

Bering Sea Daily Ice Extent

Contributed by Rick Thoman, *rthoman@alaska.edu*

Tracking the seasonal progression and retreat of sea ice highlights the interactive roles of water temperature (i.e., warmth in the system) and winds (Figure 37). Delayed sea ice formation in the fall 2023 was followed by a dramatic increase starting in early December. Between February and April, "wiggles" (i.e., advance and retreat) in the extent of sea ice were due to repeated shifts in weather patterns. Sea ice persisted in spring, with 2024 having the highest May ice extent since 2013. However, the maximum ice extent was 14% below the 1991–2020 mean.

Sea Ice Thickness

Contributed by Rick Thoman, *rthoman@alaska.edu*

Ice thickness is evaluated at five regions (Figure 38) in the Bering Sea from March 15-21, as this is generally the week with the greatest areal extent of sea ice. This year's report uses version 2.06 of the combined CryoSat-2/SMOS sea ice thickness from the Alfred Wegener Institute. There are only very minor differences from version 2.05 that was used last year.

Similar to late-season Bering Sea ice extent, the thickness of sea ice was also near average, though the period of record is shorter (2011–2024). In 2024 sea ice thickness in most regions was slightly lower

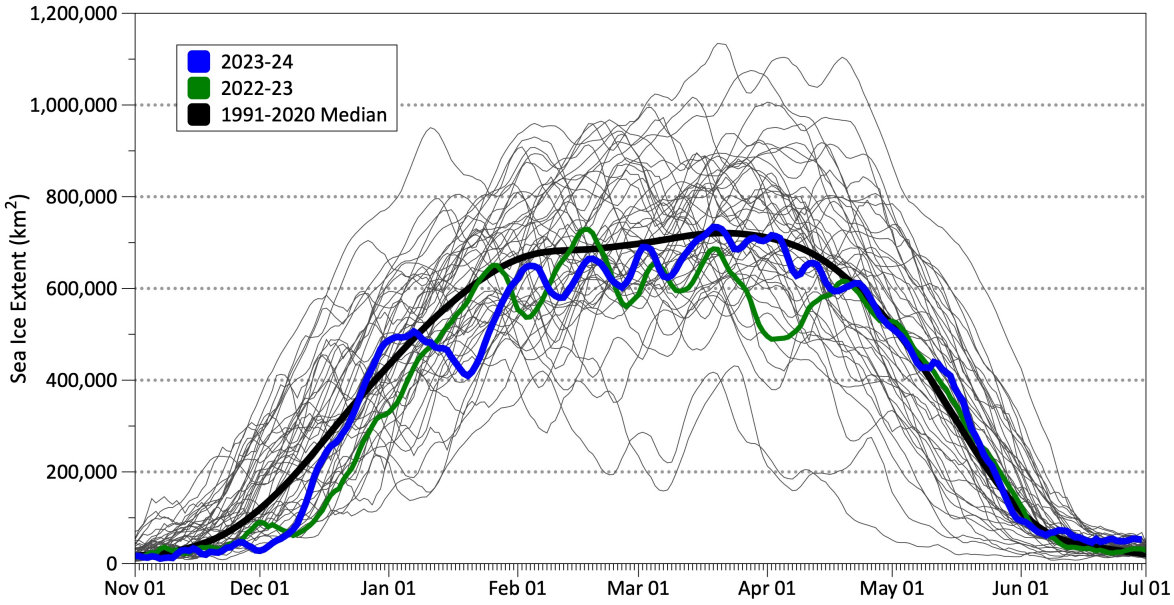

Figure 37: Daily ice extent in the Bering Sea. The most recent year (2023–2024) is shown in blue, 2022–2023 in green, and the historical median in black. Individual years in the time series are shown in gray.

than the same week in 2023, but near to above the median, except Norton Sound, where ice thickness was just below the median (Figures 39 and 40). For 2024, every region had significantly greater ice thickness than the lows observed circa 2018–2019, and was on par with the thicknesses observed in the early 2010s.

Figure 38: Map showing the five areas over the Bering Sea within which sea ice thickness indices were calculated: Gulf of Anadyr (Bering W), Bering Strait, Norton Sound (Bering E), St. Lawrence Island to St. Matthew Island (Bering NC), and St. Matthew Island to St. Paul Island (Bering S).

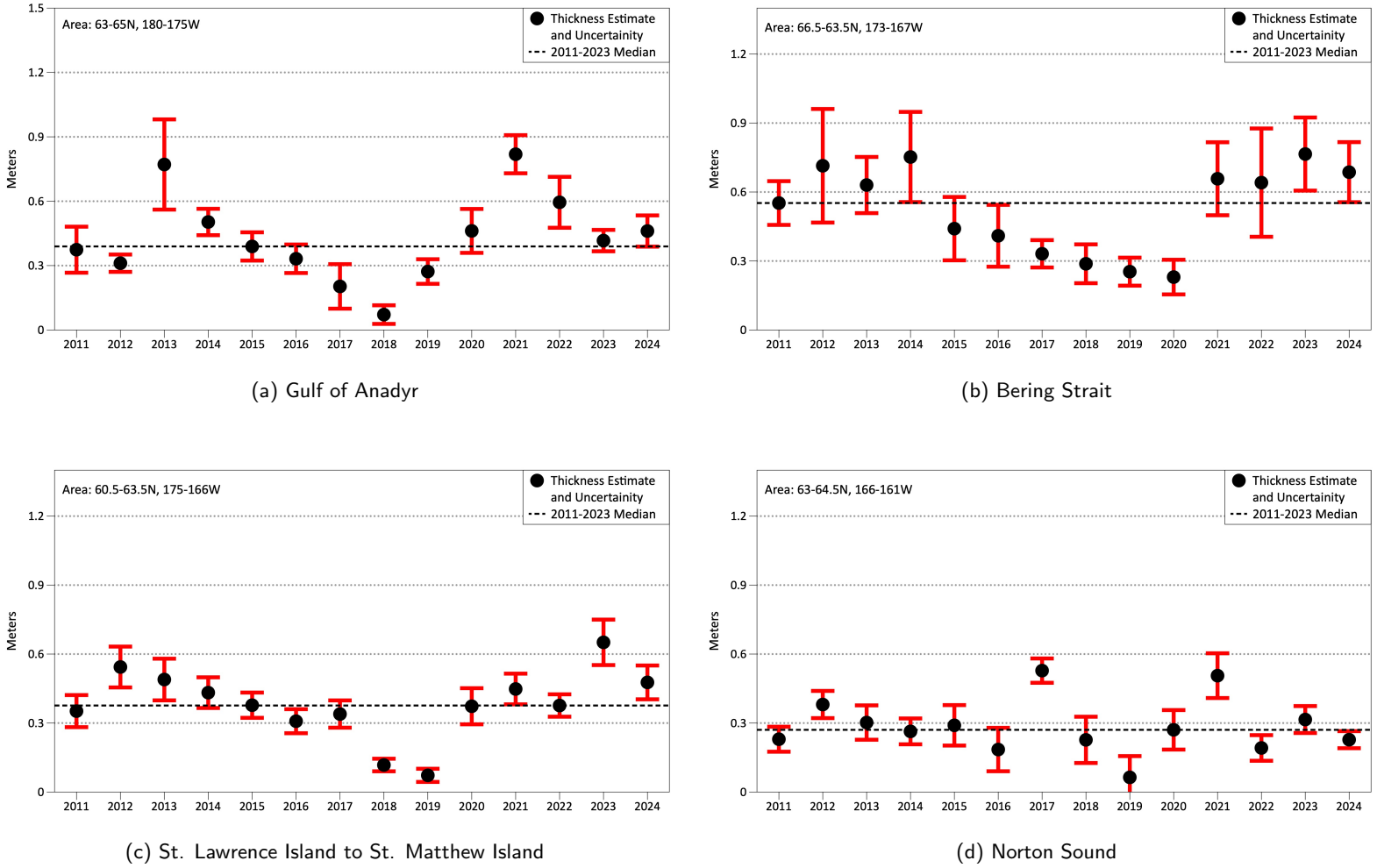

(a) Gulf of Anadyr

(b) Bering Strait

(c) St. Lawrence Island to St. Matthew Island

(d) Norton Sound

Figure 39: Sea-ice thickness in the Bering Sea for (a) Gulf of Anadyr, (b) Bering Strait, (c) St. Lawrence Island to St. Matthew Island, and (d) Norton Sound. Source: Alfred Wegener Institute. Details on how uncertainty in sea-ice thickness was quantified are available at: `https://www.meereisportal.de/en/`.

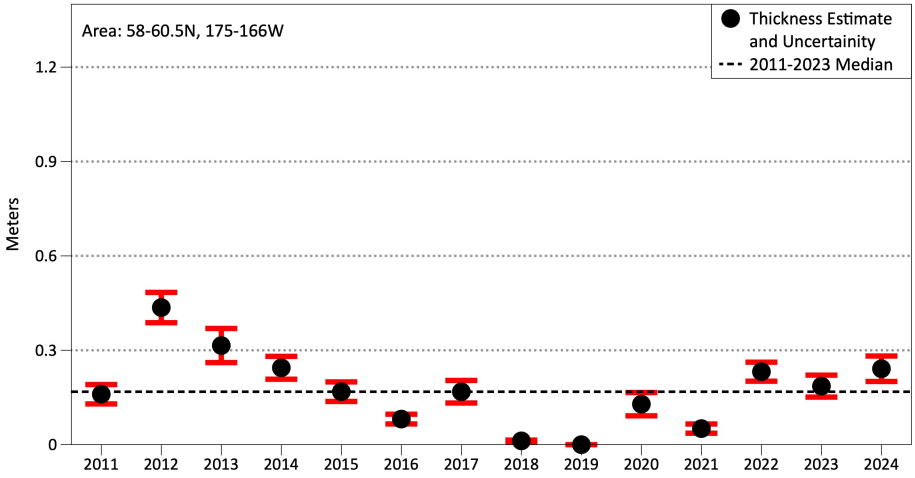

Figure 40: Sea-ice thickness between St. Matthew Island and St. Paul Island. Source: Alfred Wegener Institute. Details on how uncertainty in sea-ice thickness was quantified are available at: `https://www.meereisportal.de/en/`.

(e) Cold Pool Extent

Cold Pool Extent - AFSC Bottom Trawl Survey

Contributed by Sean Rohan, *sean.rohan@noaa.gov*, and Lewis Barnett

The spatial footprint of the cold pool (waters <2°C) in 2024 was 12.7% smaller than the last two near-average years in 2022 and 2023 (Figures 2 and 41). Compared to 2023, the extent of ≤-1°C (6,650 km^2) and ≤0°C (28,450 km^2) isotherms decreased by 54.4% and 75.0%, respectively. Despite the near-average cold pool extent, the extent of ≤-1°C and ≤0°C was similar to those observed during warm years, such as 2005, 2014, and 2016. The extents of the ≤-1°C, ≤0°C, and ≤1°C isotherms were all smaller than their time series (1982–2024) averages of 23,176 km^2, 53,545 km^2, and 102,077 km^2, respectively.

Cold Pool Extent - ROMS

Contributed by Kelly Kearney, *kelly.kearney@noaa.gov*

The Bering 10K Regional Ocean Modeling System (ROMS) hindcast simulation was extended to the near-present, using reanalysis-based input forcing. This hindcast simulation now extends from Jan 15, 1970–Aug 24, 2024.

2024 bottom temperature across the Bering Sea shelf showed mixed characteristics of a neutral or warm year. The mean simulated southeastern Bering Sea shelf bottom temperature on July 1, 2024 was 2.82°C, only 0.05°C above the climatological (1970–2024) mean of 2.76°C. Likewise, the model maintained a narrow tongue of water just below 2°C along the middle shelf (Figure 42), resulting in a 2°C cold pool index of 0.26, a value characteristic of neutral/warm years (relative to the climatological mean of 0.36).

However, the coldest waters were isolated to the northern part of the southeastern shelf, as is more characteristic of a warm year, with a 0°C cold pool index of only 0.02 (versus 0.11 mean). Our year-by-year cluster analysis was somewhat inconclusive; as a non-extreme year, 2024 shared many characteristics with other near-neutral years but we found no particularly strong analogue years for easy comparison.

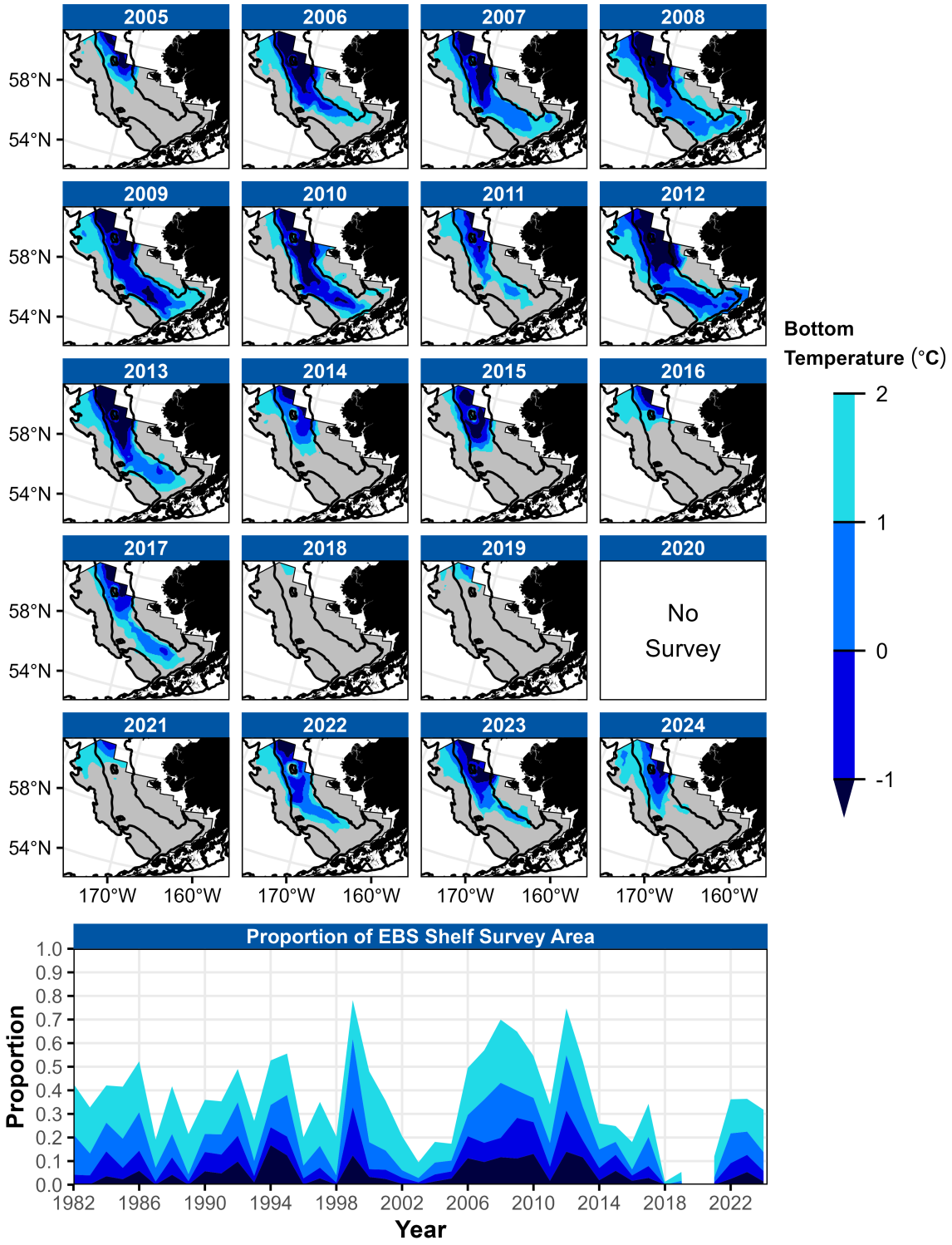

Figure 41: Cold pool extent in the eastern Bering Sea (EBS), as measured using observations from the EBS bottom trawl survey. Upper panels: Maps of cold pool extent in the EBS shelf survey area from 2005–2024. Lower panel: Extent of the cold pool in proportion to the total EBS shelf survey area from 1982–2024. Fill colors denote bottom temperatures $\leq$2°C, $\leq$1°C, $\leq$0°C, and $\leq$-1°C.

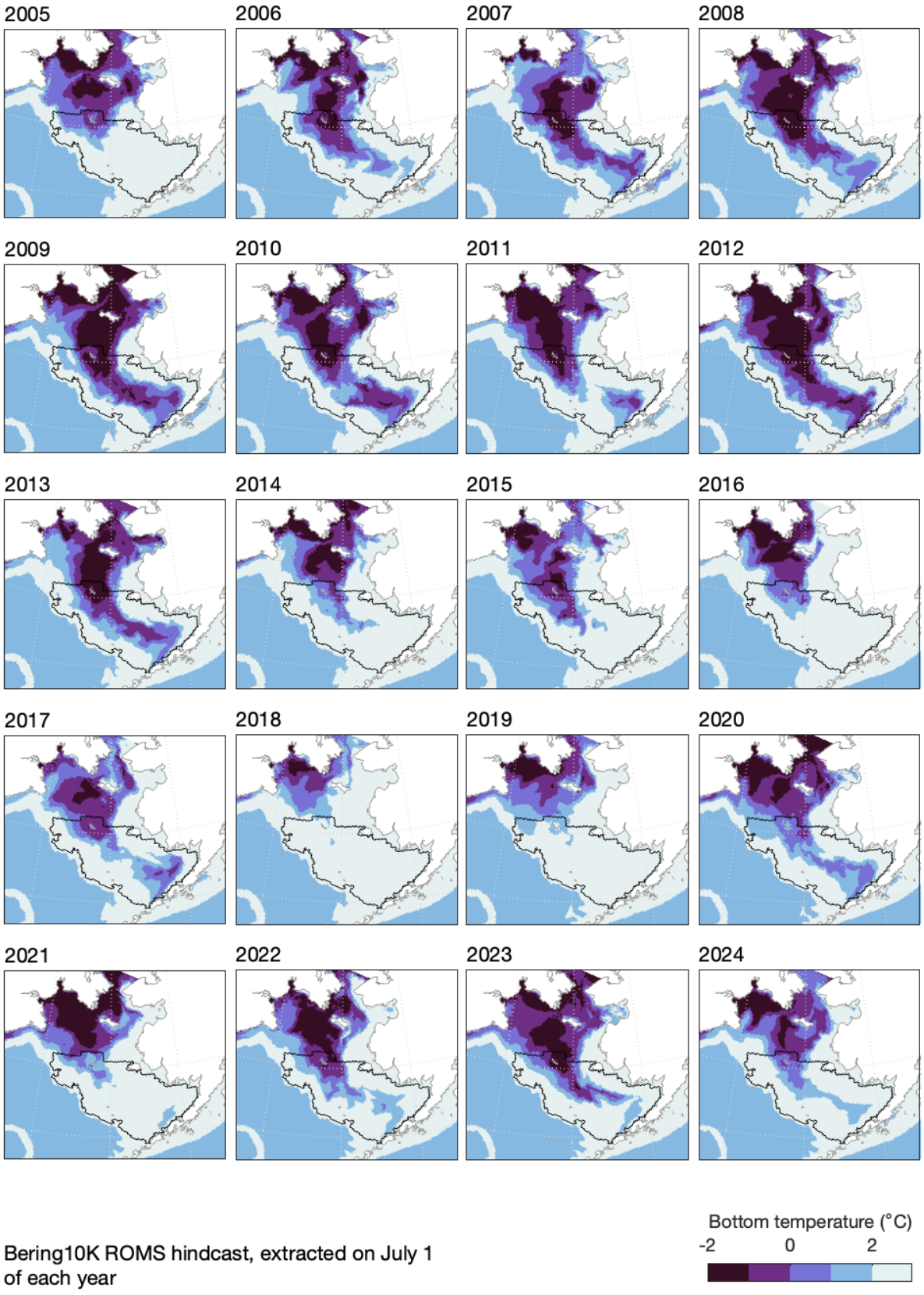

Figure 42: Bering 10K ROMS hindcast, extracted on July 1 of each year, for the Bering Sea, 2005–2024. The black outline denotes the standard bottom trawl survey grid.

Habitat

Eastern Bering Sea – Structural Epifauna

Contributed by Thaddaeus Buser and Sean Rohan
Resource Assessment and Conservation Engineering Division, Alaska Fisheries Science Center, NOAA Fisheries
Contact: thaddaeus.buser@noaa.gov
Last updated: September 2024

Description of indicator: Groups considered to be structural epifauna include: sea pens, corals, anemones, and sponges. Corals are rarely encountered in the eastern Bering Sea so they were not included here. For each group, biomass indices were updated for 2024 from the eastern Bering Sea shelf survey.

Since 1982, the RACE Groundfish Assessment Program (GAP) and Shellfish Assessment Program (SAP) have conducted annual fishery-independent summer bottom trawl surveys on the EBS shelf using standardized trawl gear and methods. Biomass index trends from the survey are likely to reflect changes in the abundance of species and life history stages that are available to the survey, especially if trends are sustained over time.

Regional and stratum indices of abundance (biomass in kilotons) and confidence intervals were estimated for each taxonomic group by fitting a multivariate random effects model (REM) to stratum-level design-based abundance index time series calculated from AFSC summer bottom trawl survey catch and effort data. Indices were calculated for the entire standardized survey time series (1982–2024). Design-based indices of abundance were calculated using the gapindex R package (Oyafuso, 2024) and REM were fitted to survey time series using the rema R package (Sullivan and Balstad, 2022). Code and data used to produce these indicators are provided in the esrindex R package and repository (Rohan, 2024).

Methodological Changes: Methods for producing this indicator have been updated this year to account for process error in survey abundance estimates, facilitate interpretation of indicator trends, utilize consistent statistical methods across ESR regions, and ensure consistent species group composition across regions. Previously, time series for this indicator were calculated as the average bottom trawl survey catch-per-unit effort for the full survey area (CPUE, kg ha^{-1}) that were scaled proportionally to the maximum CPUE in the bottom trawl survey time series.

This year, stratum biomass estimates were calculated using the gapindex R package (Oyafuso, 2024), which uses the Wakabayashi (1985) method to estimate design-based abundance index means and coefficients of variation (CVs) from catch (kg) and effort data (area swept; ha) collected during EBS summer bottom trawl surveys. Abundance index time series means and confidence intervals were estimated by fitting a multivariate random effects model (REM) to stratum biomass estimates and CVs using the R package rema (Sullivan and Balstad, 2022; Sullivan et al., 2022) to account for process error in indicator time series. The code and methods to calculate abundance indices and fit REM to time series are implemented in the R package esrindex (Rohan, 2024).

In this update, we also provide figures showing REM estimates of abundance, by stratum, to improve the characterization of spatial abundance patterns and trends, similar to subarea trends that have been presented in the AI and GOA ESRs.

Switching to REM addresses an issue raised during the November 2023 BSAI Groundfish Plan Team meeting pertaining to statistical methods to estimate Structural Epifauna abundance in the EBS:

"*The Team had a conversation about utilizing random effects models to deal with process error in the indicator and standardizing the index for variables such as bottom contact time.*"

We note that bottom contact time is already accounted for in bottom trawl survey effort data because effort is only calculated for the period of time that the net is on bottom as determined from bottom contact sensor data.

Status and trends: Sponges have undergone cyclical variability in abundance throughout the time series (Figure 43). The biomass of sponges (Porifera) in 2024 remains >1 standard deviation below the time series average, which is a continuation of the extremely low biomass level observed since 2021. Similarly low biomass was also observed intermittently early in the time series (1984–1992). Sponges have primarily been observed in stratum 30, the southern middle shelf, at 50–100 m bottom depth (Figure 44).

The biomass of sea anemones (Actiniaria) has been above average from 2022–2024, similar to 2010–2015. The recent period of above-average biomass contrasts with the period of near-average biomass observed from 2016–2021. Sea anemones are regularly encountered in all EBS survey strata, except stratum 20, the inner shelf (<50 m) north-northwest of Kuskokwim Bay, near Nunivak Island.

Sea pen (Pennatulacea) biomass has increased since 2019 and has remained above the time series average since 2019. Sea pens are most abundant on the outer shelf (100-200 m bottom depth) in strata 50 and 60.

Factors influencing observed trends: Further research in several areas would facilitate the interpretation of structural epifauna trends including systematics and taxonomy of Bering Sea shelf invertebrates, better characterization of survey gear efficiency, and the life history characteristics of the epibenthic organisms captured by the survey trawl.

Implications: Structural epifauna are utilized as habitat by commercial groundfish species in Alaska (Rooper et al., 2019), although associations on the Bering Sea shelf are not well understood. Sponges can be extremely long-lived and have slow recovery times from disturbance, meaning they may be vulnerable to impacts from fishing gear (Montero-Serra et al., 2018; Malecha and Heifetz, 2017). However, very little is known about the longevity and growth rates of most sponge taxa in Alaska. Generally, sponge longevity increases with depth (Stone et al., 2019). Understanding the trends as well as the distribution patterns of structural epifauna is important for modeling habitat to develop spatial management plans for protecting habitat, understanding fishing gear impacts, and predicting responses to future climate change (Rooper et al., 2016). More research on the eastern Bering Sea shelf will be needed to determine if there are definitive links.

Research priorities: The bottom trawl survey uses standardized survey protocols aimed at ensuring consistent sampling efficiency. However, additional research is needed to better characterize the catchability and selectivity of structural epifauna groups by the bottom trawl survey.

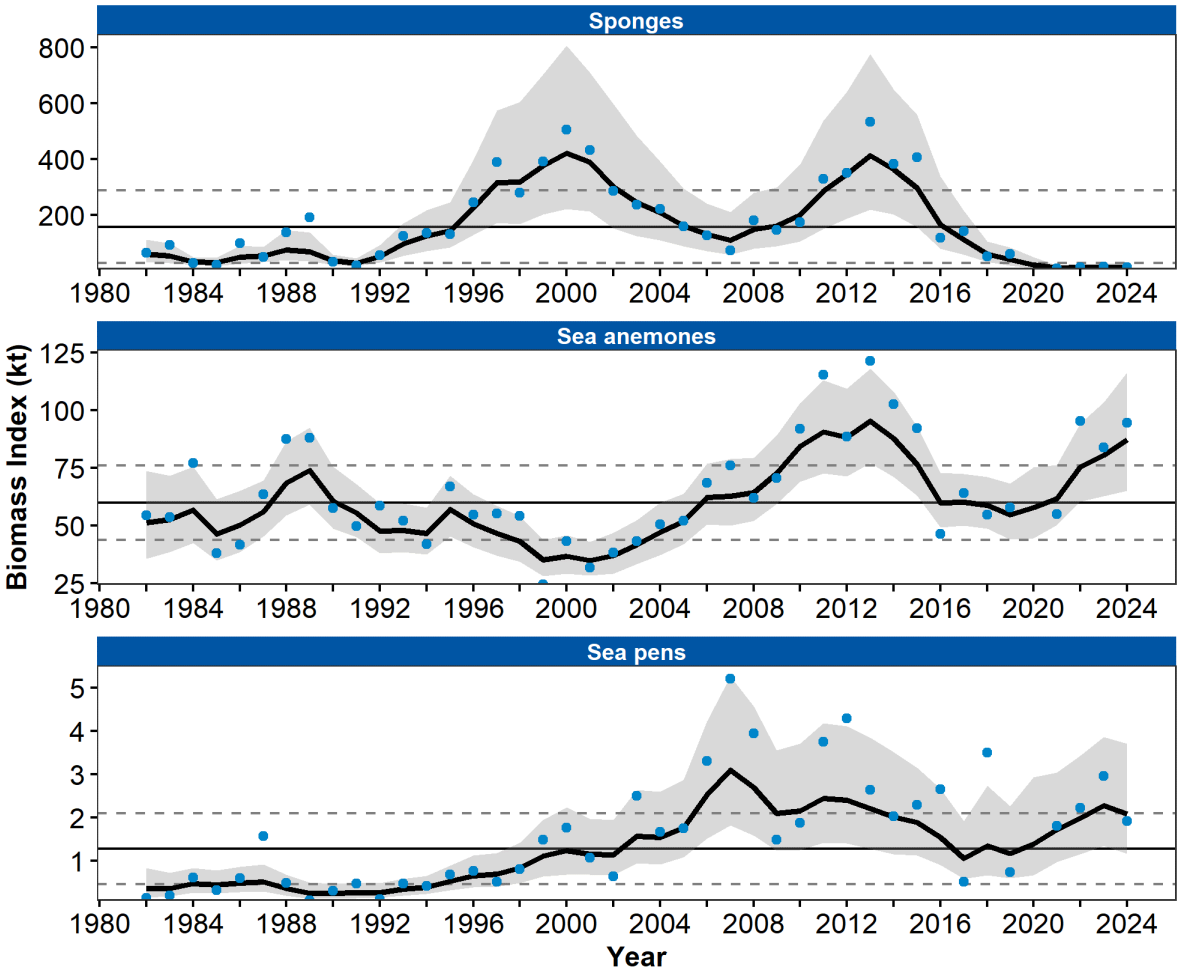

Figure 43: Biomass index of structural epifauna (sponges, sea anemones, and sea pens) from RACE Groundfish Assessment Program and Shellfish Assessment Program summer bottom trawl surveys of the eastern Bering Sea continental shelf from 1982 to 2024. Panels show the observed survey biomass index mean (blue points), random effects model fitted mean (solid black line), 95% confidence interval (gray shading), overall time series mean (solid gray line), and horizontal dashed gray lines representing one standard deviation from the mean.

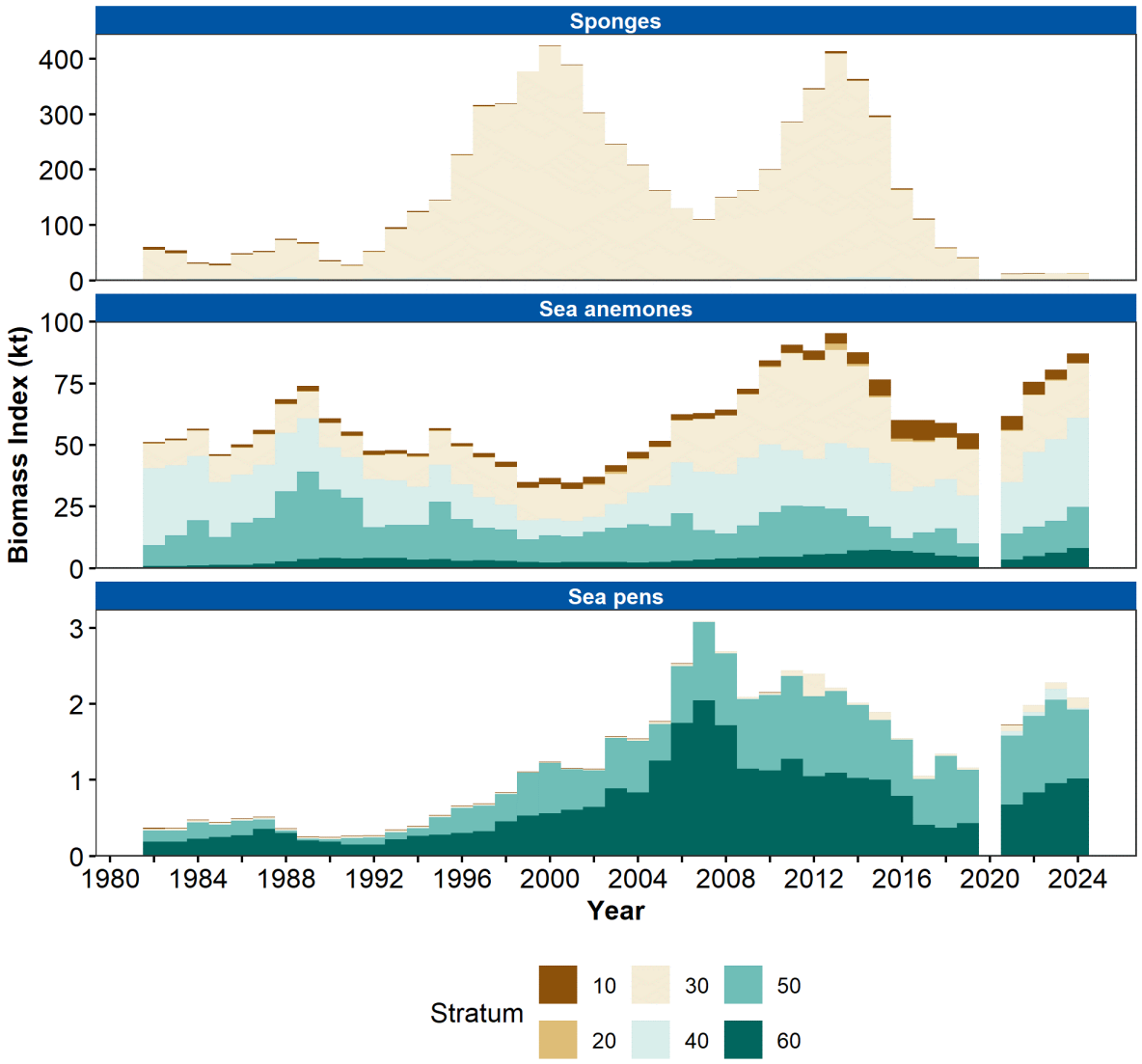

Figure 44: Biomass index of structural epifauna (sponges, sea anemones, and sea pens) in eastern Bering Sea continental shelf survey strata (10-60) estimated from RACE Groundfish Assessment Program and Shellfish Assessment Program summer bottom trawl survey data from 1982 to 2024.

Primary Production

Note: Contributors of satellite-derived chlorophyll a (chla) indicators continued to cross-validate data from both single sensor data (e.g., VIIRS) and another combined product (i.e., OC-CCI). In 2024, new cross-product comparisons showed relatively larger discrepancies among products than those from previous year comparisons. Consequently, contributors have paused contributions of satellite-derived chla trends to this year's ESRs until these discrepancies are confidently resolved. We appreciate their diligence in taking the necessary time to ensure the accuracy of the data.

St. Paul Island Chlorophyll a

Contributed by Lauren Divine[1], Aaron Lestenkof[1], and Tyler Hennon[2]
[1]Aleut Community of St. Paul Island, Ecosystem Conservation Office
[2]University of Alaska Fairbanks, College of Fisheries and Ocean Sciences
Contact: tdhennon@alaska.edu
Last updated: August 2024

Description of indicator: The community of St. Paul Island has been collecting regular (∼weekly) CTD observations for nearly the past decade. Using an RBR Concerto CTD with temperature, conductivity, and fluorescence channels, an observer conducts short vertical casts from North Dock. Water depth at the sample site is approximately 8 m, therefore measured values of temperature, salinity, and chlorophyll a are vertically averaged into single values. Figure 45 presents these values averaged into monthly bins.

Status and trends: Due to an instrument malfunction, no good data were recorded during spring 2024. However, the values obtained from June through August 2024 indicate some of the highest chlorophyll concentrations on record with values ∼10 μg/L in June and July. This is considerably higher than 2023, where there were no months with average chlorophyll a concentrations >4 μg/L.

Factors influencing observed trends: Factors that influence phytoplankton productivity include levels of photosynthetically active radiation (PAR), water temperature, stratification, and availability of micro- (e.g., iron) and macro-nutrients (e.g., nitrate). Persistent storminess in spring through summer 2024, resulting in a deeper mixed layer (Figure 27), entrained cooler and more nutrient-rich waters from below, potentially contributing to higher chlorophyll concentrations.

Implications: Phytoplankton are the base of the food web, therefore higher chlorophyll concentrations may provide better food availability for zooplankton, which could in turn positively impact higher trophic levels.

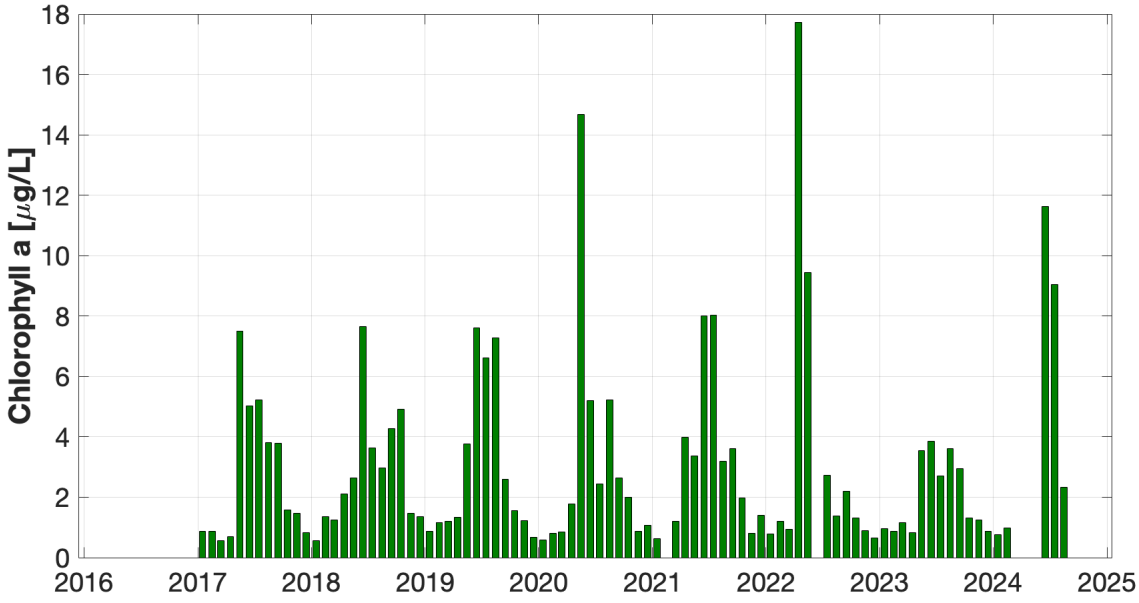

Figure 45: Monthly average chlorophyll a concentrations at St. Paul Island, January 2017 – August 2024.

Mooring M2 Chlorophyll a

Contributed by Phyllis Stabeno[1], Jens Nielsen[2,3], and Shaun Bell[1]
[1]NOAA Pacific Marine Environmental Lab [PMEL]
[2]NOAA Alaska Fisheries Science Center, Seattle, WA
[3]Cooperative Institute for Climate, Ocean, and Ecosystem Studies, University of Washington, Seattle, WA
Contact: Phyllis.Stabeno@noaa.gov
Last updated: August 2024

Description of indicator: Seasonal (early May–early October) observations of chlorophyll a were collected at the M2 mooring site (56.87°N, -164.07°W). This site provides a good representation of the biophysical conditions over the middle domain of the eastern Bering Sea shelf. A surface buoy adjacent to M2 is equipped with a Profiling Crawler (Prawler) attached to the mooring line that continuously collects high-resolution vertical profiles of physical and biological data (Figure 46. The Prawler data were used to understand phytoplankton phenology during 2024.

Status and trends: The peak of the spring bloom was slightly later than the average long-term mean (1998–2022, Nielsen et al., 2024). However, the fall bloom was unusually early in 2024, starting in early September. Sigler et al., 2014 reported fall bloom peak timing for 1997–2011 from M2, and only in 1 year (1999) did the fall bloom occur in early September. Commonly, the fall bloom occurs closer to Oct 1 (Sigler et al., 2014).

Factors influencing observed trends: Water column temperature data from M2 showed an unusually deep mixed layer (Figure 27), and stratification appeared below average (P. Stabeno, pers comm), due to frequent storm events during summer 2024. A large storm in late August likely caused water column mixing and overturning to occur early, which introduced nutrients to the surface and initiated the fall bloom.

Implications: Both the magnitude and the phenology of phytoplankton play a major role in marine food webs, with ocean primary producers accounting for about half of the world's carbon fixation. The early fall bloom observed in 2024 was likely a factor in the reduced coccolithophore bloom in September. Recent years have had substantial coccolithophore blooms in the region. The lack of a coccolithophore bloom in 2024 was corroborated by satellite images and survey-based phytoplankton imaging data (data not shown). The early fall bloom is likely to provide prey resources for zooplankton earlier than is typical. However, it is unknown at the time of writing how this event will impact zooplankton, which are important prey for fish.

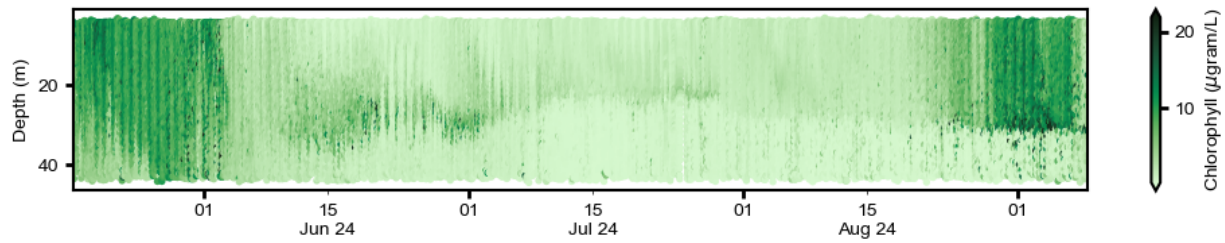

Figure 46: Observed chlorophyll a concentrations measured using the profiling crawler (Prawler) at mooring M2 in the southeastern Bering Sea.

Zooplankton

Continuous Plankton Recorder Data from the Eastern Bering Sea

Contributed by Clare Ostle[1] and Sonia Batten[2]
[1]CPR Survey, The Marine Biological Association, The Laboratory, Citadel Hill, Plymouth, Devon, PL1 2PB, UK
[2]PICES, 4737 Vista View Cr, Nanaimo, BC, V9V 1N8, Canada
Contact: claost@mba.ac.uk
Last updated: July 2024

Description of indicator: Continuous Plankton Recorders (CPRs) have been deployed in the North Pacific routinely since 2000. Two transects are sampled seasonally, both originating in the Strait of Juan de Fuca, one sampled monthly (~April-September) which terminates in Cook Inlet, the second sampled 3 times per year (in spring, summer, and fall) which follows a great circle route across the Pacific terminating in Asia. Several indicators are now routinely derived from the CPR data and updated annually.

As well as the regular Pacific CPR sampling, the icebreaker *Sir Wilfrid Laurier* (SWL) has now sampled a transect through the Bering Strait, and the western Chukchi and Beaufort Seas during the summer months since 2018.

We present CPR data from the eastern Bering Sea region (Figure 47) as the following indices: the abundance per sample of large diatoms (the CPR only retains large, hard-shelled phytoplankton so while a large proportion of the community is not sampled, the data are internally consistent and may reveal trends), mean Copepod Community Size (see Richardson et al., 2006 for details but essentially the length of an adult female of each species is used to represent that species and an average length of all copepods sampled calculated) as an indicator of community composition, and mesozooplankton biomass (estimated from taxon-specific weights and abundance data). Annual anomaly time series of each index have been calculated using a standard z-score calculation: z-score = $(x - \mu)/\sigma$ where x is the value and μ is the mean, and σ is the standard deviation (Glover et al., 2011). Scores of zero are equal to the mean, positive scores signify values above the mean, and negative scores values below the mean.

Status and trends: Figure 48 shows that the copepod community size and diatom abundance anomalies were positive in 2023 where they had been negative in 2022. The mean meso-zooplankton biomass anomaly remained negative in 2023, and has shown a decline each year since 2019.

Factors influencing observed trends: As there are only 6 years of consistently sampled data it is difficult to determine any trends yet. Analysis of summer CPR data in this region has revealed a general alternating pattern of high and low copepod size (indicated in Figure 48 by copepod community size). This could be a similar finding to the analysis from Batten et al. (2018) which was carried out in the southern Bering Sea and Aleutian Islands and concluded that this was the result of a trophic cascade caused by maturing pink salmon present in the region. However, this trophic cascade is not reflected in the diatom abundance.

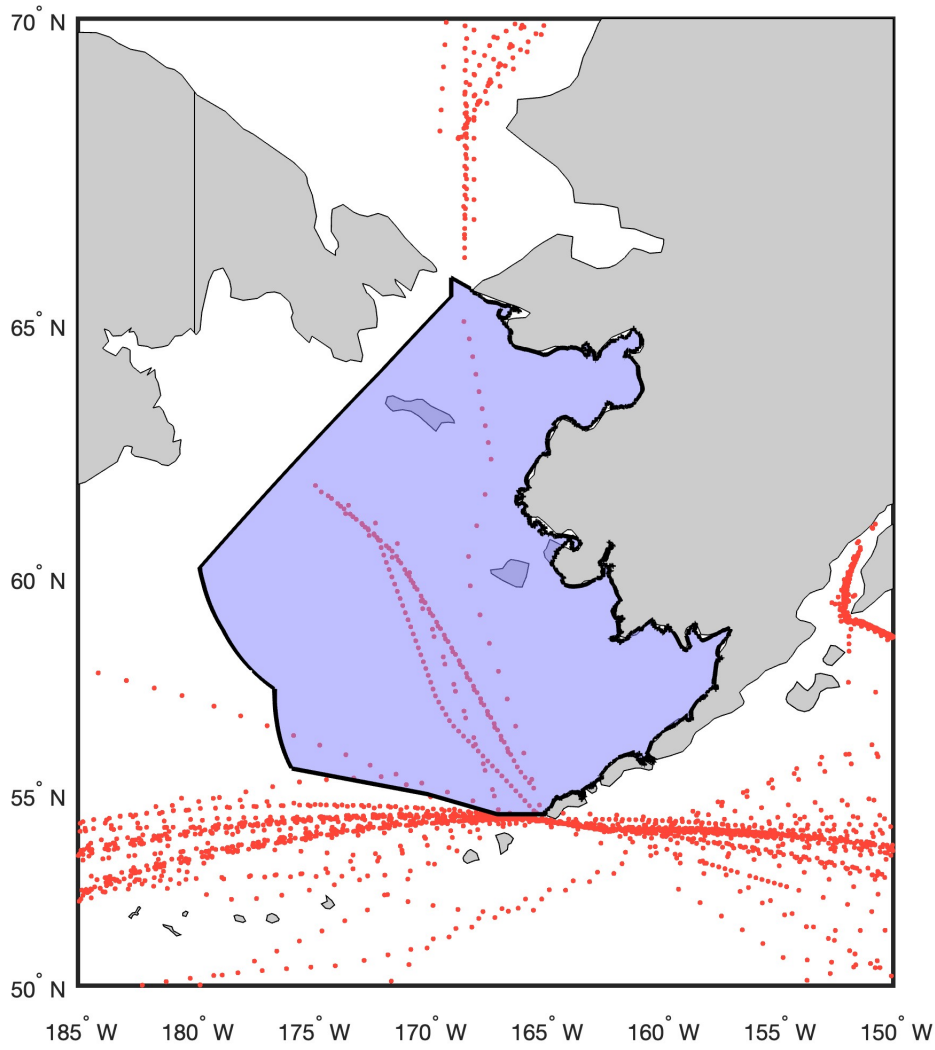

Figure 47: Location of CPR data. The EBS region selected for analysis is shaded in purple. Red dots indicate actual sample positions and may overlay each other.

Implications: This region appears to be subjected to top-down influence as well as bottom up forcing by ocean climate, which is particularly challenging to interpret. Changes in community composition (e.g., abundance and composition of large diatoms, prey size as indexed by mean copepod community size) may reflect changes in the nutritional quality of the organism to their predators. Changes in abundance or biomass, together with size, influences availability of prey to predators.

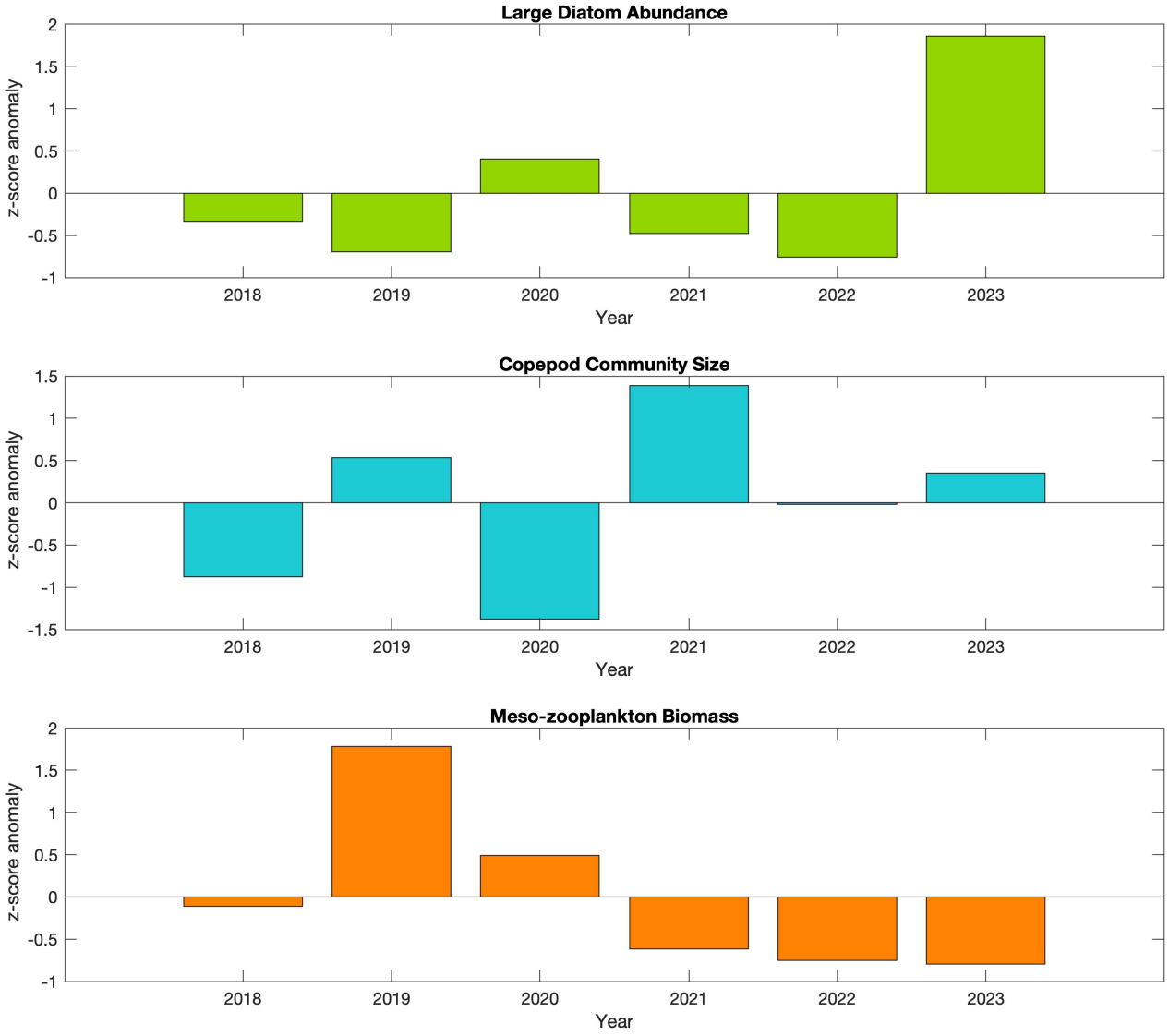

Figure 48: Annual anomalies of three indices of lower trophic levels (see text for description and derivation) for the region shown in Figure 47.

Current and Historical Trends for Zooplankton in the Bering Sea

Contributed by David Kimmel[1], Kelia Axler[1], Deana Crouser[1], H. William Fennie[1], Alicia Godersky[1], Jesse Lamb[1], James Murphy[2], Steven Porter[1], and Brooke Snyder[1]
[1]Resource Assessment and Conservation Engineering Division, Alaska Fisheries Science Center, NOAA Fisheries
[2]Auke Bay Laboratories, Alaska Fisheries Science Center, NOAA Fisheries
Contact: david.kimmel@noaa.gov
Last updated: October 2024

Description of indicator: In 2015, NOAA's Alaska Fisheries Science Center (AFSC) implemented a method for an at-sea Rapid Zooplankton Assessment (RZA) to provide leading indicator information on zooplankton composition in Alaska's Large Marine Ecosystems. The rapid assessment, which is a rough count of zooplankton (from paired 20/60 cm oblique bongo tows from 10 m from bottom or 300 m, whichever is shallower), provides preliminary estimates of zooplankton abundance. The method employed uses coarse categories and standard zooplankton sorting methods (Harris et al., 2000). The categories are small copepods (<2 mm; example species: *Acartia* spp., *Pseudocalanus* spp., and *Oithona* spp.), large copepods (>2 mm; example species: *Calanus* spp. and *Neocalanus* spp.), and euphausiids (<15 mm; example species: *Thysanoessa* spp.). Small copepods were counted from the 153 μm mesh, 20 cm bongo net. Large copepods and euphausiids were counted from the 505 μm mesh, 60 cm bongo net. Other, rarer zooplankton taxa were present but were not sampled effectively with the on-board sampling method.

RZA abundance estimates may not closely match historical estimates of abundance as methods differ between laboratory processing and ship-board RZA, particularly for euphausiids which are difficult to quantify accurately (Hunt et al., 2016). Rather, RZA abundances should be considered estimates of relative abundance trends overall. Detailed information on these taxa is provided after in-lab processing protocols have been followed (1 year post survey).

Here, we show RZA maps for four surveys: (1) the spring larval survey (May 2024), (2) the summer age-0 survey (Aug 2024), (3) the fall 70 m isobath survey (Sept 2024), and (4) the northern Bering Sea survey (Aug/Sept 2024). Note that the spring 70 m isobath survey was not conducted in 2024. We also show corresponding time-series derived from the south middle shelf region (Ortiz et al., 2012) for each survey and a time-series for the northern Bering Sea. Total lipid content for the zooplankton categories of large copepods and euphausiids is presented in a separate section (see Pinger et al., p. 99).

Status and trends:
Spring larval survey
Large copepods were low in abundance along the middle shelf during the spring larval survey; however, greater numbers were observed along the outer shelf (Figure 49). Average large copepod abundances were lower than in recent survey years (Figure 50). Small copepods were abundant throughout the sampling grid and were highest in the middle shelf (Figure 49). Mean abundances of small copepods remain similar to recent estimates, though slightly lower than in recent years (Figure 50). Euphausiids (<15 mm) were largely absent from RZA estimates, with only one sampling location having a high abundance near Bering Canyon (Figure 49). Mean euphausiid numbers were typical for the spring, with low numbers reported historically (Figure 50).

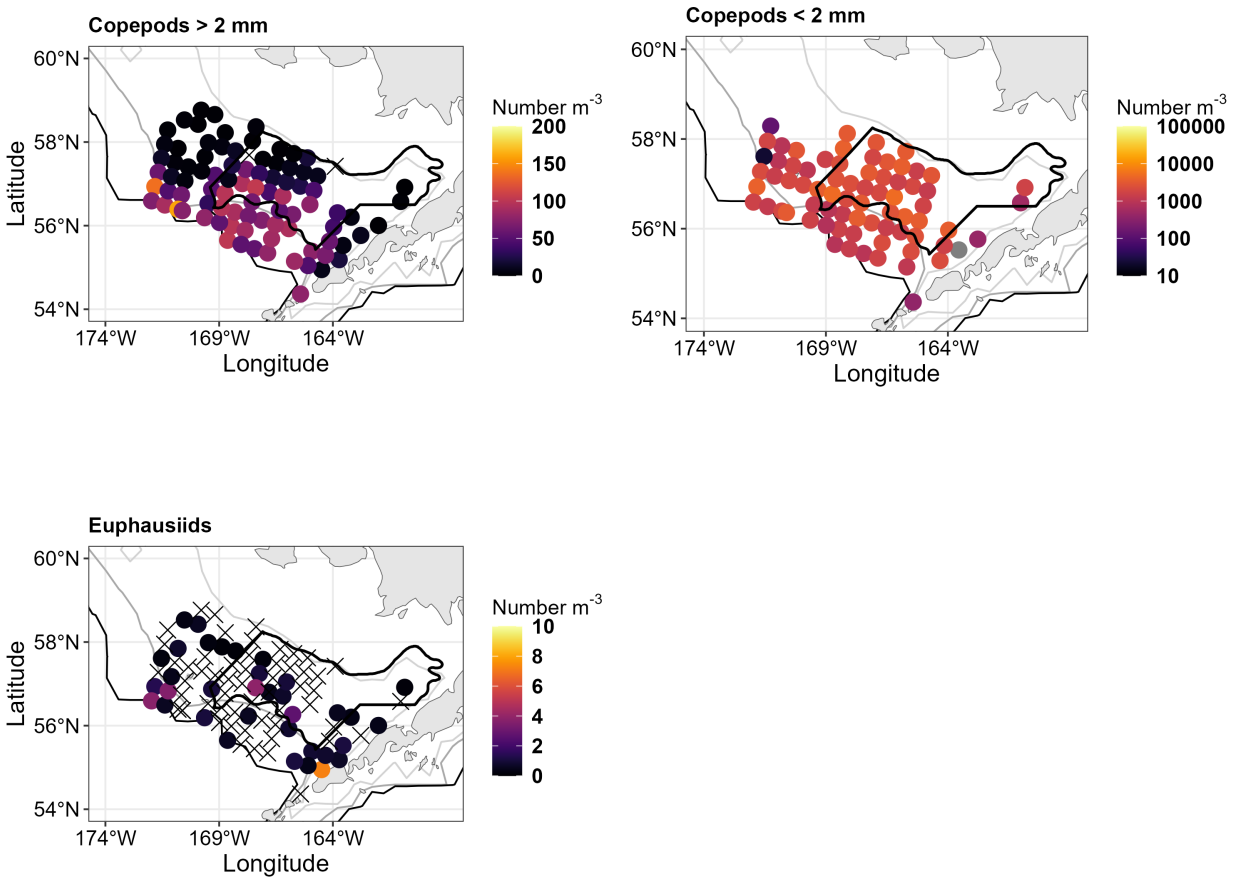

Figure 49: Maps show the abundance estimated by the RZA during the spring larval survey. Note all maps have different abundance scales (Number m^{-3}). X indicates a sample with abundance of zero individuals m^{-3}. Black polygon shows the core sampling area used to estimate the time-series. Contour lines represent the 50 m isobath (light gray), 100 m isobath (dark gray), and the 200 m isobath (black).

Summer age-0 survey

Large copepods were very low in abundance during the summer age-0 survey (Figure 51). Average large copepod abundances were near zero and far below recent observations (Figure 52). Small copepods were abundant throughout the sampling grid (Figure 51). Mean abundances of small copepods were below recent estimates, similar to the 2008–2012 period (Figure 52). Euphausiids (<15 mm) were elevated, particularly in the northern portion of the sampling grid (Figure 51). Mean euphausiid numbers were intermediate in abundance, being higher than the 2008–2012 period, but lower than those measured in 2014–2016 (Figure 52).

Fall 70 m isobath survey

Large copepod abundances were very low in the times-series sampling region, but increased in the northern portion of the fall 70 m isobath, near St. Matthew's Island (Figure 53). Small copepods followed a similar pattern (Figure 53). Euphausiid abundances were similar in pattern to those of large copepods, with low values in the southern portion of the 70 m isobath and increasing numbers in the

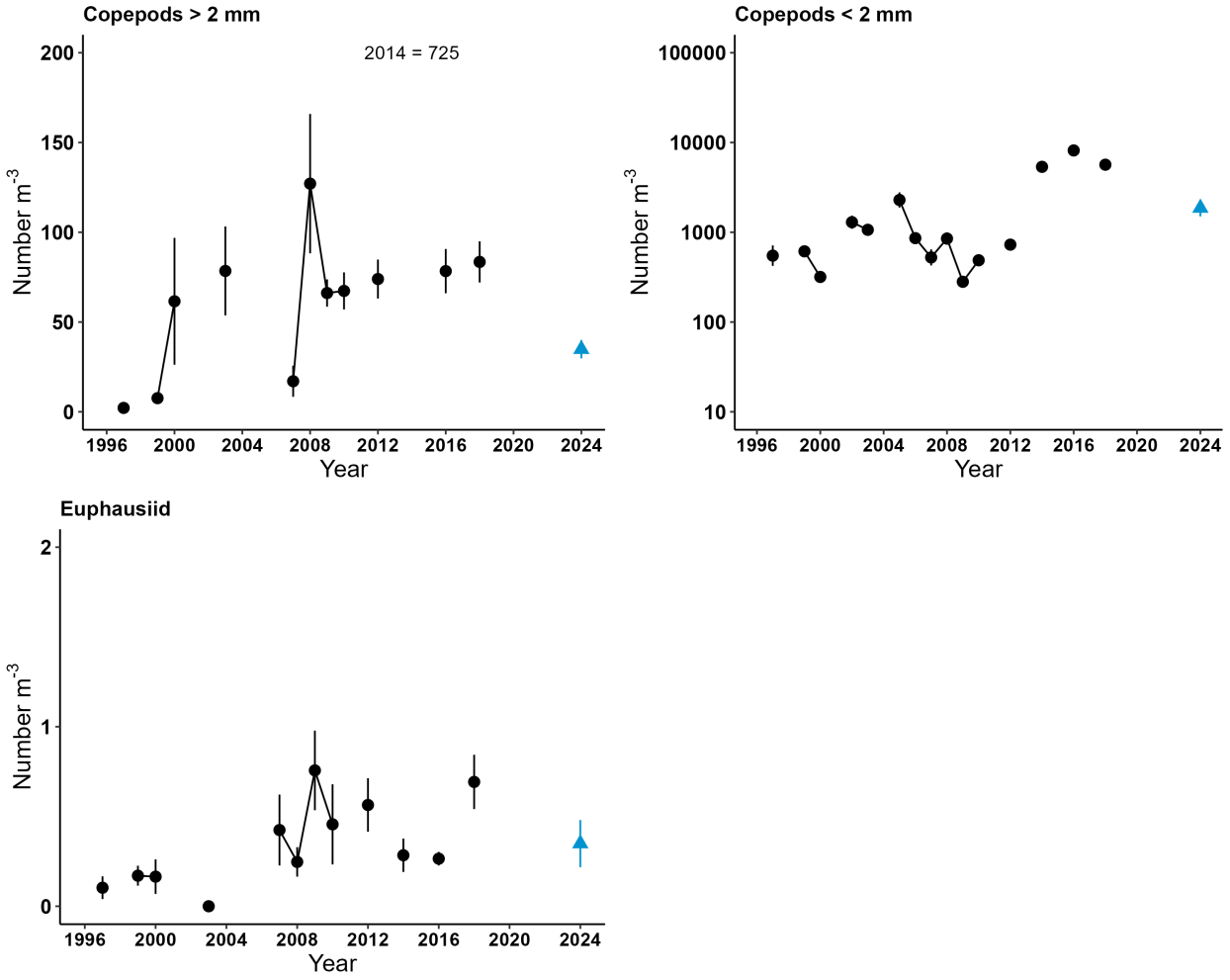

Figure 50: Mean abundance during the spring larval survey. Black circles represent laboratory processed data, blue triangle represents vessel-based RZA abundance estimate for 2024. Line ranges are the standard error of the mean. Note differences in scale.

northern portion (Figure 53). Only a total of four samples were collected within the time-series polygon, thus the estimate for the time-series should be viewed with caution. Here we place the 2024 RZA estimate on the time-series to provide some information about the status and trend. Large copepod numbers were very low on the southeastern shelf, well-below the peak values observed during the cold period (2006–2013) (Figure 54). These values are similar to the low numbers observed during recent warm periods. Small copepod abundances were about average relative to the historical record, above those of the cold period (2006–2013) and below those of the recent warm period, with the exception of 2017 (Figure 54). Euphausiid abundances were similar to most years in the data record, having low abundance in the fall, but slightly elevated compared to the last four observations (Figure 54).

Northern Bering Sea survey

Large copepod abundances in the northern Bering Sea were patchy throughout the sampling region with the highest values north and south of St. Lawrence Island, as has been observed in the past (Figure 55). However, a couple of large abundance estimates (annotated on Figure 55) produced an overall average that was similar to last year and higher than most observations in the data record (Figure 56). Small

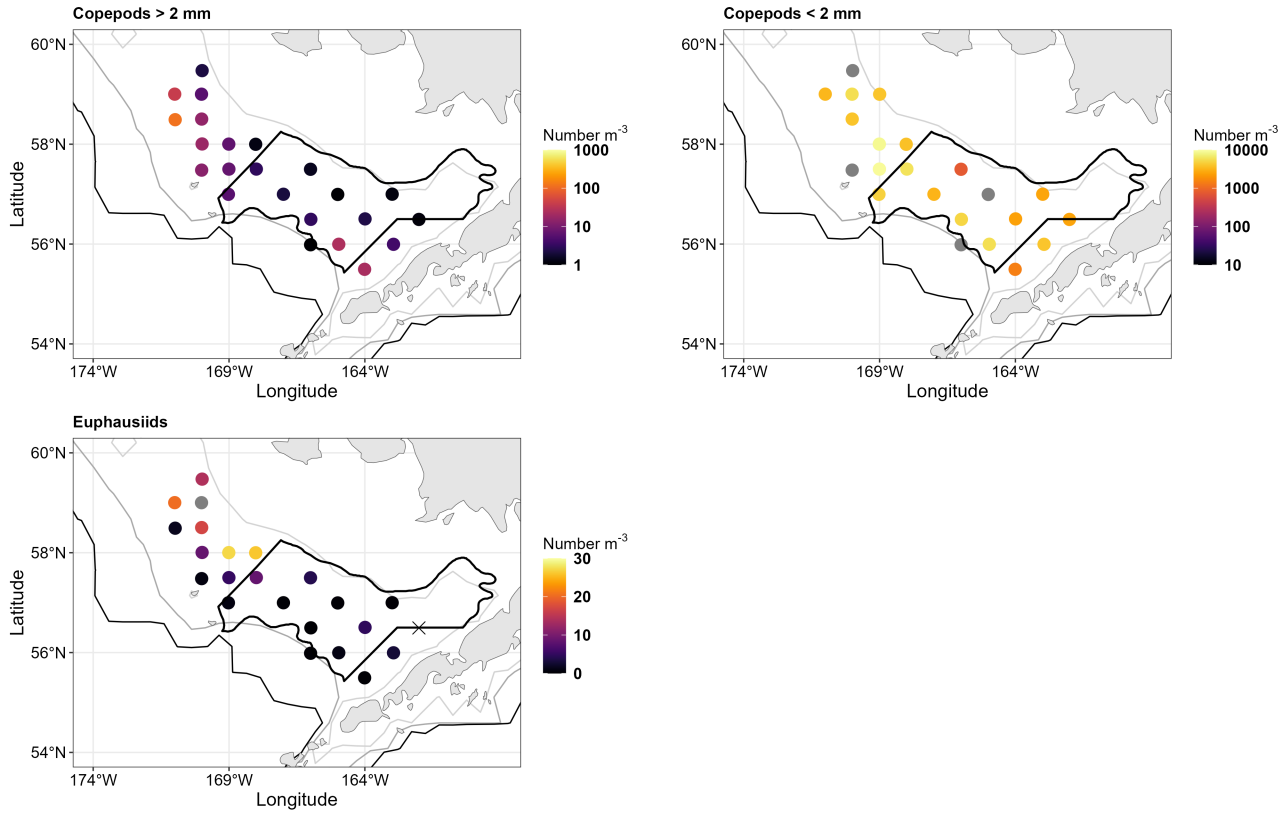

Figure 51: Maps show the abundance estimated by the RZA during the summer age-0 survey. Note all maps have different abundance scales (Number m^{-3}). X indicates a sample with abundance of zero individuals m^{-3}. Black polygon shows the core sampling area used to estimate the time-series. Contour lines represent the 50 m isobath (light gray), 100 m isobath (dark gray), and the 200 m isobath (black).

copepods had similar abundances throughout the sampling grid (Figure 55) and average abundances remained fairly similar over time (Figure 56). Euphausiids were very low in the sampling grid overall (Figure 55) and this was reflected in the average abundance estimate for 2024, which was near zero (Figure 56).

Factors influencing observed trends: Moderate ice cover and colder temperatures in the spring (May) relative to recent years suggested that a cold pool had a chance to form during 2024. Conditions appeared favorable for *Calanus* spp. population accumulation in summer/fall. This is based on the average abundances of large copepods observed in spring as warmer years tend to have higher large copepod abundances (Figure 50). Small copepod numbers were also slightly reduced compared to the very high values observed during the past warm years (Figure 50), another indicator that colder conditions were reducing development rates and slowing the population increase for small copepods (Kiorboe and Sabatini, 1995).

Though conditions did appear favorable in the spring, very low numbers of large copepods (*Calanus* spp.) were seen on the southeastern shelf during the summer age-0 and fall mooring surveys (Figures 51 and 53). This can be attributed to bottom temperatures in excess of 3°C on the southeastern shelf. When bottom temperatures decreased below 2°C in the northern portion of the age-0 sampling grid or 70 m isobath line, *Calanus* spp. were present in greater numbers, particularly near 60°N on the fall 70 m isobath survey (Figure 53). However, it appeared that the cold pool did not persist on the

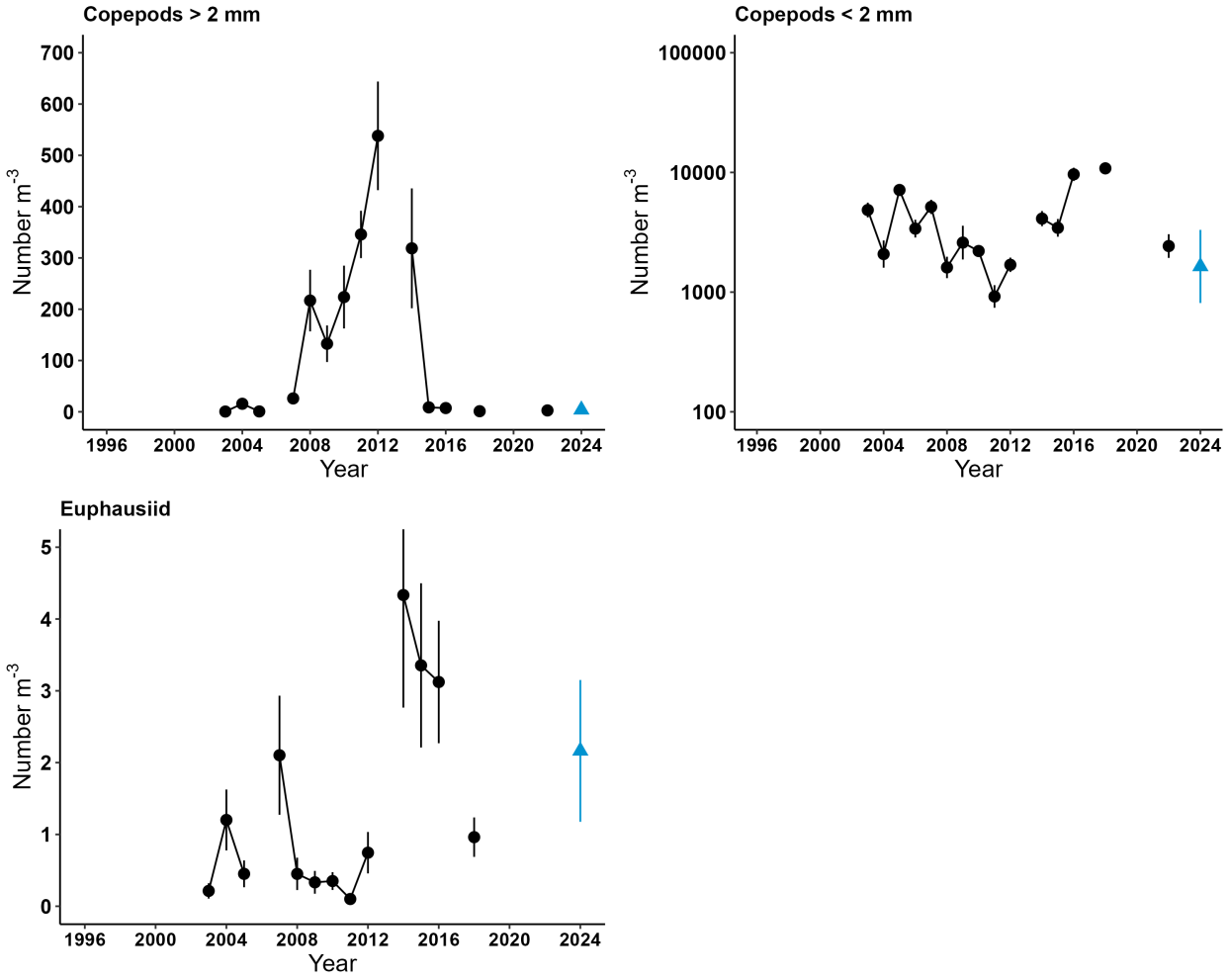

Figure 52: Mean abundance during the summer age-0 survey. Black circles represent laboratory processed data, blue triangle represents vessel-based RZA abundance estimate for 2024. Line ranges are the standard error of the mean. Note differences in scale.

southeastern shelf and cold pool extent is one of the most important factors that correlates to the presence of *Calanus* spp. (Eisner et al., 2018; Kimmel et al., 2018). Small copepod abundances in late summer were moderate and did not show a spatial gradient from south to north (Figures 51 and 53). The lower abundances of small copepods compared to more recent warm years suggests water temperatures were lower than prior years, but still elevated relative to very cold years (Figures 52 and 54). Euphausiid abundances were higher than those observed in spring and this suggests that euphausiids had reproduced in spring and euphausiids <15 mm were present in late-summer. Their numbers also appeared to increase with declining bottom water temperatures; however, correlations with euphausiids and temperature are not strong (Bi et al., 2015) and population dynamics of euphausiids remain difficult to estimate (Hunt et al., 2016).

The lack of large copepods on the southeastern shelf was in contrast to the northern Bering Sea survey which found higher abundances overall (Figure 55), albeit the distribution of these large copepods was patchy. Average abundances were similar to last year, but below those of the cold period (2006–2013) (Figure 56) and can be attributed to a few stations with very high abundances (Figure 55). The northern

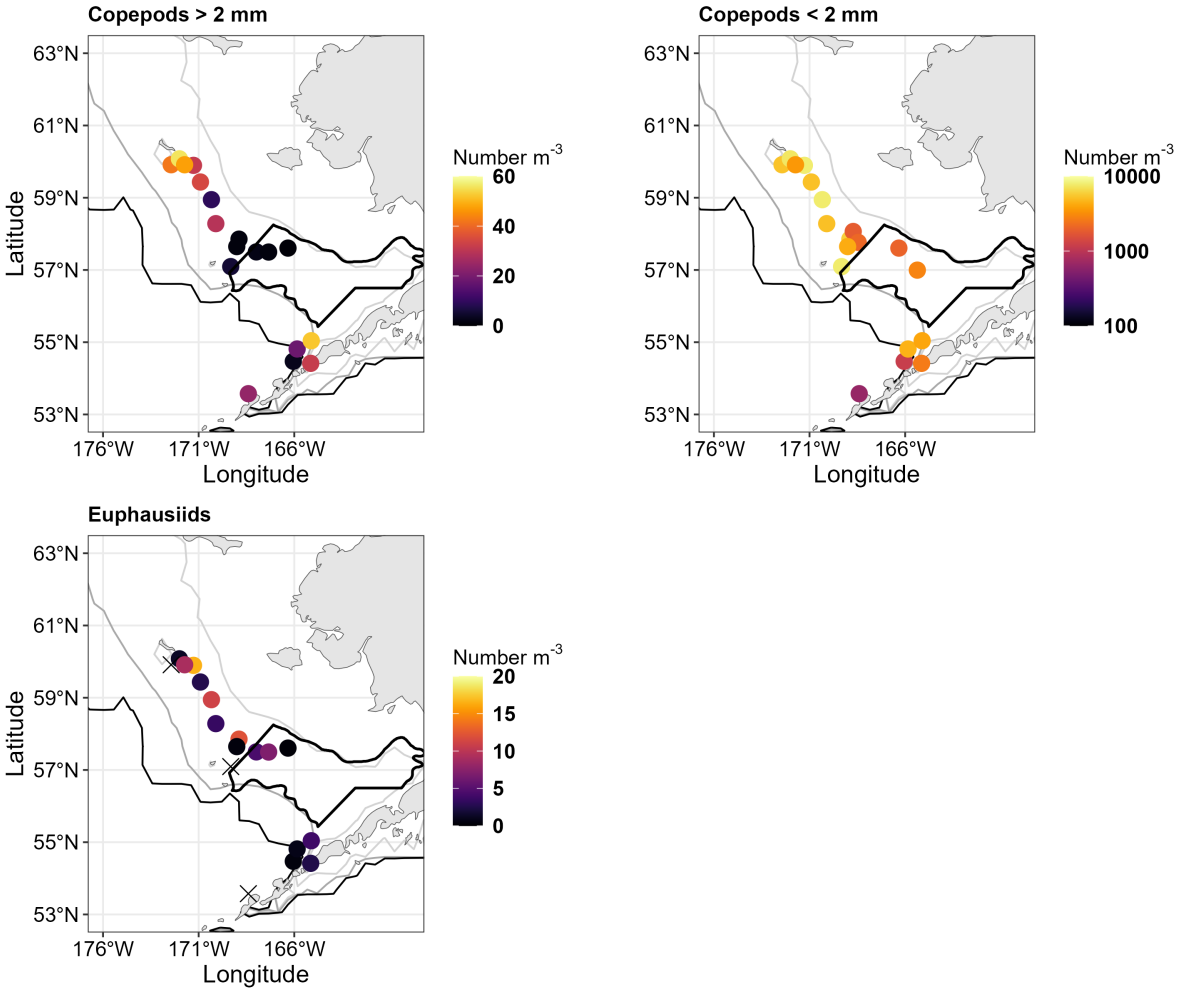

Figure 53: Maps show the abundance estimated by the RZA during the fall 70 m isobath survey. Note all maps have different abundance scales (Number m^{-3}). X indicates a sample with abundance of zero individuals m^{-3}. Black polygon shows the core sampling area used to estimate the time-series. Contour lines represent the 50 m isobath (light gray), 100 m isobath (dark gray), and the 200 m isobath (black).

Bering Sea appears to be more stable across warm and cold periods in comparison to the southeastern shelf, with at least a small population of *Calanus* spp. present annually. It should be noted that the *Calanus* spp. numbers are also lower in this inner shelf region compared to middle shelf numbers. Small copepod numbers were elevated in the northern Bering Sea as would be expected in inner shelf waters (Figure 55) and the average time-series shows little variability over time (Figure 56). Euphausiid values were near zero in the northern Bering Sea (Figure 55) in contrast to recent years (Figure 56). This observation resulted in the end of a recent upward trend in euphausiid numbers (Figure 56).

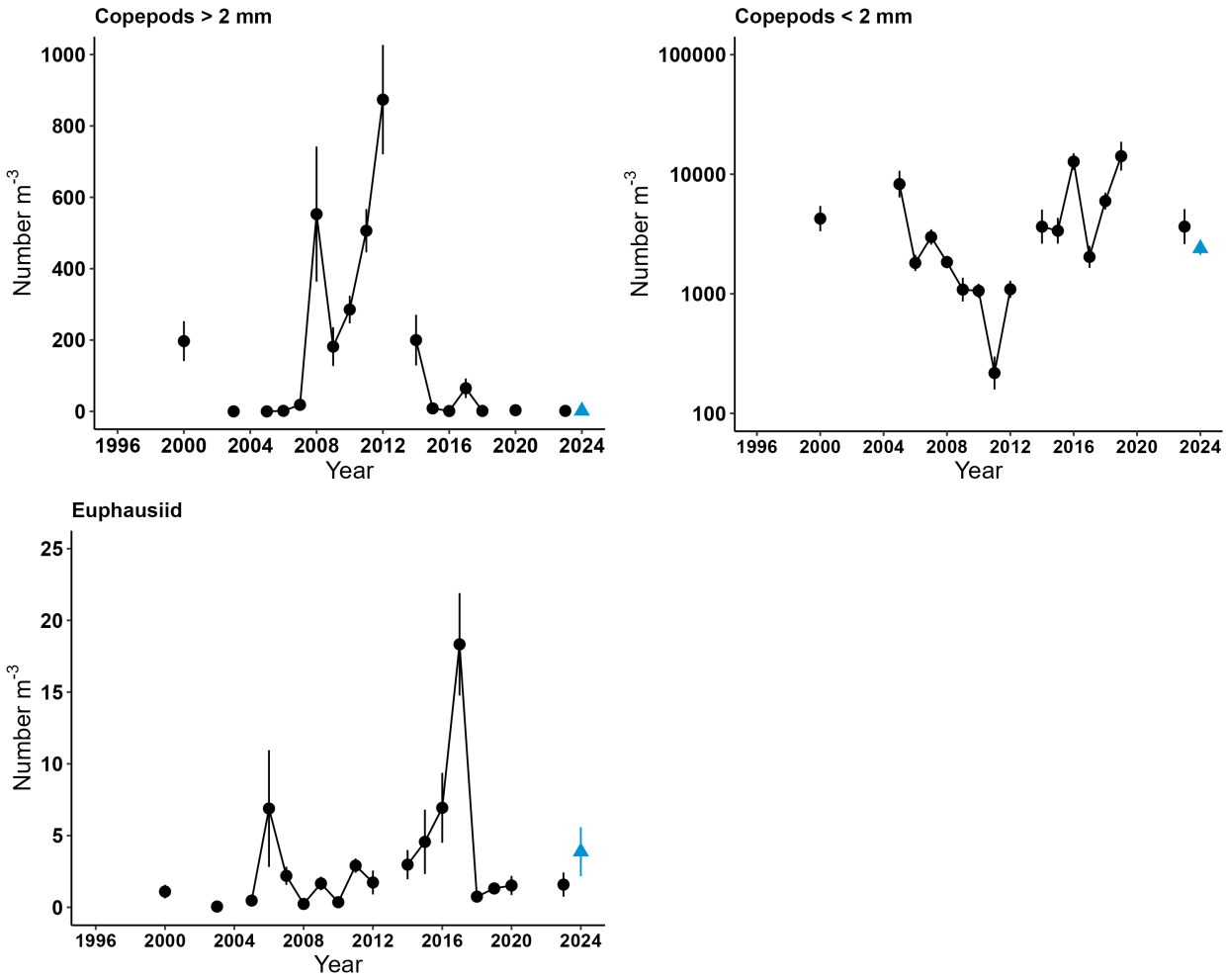

Figure 54: Mean abundance during the fall 70 m isobath survey. Black circles represent laboratory processed data, blue triangle represents vessel-based RZA abundance estimate for 2024. Line ranges are the standard error of the mean. Note differences in scale.

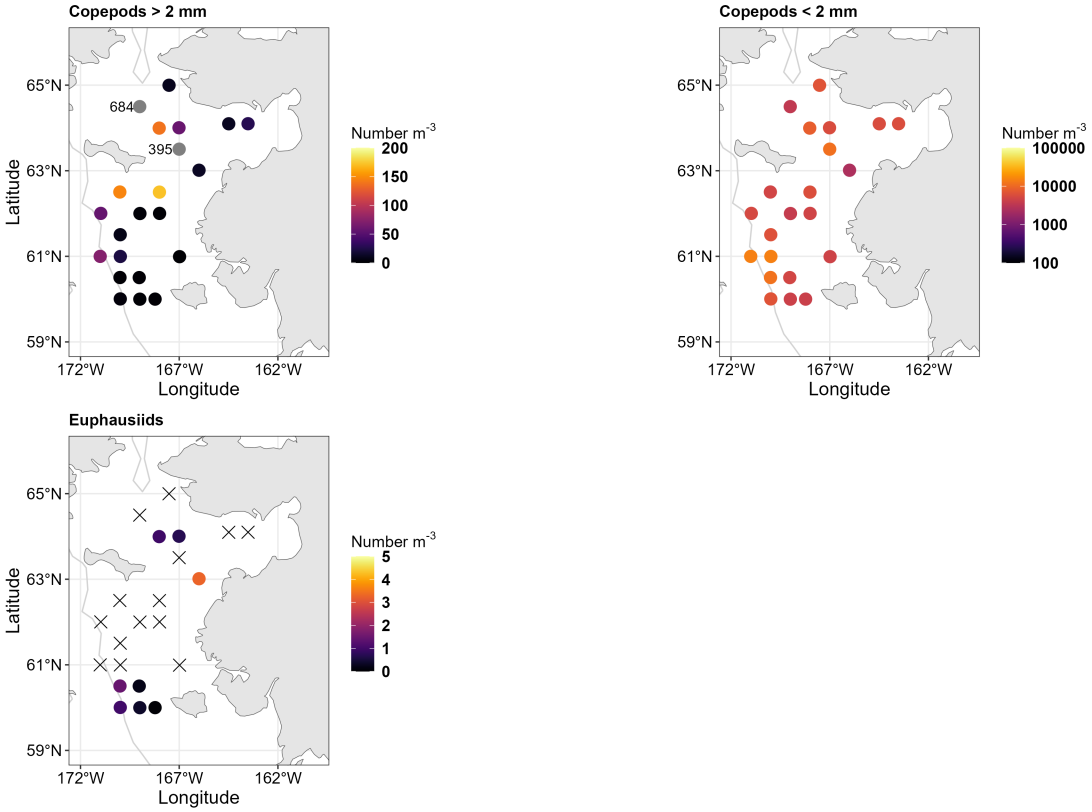

Figure 55: Maps show the abundance estimated by the RZA during the northern Bering Sea survey in fall. Note all maps have different abundance scales (Number m^{-3}). X indicates a sample with abundance of zero individuals m^{-3}. Time-series is estimated from the whole sample region. Note two values for copepods >2 mm was beyond the legend scale and their values are indicated on the map. Contour line represents the 50 m isobath (light gray).

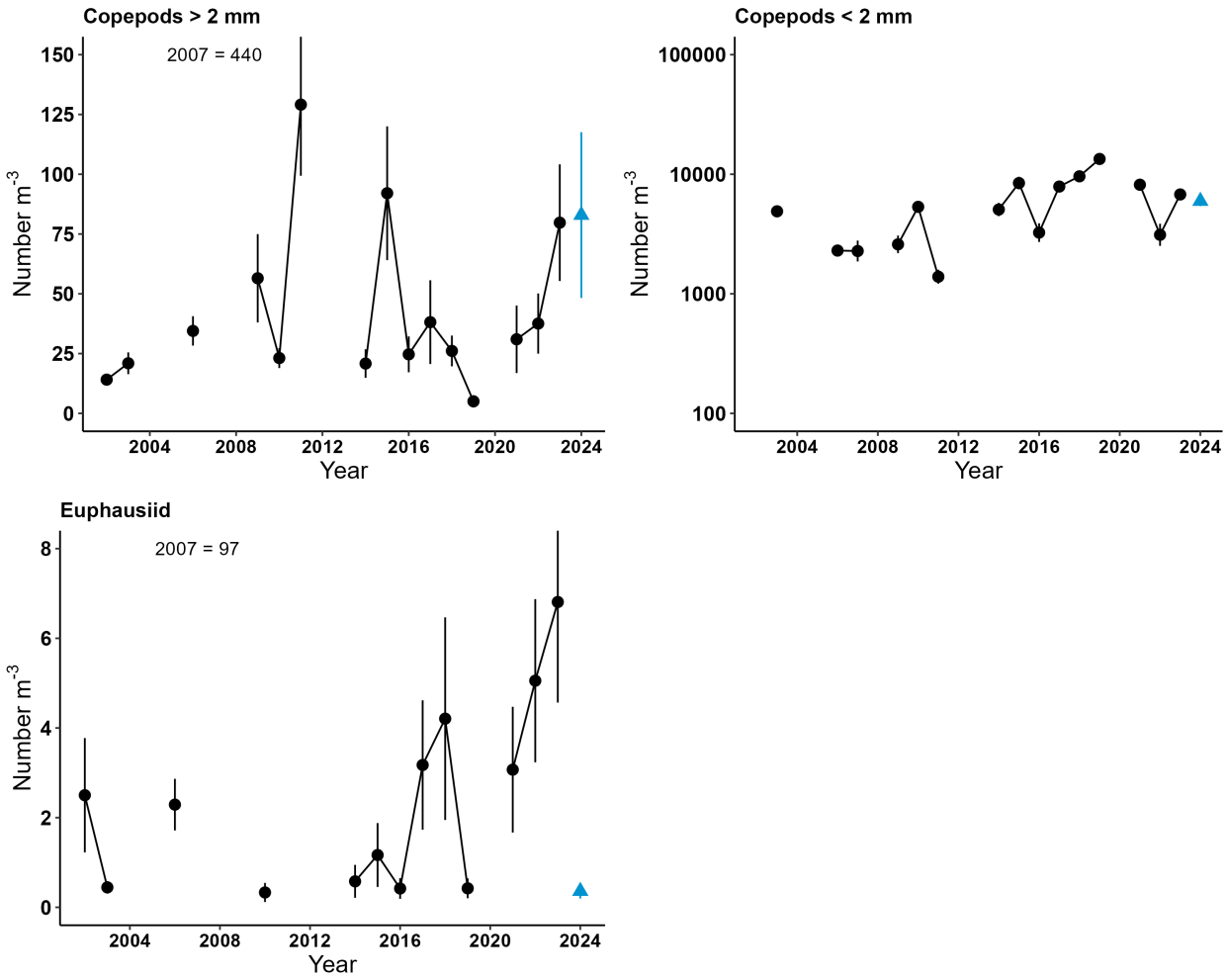

Figure 56: Mean abundance during the northern Bering Sea survey in fall. Black circles represent laboratory processed data, blue triangle represents vessel-based RZA abundance estimate for 2024. Line ranges are the standard error of the mean. Note differences in scale.

Implications: Smaller copepods and their early life history stages (nauplii) form the prey base for larval to early juvenile walleye pollock, as well as other fish species, during spring (Figures 49 and 50) on the eastern Bering Sea middle shelf. Warm years result in larger abundances of small copepods in the spring (Figure 50) and this led to the formulation of the first Oscillating Control Hypothesis (OCH) (Hunt et al., 2002) as this supports larval pollock production. Small copepod numbers observed in 2024 were intermediate between warm and cold year estimates and this suggests that adequate food for larval fish was present during spring 2024.

Large copepods and euphausiids are more important to juvenile pollock as shown in the second iteration of the OCH (Hunt et al., 2011). While large copepods were absent on the southeastern shelf in late summer, they were present in moderate abundances further north in both the summer age-0 and fall 70 m isobath surveys (Figures 51 and 53) and northern Bering Sea surveys (Figure 55). This suggests forage for juvenile pollock would be present in the northern portion of the Bering Sea on the middle shelf, but scarce in the southeastern shelf.

Euphausiid numbers were moderate during summer in the summer age-0 and fall 70 m isobath surveys, but numbers were very low in the northern Bering Sea survey relative to prior years (Figures 51, 53, 55, and 56). Euphausiids have been more prevalent in age-0 pollock diets during warm years, thus have been proposed as an alternative diet item in the absence of *Calanus* spp. (Duffy-Anderson et al., 2017). Exact estimates of euphausiid abundances remain semi-quantitative. Euphausiid estimates should be treated with caution as the bongo nets are effectively avoided by euphausiids (Hunt et al., 2016).

In summary, the cooler conditions during spring had differing impacts on the zooplankton community. It moderately reduced zooplankton levels early in the year, particularly for small copepods which had been elevated during the recent warm period (Figure 50). Despite this, adequate numbers appeared to be present, suggesting that larval fish in the early portion of the year experienced sufficient forage. The cooler conditions did not translate into an extension of the cold pool over the southeastern shelf during late summer, but colder bottom temperatures were present further north along with increased abundances of large copepods and euphausiids (Figure 53). The *Calanus* spp. that were found during the summer age-0 survey and northern Bering Sea survey were rich in lipid (see Pinger et al., p. 99). Cold pool dynamics continue to play a key role in the degree of spatial overlap between age-0 pollock and these prey species that are important to their survival (Siddon et al., 2013; Eisner et al., 2020).

Lipid Content of Copepods and Euphausiids in the Bering Sea

Contributed by Cody Pinger[1], Bryan Cormack[1], Dave Kimmel[2], Jesse Lamb[2], Jacek Maselko[1], Todd Miller[1], Drew Porter[1], Rob Suryan[1]
[1]Auke Bay Laboratories, NOAA Fisheries, Alaska Fisheries Science Center, Juneau, AK
[2]Resource Assessment and Conservation Engineering Division,NOAA Fisheries, Alaska Fisheries Science Center, Seattle, WA
Contact: Cody.Pinger@noaa.gov
Last updated: October 2024

Description of indicator: Large copepods (*Calanus* spp.) and euphausiids are important prey for fishes in the Bering Sea, including age-0 walleye pollock (*Gadus chalcogrammus*), juvenile salmon (*Oncorhynchus* spp.), and capelin (*Mallotus catervarius*), because they provide a valuable source of dietary lipids (Heintz et al., 2013; Farley et al., 2016; Kimmel et al., 2018). Consumption of a high lipid diet prior to winter is important for age-0 fishes, as higher growth and lipid reserves can reduce starvation mortality and predation over prolonged winter months of low prey availability and quality. The lipid content of large copepods and euphausiids collected in early spring are at their seasonal lowest and show little variability, however samples from late summer/fall collections that are reflective of summer production vary annually and are therefore the focus of this indicator. This indicator provides insight into environmental drivers of diet quality affecting the future health and recruitment success of age-0 fish.

Mean annual lipid content of large copepods and euphausiids collected from the NMFS northern Bering Sea (NBS; annual) and southeastern Bering Sea (SEBS; biennial) surface trawl survey grids occurring in late August and September are presented. Samples were collected by bongo net tows as part of the Rapid Zooplankton Assessment (RZA, Kimmel et al., 2023) method. Samples consisted of composites of 2–10 individuals, with copepods >2 mm (primarily stage IV and V *Calanus glacialis*) and for euphausiids ≥15 mm or the largest available individuals (primarily *Thysanoessa* spp. and *Euphausia* spp.). Once picked from the RZA, zooplankton were placed in glass vials, frozen at -80°C, and transported to NOAA Auke Bay Laboratories immediately after the survey for analysis of lipid content. Lipid content was measured as a percent of the total wet weight via the sulfo-phospho-vanillin (SPV) assay as described in Pinger et al. (2022).

Status and trends: So far, this new time series shows similar interannual trends in copepod lipid content in the SEBS (Figure 57) and NBS (Figure 58), with lower values in 2018 and 2019, reflecting the unusually warm conditions in the Bering Sea during those years. Copepod lipids were significantly higher in 2024 compared to last year (2023), and were more similar to those observed in 2022. Interestingly, although the mean lipid content was high, the variability was also large. Surprisingly, 2023 had considerably lower values than both 2022 and 2024, despite similarly favorable (near average) temperature and sea ice conditions. Euphausiids collected in the SEBS had significantly higher lipid content in 2024 relative to 2022 (Figure 59).

Factors influencing observed trends: *Calanus* copepods and euphausiids store energy in the form of lipids for future use in survival, growth, and reproduction. The lipid content observed in this time series may be driven in part by water temperature, food availability (phytoplankton), competition, sea ice extent, and timing of sea ice retreat.

Implications: Large lipid-rich copepods are less abundant during warm years in the Bering Sea (Kimmel et al., 2023). Our time series shows that copepods and euphausiids also contain less lipid during warm years, suggesting there is less energy available at the base of the food web in these years. Data from 2023 suggest that temperature may not be the only factor influencing summer/fall copepod lipid content, with other oceanographic factors, such as food availability, also playing a role.

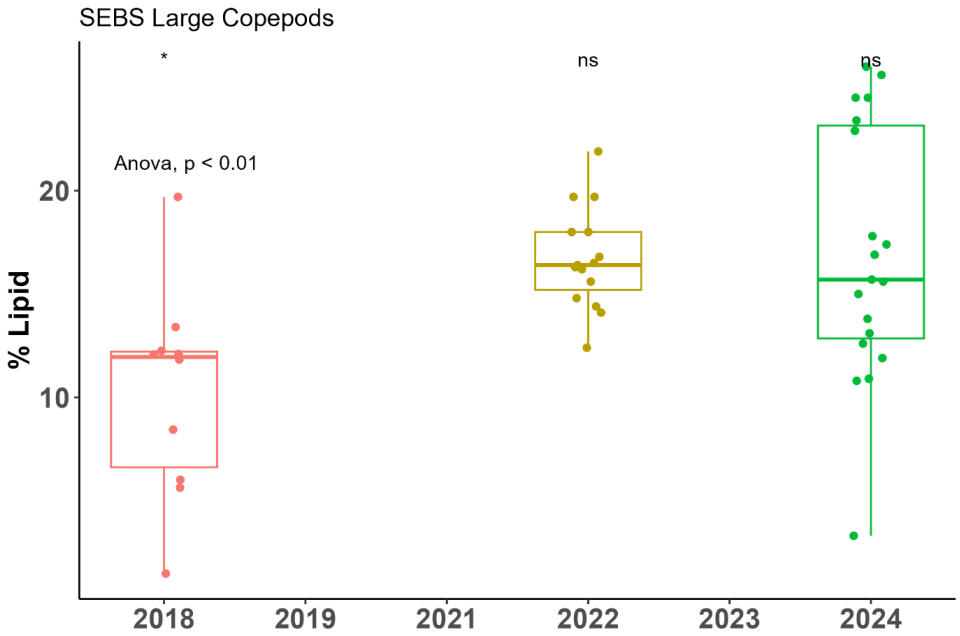

Figure 57: Annual lipid content (% lipid per wet mass) of large copepods from the southeastern Bering Sea surface trawl survey. The stars above each group indicate the significance of the difference of that group mean from the overall mean.

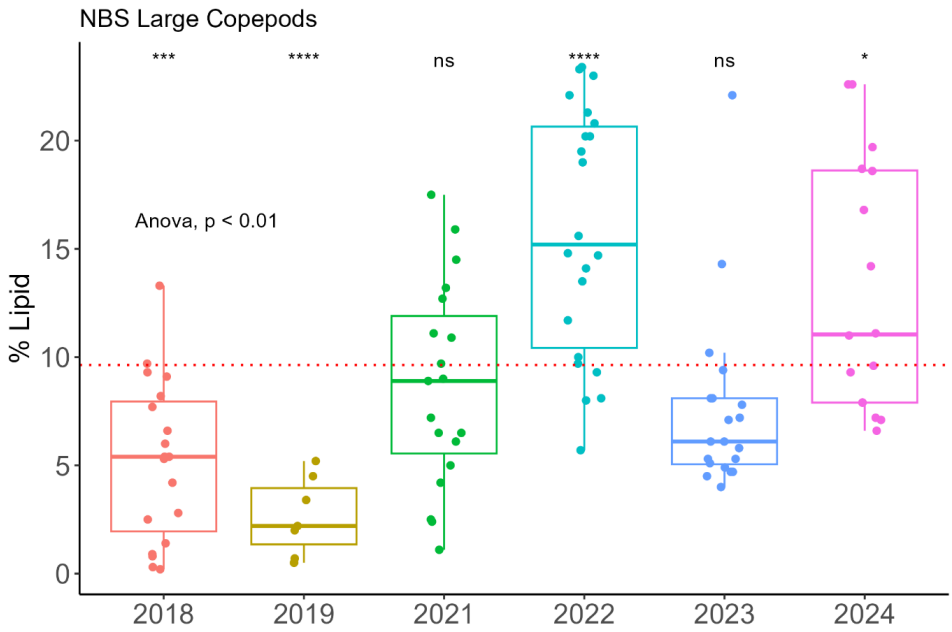

Figure 58: Annual lipid content (% lipid per wet mass) of large copepods from the Northern Bering Sea surface trawl survey. The stars above each group indicate the significance of the difference of that group mean from the overall mean which is indicated by the horizontal red line.

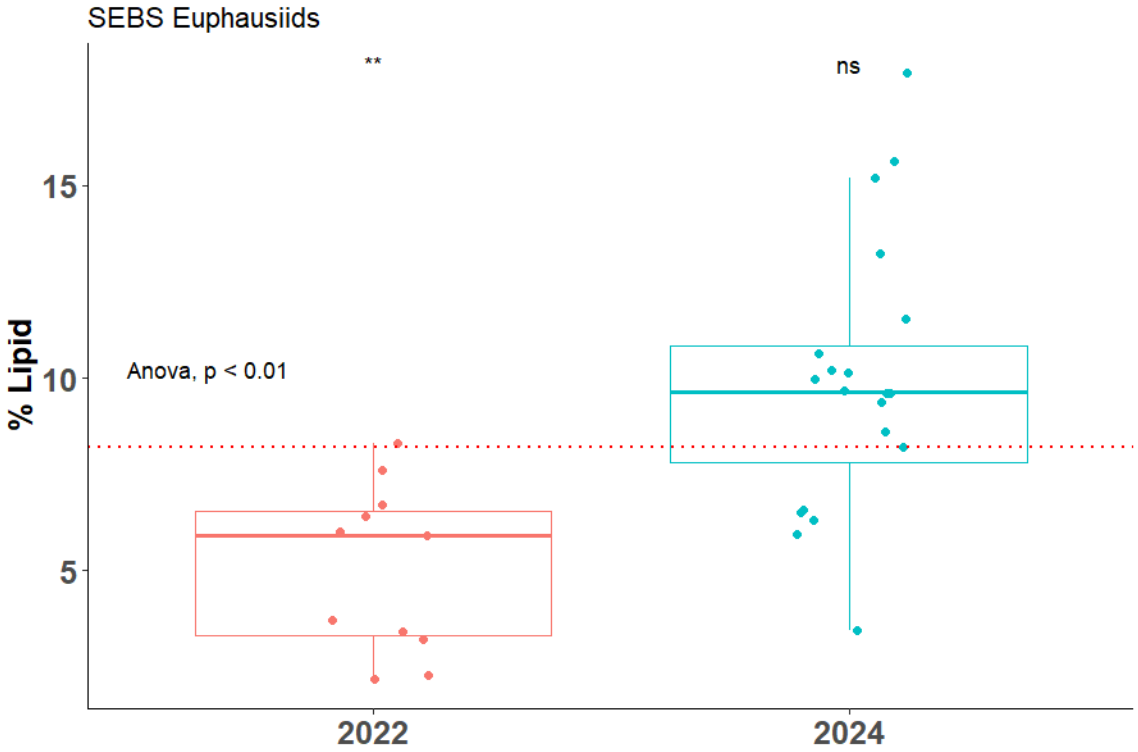

Figure 59: Annual lipid content (% lipid per wet mass) of euphausiids from the southeastern Bering Sea surface trawl survey. The stars above each group indicate the significance of the difference of that group mean from the overall mean which is indicated by the horizontal red line.

Eastern Bering Sea Euphausiids ('Krill')

Contributed by Mike Levine and Patrick Ressler
Resource Assessment and Conservation Engineering Division, Alaska Fisheries Science Center (AFSC), NOAA Fisheries
Contact: patrick.ressler@noaa.gov
Last updated: September 2024

Description of indicator: Ressler et al. (2012) developed a survey of the abundance and biomass of euphausiids on the middle and outer shelf of the eastern Bering Sea using acoustic and Methot trawl data from 2004–2010 surveys of midwater walleye pollock (*Gadus chalcogrammus*, e.g., McCarthy et al., 2020). The method has been used to estimate an index of euphausiid abundance on a biennial schedule since that time. Acoustic backscatter at 120 kHz classified as euphausiids was used to compute the mean numerical density (no. m^3) of euphausiids in 0.5 nmi intervals along acoustic-trawl survey transects (Figure 60); these values were then averaged across the surveyed area to produce annual averages (Figure 61). Because few trawl samples were available in the early years of the times series, the parameter used to convert euphausiid backscatter to numerical density (target strength; Smith et al., 2013) was modeled using the average of length and species composition from samples collected over the time series. There is large uncertainty about the abundance of euphausiids in the eastern Bering Sea, with acoustic estimates being much higher than those from net capture in an absolute sense (Hunt et al., 2016), but the relative trends in the index presented here are probably robust. Error bars on annual values indicate 95% confidence intervals computed from geostatistical estimates of relative estimation error due to sampling variability (Petitgas, 1993).

Since the previous update to this index, euphausiid backscatter observations from the 2020 Saildrone uncrewed surface vehicle survey (analyzed using a modified but functionally equivalent method; Levine and De Robertis, submitted) as well as the 2024 acoustic-trawl survey of pollock (McCarthy et al., in prep.) were added to the time series. Net catches collected from 2004–2016 were used to estimate the average length and species composition of euphausiids (length and species composition from trawl samples collected in 2018, 2022, and 2024 are not yet available); they indicated euphausiid layers in 2004–2016 were dominated numerically by euphausiids (mean 87%) of average length between 18 and 20 mm, and that euphausiid species *Thysanoessa inermis* dominated species composition on the outer shelf, and *T. raschii* dominated inshore. These observations of length and species composition are consistent with what is known from the literature (Smith, 1991; Coyle and Pinchuk, 2002). There is some indication that euphausiids were smaller in 2004–2009 and in 2016 (by 1-2 mm), and that there was an increase in relative abundance of *T. spinifera* in 2016, compared to other years in the time series. Overall though, no radical changes in length or species composition of euphausiid scattering layers have been indicated in our samples. De Robertis et al. (2010) advocated the use of a mean normal deviate (z-score) of the frequency response to judge the quality of the multifrequency backscatter classification process used here, where a value of 1 indicates that the observed frequency response is within 1 standard deviation of the known response for a given class of acoustic targets. For euphausiids, this value has averaged 0.86 (range 0.75–1.15) from 2004–2022; the 2024 value was 0.86, indicating consistent performance of the method.

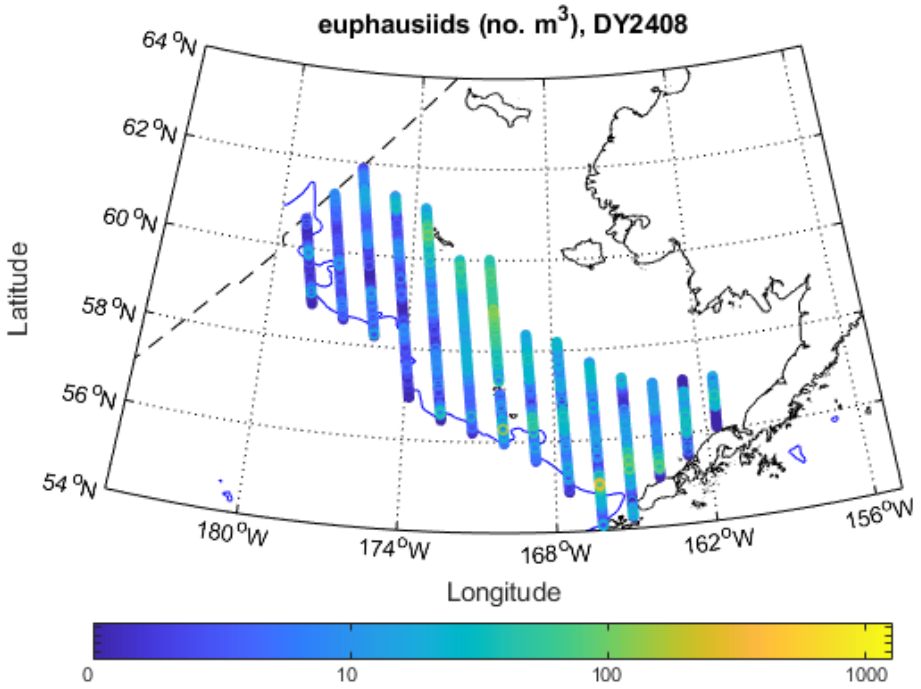

Figure 60: Water column averages of estimated euphausiid density (no. m^3) in the 2024 NOAA-AFSC eastern Bering Sea summer acoustic-trawl survey.

Status and trends: Summertime euphausiid density increased in the eastern Bering sea from 2004–2009, then subsequently declined 2010 through 2016, when the lowest value in the time series was reported. Euphausiid density increased in summers 2018 through 2022, but declined again in 2024 to the second-lowest value in the time series (8.18 $\pm$ 0.83 euphausiids m^3; Figure 61).

Factors influencing observed trends: Factors controlling annual changes in euphausiid abundance in the north Pacific are not well understood; possible candidates include bottom-up forcing by temperature and food supply, and top-down control through predation (Hunt et al., 2016). When factors including temperature, pollock abundance, primary production, and spatial location have been considered in spatially-explicit multiple regression models, temperature has been the best predictor, with increases in euphausiid abundance associated with cold temperatures in the eastern Bering Sea (Ressler et al., 2014), but not in the Gulf of Alaska (Simonsen et al., 2016). The summers of 2014–2019 were warmer than average on the Bering Sea shelf (Hennon et al., 2023) and in the acoustic-trawl survey area (McCarthy et al., 2020), but 2022 and 2024 were more moderate and a substantial cold pool was observed (Stienessen et al., in prep.). The biomass of eastern Bering Sea pollock (an abundant predator of euphausiids) has been near or above the historical mean over the past decade (Ianelli et al., 2023), though euphausiid abundance has not been strongly correlated with pollock biomass in multiple regression models of euphausiid biomass in either the eastern Bering Sea or the Gulf of Alaska (Ressler et al., 2014; Simonsen et al., 2016).

Implications: Euphausiids are food for many species of both ecological and commercial importance in the eastern Bering Sea, including pollock (Aydin and Mueter, 2007). The data presented here suggest that euphausiid prey availability is below average in 2024.

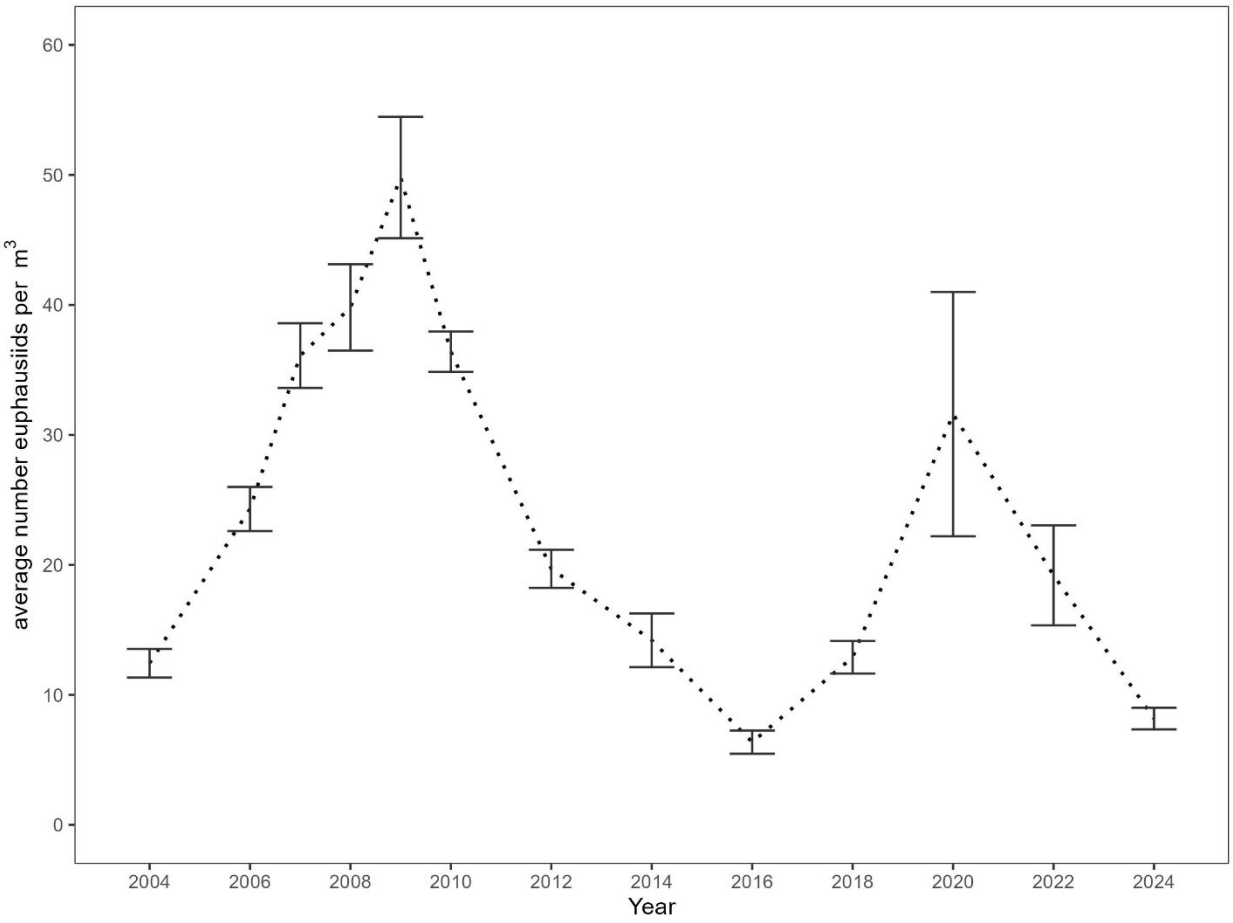

Figure 61: Acoustic estimate of average euphausiid abundance (no. m^3) from NOAA-AFSC EBS summer acoustic-trawl surveys. Error bars are approximate 95% confidence intervals computed from geostatistical estimates of sampling error (Petitgas, 1993).

Jellyfish

Jellyfish from Surface Trawl Surveys, 2004–2024

Contributed by Ellen Yasumiishi, Alex Andrews, Jim Murphy, and Andrew Dimond
Auke Bay Laboratories, Alaska Fisheries Science Center, NOAA Fisheries, Juneau, AK
Contact: ellen.yasumiishi@noaa.gov
Last updated: October 2024

Description of indicator: Annual indices of juvenile groundfish, juvenile salmon, forage fish, and jellyfish biomass (metric tonnes) and abundance (numbers) of juvenile sockeye salmon (*Oncorhynchus nerka*) in surface waters were estimated for the Alaska Fisheries Science Centers' (AFSC) Bering Arctic Subarctic Integrated Survey (BASIS). BASIS is an integrated fisheries oceanography survey in the south- and northeastern Bering Sea during late summer.

Pelagic fish and jellyfish were sampled using a trawl net towed in the upper 25 m. For the estimates of species abundance, the BASIS survey (373,404 km^2) was south to north from 54.54° to 59.50° and from -173.08° to -159.00° west to east for years 2002–2012, 2014, 2016, 2018, 2022, and 2024. The northern Bering Sea survey (197,868 km^2) was south to north from 59.97° to 65.50° and from -172.00° to -161.50° west to east for years 2003–2007, 2009–2019, 2021–2024. A trawl was towed for approximately 30 minutes. Area swept was estimated from horizontal net opening and distance towed.

Annual indices of relative densities were estimated using a single-species spatio-temporal model with the VAST package version 3.11.1, and R software version 4.3.1 (RTeam, 2023; Thorson et al., 2015; Thorson and Kristensen, 2016; Thorson, 2019*a*). We used the VAST package to reduce bias in density estimates due to spatially unbalanced sampling across years, while propagating uncertainty resulting from predicting density in unsampled areas. Spatial and spatio-temporal variation for both encounter probability and positive catch rate components were specified at a spatial resolution of 500 knots. We used a Poisson-link, or conventional, delta model and a gamma distribution to model positive catch rates and specified a bias-corrected estimate (Thorson et al., 2019). Parameter estimates were within the upper and lower bounds and final gradients were less than 0.0005. Julian day was added as a normalized covariate with a spatially constant and linear response due to changes in the timing of the survey among years.

Primary fish caught and included in the forage fish species aggregate are age-0 pollock (*Gadus chalcogrammus*), age-0 Pacific cod (*Gadus macrocephalus*), capelin (*Mallotus villosus*), Pacific herring (*Clupea pallasii*), juvenile Chinook (*O. tshawytscha*), sockeye (*O. nerka*), chum salmon (*O. keta*), pink (*O. gorbuscha*), and coho salmon (*O. kisutch*), rainbow smelt (*Osmerus mordax*), and saffron cod (*Eleginus gracilis*). Primary jellyfish taxa include *Chrysaora melanaster*, *Cyanea* sp., *Aequorea* sp., *Aurelia labiata*, *Phacellophora camtschatica*, and *Staurophora mertensii*. Unidentified or non-dominant jellyfish species were included in the total jellyfish catch. Jellyfish sampling began in 2004.

Status and trends: During 2024, the CPUE estimate of jellyfish in pelagic waters was high in the north, but low in the southeastern Bering Sea during late summer (Figure 62). Trends in jellyfish densities were similar in the north and south, except from 2012–2018. The higher levels of jellyfish densities in the south occurred during 2012, 2014, and 2016.

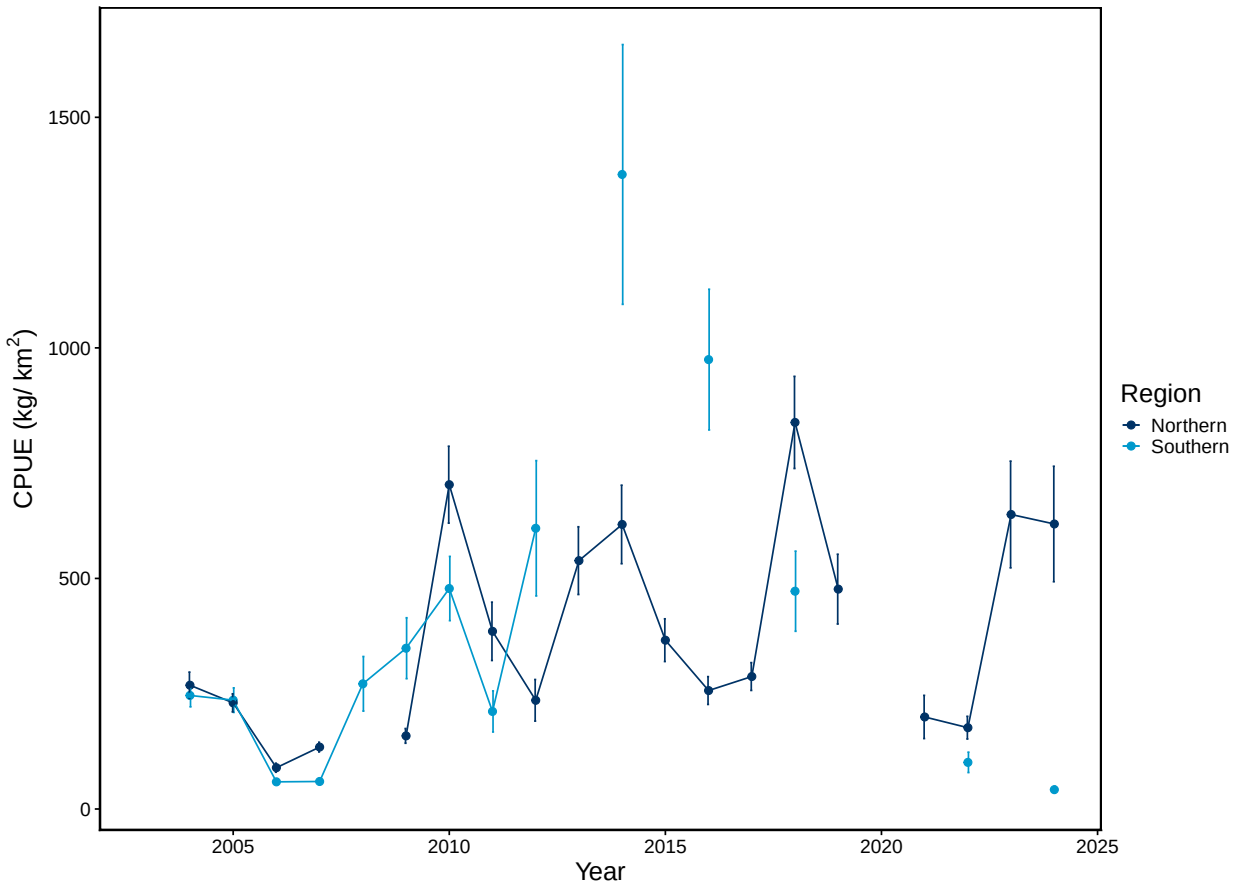

Figure 62: Estimated CPUE (kg/km^2) of jellyfish in surface waters surveyed in the eastern Bering Sea during late summer, 2004–2024.

Factors influencing observed trends: Jellyfish feed primarily on small fish and zooplankton, and jellyfish production tracks forage fish production and climate (Yasumiishi et al., 2023). CPUE estimates of jellyfish were relatively higher during warm years and lower during cool years in the south. Similarly, in the north, densities were higher during warm years and lower in cool years, except estimates were higher during the recent cool years of 2023 and 2024. In the south, lower forage fish CPUE estimates, such as age-0 pollock, during 2022–2024 may contribute to lower jellyfish production. However in 2023 and 2024, cool years, jellyfish estimates were high and forage fish estimates low in the north (Figure 3). In addition, the higher levels of jellyfish densities in the south in 2014 and 2016 corresponded with heat wave years and higher densities of age-0 pollock (Figure 71) and forage fish (Figure 2), prey items of jellyfish.

Implications: Jellyfish are competitors, predators, and act as shelters for forage fishes. During 2024, the higher densities of jellyfish in the north may indicate favorable environmental conditions for the growth and survival of jellyfish and other species, while the lower densities in the south may indicate less favorable conditions in the southeastern Bering Sea during late summer. Higher jellyfish densities may also not favor other species by increased competition for food and predation pressure.

Eastern Bering Sea – Jellyfishes

Contributed by Thaddaeus Buser and Sean Rohan
Resource Assessment and Conservation Engineering Division, Alaska Fisheries Science Center, NOAA Fisheries
Contact: thaddaeus.buser@noaa.gov
Last updated: September 2024

Description of indicator: The index of abundance time series for jellyfishes (Scyphozoa, but primarily *Chrysaora melanaster*) was updated for 2024 from the eastern Bering Sea shelf survey (Figures 63, 64).

Since 1982, the RACE Groundfish Assessment Program (GAP) and Shellfish Assessment Program (SAP) have conducted annual fishery-independent summer bottom trawl surveys on the EBS shelf using standardized trawl gear and methods. Biomass index trends from the survey are likely to reflect changes in the abundance of species and life history stages that are available to the survey, especially if trends are sustained over time.

Regional and stratum indices of abundance (biomass in kilotons) and confidence intervals were estimated for jellyfish by fitting a multivariate random effects model (REM) to stratum-level design-based abundance index time series calculated from GAP summer bottom trawl survey catch and effort data. The index was calculated for the entire standardized survey time series (1982–2024). The design-based index of abundance was calculated using the gapindex R package (Oyafuso, 2024) and REM were fitted to survey time series using the rema R package (Sullivan and Balstad, 2022). Code and data used to produce these indicators are provided in the esrindex R package and repository (Rohan, 2024).

Methodological Changes: see Eastern Bering Sea – Structural Epifauna (p. 78).

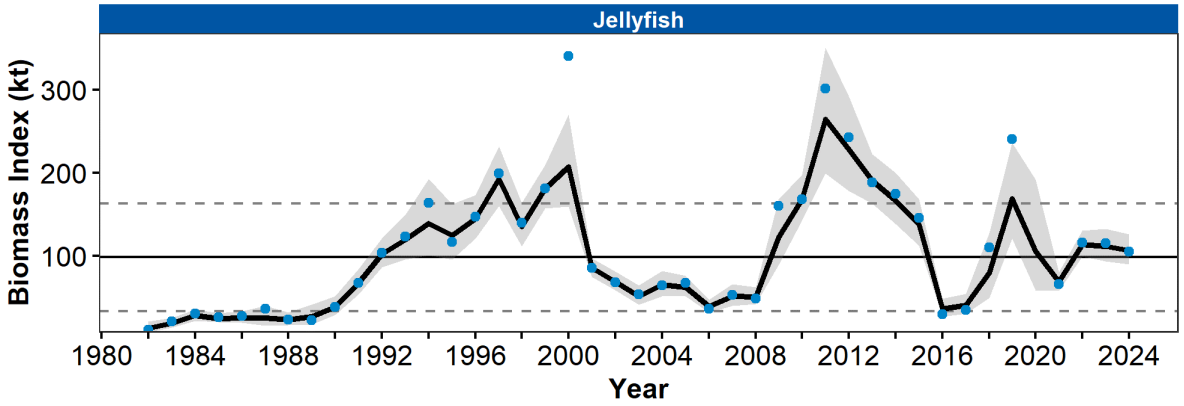

Figure 63: Biomass index of jellyfishes from RACE Groundfish Assessment Program and Shellfish Assessment Program summer bottom trawl surveys of the eastern Bering Sea continental shelf from 1982 to 2024 showing the observed survey biomass index mean (blue points), random effects model fitted mean (solid black line), 95% confidence interval (gray shading), overall time series mean (solid gray line), and horizontal dashed gray lines representing one standard deviation from the mean.

Status and trends: The abundance of jellyfishes in the eastern Bering Sea in 2024 was near the time series average and similar to estimates from 2022 and 2023 (Figure 63). There is an apparent pattern of cyclical rise and fall in jellyfish abundance throughout the time series. The relatively low abundance

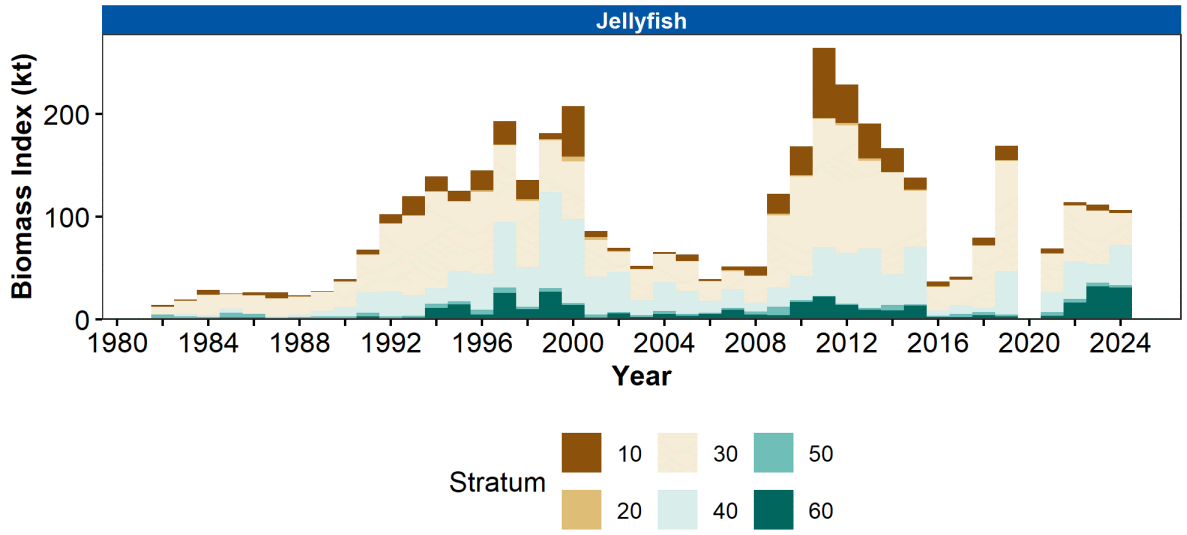

Figure 64: Biomass index of jellyfish in eastern Bering Sea survey strata (10-60) estimated from RACE Groundfish Assessment Program and Shellfish Assessment Program summer bottom trawl survey data from 1982 to 2024.

estimated from 1982 to 1988 was followed by a period of increasing biomass throughout the 1990s. A second period of relatively low biomass from 2001 to 2008 was followed by a period with relatively high abundance from 2009 to 2015. Jellyfish occur throughout the survey area, but their biomass is highest in strata 10 (southern inner shelf at bottom depth <50 m), 30 (southern middle shelf at 50-100 m), 40 (northern middle shelf at 50-100 m), and 60 (northern outer shelf at 100-200 m; Figure 64).

Factors influencing observed trends: Cyclic fluctuations in jellyfish abundance in the EBS are associated with jellyfish biomass during the preceding year and environmental and climatological factors, including the timing of sea ice retreat, sea surface temperature, wind mixing, and currents (Brodeur et al., 2008; Decker et al., 2023).

Implications: Jellyfishes are pelagic consumers of zooplankton, larval and juvenile fishes, and small forage fishes. At high levels of abundance, jellyfishes can limit fish productivity through competition for prey and predation on larval fish (Purcell and Arai, 2001)). ECOTRAN model suggests that the predominant jellyfish species in the EBS, *Chrysaora melanaster*, utilized 1% of consumer production over the middle shelf (51–100 m) during a period of high abundance (2009–2014; Ruzicka et al., 2020). This level of consumption corresponds with roughly a quarter of production required to support predominant forage fish in the EBS (age-0 walleye pollock, age-0 Pacific cod, Pacific herring, capelin; Ruzicka et al., 2020).

Research priorities: The bottom trawl survey uses standardized survey protocols aimed at ensuring consistent sampling efficiency. However, additional research is needed to better characterize the catchability and selectivity of jellyfish by the bottom trawl survey.

Ichthyoplankton

Abundance and Distribution of Larval Fishes in the Southeastern Bering Sea 2012–2024

Contributed by Lauren Rogers, Kelia Axler, Will Fennie, Laurel Nave-Powers, Brooke Snyder, and Nancy Roberson
Resource Assessment and Conservation Engineering Division, Alaska Fisheries Science Center, NOAA Fisheries
Contact: lauren.rogers@noaa.gov
Last updated: August 2024

Description of indicator: The southeastern Bering Sea (SEBS) shelf ichthyoplankton survey is conducted biannually in late spring (May) to assess the abundance and spatial distribution of early life stages of fishes. Ichthyoplankton (fish eggs and larvae) were sampled using a paired 60 cm bongo array with 505 μm mesh nets towed to 10 m off bottom or 300 m maximum depth. A Sea-Bird FastCat CTD was mounted above the bongo array to acquire gear depth, temperature, and salinity profiles. Larval fish abundance (number/10 m^2) for 2012–2018 was calculated from laboratory-processed and verified quantitative data on number of larvae, standardized by the volume of water filtered during a tow. For 2024, a Rapid Larval Assessment was conducted for five commercially-important taxa by sorting samples at sea, enabling provisional time-series updates in the year of collection. Mean larval abundance (number/10 m^2) was estimated using spatial-temporal generalized linear mixed models with the R package sdmTMB (Anderson et al., 2022). A Tweedie error distribution was used, and the mean larval abundance was calculated over the standardized survey area outlined in (Figure 65). Model-derived estimates of pollock egg abundance (2012–2018) are shown for context. Note, no survey occurred in 2020 or 2022.

Status and trends: Walleye pollock (*Gadus chalcogrammus*) were the most abundant larvae of the five taxa examined, and their estimated abundance increased from near the end of the last cold stanza (2012) through the warm stanza (2014, 2016, 2018), to a time-series maximum in 2024 (Figure 66). Pollock larvae were distributed throughout the area surveyed, and their highest abundance was consistently near the Pribilof Islands and the Alaska Peninsula (Figure 65). In contrast, the abundance of Pacific cod (*G. macrocephalus*) larvae was highest in 2012, yet declined and remained low through the following sampled years, with 2024 abundance being the lowest of the time series. Pacific cod larvae were concentrated in the northwest portion of the survey grid in 2012, all along the 100 m isobath in 2014, and patchily distributed near the Alaska Peninsula in more recent sampled years. Northern rock sole (*Lepidopsetta polyxystra*) larvae were most abundant in 2012 and 2014, and less abundant in subsequent years. These larvae were distributed similarly to pollock, often present at pollock hotspots, albeit at lower densities. Southern rock sole (*L. bilineata*) larvae were the least abundant of all the species examined, with notable catches only in 2014, clustered east of the Pribilof Islands. Rockfish (*Sebastes* spp.) larvae have been relatively stable in abundance, with relatively higher abundance in 2014 compared to the other years. They were present on the outer domain primarily in waters deeper than 100 m, and this pattern was consistent through time.

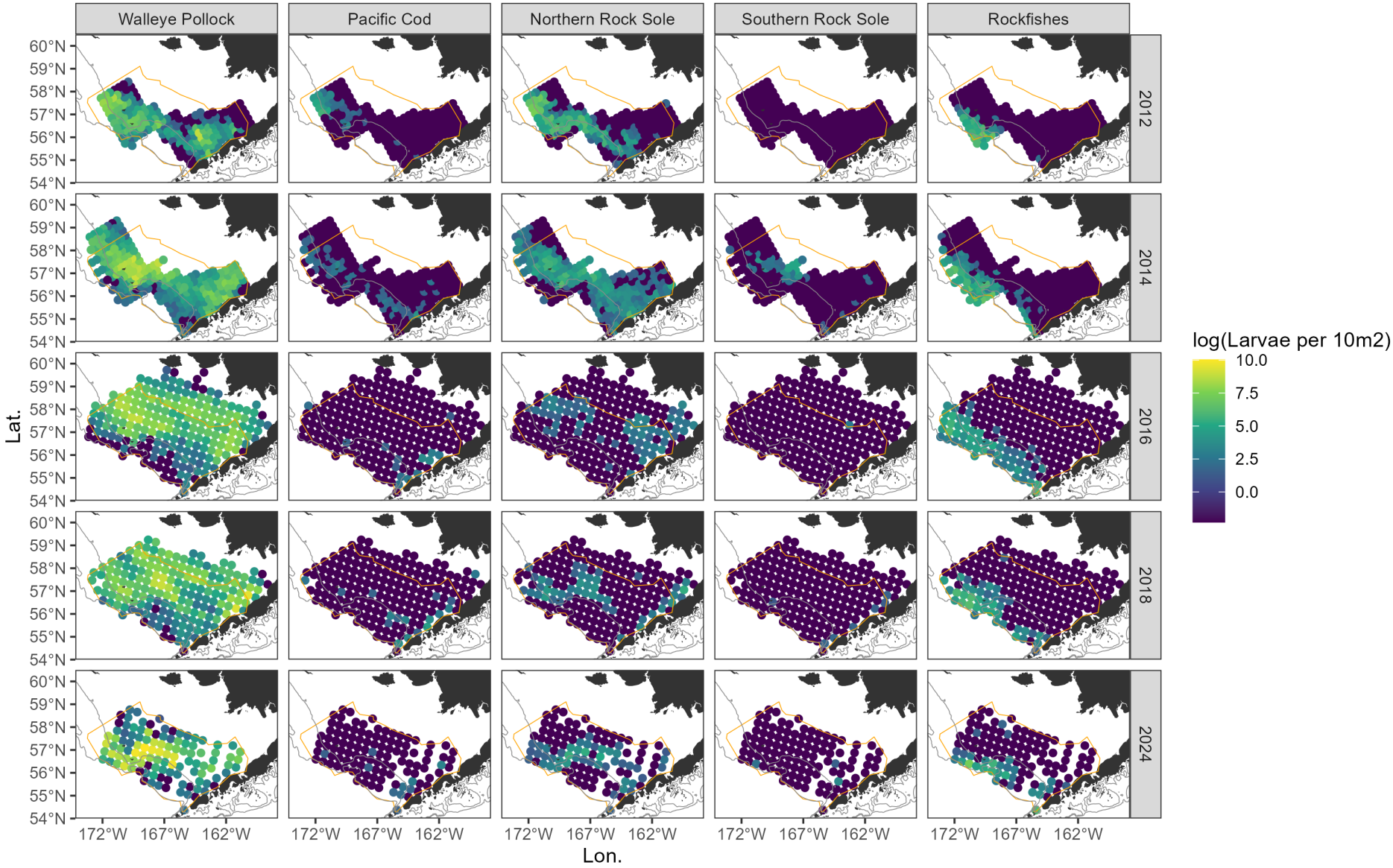

Figure 65: Distribution of larval catch per 10 m^2 in the SEBS for five taxa during spring ichthyoplankton surveys, 2012–2024. Gray lines show the 100 m and 200 m isobaths, and the standardized index area is outlined in orange. Data from 2024 are provisional pending laboratory processing.

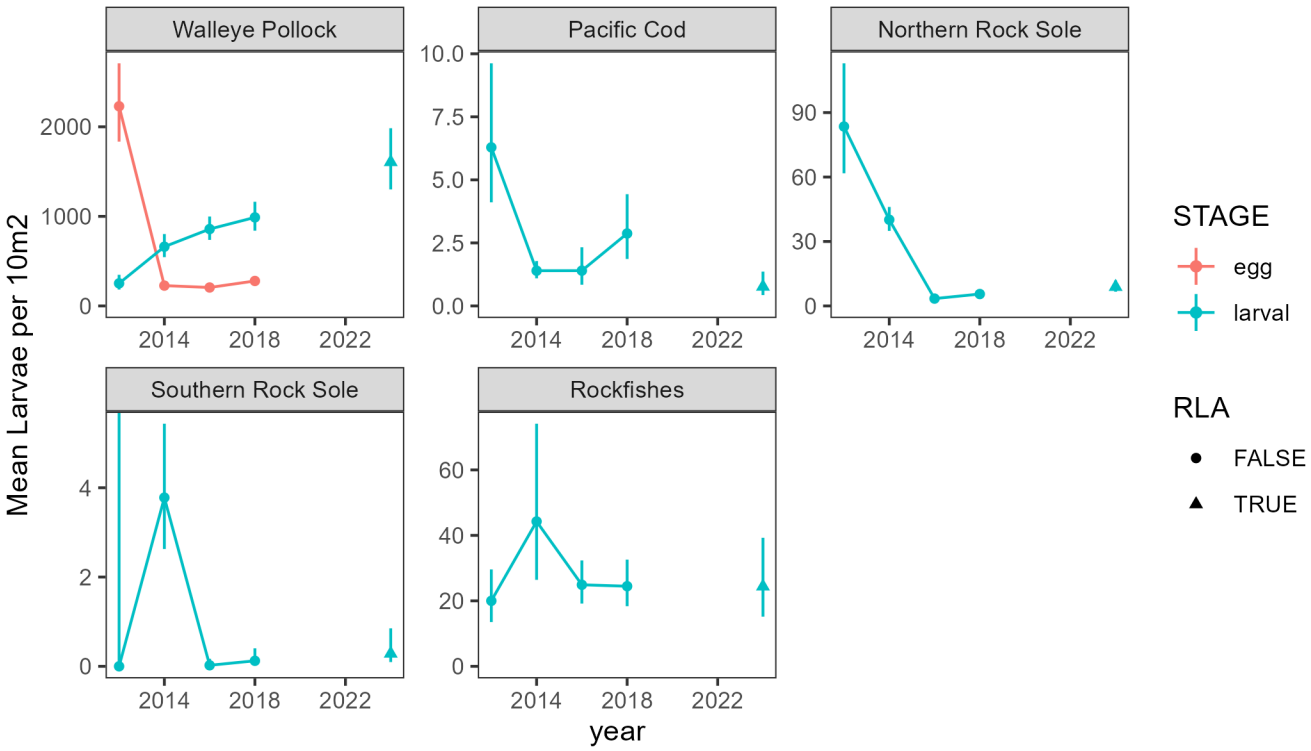

Figure 66: Estimates of mean larval (and egg) catch per 10 m^2 in the standardized area outlined in orange in Figure 65. Bars show 95% confidence intervals. In 2024, estimates were based on a Rapid Larval Assessment (RLA) conducted at sea and data are subject to revision upon laboratory processing.

Factors influencing observed trends: Interannual variation in ocean temperature in early spring can shift phenology of fishes and the timing of the spring phytoplankton bloom that is important for the production of zooplankton prey for fish larvae. This can lead to a temporal mismatch between fish larvae and their prey resulting in poor larval survival. In addition, temperature can affect the timing of spawning and rate of egg development, which can affect whether larvae are present in the study region during the survey. In 2012, larval pollock were relatively scarce, but eggs were abundant (Figure 66), indicating that hatching was relatively late during that cold year, at least partly explaining the low larval abundance in 2012. The abundance of Pacific cod and northern rock sole declined when conditions on the SEBS shelf changed from cold to warm. However, northern rock sole recruitment is typically higher in warmer years relative to cold years, a pattern which is linked to differential use of a northern nursery area (Cooper and Nichol, 2016), highlighting the importance of settlement processes for this stock. Southern rock sole is at the northernmost extent of its range in the Bering Sea and this may account for its low abundance.

Implications: Ichthyoplankton surveys can provide early-warning indicators for ecosystem conditions, spawning phenology, and recruitment patterns in marine fishes. In 2024, pollock larval abundance was high, Pacific cod abundance was relatively low, while abundance for the three other taxa was similar to 2018 and 2016. Ongoing research is focused on the importance of larval phenology, condition (see Porter et al., this report), geographic distribution, and overlap with zooplankton prey for eventual recruitment success.

Morphometric Condition of Walleye Pollock Larvae

Contributed by Steven Porter, Kelia Axler, Will Fennie, David Kimmel, Laurel Nave-Powers, Nancy Roberson, Lauren Rogers, and Brooke Snyder
Resource Assessment and Conservation Engineering Division, Alaska Fisheries Science Center, NOAA Fisheries
Contact: steve.porter@noaa.gov
Last updated: August 2024

Description of indicator: The morphometric condition of walleye pollock larvae in the southeastern Bering Sea (SEBS) was assessed using the ratio of the body depth at anus (BDA) to standard length (SL). The BDA:SL ratio, hereafter called Condition Ratio (CR), was used to show the spatial distribution of larval condition. The CR is based on the observation that for two fish larvae of similar size, the larva in poorer condition is "skinnier" (smaller BDA) than the larva in better condition (larger BDA), resulting in a smaller CR. For Atlantic cod (*Gadus morhua*) larvae, CR was sensitive to environmental surroundings, including prey abundance (Koslow et al., 1985). The CR for pollock larvae was calibrated using fed (good condition) and starved (poor condition) larvae reared in the laboratory at 3° and 6°C (n=263). The CR of larvae in good condition (mean=0.0635 $\pm$ 0.0088, SL=5.96-11.17 mm) was significantly larger than the ratio of larvae in poor condition (mean=0.0525 $\pm$ 0.0053, SL=4.89-6.15 mm; t-Test, $p<0.001$). The mean ratio for larvae in good condition was used to classify condition of Bering Sea larvae, with CRs $\geq$0.0635 indicating good condition and larvae in poor condition having smaller CRs. In May 2024, EcoFOCI conducted an ichthyoplankton survey in the SEBS. At each station, digital photographs were taken of up to 15 randomly selected pollock larvae collected from a 60 cm bongo net tow, and later measured using image analysis software. Mean ratio for larvae measured at a station was used to determine larval condition at that location.

Status and trends: Morphometric condition of pollock larvae (n=352) was assessed from 78 stations located across the SEBS. Larvae with the largest ratios were located in the southeast where the warmest temperatures in the upper 40 m of the water column occurred (depth range where a majority of pollock larvae are located, Smart et al. (2013); Figures 67, 68). Larvae in the western most area tended to have the smallest CRs corresponding with the coldest temperatures (Figures 67, 68). Larvae in poor condition occurred at six stations, and five of those stations were located in the western most area (Figure 67).

Factors influencing observed trends: Pollock larval condition and water temperature were correlated (r=0.73, $p<0.001$). Larvae tended to be in better condition (larger CR) in warmer areas, and this is consistent with previous observations that suggest relatively warm water temperatures in the Bering Sea are beneficial for larval pollock survival (Hunt et al., 2011). Most of the larvae with small CRs and the stations classified as poor larval condition were located in the west where the coldest temperatures occurred. Size of larvae tended to decrease from east to west across the survey area, those differences may be due pollock spawning later in the west, and slower larval growth in colder water. Pollock spawning in the Bering Sea begins near Bogoslof Island, progresses to near Unimak Island, and then to near the Pribilof Islands (Bacheler et al., 2010).

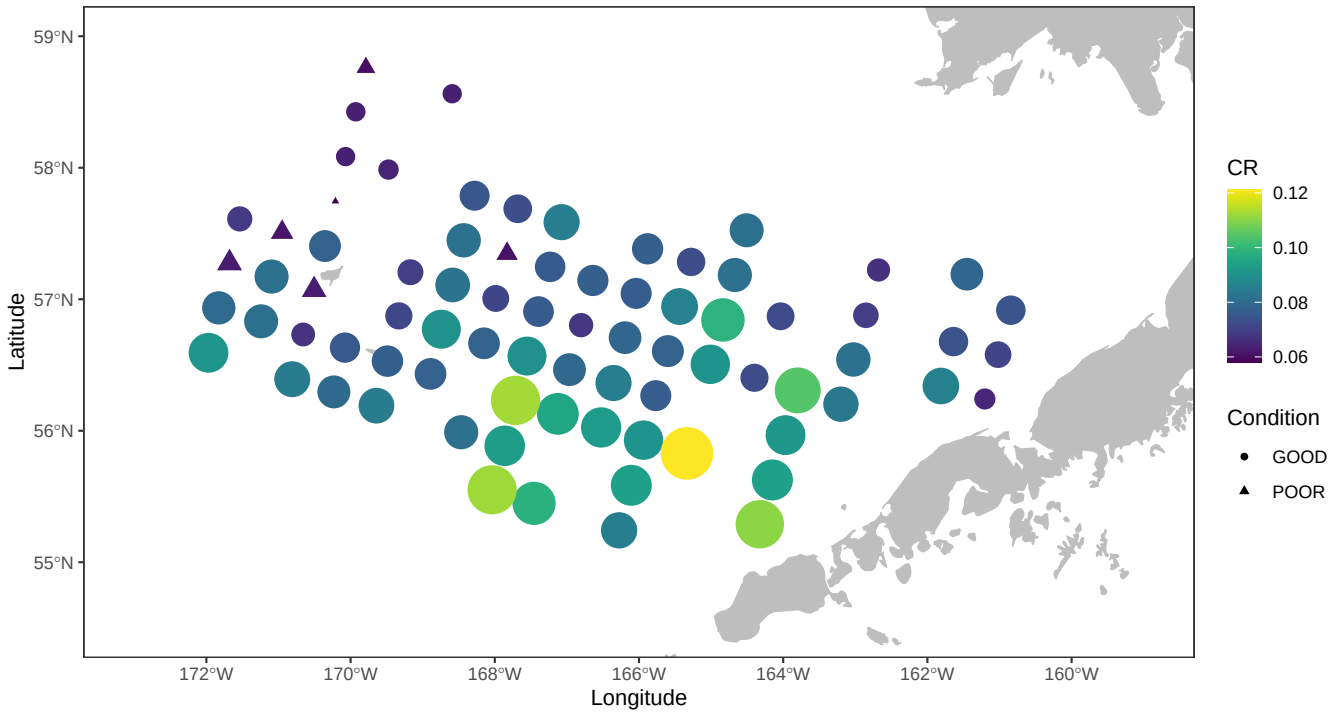

Figure 67: Mean condition ratio (CR) and location of pollock larvae in good or poor condition in the southeastern Bering Sea. Station mean CR was used to classify that location as having larvae in good or poor condition.

Implications: Larval condition may indicate the likelihood of survival to later life stages (Theilacker et al., 1996). Springtime environmental conditions were most favorable for pollock larvae in the southeastern area of the shelf as indicated by larvae having the largest CRs there. Relatively warm temperatures are beneficial for pollock larvae survival and growth (Hunt et al., 2011; Koenker et al., 2018). The southeast may have been a better feeding environment for larvae because of a greater abundance of copepod nauplii prey due to faster reproduction rates of smaller-sized copepods in warm water assuming prey are not food limited (Huntley and Lopez, 1992). Environmental conditions in the western most area (coldest temperatures) were less favorable for larvae as nearly all of the larvae in poor condition occurred there and larvae had smaller CRs than other areas surveyed. Cold temperatures are associated with slower growth of pollock larvae and decreased survival (Koenker et al., 2018). Mean SL at three of the five western most stations where larvae in poor condition occurred showed early feeding-stage pollock larvae (<6.5 mm SL) there, and larvae of that size are more vulnerable to starvation than larger, later stage larvae (Theilacker et al., 1996). Nauplii prey may be less abundant in the west due to cold temperatures slowing copepod growth and development rates (Gillooly, 2000; Hirst and Bunker, 2003), this would negatively affect larval feeding and cause larvae to be in poorer condition.

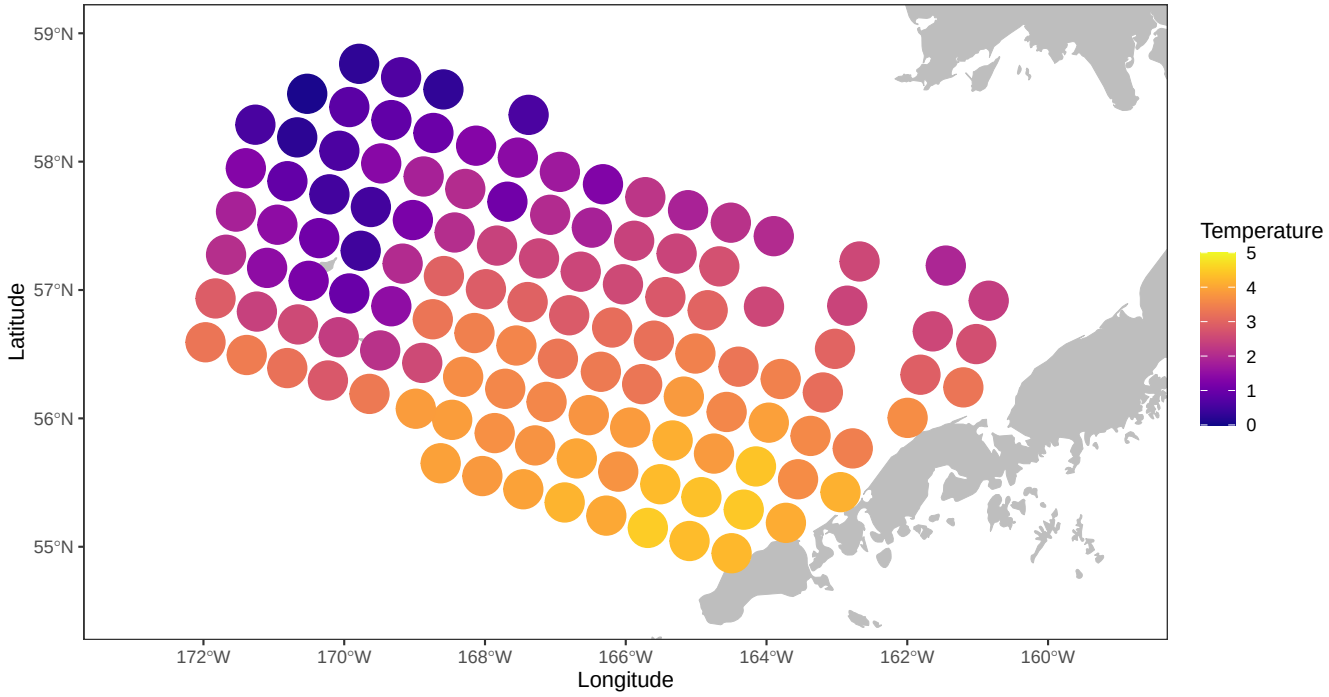

Figure 68: Mean water temperature in the upper 40 m of the water column in the southeastern Bering Sea. That depth range is where a majority of pollock larvae are located (Smart et al., 2013).

Forage Fish

Forage Fish Dynamics in the Eastern Bering Sea

Forage fish, such as age-0 pollock, capelin, and herring, are a critical trophic link in the Bering Sea ecosystem. Exploring quantitative linkages among ecosystem drivers and forage fish biomass illustrates how environmental changes might affect the availability of different forage fish species. Here, we use dynamic structural equation modeling (DSEM) to identify emergent trends in forage fish dynamics.

First, to understand ecosystem structure and function, a simplified conceptual model was developed (not shown), representing physical, zooplankton, and forage variables as boxes and interactions as arrows. This "box-and-arrow" conceptual model is used in qualitative network models (QNM; Levins, 1974) to summarize the relationships among multiple variables (represented as boxes) that are linked by hypothesized mechanisms (represented as arrows), where mechanisms are specified as a positive or negative impact. QNMs have been successfully used at the Alaska Fisheries Science Center to identify likely consequences of hypothetical ecosystem changes (Reum et al., 2020, 2021), and can incorporate stakeholder input regarding relevant variables and interactions. In this example, we did not elicit structured stakeholder input about whether interactions are positive or negative; future research could incorporate this information as Bayesian priors to fully bridge from a QNM to the DSEM.

Extending QNMs, we develop a time-series model that includes ecosystem indicators (time-series variables shown as icons or boxes) and hypothesized linkages (path coefficients shown as arrows), where the sign and strength of a path coefficient can either be specified *a priori* (i.e., specifying that a 10% increase in a predator drives a 10% decrease in per-capita production for a prey species) or estimated from available time-series data. This approach - dynamic structural equation modeling (DSEM) - has been demonstrated via application to recruitment modeling for walleye pollock (among other uses) (Thorson et al., 2024). DSEM can accommodate a combination of lagged and simultaneous impacts of any variable on any other variable and jointly estimates the strength of impacts (termed "path coefficients").

Additionally, DSEM can estimate missing values within indicator time series, thereby accommodating biennial survey structures, for example. DSEM also addresses potential correlations and complementarity (i.e., trade-offs) among indicators.

In this species-specific application of DSEM, the structure is based upon the following design choices:

1. We include the physical variable of sea ice ("Sea.Ice.Extent") and assume greater sea ice extent results in a lower proportion of open-water-associated phytoplankton blooms ("Bloom.Type") and greater proportion of early, ice-associated blooms (Eisner et al., 2016; Sigler et al., 2014; Hunt et al., 2011; Hare et al., 2007).
2. Whether the phytoplankton bloom is associated with open water (higher "Bloom.Type" values) or sea ice (lower "Bloom.Type" values) is hypothesized to cause changes in pelagic secondary producers (e.g., summer euphausiids ["Euphausiids"] and fall zooplankton ["Small.Copepods" and "Large.Copepods"]), with a higher proportion of ice-associated blooms thought to result in higher abundance of pelagic secondary producers in the summer and fall (Kimmel et al., 2018; Coyle et al., 2008).
3. We include both BASIS and 70 m isobath surveys as separate measures of fall densities for small and large copepods. Small, lipid-poor species of copepods are a relatively poor prey resource

for forage fish, while large-bodied, lipid-rich copepods and euphausiids are characteristic of fish diets during years of enhanced fish abundance of all three fishes evaluated, as well as enhanced body condition in YOY pollock (Andrews III et al., 2016; Heintz et al., 2013). We initially explored estimating latent variables for small and large copepods, with both surveys as independent measurements. However, this structure was numerically unstable, so we instead treat BASIS as the primary measure of fall copepod densities and used the 70 m isobath as a correlated measurement to inform missing values (e.g., in 2000 when data from the 70 m isobath survey was available but BASIS data was not).

4. Euphausiids are assumed to drive changes in forage fishes including herring ("Herring"), capelin ("Capelin"), and juvenile gadids, including "Age.0.Pollock" (Andrews III et al., 2016; Heintz et al., 2013) and "Age.1.Pollock" as estimated in the pollock stock assessment in the following year.

We fitted this model by testing a potential link from every zooplankton (small copepods, large copepods, and euphausiids) to every forage species tested (herring, capelin, age-0 pollock, and age-1 pollock with a one-year lag). This included 12 potential path coefficients, and we did a factorial test of including or excluding each path coefficient, which involved fitting 2^{12}=4096 models. We then used marginal AIC to select the most parsimonious model presented here. Future research could reevaluate this approach and could explore AIC-weighted model ensembles to better represent model-selection uncertainty.

The most parsimonious model (Figure 69) estimated some linkage strengths that were in line with prior expectations. For example, increased sea ice extent drives a decrease in the proportion of open water blooms, as predicted by other studies (Eisner et al., 2016; Sigler et al., 2014; Hunt et al., 2011; Hare et al., 2007). Open water blooms, in turn, are positively associated with small copepods and negatively associated with large copepods and euphausiids, also in agreement with the literature (Kimmel et al., 2018; Hunt et al., 2011; Coyle et al., 2008). Large copepods were more responsive than euphausiids to open-water blooms (i.e., had a stronger relationship), such that the ratio of euphausiids to large copepods is higher in warm than cold years. In agreement with previous studies, the model found significant impacts of euphausiid density on herring abundance. Euphausiid contribution to herring diets has been shown to fluctuate with changing ocean temperatures, which also appears as a positive effect in our model results (Andrews III et al., 2016). Finally, the model estimated that small copepods are positively associated with herring. This supports the overall expectation that warm years (with low sea ice extent) have more open-water blooms, more small copepods, and more herring.

Several of the model results were contrary to expectations, however, most notably the lack of an effect of large copepods on age-0 pollock and capelin dynamics. Much work has connected consumption of large copepods with better body condition and overwinter survival for age-0 pollock, so much so that the linkages have been coined the "Oscillating Control Hypothesis" (Hunt et al., 2011; Heintz et al., 2013; Siddon et al., 2013; Buckley et al., 2016). Similarly, capelin abundance has been found to vary significantly between warm and cool periods, with higher abundance and a larger proportion of large copepods in their diets in cold years (Andrews III et al., 2016). The estimated negative effect of euphausiids on age-0 pollock was also unexpected. Euphausiids are a major component of the diets of age-0 pollock in cold years (Andrews III et al., 2016; Buckley et al., 2016), but the most parsimonious model estimated a negative response of age-0 pollock abundance to euphausiids.

We conclude that DSEM provides an avenue to combine a conceptual model for ecosystem function with time-series indicators that are compiled in the ESRs, while compensating for (and interpolating) missing data. Building from an original application to Report Card indicators in the 2023 EBS ESR (Thorson and Siddon, 2023), this species-specific example provides a high-level and transparent synthesis

of environmental drivers of forage fish. The DSEM framework can be applied in fisheries management for several purposes:

1. It provides a quantitative way to synthesize sets of linear interactions between ecosystem components, including lagged interactions, even when covariates are collinear. This is relevant for ESRs because many environmental processes are correlated with each other (e.g., sea ice and cold pool extent) and likely to drive the dynamics of higher trophic levels at multiple scales.

2. It provides a way to interpolate missing values while accounting for ecological relationships among variables (Figure 70). For example, large and small copepod density estimated by DSEM is relatively precise (has smaller confidence intervals) in 2000, despite there being no BASIS data in that year, due to the estimated correlation between the zooplankton densities from BASIS and those from the 70 m isobath survey, which is available in that year. Using a more frequent survey (i.e., the 70 m isobath transect) to interpolate a correlated but higher-quality survey (i.e., the BASIS survey, which has greater spatial coverage) could provide information about zooplankton densities when data are sparse, based on shared drivers. This could be particularly useful when survey frequency is reduced, although higher quality data will improve the reliability of these predictions.

3. It provides a formal process to elicit expertise and input from scientists, stakeholders, and local and traditional knowledge holders about which ecological variables are interacting, as well as the sign and strength of these interactions (arrows in Figure 69). This input can be used to create Bayesian priors as well as identify potential linkages (which path coefficients to include during model selection). This information could also be incorporated into the forage fish SAFE report to help inform fishery management decisions.

4. It allows scientists to communicate "expected" relationships between multiple ecosystem variables. This allows us to identify situations where ecosystem conditions are different from expectations. If fishery managers are interested, we could develop a time-series of how "unexpected" each variable is relative to the DSEM (i.e., using statistical residuals to define "unexpected" values), and provide this time series as a future ESR indicator. This would involve calculating the "leave-one-out" or "one-step-ahead" residual for an observation given other (or past) observations and model predictions, where the statistical residual is then an indicator of how a given measurement differs from its expected value given estimated ecological interactions.

Contributed by
James T. Thorson[1], Margaret Siple[1], Jens Nielsen[1,2], Jonathan Reum[1], Elizabeth Siddon[3], and Johanna Page[3]

[1]NOAA Fisheries, Alaska Fisheries Science Center, Seattle, WA
[2]Cooperative Institute for Climate, Ocean, and Ecosystem Studies (CICOES), University of Washington, Seattle, WA
[3]NOAA Fisheries, Alaska Fisheries Science Center, Juneau, AK

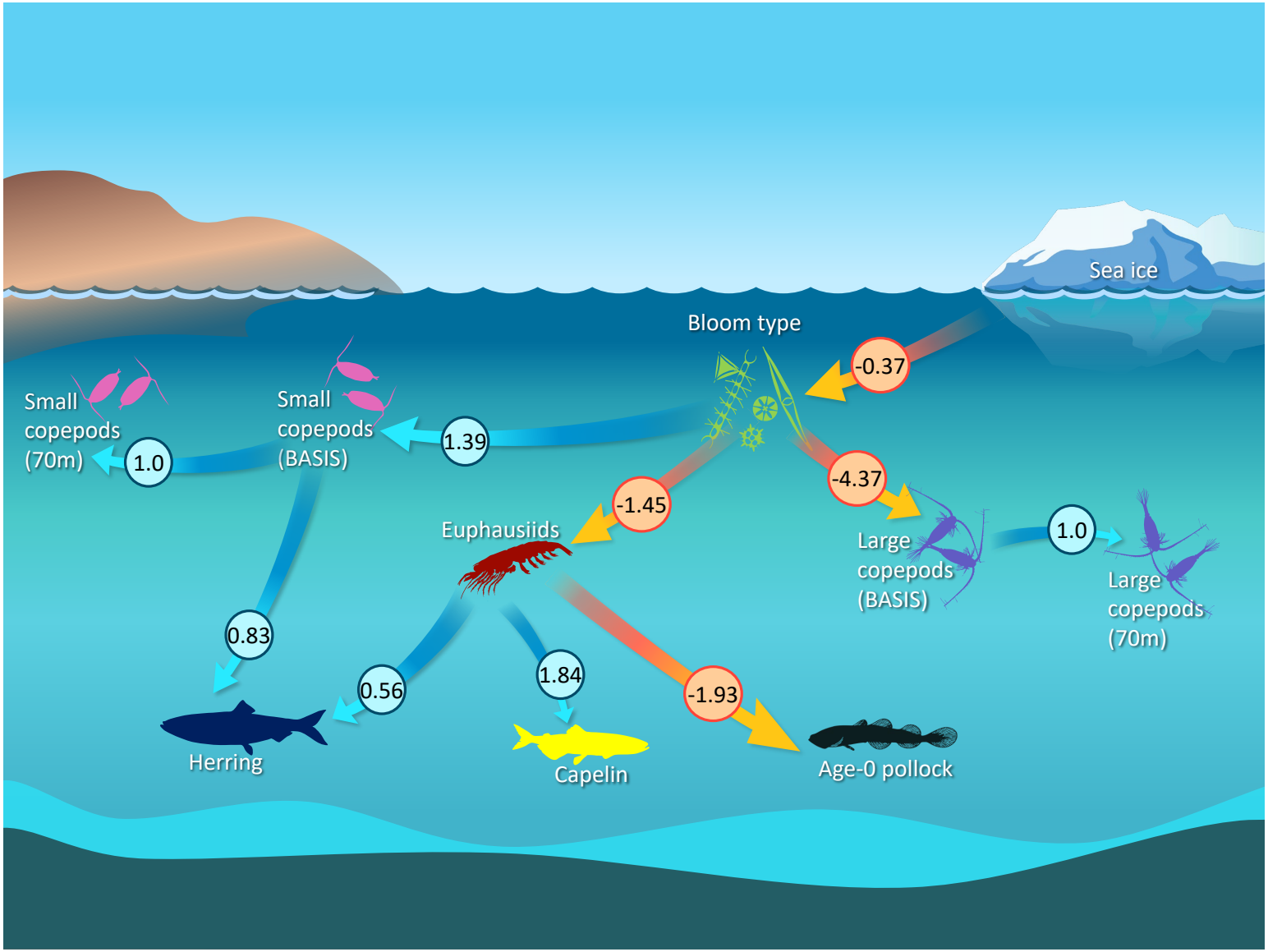

Figure 69: A path diagram showing estimated quantitative linkages among ecosystem variables. Arrows correspond to hypothesized relationships, where an arrow pointing from X to Y indicates that a change in X is estimated to cause a change in Y. The number listed in each arrow shows the estimated path coefficient, where e.g., the value of 0.83 from small copepods to herring indicates that a 10% increase in small copepod biomass is associated with a 8.3% increase in herring. We performed backwards model selection using marginal AIC, and all listed coefficients are statistically significant. We also estimated additional first-order autocorrelation for each variable.

Data sources
* indicates the data source is also a Report Card indicator, with further details available on p. 261.

Sea Ice Extent: The Bering Sea ice year is defined as 1 August–31 July. Bering Sea ice extent data are from the National Snow and Ice Center's Sea Ice Index, version 3 (Fetterer et al., 2017), and use the Sea Ice Index definition of the Bering Sea, effectively south of the line from Cape Prince of Wales to East Cape, Russia (i.e., this index includes ice extent in both the western and eastern Bering Sea). The daily mean annual ice extent integrates the full ice season into a single value. Data courtesy of Rick Thoman, *rthoman@alaska.edu*

***Proportion of Open Water Blooms:** The timing of ice retreat and bloom peak was used to estimate bloom type over the southeastern Bering Sea shelf ($<$60°N). Bloom type differentiates between open-water blooms (i.e., ice retreat occurred $\geq$21 days prior to bloom peak) and ice-associated blooms (i.e., ice retreat occurred $<$21 days prior to bloom peak) for each year (Perrette et al., 2011). Timing of sea-ice retreat was determined as the date when ice coverage remained below 15% based on the 15-day running mean of the daily sea-ice fraction data. Bloom peak timing was estimated using standardized merged ocean color satellite data of 8-day satellite chlorophyll-a (chl-a, μg/L) at a 4 km-resolution from The Hermes GlobColour website covering the years 1998–2024. Data courtesy of Jens Nielsen, *Jens.Nielsen@noaa.gov*

Small Copepods from BASIS: Small copepods (*Acartia* spp., *Pseudocalanus* spp., and *Oithona* spp.) were quantified from 153 μm mesh, 20 cm bongo net samples taken during the fall (Aug/Sept) BASIS surface trawl survey over the southern Bering Sea shelf. Data courtesy of David Kimmel, *David.Kimmel@noaa.gov*

Small Copepods from Fall Mooring 70 m isobath: Small copepods were quantified from 153 μm mesh, 20 cm bongo net samples taken during the fall (Aug/Sept) 70 m isobath survey over the southern Bering Sea shelf. Data courtesy of David Kimmel, *David.Kimmel@noaa.gov*

Large Copepods from BASIS: Large copepods (predominantly *Calanus* spp.) were quantified from 505 μm mesh, 60 cm bongo net samples taken during the fall (Aug/Sept) BASIS surface trawl survey over the southeastern Bering Sea shelf. Data courtesy of David Kimmel, *David.Kimmel@noaa.gov*

***Large Copepods from Fall 70 m isobath:** Large copepods (predominantly *Calanus* spp.) were quantified from 505 μm mesh, 60 cm bongo net samples taken during the fall (Aug/Sept) 70 m isobath survey over the southeastern Bering Sea shelf. Data courtesy of David Kimmel, *David.Kimmel@noaa.gov*

***Euphausiids:** An estimate of euphausiid biomass was determined by acoustic backscatter and midwater trawl data collected during biennial pollock surveys. Data courtesy of Mike Levine, *Mike.Levine@noaa.gov*

Capelin: Fish were sampled using a surface trawl net towed in the upper 25 m during the fall (Aug/Sept) BASIS survey in the southeastern Bering Sea. Annual indices of relative biomass were estimated using a single-species spatio-temporal model with the VAST package version 3.10.1. Data courtesy of Ellen Yasumiishi, *Ellen.Yasumiishi@noaa.gov*

Herring: see methods for capelin above. Data courtesy of Ellen Yasumiishi, *Ellen.Yasumiishi@noaa.gov*

Age-0 pollock: see methods for capelin above. Data courtesy of Ellen Yasumiishi, *Ellen.Yasumiishi@noaa.gov*

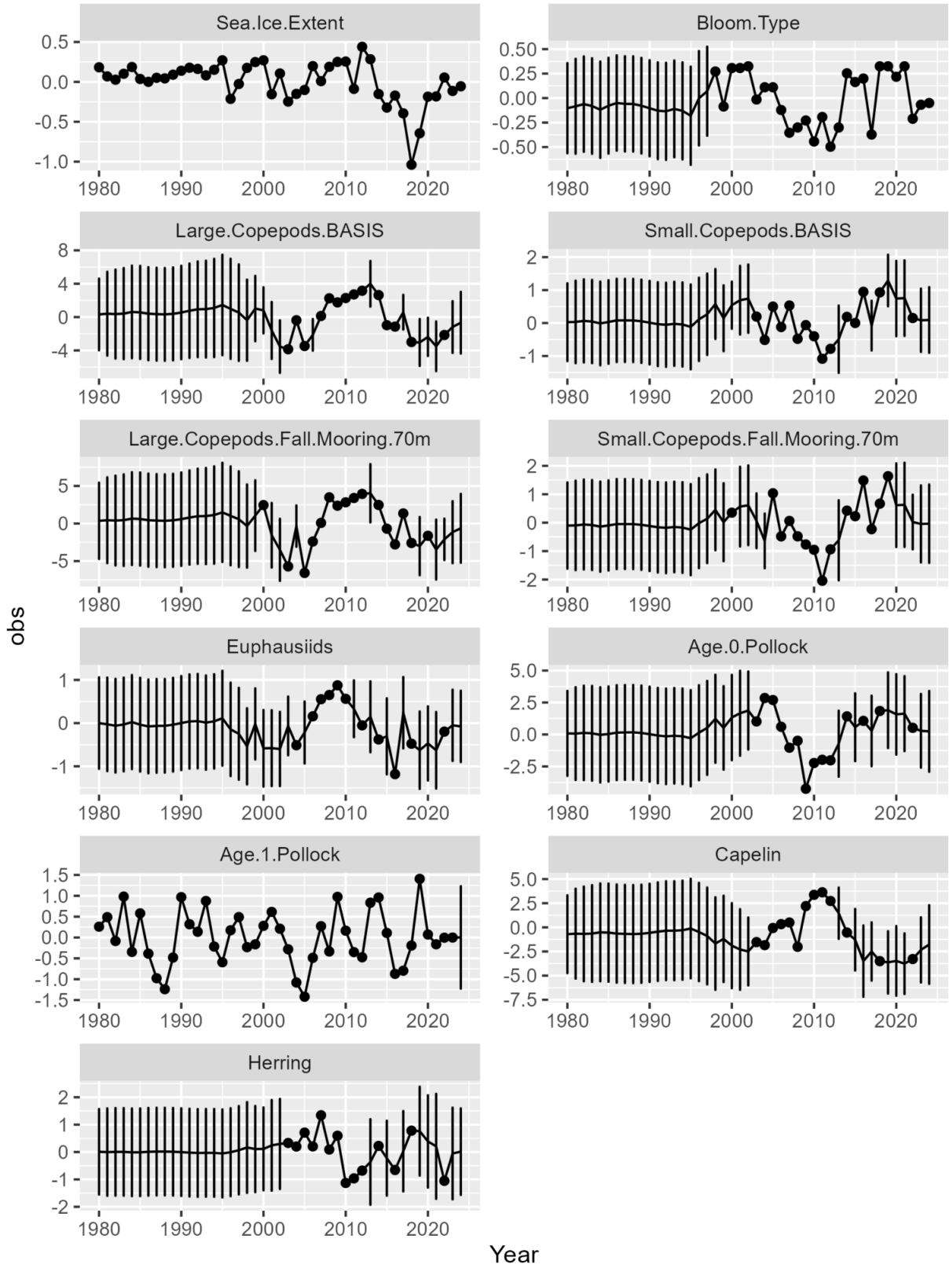

Figure 70: Values from a 24-year time series showing observed (black dot) and estimated (black line with 95% confidence interval as vertical bars) value for each ecosystem variable included in the Dynamic Structural Equation Model. Note that the model is specified to exactly fit observations, such that estimates (lines) are equal to observations (dots) when observations are available in a given year. See detailed list of data sources below.

Catch Estimates of Age-0 Walleye Pollock from Surface Trawl Surveys, 2003–2024

Contributed by Alex Andrews[1], Ellen Yasumiishi[1], Adam Spear[2], Jim Murphy[1], and Andrew Dimond[1]
[1]Auke Bay Laboratories, Alaska Fisheries Science Center, NOAA Fisheries
[2]Resource Assessment and Conservation Engineering Division, Alaska Fisheries Science Center, NOAA Fisheries
Contact: alex.andrews@noaa.gov
Last updated: October 2024

Description of indicator: See p. 105.

Status and trends: The 2024 age-0 pollock CPUE estimates (kg/km^2) in the SEBS and NBS regions were lower than estimates from the recent warm period (2014–2021), and were slightly higher than estimates from the cold period (2007–2013; Figure 71). Higher estimates appear to be related to warm periods with reduced cold pool extents. In the NBS, CPUE estimates increased in 2014, 2015, and 2018 (three warm years; Figure 72), but have otherwise remained low compared to the SEBS.

Factors influencing observed trends: Changes in climate-mediated oceanographic conditions, such as water column temperatures, may influence the vertical and spatial distribution of age-0 pollock and therefore the resulting surface trawl catches. Results from water column trawls (i.e. oblique trawls; not shown) demonstrated that age-0 pollock densities were higher in representative warm years (2014, 2016) than in cold years (2011, 2012), and age-0 pollock were found closer to the surface in warm years (see p. 124). However, warm periods with increased age-0 pollock biomass do not always correlate with strong recruitment, which is likely a result of the lack of high quality prey during warm years (Heintz et al., 2013).

Implications: Consistent with historical estimates during average to cold ocean conditions, the CPUE estimates of age-0 walleye pollock in the NBS remained relatively low during 2024. A large increase in estimates of age-0 pollock in the NBS relative to the SEBS region would reflect northward movement of adult spawning aggregations or improved juvenile habitat in the NBS. Monitoring changes in CPUE estimates along with vertical distribution provides a better understanding of overall biomass and spatial distribution of age-0 pollock in the EBS. Age-0 pollock are part of the forage fish group and are a major source of prey for upper trophic level guilds including fish, birds, and mammals.

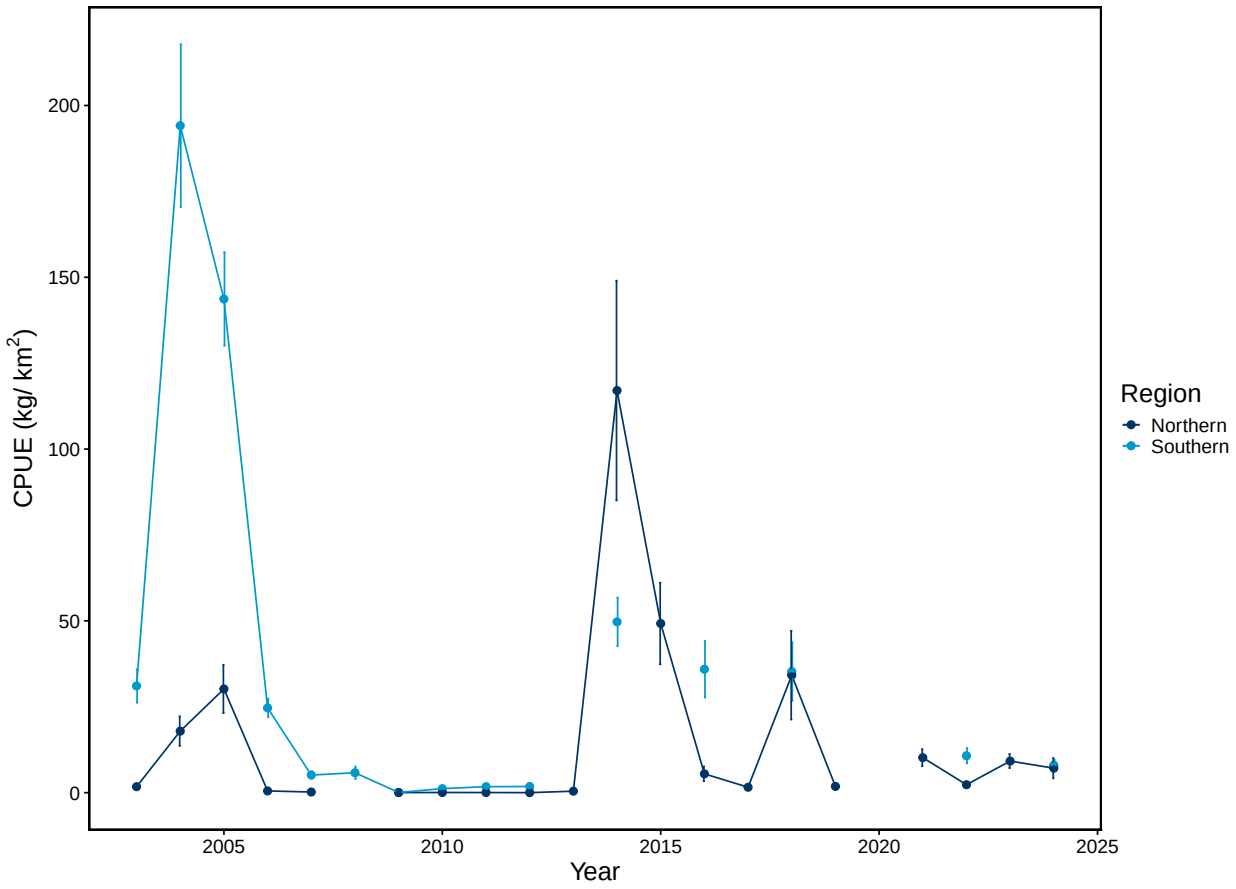

Figure 71: Estimated CPUE (kg/km^2) of age-0 pollock in surface waters surveyed in the eastern Bering Sea during late summer, 2003–2024.

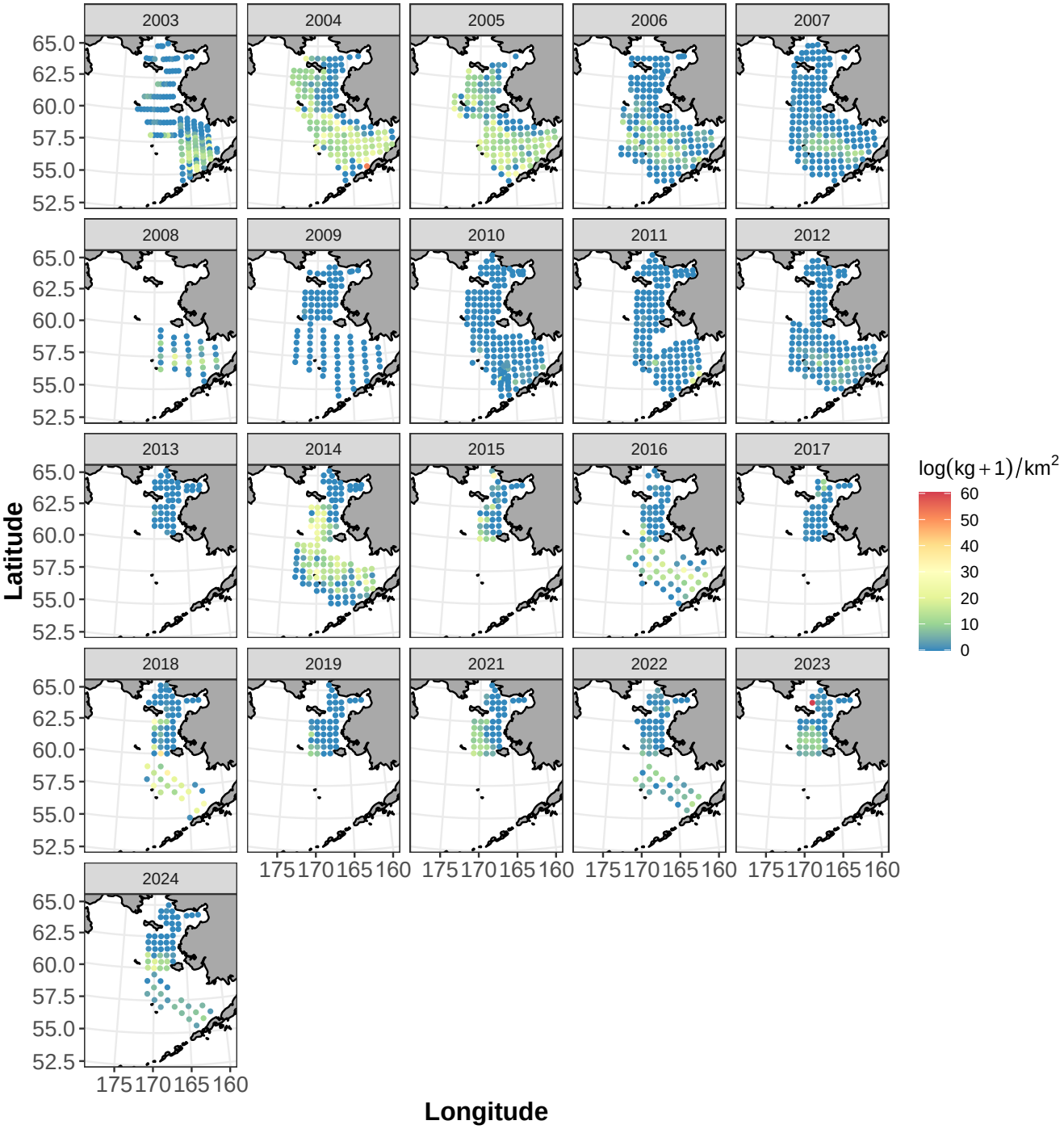

Figure 72: Maps illustrating the spatial distribution of age-0 pollock CPUE estimates [log(kg + 1)/km^2] in surface waters surveyed in the eastern Bering Sea during late summer, 2003–2024.

Vertical Distribution of Age-0 Pollock in the Southeastern Bering Sea

Contributed by Adam Spear[1] and Alexander G. Andrews III[2]
[1]Resource Assessment and Conservation Engineering Division, Alaska Fisheries Science Center, NOAA Fisheries
[2]Auke Bay Laboratories, Alaska Fisheries Science Center, NOAA Fisheries
Contact: adam.spear@noaa.gov
Last updated: October 2024

Description of indicator: Vertical distribution of age-0 pollock was estimated through the calculation of an abundance-weighted mean depth during two cold years (2011, 2012) and two warm years (2014, 2016). The abundance of age-0 walleye pollock in the southeastern Bering Sea was estimated using acoustic-trawl methods. The process involved assigning trawl-catch data to acoustic-backscatter data that was measured along the transect line. The trawl catch information was manually assigned to backscatter from a single surface, oblique, or midwater-trawl depending on proximity, tow depth, and backscatter characteristics. Scrutinized backscatter was echo-integrated into 0.5 nautical mile (nmi) by 5 m bins, and output as nautical area scattering coefficient, m^2/nmi^2 (NASC). The species-specific compositions from each catch were used to convert NASC to species-specific abundance (individuals/nmi^2) using published measurements of the acoustic properties of these species. The middle domain (50 to 100 m isobath; Coachman, 1986) was the most consistent region surveyed across all years. Thus, to account for survey bias, values were constrained to those sampled over the middle domain. Age-0 pollock abundance was summed over each depth bin to calculate the weighted mean depth. Here, we show yearly abundance-weighted mean depths during the late summer over the southeastern Bering Sea middle domain.

Status and trends: Age-0 pollock were deeper in the water column in 2011 (~37 m) and 2012 (37 m; cold years), and closer to the surface in 2014 (~32 m; warm year) by 10 and 5 meters, respectively. The trend was less apparent in 2016 (warm year) with a weighted mean depth of 39 m, which was similar to colder years. In 2022 (average temperatures), the weighted mean depth was 38 m, which was also similar to colder years. The trend was less apparent in 2024 (cold year) with a weighted mean depth was 33 m, which was more comparable to a warm year (Figure 73).

Factors influencing observed trends: From the six data points, 2011, 2012, and 2024 represent three anomalously colder years, while 2014 and 2016 represented two warmer years, and 2022 represented an average year in the southeastern Bering Sea. These two oceanographic temperature phases resulted in a change in the vertical distribution of age-0 pollock (Spear et al., 2023). Energy densities of age-0 pollock collected in trawls from these surveys showed that pollock collected in cold years had higher energy densities than those collected in warm years, suggesting improved feeding and provisioning conditions at depth in colder-than-average thermal conditions. Colder years have greater abundances of larger lipid-rich prey which result in higher dietary percentages of lipid and energy densities of age-0 pollock (Coyle et al., 2011; Heintz et al., 2013; Kimmel et al., 2018). This is partially explained by larger lipid-rich prey vertically migrating deeper in the water column during the day. Deeper age-0 pollock in 2016 is likely attributed to extreme surface temperatures that reached >15°C in the southeastern Bering Sea (Stabeno et al., 2017), which is within the range where they exhibit thermal stress (Laurel et al., 2016). Shallower age-0 pollock in 2024 is likely the result of shorter lengths and ontogeny playing a much larger role compared to previous years.

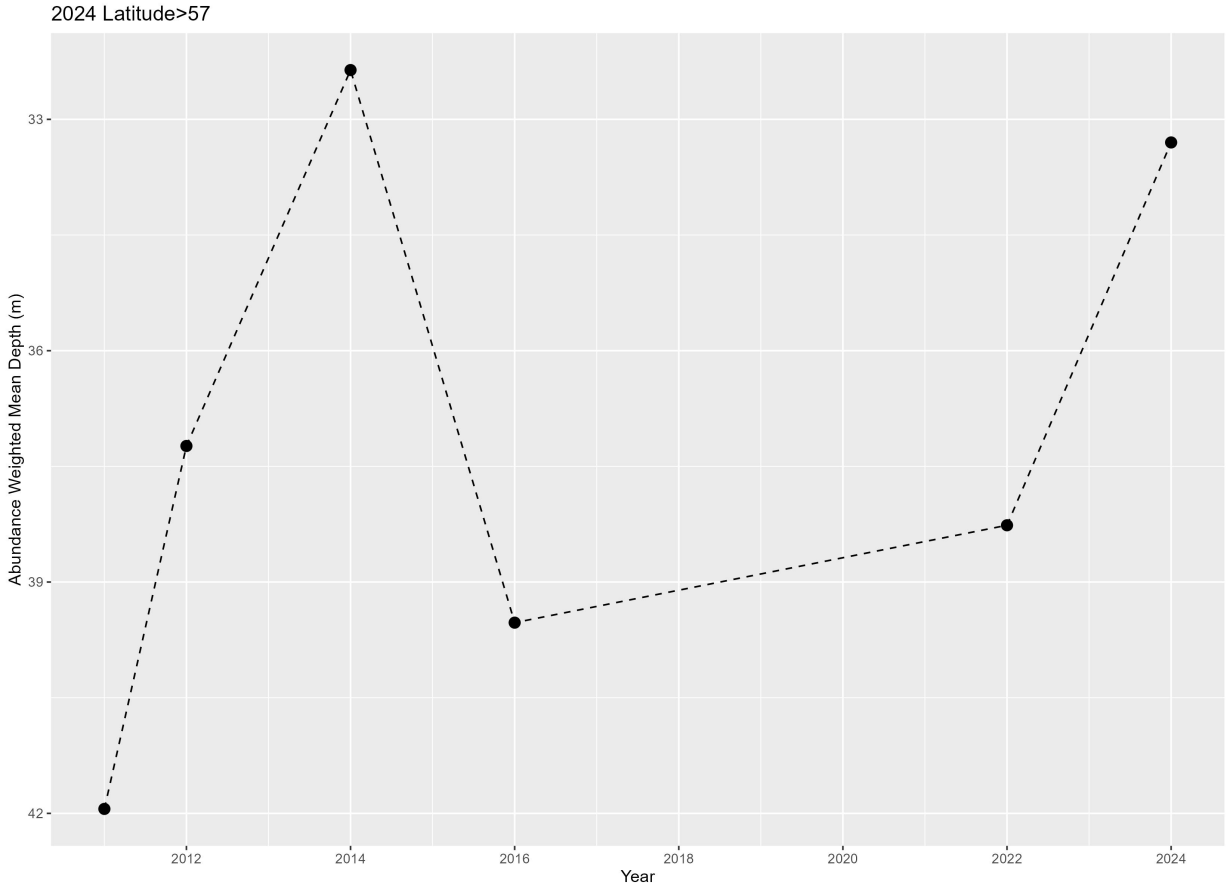

Figure 73: Annual abundance-weighted mean depth of age-0 pollock during late summer in the southeastern Bering Sea.

Implications: Vertical distribution shifts may impact predator-prey overlap between age-0 pollock and their lipid-rich prey, Calanoid copepods and euphausiids, resulting in different feeding conditions that ultimately define fish body condition prior to winter onset. As the climate warms further, or these warm phases potentially lengthen in time, there may be a compounding problem of poor condition and recruitment, thus significantly reducing standing stocks.

Fall Condition of Young-Of-The-Year Walleye Pollock in the Southeastern and Northern Bering Sea, 2002–2024

Contributed by Johanna Page, Jacek Maselko, Rob Suryan, Todd Miller, Elizabeth Siddon, Emily Fergusson, Cathy Mattson, Annie Masterman, Bryan Cormack, Alex Andrews, and Jim Murphy
Auke Bay Laboratories, Alaska Fisheries Science Center, NOAA Fisheries, Juneau, AK
Contact: johanna.vollenweider@noaa.gov
Last updated: October 2024

Description of indicator: Time series of several body condition metrics of young-of-the-year (YOY) walleye pollock (*Gadus chalcogrammus*) in the southeastern Bering Sea (SEBS) and Northern Bering Sea (NBS) are presented, including length-weight residuals, percent lipid, and energy density residuals. **Note:** values from the NBS in 2024 are from a preliminary subsample of fish and the SEBS is complete. Fish for this time series were sampled primarily by surface trawl from the late-summer BASIS (Bering Arctic Subarctic Integrated Survey) and NBS surface trawl surveys, with a relatively small number of fish from opportunistic surveys. Fish <100 mm total length were assumed to be YOY (Bailey, 1989).

Multiple YOY pollock condition metrics were evaluated across an 18-year time series to assess latitudinal effects. Condition metrics considered include energy density (ED; kJ/g), % moisture, % lipid, % protein, RNA:DNA (RNA/DNA; an index of growth), and % carbon:nitrogen ratios (C/N; a lipid to protein indicator) (Figure 74). Hockey stick regressions show a clear inflexion point in condition metric trends at an average latitude of 60.085°N. Consequently, ESR condition metric time series presented here are split into southeastern and Northern Bearing Sea delineated at 60°N, which coincides with oceanographic delineations (Stabeno et al., 2012*a*). Annual length-weight residuals were calculated from the linear regression of log transformed length (total length, mm) and weight (whole wet mass, g) (Figure 75). Percent lipid (wet mass; Figure 76) and ED (Figure 77) were measured in the analytical chemistry laboratory at Auke Bay Laboratories, Juneau, AK, following standard protocols described in Pinger et al. (2024) and Vollenweider et al. (2011), respectively. Length-adjusted weight and ED were based on residuals obtained from the regression of weight and ED on length, respectively.

Status and trends: Trends in YOY pollock condition diverge at latitude 60°N, with different energetic processes in the SEBS and NBS. In the SEBS, pollock condition fluctuates in response to temperature-mediated processes, with below-average body condition during periods with positive sea surface temperature anomalies, and above-average body condition during periods with negative sea surface temperature anomalies (Figures 75, 76, 77). During the relatively cool period from 2006–2012, YOY pollock body weights were average or above average, and their lipid stores and ED were above average. During the ensuing warm period that began in 2014, all three condition metrics were generally below average. Since 2022, sea surface temperatures have cooled to near-average in 2024 (Figure 31) with low pollock weights and ED, and average % lipid.

In the NBS, YOY pollock body condition metrics had lower residuals than in the SEBS, and condition did not respond similarly to the same range of temperatures as they did in the SEBS. In 2024, ocean temperatures cooled and were slightly below average (Figure 31) while YOY pollock were lighter than average with average lipid stores and low energy densities (Figures 75, 76, 77).

Factors influencing observed trends: The NBS and SEBS are characterized by distinct physical oceanography with consequences on their respective biological communities. The NBS has more stable,

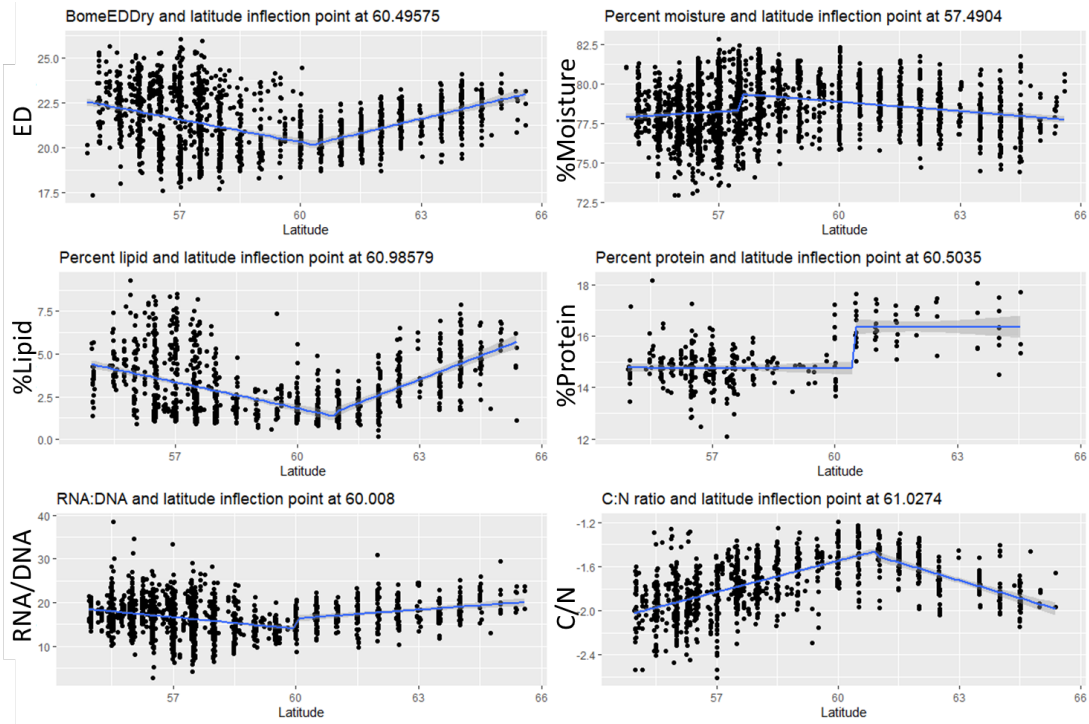

Figure 74: Latitudinal trends in body condition metrics of young-of-the-year walleye pollock in the Bering Sea, with a mean inflection point at latitude 60.085°N. ED = energy density (kJ/g dry mass); RNA/DNA = ratio of RNA to DNA content indexing growth; % C/N = ratio of carbon to nitrogen content.

cold conditions with extensive sea ice cover while the SEBS undergoes large interannual and multiyear variability in sea ice cover and ocean temperature (Stabeno et al., 2012*a*). During relatively cool periods in the SEBS, zooplankton assemblages include large, energy-rich *Calanus* spp. and *Thysanoessa raschii* (Coyle et al., 2008; Stabeno et al., 2012*b*). In combination, an abundance of high-quality prey and reduced metabolic demands maximize growth and lipid storage of YOY pollock for winter survival (Andrews et al., 2019; Koenker et al., 2018; Laurel et al., 2016; Siddon et al., 2013). Though similar processes have occurred more recently in the NBS (Kimmel et al., 2023), the stability of ice cover dampens physical and biological variability.

Implications: Summer environmental conditions and the ability of YOY pollock to balance the synonymous energetic demands to grow and store lipid is reflected in their body condition prior to winter. Winter survival is dependent on their ability to grow large enough for predator avoidance while simultaneously having acquired sufficient lipid stores to sustain them through winter when food is relatively scarce. In the Bering Sea, the first winter survival of YOY pollock to age-1 recruits has been shown to vary during cold and warm regimes (Heintz et al., 2013).

Acknowledgements: Thanks to the many sea-going scientific staff that collected, preserved, and delivered samples and associated metadata to the Recruitment Ecology and Coastal Assessment group at Auke Bay Labs, particularly Jim Murphy and Andrew Dimond. And thanks to the group of people that conducted biological and analytical chemical analysis of the samples with the utmost expediency for timely inclusion in the ESR, including Wil Licht and Cody Pinger.

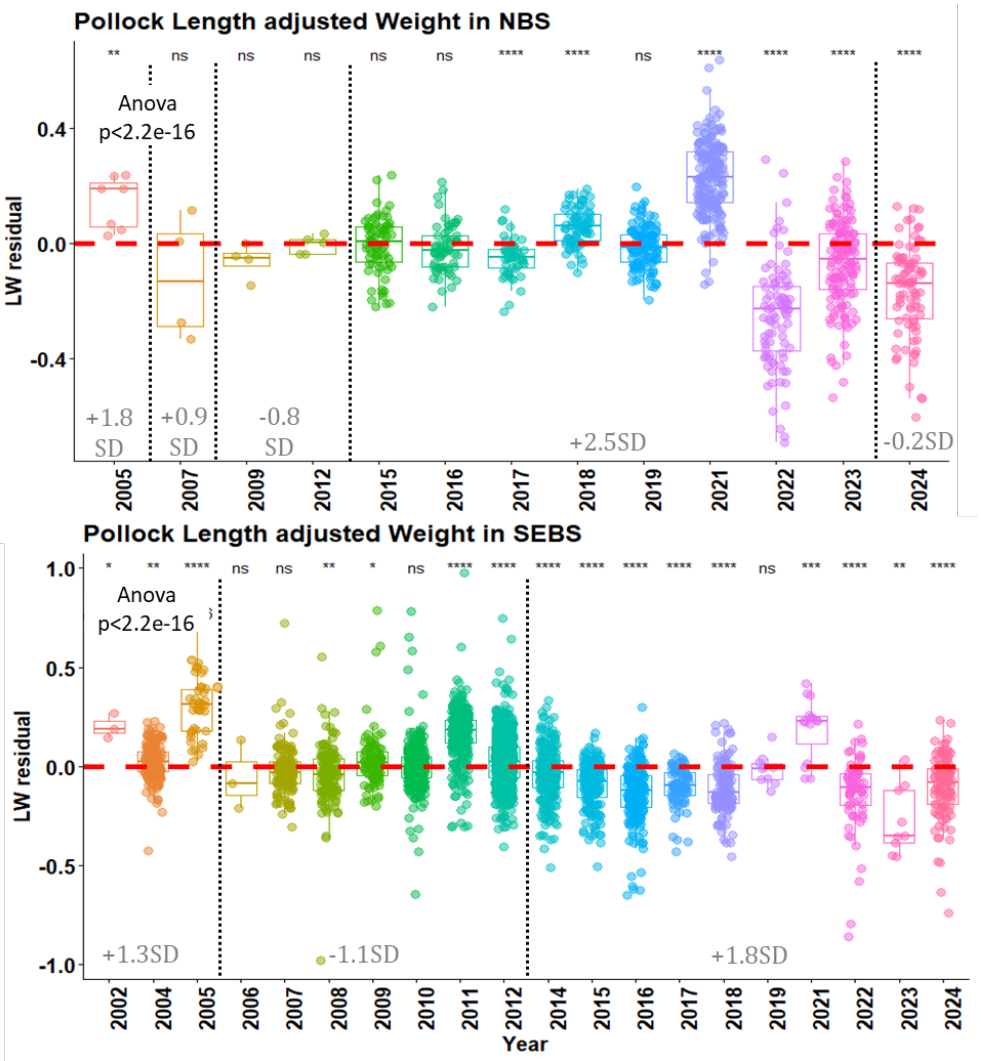

Figure 75: Annual length-weight residuals from log-transformed length-weight regressions of young-of-the-year walleye pollock in the Northern Bering Sea (NBS; top) and southeastern Bering Sea (SEBS; bottom). The horizontal dashed red line indicates the mean of all residuals. The significance of deviations from the mean are denoted by stars above the given year where ns = not significant. The dashed vertical black lines delineate periods of positive (+) and negative (–) sea surface temperature anomalies (Figure 31), and the average annual anomaly standard deviation (SD) for that period is presented.

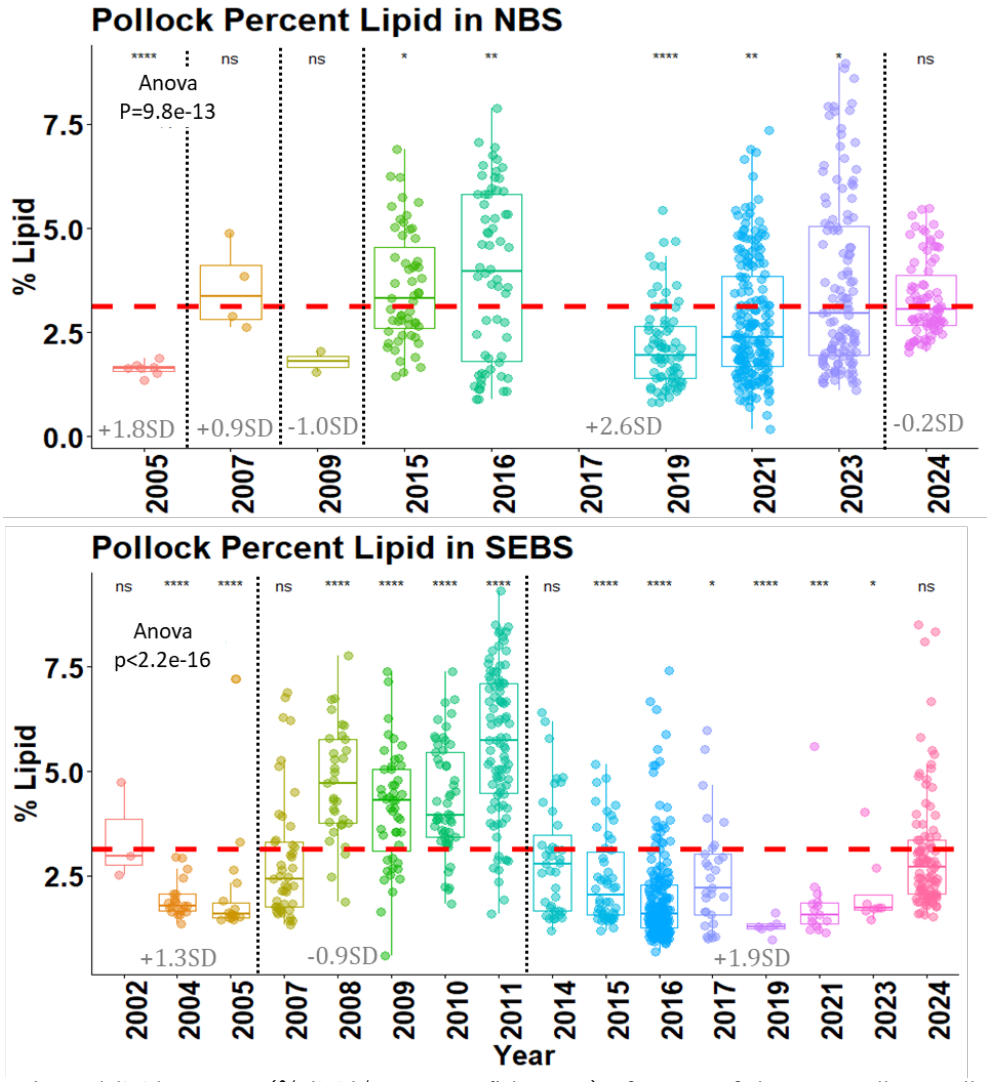

Figure 76: Annual lipid content (% lipid/gram wet fish mass) of young-of-the-year walleye pollock in the Northern Bering Sea (NBS; top) and southeastern Bering Sea (SEBS; bottom). The horizontal dashed red line indicates the mean of all residuals. The significance of deviations from the mean are denoted by stars above the given year where ns = not significant. The dashed vertical black lines delineate periods of positive (+) and negative (–) sea surface temperature anomalies (Figure 31), and the average annual anomaly standard deviation (SD) for that period is presented. The asterix above NBS 2024 data indicates that these are preliminary results.

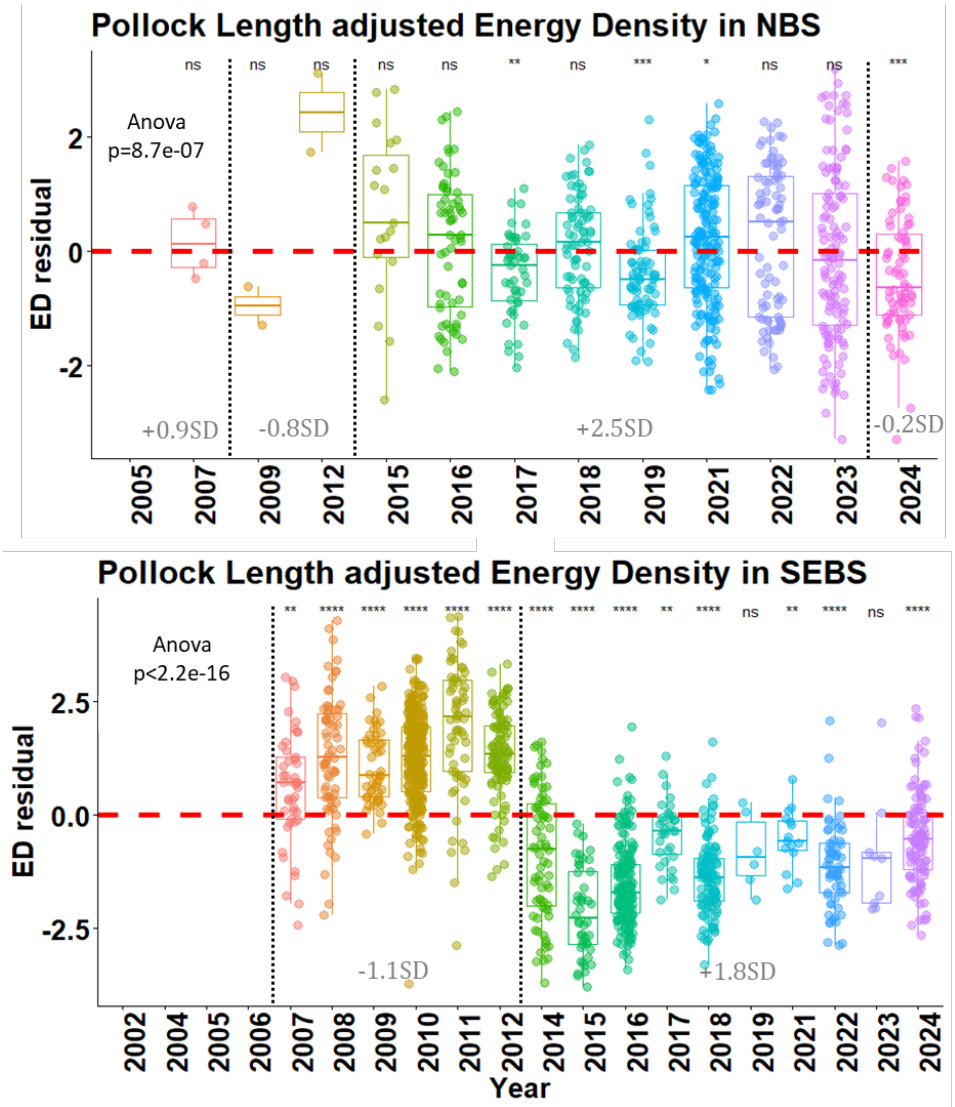

Figure 77: Annual length-adjusted energy density (ED; kJ/gram fish dry mass) of young-of-the-year walleye pollock in the Northern Bering Sea (NBS; top) and southeastern Bering Sea (SEBS; bottom). The horizontal dashed red line indicates the mean of all residuals. The significance of deviations from the mean are denoted by stars above the given year where ns = not significant. The dashed vertical black lines delineate periods of positive (+) and negative (–) sea surface temperature anomalies (Figure 31), and the average annual anomaly standard deviation (SD) for that period is presented. The asterix above NBS 2024 data indicates that these are preliminary results.

Herring

Catch Estimates of Pacific Herring and Capelin from Surface Trawl Surveys, 2003–2024

Contributed by Alex Andrews, Ellen Yasumiishi, Jim Murphy, Andrew Dimond, and Rob Suryan
Auke Bay Laboratories, Alaska Fisheries Science Center, NOAA Fisheries, Juneau, AK
Contact: alex.andrews@noaa.gov
Last updated: October 2024

Description of indicator: See 'Description of indicator' on p. 105.

Status and trends: Juvenile and adult Pacific herring (i.e., age-0 and age-1+) and capelin are predominantly caught in the NBS (Andrews et al., 2015). Pacific herring CPUE (kg/km^2) estimates remained at lower levels in the SEBS through 2024, while CPUE estimates have increased gradually then stabilized from 2021–2024 in the NBS (Figure 78). Overall, CPUE estimates from 2021–2024 remained lower than previous estimates in the time series. Capelin CPUE estimates from 2021–2023 were lower than previous estimates in the time series; CPUE estimates increased significantly in the NBS in 2024 (Figure 79).

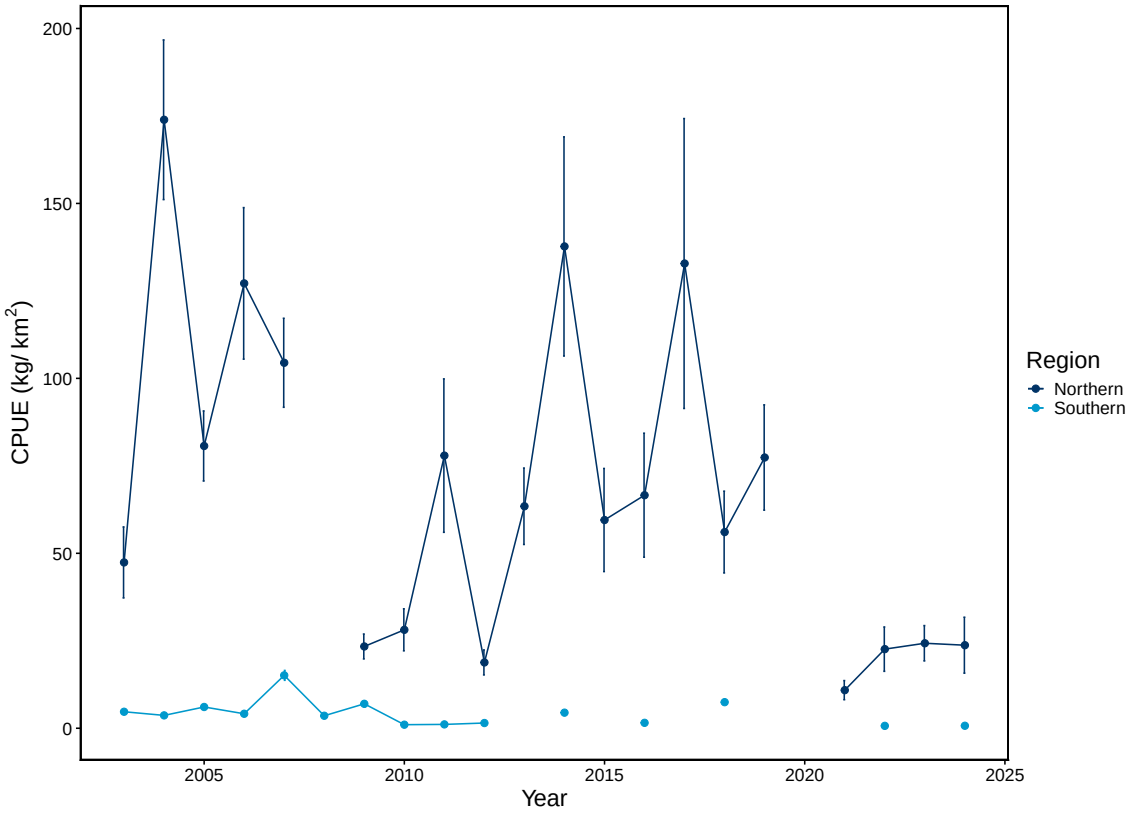

Figure 78: Estimated CPUE (kg/km^2) of herring in surface waters surveyed in the eastern Bering Sea during late summer, 2003–2024.

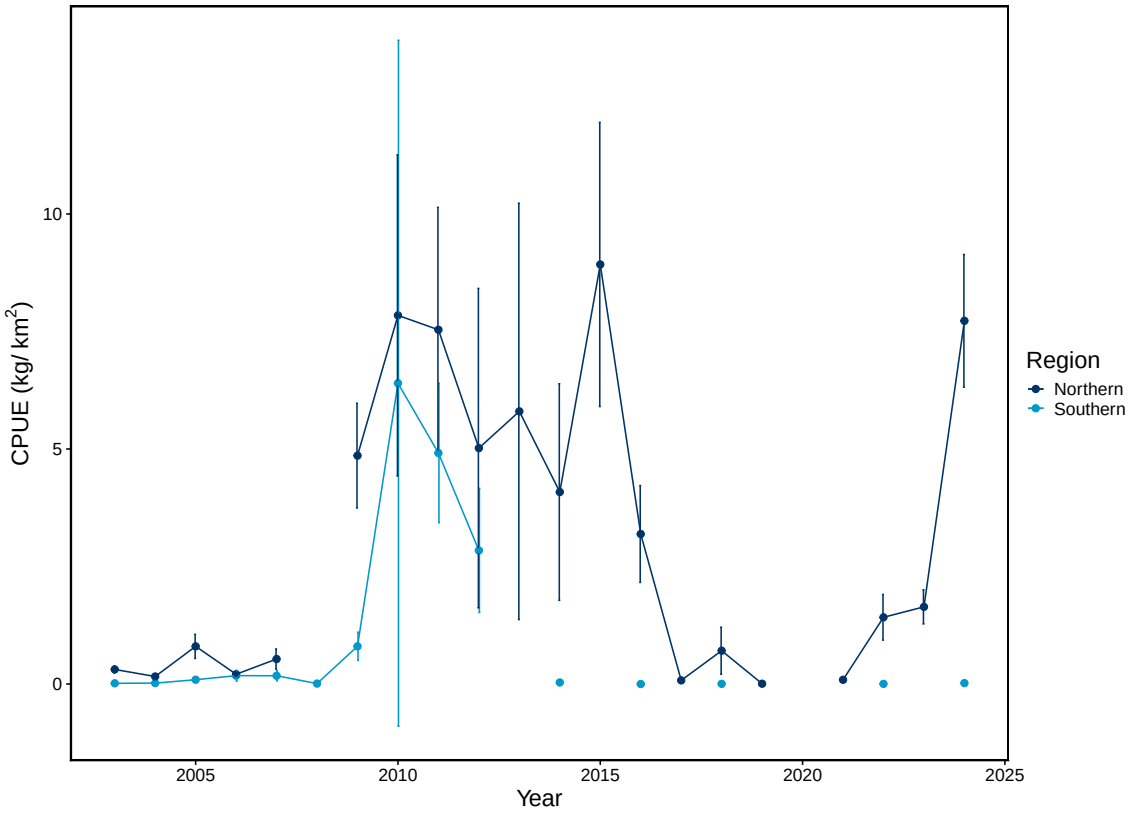

Figure 79: Estimated CPUE (kg/km^2) of capelin in surface waters surveyed in the eastern Bering Sea during late summer, 2003–2024.

Factors influencing observed trends: Favorable conditions for herring recruitment are linked to warm temperatures, wind direction, and prey availability (see Dressel et al., p. 134, Williams and Quinn (2000); Wespestad and Gunderson (1991)). High CPUE estimates in 2014, 2017, and 2019 occurred during a series of warm years in the EBS (Figure 78, Figure 80). In the NBS, catches of herring in the surface trawl are predominantly age-0s and juveniles. Therefore, the high CPUE estimates in 2017 may have been an early indicator of a high model estimate for age-4 recruit strength in 2021 (see Dressel et al., p. 134). Thus, relatively low juvenile herring CPUE in 2022–2024 indicate that age-4 recruits in 2026–2028 may be at or below average.

Capelin relative biomass estimates are generally higher in the during cold periods when the cold pool extends into the SEBS. The highest estimates in the time series occurred in the NBS and the SEBS between 2009–2016, either during a cold year or closely following a series of cold years. In 2024 (an average to cold year), CPUE estimates in the NBS rebounded.

Implications: Herring and capelin are both important prey species for upper trophic level guilds including groundfish (Ciannelli and Bailey, 2005; Aydin and Mueter, 2007), birds, and mammals (Sinclair et al., 2008). In addition, herring is an important resource for both subsistence and commercial harvesters. Monitoring CPUE estimates can provide important information for changes in distribution patterns and abundance and the impacts of climate change in the EBS.

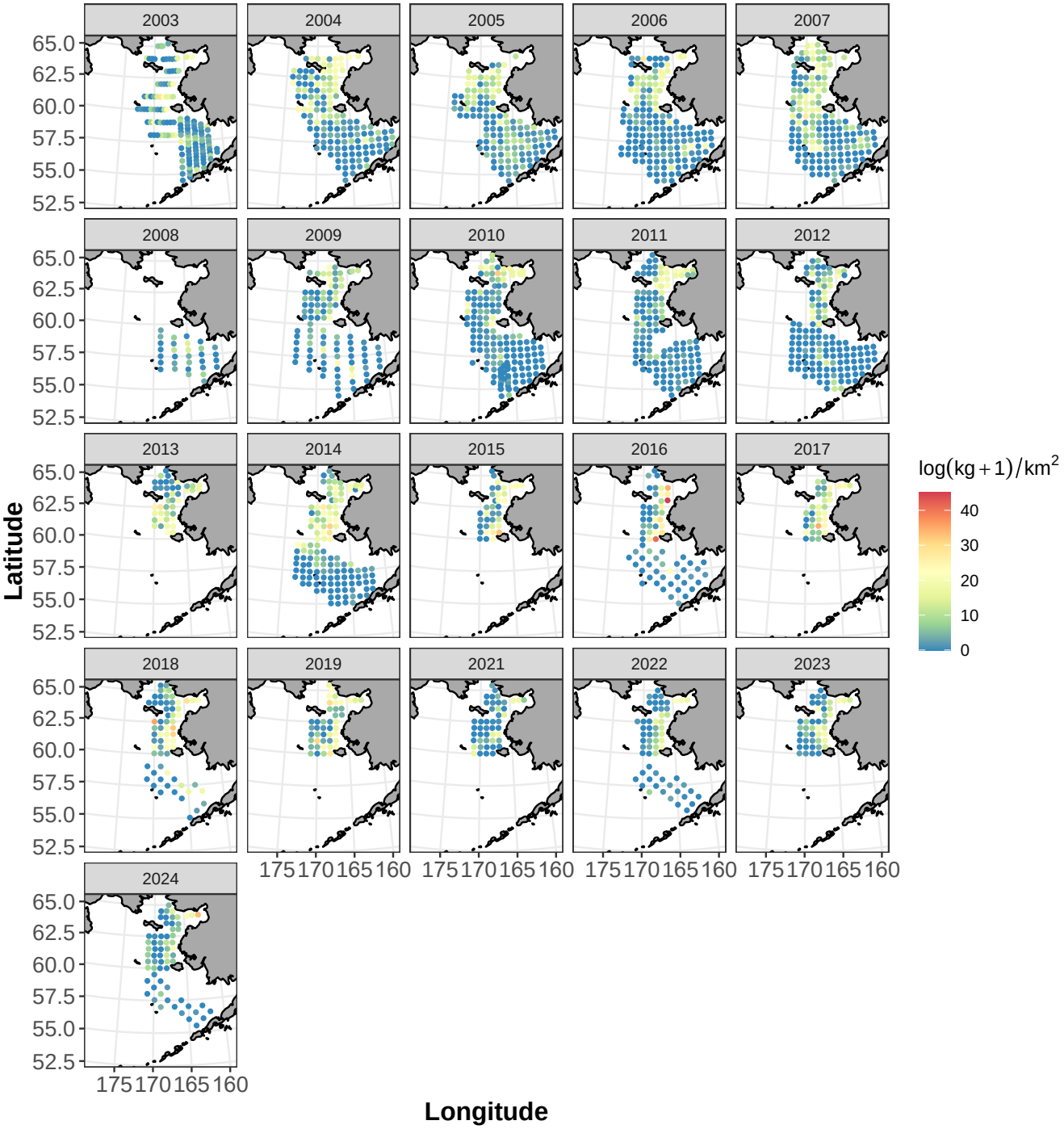

Figure 80: Maps illustrating the spatial distribution of herring CPUE estimates [log(kg + 1)/km^2] in surface waters surveyed in the eastern Bering Sea during late summer, 2003–2024.

Togiak Herring Population Trends

Contributed by Sherri Dressel[1], Sara Miller[1], Caroline Brown[2], and Jack Erickson[1]
[1]Alaska Department of Fish & Game, Commercial Fisheries Division
[2]Alaska Department of Fish & Game, Subsistence Section
Contact: Sherri.Dressel@alaska.gov
Last updated: September 2024

Description of indicator: A time-series of aerial survey biomass estimates (Lebida and Whitmore, 1985) of mature Pacific herring biomass (1980–2023) in the Togiak District of Bristol Bay serves as an index of mature population size (Figure 81, black dots). A simple moving average of aerial survey estimates with confidence ratings greater than 0.25 over an eight-year period (estimated generation time for Togiak herring) is used to show the trend of the indicator. The confidence rating for each aerial biomass estimate ranges from zero (representing no confidence) to one (representing perfect confidence) and is based on criteria such as the number of surveys flown over the season, the number of surveys flown relative to the date of peak biomass and the occurrence of spawn, quality of individual surveys based largely on visibility of schools due to air and water conditions, and extent of the survey area covered per survey. Aerial surveys that receive biologists' overall confidence rating of 0.25 or less are believed to greatly underestimate spawning biomass as a result of poor survey conditions.

In previous years' contributions, the indicator for Togiak mature biomass was a time-series of statistical catch-at-age (SCAA) model estimates (Figure 82, black line). The SCAA model incorporated a time-series of aerial survey biomass estimates, age composition estimates of both the mature population and the commercial harvest, weight at age, and commercial harvest. The SCAA model was also used to forecast biomass through 2023. However, the 2024 Togiak herring forecast was calculated as a median of aerial survey biomass estimates with confidence ratings greater than 0.25 in the last ten years (Figure 81). Last year (2023) marks the first time since the early days of the fishery (fishery began in 1967) that sac roe harvest did not occur in Togiak, precluding the collection of age composition data and necessitating the change in assessment methodology.

Togiak herring are an important prey species for piscivorous fish, seabirds, and marine mammals. They are also an important resource for subsistence harvesters and the basis for a directed Togiak commercial herring sac roe fishery and a directed commercial Dutch Harbor bait fishery. Additionally, they are a prohibited species catch (PSC) in the eastern Bering Sea (EBS) groundfish fisheries. The PSC limit for BSAI groundfish fisheries is set at 1% of the EBS mature herring biomass (age 4+) forecast. The Togiak herring forecast comprises a majority of the nine-stock combined EBS mature herring biomass (Siddon, 2020).

Status and trends: Aerial survey biomass estimates of mature Togiak herring decreased from the early 1980s through approximately 2000 and remained stable through the early 2000s before increasing to the highest survey estimate in the time-series in 2023 (Figure 81, Figure 82). Both the eight-year simple moving average (Figure 81, dashed line) used to show a trend in 1980–2023 aerial survey estimates and a previous model run with the SCAA model (based on 1980–2022 data; Figure 82, black line) show this general trend, however the SCAA model that includes age composition information captures a more dramatic increase since 2020 as a result of strong age-4 recruitment in 2020 and 2021 (Figure 82, Figure 83). Estimates from the SCAA model indicate that recruitment was near or above the long-term median (128 million fish) during 2017–2022 with two of the largest recruitment events since the 1980s occurring

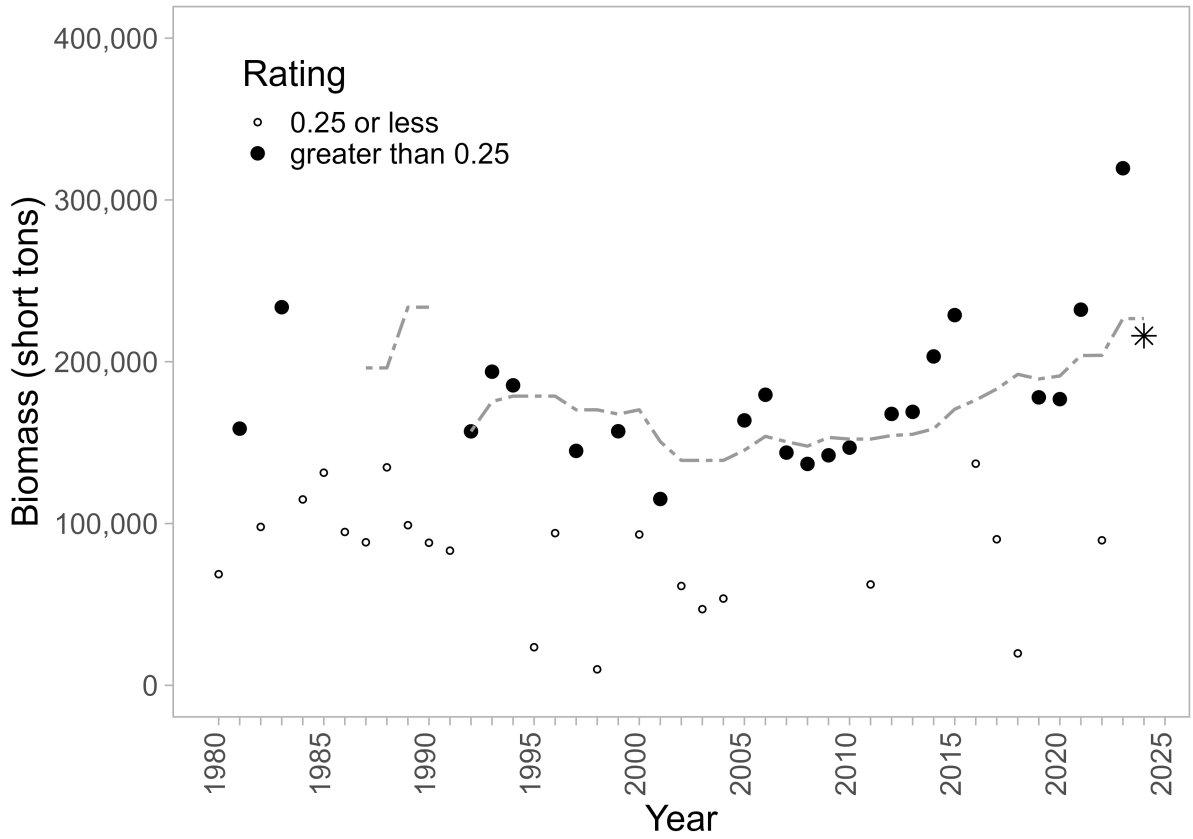

Figure 81: Aerial survey biomass estimates (sum of aerial observed biomass and pre-peak harvest) of Togiak herring (points), trend (dashed line), and forecast (asterisk). The size and fill of the points reflect whether the confidence rating, which was based on weather, number of surveys, quality of surveys, and timing of surveys relative to the spawn, was greater than 0.25 and included in the trend and forecast or whether it was rated 0.25 or less. The trend was calculated with an eight-year simple moving average of aerial survey biomass with confidence ratings greater than 0.25. The 2024 forecast (216,037 short tons or 195,988 metric tons) was calculated as the median aerial survey biomass rated greater than 0.25 within the last ten years (2014–2023).

in 2020 and 2021 (the 2016- and 2017-year classes; Figure 83). The growth and maturation of these fish explains the increase in biomass and high forecasted biomass in 2023 (Figure 82). The 2023 aerial survey estimate (Figure 81, black dot) came in as forecasted and was the highest on record since 1980. The forecast of biomass for 2024, using a median of the last 10 years of aerial surveys with confidence ratings greater than 0.25 (Figure 81, asterisk), was considerably lower and the returning biomass in 2024 is unknown due to poor weather during the Togiak spawn event and poor resultant survey confidence rating. ADF&G subsistence surveys show variable harvest lbs per capita from 1999–2019 (Coiley-Kenner et al., 2003; Fall et al., 2012; Jones et al., 2021), which appears to reflect the oscillating biomass trend during that time as reflected in the SCAA model, but Togiak respondents noted that the quantity of herring spawn on kelp available for harvest was improved in 2019 in comparison to resource availability since the early 1990s. There is no subsistence harvest data to report from 2020–2024.

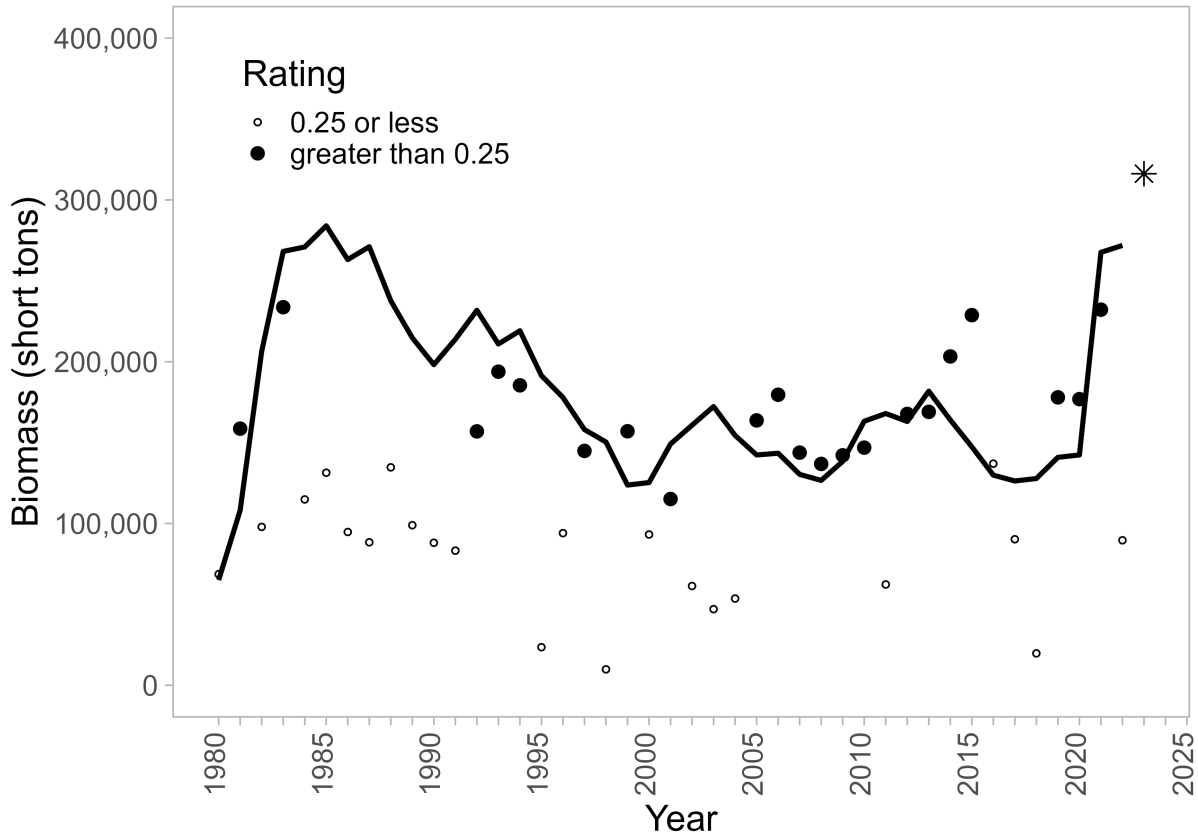

Figure 82: Aerial survey biomass estimates (sum of aerial observed biomass and pre-peak harvest) of Togiak herring biomass (points), model-estimated mature biomass (black solid line), and model-estimated mature biomass forecast (black asterisk) for 2023. The size and fill of the points reflect whether the confidence rating, which was based on weather, number of surveys, quality of surveys, and timing of surveys relative to the spawn, was greater than 0.25 and included in the model and forecast or whether it was rated 0.25 or less. The 2023 forecast from the integrated statistical catch-at-age model for the Togiak herring stock was 316,203 short tons (286,855 metric tons).

Factors causing observed trends: Togiak herring biomass trends are dependent upon highly variable recruitment and are influenced by the environment. The SCAA model, used for previous contributions, indicates that the large biomass estimates in the mid-1980's and in recent years (Figure 82) resulted from the large age-4 recruitments in 1981, 1982, 2020, and 2021 (Figure 83). Williams and Quinn (2000) demonstrated that Pacific herring populations in the North Pacific are closely linked to environmental conditions, particularly water temperature. Tojo et al. (2007) demonstrated how the complex reproductive migration of EBS herring is related to temperature and the retreat of sea ice and how it has changed since the 1980s. Wespestad and Gunderson (1991) suggest that recruitment variation in the EBS relates to the degree of larval retention in near-coastal nursery areas where temperatures and feeding conditions are optimal for rapid growth. Specifically, they indicate that above average year-classes occur in years with warm sea surface temperatures when the direction of transport is north to northeast (onshore) and wind-driven transport velocity is low. The shift to warm sea surface temperatures from 2014 to 2021 (e.g., Figures 20 and 31) and the northward onshore springtime drift in June 2017 (Wilderbuer, 2017) may have contributed to support the exceptional 2016- and 2017-year classes.

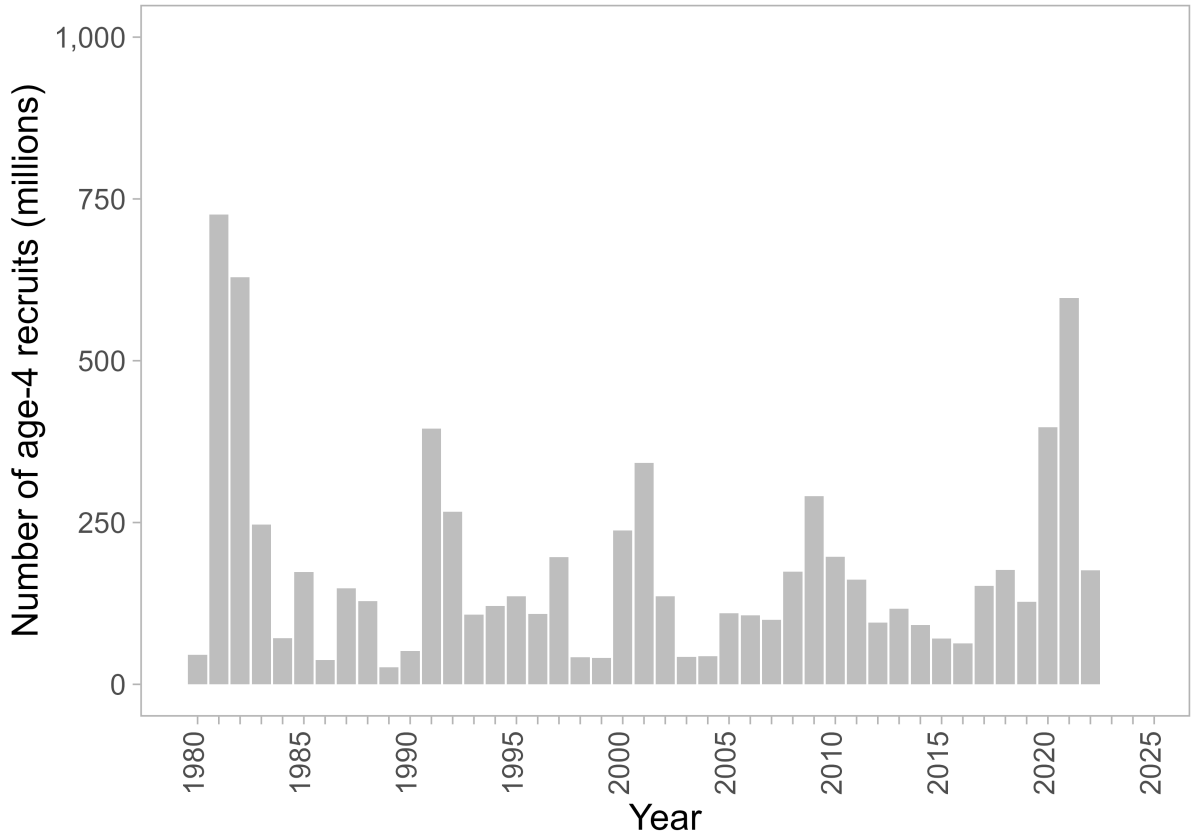

Figure 83: Togiak 2023-forecast model estimates of 1980–2022 age-4 herring recruit strength (millions of age-4 mature and immature fish).

Implications: The high aerial survey estimate of mature herring biomass in 2023 (Figure 81) corroborates the large 2023 forecast of Togiak herring (Figure 82) and the strength of the 2016- and 2017-year classes that have contributed to the population (Figure 83). A large population biomass in 2023 allowed for increased opportunity for directed commercial fisheries (Togiak sac roe and Dutch harbor food and bait), the second highest prohibited species catch limit for the EBS groundfish fisheries since at least 2003, and more forage for the ecosystem. While the large biomass supported greater opportunity for directed herring fisheries in 2023, a lack of a market for Togiak sac roe product resulted in no 2023 sac roe harvest for the first time in over 50 years. While the PSC allowance was the second highest since the herring savings areas (HSAs) were established under Amendment 16a in 1991, the PSC limit was limiting for some groundfish sectors in 2023 (the rock sole/flathead sole/other flatfish trawl sector exceeded their 135 mt PSC allocation by 36 tons and the directed pollock fishery caught 3,049 mt of their 3,066 mt allocation).

Because age, size, and sex data for the spawning population is collected from commercially caught herring and age or size composition data is necessary for the SCAA model, the forecast for 2024 Togiak herring was based on aerial survey data alone (Figure 81). Using a 10-year median is a relatively stable forecast estimator, but as such, is less responsive to large and quick changes in population size. So, while the 2024 forecast was the fifth highest forecast on record for Togiak herring, it was 32% lower than the 2023 forecast. The lower 2024 forecast continued to provide opportunity for directed herring fisheries, but the lack of market and no Togiak sac roe harvest continued in 2024. The lower 2024 forecast led to an approximate 1,000 mt decrease in the PSC limit from 2023 (3,444 mt in 2023 and 2,535 mt in 2024). Despite this decrease, EBS groundfish fisheries have been successful at avoiding herring in 2024 to date with none nearing their PSC allocations (reported harvest as of September 23, 2024). The relatively large mature biomass forecast for 2024 suggests continued benefits for the ecosystem and continued biomass and spawn for subsistence harvest.

If market conditions continue to lead to no directed Togiak herring fishery, future aerial surveys and age/size sampling of the Togiak spawning population are uncertain. If aerial surveys continue without a directed fishery, trends in the Togiak mature population biomass can be tracked, but cohort sizes that contribute to the population biomass will not be known. Although using a 10-year median to forecast Togiak biomass (Figure 81) is less responsive to population trends than forecasting with the SCAA model (Figure 82), using the 10-year median allows more responsiveness to recent population changes than the long-term median (greater than 30 years) used for the other eight less frequently surveyed EBS herring stocks. If aerial surveys do not continue in Togiak, using a 10-year median for forecasting mature Togiak herring biomass may be reconsidered.

Acknowledgements: The authors would like to thank Phil Joy for his primary authorship on the Togiak 2023- and 2024-forecast herring stock assessments. We also thank the ADF&G Togiak herring research and management staff and Mark, Tag, and Age Laboratory staff for their survey, sampling, and data collection efforts without which the Togiak stock assessments would not be possible.

Salmon

Salmon Summary and Synthesis

Contributions to the 2024 Eastern Bering Sea Ecosystem Status Report (ESR) provide information on the status of both adult and juvenile salmon (*Oncorhynchus* spp.) of all species. Due to the variable age structure and complex life cycles of Pacific salmon which span multiple habitats, it can be difficult to disentangle the impacts of environmental conditions experienced across different life stages on their population dynamics. However, some salient patterns do emerge from the contributions to the 2024 ESR, including contrasting, species-specific responses to the recent return to cool/average temperatures following a period of anomalously warm conditions spanning from ∼2014–2021.

Adult returns of western Alaska chum salmon (*O. keta*) stocks experienced precipitous declines during the recent marine heatwave period. Poor juvenile energetic condition driven by dietary shifts to poorer quality prey items during this time period indicate that negative bottom-up effects associated with warmer conditions were likely responsible for these declines (Farley Jr et al., 2024). Juvenile condition of chum salmon in the NBS survey improved in 2021, and remained above-average through 2023, with 2024 reflecting closer to average juvenile condition. However, the abundance of juvenile chum salmon in 2024 is the highest on record for the NBS survey. Such elevated abundance in combination with a decline from above-average to average bioenergetic condition may reflect a possible density-dependent response among the juvenile population. The elevated abundance of juvenile chum salmon in the 2024 juvenile survey may be the result of a combination of favorable environmental conditions, as well increasing spawner abundance. While still below-average, the spawner escapement in 2023 (the parents of the juveniles encountered in the 2024 NBS survey) for western Alaska chum salmon stocks improved compared to previous years (2021–2022). Collectively, the trend of increasing adult returns, juvenile abundance, and above-average to average juvenile condition in recent years point to signs of recovery in western Alaska chum salmon populations. However, a consistent relationship between juvenile chum salmon abundance and future adult returns has not been established, and continued recovery likely depends on environmental conditions remaining favorable.

In contrast to chum salmon, western Alaska Chinook salmon (*O. tshawytscha*) do not appear to show signs of recovery in response to the recent cooler conditions. While western Alaska Chinook salmon runs also declined substantially during the recent marine heatwaves, these populations have been declining more broadly since the early 2000s, pointing to a more complex set of stressors that may be constraining production of these stocks. Available evidence points to demographic shifts towards reduced size and age-at-maturity and concomitant reductions in fecundity, as well as freshwater factors such as river discharge and temperature as important drivers of the observed declines (Cunningham et al., 2018; Howard and von Biela, 2023; Neuswanger et al., 2015; Ohlberger et al., 2020; Feddern et al., 2024). As such, the population dynamics of Chinook salmon do not appear to be as straightforwardly linked to marine temperatures as for chum salmon. In particular, demographic shifts to reduced size-and-age-at maturity may likely involve a genetic component that would not be expected to rapidly reverse in response to environmental conditions (e.g., Ohlberger et al., 2019). The mixed stock abundance of juvenile Chinook salmon encountered in the 2024 NBS survey was the lowest ever recorded, likely reflecting correspondingly low adult spawner escapements in 2022 (the spawning event from which the juveniles in 2024 originated). While the bioenergetic condition of these juveniles was above-average, the relationship between body condition and survival for NBS Chinook salmon is unclear. However, there is a consistent relationship between the juvenile abundance of Chinook in the NBS survey and subsequent

adult returns (Murphy et al., 2017), suggesting that poor run sizes may be expected in the next three to four years (when most juvenile Chinook present in 2024 would be expected to mature and return to freshwater to spawn).

While the abundance of many salmon stocks declined during the recent marine heatwave, Bristol Bay sockeye salmon (*O. nerka*) exhibited an opposite response, with record-high run sizes observed during this time-period. The abundance of Bristol Bay sockeye peaked in 2021–2022, reflecting a strong 2017 year-class and positive ocean entry conditions in 2019. The contrasting response of Bristol Bay sockeye to marine temperature conditions likely reflects their freshwater rearing and marine migratory life histories. While other anadromous salmon rear in riverine habitats as juveniles, sockeye salmon juveniles typically rear in lakes for 1–2 years before migrating to the ocean. Warming temperatures have been shown to increase the productivity of lake ecosystems in Bristol Bay watersheds (Rogers and Schindler, 2011) with corresponding increases in juvenile size and growth (Cline et al., 2019). As such, juvenile sockeye salmon may be better equipped to survive the size-dependent mortality typically experienced during early marine residency after enjoying better growing conditions in freshwater during warmer years. Moreover, there is evidence that Bristol Bay sockeye salmon modulate their marine migration pathways in response to ocean temperature conditions. In cooler years, Bristol Bay sockeye are thought to delay offshore migration in favor of remaining in comparatively warm nearshore habitats of the Bering Sea shelf (Farley Jr et al., 2007). Conversely, in warmer years, Bristol Bay sockeye migrate offshore more rapidly, which has been shown to increase survival rates, and likely allows them to avoid heatwave conditions on the shelf. Thus, it is not necessarily surprising that Bristol Bay sockeye experienced high ocean survival and adult returns during recent warm conditions. Consistent with these expectations, the recent return to cooler conditions also resulted in smaller adult run sizes closer to long-term averages in Bristol Bay in 2023–2024. Given these responses to temperature variation, continued Bering Sea temperatures near or below average may be expected to result in more modest Bristol Bay run sizes in the near future. These expectations are supported by reduced abundance of sockeye salmon encountered in the SEBS survey, as well as below average juvenile condition of sockeye salmon in 2024.

Compiled by Lukas DeFilippo
NOAA Fisheries
Alaska Fisheries Science Center
Last updated: October 2023

Abundance of Juvenile Sockeye Salmon from Surface Trawl Surveys, 2003–2024

Contributed by Alex Andrews, Ellen Yasumiishi, Jim Murphy, and Andrew Dimond
Auke Bay Laboratories, Alaska Fisheries Science Center, NOAA Fisheries, Juneau, AK
Contact: alex.andrews@noaa.gov
Last updated: October 2024

Description of indicator: See 'Description of indicator' on p. 105.

Status and trends: Juvenile sockeye relative abundance remained high in the SEBS (Figure 84) through 2022, following a series of warm years. In 2024 (an average to cold year), the relative abundance decreased from the warm year relative abundances. Relative abundances in the NBS tend to be low, with the exception of 2019, when SSTs were high and the cold pool extent was at a near minimum extent. In 2024, relative abundance remained low in the NBS; Bristol Bay juvenile sockeye tend to remain nearshore and further south in cold years (Figure 85).

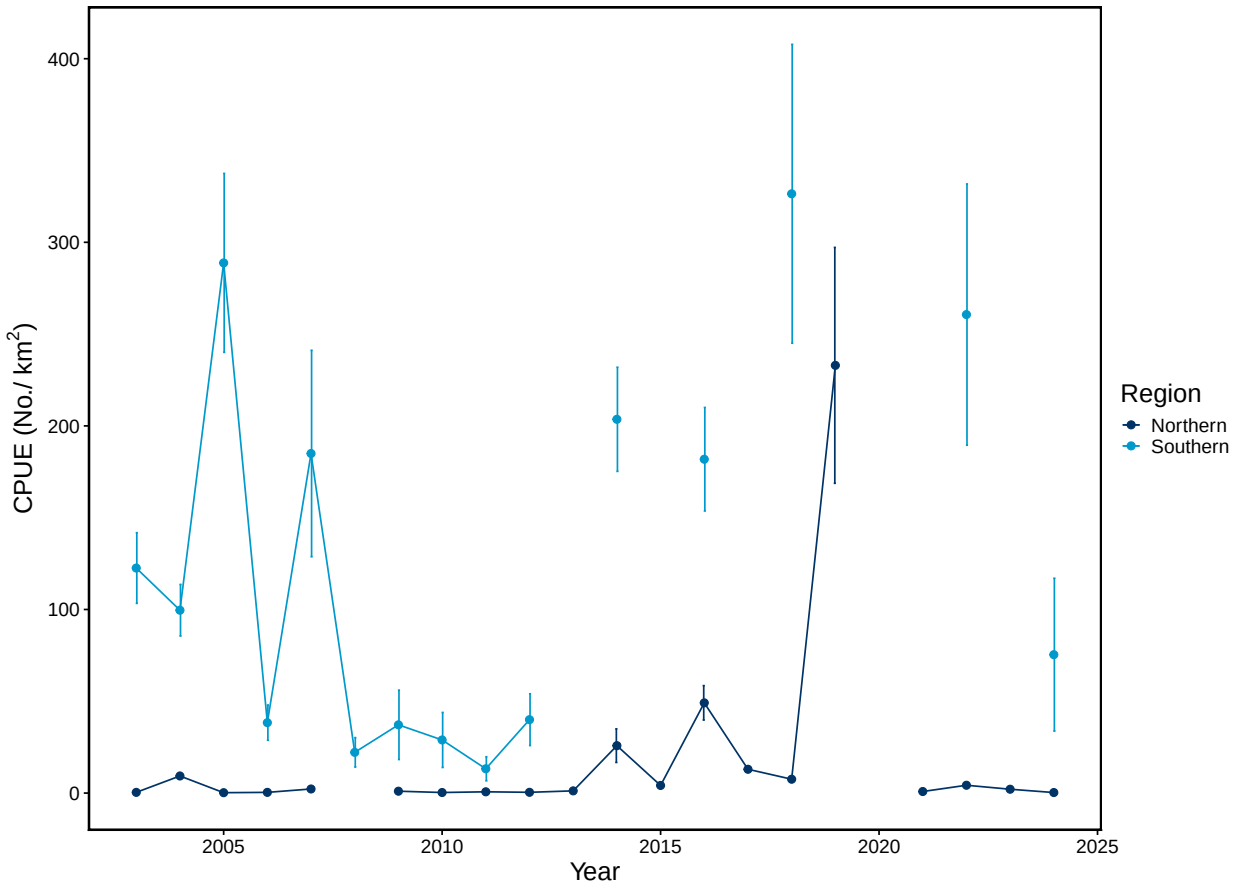

Figure 84: Estimated abundance [No./km^2] of juvenile sockeye salmon in surface waters during late summer, 2003–2024.

Factors influencing observed trends: Bristol Bay sockeye adult returns in the last 5–10 years have been above long-term averages, with a record high in 2022 (see p. 150). Juvenile sockeye are likely benefiting from a combination of good freshwater rearing habitat and good early marine survival (Farley et al., 2011), and high abundances of age-0 pollock in surface waters during warm years, a major prey item of juvenile sockeye salmon (Yasumiishi et al., 2024). From 2003–2018, juvenile sockeye salmon in these surveys incurred warming related increases in abundance, shifts in their distribution northward and westward, and increases in area occupied (Yasumiishi et al., 2020). Further research into the predominant age classes of the juvenile salmon encountered during this survey would benefit the interpretation of these relative abundances. In addition, genetic analyses confirming the juvenile sockeye captured in the NBS, are of Bristol Bay origin, would help to determine if during periods of warm SSTs and reduced cold pool extent, Bristol Bay juvenile sockeye are able to benefit from expanding distributions into the NBS.

Implications: Less favorable ocean conditions with lower SSTs and a larger cold pool extent may lead to reduced relative abundances in the SEBS. Low relative abundances in the NBS are to be expected under these conditions.

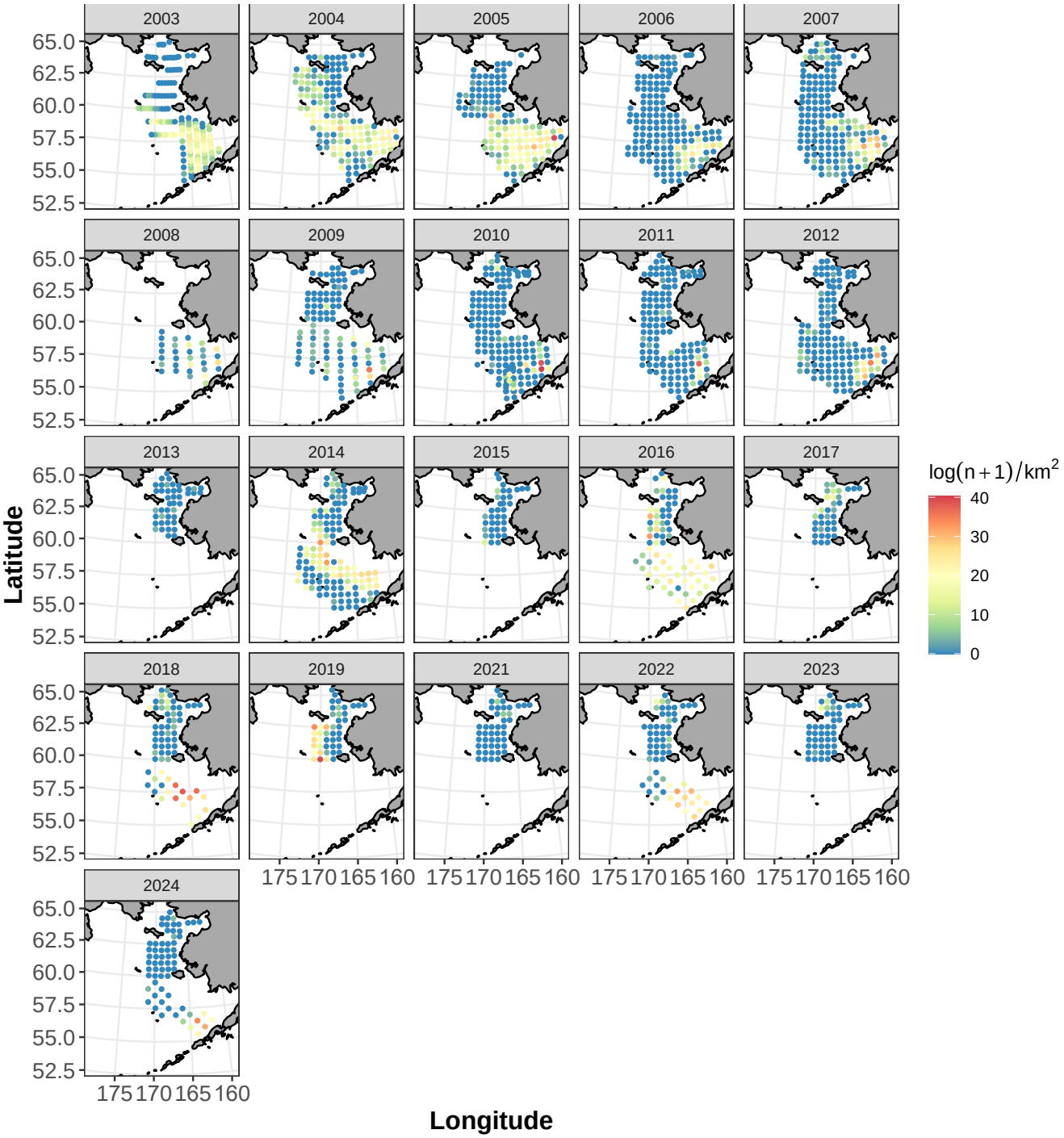

Figure 85: Maps illustrating the spatial distribution of juvenile sockeye salmon abundance [No./km^2] in surface waters surveyed in the eastern Bering Sea during late summer, 2003–2024.

Juvenile Salmon Condition Trends in the Eastern Bering Sea

Contributed by Emily Fergusson, Rob Suryan, Todd Miller, Jim Murphy, and Alex Andrews
Auke Bay Laboratories, Alaska Fisheries Science Center, NOAA
Contact: emily.fergusson@noaa.gov
Last updated: September 2024

Description of indicator: The eastern Bering Sea surface trawl surveys consist of multidisciplinary research in the southeastern Bering Sea (SEBS) and northern Bering Sea (NBS) that support sampling of fish, zooplankton and lower trophic levels, and oceanographic conditions. The SEBS survey occurs biennially in late summer (even years, Aug-Sept) within the middle to outer domains (50-200 m, 55°N–60°N). The NBS survey occurs annually in late summer (Sept) and covers the inner domain (bottom depths generally less than 55m) waters between 60°N–66.5°N.

Juvenile pink (*Oncorhynchus gorbuscha*), chum (*O. keta*), sockeye (*O. nerka*), coho (*O. kisutch*), and Chinook (*O. tshawytscha*) salmon nutritional condition data have been collected from the two fisheries-independent surveys. This report presents energy density (ED, kJ/g dry weight) anomalies of juvenile salmon in relation to the time series of fish condition from these surveys, updated with 2024 samples from the SEBS, and 2023 and 2024 samples from the NBS. Energy density trends over time can represent the condition of juvenile salmon and other taxa in response to climate and ocean conditions during their early marine residency.

Status and trends: For the SEBS in 2024, ED anomalies were negative for chum and sockeye salmon (Figure 86). No juvenile pink, coho, or Chinook salmon samples were available for ED analysis in the SEBS in 2024.

For the NBS in 2024, ED anomalies varied among species (Figure 87). For juvenile pink, chum, and coho salmon, ED anomalies all decreased from positive 2023 values to average. Juvenile Chinook salmon ED anomalies increased from average to positive. There were no sockeye salmon samples available for analysis.

Factors influencing observed trends: During early marine entry and residency, juvenile salmon must grow quickly to avoid predation while also acquiring enough lipid reserves to survive winter when food is severely limited (Beamish and Mahnken, 2001; Moss et al., 2005). The SEBS ED anomaly trends were not in-step with NBS salmon, with SEBS ED anomalies responding more variably to SST conditions.

For the NBS, the anomalously high ED values from all salmon species in 2021 and 2022, and relatively lower values from 2018 and 2019, indicate a shared functional response to variable sea surface temperature (SST) values in the Bering Sea. As a mechanism for salmon condition, direct effects of SST on metabolic demands reduce energy available for reserves, while indirect effects of reduced availability of lipid-rich prey further constrains the capacity to build reserves for overwinter survival.

Implications: Juvenile pink, chum, coho, and Chinook salmon in the SEBS showed ED anomaly values that were more consistent with lower energy stores and a reduced capacity for overwinter survival. The juvenile salmon entered the NBS in 2024 with average to positive energy stores, which may contribute to higher overwinter survival (when food is limited) and higher adult returns.

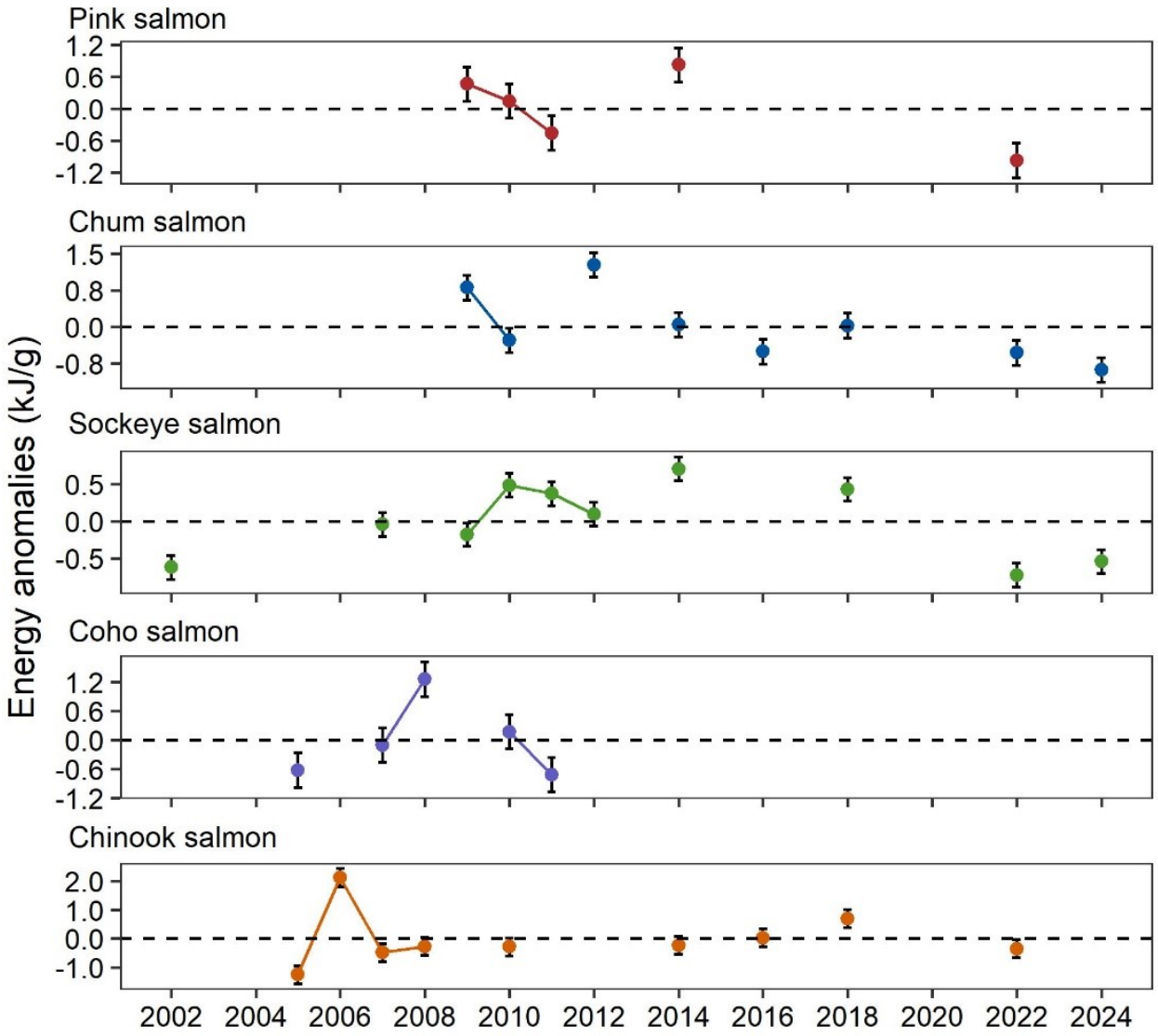

Figure 86: Energy density anomalies (kJ/g, dry weight; ±1 SE) of juvenile salmon captured in the south-eastern Bering Sea, 2002–2024. Time series average is indicated by the dashed line.

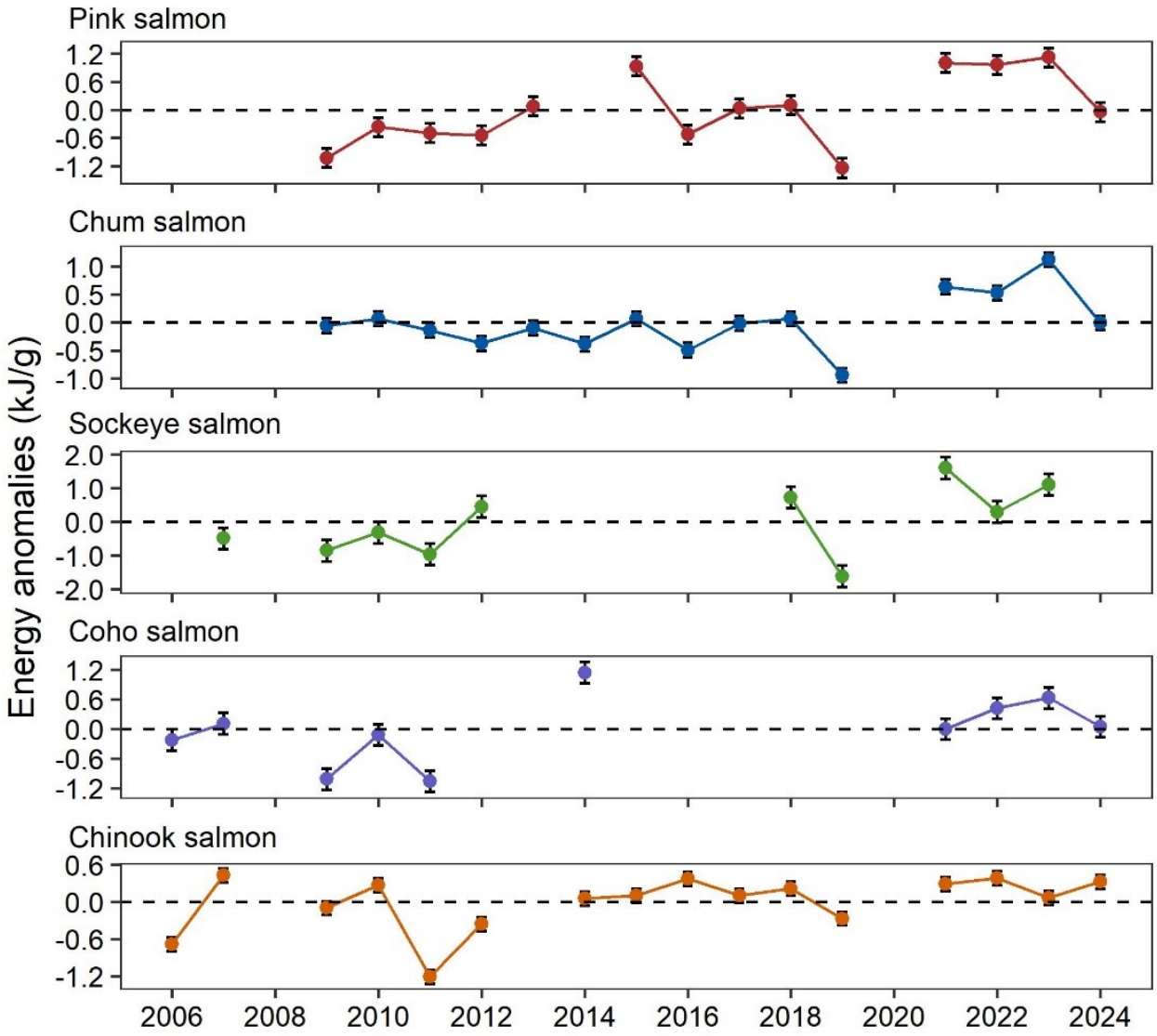

Figure 87: Energy density anomalies (kJ/g, dry weight; ±1 SE) of juvenile salmon captured in the northern Bering Sea, 2006–2024. Time series average is indicated by the dashed line.

Northern Bering Sea Juvenile Salmon Abundance Indices

Contributed by Jim Murphy[1], Sabrina Garcia[2], Dan Cooper[3], Andrew Dimond[1], Elizabeth Lee[2], Lukas DeFilippo[1], and Kathrine Howard[2]
[1]Auke Bay Laboratories, Alaska Fisheries Science Center, NOAA Fisheries, Juneau, AK
[2]Alaska Department of Fish & Game, Anchorage, AK
[3]Resource Assessment and Conservation Engineering Division, Alaska Fisheries Science Center, NOAA Fisheries, Seattle, WA
Contact: jim.murphy@noaa.gov
Last updated: October 2024

Description of indicator: Mixed-stock juvenile (first year at sea) Chinook salmon (*Oncorhynchus tshawytscha*) abundance indices are estimated from late summer (September) surface trawl catch-per-unit-effort (CPUE) data and adjusted for mixed-layer depth in the northern Bering Sea (NBS). This mixed-stock index provides a rapid assessment of all juvenile Chinook salmon stocks present in the NBS and is different from the stock-specific abundance estimates of Yukon River Chinook salmon that are used to forecast future run sizes.

Abundance indices for Yukon River fall chum salmon (Upper Yukon River genetic stock group) are based on CPUE data from surveys in both the northern and southern Bering Sea through 2023 and for northern Bering Sea data only in 2024. The preliminary 2024 abundance index was generated using the average genetic stock proportion from 2021 to 2023 and will change once stock compositions from 2024 become available.

Status and trends: The mixed-stock abundance of juvenile Chinook salmon in the NBS was at a record low in 2024 (1.01 million), and has varied from 1.01 million to 5.82 million with an overall average of 2.80 million since 2003 (Figure 88). The stock-specific CPUE index for the fall chum salmon stock group ranged from a low of 22 in 2017 to a high of 154 in 2024, with an average of 59 (Figure 89).

Factors influencing observed trends: Early life-history (freshwater and early marine) survival and adult spawning escapement are the key factors that determine juvenile salmon abundance in the northern Bering Sea. The parent year spawning escapement for Yukon River Chinook salmon was at a record low level in 2022 (JTC, 2024) and is a key factor contributing to the record low abundance of juvenile Chinook salmon in NBS during 2024.

Implications: Juvenile Chinook salmon abundance is significantly correlated with adult returns (Murphy et al., 2017; Howard et al., 2019, 2020; Murphy et al., 2021); therefore record low juvenile abundance is expected to contribute to record low returns to the Yukon River three to four years in the future (juveniles typically remain at sea for three to four years before returning to freshwater to spawn). Although the condition (energy density) of juvenile Chinook was slightly above average in 2024 (see p. 144) it is unlikely to improve the abundance-based outlook as we have not observed a significant connection between their condition and survival. The survival of juvenile chum salmon is linked to their condition (Farley Jr et al., 2024), but chum salmon were in average condition during 2024 (see p. 144). The record-high abundance of juvenile fall chum salmon in 2024 and average condition indices are expected to result in improved run sizes to the Yukon River three to four years in the future.

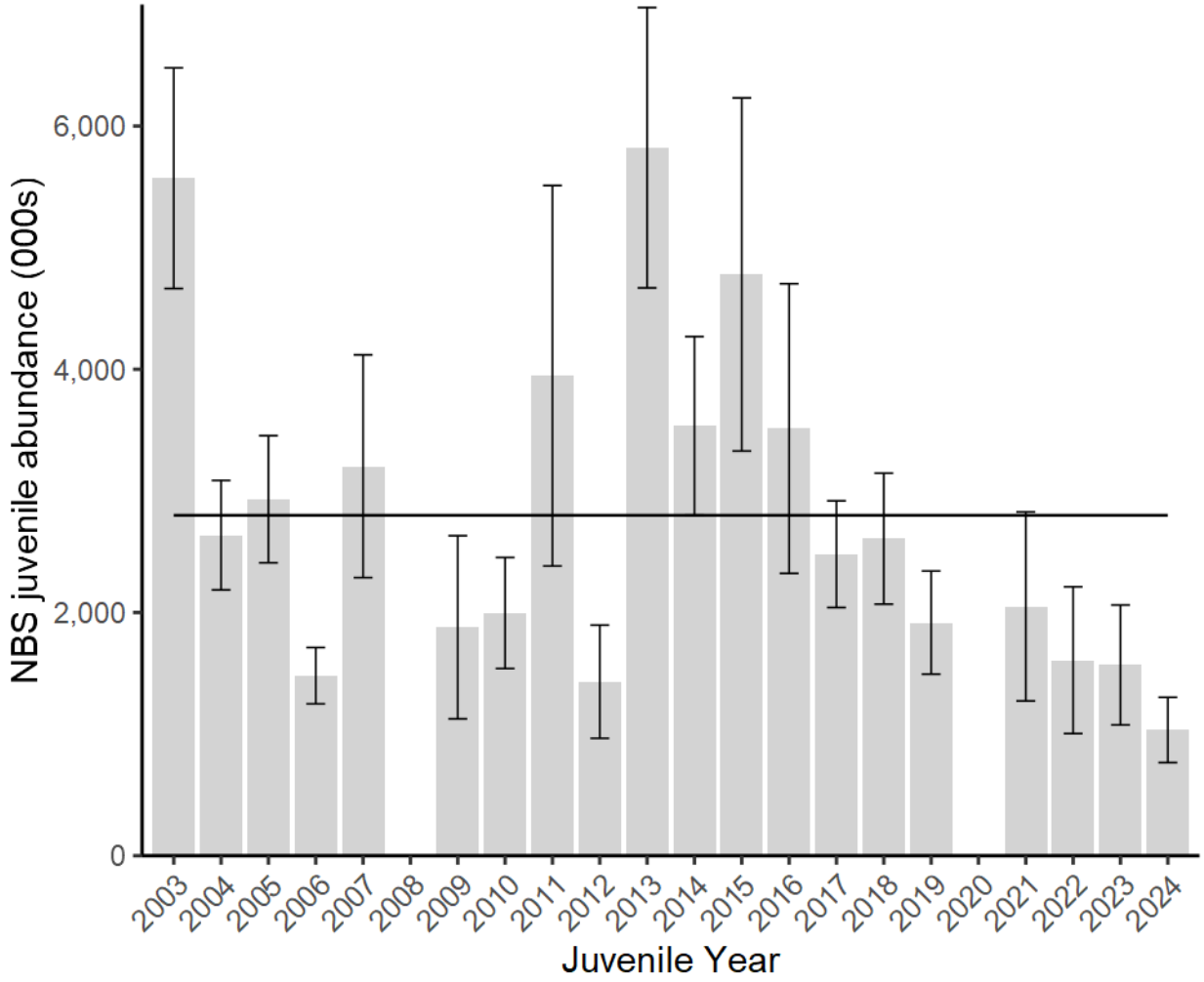

Figure 88: Juvenile Chinook salmon abundance estimates in the northern Bering Sea (NBS), 2003–2024. Error bars are one standard deviation above and below juvenile abundance estimates. The solid black line identifies the average abundance of juvenile Chinook salmon in the NBS (2.8 million).

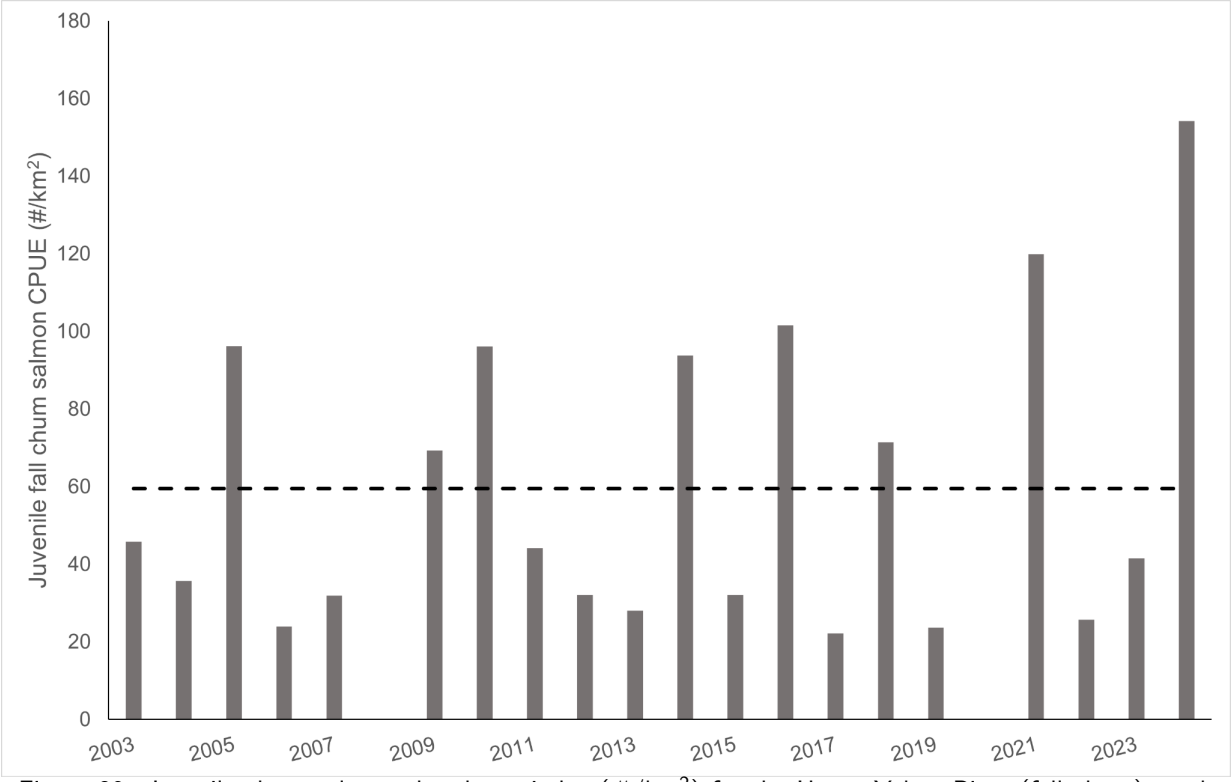

Figure 89: Juvenile chum salmon abundance index (#/km^2) for the Upper Yukon River (fall chum) stock group, 2003–2024. No surveys occurred in 2008 and 2020. The 2024 CPUE only includes data from the Northern Bering Sea survey. Additionally, the 2024 abundance index was generated using the average genetic stock proportion from 2021 to 2023 and will change once stock compositions from 2024 become available. Dashed line indicates the average juvenile chum salmon index across years 2003–2024.

Temporal Trend in the Annual Inshore Run Size of Bristol Bay Sockeye Salmon (Oncorhynchus nerka)

Contributed by Curry J. Cunningham[1], Stacy Vega[2], and Jasmine Terry-Shindelman[2]
[1]College of Fisheries and Ocean Sciences, University of Alaska Fairbanks, Juneau, Alaska
[2]Alaska Department of Fish & Game, Anchorage, Alaska
Contact: cjcunningham@alaska.edu
Last updated: October 2024

Description of indicator: The annual abundance of adult sockeye salmon (*Oncorhynchus nerka*) returning to Bristol Bay, Alaska is enumerated by the Alaska Department of Fish and Game (ADF&G). The total inshore run in a given year is the sum of catches in five terminal fishing districts plus the escapement of sockeye to nine major river systems. Total catch is estimated based on the mass of fishery offloads and the average weight of individual sockeye within time and area strata. Escapement is the number of fish successfully avoiding fishery capture and enumerated during upriver migration toward the spawning grounds, or through post-season aerial surveys of the spawning grounds (Elison et al., 2018). Although there have been slight changes in the location and operation of escapement enumeration projects and methods over time, these data provide a consistent index of the inshore return abundance of sockeye salmon to Bristol Bay since 1963.

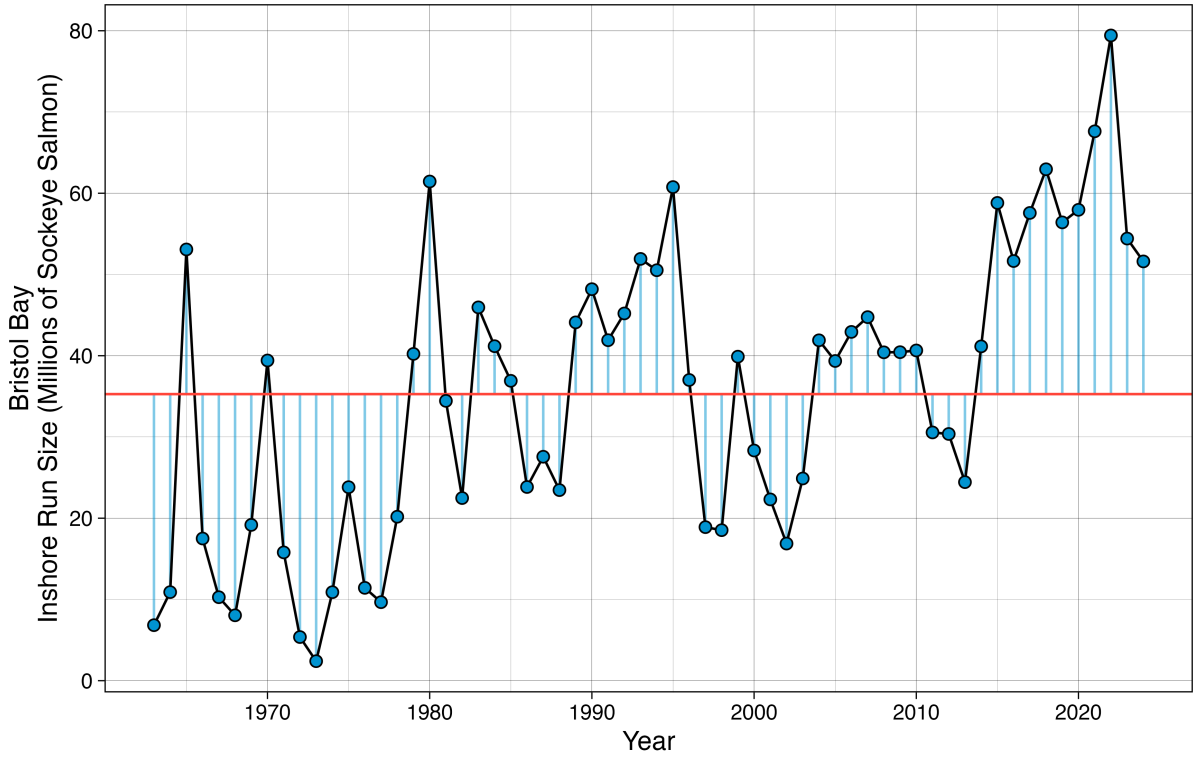

Figure 90: Annual Bristol Bay sockeye salmon inshore run size 1963–2024. Red line is the time series average of 35.3 million sockeye.

Status and trends: The 2024 Bristol Bay preliminary inshore run estimate of 51.6 million sockeye salmon is 12.2% lower than the recent 10-year average of 58.8 million sockeye, and 46.3% higher than the 1963–2023 average of 35.3 million sockeye salmon. The 2024 inshore run represents a continued decrease from the record high Bristol Bay runs sizes observed in 2021–2022 (Figure 90). Despite the decline in run sizes observed in 2023 and 2024, run sizes in each of the last ten years (2015–2024) have all exceeded 50 million salmon and are above the long-term average.

Note: *At this time 2024 Bristol Bay inshore run size numbers are preliminary and subject to change.*

Factors influencing observed trends: The return abundance of Bristol Bay sockeye salmon is positively correlated with the Pacific Decadal Oscillation (Hare et al., 1999), specifically with Egegik and Ugashik district run sizes increasing after the 1976/1977 regime shift (Figure 91). However, recent research has highlighted that relationships between salmon population dynamics and the PDO may not be as consistent as once thought, and may in fact vary over time (Litzow et al., 2020*a*,*b*). The abundance and growth of Bristol Bay sockeye salmon has also been linked to the abundance of pink salmon (*Oncorhynchus gorbuscha*) in the North Pacific (Ruggerone and Nielsen, 2004; Ruggerone et al., 2016).

Implications: The record high inshore runs of Bristol Bay sockeye salmon in 2021–2022, and above-average run sizes 2015–2024, indicate overall positive survival conditions for these stocks while in the ocean. Given evidence that the critical period for sockeye salmon survival occurs during the first summer and winter at sea (Beamish and Mahnken, 2001; Farley et al., 2007, 2011) and the predominant age classes observed for Bristol Bay stocks are 1.2, 1.3, 2.2, and 2.3 (European designation: years in freshwater – years in the ocean), the extremely large 2021–2022 inshore run sizes suggests these salmon experienced positive conditions at entry into the eastern Bering Sea in the summers of 2019 and 2020, and winters of 2019–2020 and 2020–2021. However, the predominance (>80%) of age 1.3 sockeye salmon in the 2023 Bristol Bay run and age 1.2 sockeye salmon in the 2024 run (>80%), combined with the decline in overall run size from 2022 to 2023–2024 suggests that survival for the brood year 2019 cohort was lower than that of the 2017–2018 cohorts. This may reflect less favorable spawning conditions in 2019, freshwater rearing conditions in 2020, or conditions within the eastern Bering Sea at ocean entry in 2021 or the winter of 2021–2022.

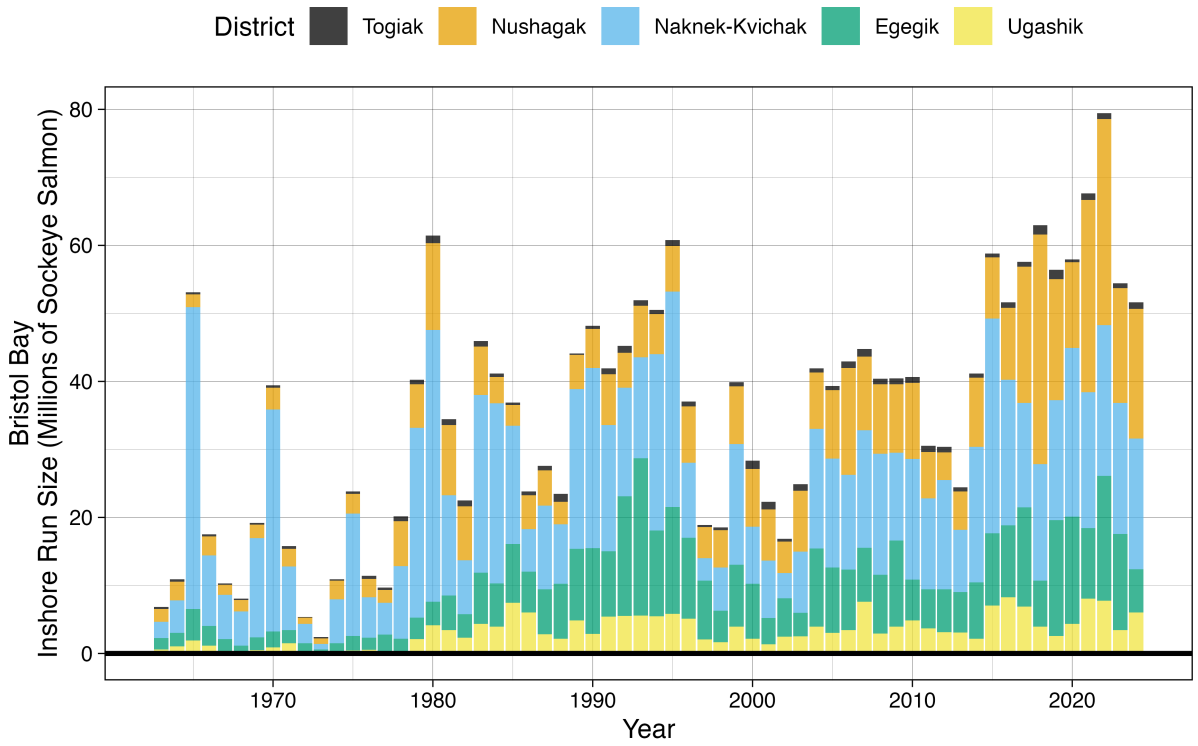

Figure 91: Annual Bristol Bay sockeye salmon inshore run size 1963–2024 by commercial fishing district.

Trends in Alaska Commercial Salmon Catch – Bering Sea

Contributed by George A. Whitehouse
Cooperative Institute for Climate, Ocean, and Ecosystem Studies (CICOES), University of Washington, Seattle WA
Contact: andy.whitehouse@noaa.gov
Last updated: September 2024

Description of indicator: This contribution provides historic and current commercial catch information for salmon of the Bering Sea; it summarizes data and information available in current Alaska Department of Fish & Game (ADF&G) agency reports (e.g., Donnellan, 2024) and on their website[11].

Pacific salmon in Alaska are managed in four regions based on freshwater drainage basins[12]: Southeast/Yakutat, Central (encompassing Prince William Sound, Cook Inlet, and Bristol Bay), Arctic-Yukon-Kuskokwim, and Westward (Kodiak, Chignik, and Alaska peninsula). ADF&G prepares harvest projections for all areas rather than conducting run size forecasts for each salmon run. There are five Pacific salmon species with directed commercial fisheries in Alaska; they are sockeye (*Oncorhynchus nerka*), pink (*O. gorbuscha*), chum (*O. keta*), Chinook (*O. tshawytscha*), and coho (*O. kisutch*) salmon.

Status and trends:
Statewide
Combined catches from directed fisheries on the five salmon species have fluctuated over recent decades but in total have been generally strong statewide (Figure 92). The salmon commercial harvests from 2023 totaled 232.2 million fish, which was 42.8 million more than the preseason forecast of 189.4 million fish. The 2023 total commercial harvest was elevated by the harvest of 154 million pink salmon, primarily from Prince William Sound and Southeast Alaska. While the 2024 harvest data are not yet final, preliminary data from ADF&G for 2024 indicates a statewide total commercial salmon harvest of about 98 million fish (as of 23 September 2024), which is below the preseason projection of 135.7 million fish. In particular, the preliminary statewide pink salmon harvest of 38 million fish is below the harvest projection of 69 million pink salmon.

Bering Sea
Salmon harvests in the Bering Sea are numerically dominated by the catch of sockeye in Bristol Bay (Figure 93). The 2023 Bristol Bay sockeye salmon run of 54.5 million and the harvest of 40.6 million were both greater than the preseason forecast. Escapement goals for sockeye salmon in 2023 were met or exceeded in every drainage in Bristol Bay where escapement was defined. Preliminary data for 2024 from ADF&G indicates that the commercial harvest of Bristol Bay sockeye salmon is strong again, at about 31.6 million fish. For more information on 2024 Bristol Bay sockeye salmon, see Cunningham et al., p. 150. The 2023 commercial harvest of other species in the Bering Sea were 6,900 Chinook salmon, 504,000 chum salmon, 79,800 pink salmon, and 44,500 coho salmon.

Chinook salmon abundance in the Arctic-Yukon-Kuskokwim region has been low since the mid-2000s and remains low. From 2008 to 2023 no commercial periods targeting Chinook salmon were allowed in the Yukon Management Area. In 2023, Chinook salmon did meet the drainage-wide sustainable escapement goal for the Kuskokwim River. Preliminary data for 2024 indicate that Chinook salmon escapement goals will not likely be met for the Yukon Area.

[11] https://www.adfg.alaska.gov/
[12] https://www.adfg.alaska.gov/index.cfm?adfg=commercialbyfisherysalmon.salmonareas

Summer chum salmon did meet the drainage-wide escapement goal in the Yukon Area in 2023, however there was no commercial harvest. There were no commercial harvests for salmon in 2023 on the Yukon River due to the low abundance of Chinook and summer chum salmon. Preliminary data for the Yukon River in 2024 indicates that fall chum salmon are again unlikely to meet escapement goals.

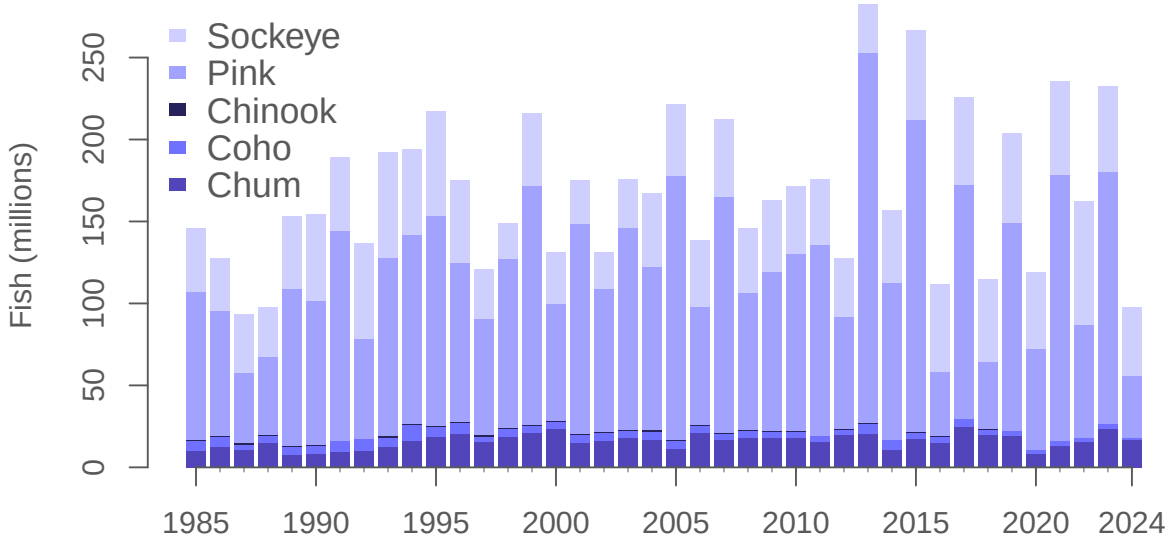

Figure 92: Alaska statewide contemporary commercial salmon catches, 2024 values are preliminary. Source: ADF&G, `http://www.adfg.alaska.gov`. ADF&G is not responsible for errors or deficiencies in the reproduction, subsequent analysis, or interpretation of data.

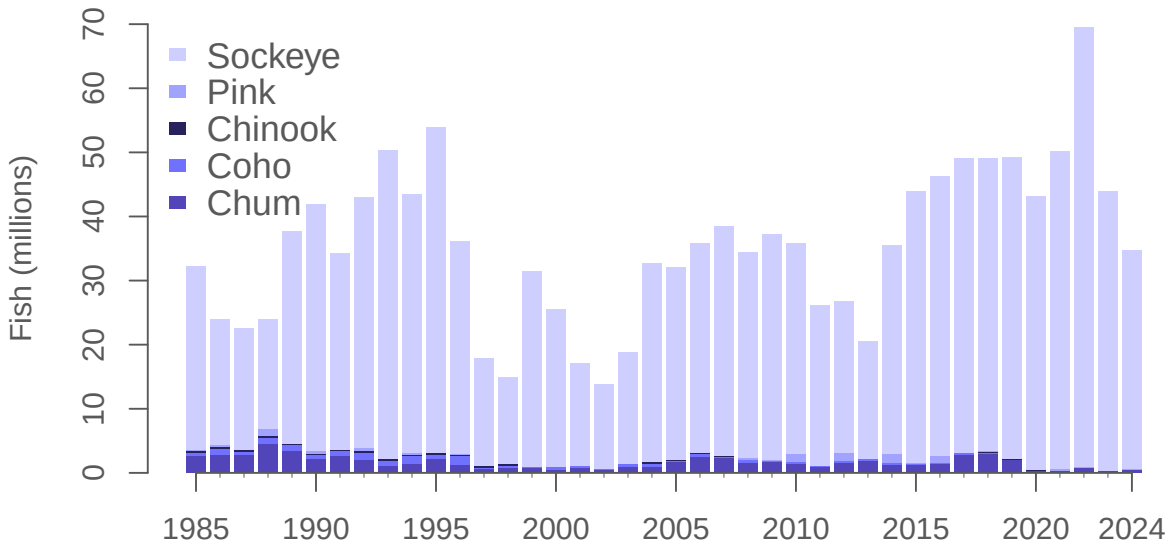

Figure 93: Contemporary commercial salmon catches in the eastern Bering Sea, 2024 values are preliminary. Source: ADF&G, `http://www.adfg.alaska.gov`. ADF&G is not responsible for errors or deficiencies in the reproduction, subsequent analysis, or interpretation of data.

Factors influencing observed trends: Salmon have complex life histories and are subject to stressors in the freshwater and marine environments, and anthropogenic pressures. These forces do not affect

all species and stocks equally or in the same direction, and resolving what is driving the population dynamics of a particular stock is challenging (Rogers and Schindler, 2011). Interannual variation in Alaska statewide total salmon abundance is partly due to the even-year, odd-year cycle in pink salmon, particularly production from the Prince William Sound stock of pink salmon, which typically have larger runs in odd years. Chinook salmon runs have been declining statewide since 2007. Size-dependent mortality during the first year in the marine environment is thought to be a leading contributor to low Chinook run sizes (Beamish and Mahnken, 2001; Graham et al., 2019). Rising sea temperatures and loss of sea ice may be contributing factors leading to slower growth for juvenile Chinook salmon in the eastern Bering Sea (Yasumiishi et al., 2020). Additionally, warming water temperatures and low stream discharges during adult spawner migrations may reduce Chinook salmon reproductive success (Howard and von Biela, 2023). Warming water temperatures have also been linked to lower quality prey and lower energy density of juvenile chum salmon (Kaga et al., 2013; Farley Jr et al., 2024).

Salmon may also be caught as bycatch in Bering Sea groundfish trawl fisheries, most of which are Chinook and chum salmon. The North Pacific Fishery Management Council has implemented a number of management measures and incentives that have largely been successful at reducing Chinook salmon bycatch in groundfish trawl fisheries since their peak in 2007 (Stram and Ianelli, 2015). However, the bycatch of non-chinook salmon (i.e., chum) has trended upward since 2012 and in 2021 was at its highest level since 2005[13].

In the Bering Sea, sockeye salmon are the most abundant salmonid and since the early 2000s, they have had consistently strong runs, which have supported large harvests. Bristol Bay sockeye salmon display a variety of life history types and utilize a diverse range of habitats for spawning (Hilborn et al., 2003). Productivity within these various habitats may be affected differently depending upon varying conditions, such as climate (Mantua et al., 1997), so more diverse sets of populations provide greater overall stability (Schindler et al., 2010). The abundance of Bristol Bay sockeye salmon may also vary over centennial time scales, with brief periods of high abundance separated by extended periods of low abundance (Schindler et al., 2006).

Implications: Salmon have important influences on Alaska marine ecosystems through interactions with marine food webs as predators on lower trophic levels and as prey for other species such as Steller sea lions. In years of great abundance, salmon may exploit prey resources more efficiently than their competitors. In odd years when pink salmon are most abundant they can initiate pelagic trophic cascades (Batten et al., 2018) which may negatively impact the growth and population dynamics of several other species, including other salmonids, forage fishes, seabirds, and whales (Ruggerone et al., 2023; Rand and Ruggerone, 2024). A biennial pattern in seabird reproductive success has been attributed to a negative relationship with years of high pink salmon abundance (Springer and van Vliet, 2014). Directed salmon fisheries are economically important for the state of Alaska. The trend in total statewide salmon catch in recent decades has been for generally strong harvests, despite annual fluctuations and lower catches for some species in specific management areas.

Measures to reduce salmon bycatch can affect the spatial distribution of groundfish trawl fisheries through area closures and incentives to avoid bycatch. When the aggregate Chinook salmon run size in the Kuskokwim, Unalakleet, and Upper Yukon Rivers is less than 250,000, a lower limit to Chinook bycatch is imposed on the pollock fishery.

[13] https://www.npfmc.org/wp-content/PDFdocuments/bycatch/BeringSeaSalmonBycatchFlyer.pdf

Groundfish

Eastern and Northern Bering Sea Groundfish Condition

Contributed by Bianca Prohaska, Rebecca Howard, and Sean Rohan
Resource Assessment and Conservation Engineering Division
Alaska Fisheries Science Center, NOAA Fisheries
Contact: sean.rohan@noaa.gov
Last updated: September 2024

Description of indicator: Length-weight residuals represent how heavy a fish is per unit body length and are an indicator of somatic growth variability (Brodeur et al., 2004). Therefore, length-weight residuals can be considered indicators of prey availability, growth, general health, and habitat condition (Blackwell et al., 2000; Froese, 2006). Positive length-weight residuals indicate better condition (i.e., heavier per unit length) and negative residuals indicate poorer condition (i.e., lighter per unit length) (Froese, 2006). Fish condition calculated in this way reflects realized outcomes of intrinsic and extrinsic processes that affect fish growth, which can have implications for biological productivity through direct effects on growth and indirect effects on demographic processes, such as reproduction and mortality (e.g., Rodgveller, 2019; Barbeaux et al., 2020).

The groundfish morphometric condition indicator is calculated from paired fork lengths (mm) and weights (g) of individual fish that were collected during bottom trawl surveys of the eastern Bering Sea (EBS) shelf and northern Bering Sea (NBS), which were conducted by the Alaska Fisheries Science Center's Resource Assessment and Conservation Engineering (AFSC/RACE) Groundfish Assessment Program (GAP). Fish condition analyses were applied to walleye pollock (*Gadus chalcogrammus*), Pacific cod (*G. macrocephalus*), arrowtooth flounder (*Atheresthes stomias*), yellowfin sole (*Limanda aspera*), flathead sole (*Hippoglossoides elassodon*), northern rock sole (*Lepidopsetta polyxystra*), and Alaska plaice (*Pleuronectes quadrituberculatus*) collected in bottom trawls at standard survey stations (Figure 94). Alaska plaice were not sampled in 2024. For these analyses and results, survey strata 31 and 32 were combined as stratum 30; strata 41, 42, and 43 were combined as stratum 40; and strata 61 and 62 were combined as stratum 60. Northwest survey strata 82 and 90 were excluded from these analyses.

To calculate indicators, length-weight relationships were estimated from linear regression models based on a log-transformation of the exponential growth relationship, $W = aL^b$, where W is weight (g) and L is fork length (mm) for all areas for the period 1997–2024 (EBS: 1997–2024, NBS: 2010, 2017, 2019, 2021–2023). Unique intercepts (a) and slopes (b) were estimated for each survey stratum, sex, and interaction between stratum and sex to account for sexual dimorphism and spatial-temporal variation in growth and bottom trawl survey sampling. Length-weight relationships for 100-250 mm fork length walleye pollock (corresponding with ages 1–2 years) were calculated separately from adult walleye pollock ($>$250 mm). Residuals for individual fish were obtained by subtracting observed weights from bias-corrected weights-at-length that were estimated from regression models. Length-weight residuals from each stratum were aggregated and weighted proportionally to total biomass in each stratum from area-swept expansion of mean bottom-trawl survey catch per unit effort (CPUE; i.e., design-based stratum biomass estimates). Variation in fish condition was evaluated by comparing average length-weight residuals among years. To minimize the influence of unrepresentative samples on indicator calculations, combinations of species, stratum, and year with a sample size $<$10 were used to fit length-weight regressions, but were excluded

from calculating length-weight residuals for both the EBS and NBS. Morphometric condition indicator time series, code for calculating the indicators, and figures showing results for individual species are available through the *akfishcondition* R package and GitHub repository[14].

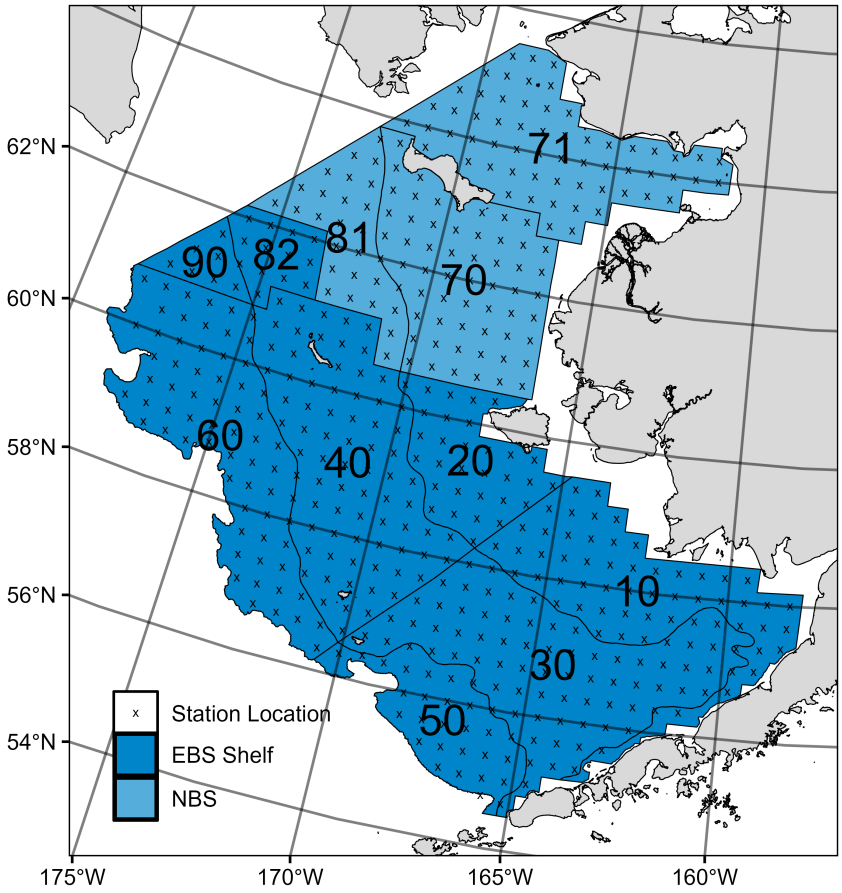

Figure 94: NOAA Alaska Fisheries Science Center summer bottom trawl survey strata (10–90) and station locations (x) on the eastern Bering Sea (EBS) shelf and in the northern Bering Sea (NBS).

Status and trends: Fish condition, indicated by length-weight residuals, has varied over time for all species examined in the EBS (Figures 95 and 96). Since 2022, a declining trend in condition was observed in small walleye pollock (100-250 mm), northern rock sole, and Pacific cod; however, these species were still within one standard deviation of the historical mean. Large walleye pollock (>250 mm), yellowfin sole, and arrowtooth flounder exhibited an increase in condition from 2023 to 2024, while little to no change in condition was observed in flathead sole. Despite observing increasing or decreasing trends in condition among most of the species examined, the 2024 mean condition of all species, except for northern rock sole, fell within two standard errors of the mean condition in 2023. Furthermore, the mean condition of every species fell within one standard deviation of the historical mean in 2024 (Figure 95).

In the EBS in 2024, condition was negative for all species examined across most strata, except for yellowfin sole on the inner and middle shelf (strata 10 and 30), and arrowtooth flounder on the southern outer shelf (stratum 50) (Figure 96).

[14] `https://github.com/afsc-gap-products/akfishcondition`

The NBS was not surveyed in 2024; however, in the NBS in 2023, positive condition was observed for large walleye pollock (>250 mm), which has been increasing since 2021. The remaining species exhibited near-average condition in the NBS in 2023, except for yellowfin sole, which exhibited negative condition and has been declining since 2019 (Figure 97).

In 2023 large walleye pollock (>250 mm) condition was positive in all NBS strata, whereas condition was previously negative in all strata from 2021–2022. Pacific cod, small walleye pollock (100-250 mm), Alaska plaice, and yellowfin sole condition have been consistently negative across all strata since 2021, with a notable exception in 2023 of positive condition for Pacific cod in the inner southern NBS shelf, and Alaska plaice in the northern inner NBS shelf and Norton Sound (Figure 98).

Factors influencing observed trends: Similar to trends observed in 2023, temperature appears to influence morphological condition of species in the EBS, so near-average cold pool extent and water temperatures in 2024 likely played a role in the near-average condition (within 1 SD of the mean) for all species examined in the EBS. Historically, particularly cold years tend to correspond with negative condition, while particularly warm years tend to correspond to positive condition. For example, water temperatures were particularly cold during the 1999 Bering Sea survey, a year in which negative condition was observed for all species for which data were available. In addition, spatiotemporal factor analyses suggest the morphometric condition of age-7 walleye pollock is strongly correlated with cold pool extent in the EBS (Grüss et al., 2021). In recent years, warm temperatures across the Bering Sea shelf, since the record low seasonal sea ice extent in 2017–2018 and historical cold pool area minimum in 2018 (Stabeno and Bell, 2019), may have influenced the positive trend in the condition of several species from 2016 to 2019. However, despite near-average temperature in 2023 large walleye pollock (>250 mm) condition in the EBS was the second lowest recorded over the time series. In 2024 temperature was near-average again, and while large walleye pollock (>250 mm) condition was still negative, it was less negative than that observed in 2023.

Although warmer temperatures may increase growth rates if there is adequate prey to offset temperature-dependent increases in metabolic demand, growth rates may also decline if prey resources are insufficient to offset temperature-dependent increases in metabolic demand. The influence of temperature on growth rates depends on the physiology of predator species, prey availability, and the adaptive capacity of predators to respond to environmental change through migration, changes in behavior, and acclimatization. For example, elevated temperatures during the 2014–2016 marine heatwave in the Gulf of Alaska led to lower growth rates of Pacific cod and lower condition because available prey resources did not make up for increased metabolic demand (Barbeaux et al., 2020).

Other factors that could affect morphological condition include survey timing, stomach fullness, fish movement patterns, sex, and environmental conditions (Froese, 2006). The starting date of annual length-weight data collections has varied from late May to early June and ended in late July-early August in the EBS, and mid-August in the NBS. Although we account for some of this variation by using spatially-varying coefficients in the length-weight relationship, variation in condition could relate to variation in the timing of sample collection within survey strata. Survey timing can be further compounded by seasonal fluctuations in reproductive condition with the buildup and depletion of energy stores (Wuenschel et al., 2019). Another consideration is that fish weights sampled at sea include gut content weights, so variation in gut fullness may influence weight measurements. Since feeding conditions vary over space and time, prey consumption rates and the proportion of total body weight attributable to gut contents may be an important factor influencing the length-weight residuals.

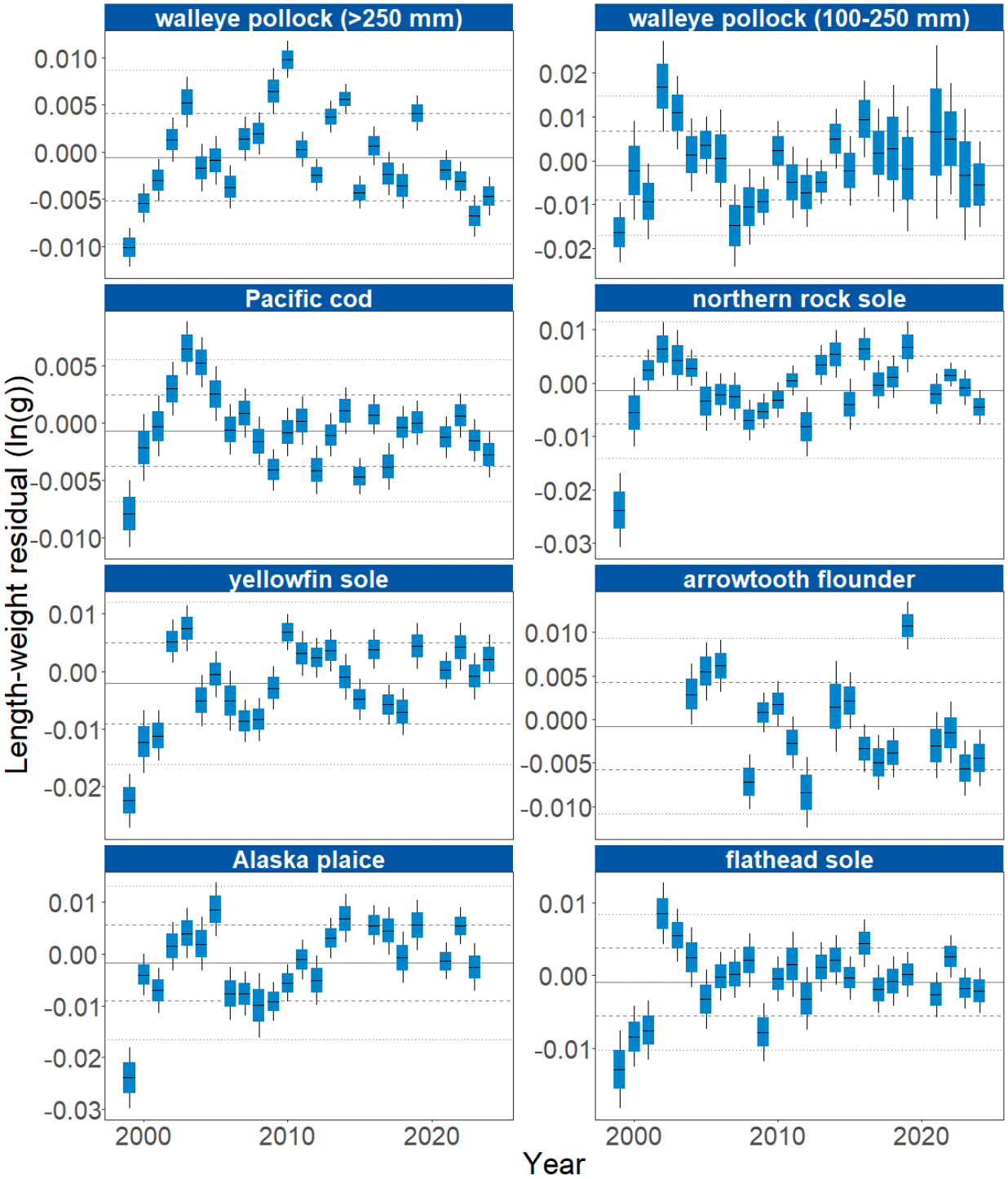

Figure 95: Morphometric condition of groundfish species collected during AFSC/RACE GAP standard summer bottom trawl surveys of the eastern Bering Sea shelf (1999–2024) based on residuals of length-weight regressions. The dash in the blue boxes denote the mean for that year, the box denotes one standard error, and the lines on the boxes denote two standard errors. Lines on each plot represent the historical mean, dashed lines denote one standard deviation, and dotted lines denote two standard deviations.

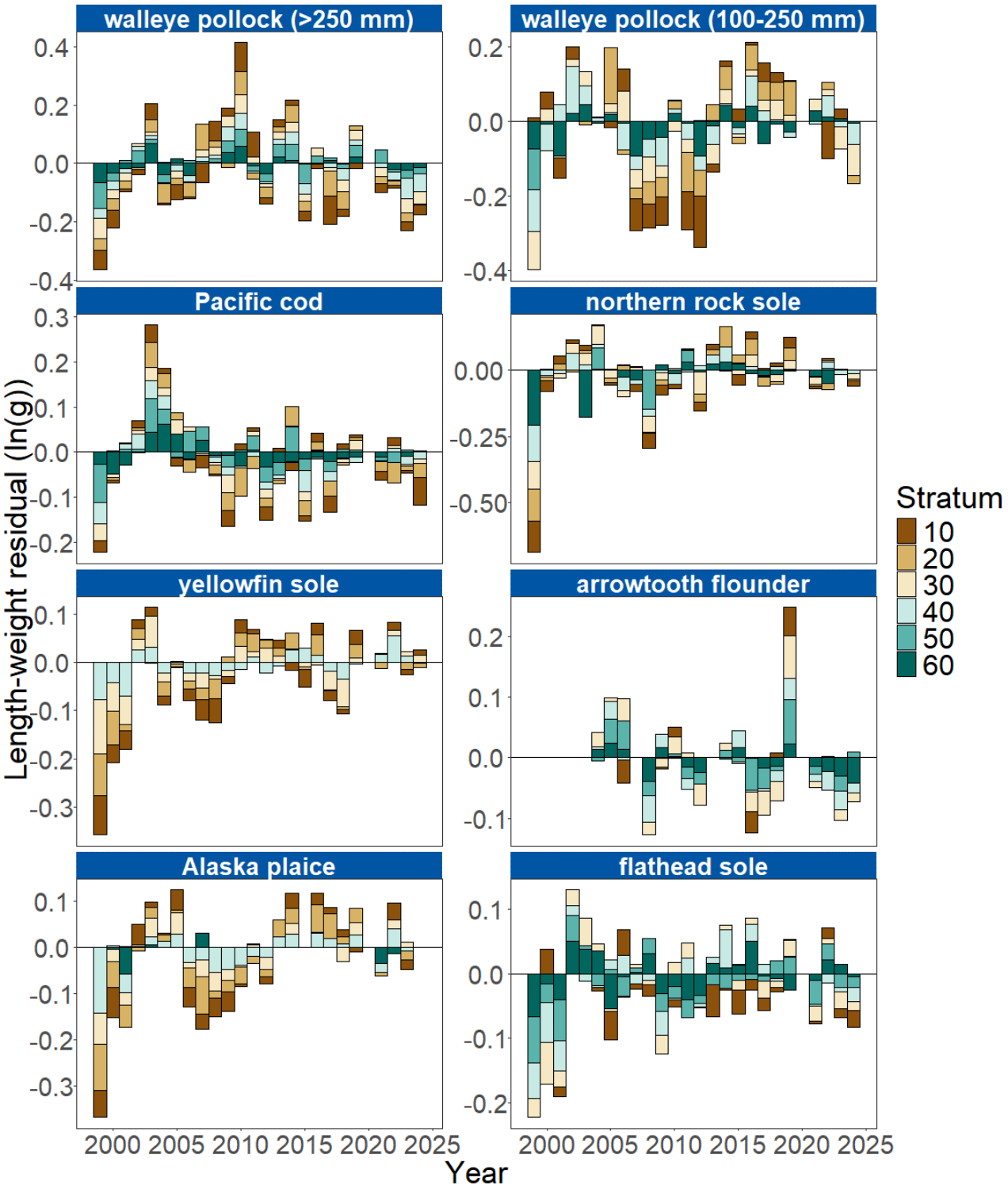

Figure 96: Length-weight residuals by survey stratum (10–60) for seven eastern Bering Sea shelf groundfish species and age 1–2 walleye pollock (100–250 mm) sampled in the AFSC/RACE GAP standard summer bottom trawl survey, 1999–2024. Length-weight residuals are not weighted by stratum biomass.

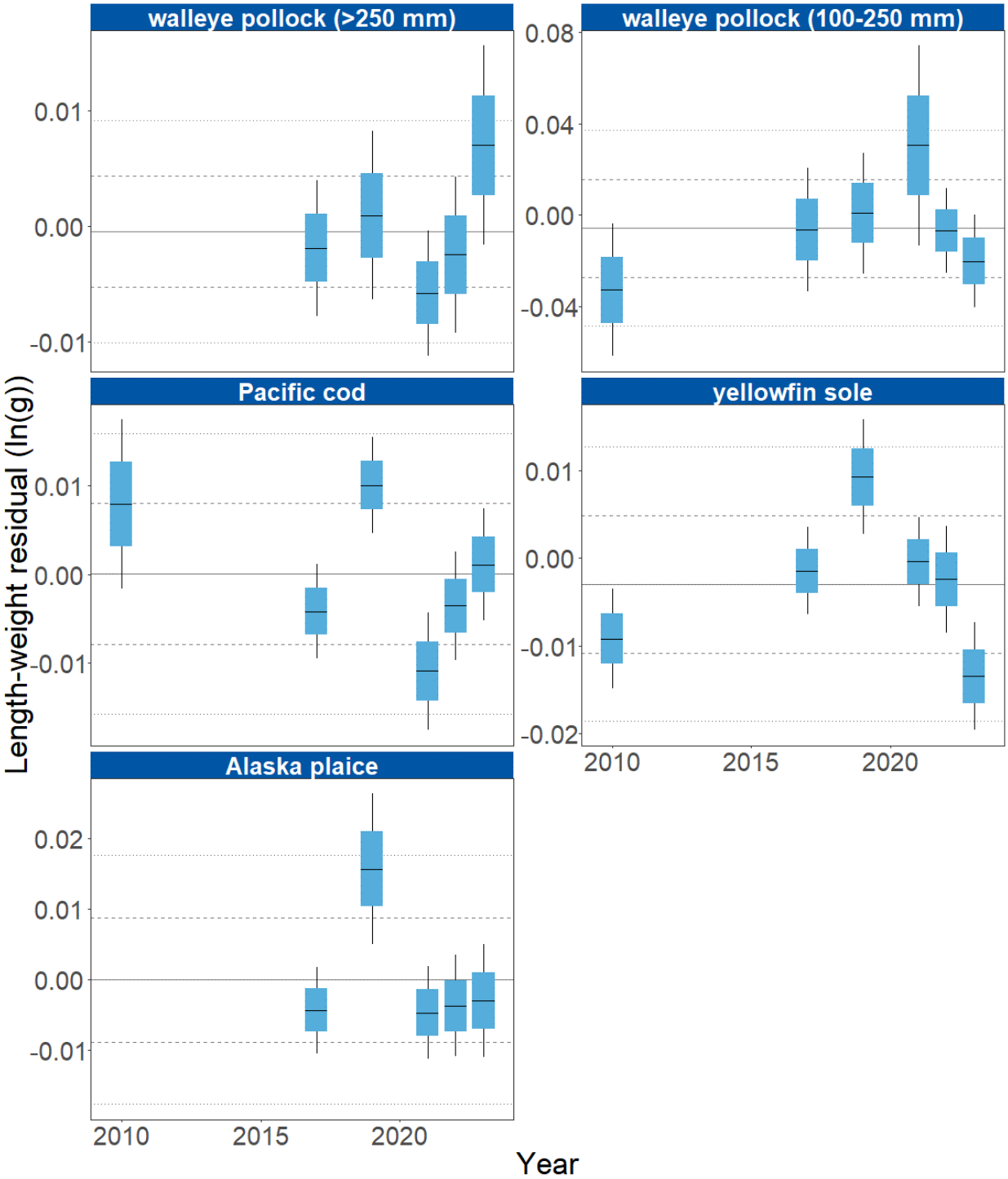

Figure 97: Morphometric condition of groundfish species collected during AFSC/RACE GAP standard summer bottom trawl surveys of the northern Bering Sea shelf (2010, 2017, 2019 and 2021–2023) based on residuals of length-weight regressions. The dash in the blue boxes denote the mean for that year, the box denotes one standard error, and the lines on the boxes denote two standard errors. Lines on each plot represent the historical mean, dashed lines denote one standard deviation, and dotted lines denote two standard deviations.

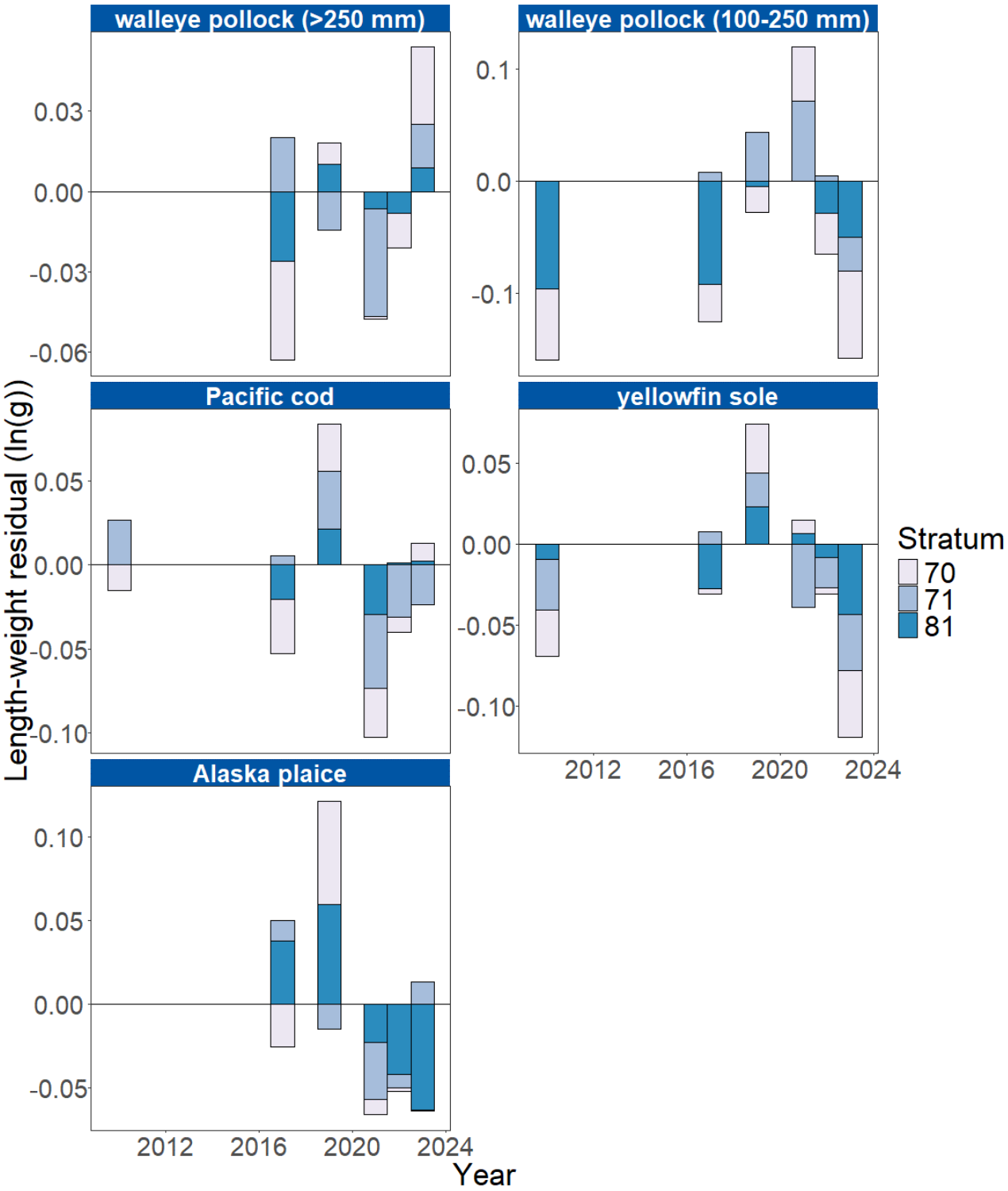

Figure 98: Length-weight residuals by survey stratum (70, 71, and 81) for four northern Bering Sea shelf groundfish species and age 1–2 walleye pollock (100–250 mm) sampled in the AFSC/RACE GAP standard summer bottom trawl survey during 2010, 2017, 2019, and 2021–2023. Length-weight residuals are not weighted by stratum biomass.

Finally, although the condition indicators characterize temporal variation in morphometric condition for important fish species in the EBS and NBS, they do not inform the mechanisms or processes behind the observed patterns.

Implications: Fish morphometric condition can be considered an indicator of ecosystem productivity with implications for fish survival, maturity, and reproduction. For example, in Prince William Sound, the pre-winter condition of herring may determine their overwinter survival (Paul and Paul, 1999), differences in feeding conditions have been linked to differences in morphometric condition of pink salmon in Prince William Sound (Boldt and Haldorson, 2004), variation in morphometric condition has been linked to variation in maturity of sablefish (Rodgveller, 2019), and lower morphometric condition of Pacific cod was associated with higher mortality and lower growth rates during the 2014–2016 marine heat wave in the Gulf of Alaska (Barbeaux et al., 2020). Condition can also be an indicator of stock status relative to carrying capacity because morphometric condition is expected to be high when the stock is at low abundance and low when the stock is at high abundance because of the effects of density-dependent competition (Haberle et al., 2023). Thus, the condition of EBS and NBS groundfishes may provide insight into ecosystem productivity as well as fish survival, demographic status, and population health. However, survivorship is likely affected by many factors not examined here.

Another important consideration is that fish condition was computed for all sizes of fishes combined, except in the case of walleye pollock. Examining condition of early juvenile stage fishes not yet recruited to the fishery, or the condition of adult fishes separately, could provide greater insight into the value of length-weight residuals as an indicator of individual health or survivorship (Froese, 2006), particularly since juvenile and adult walleye pollock exhibited opposite trends in condition in the EBS this year.

The near-average condition for most species in 2024 may be related to the near historical average temperatures observed. However, trends in recent years such as prolonged warmer water temperatures following the marine heat wave of 2014–2016 (Bond et al., 2015) and reduced sea ice and cold pool areal extent in the eastern Bering Sea (Stabeno and Bell, 2019) may affect fish condition in ways that have not yet been determined. Additionally, periods of high fishing mortality that reduce population biomass are likely to increase body condition because of the compensatory alleviation of density-dependent competition (Haberle et al., 2023). As we continue to add years of length-weight data and expand our knowledge of relationships between condition, growth, production, survival, and the ecosystem, these data may increase our understanding of the health of fish populations in the EBS and NBS.

Research priorities:
Recent studies have sought to improve the understanding of factors that affect fish growth and morphometric condition in the EBS (e.g., Oke et al., 2022) although significant knowledge gaps remain for numerous species and life history stages. Research is underway to evaluate connections between morphometric condition indices, temperature, and density-dependent competition.

Summer Food Habits of Walleye Pollock and Pacific Cod

Contributed by Kerim Aydin
Resource Ecology and Fishery Management Division
Alaska Fisheries Science Center, NOAA Fisheries
Contact: kerim.aydin@noaa.gov
Last updated: October 2024

Description of indicator: Stomachs of walleye pollock (*Gadus chalcogrammus*) and Pacific cod (*G. macrocephalus*) have been collected on the Alaska Fisheries Science Center's eastern Bering Sea (EBS) shelf survey between 1984–2024; samples were preserved in formalin and prey contents identified to the lowest resolvable taxonomic category and weighed. For key prey items such as snow crab (*Chionoecetes opilio*), prey size (standard length for fish and carapace width for crabs) was measured when sufficiently intact prey samples were present in predator stomach samples. To estimate diet proportions for the population, samples are stratified by length and survey stratum and weighted by the survey biomass for each length class and stratum and estimated ration for each size class. Collection, analysis, and stratification methods are described in Livingston et al., 2017 while ration estimation is described in Holsman and Aydin, 2015.

Status and trends: Summer pollock diets for the EBS primarily consist of euphausiids, copepods, and other plankton throughout the time series (Figure 99). Euphausiids were lower in importance from 2004–2011; in particular in 2010–2011 both euphausiids and copepods were low compared to "other" plankton, which was dominated by amphipods in 2010–2011. In 2024, euphausiids declined in region-wide diets compared to copepods. Cannibalism was a larger diet component in the 1990s and declined to historic lows in 2018 and 2022–2024.

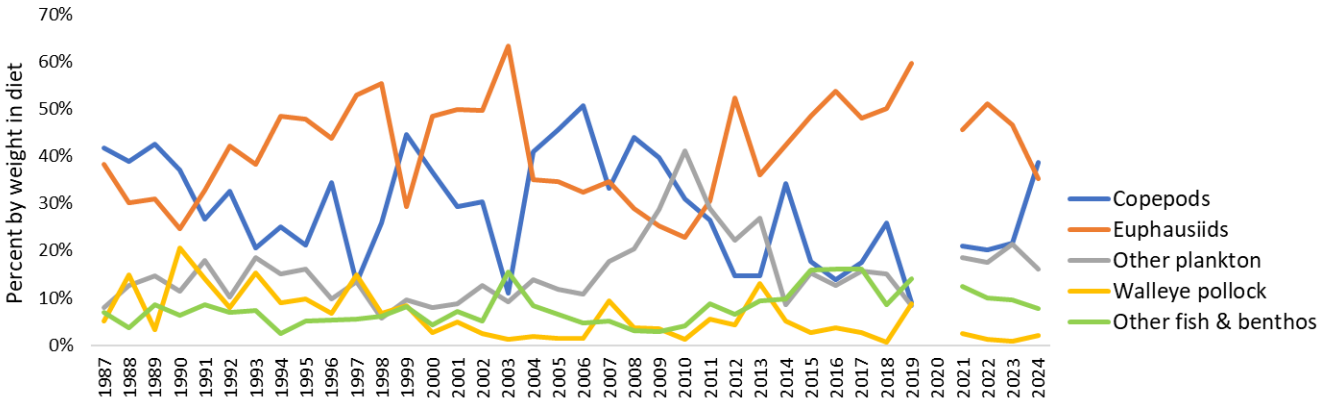

Figure 99: Percent by weight in diet of major prey types of walleye pollock in the eastern Bering Sea, weighted by survey stratum and predator survey biomass in each stratum.

Pacific cod diets include a range of fish and crab species (Figure 100). Feeding on walleye pollock was highest in the late 1980s, declined significantly from 2006–2016, before increasing again in 2019–2024. Consumption of snow crab was at a high level from 2014–2018 and generally average from 2021–2024.

When multiplied by Pacific cod diet and ration, the snow crab consumption rate (Figure 101) showed particularly high consumption from 2014–2016 and in 2018. The size of crab in cod stomachs (Figure 102) show sizes classes corresponding with crab measured directly during the bottom trawl survey, with the addition of potential early signs of crab recruitment showing in cod stomachs before appearing in the survey (e.g., in 2021).

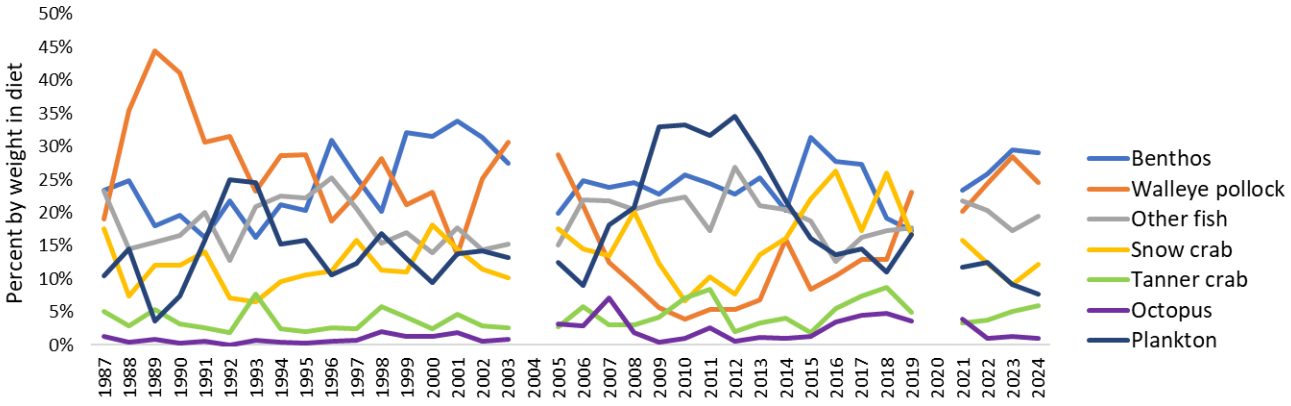

Figure 100: Percent by weight in diet of major prey types of Pacific cod in the eastern Bering Sea, weighted by survey stratum and predator survey biomass in each stratum.

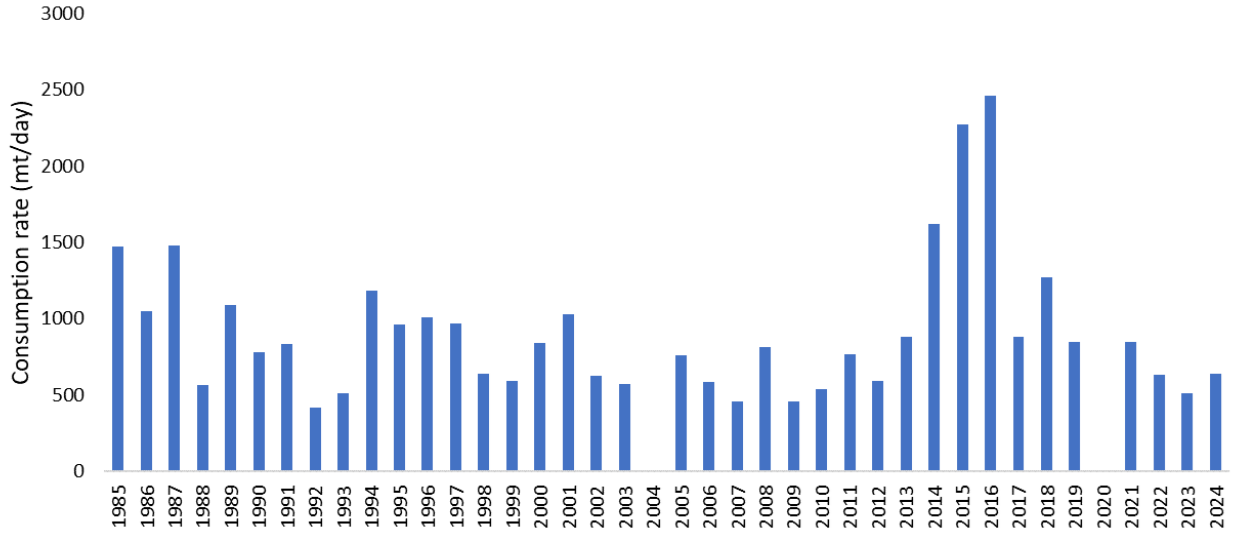

Figure 101: Daily consumption rate of snow crab by Pacific cod, calculated by multiplying the diet proportion in each survey strata with cod biomass-at-length from the survey data and temperature-specific cod daily ration-at-length using methods described in Holsman and Aydin, 2015.

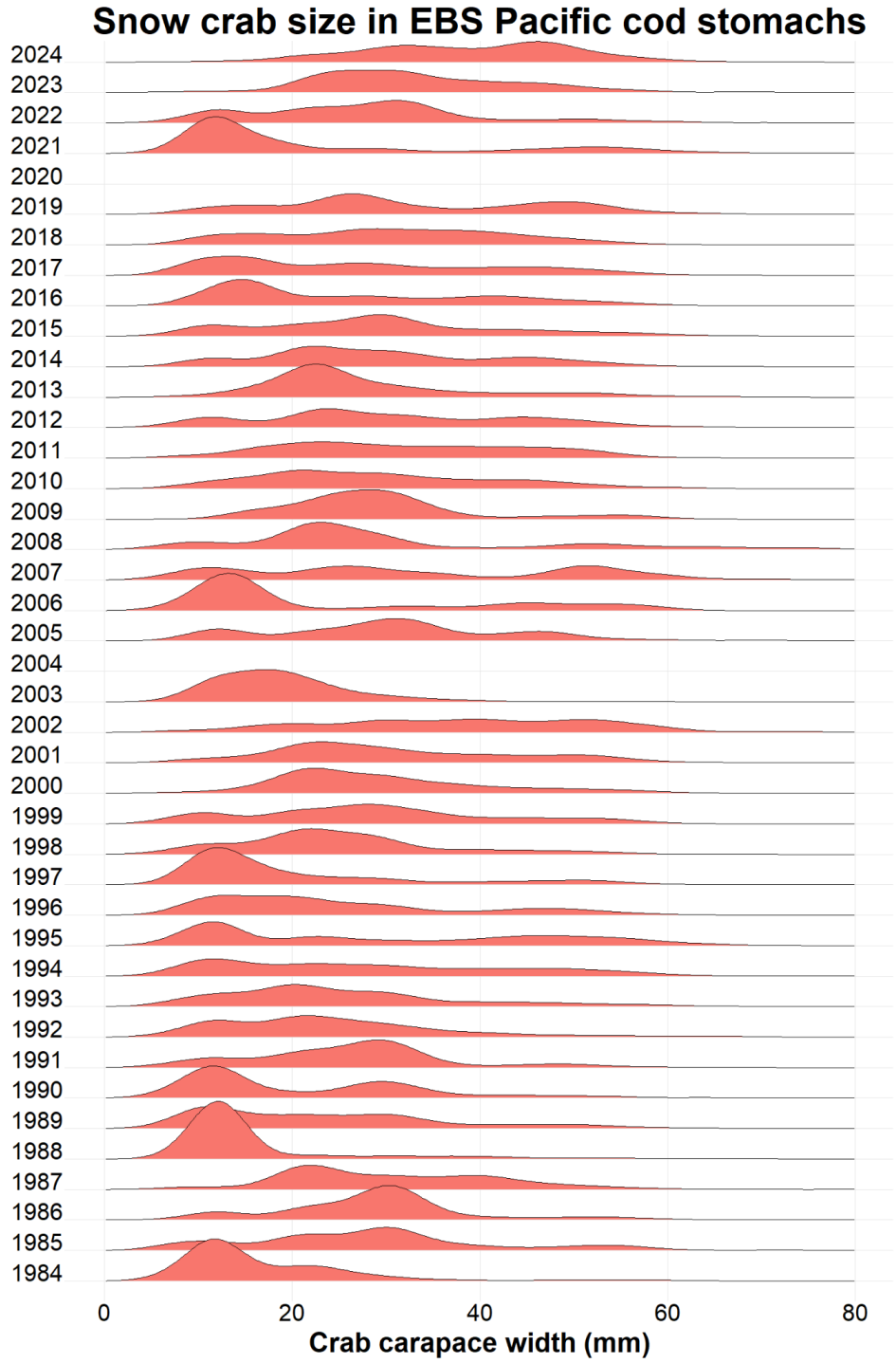

Figure 102: Carapace width of measurable snow crab (*Chionoecetes opilio*) and unidentified *Chionoecetes* spp. removed from Pacific cod stomachs in the EBS, 1984–2024. Species identification is size-dependent; unidentified *Chionoecetes* spp. represent the smallest carapace widths and were mostly found in areas overlapping with snow crab.

Factors influencing observed trends: When viewing population-level consumption across the entire EBS, shifts in diet proportion may come from changes in prey populations within a single strata; however, the shifts may also be due to changes in predator distribution between strata or differences in the size composition of the predator population as age classes with differing feeding ontogeny move through the ecosystem.

In particular, in 2024 the high proportion of copepods in pollock diets (Figure 99) was due to a larger proportion of the total pollock biomass being distributed over the northwest outer shelf, where larger oceanic copepods from the Bering Sea shelf break and basin form the bulk of diets in most years. It is not known if this distribution shift is due to better-than-typical foraging of copepods on the outer shelf versus poorer production in the middle domain, where euphausiids are the prominent diet item. The other major ecosystem shift visible in the data came in 2009–2011 when both euphausiids and copepods were lower in diets in favor of "other" zooplankton, primarily consisting of amphipods. This shift came with historic highs in the EBS cold pool volume and represents the influence of more Arctic zooplankton species associated with the larger cold pool.

For Pacific cod, there was a notable decline of pollock in diets from 2008–2013, again likely due to the large cold pool limiting overlap between these species (Figure 100). Pacific cod diets showed increased plankton consumption during these years, in particular focusing on colder-water shrimp species. From 2014–2019, the prominence of snow crab in diets (Figure 101) was likely a bottom-up effect, as a large cohort of crab were observed in both the stomachs and survey data. Similarly, the changes in crab carapace width distribution over time (Figure 102) was likely driven by these crab recruitment events.

Implications: Changes in diet composition of fish may be an indicator of fish health and condition, growth, or later recruitment, and may also signal potential changes in productivity that would come with longer-term climate change. Snow crab consumption by Pacific cod may be an early indicator of the recruitment strength of incoming crab cohorts.

Patterns in Foraging and Energetics of Bering Sea Walleye Pollock, Pacific Cod, Arrowtooth Flounder, and Pacific Halibut

Contributed by Kirstin K. Holsman[1], Cheryl Barnes[2], Kerim Aydin[1], Ben Laurel[3], Jon Reum[1], and Anna Sulc[4]
[1]Resource Ecology and Fishery Management Division, Alaska Fisheries Science Center, NOAA Fisheries, Seattle, WA
[2]Coastal Oregon Marine Experiment Station, Oregon State University, Newport, OR
[3]Resource Assessment and Conservation Engineering Division, Alaska Fisheries Science Center, NOAA Fisheries, Newport, OR
[4]University of Washington, Seattle, WA
Contact: kirstin.holsman@noaa.gov
Last updated: October 2024

Description of indicator: We report trends in metabolic demand from an adult bioenergetics model for groundfish in the eastern Bering Sea (EBS) (Ciannelli et al., 1998; Holsman et al., 2019; Holsman and Aydin, 2015) and patterns in diet composition from the NOAA Fisheries Alaska Fisheries Science Center's Food Habits database of fish diets collected during summer bottom trawl surveys in the SEBS and NBS. Bioenergetics-based indices were calculated for individual predator stomach samples using bioenergetics models. Samples were averaged by 1-cm predator length bins across stations within a strata and then extrapolated to the population level using annual proportional biomass for each bin in each strata based on bottom trawl surveys (see Ciannelli et al., 1998; Holsman et al., 2019; Holsman and Aydin, 2015, and Livingston et al., 2017 for more information).

Bioenergetic diet indices collectively indicate changes in foraging and growing conditions; relative foraging rate (RFR) reflects the ratio of observed food consumption (specific consumption rate; C_ggd) to a theoretical temperature and size-specific maximum consumption rate from laboratory feeding experiments. Declines in this index can reflect decreases in prey availability or prey switching to more energetically valuable prey. Therefore we also present mean diet energy density (mnEDJ_g) (J per gram) which reflects the average energetic density of prey in stomachs sampled from across the EBS in a given year. Less favorable foraging patterns would be reflected in declines in RFR when average diet energy density (mnEDJ_g) remains the same or also declines in a given year. Metabolic demand (R_ggd; g per g predator per day) generally increases with temperature and indicates the basal energetic requirements of the fish. Finally, scope for growth (G_ggd) integrates metabolic demand, prey energy, and relative consumption rates to indicate how changes in temperature and foraging collectively influence (potential) growth.

More information can be found at `https://github.com/kholsman/AK_climate_engergetics`.

Status and trends: We observe directional trends in consumption and potential growth that reflect climate-driven changes to metabolic demand and trophic interactions and which indicate declining conditions for groundfish in the SEBS and NBS during recent marine heatwave (MHW) years. All six indices suggest that MHWs across the EBS resulted in poor foraging conditions for pollock (*Gadus chalcogrammus*; hereafter "pollock") and Pacific cod (*Gadus macrocephalus*; hereafter "P. cod"). For adult pollock, prey limitation during MHW years is indicated by multiple consumption indices including observed and relative foraging rates ('C_ggd' and 'RFR', respectively), and is reflected in a low scope for

growth (i.e., 'G_ggd' or "growth potential") index for pollock. In recent years cooler conditions appear favorable for foraging and growth, with most indices, except scope for growth, returning to long-term averages (1990–2010). Growth potential for adult pollock and juvenile P. cod remains below the historical averages, while Pacific halibut (*Hippoglossus stenolepis*), and to a lesser extent adult P. cod, appears to have offset warming impacts with increases in consumption of energetically valuable prey and continue to forage on energetically valuable prey through cooler, more favorable conditions.

Thermal experience (species-specific survey biomass weighted mean bottom temperature; 'TempC') of all four groundfish species in the EBS increased during MHW years (Figure 103), with thermal experience in 2018 being the highest in the 30+ year time series (Figure 104). Relative metabolic demand ('R_ggd') reflects the climate- and behaviorally- mediated changes to thermal experience. Accordingly, we observe divergent trends in metabolic demand in the SEBS relative to the NBS, and between juvenile and adults of each species. In the SEBS, metabolic demand for adult groundfish has returned to more average conditions (1982–2010) (Figure 105) and is lower than in the recent warm period with 2020–2023 rates approximately 5% and -2% different than historical values for pollock and P.cod, respectively. In the NEBS, metabolic demand for adult groundfish has returned from extremely high rates during the MHW to near average historical (1982–2010) rates with 2020–2023 rates approximately -2% and 8% different than historical mean values for pollock and P. cod, respectively.

There is evidence of MHW induced declines in foraging efficiency of multiple groundfish species in the SEBS (Figures 104 and 105). Specifically, observed consumption rates (g of prey consumed per g body weight of the predator per day) and Relative Foraging Rates (i.e., the ratio of observed consumption rates relative to theoretical maximum consumption rates given the size and thermal experience of the fish) declined markedly during MHW years and have partially recovered more recently (2020–2023) except for juvenile and adult pollock (Figures 104 and 105). In contrast, adult P. cod continue to exhibit foraging rates near the long-term average, suggesting redistribution to the NBS during MHW years may have helped reduce metabolic demand and maintained sufficient access to prey.

Observed consumption rates for pollock and P. cod tend to exhibit a dome shaped relationship with bottom temperature, peaking around 2.5-2.75°C and declining at higher and lower temperatures. Arrowtooth flounder similarly exhibits this pattern but with a peak at 3.5°C. Combined with exponential increases in metabolism with warming, the integrated outcome of these changes is a peak in adult P. cod and halibut scope for growth around 2.8°C, while for juvenile P. cod and juvenile and adult pollock, the scope for growth declines with increasing temperatures (Figure 106). This is reflected in annual patterns, where we observed an overall decline in scope for growth for juvenile pollock and P. cod during the MHW years (2016–2019), and low scope for growth of adult P. cod since 2010, and adult pollock since 2015; Figures 104 and 105). Recent diet patterns indicate higher growth potential for pollock in recent years.

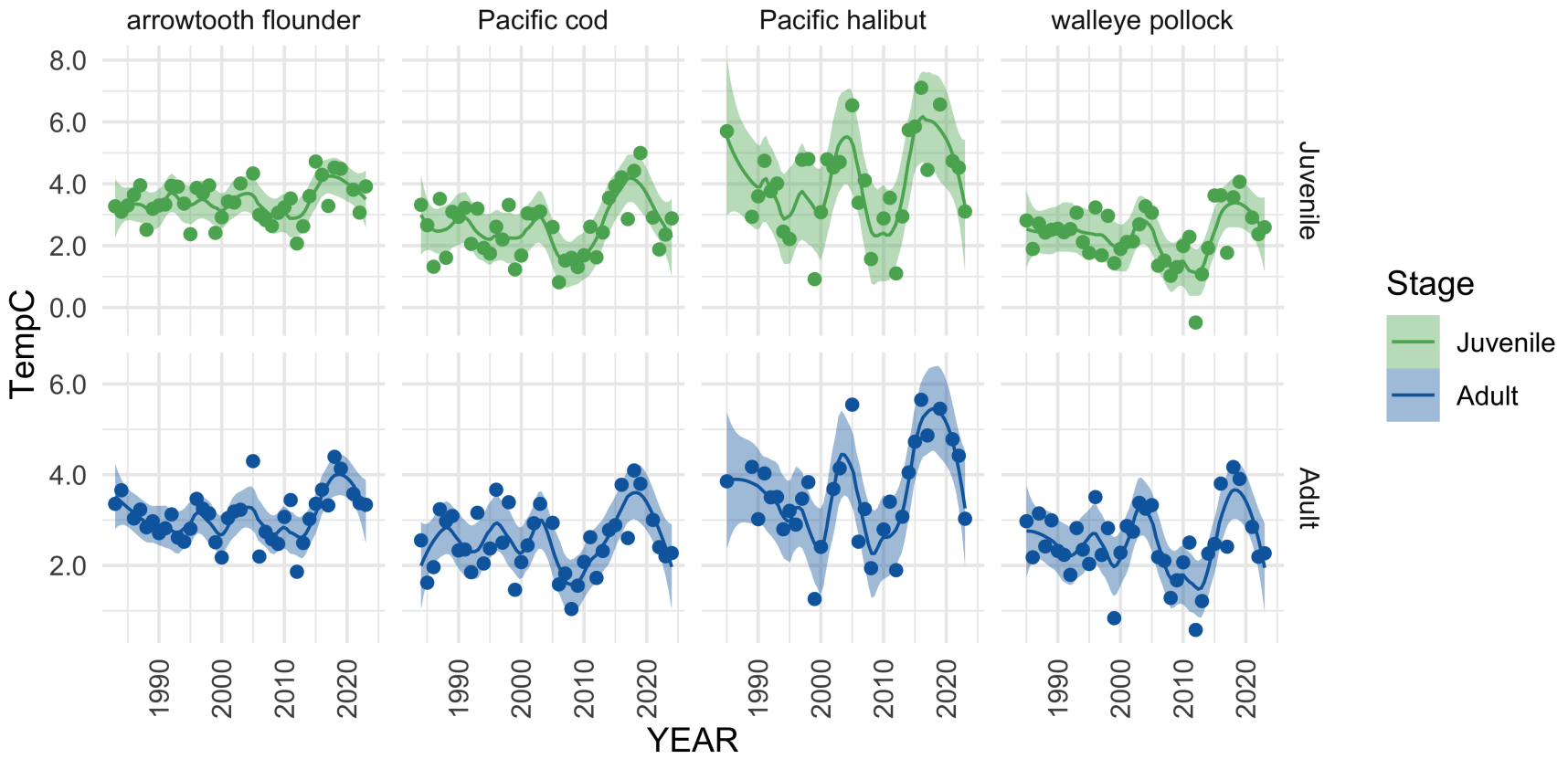

Figure 103: Average thermal experience (TempC) groundfish species in the EBS (dots). The spline represents a loess smoother for juvenile (top row) and adult (bottom row) fish. Data are based on biomass-weighted bottom temperature for samples collected during NOAA NMFS AFSC bottom-trawl summer surveys.

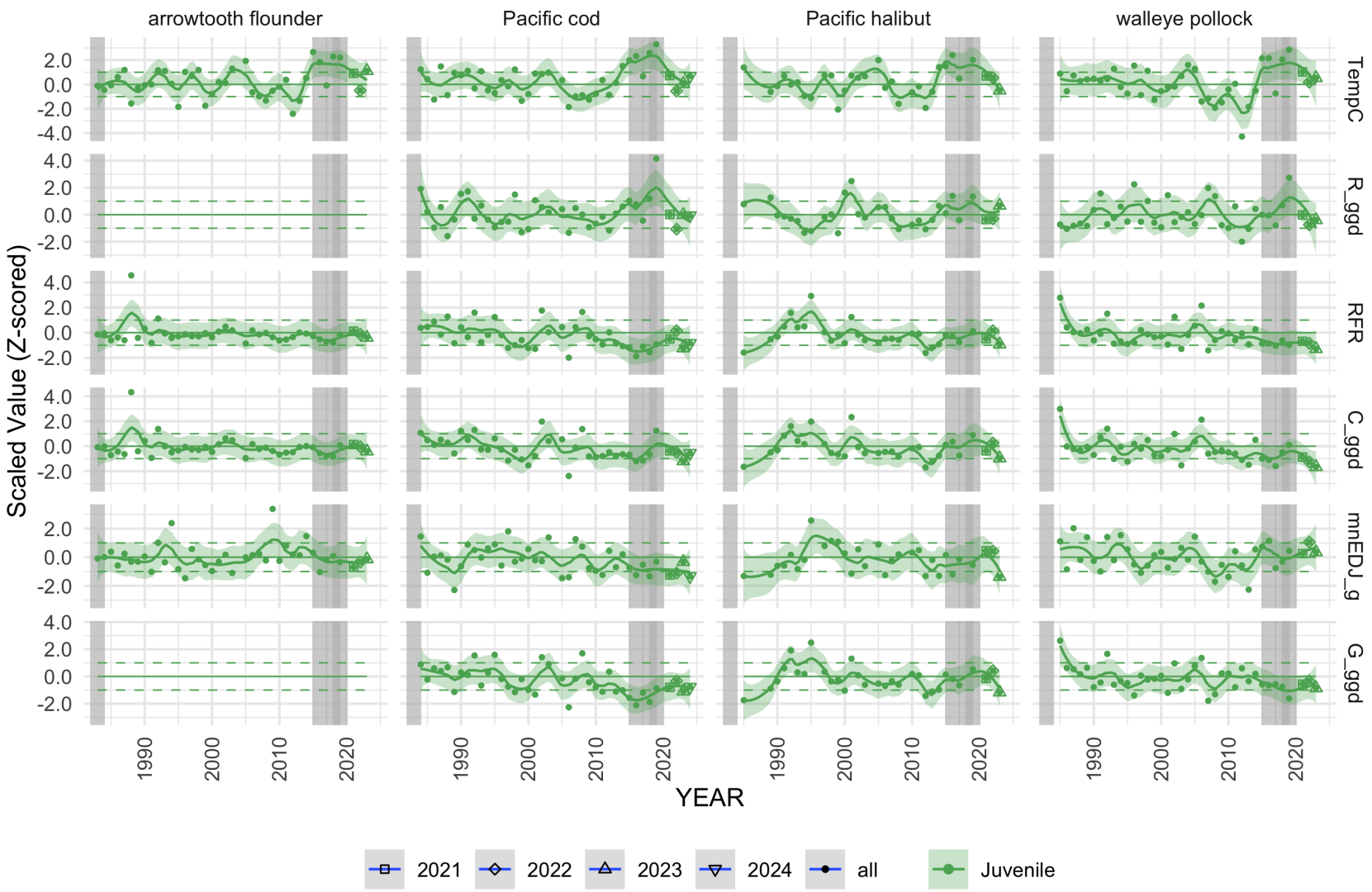

Figure 104: Normalized (i.e., Z-score scaled) bioenergetic diet indices for juvenile (<45 cm) groundfish species over time including thermal experience ('TempC'), metabolic demand ('R_ggd'), Relative Foraging Rate ('RFR'), observed specific consumption rate ('C_ggd'), mean diet energy density ('mnEDJ_g'), and scope for growth ('G_ggd'). Mean values for each year and bin are shown as dots, while recent sampled years are highlighted for reference (large triangles and squares). The spline represents a LOESS smoother. Data is based on biomass-weighted indices for samples collected during NOAA NMFS AFSC bottom-trawl summer surveys.

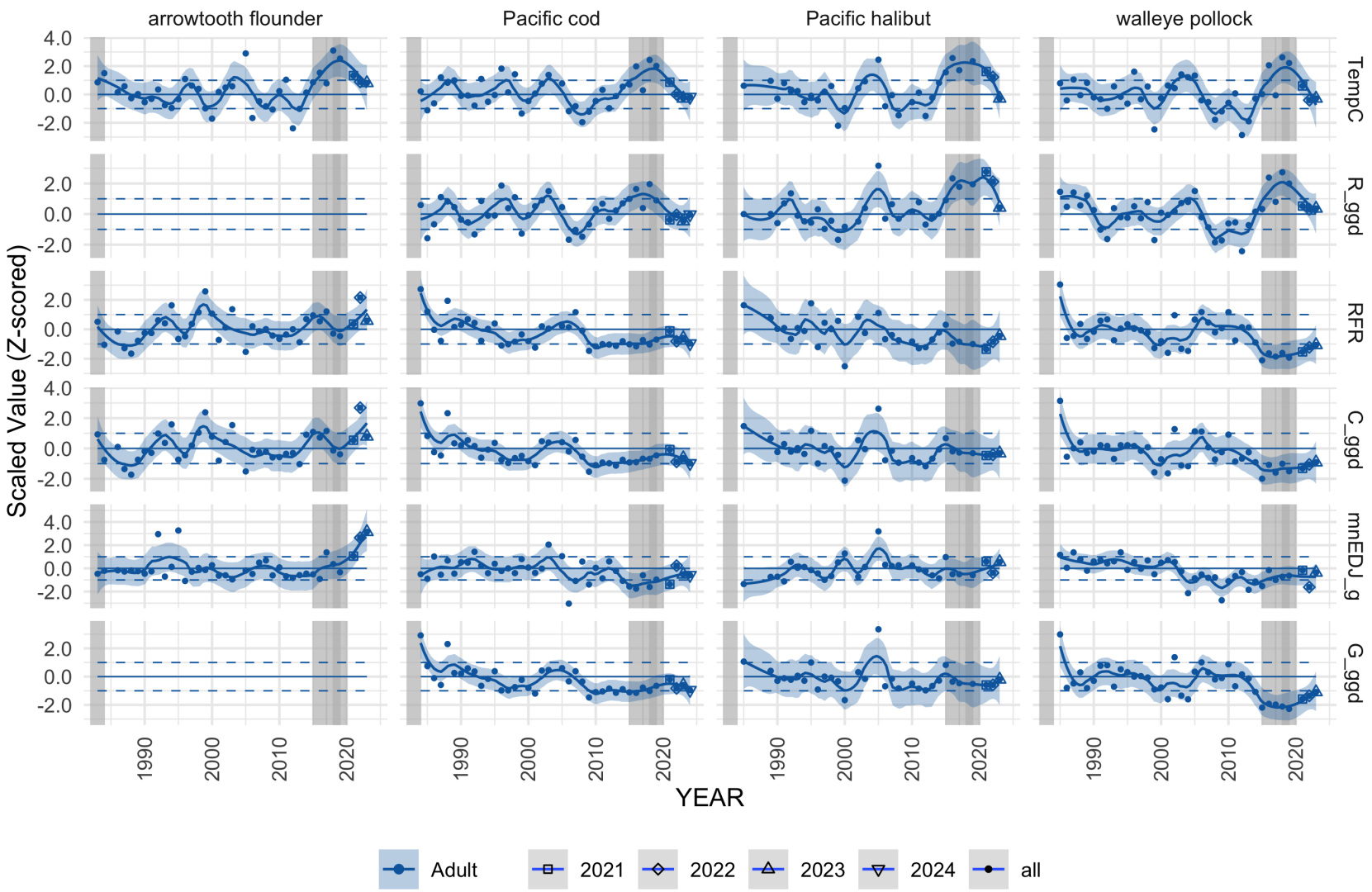

Figure 105: Normalized (i.e., Z-score scaled) bioenergetic diet indices for adult groundfish species over time including thermal experience ('TempC'), metabolic demand ('R_ggd'), Relative Foraging Rate ('RFR'), observed specific consumption rate ('C_ggd'), mean diet energy density ('mnEDJ_g'), and scope for growth ('G_ggd'). Mean values for each year and bin are shown as light as dots, while recent sampled years are highlighted for reference (large triangles and squares). The spline represents a loess smoother. Data is based on biomass-weighted indices for samples collected during NOAA NMFS AFSC bottom-trawl summer surveys.

The average energetic content of sampled diets generally increases linearly with thermal experience for juvenile and adult arrowtooth flounder, P. cod, and P. halibut, but while this holds true for juvenile pollock, adult pollock diets have exhibited considerably little variation across years or EBS bottom temperatures. Similarly, observed consumption rates for these species also tend to increase linearly with increasing bottom temperature, again except for pollock where consumption rates decline above 1.5°C (bottom temperature) and to a lesser extent for juvenile P. cod. The integrated outcome of these changes, combined with exponential increases in metabolism with warming, is a linear increase in adult P. cod and halibut scope for growth with increasing bottom temperature, while juvenile P. cod and adult and juvenile pollock scope for growth decreases with warming temperatures (Figure 106). This is reflected in annual patterns, where we observed an overall decline in scope for growth for both pollock and P. cod in recent years, especially for juvenile pollock and P. cod during the MHW (2016–2019), adult P. cod since 2010, and adult pollock in 2021; Figures 104 and 105). Initial limited sampling from 2022 collections suggest higher growth potential for pollock in that year, although these early samples should be interpreted cautiously.

Trends in energetic densities in recent years may reflect temporal shifts in diet composition of groundfish in response to changing climate conditions (Figure 107. In particular, for P. cod (as predators), there was a notable increase in the proportion diets composed of snow and tanner crab (*Chionoecetes* sp.) and decrease in the proportion composed of pollock during the MHW years (2016–2019), but recently P.cod have shifted back to consuming more pollock.

Factors influencing observed trends: Metabolic demands for ectothermic fish like pollock, P. cod, arrowtooth flounder, and P. halibut are largely a function of thermal experience and body size and tend to increase exponentially with increasing temperatures. Fish can minimize metabolic costs through behaviors such as movement to thermally optimal temperatures (e.g., movement to climate refugia in the NBS or at depth), or can increase consumption of food energy (quality and/or quantity of prey) to meet increasing metabolic demands. The latter requires sufficient access to abundant or high energy prey resources. By examining patterns in diets of fish across the EBS we are able to derive indices of potential increases in metabolic demand, foraging rate, and growth potential (or "scope for growth") which provides insight into ecological changes associated with marine heatwaves and long-term warming in the region.

Implications: For both species in the EBS, during recent anomalously warm years, metabolic demands were elevated while foraging rates and scope for growth were reduced (Figures 103 and 104). This pattern was most pronounced for juvenile and adult pollock, and juvenile P. cod (Figure 105). This has important implications, as to offset metabolic demands these fish would have had to (1) consume more food or more energetically rich food, (2) access energetic reserves leading to net body mass loss, or (3) move to more energetically favorable foraging grounds. There are a few lines of evidence to support all three of these potential responses to climate-driven changes in the EBS, including observations of large numbers of P. cod in the NBS surveys in 2017–2023.

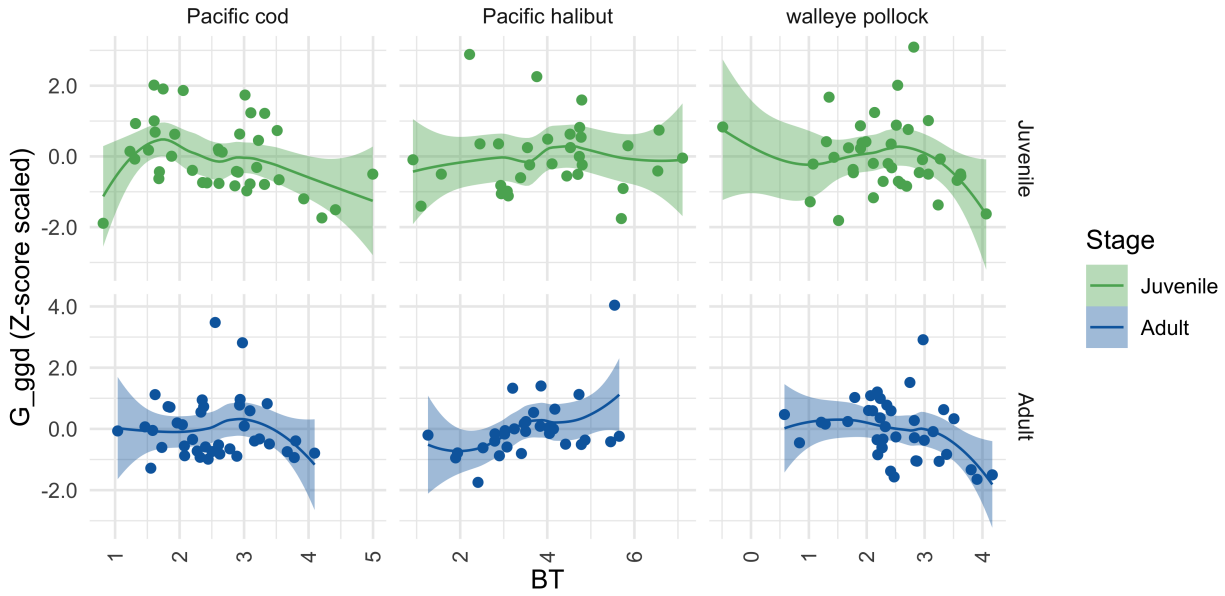

Figure 106: Normalized (i.e., Z-score scaled) bioenergetic (potential) scope for growth ('G_ggd') for juvenile and adult fish as a function of survey bottom temperature (BT; °C). Data is based on biomass-weighted indices for samples collected during NOAA NMFS AFSC bottom-trawl summer surveys for the SEBS and NBS.

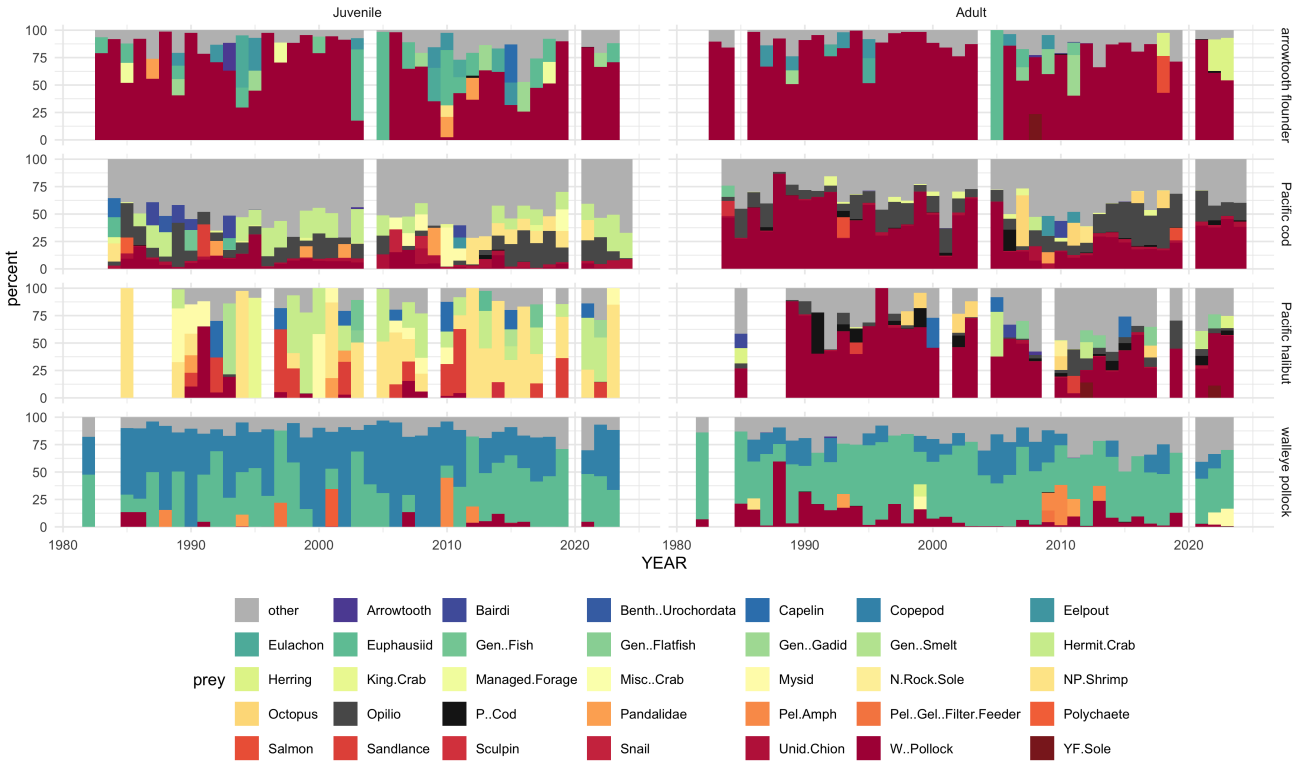

Figure 107: Diet composition of juvenile and adult groundfish across the Bering Sea. Data is based on biomass-weighted indices for samples collected during NOAA NMFS AFSC bottom-trawl summer surveys for the SEBS and NBS. **Note** that recent years (2021–present) have fewer processed samples.

Multispecies Model Estimates of Time-Varying Natural Mortality

Contributed by Kirstin K. Holsman[1], Jim Ianelli[1], Kerim Aydin[1], Kalei Shotwell[1], Kelly Kearney[1], Steve Barbeaux[1], Grant Adams[1], Anna Sulc[2], and Sophia Wassermann[1]
[1]Resource Ecology and Fishery Management Division, Alaska Fisheries Science Center, NOAA Fisheries, Seattle, WA
[2]University of Washington, Seattle, WA
Contact: kirstin.holsman@noaa.gov
Last updated: October 2024

Description of indicator: We report trends in age-1 total mortality for walleye pollock (*Gadus chalcogrammus*, 'pollock'), Pacific cod (*Gadus macrocephalus*, 'P. cod'), and arrowtooth flounder (*Atheresthes stomias*, 'arrowtooth'), from the eastern Bering Sea (EBS). Total mortality rates are based on residual mortality inputs (M1) and model estimates of annual predation mortality (M2) produced from the multi-species statistical catch-at-age assessment model (known as CEATTLE: Climate-Enhanced, Age-based model with Temperature-specific Trophic Linkages and Energetics). See the BSAI multi-species stock assessment (Holsman et al., 2016, 2020, 2024), Adams et al., 2022, Holsman and Aydin, 2015, Ianelli et al., 2016, and Jurado-Molina et al., 2005 for more information.

Status and trends: The CEATTLE model estimates of age-1 natural mortality (i.e., M1+M2) for pollock, P. cod, and arrowtooth flounder continue to decline from the 2016 peak mortality. For all three species, age-1 predation mortality rates have remained similar to 2023. At 1.42 yr^{-1}, age-1 mortality estimated by the model was greatest for pollock and lower for P. cod and arrowtooth, with total age-1 natural mortality at around 0.71 and 0.7 0.66 yr^{-1} for P. cod and arrowtooth, respectively. The 2024 age-1 natural mortality across species is 12% to 38% lower than in 2016 and is near average for pollock (relative to the long-term mean) (Figure 108) while P. cod and arrowtooth age-1 mortality rates are well below the long-term mean.

Patterns in the total biomass of each species consumed by all three predators in the model (typically 1-3 yr old fish) exhibit divergent trends from predation mortality in 2024. Pollock biomass consumed by all predators in the model is above the long-term mean (indicating more 1-3 year old pollock were consumed in the last few years than on average), while P. cod consumed is approximately the mean, and juvenile arrowtooth consumed is trending downward (Figure 109).

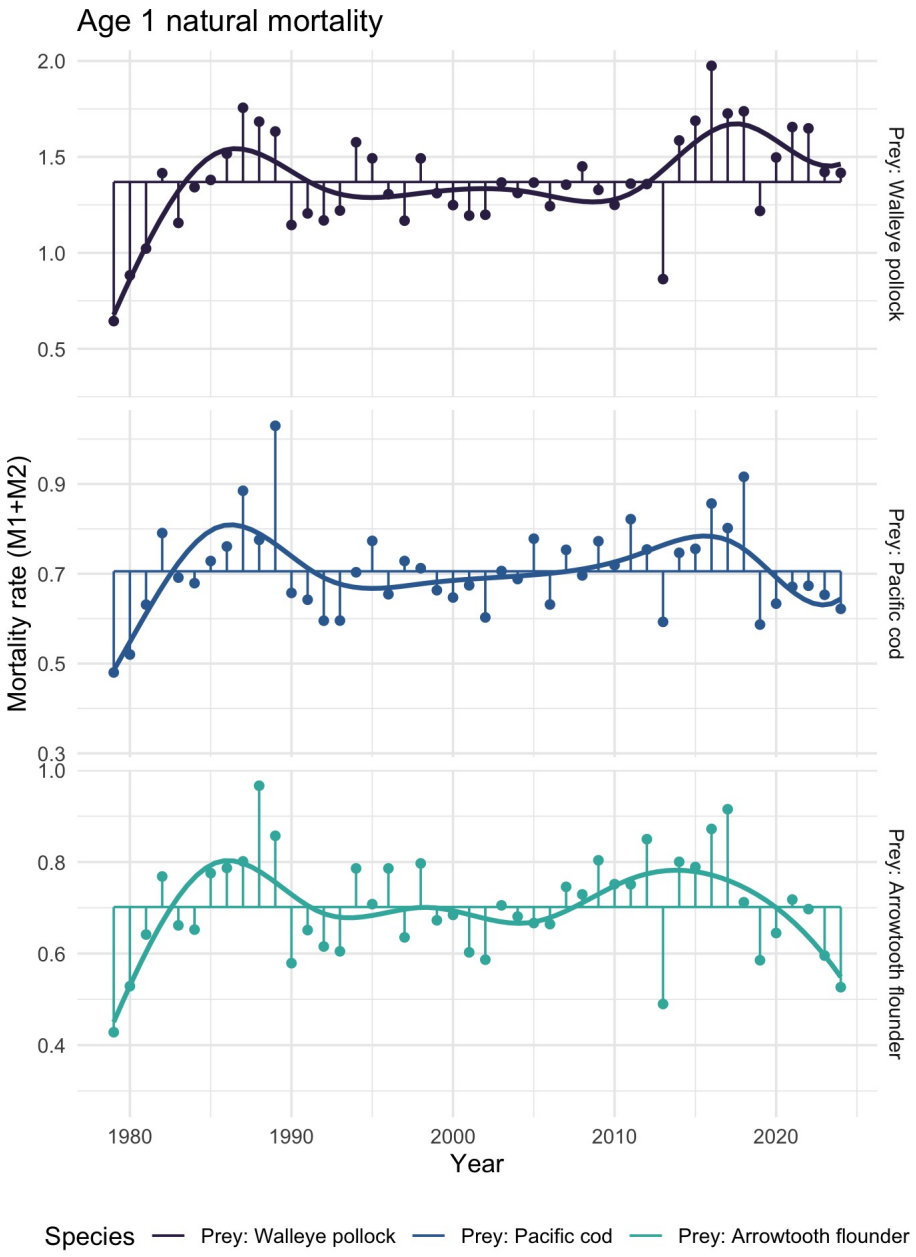

Figure 108: Annual variation in total mortality ($M1_{i1} + M2_{i1,y}$) of age-1 pollock (as prey) (a), age-1 P. cod (as prey) (b), and age-1 arrowtooth flounder (as prey) (c) from the single-species models (dashed) and the multi-species models with temperature (points and solid line). Updated from Holsman et al., 2016; more model detail can be found in Appendix 1 of the BSAI pollock stock assessment (Ianelli et al., 2024). Solid lines are a 10-y (symmetric) loess polynomial smoother indicating trends in age-1 mortality over time.

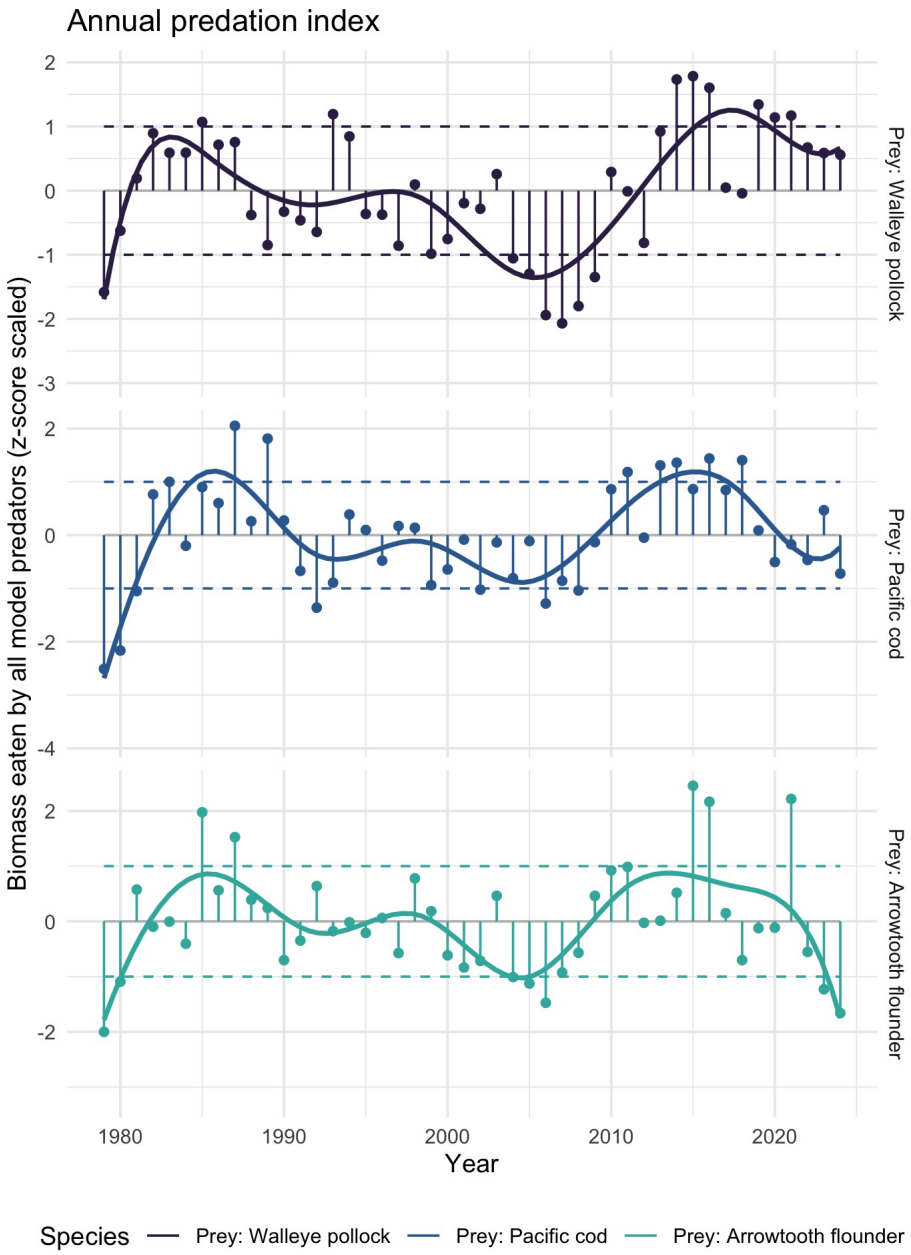

Figure 109: Multispecies estimates of prey species biomass consumed by all predators in the model (points): a) total biomass of pollock consumed by predators annually, b) total biomass of P. cod consumed by predators annually, c) total biomass of arrowtooth flounder consumed by predators annually. Gray lines indicate 1979–2024 mean estimates for each species; dashed lines represent 1 standard deviation of the mean. Solid lines are a 10-y (symmetric) loess polynomial smoother indicating trends in biomass consumed over time.

Factors influencing observed trends: Temporal patterns in natural mortality reflect annually varying changes in predation mortality that primarily impact age- fish (and to a lesser degree impact ages 2 and 3 fish in the model). Pollock are primarily consumed by older conspecifics, and pollock cannibalism accounts for 54% (on average) of total age-1 predation mortality, with the exception of the years 2006–2008 when predation by arrowtooth marginally exceeded cannibalism as the largest source of predation mortality of age-1 pollock (Figure 110). The relative proportion of age-1 pollock consumed by older pollock increased in 2024 relative to previous years, while the relative proportion consumed by P. cod declined.

Combined annual predation demand (annual ration) of pollock, P. cod, and arrowtooth flounder in 2024 was 8.22 million tons, down slightly from the 10.68 million t annual average during the warm years and large maturing cohorts of 2014–2016. Pollock represent approximately 76% of the model estimates of combined prey consumed with a long-term average of 5.98 million tons of pollock consumed annually by all three predators in the model. From 2015–2019, individual annual rations were above average for all three predator species, driven by anomalously warm water temperatures in the Bering Sea during during those years. However, cooler temperatures in 2024 relative to the recent warm years has resulted in annual rations at or below the long-term average (Figure 111).

Implications: We find evidence of continued declines in predation mortality of age-1 pollock, P. cod, and arrowtooth flounder relative to recent high predation years (2014–2016). While warm temperatures continue to lead to high metabolic (and energetic) demand of predators, declines in total predator biomass, in particular P. cod, are contributing to a net decrease in total consumption (relative to 2016) and therefore reduced predation rates and mortality in 2022–2024. This pattern indicates continued favorable top-down conditions for juvenile groundfish survival in 2024 through predator release due to declining biomass of groundfish.

Between 1980 and 1993, relatively high natural mortality rates for pollock reflect patterns in combined annual demand for pollock prey by all three predators that was high in the mid 1980's (collectively 9.87 million t per year). The peak in predation mortality of age-1 pollock in 2016 corresponds to warmer than average conditions and higher than average energetic demand of predators combined with the maturation of the large 2010–2012 year classes of pollock and P. cod (collectively with arrowtooth 10.62 million t per year).

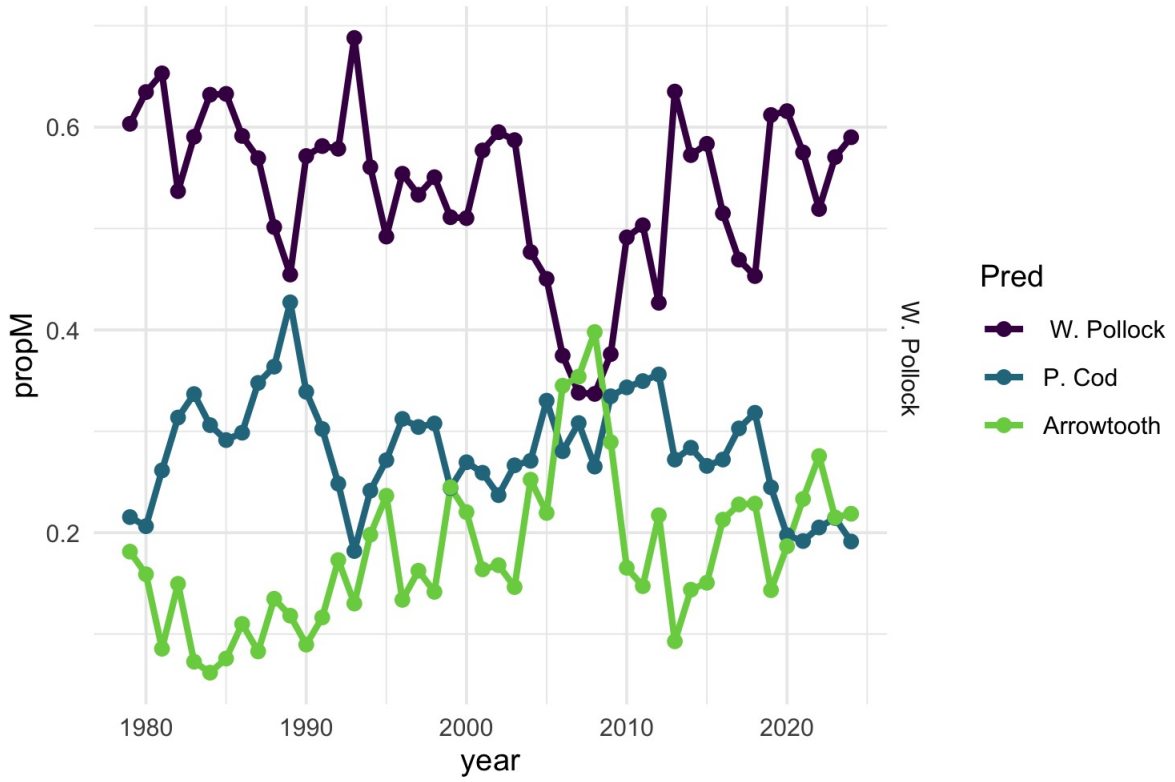

Figure 110: Proportion of total predation mortality for age-1 pollock from pollock, P. cod, and arrowtooth flounder predators across years. Updated from Holsman et al. (2016); more model detail can be found in Appendix 1 of the BSAI pollock stock assessment (Ianelli et al., 2024).

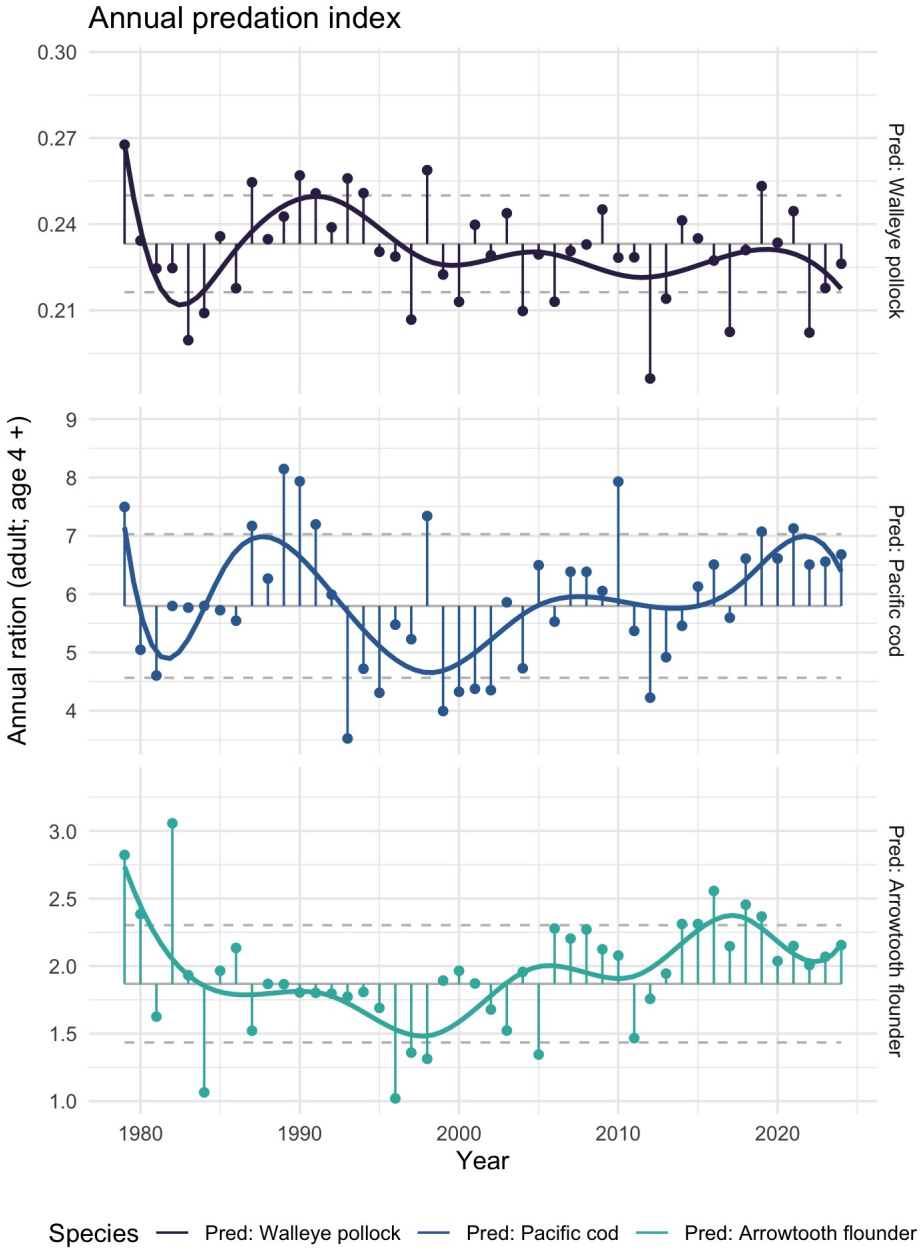

Figure 111: Multispecies estimates of annual ration (kg consumed per individual per year) for adult (age-4+) predators: a) pollock, b) P. cod, and c) arrowtooth flounder. Gray lines indicate 1979–2024 mean estimates for each species; dashed lines represent 1 standard deviation of the mean. Solid lines are a 10-y (symmetric) loess polynomial smoother indicating trends in ration over time.

Groundfish Recruitment Predictions

Pre- and Post-Winter Temperature Change Index and the Recruitment of Bering Sea Pollock

Contributed by Ellen Yasumiishi
Auke Bay Laboratories, Alaska Fisheries Science Center, NOAA Fisheries
Contact: ellen.yasumiishi@noaa.gov
Last updated: August 2024

Description of indicator: The temperature change (TC) index is a composite index for the pre- and post-winter thermal conditions experienced by walleye pollock (*Gadus chalcogrammus*) from age-0 to age-1 in the eastern Bering Sea (Martinson et al., 2012). The TC index (year t) is calculated as the difference in the average monthly sea surface temperature in June (t+1) and August (t) (Figure 112) in an area of the southern region of the eastern Bering Sea (56.2°N to 58.1°N by 166.9°W to 161.2°W). Time series of average monthly sea surface temperatures were obtained from the NOAA Earth System Research Laboratory Physical Sciences Division website. Sea surface temperatures were based on NCEP/NCAR gridded reanalysis data (Kalnay et al., 1996, data obtained from `http://www.esrl.noaa.gov/psd/cgi-bin/data/timeseries/timeseries1.pl` (accessed August 8, 2023)). We specify Variable SST and Analysis level Monolevel Variables. Less negative values represent a cool late summer during the age-0 phase followed by a warm spring during the age-1 phase for pollock.

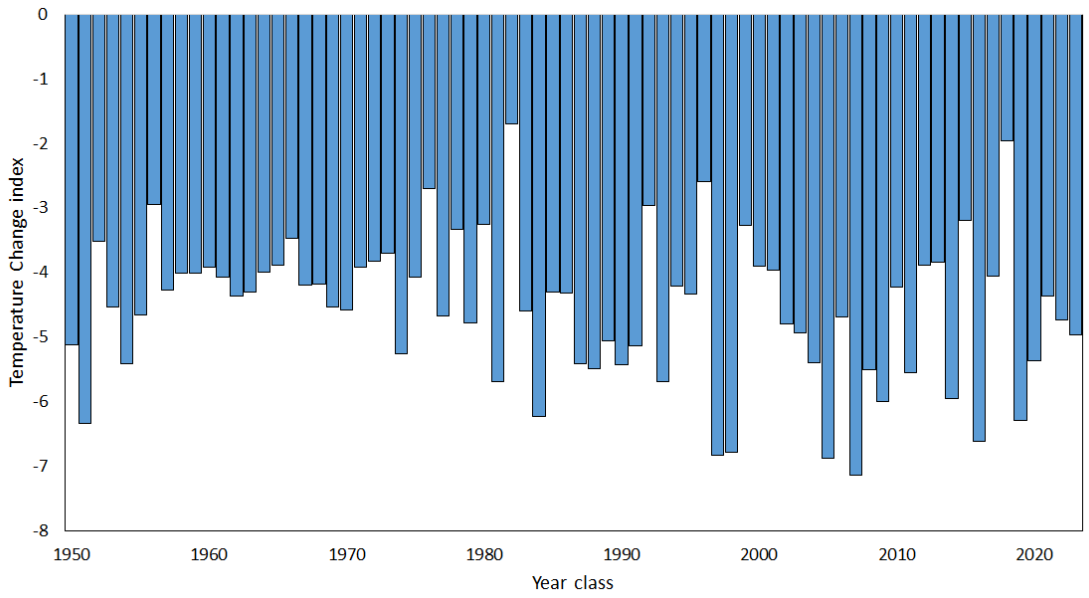

Figure 112: The temperature change index values for the 1950 to 2023 year classes of pollock. Values represent the differences in sea temperatures on the southeastern Bering Sea shelf experienced by the 1950–2022 year classes of pollock. Less favorable conditions (more negative values) represent a warm summer during the age-0 life stage followed by a relatively cool spring during the age-1 life stage. More favorable conditions (less negative values) represent a cool summer during the age-0 life stage followed by a relatively warm spring during the age-1 life stage.

Status and trends: The 2023 year class TC index value is -4.97, slightly lower than the 2022 year class TC index value of -4.74, indicating slightly better conditions for pollock survival from age-0 and age-1 from 2023 to 2024 than from 2022 to 2023. The average expected survival is due to the smaller relative difference in sea temperature from late summer (average) to the following spring (cool). The late summer sea surface temperature (August 9.8°C) in 2023 was 0.1°C lower than the long term average (9.9°C) and spring sea temperature (June 4.8°C) in 2024 was cooler than the long-term average of 5.3°C since 1949.

Factors influencing observed trends: According to the original Oscillating Control Hypothesis (OCH), warmer spring temperatures and earlier ice retreat led to a later oceanic and pelagic phytoplankton bloom and more food in the pelagic waters at an optimal time for use by pelagic species (Hunt et al., 2002). The revised OCH indicated that age-0 pollock were more energy-rich and have higher over wintering survival to age-1 in a year with a cooler late summer (Coyle et al., 2011; Heintz et al., 2013). The 2023 year class of pollock experienced average late summer temperatures in 2023 during the age-0 stage and cooler spring temperatures in 2024 during the age-1 stage indicating average conditions for the overwintering survival from age-0 to age-1.

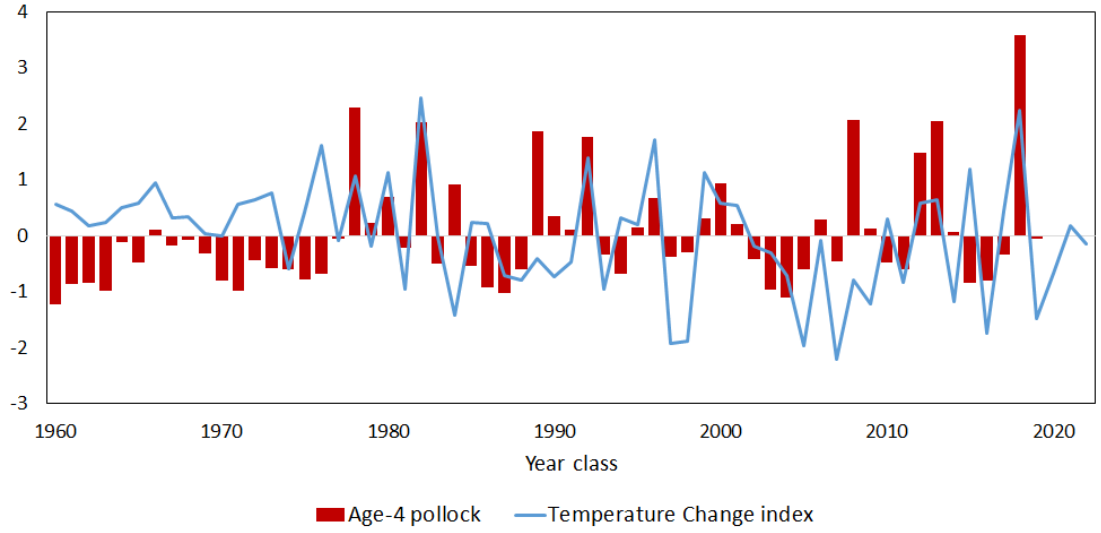

Figure 113: Normalized time series values of the temperature change index indicating conditions experienced by the 1960–2023 year classes of pollock during the summer age-0 and spring age-1 life stages. Normalized values of the estimated abundance of age-4 pollock in the eastern Bering Sea from 1964–2023 for the 1960–2019 year classes. Age-4 pollock estimates are from Table 1-24 in Ianelli et al. (2023). The TC index indicate average conditions for the 2023 year class of pollock.

Implications: The 2023 TC index value of -4.97 was similar to the long-term average of -4.59, therefore we expect average recruitment of pollock to age-4 in 2027 from the 2023 year class (Figure 113).

Implications for Pollock Recruitment to Age-1 Based on Late Summer Surface Silicic Acid and Age-0 Pollock Weights

Contributed by Jeanette C. Gann and Lisa B. Eisner (retired)
Auke Bay Laboratories, Alaska Fisheries Science Center, NOAA Fisheries
Contact: jeanette.gann@noaa.gov
Last updated: September 2024

Description of indicator: Nitrogen (nitrate, nitrite, or ammonium) is usually the principal limiting nutrient in the eastern Bering Sea (EBS) for phytoplankton growth. It is, however, often near detection limits during late summer/early fall for stratified surface waters. Therefore, inter-annual variations in surface nitrogen are difficult to measure during this time. In contrast, surface silicate (silicic acid) is found in higher concentrations than nitrogen and inter-annual variations are reliably detectable, making silicate a possible indicator of nutrient availability in surface waters.

The condition of age-0 pollock during late summer/early fall, can be an indicator for recruitment to age-1 (Heintz et al., 2013), where pollock weight is sometimes used as a general proxy for condition. Surface silicic acid is observed during late summer/early fall, in conjunction with age-0 pollock weights, to look for possible connections between nutrients, phytoplankton growth, and young of the year (age-0) pollock condition as they approach their first winter at sea (Gann et al., 2016).

Status and trends: Pollock weight and silicic acid values vary interannually; both trended slightly upwards from 2012–2016 when viewed within the years 2003–2022. Normalized values for 2022 pollock weights were the lowest in the time series, while silicic acid was second lowest overall. Pollock recruitment to age-1 was among the highest from the 2018 year class, while the 2022 year class and recruitment to age-1 in 2023 appear to have been average (Ianelli et al., 2023). It should be noted that the stock assessment surveys cover a larger geographic area into the northern Bering Sea, while this assessment accounts for only the southern middle domain. The year with the lowest surface silicic acid concentrations within the time series by the end of summer was 2007, with 2022 the next lowest. Pollock weights over the southern middle domain in 2022 were the lowest in the time series. A scatterplot showing normalized age-0 pollock weight with silicic acid values reveals a positive relationship (Figure 114) while a line plot shows a general positive co-variance between the two (Figure 115).

Factors influencing observed trends: During summer, the strength and frequency of storm events and water column stratification will influence the amount of nutrients (including silicic acid) that are brought to surface waters from depth. Late summer concentrations of surface silicic acid may serve as an indicator of nutrient availability, with higher concentrations seen during windy years and lower stratification, and low concentrations seen when storm activity is minimal and stratification is high (Eisner et al., 2016). Diminished nutrient stores leading to lower production in the upper water column may directly affect food stores for higher trophic levels and lead to slowed growth of age-0 pollock during summer months.

Implications: The significant decline in pollock weight observed in 2022 may signal poorer recruitment to age-1 (for the 2022 year class in the southern Bering Sea) compared with other recent years. It is notable that silicate values dropped considerably as well, compared with previous years. Surface silicate concentrations during the age-0 life stage has potential to be an asset in estimating pollock recruitment to age-1.

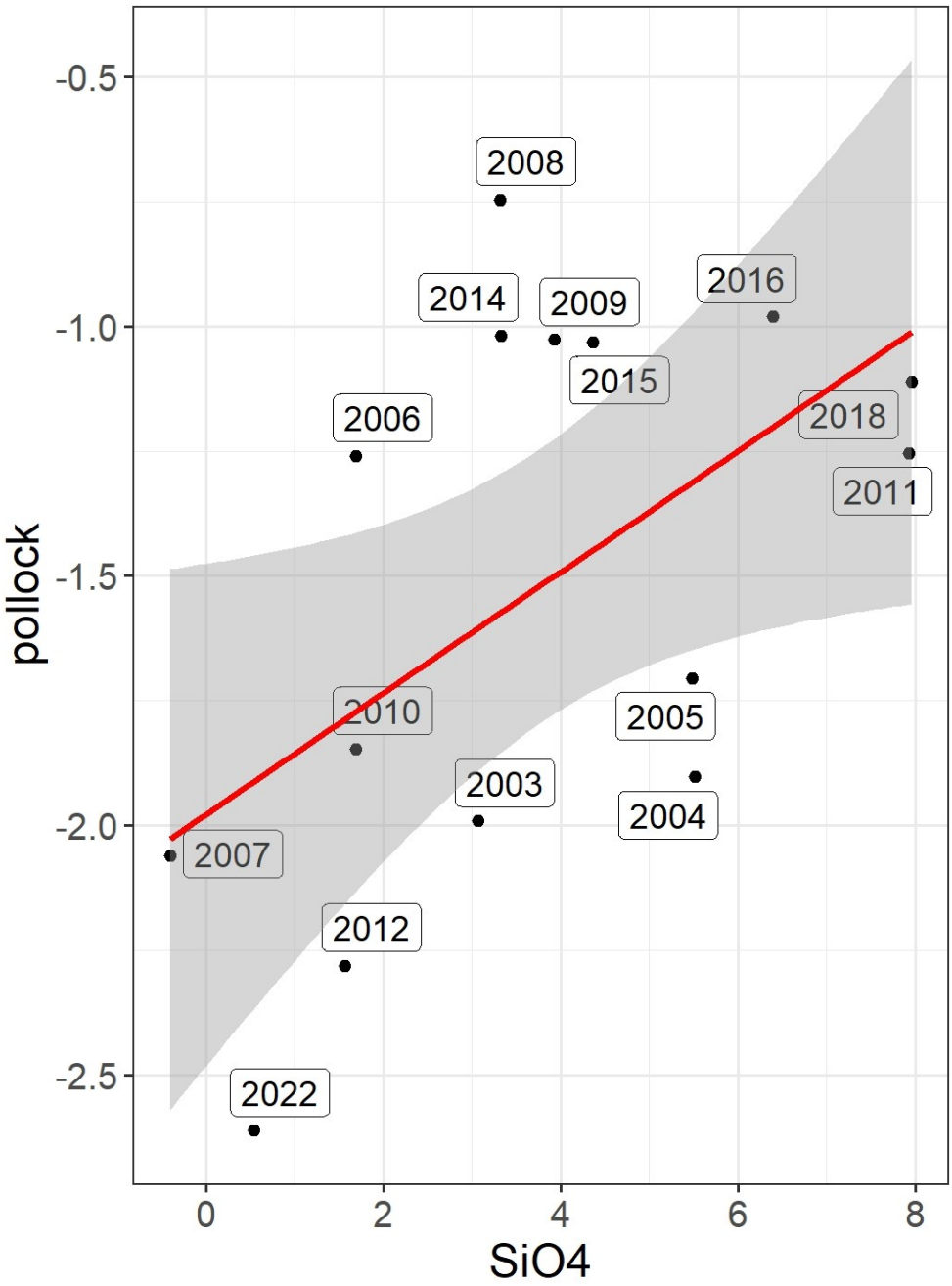

Figure 114: Plot of normalized yearly averages for age-0 pollock weight and silicic acid ($Si(OH)_4$), with regression line (red) and 95% confidence intervals shown in gray. Values were normalized by subtracting the mean from the value for each year and dividing by the standard deviation. Silicic acid was significant ($p<0.05$) in the linear model.

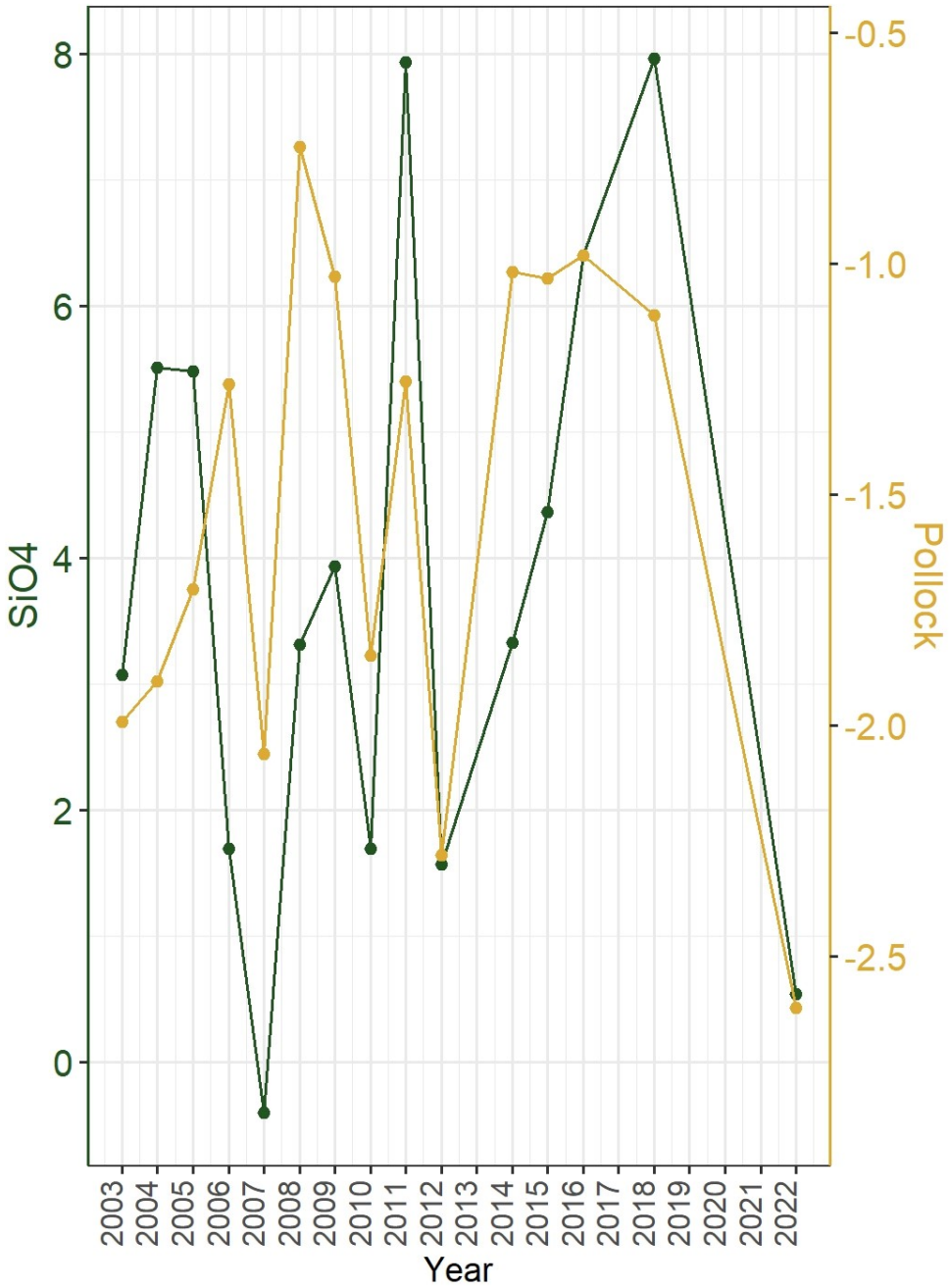

Figure 115: Interannual variability of normalized surface silicic acid ($Si(OH)_4$) (see explanation of normalization under Figure 114) from the southern middle domain and concurrently collected normalized mean weights of age-0 pollock. *Note: data points missing in 2013, 2017, and 2019–2021 due to lack of surveys in those years.*

Benthic Communities and Non-target Fish Species

Eastern Bering Sea – Miscellaneous Benthic Fauna

Contributed by Thaddaeus Buser and Sean Rohan
Resource Assessment and Conservation Engineering Division, Alaska Fisheries Science Center, NOAA Fisheries
Contact: thaddaeus.buser@noaa.gov
Last updated: September 2024

Description of indicator: "Miscellaneous" species fall into three groups: eelpouts (fishes of the Family Zoarcidae), poachers (fishes of the Family Agonidae), and sea stars (Class Asteroidea). The three species comprising the bulk of the eelpout group are the wattled eelpout (*Lycodes palearis*) and shortfin eelpout (*L. brevipes*) and to a lesser extent the marbled eelpout (*L. raridens*). The biomass of poachers is dominated by the sturgeon poacher (*Podothecus acipenserinus*) and to a lesser extent the sawback poacher (*Leptagonus frenatus*). The composition of sea stars is dominated by the purple-orange sea star (*Asterias amurensis*), found primarily in the inner/middle shelf (strata 10-40), and the common mud star (*Ctenodiscus crispatus*), primarily in the outer shelf (strata 50 and 60).

Since 1982, the RACE Groundfish Assessment Program (GAP) and Shellfish Assessment Program (SAP) have conducted annual fishery-independent summer bottom trawl surveys on the EBS shelf using standardized trawl gear and methods. Biomass index trends from the survey are likely to reflect changes in the abundance of species and life history stages that are available to the survey, especially if trends are sustained over time.

Regional and stratum indices of abundance (biomass in kilotons) and confidence intervals were estimated for each taxonomic group by fitting a multivariate random effects model (REM) to stratum-level design-based abundance index time series calculated from AFSC summer bottom trawl survey catch and effort data. Indices were calculated for the entire standardized survey time series (1982–2024). Design-based indices of abundance were calculated using the gapindex R package (Oyafuso, 2024) and REM were fitted to survey time series using the rema R package (Sullivan and Balstad, 2022). Code and data used to produce these indicators are provided in the esrindex R package and repository (Rohan, 2024).

Methodological Changes: see Eastern Bering Sea – Structural Epifauna (p. 78).

Status and trends: The 2024 biomass estimate for eelpouts increased from 2023, continuing an increasing trend that began in 2021 (Figure 116). The 2024 estimate is >1 standard deviation above the time series average and represents the largest biomass estimate since 1983. Eelpout biomass is concentrated on the outer shelf in strata 50 and 60 (100-200 m bottom depth) and southern middle shelf in stratum 30 (50-100 m bottom depth; Figure 117).

Poacher biomass increased from 2023 and is near the time series average (Figure 116). Poacher biomass is concentrated in inner (<50 m) and middle (50-100 m) shelf strata (10-40), although lower abundances of deeper species are encountered in strata 50 and 60 (Figure 117).

The biomass for sea stars in 2024 was similar to 2023, which marked the apparent end of a multi-year period of above average biomass from 2017 to 2022. The 2023 and 2024 sea star biomass estimates are near the time series average and are a return to levels last seen in 2016 (Figure 116). Sea stars are

observed in all survey strata, although their biomass in stratum 50 is much lower than in other strata (Figure 117).

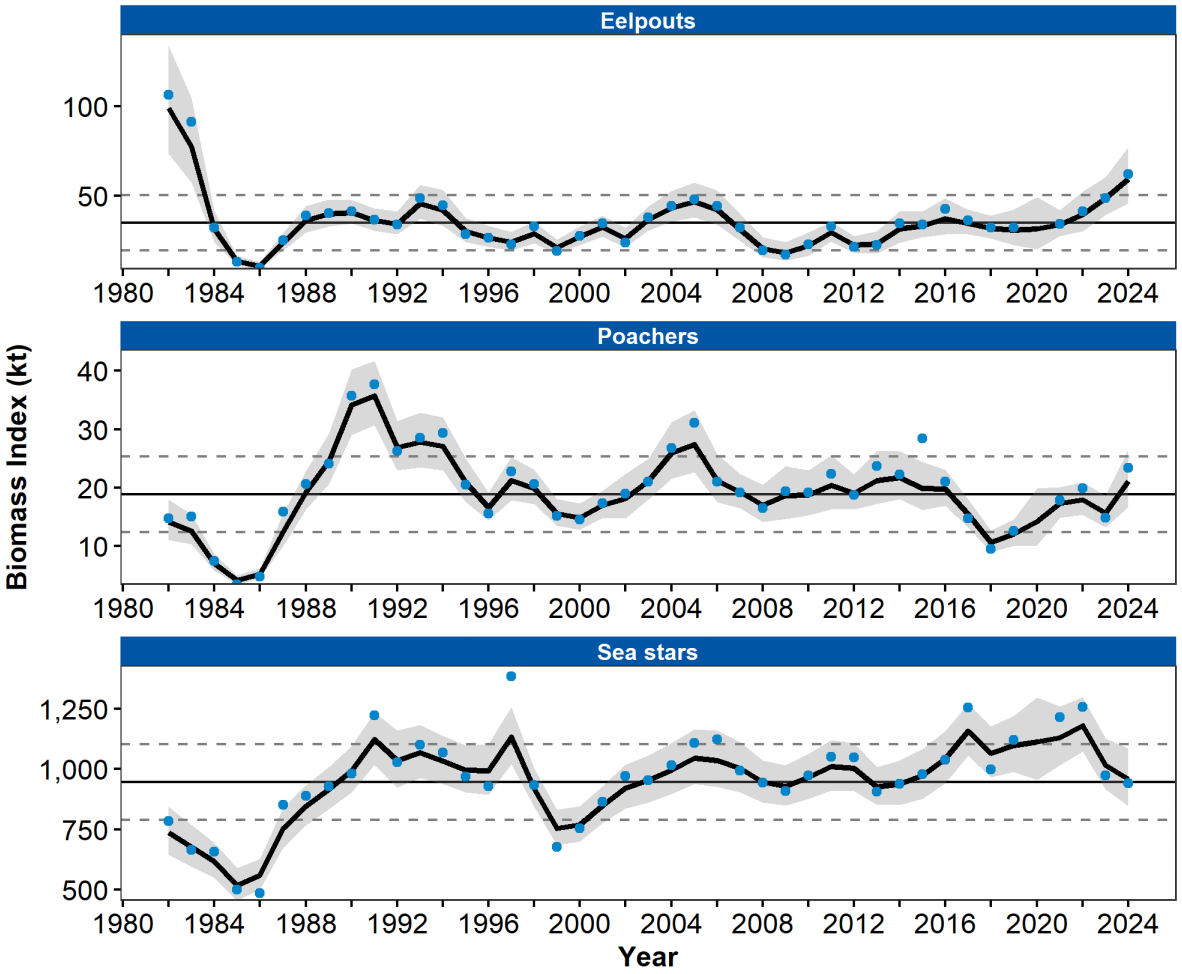

Figure 116: Biomass index of benthic fauna (eelpouts, poachers, sea stars) from RACE Groundfish Assessment Program and Shellfish Assessment Program summer bottom trawl surveys of the eastern Bering Sea continental shelf from 1982 to 2024. Panels show the observed survey biomass index mean (blue points), random effects model fitted mean (solid black line), 95% confidence interval (gray shading), overall time series mean (solid gray line), and horizontal dashed gray lines representing one standard deviation from the mean.

Factors influencing observed trends: It is difficult to identify trends. Determining whether, for example, the low abundance after 2018 in poachers represent changes in abundance, demographic structure, distributional changes, or selectivity will require more specific research on survey trawl gear selectivity relative to interannual differences in bottom temperatures and on the life history characteristics of these epibenthic species.

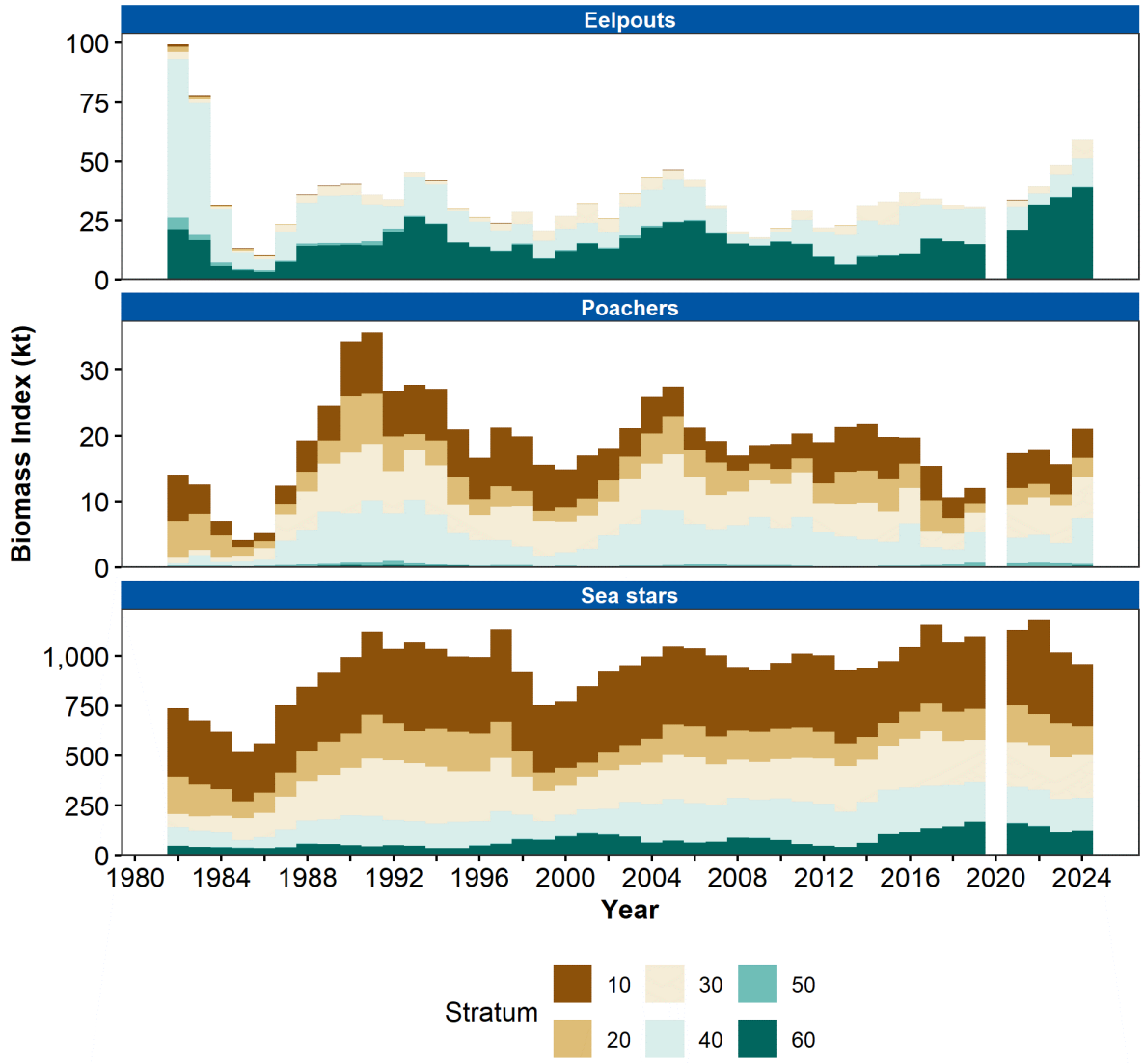

Figure 117: Biomass index of benthic fauna (eelpouts, poachers, sea stars) in eastern Bering Sea continental shelf survey strata (10-60) estimated from RACE Groundfish Assessment Program and Shellfish Assessment Program summer bottom trawl survey data from 1982 to 2024.

Implications: Eelpouts, poachers, and sea stars have important roles in the energy flow within benthic communities. For example, eelpouts are a common prey item of arrowtooth flounder (*Atheresthes stomias*). However, it is not known at present whether these changes in CPUE are related to changes in energy flow.

Research priorities: The bottom trawl survey uses standardized survey protocols aimed at ensuring consistent sampling efficiency. However, additional research is needed to better characterize the catchability and selectivity of structural epifauna groups by the bottom trawl survey.

Eastern Bering Sea Commercial Crab Stock Biomass Indices

Contributed by Jon Richar
Kodiak Laboratory, Alaska Fisheries Science Center, NOAA Fisheries
Contact: jon.richar@noaa.gov
Last updated: August 2024

Description of indicator: This indicator is the commercial crab species biomass time series in the eastern Bering Sea. The eastern Bering Sea bottom trawl survey has been conducted annually since 1975 by the Resource Assessment and Conservation Engineering Division of the Alaska Fisheries Science Center. The purpose of this survey is to collect data on the distribution and abundance of crab, groundfish, and other benthic resources in the eastern Bering Sea. The data provided here include the time series of results from 1998 to the present. In 2024, 349 standard stations were sampled on the eastern Bering Sea shelf from 2 June to 5 August. This constitutes a reduction in sampling effort relative to previous years, and results from the elimination of corner stations near the Pribilofs and St. Matthew Is. The observed trends in crab biomass may be indicative of trends in either benthic production or benthic response to environmental variability. The commercial crab biomass is also indicative of trends in exploited resources over time.

Status and trends: The historical trends of commercial crab biomass and abundance are highly variable (Figure 118). Pribilof Island crab stocks remain extremely depressed with highly variable survey biomass estimates due to trawl survey limitations related to crab habitat and the patchy crab distribution. Of note, while no mature males were caught in 2023, 2024 was the first year in the history of the survey in which no Pribilof Island blue king crab of any sex/maturity classification were caught during the standard survey. The Pribilof red king crab stock saw declines of -57% in both mature and legal male stocks, while mature females declined by -77% (not shown). No immature males or females were caught.

The St. Matthew blue king crab adult male biomass decreased by -4% relative to 2023 estimates, continuing a declining trend decline observed since 2014. Female blue king crab biomass is not adequately sampled during this survey due to a nearshore distribution around St. Matthew Island.

Mature female Tanner biomass increased substantially in both the western district (+273%) and the eastern district (+106%). Mature male Tanner biomass trends were positive, with the eastern district seeing a 44% increase and a 90% increase occurring in the western district. Although the increase in the eastern district mature male biomass constitutes a reversal in the recent declining trend, biomass remains down by -77% since 2014.

Total snow crab biomass increased by 277% relative to 2023, although it still represents a 56% decline since 2018. Across the board increases were seen in mature females (+173%), immature females (+462%), mature males (+50%), immature males (+303%), legal males (+114%), and industry-preferred (49%). Increases in population biomass were driven by a combination of increased abundance and larger crab relative to prior years.

In 2024, Bristol Bay mature female red king crab biomass decreased by 14%, while abundance declined by -0.15%, with the discrepancy being due to an increasing proportion of smaller crab. Numbers remain near the historical low points. Conversely, mature male red king crab biomass increased by 44% relative to 2023 estimates, reversing the decline seen in 2023.

Factors influencing observed trends: Environmental variability and exploitation affect trends in commercial crab biomass over time. Recent modeling analyses suggest that environmental variability is largely driving inter-annual variability in crab stock recruitment. Trends in 2024 estimates relative to those for prior years are likely to be influenced by the aforementioned reduction in survey effort, particularly those for Pribilof Island red king crab and blue king crab, and St. Matthew blue king crab. Analyses suggest that impacts on estimates for stocks other than these are likely to be minor ($<<<$10%).

Implications: The implications of the observed variability in crab stocks are dramatic inter-annual and inter-decadal variability in benthic predators and ephemeral (seasonal) pelagic prey resources when crab are in larval stages in the water column or as juveniles in the benthos. Although it is unclear at what life stage crab stock variability is determined, it is likely that environmental variability affecting larval survival and changes in predation affecting juvenile survival are important factors. As such, the environmental conditions affecting larval crab may also be important for larval demersal groundfish and the availability of crab as prey may be important for demersal fish distributions and survival. Disease may also be a factor, although this is speculative.

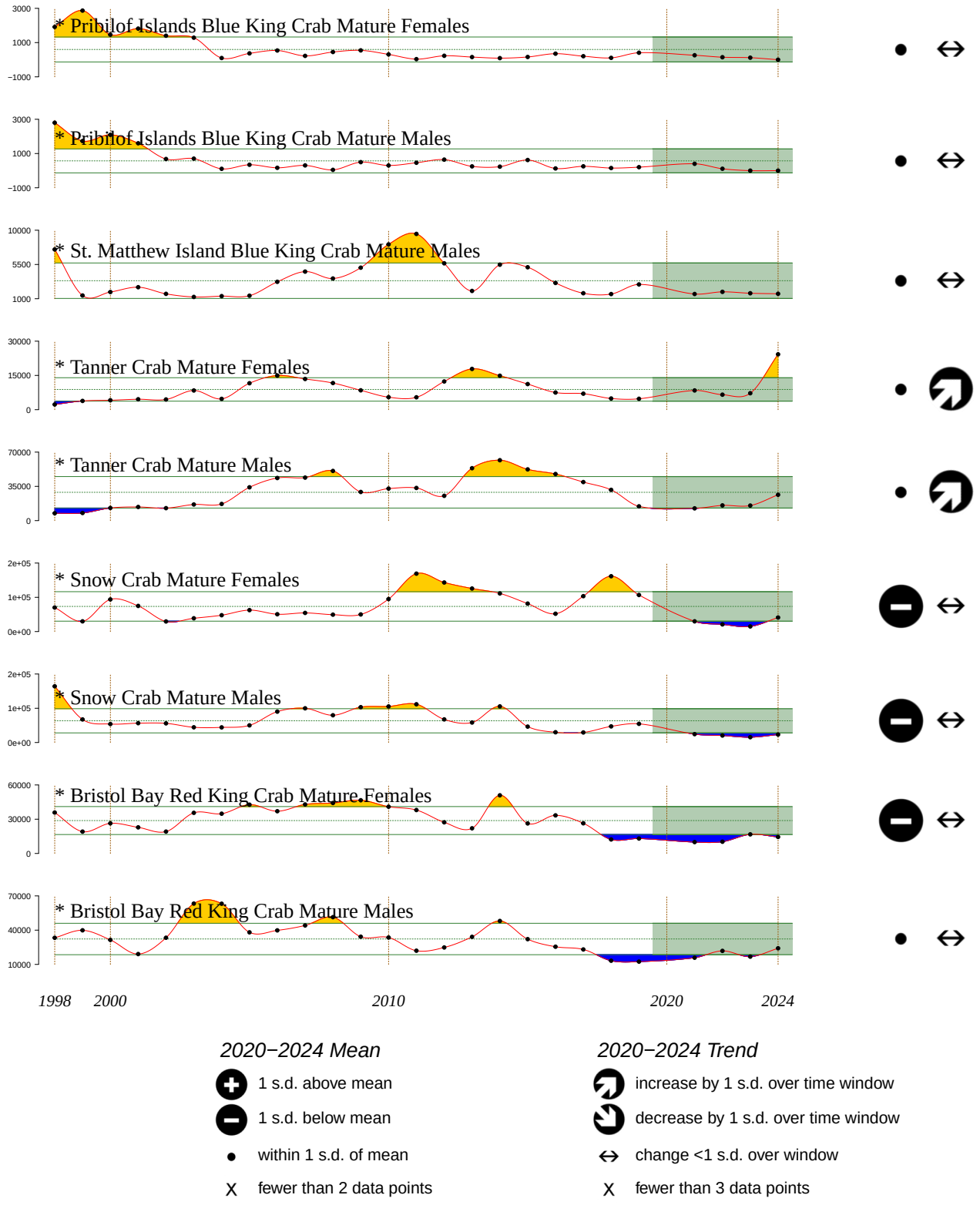

Figure 118: Biomass of commercial crab stocks caught on the NOAA eastern Bering Sea bottom trawl survey, 1998–2024.

Seabirds

Integrated Seabird Information

This integration is in response to ongoing collaborative efforts within the seabird community and contains contributions from (in alphabetical order):

Jackie Lindsey – Coastal Observation and Seabird Survey Team [COASST], WA
Matthew Rustand – U.S. Fish & Wildlife Service, Alaska Maritime National Wildlife Refuge, Homer, AK
Stephanie Zador – NOAA Fisheries, Alaska Fisheries Science Center, Seattle, WA

Last updated: October 2024

Summary Statement
Seabirds at the Pribilof Islands in the southeastern Bering Sea were monitored by Alaska Maritime National Wildlife Refuge in 2024. Monitored species (common and thick billed murres, black-legged and red-legged kittiwakes, and red-faced cormorants) at the Pribilof Islands had a mixed year in terms of reproductive success. On St. George Island, productivity for common and thick-billed murres was average, black- and red-legged kittiwakes was slightly below average, and above average for least auklets. On St. Paul Island, productivity was well below average for common and thick-billed murres and average for black- and red-legged kittiwakes. Murres generally bred later and kittiwakes earlier, with murres seeming to experience chick failure later in the summer. Comparisons of reproductive success between 2023 and 2024 are mixed across islands and species. Reproductive success can represent food availability around the colony during the breeding season (summer), therefore indicating sufficient prey abundance and/or high-quality prey over the southeastern Bering Sea shelf. Compared to 2023, colony attendance counts in 2024 were lower for most species.

Introduction
Seabirds can be viewed as indicators of ecosystem changes in productivity, therefore population-level responses can signal shifts in prey availability that may similarly affect commercial fish populations. In this Seabird Integration section, we synthesize information and observations from a variety of sources to provide an overview of environmental impacts to seabirds and what that may indicate for ecosystem productivity as it pertains to fisheries management. We merge across information sources to derive a regional summary for the southeastern Bering Sea and interpret changes in seabird dynamics with respect to understanding ecosystem productivity.

Approach
We focused on several attributes of seabirds that may serve as broader ecosystem indicators important to fisheries managers. We interpret these attributes as reflective of seabirds' life history and how they sample the ecosystem, either as fish-eating or plankton-eating species.

1. *Breeding timing* can represent conditions prior to breeding and/or phenological variation in the environment. Birds arriving to breed at an earlier date can reflect favorable winter and/or spring foraging conditions, or earlier peaks in ocean productivity.

2. *Reproductive success* can represent food availability around the colony during the breeding season, with a higher number of fledged chicks generally reflecting an increase in the local abundance of high-quality prey.

3. *Mortality* gives insight into environmental conditions and ecosystem impacts beyond breeding colonies and the breeding season.

Breeding and Reproductive Success
Southeastern Bering Sea (Pribilof Islands)
Common murres had the lowest reproductive success on St. Paul Island since the marine heatwave in 2015–2016 with most loss occurring during the chick rearing period. St. George Island common murre productivity was slightly above average (Figures 119 and 120). The mean hatch date was eight days later on St. George and five days later on St. Paul than the long-term average.

Thick-billed murres had below average reproductive success on St. Paul Island and average success on St. George Island. The mean hatch date was twelve days later on St. George and nine days later on St. Paul than the long-term average.

Least auklets mean hatch date on St. George Island was five days later than the mean. Colony attendance was higher than in 2023, however, was very low when compared to the historical average. Least auklets experienced an above average reproductive year but the number of nesting crevices remained low as biologists struggled to locate nests to follow.

Black-legged and red-legged kittiwake overall reproductive success was slightly above average in 2024 on the Pribilof Islands. On St. George, both kittiwake species experienced above average reproductive success when compared to the long-term mean. On St. Paul, red-legged kittiwakes had above average and black-legged kittiwakes had below average reproductive success. Overall, the hatch date of both species overlapped the mean. Although there was indication that black-legged kittiwakes were slightly late and red-legged kittiwakes were slightly early.

Red-faced cormorants had a below average year in regards to reproductive success at St. Paul Island in 2024. While monitored less intensively at St. George, cormorants did well, with all metrics near the long-term averages.

A multivariate seabird breeding index (Figure 2) indicated that, on the whole, seabird reproductive timing and success at the Pribilof Islands was slightly below average in 2024, although there were differences between islands and species that may reflect local-scale processes and/or diversity in foraging strategies. Both thick-billed and common murres nesting on St. Paul had particularly low reproductive success, while kittiwakes and red-faced cormorants fared better. Both murres and kittiwakes had about average reproductive success at St. George. The poor reproductive success of murres on St Paul may reflect more vulnerability to disturbance and predation at the colony due to their smaller population sizes following mass mortality during the 2014–2016 heatwave in the Gulf of Alaska (where the murres over winter) (H. Renner, pers comm). All species at both islands hatched chicks later than average. Reproductive success and/or hatch timing can be influenced by their food supply, therefore below-average values may indicate lower than average recruitment of year classes that seabirds feed on (e.g., age-0 pollock), or lower than average supply of forage fish that commercially fished species feed on (e.g., capelin eaten by both seabirds and Pacific cod).

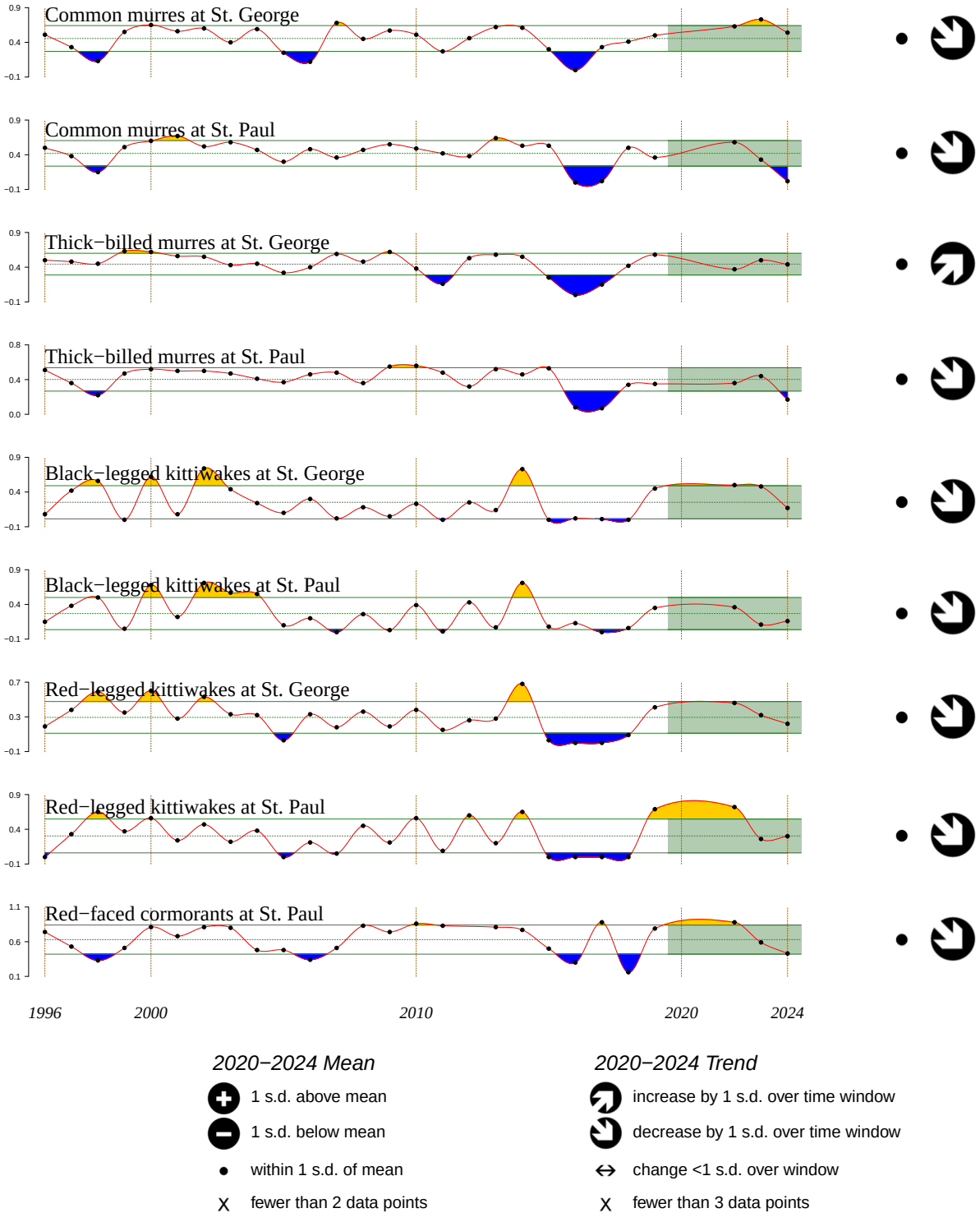

Figure 119: Reproductive success of five seabird species at St. George and St. Paul Islands between 1996–2024. Trends should be interpreted with caution as only 3 data points are available in the 5-year time window.

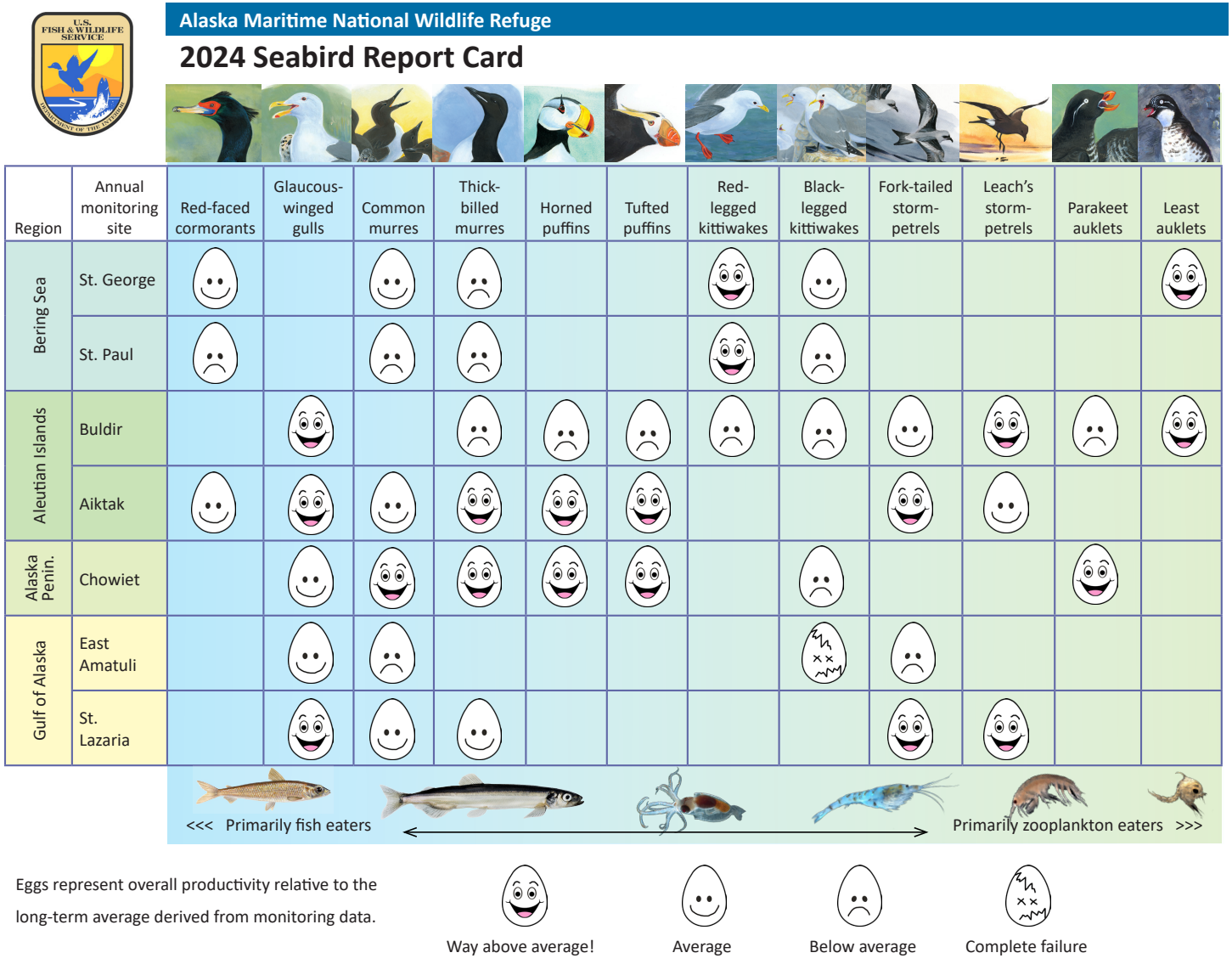

Figure 120: 2024 Alaska Maritime National Wildlife Refuge Seabird Report Card showing a summary of seabird productivity across monitored colonies. Conclusions are drawn from productivity observations made dating to the 1970s and therefore may differ from conclusions made in Figure 119 above.

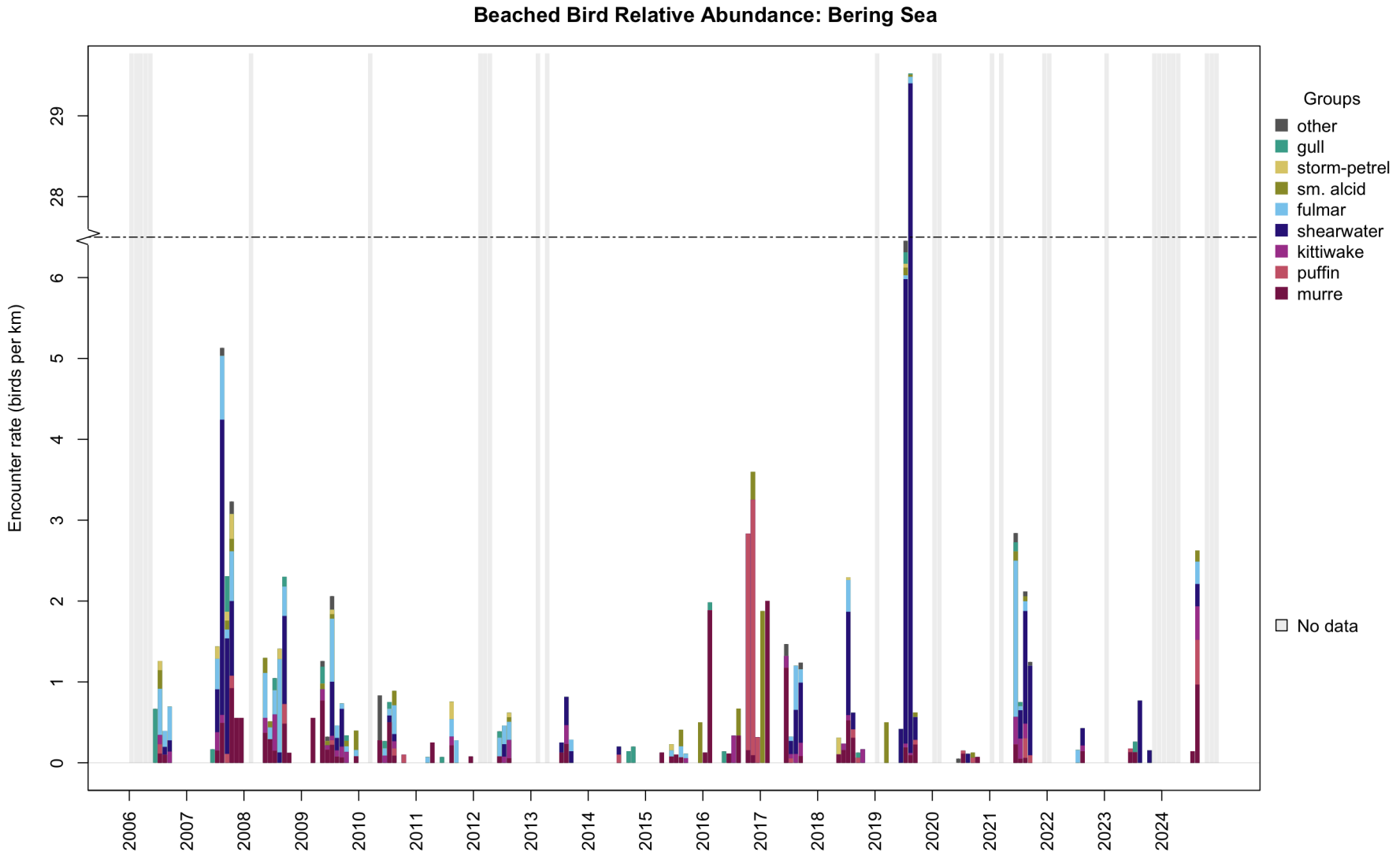

Figure 121: Month-averaged beached bird abundance, standardized per km of survey effort, for the eastern Bering Sea. Species groups (gull, storm-petrel, small alcid, fulmar, shearwater, kittiwake, puffin, murre) are depicted with different colors within each bar, with gray bars indicating months where no survey was conducted. **Note:** that a break in the y-axis between 6 and 28 birds/km, indicated by the dashed line, shows the magnitude of the 2019 die-off while still being able to distinguish patterns among other years. Credit: COASST.

Mortality

Eastern Bering Sea

Monitoring by the Coastal Observation and Seabird Survey Team (COASST) and regional partners provides a standardized measure of relative beached bird abundance. Surveys began in the eastern Bering Sea in 2006, and since that time over 1400 surveys have taken place across 25 beaches; in 2024, 33 surveys took place across 4 beaches, mostly concentrated on the Pribilof Islands, but sites in Bristol Bay and near Nome were also surveyed. Detailed methods for beached bird surveys can be found in Jones et al. (2019).

In 2024, surveyors reported relatively few carcasses across beaches in the Bering Sea. Encounter rates (all <1 per km) were not indicative of a die-off event. See monthly encounter rates for 2007 and 2019 in Figure 121 for examples of elevated encounter rates indicative of an unusual mortality event (typically defined as 5x the baseline rate). There were also relatively few opportunistic reports of additional beached bird carcasses in the eastern Bering Sea. Overall, the relatively few opportunistic reports received, in conjunction with low encounter rate on regular beached bird surveys performed by COASST, suggests that there was no major die-off event in this region in 2024.

Implications

Fish-eating, surface feeding seabirds include black-legged kittiwakes who feed on small schooling fish that are available at the surface (e.g., capelin, Arctic cod, juvenile pollock and juvenile herring), making them potential indicators of processes affecting juvenile groundfish that migrate to the surface to feed. Fish eating, diving seabirds include common murres who feed on small schooling fish (age-0 and age-1 pollock) to depths up to 90 m, thus they have access to fish throughout the water column and to the ocean bottom in shallow areas. These species had mixed reproductive success at the Pribilof Islands in 2024 when compared to the long-term average, with both species having greater reproductive success at St. George Island than at St. Paul Island. This may indicate differences in local availability of small schooling forage fish in feeding areas utilized by seabirds of each island.

Planktivorous seabirds include least and crested auklets, which feed primarily on copepods and euphausiids. Shearwaters and thick-billed murres also consume euphausiids, along with larvae and small fish. All of these species are indicators of feeding conditions for planktivorous groundfish species, including the larvae and juveniles of fish-eating species. Least auklets had above average reproductive success at the Pribilof Islands, however colony attendance was very low. Thick-billed murres had mixed reproductive success across islands, greater at St. George Island than at St. Paul Island. This may also indicate differences in local availability of zooplankton in feeding areas utilized by seabirds of each island.

Marine Mammals

Marine Mammal Stranding Network: Eastern Bering Sea

Contributed by Mandy Keogh
NOAA Fisheries, Protected Resources Division, Alaska Regional Office
Contact: mandy.keogh@noaa.gov
Last updated: September 2024

Description of indicator: Since 1985, members of the NMFS Alaska Marine Mammal Stranding Network (AMMSN) have collected and compiled reports on marine mammal strandings throughout the state. These reports are indices of events witnessed by members of the stranding network, the scientific community, and the general public, with varying degrees of knowledge regarding marine mammal biology and ecology. A marine mammal is considered "stranded" if it meets one of the following criteria: 1) dead, whether found on the beach, ice, or floating in the water; 2) alive on a beach (or ice) but unable to return to the water; 3) alive on a beach (or ice) and in need of apparent medical attention; or 4) alive in the water and unable to return to its natural habitat without assistance. The causes of marine mammal strandings are often unknown but some causes include disease, exposure to contaminants or harmful algal blooms, vessel strikes, and entanglement in or ingestion of human-made gear or debris.

When a stranded marine mammal is reported, information is collected including species, location, age class or size. In some cases, the initial photos and observations reported to AMMSN may be the only opportunity to collect information on the event. When possible, trained and authorized AMMSN members respond and collect life history data and samples as part of a postmortem examination. Photos and carcasses are evaluated for potential human interactions such as entanglement. These responses are conducted under the Marine Mammal Protection Act authorization either under a 112(c) agreement issued by NMFS to AMMSN members through a Stranding Agreement or under 109(h) authority exercised by local, state, federal or tribal entities. All responses involving ESA-listed species and some enhanced responses (e.g., remote sedation) are authorized under the NOAA Permit No. 24359.

Status and trends: The number of reported strandings in Alaska has increased over time. As of September 18, 2024, 189 stranded marine mammals have been reported for the year within Alaska, of which 80 were in the eastern Bering Sea region (Table 1). These numbers do not include entangled pinnipeds with no response or live, entangled baleen whales. The majority of reports were from more populated areas where AMMSN members are located (Figure 122). Further, increased outreach and dedicated surveys associated with high priority species or events (e.g., northern fur seal entanglement survey and response on St. Paul Island) also contributed to reported strandings in some areas and years. Reported strandings in the eastern Bering Sea region since 2020 varied between years without an overall pattern or consistent increase in reports (Table 1). The 2024 stranding data includes confirmed strandings reported between January 1, 2024 and September 18, 2024. These data are preliminary and the details may change as we review reports and receive additional information.

Factors influencing observed trends: It is important to recognize that stranding reports represent effort that has varied substantially over time and location. Human population and activity in an area influences the potential for a carcass or stranded marine mammal to be observed and reported. Overall, this effort has increased across Alaska and particularly in areas with higher human population densities. Unusual Mortality Events (UME), including the 2019 gray whale UME, can have a large influence on

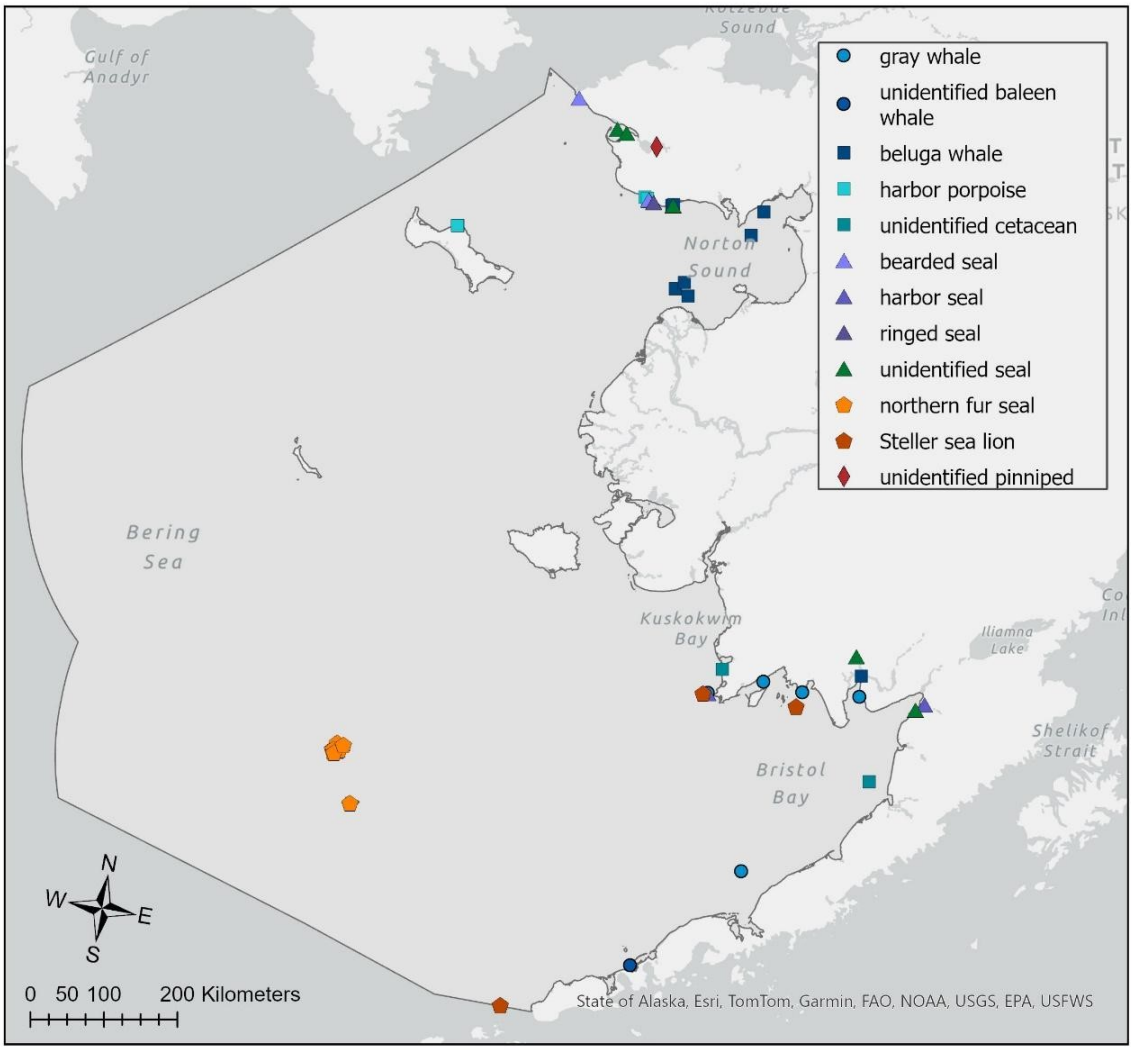

Figure 122: Reported stranded marine mammals between January 1, 2024 and September 18, 2024.

variability between years in this area (Table 1). Under the Marine Mammal Protection Act, an UME is defined as "a stranding that is unexpected; involves a significant die-off of any marine mammal population; and demands immediate response."

Other factors that may influence the number and species of marine mammals being reported include changing populations of some species including the increase in northern fur seals using Bogoslof Island for breeding prior to its most recent eruption. Further, the number of stranded marine mammals in an area can vary due to the potential conflict with fishery resources either directly through prey competition or indirectly through interactions with fishing gear such as increased entanglements (e.g., harbor porpoise caught in subsistence salmon nets). Within the eastern Bering Sea region, there has been a dramatic increase in stranded northern fur seals since 2022 (Table 1). Nearly all of these fur seals were alive and disentangled by the Ecosystem Conservation Office (ECO) of the Aleut Community of St. Paul

Island, an AMMSN member. Under the Examiners Guide[15] the level A and human interaction forms are completed for entangled pinnipeds when a response is conducted and the animal is in-hand. Observations of entangled pinnipeds with no response are captured in the Alaska Region dataset and by ECO database but these observations are not part of the national stranding database. In 2021, the Aleut Community of St. Paul Island increased ECO team efforts which allowed entangled northern fur seals observed during their weekly entanglement surveys or subsistence efforts to be captured and disentangled (Table 1, Figure 122). Therefore, the increase in stranded northern fur seals since 2022 in this region is due, at least in part, to reporting requirements and the successful capture and disentanglement of northern fur seals by the Aleut Community of St. Paul Island, rather than solely do to an increase in entanglements.

Implications: Across Alaska, reported marine mammal strandings have varied by year and location. In 2019, the increase in gray whale starndings across the migration route between Mexico and Alaska led to the declaration of an UME which continued until its closing on November 9, 2023. There were 146 stranded gray whales in Alaska during this UME. The UME Investigative Team concluded that the preliminary cause of this UME was localized ecosystem changes in the whale's subarctic and Arctic feeding areas that led to changes in food, malnutrition, decreased birth rates, and increased mortality. All these factors were documented during the gray whale UME. Increases in strandings of marine mammals may signal changes in the environment or other stressors (e.g., entanglements). Marine mammal stranding data can be paired with other datasets and may give clues to ecosystem-wide changes.

[15] https://media.fisheries.noaa.gov/2021-07/EXAMINERS%20GUIDE_2024%20FINAL.pdf?

Table 1: Reported stranded NMFS marine mammal species for 2024 and the previous five years in the eastern Bering Sea by species and year. The number of live stranded animals is reported in parenthesis by species and year.

	2020	2021	2022	2023	2024[16]
Bowhead whale			1		
Fin whale	1				
Gray whale	15	4	4	3	5
Humpback whale		1	3	1	
Minke whale	2		1	1	
Unidentified baleen whale	1	3	1	4	1
Baird's beaked whale				1	
Beluga whale	13	7 (1)	6	5	8 (2)
Harbor porpoise	3		3	3	6
Killer whale	1	3	1	1	
Pacific white-sided dolphin				1	
Unidentified cetacean	3	1	4	2	2
Total cetaceans	39	19	24	22	22
Bearded seal	9	3	7	1	3
Harbor seal	1	2 (2)		5 (1)	3 (2)
Ringed seal	3 (1)		4 (3)	2 (1)	1 (1)
Spotted seal	4 (1)	1	2		
Unidentified seal	5		2		5 (1)
Northern fur seal	2 (1)	8 (8)	49 (49)	57 (57)	42 (31)[17]
Steller sea lion	1	1	3	5	3
Unidentified pinniped	3				1
Total pinnipeds	28	15	67	70	58
Unidentified marine mammal		1			
Total cetaceans and pinnipeds	67	35	91	92	80

[16] 2024 stranding data includes confirmed strandings reported between January 1, 2024 and September 18, 2024.

[17] Most of the northern fur seals in the eastern Bering Sea region in 2024 were alive and entangled in fishing gear or debris. Seals were captured, disentangled, and immediately released by the Aleut Community of St. Paul Island. There was a group event of ten dead northern fur seals and a large number of cod and sole observed on Benson Beach, a known catcher beach on St. Paul Island on August 18, 2024.

Ecosystem or Community Indicators

Mean Lifespan of the Fish Community

Contributed by George A. Whitehouse[1] and Geoffrey M. Lang[2]
[1]Cooperative Institute for Climate, Ocean, and Ecosystem Studies (CICOES), University of Washington, Seattle WA
[2]Resource Ecology and Fisheries Management Division, Alaska Fisheries Science Center, NOAA Fisheries
Contact: andy.whitehouse@noaa.gov
Last updated: October 2024

Description of indicator: The mean lifespan of the community is a proxy for the turnover rate of species and communities and reflects the resistance of the community to perturbations (Shin et al., 2010). Lifespan estimates of groundfish species regularly encountered during the NMFS/AFSC annual summer bottom-trawl survey of the eastern Bering Sea were retrieved from the AFSC Life History Database[18]. The groundfish community mean lifespan is weighted by biomass indices calculated from the bottom-trawl survey catch data.

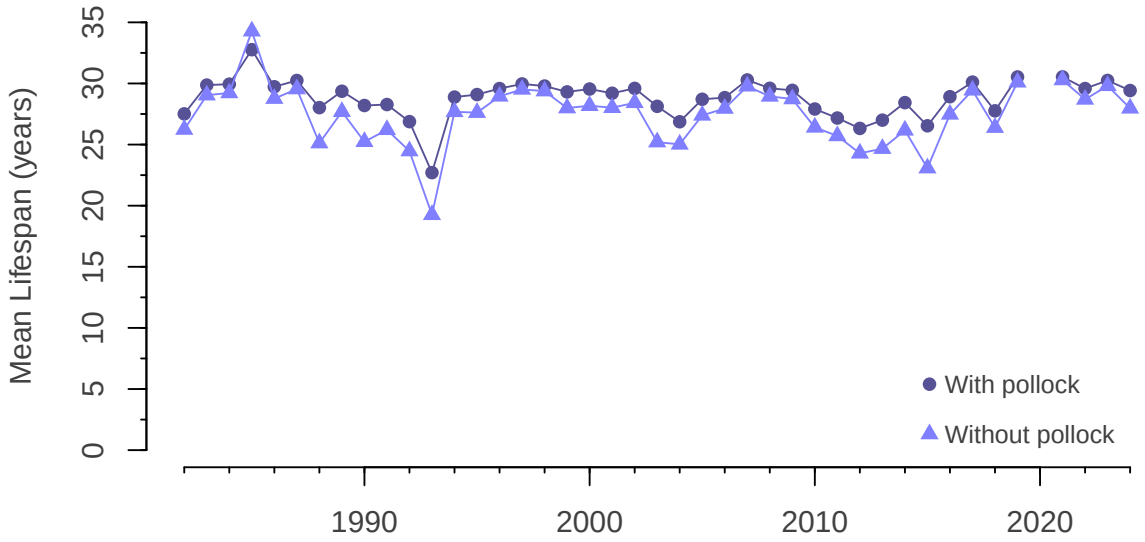

Figure 123: The mean lifespan of the eastern Bering Sea demersal fish community, weighted by biomass indices calculated from the NMFS/AFSC annual summer bottom-trawl survey. The circles are the series with pollock included and the triangles are the series without pollock included.

This indicator specifically applies to the portion of the demersal groundfish community that is efficiently sampled by the trawling gear used by NMFS during this survey at the standard survey sample stations (for survey details see Markowitz et al., 2023). Species that are infrequently encountered or not efficiently caught by the bottom-trawling gear are excluded from this indicator (e.g., sharks, grenadiers, myctophids, pelagic smelts). The survey index used here is the same as that used for foraging guild biomass indices on the report card (Figure 2).

[18]https://apps-afsc.fisheries.noaa.gov/refm/reem/lhweb/index.php

Walleye pollock is a biomass dominant species in the eastern Bering Sea and may drive the value of community indicators. Therefore this indicator is presented as two time series, one that includes and one that excludes pollock.

Status and trends:
With pollock included: The mean lifespan of the eastern Bering Sea demersal fish community in 2024 is 29.4, down from 30.2 years in 2023, and is above the time series mean of 28.8 years (Figure 123, circles). Mean groundfish lifespan has generally been stable over the time series with only a small amount of year-to-year variation, and shows no indication of a long-term trend.

Without pollock included: The mean lifespan of the eastern Bering Sea groundfish community without pollock in 2024 is 28.0, down from 29.8 years in 2023. Over the times series, the patterns and trends are similar between the two series with the values being slightly lower for the series without pollock (Figure 123, triangles). The exception to this pattern was 1985 when the mean lifespan was 32.8 with pollock included and 34.3 without pollock.

Factors influencing observed trends: Fishing can affect the mean lifespan of the groundfish community by preferentially targeting larger, older fishes, leading to decreased abundance of longer-lived species and increased abundance of shorter-lived species (Pauly et al., 1998). Interannual variation in mean lifespan can be influenced by the spatial distribution of species and the differential selectivity of species and age classes to the trawling gear used in the survey. Strong recruitment events or periods of weak recruitment could also influence the mean community lifespan by altering the relative abundance of age classes and species. For example, the low value observed in 1993 reflects a year of peak biomass index for capelin, a shorter-lived species. The peak mean lifespan for both series in 1985 was in part elevated by high biomass indices for long-lived species, such as sablefish. The lifespan of pollock is slightly higher than the mean groundfish lifespan without pollock. When pollock are removed from this indicator, there is a small decrease in value but the same overall trend is followed.

Implications: The groundfish mean lifespan has been stable over the time series of the summer bottom-trawl survey. There is no indication longer-lived species have decreased in relative abundance or are otherwise being replaced by shorter lived-species. Species that are short-lived are generally smaller and more sensitive to environmental variation than larger, longer-lived species (Winemiller, 2005). Longer-lived species help to dampen the effects of environmental variability, allowing populations to persist through periods of unfavorable conditions and to take advantage when favorable conditions return (Berkeley et al., 2004; Hsieh et al., 2006).

Mean Length of the Fish Community

Contributed by George A. Whitehouse[1] and Geoffrey M. Lang[2]
[1]Cooperative Institute for Climate, Ocean, and Ecosystem Studies (CICOES), University of Washington, Seattle WA
[2]Resource Ecology and Fisheries Management Division, Alaska Fisheries Science Center, NOAA Fisheries
Contact: andy.whitehouse@noaa.gov
Last updated: October 2024

Description of indicator: The mean length of the groundfish community tracks fluctuations in the size of groundfish over time. This size-based indicator is sensitive to the effects of commercial fisheries because larger predatory fish are often targeted by fisheries and their selective removal would reduce mean size (Shin et al., 2005). This indicator is also sensitive to shifting community composition of species with different mean sizes. Fish lengths are routinely recorded during the NMFS bottom trawl survey of the eastern Bering Sea, which has occurred each year from 1982 to 2024, except in 2020. Mean lengths are calculated for groundfish species (or functional groups of multiple species; e.g., eelpouts) from the length measurements collected during the trawl survey. The mean length for the groundfish community is calculated with the species mean lengths, weighted by biomass indices (Shin et al., 2010) calculated from the bottom-trawl survey catch data.

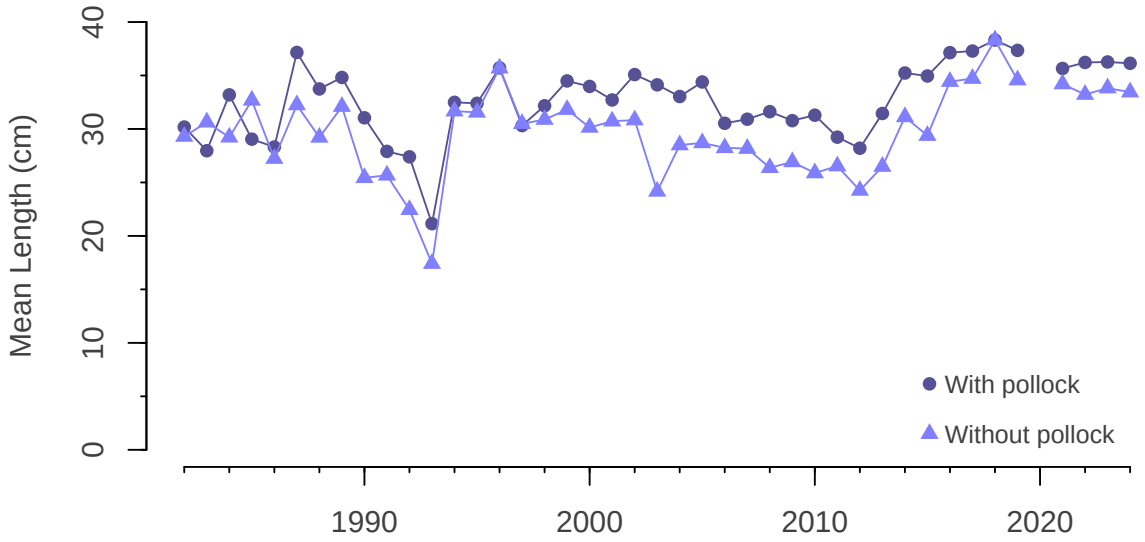

Figure 124: Mean length of the groundfish community sampled during the NMFS/AFSC annual summer bottom-trawl survey of the eastern Bering Sea (1982–2024). The groundfish community mean length is weighted by the relative biomass of the sampled species. The circles are the mean length with pollock included and the triangles are the series without pollock.

This indicator specifically applies to the portion of the demersal groundfish community that is efficiently sampled with the trawling gear used by NMFS during the summer bottom-trawl survey of the EBS at the standard survey sample stations (for survey details see Markowitz et al., 2023). Species that are infrequently encountered or not efficiently caught by the bottom-trawling gear are excluded from this indicator (e.g., sharks, grenadiers, myctophids, pelagic smelts). The survey index used here is the same as that used for foraging guild biomass indices on the report card (Figure 2).

Species (or functional groups) infrequently sampled for lengths (less than five times over the time series) are excluded from this indicator (e.g., capelin, eulachon, greenlings). Twenty-two species are included. Eleven species had their lengths sampled in all 42 years of the survey time series. Another 11 species were sampled between 11 and 39 times over the time series. In years where a species lengths were not sampled, we replaced with a long-term mean for that species.

Walleye pollock is a biomass dominant species in the eastern Bering Sea and may drive the value of community indicators. Therefore this indicator is presented as two time series, one that includes and one that excludes pollock.

Status and trends:
With pollock included: The mean length of the eastern Bering Sea groundfish community in 2024 is 36.14 cm, nearly equal to the value of 36.3 in 2023, and remains above the long term mean of 32.6 (Figure 124, circles).

Without pollock included: The mean length of eastern Bering Sea groundfish without pollock is 33.4 cm in 2024, down slightly from 33.8 cm in 2023, and above the long term mean of 29.7 cm (Figure 124, triangles). This series trended upward from 2012 to 2018 then declined each survey year to 2022 and has been relatively flat since.

Factors influencing observed trends: This indicator is specific to fishes that are routinely caught and sampled during the NMFS summer bottom-trawl survey. The estimated mean length can be biased if specific species-size classes are sampled more or less than others, and is sensitive to spatial variation in the size distribution of species. Changes in fisheries management or fishing effort could also affect this indicator. Modifications to fishing gear, fishing effort, and targeted species could affect the mean length if different size classes and species are subject to changing levels of fishing mortality. This indicator could also be influenced by fluctuations in recruitment, where a large cohort of small forage species could reduce mean length. Environmental factors could also influence fish growth and mean length by effecting the availability and quality of food or by direct temperature effects on growth rate.

Pollock is a biomass dominant component of this ecosystem and year-to-year fluctuations in their mean size and biomass have a noticeable effect on this indicator. In 1993, their biomass index was above average but their mean size was the fifth lowest of the time series. Additionally, 1993 was a pronounced peak in the biomass index of capelin. This reduced the proportional contribution of other species to total groundfish biomass index, thus reducing the indicator value in 1993. Years where this indicator attained its highest values (1987, 2016–2024) generally correspond to years of above average mean size and/or biomass index for pollock, except 2018, 2021, and 2023 where pollock mean size was above average but their biomass index was below average.

The series without pollock mirrored the overall trends in the series with pollock included, but was generally lower. This was because the mean length of pollock was generally a few cm greater than the mean length of the rest of the groundfish community. Exceptions occurred in 1983, 1985, and 2018 when the mean length of pollock was less than the mean of the rest of the groundfish community.

Implications: The mean length of the groundfish community in the EBS has been stable over the bottom-trawl time series (1982–2024) with some interannual variation. The collective stability of the combined biomass of relatively larger groundfish species has helped to maintain this indicator at its recent high values. Previous dips in this indicator were in part attributable to spikes in abundance of smaller forage species (e.g., capelin) as opposed to a sustained shift in community composition or reductions in species mean length.

Stability of Fish Biomass

Contributed by George A. Whitehouse
Cooperative Institute for Climate, Ocean, and Ecosystem Studies (CICOES), University of Washington, Seattle WA
Contact: andy.whitehouse@noaa.gov
Last updated: October 2024

Description of indicator: The stability of the groundfish community total biomass is measured with the inverse biomass coefficient of variation (CV; 1 divided by the coefficient of variation of total groundfish biomass (1/CV[B])). This indicator provides a measure of the stability of the ecosystem and its resistance to perturbations. The variability of total community biomass is thought to be sensitive to fishing and is expected to increase with increasing fishing pressure (Blanchard and Boucher, 2001). The CV is the standard deviation of the groundfish biomass index over the previous 10 years divided by the mean biomass over the same time span Shin et al. (2010). The biomass index for groundfish species was calculated from the catch of the NMFS/AFSC annual summer bottom-trawl survey of the eastern Bering Sea (EBS). Since 10 years of data are required to calculate this metric, the indicator values start in 1991, the tenth year in the trawl survey time series (1982–2024). This metric is presented as an inverse, so as the CV increases the value of this indicator decreases, and if the CV decreases the value of this indicator increases.

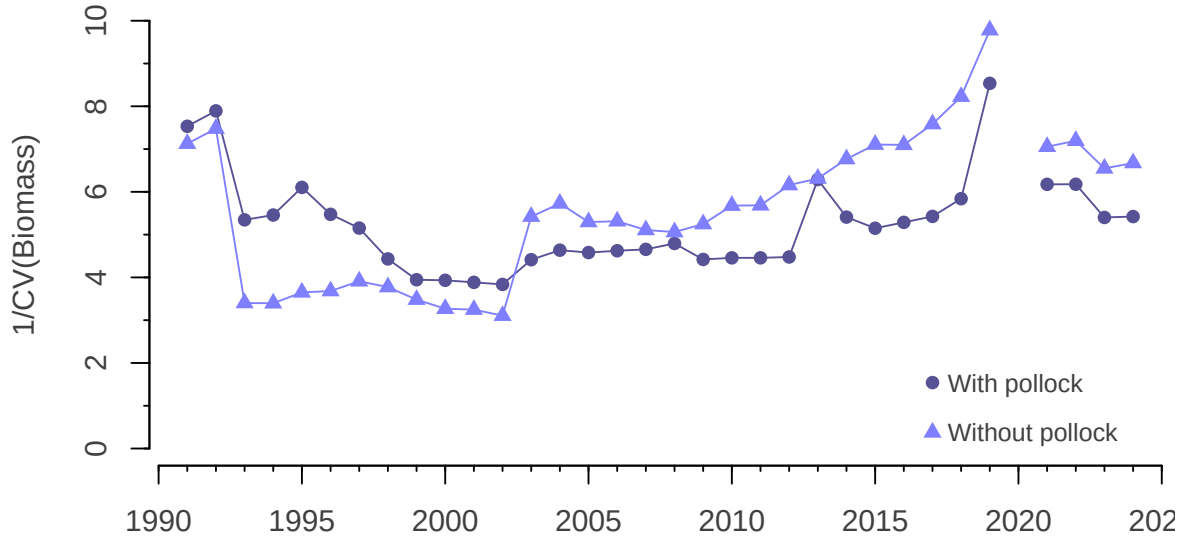

Figure 125: The stability of fish biomass in the eastern Bering Sea represented with the inverse biomass coefficient of variation of total fish biomass (1/CV[B]). The circles are the series with pollock included in the index, and the triangles are the same series but with pollock excluded.

This indicator specifically applies to the portion of the demersal groundfish community that is efficiently sampled by the trawling gear used by NMFS during the annual summer survey at the standard survey sample stations (for survey details see Markowitz et al., 2023). Species that are infrequently encountered or not efficiently caught by the bottom-trawling gear are excluded from this indicator (e.g., sharks, grenadiers, myctophids, pelagic smelts). The survey index used here is the same as that used for foraging guild biomass indices on the report card (Figure 2).

Pollock is a biomass dominant species in the EBS and may drive the value of this indicator. Therefore this indicator is presented as two time series, one that includes and one that excludes pollock.

Status and trends:
With pollock included: The state of this indicator in 2024 is 5.42 (Figure 125, circles), which is nearly equal to its time series mean of 5.26. An earlier peak of 7.90 was observed in 1992, which was followed by a steady decrease to a low of 3.84 in 2002. Since then it gradually increased to a value of 5.84 in 2018 before sharply increasing to a recent high in 2019.

Without pollock included: This indicator decreased from 7.19 in 2022 to 6.55 in 2023 and 6.67 in 2024 (Figure 125, triangles). This indicator dropped sharply from 7.49 in 1992 to 3.41 in 1993, and remained below 4 until 2003, where the value increased to 5.44. The indicator remained relatively stable until 2010, when the indicator began a steady upward trend to the series high value in 2019.

Factors influencing observed trends: Fishing is expected to influence this metric as fisheries can selectively target and remove larger, long-lived species effecting population age structure (Berkeley et al., 2004; Hsieh et al., 2006). Larger, longer-lived species can become less abundant and be replaced by smaller shorter-lived species (Pauly et al., 1998). Larger, longer-lived individuals help populations to endure prolonged periods of unfavorable environmental conditions and can take advantage of favorable conditions when they return (Berkeley et al., 2004). A truncated age-structure could lead to higher population variability (CV) due to increased sensitivity to environmental dynamics (Hsieh et al., 2006). Interannual variation in this metric could also be influenced by interannual variation in species abundance in the trawl survey catch, patchy spatial distribution for some species, or species distribution shifts (Stevenson and Lauth, 2019; Thorson, 2019*b*). This metric, as calculated here with trawl-survey data, reflects the stability of the portion of the groundfish community that is represented in the catch data of the annual summer bottom-trawl survey. Both, sharp increases or decreases in species index values can increase variability and reduce the indicator value.

The high values for this indicator in 2019 and at the start of the time series are indicative of stable groundfish biomass with a relatively low CV during the previous ten years. The CVs for both time series (with and without pollock) in 2019 were the lowest over their respective time series resulting in their highest indicator values. The sharp drop in total biomass in 2021, particularly for pollock, increased the CV resulting in lower indicator values in 2021. Previously, both series dropped sharply from 1992 to 1993. This was because the index for capelin in 1993 was anomalously high which increased variability and reduced the indicator value. In 2003, both series increased, which was in part due to the high capelin value in 1993 no longer being a part of the most recent 10 years.

In 2009, the series without pollock begins a steady increase towards its high value in 2019. The series with pollock included has a more modest positive trend over the same span, with high values in 2013 and 2019. Pollock is a biomass dominant species in the EBS and interannual fluctuations in their biomass are sufficient to increase variability for the total groundfish community and thus, reduce the indicator value. The series without pollock is more sensitive to fluctuations of other species, such as capelin. The sharp increase in the capelin index in 1993 kept this series lower than the series with pollock included from 1993–2002.

Implications: This measure indicates that the EBS groundfish community has been generally stable over the time period examined here, particularly since 2003. While the indicator values dropped from 2022 to 2023 with and without pollock, both series remain above their long term means in 2024 and indicate a maintenance of community biomass stability.

Emerging Stressors

Ocean Acidification

Contributed by Darren Pilcher[1], Jessica Cross[2], Natalie Monacci[3], Esther Kennedy[3], Elizabeth Siddon[4], and W. Christopher Long[5]
[1]NOAA Fisheries, Northwest Fisheries Science Center, Seattle, WA
[2]Pacific Northwest National Laboratory
[3]University of Alaska Fairbanks, Ocean Acidification Research Center
[4]NOAA Fisheries, Alaska Fisheries Science Center, Auke Bay Laboratories, Juneau, AK
[5]NOAA Fisheries, Alaska Fisheries Science Center, Kodiak Laboratory, Kodiak, AK
Contact: darren.pilcher@noaa.gov
Last updated: October 2024

Description of indicator: The oceanic uptake of anthropogenic CO_2 is decreasing ocean pH and carbonate saturation states in a process known as ocean acidification (OA). The cold, carbon rich waters of the Bering Sea are already naturally more corrosive than other regions of the global ocean, making this region more vulnerable to rapid changes in ocean chemistry. The projected areal expansion and shallowing of these waters with continued absorption of anthropogenic CO_2 from the atmosphere poses a direct threat to marine calcifiers and an indirect threat to other species through trophic interactions. These OA risks demonstrate a clear need to track and forecast the spatial extent of acidified waters in the Bering Sea.

Here, we present updated carbonate chemistry output from the Bering Sea ROMS model (Bering10K; Pilcher et al., 2019), which is updated annually and currently spans 1970–August 24, 2024. We show spatial plots for modeled Bering Sea bottom water pH, including both the conditions in 2024 (Figure 126, left) as well as the 2024 detrended anomaly (Figure 126, right). The detrended anomaly removes the impact of ocean acidification (otherwise a slow, consistent process) and highlights the role of natural processes, which generate most of the interannual variability in the carbon system. It is calculated as the residual after removing the linear trend over the entire 1970–2024 hindcast, similar to removing the global warming trend from a long-term temperature timeseries.

We focus on bottom waters and the late summer time frame because this is where and when we expect the most acidic waters to develop, due to the combination of ocean acidification pressures and natural seasonal biological respiration. This is also when bottom temperatures typically reach seasonal highs. Late summer is, therefore, the time most likely for synergistic negative effects on crabs to emerge (Swiney et al., 2017). This model output is used to develop indices for both pH and the aragonite saturation state (Ω_{arag}) using threshold values of biological significance (Figures 127 and 128). The growth and survival of red king and tanner crab are negatively affected at pH $\leq$7.8 (Long et al., 2013), and bivalve larvae are negatively affected at Ω_{arag} $<$1 (Waldbusser et al., 2015). The goal of this index time series, along with the spatial anomaly plot, is to provide a quick assessment of the summer water pH and Ω_{arag} conditions compared to previous years.

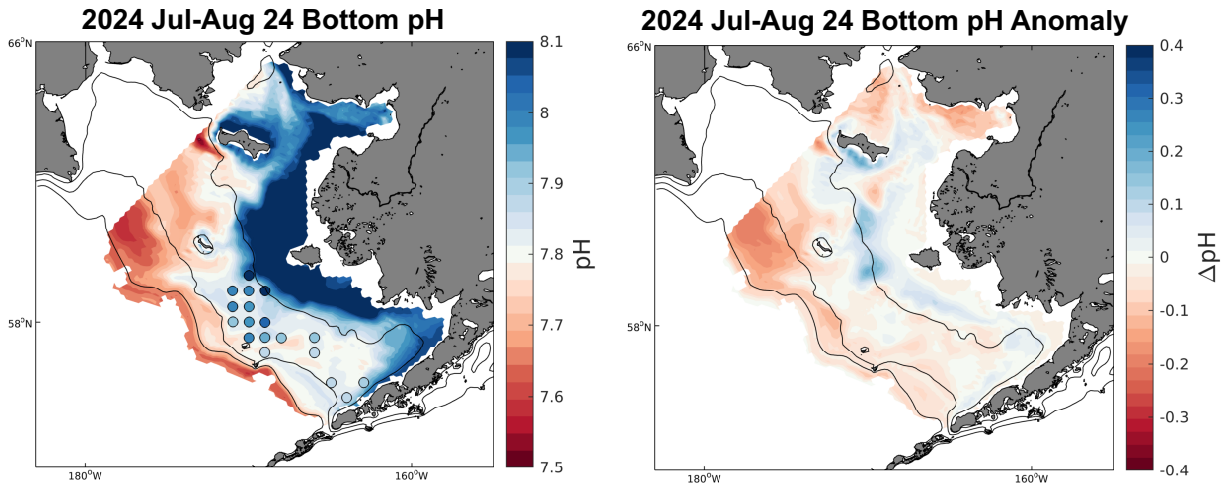

Figure 126: Model spatial maps of July-August 24 averaged bottom water pH for (left) 2024 hindcast and (right) the 2024 detrended anomaly. The circles in the left panel represent the preliminary* data collected onboard the fall 2024 BASIS cruise, plotted on the same colorbar as the model output. Contour lines denote the 50 m, 100 m, and 200 m isobaths. Regions that are outside of the eastern Bering Sea management region are omitted. Impacts of ocean acidification on fisheries are understood to be a combination of the temporal duration, biogeochemical intensity, and spatial extent. This visualization shows both the intensity and extent of acidified conditions over the Bering Sea shelf. * Data have not yet undergone quality assurance and control at the time of this writing.

Status and trends: Modeled bottom water pH and Ω_{arag} values were greater in 2024 compared to 2023, leading to a decrease in the percent of bottom waters below highlighted biological thresholds (Figures 127 and 128). Detrended pH anomalies were relatively weak in 2024 for the inner and middle shelf, with patchy regions of relatively low magnitude pH anomalies (Figure 126, right). Bottom pH values near the 50 m isobath were slightly higher compared to the detrended pH baseline. The middle shelf displayed a noticeable gradient near St. Matthew Island, with pH values to the south generally greater than 7.8, but values to the north less than 7.8. Notably, the outer shelf negative pH anomaly - a persistent anomaly in the model since 2018 - was still present, but was most prevalent in the northwest portion of the outer shelf (Figure 126, right).

Preliminary data collected onboard the fall Bering Arctic Subarctic Integrated Survey (BASIS) also indicated pH values above 7.8 for the middle shelf, with relatively higher values in the central middle shelf compared to the limited data in the southeastern middle shelf. BASIS data are similar in magnitude to modeled pH data, though the observational data suggests slightly higher pH for the central middle shelf compared to the model.

Factors influencing observed trends: Modeled bottom pH and Ω_{arag} both increased this year compared to the relatively low values of 2023. However, because the model hindcast ends in mid-August, these relatively higher values compared to 2023 are partly driven by the shorter seasonal averaging timeframe (i.e., not the complete July-September timeframe). Bottom pH and Ω_{arag} are typically lowest in September due to the seasonal accumulation of subsurface respired carbon. Overall, bottom pH and Ω_{arag} values are still low relative to the entire model timeframe, driven mainly by the long-term decreasing trend caused by ocean acidification. We anticipate that natural variability will continue to be the dominant source of interannual variability such as that illustrated between 2023–2024, and that over decadal timeframes, pH and Ω_{arag} will continue to decline with ocean acidification.

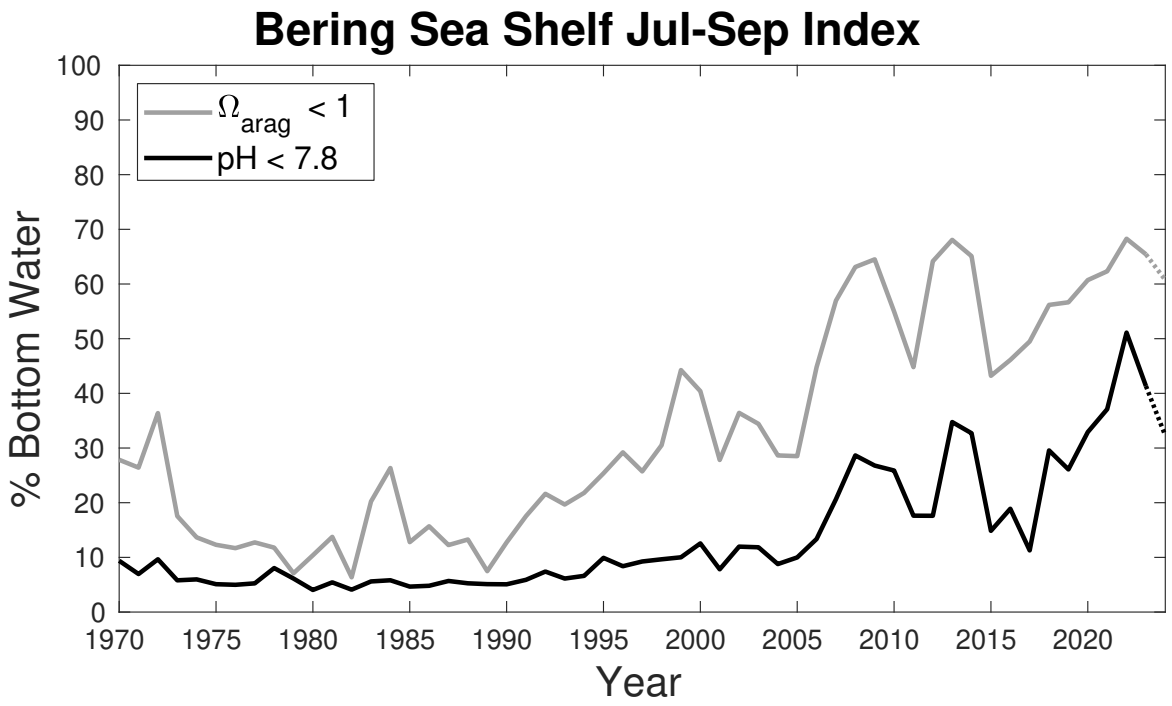

Figure 127: Model timeseries of the July-September pH index (black line) and Ω_{arag} undersaturation index (grey line). Each index is calculated as the percent of spatial area of the Eastern Bering Sea region (see Figure 126) where bottom waters have a July-September average below the denoted value. The dotted portion at the end represents the incomplete 2024 value, which is run up through August 24 at the time of writing. Impacts of ocean acidification on fisheries are a function of the temporal duration, biogeochemical intensity, and spatial extent. This visualization shows the percent area (spatial extent) of the shelf that is exposed to potentially harmful biogeochemical conditions.

Implications: Based on the sensitivity of red king crab to pH, previous work suggests that OA may have significant negative impacts to the red king crab fishery (Seung et al., 2015; Punt et al., 2016). In 2024, modeled pH and Ω_{arag} water conditions in Bristol Bay are near or slightly above the detrended average conditions and the shallower inner shelf waters that serve as habitat for juvenile red king crab are relatively well buffered. Although portions of the outer and middle shelf contain model pH values less than 7.8, the anomaly is relatively low as these waters contain higher acidity at baseline. Furthermore, a recent experimental study suggests that snow crab are resilient to OA (Long et al., 2023).

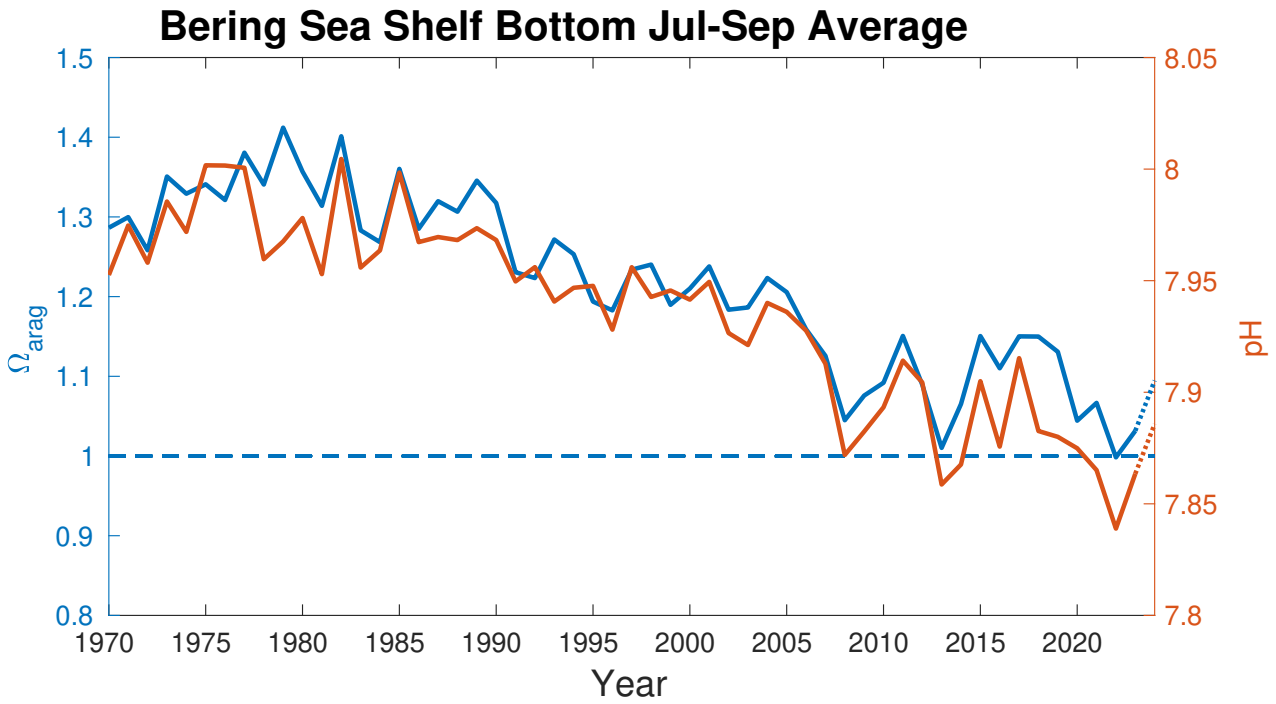

Figure 128: Model timeseries of the Jul-Sept average bottom water Ω_{arag} (left vertical axis, blue) and pH (right vertical axis, orange). The dotted portion at the end represents the incomplete 2024 value, which is run up through August 24 at the time of writing. Impacts of ocean acidification on fisheries are understood to be a combination of the temporal duration, biogeochemical intensity, and spatial extent. Visualizing the net shelf-wide average, rather than scaling these variables spatially (see Figure 127), helps show the intensity of aggregate conditions. However, it is important to consider this figure in context with Figures 126 and 127, as a shelf-wide average may disguise some areas of resilience (e.g., cool colors, Figure 126) and ocean acidification hotspots (e.g., warmer colors, Figure 126).

Harmful Algal Blooms

Contributed by Thomas Farrugia
Alaska Ocean Observing System, Anchorage, AK
Contact: farrugia@aoos.org
Last updated: October 2024

Description of indicator: Alaska's most well-known and toxic harmful algal blooms (HABs) are caused by *Alexandrium* spp. and *Pseudo-nitzschia* spp. *Alexandrium* produces paralytic shellfish toxins (PST) which can cause paralytic shellfish poisoning (PSP) and has been responsible for five deaths and over 100 cases in Alaska since 1993[19]. Analyses of PSTs are commonly reported as µg of toxin/100 g of tissue, where the FDA regulatory limit is 80 µg/100 g. Toxin levels between 80 µg–1000 µg/100 g are considered to potentially cause non-fatal symptoms, whereas levels >1000 µg/100 g (∼12x regulatory limit) are considered potentially fatal.

Pseudo-nitzschia produces domoic acid which can cause amnesic shellfish poisoning and inflict permanent brain damage. *Pseudo-nitzschia* has been detected in 13 marine mammal species and has the potential to impact the health of marine mammals and birds in Alaska. No human health impacts of domoic acid have been reported in Alaska, although both acute and chronic amnesic shellfish poisoning has been reported in several states, including Washington and Oregon.

Another organism, *Dinophysis* spp., produces okadaic acid which can lead to diarrhetic shellfish poisoning. This primarily impacts the gastrointestinal system and is not usually life-threatening but can lead to nausea, vomiting, abdominal cramping, and diarrhea. Although there have not been recorded cases of diarrhetic shellfish poisoning in Alaska, *Dinophysis* has been detected throughout Alaska, and okadaic acid is at times detected in shellfish.

The Alaska Department of Environmental Conservation (DEC) tests bivalve shellfish harvested from classified shellfish growing areas meant for commercial market for marine biotoxins including PST in all bivalve shellfish and domoic acid (DA) specifically in razor clams. The Environmental Health Laboratory (EHL) is the sole laboratory in the state of Alaska certified by the FDA to conduct regulatory tests for commercial bivalve shellfish. The EHL also does testing for research, tribal, and subsistence use.

The State of Alaska tests all commercial shellfish harvest, however there is no state-run shellfish testing program for recreational and subsistence shellfish harvest. Regional programs, run by Tribal, agency, and university entities, have expanded over the past five years to provide test results to inform harvesters and researchers and reduce human health risk. All of these entities are partners in the Alaska Harmful Algal Bloom (AHAB) Network which was formed in 2017 to provide a statewide approach to HAB awareness, research, monitoring, and response in Alaska. More information can be found on the Alaska HAB Network website[20].

Nurse consultants from the Alaska Department of Health, Section of Epidemiology (SOE) join monthly AHAB meetings and collaborate with stakeholders so they can be made aware of reportable illness such as PSP. More information about PSP and other shellfish poisoning can be found on the SOE website[21].

[19] State of Alaska. Epidemiology Bulletin. 2022. Available at: http://www.epi.alaska.gov/bulletins/docs/b2022_05.pdf

[20] https://ahab.aoos.org

[21] https://health.alaska.gov/dph/Epi/id/Pages/dod/psp/default.aspx

Status and trends:
Alaska Region: Results from shellfish and phytoplankton monitoring showed a slight downtick in the presence of harmful algal blooms (HABs) and toxins throughout all regions of Alaska in 2024 compared to 2023, and the overall levels were lower than in 2019–2021. Bivalve shellfish from areas that are well known for having PSP levels above the regulatory limit, including Southeast Alaska and the Aleutians, continued to have samples that tested above the regulatory limit, albeit less frequently than since 2019 and 2020. Overall, 2024 seems to have been slightly less active for blooms and toxin levels than 2021, 2020, and 2019, but areas continue to have HAB organisms in the water, and shellfish testing well above the regulatory limit, primarily between May and September in 2024. Over the last few years, the dinoflagellate *Dinophysis* has become more common and abundant in water samples, and 2024 continued that trend. We are also seeing a geographic expansion of areas that are sampling for phytoplankton species. In the Bering Sea, HABs were being monitored through the opportunistic placement of Imaging FlowCytobots (IFCB) on the USCGC Healy as it transited the Bering, Chukchi, and Beaufort Seas on research cruises.

Bering Sea: No toxin results from 2024 are available yet for the Bering Sea region, but invertebrate samples have been taken and will be analyzed in the near future. However, the Alaska Ocean Observing System was able to deploy an Imaging FlowCytobot (IFCB) on the Arctic Observing Network cruise aboard the USCGC Healy in July 2024. The IFCB collected imagery of the plankton community through the underway seawater system of the vessel, allowing near real-time identification and counts of different algal types. The research cruise transited through the Bering Sea from Dutch Harbor to the Bering Strait in early July. On July 5th, the IFCB detected elevated levels of *Alexandrium catenella* cells (Figure 129). Maximum concentrations of this algae were estimated to be between 200 and 4,600 cells per liter of seawater, recorded approximately 160 nautical miles (nm) east of St. Paul Island and 120 nm from the Alaskan mainland. The relatively small patch of elevated cells consisted of six seawater samples with high cell counts of $>$1,000 cells/L while the vessel transited approximately 35 nm.

For more HAB results from the Northern Bering Sea, see the ECOHAB section of this report on p. 215.

Factors influencing observed trends: HABs are likely to increase in intensity and geographic distribution in Alaska waters with warming water temperatures. Observations in Southeast and Southcentral Alaska suggest *Alexandrium* blooms occur at temperatures above 10°C and salinities above 20 (Vandersea et al., 2018; Tobin et al., 2019; Harley et al., 2020). As waters warm throughout Alaska, blooms may increase in frequency and geographic extent.

Implications: HABs pose a risk to human health when present in wildlife species that people consume, including shellfish, birds, and marine mammals. Research across the state is attempting to better understand the presence and circulation of HABs in the food web. HAB toxins have been detected in stranded and harvested marine mammals from all regions of Alaska in past years (Lefebvre et al., 2016). A multi-disciplinary statewide study funded by NOAA's ECOHAB program is underway and encompasses ship-based sediments samples, water samples, zooplankton samples, krill samples, copepod samples, multiple species of fish, bivalves, and the continuation of sampling subsistence-harvested and dead stranded marine mammals.

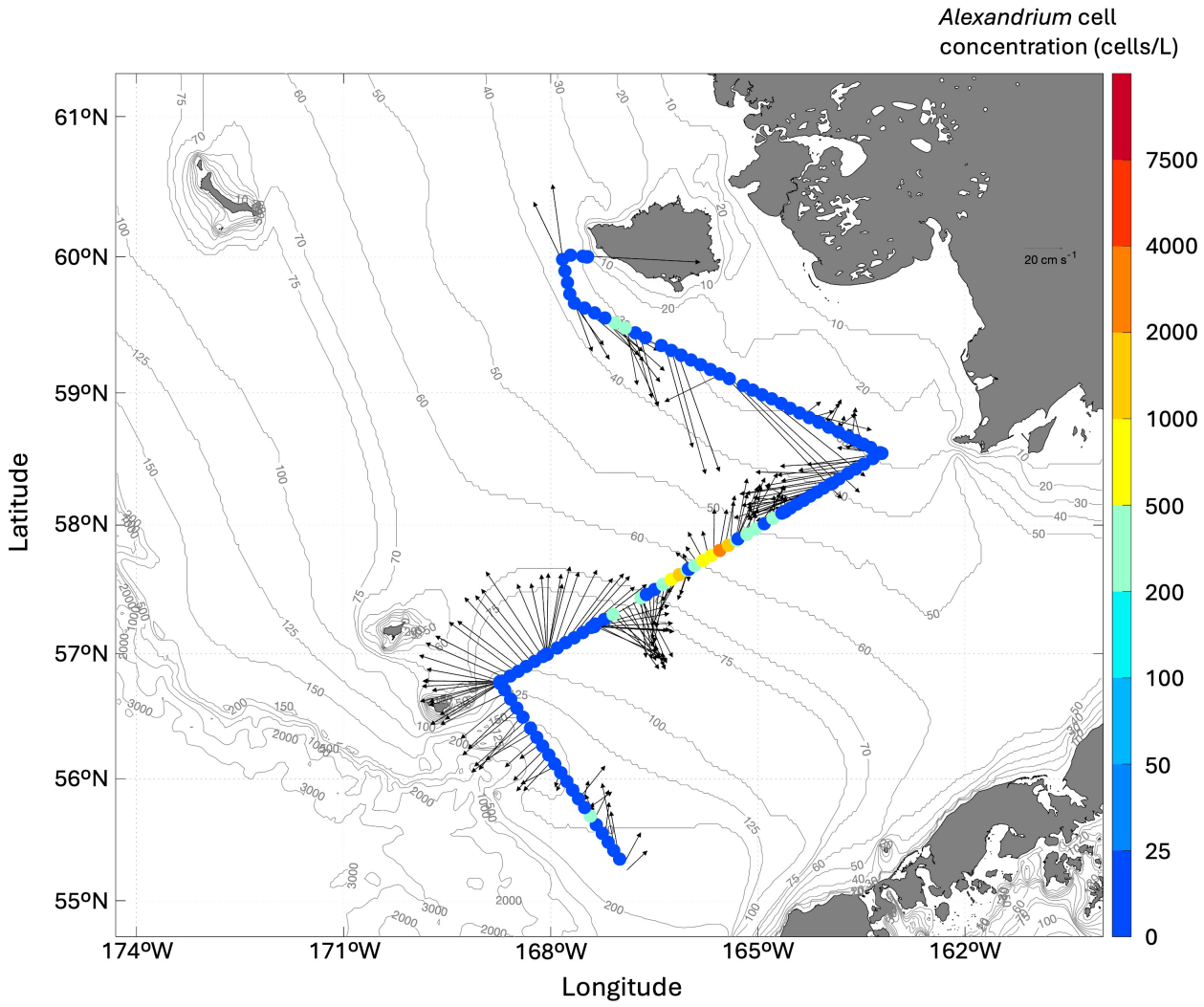

Figure 129: Estimated cell concentrations of the marine algae *Alexandrium catenella* sampled July 4–6, 2024 based on data collected by the Imaging FlowCytobot (IFCB) onboard the USCGC Healy. The color of the dots represents the concentration of *Alexandrium* cells in the samples (cells/L). Arrows indicate current direction and strength at the time of sampling, measured by shipboard instrumentation.

ECOHAB: Harmful Algal Bloom (HAB) Toxins in Arctic Food Webs

Contributed by Kathi Lefebvre[1], Donald M. Anderson[2], Gay Sheffield[3], Raphaela Stimmelmayr[4], Evangeline Fachon[2], Patrick Charapata[1], Robert Pickart[2], Thomas Farrugia[5], and Emily Bowers[1]
[1]Environmental and Fisheries Science, Northwest Fisheries Science Center, National Marine Fisheries Service, NOAA, Seattle, WA
[2]Woods Hole Oceanographic Institution, Woods Hole, MA
[3]University of Alaska Fairbanks, Alaska Sea Grant, Nome, AK
[4]North-Slope Borough Department of Wildlife Management, Utqiagvik, AK
[5]Alaska Ocean Observing System, Anchorage, AK
Contact: kathi.lefebvre@noaa.gov
Last updated: October 2024

Description of indicator: *Alexandrium* and *Pseudo-nitzschia* are two common harmful algal bloom (HAB) species in Alaskan waters that produce neurotoxic compounds such as saxitoxin (STX; generated by *Alexandrium* species; causes Paralytic Shellfish Poisoning PSP) and domoic acid (DA; generated by *Pseudo-nitzschia* species; causes Amnesic Shellfish Poisoning ASP). Monitoring the presence and abundance of HAB cell (i.e., *Alexandrium* and *Pseudo-nitzschia*) densities and toxin (STX and DA) prevalence in marine food webs are useful indicators of ecosystem health and potential threats to wildlife and human health. Multiple years of sampling via the ECOHAB: Arctic Food Webs study confirm that HAB toxins are present in Arctic and Subarctic food webs on a regular basis and at varying concentrations (Figure 130). The risks of these toxins include human illness and death associated with seafood consumption as well as health impacts to marine wildlife at multiple trophic levels. Many commercially valuable shellfish and finfish are impacted by these toxins, as well as marine mammals, invertebrates, seabirds, and filter-feeding fishes that are harvested for subsistence purposes and consumed by Alaska's coastal communities.

Status and trends: As the climate has warmed over the past few decades, the Pacific sector of the Arctic Ocean has warmed with dramatic consequences. The quality, quantity, and duration of sea ice has decreased markedly due to earlier melting and a delayed freeze-up (Frey et al., 2014). The input of Pacific water northwards through the Bering Strait has increased, warmed, and freshened (Woodgate et al., 2012). Warmer air temperatures are peaking earlier in the season and have led to increased summer ocean warming (Pickart et al., 2013). Stronger summertime northeasterly winds have led to upwelling-favorable conditions along the western Alaskan coast (Pickart et al., 2011). Combined, these physical changes have made conditions more favorable for HAB species, particularly the dinoflagellate *Alexandrium catenella* and diatoms in the genus *Pseudo-nitzschia* (Anderson et al., 2012).

Recent studies reveal increasing toxin prevalence in food webs (Hendrix et al., 2021) and the potential for increased *Alexandrium* cyst germination in certain cyst-dense areas, such as the seafloor in the northeastern Chukchi Sea, directly linked to warmer ocean bottom temperatures (Anderson et al., 2021). Saxitoxin doses were estimated during an anomalously warm year (2019) in the Arctic revealing that walruses were exposed to toxin concentrations at levels known to impact human health during shellfish poisoning events, as well as rodents in controlled laboratory studies (Lefebvre et al., 2022). In October of 2023, no harvested bowhead whales contained domoic acid, but 90% contained low levels of saxitoxin (Figure 131). This confirms a consistent trend of higher prevalence of saxitoxin than domoic acid in Arctic food webs observed in all regions including the Bering Strait.

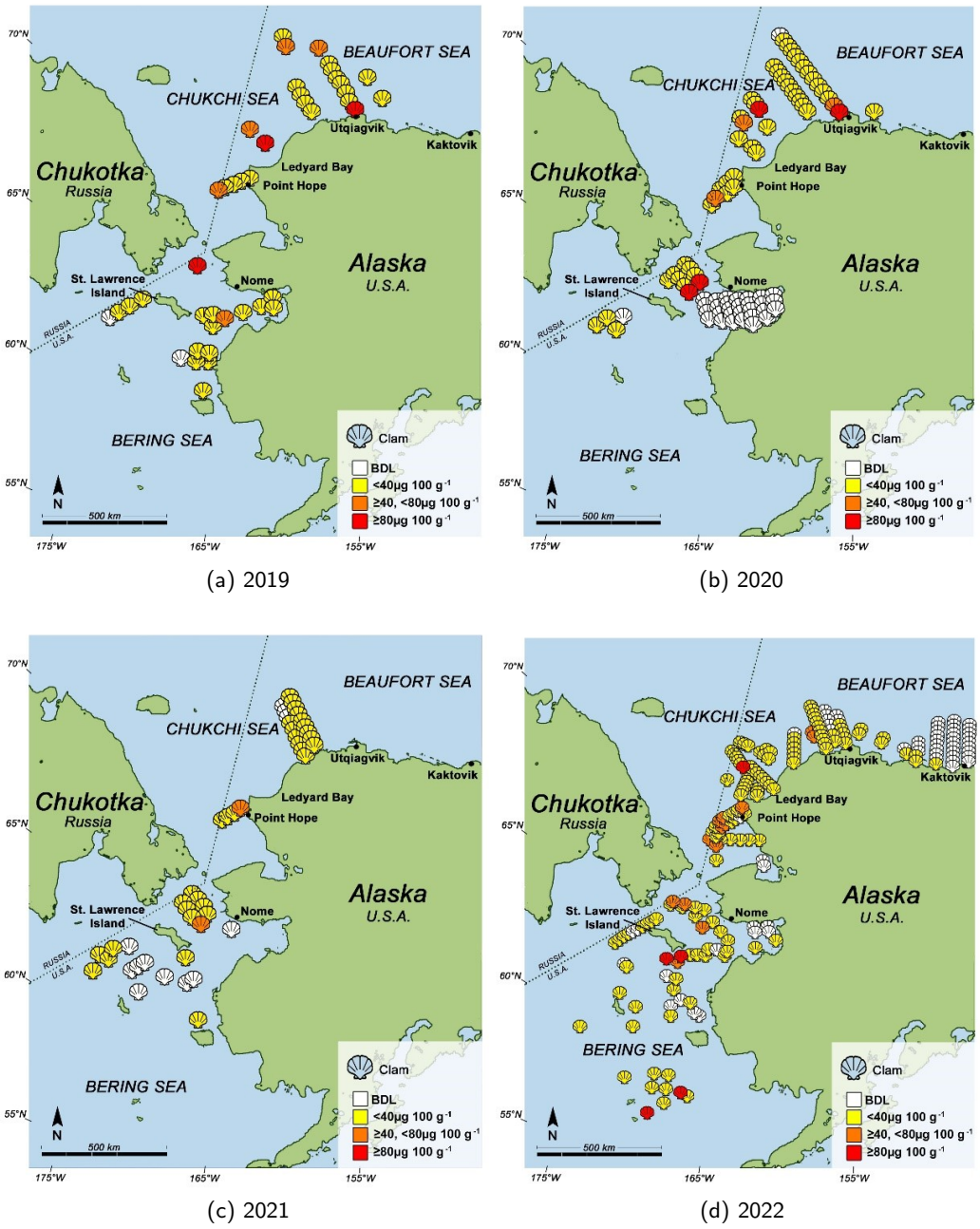

(a) 2019 (b) 2020

(c) 2021 (d) 2022

Figure 130: Saxitoxins detected in clams sampled during summers of (a) 2019, (b) 2020, (c) 2021, and (d) 2022. Red = high concentrations at or above seafood safety regulatory limit of 80 µg/100 g; Orange = moderate concentrations; Yellow = low concentrations; white = below toxin detection limits (BDL).

In July 2022 and 2023, dense blooms of *Alexandrium* were detected in the Bering Strait region, prompting public advisories and regional event response. These events have motivated continued efforts to implement and expand real-time shipboard HAB monitoring through Imaging FlowCytobot (IFCB) deployments. During the summer 2024 field season, a research cruise in July detected elevated levels of *Alexandrium* (∼4500 cells/L) ∼160 nautical miles east of St. Paul, leading to the release of a risk

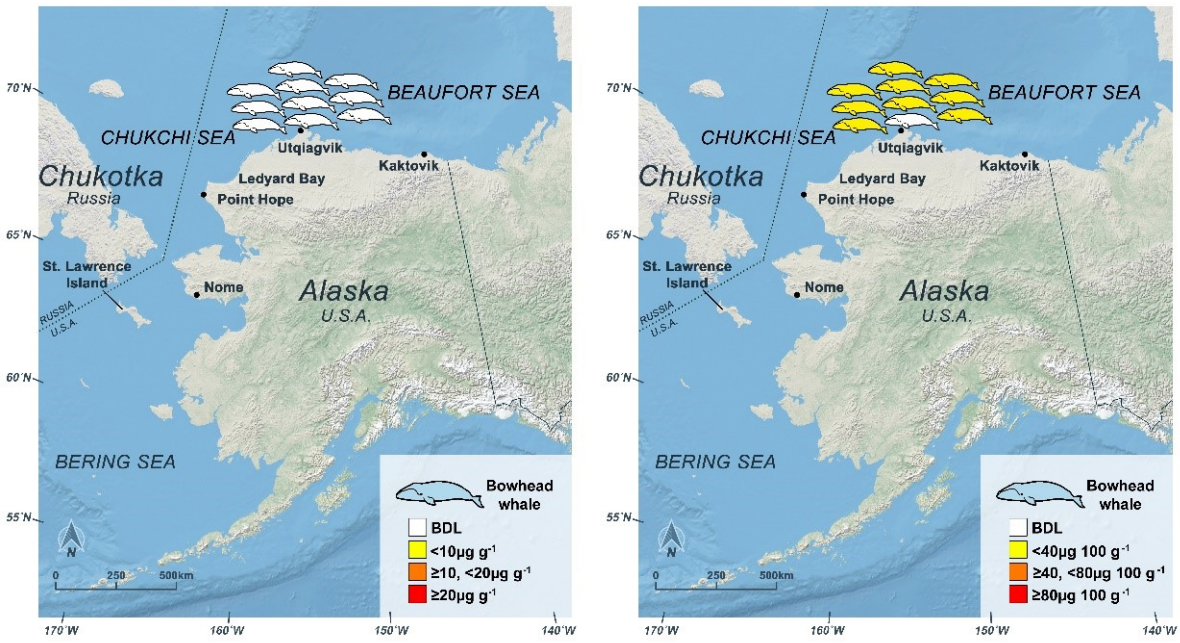

Figure 131: Low levels of harmful algal bloom toxins were detected in bowhead whales harvested for subsistence purposes during Fall 2023: Left: domoic acid (DA) was below detection limits (BDL) in all animals tested; Right: low concentrations of saxitoxins (STX) were found in 90% of animals tested (unpublished data from K. Lefebvre). This trend of higher STX prevalence compared to DA also occurs in the Bering Strait region.

advisory (Figure 129). However, shipboard observing efforts in August did not detect any significant *Alexandrium* presence in the Bering Strait region where blooms had been detected previously. Further analysis of data collected during these cruises, as well as ocean reanalysis fields, will be used to investigate what environmental factors may be contributing to the broad differences in bloom occurrence between years.

Factors influencing observed trends: Increasing HAB events and toxin prevalence is linked to warming ocean temperatures throughout the water column (both surface and bottom) and increased sunlight associated with the loss of sea-ice cover. Analysis of pathways from the 2022 Bering Strait region bloom event indicated that the *Alexandrium* likely entered the region from western waters in the Gulf of Anadyr. Therefore, understanding conditions in western waters is an important component in predicting and interpreting bloom occurrence.

Implications: The impacts of increased biotoxin exposure include increased risks to ecosystem, wildlife, and public health in Northern Arctic regions. As ocean temperatures continue to rise, algal growth and cyst germination rates of toxic *Alexandrium* will continue to increase. Recurrent high *Alexandrium* cell counts confirm the regular occurrence of HABs in the region that can contaminate food webs. Results indicate that HAB events are intensifying in Alaskan waters and there is a clear need to monitor HAB densities and toxin concentrations throughout the food web. Impacts also include food security concerns to Arctic coastal peoples as well as conservation concerns for many species of marine resources, including several marine mammals currently listed under the Endangered Species Act (ESA). Arctic coastal people sampling efforts are being developed, but consistent funding is needed to sustain temporal and spatial monitoring coverage of HAB activity in the Alaskan ecosystem.

Future Steps:
Ongoing research projects include the continuous monitoring of *Alexandrium* and *Pseudo-nitzschia* within Alaskan waters and their biotoxins among marine trophic levels. Innovative technology such as the IFCB allows continuous 24/7 underway sampling during extended research cruises (>1 month). The IFCB can identify *Alexandrium* and *Pseudo-nitzschia* cells and provide cell densities using machine learning based algorithms. This has continued to be useful for providing real time updates on bloom activity in sampled areas.

Currently, models for quantifying toxin exposure risks in Arctic marine ecosystems are being developed. Thus, cruises will continue to collect samples from organisms throughout different components of the food web (phytoplankton, zooplankton, invertebrates, fish, and marine mammals) to develop toxin trophic transfer models that will estimate biotoxin exposure to commercially important marine resources and Alaska Native food resources during HABs of different intensities. Specifically, cell and cyst [*A. catenella* only] densities and toxicities, secondary trophic level taxa (e.g., invertebrates and zooplankton) morphometrics and measured toxicities, and data from published literature will be used to develop algal toxin trophic transfer models. Model parameters include consumption rates (e.g., clams; cells/day), diet composition (e.g., proportion of diet composed of *A. catenella* cells), mass of predators, and elimination rate of toxins. Once parameters have been validated using established methods (Hoondert et al., 2020), these models will provide estimates of algal toxins in these secondary trophic level taxa during bloom events, which will be used to estimate algal toxin oral dose estimates to higher trophic level predators, including marine mammals harvested for subsistence purposes (e.g., walruses).

Current work focuses on using all available data from years of greatest spatiotemporal coverage (2019 and 2022) to validate parameters in a trophic transfer model that assesses movement of saxitoxins produced during *A. catenella* bloom events to benthic invertebrates including worms, gastropods, and clams and subsequently to walruses. Models for estimating saxitoxin oral dose estimates to walruses are based on the foraging ecology and bioenergetics of walruses and include similar parameters (e.g., consumption rates) to secondary trophic level models that are retrieved from published literature. Benthic invertebrate trophic transfer model parameters have undergone validations and future work will include incorporating results of model predictions into walrus saxitoxin oral dose estimate models. Data are available from 2019–2024 and various analyses relating to HAB species abundances and the development of other trophic transfer models are underway. The implementation of continuous HAB monitoring efforts such as IFCB deployments are needed to provide early warning and ensure future ecosystem and Alaska Native community health.

Maintaining Diversity: Discards and Non-Target Catch

Time Trends in Non-Target Species Catch

Contributed by George A. Whitehouse[1] and Sarah Gaichas[2]
[1]Cooperative Institute for Climate, Ocean, and Ecosystem Studies (CICOES), University of Washington, Seattle WA
[2]Ecosystem Assessment Program, Northeast Fisheries Science Center, NOAA Fisheries, Woods Hole MA
Contact: andy.whitehouse@noaa.gov
Last updated: August 2024

Description of indicator: This indicator reports the catch of non-target species in groundfish fisheries in the eastern Bering Sea (EBS). Catch since 2003 has been estimated using the Alaska Region's Catch Accounting System (Cahalan et al., 2014). This sampling and estimation process does result in uncertainty in catches, which is greater when observer coverage is lower and for species encountered rarely in the catch. Since 2013, the three categories of non-target species tracked here are:

1. Scyphozoan jellyfish
2. Structural epifauna (seapens/whips, sponges, anemones, corals, tunicates)
3. Assorted invertebrates (bivalves, brittle stars, hermit crabs, miscellaneous crabs, sea stars, marine worms, snails, sea urchins, sand dollars, sea cucumbers, and other miscellaneous invertebrates).

The catch of non-target species/groups from the Bering Sea includes the reporting areas 508, 509, 512, 513, 514, 516, 517, 521, 523, 524, and 530[22].

Status and trends: The catch of jellyfish more than doubled from 2020 to 2021 (Figure 132, top). Previous high catches of jellyfish occurred in 2011, 2014, and 2018 and were each followed by a sharp decrease in jellyfish catch the following year. The catch of jellyfish has had a slight downward trend from 2021 to 2023. Jellyfish are primarily caught in the pollock fishery.

The catch of structural epifauna trended downward from 2015 to 2020, and has remained low from 2021 to 2023 (Figure 132, middle). Benthic urochordate caught in non-pelagic trawls were the dominant component of the structural epifauna catch in 2012 and 2015–2023. In 2013 and 2014, anemones caught in the Pacific cod fishery were the dominant part of the structural epifauna catch. Sponge were the dominant component of the structural epifauna catch in 2011 and were primarily caught in non-pelagic trawls.

Sea stars comprise more than 85% of the assorted invertebrate catch in all years (2011–2023) and are primarily caught in flatfish fisheries (Figure 132, bottom). The catch of assorted invertebrates generally trended upward from 2011 to 2015, then declined from 2015 to 2023.

[22]https://www.fisheries.noaa.gov/alaska/sustainable-fisheries/alaska-fisheries-figures-maps-boundaries-regulatory-areas-and-zones

Factors influencing observed trends: The catch of non-target species may change if fisheries change, if ecosystems change, or both. Because non-target species catch is unregulated and unintended, if there have been no large-scale changes in fishery management in a particular ecosystem, then large-scale signals in the non-target catch may indicate ecosystem changes. Catch trends may be driven by changes in biomass or changes in distribution (overlap with the fishery) or both. Fluctuations in the abundance of jellyfish in the EBS are influenced by a suite of biophysical factors affecting the survival, reproduction, and growth of jellies including temperature, sea ice phenology, wind-mixing, ocean currents, and prey abundance (Brodeur et al., 2008). The lack of a clear trend in the catch of scyphozoan jellies may reflect interannual variation in jellyfish biomass and/or changes in the overlap with fisheries.

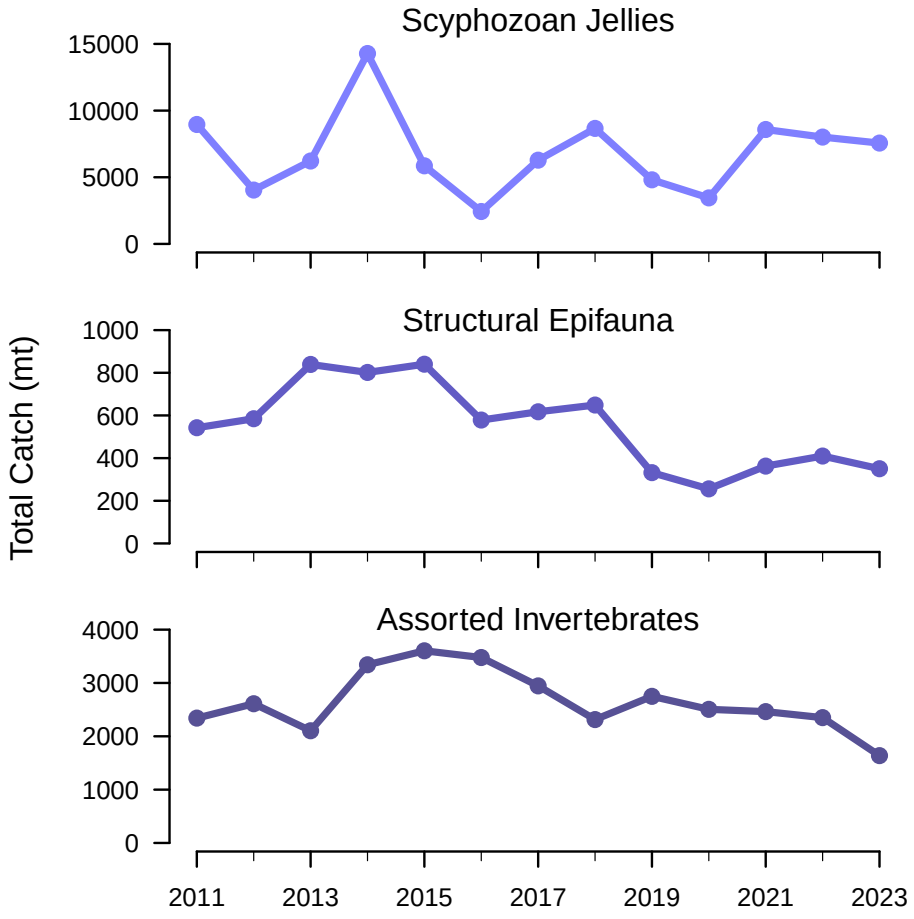

Figure 132: Total catch of non-target species (tons) in EBS groundfish fisheries (2011–2023). **Please note the different y-axis scales** between the species groups.

Implications: The catches of structural epifauna species and assorted invertebrates are very low compared with the catch of target species. Structural epifauna species may have become less available to the EBS fisheries or the fisheries avoided them more effectively. Abundant jellyfish may have a negative impact on fishes as they compete with planktivorous fishes for prey resources (Purcell and Arai, 2001; Ruzicka et al., 2020), and may prey upon the early life history stages (eggs and larvae) of fishes (Purcell and Arai, 2001; Robinson et al., 2014). Additionally, jellyfish may be an important prey resource for predators, including commercially important groundfishes (Brodeur et al., 2021).

Seabird Bycatch Estimates for Groundfish and Halibut Fisheries in the Eastern Bering Sea, 2013–2023

Contributed by Jessica Beck[1], Adam Zaleski[2], and Cathy Tide[2]
[1] Resource Ecology and Fisheries Management Division, Alaska Fisheries Science Center, National Marine Fisheries Service, NOAA
[2] Sustainable Fisheries Division, Alaska Regional Office, NOAA Fisheries
Contact: jessica.beck@noaa.gov
Last updated: September 2024

Description of indicator: This report provides estimates of the number of seabirds caught as bycatch in commercial groundfish and halibut fisheries operating in waters off of Alaska in the eastern Bering Sea for the years 2013 through 2023. Data collection on the Pacific halibut longline fishery began in 2013 with the restructured North Pacific Observer Program. Estimates of seabird bycatch from earlier years using different methods are not included here (see previous Ecosystem Status Reports). Fishing gear types represented are demersal longline, pot, pelagic trawl, and non-pelagic trawl. These numbers do not apply to jig, gillnet, seine, or troll fisheries[23].

The NMFS Alaska Regional Office Catch Accounting System (CAS) produces estimates (Cahalan et al., 2010, 2014) and provides near real-time delivery of accurate groundfish and prohibited species catch and bycatch information for inseason management decisions. These estimates are based on three sources of information: (1) data provided by NMFS-certified fishery observers deployed to vessels and floating or shoreside processing plants, (2) video review of electronically monitored (EM) fixed gear vessels, and (3) industry reports of catch and production. CAS also estimates non-target species (such as invertebrates) and seabird bycatch in the groundfish fisheries. The three data sets used by CAS are subject to change over time. Observer deployment plans are reviewed and updated annually in the Annual Deployment Plan (the 2023 plan is available at: `https://www.fisheries.noaa.gov/resource/document/2023-annual-deployment-plan-observers-and-electronic-monitoring-groundfish-and`).

This report delineates and separately discusses estimates of seabird bycatch in the southeastern Bering Sea and the northern Bering Sea. Estimates of seabird bycatch from the southeastern Bering Sea include the reporting areas 508, 509, 512, 513, 514, 516, 517, 521, and 524 (estimates for 514 and 524 only include data south of 60°N). Estimates from the northern Bering Sea include areas north of 60°N and south of 65°N in reporting areas 514 and 524[24]. Estimates of seabird bycatch north of 65°N are not included in this report. In previous versions of this report, bycatch estimates in the southeastern Bering Sea, northern Bering Sea, and waters north of 65°N were all included as the eastern Bering Sea summaries.

[23] This report does not include estimates of seabird bycatch in fisheries using jig, gillnet, seine, or troll gear because NOAA Fisheries does not have independent observer data from these fisheries. These estimates also do not apply to State of Alaska-managed salmon, herring, shellfish (including crab), or dive fisheries.

[24] `https://www.fisheries.noaa.gov/alaska/commercial-fishing/alaska-fisheries-figures-maps-boundaries-regulatory-areas-and-zones`

Status and trends:

Southeastern Bering Sea

The numbers of seabirds estimated to be caught incidentally in the southeastern Bering Sea fisheries in 2023 (2,586 birds) decreased from 2022 (3,236 birds) by 20%, and was below the 2013–2022 average of 3,654 birds by 29% (Table 2, Figure 133). Northern fulmars (*Fulmarus glacialis*), shearwaters (*Ardenna* spp.), and gulls (*Larid* spp.) were the most common species or species groups caught incidentally in the southeastern Bering Sea fisheries in 2023 that could be identified. In 2023, the number of northern fulmars was about equal to 2022 (1,500 vs. 1,507) and the number of shearwaters increased by 47%, compared to 2022. The estimated number of northern fulmars and shearwaters in 2023 were below the 2013–2022 average of 2,106 and 846 birds by 29% and 14%, respectively. In 2023, the number of gulls decreased by 80% compared to 2022 and was below the 2013–2022 average of 419 birds by 68%.

Northern Bering Sea

The numbers of seabirds estimated to be caught incidentally in the northern Bering Sea fisheries in 2023 (175 birds) decreased from 2022 (403 birds) by 57%, and was below the 2013–2022 average of 624 birds by 72% (Table 3, Figure 133). Northern fulmars, shearwaters, and gulls were the most common species or species groups caught incidentally in the northern Bering Sea fisheries in 2023 that could be identified. In 2023, the number of northern fulmars decreased by 62% compared to 2022, and was below the 2013–2022 average of 358 by 72%. In 2023, the number of shearwaters decreased by 66% compared to 2022 and was below the 2013–2022 average of 191 birds by 83%. In 2023, the number of gulls increased 4x compared to 2022 and was above the 2013–2022 average of 32 birds by 33%.

Pacific cod fisheries using demersal longline are responsible for the majority of seabird bycatch in the eastern Bering Sea. The average annual seabird bycatch across all fisheries in the eastern Bering Sea (north and southeastern reporting areas combined) for 2013 through 2022 was 4,278 birds per year (Table 2, Table 3). The 2023 estimated seabird bycatch in the eastern Bering Sea (2,761 birds) was below the 2013–2022 average by 35%.

Focusing solely on the bycatch of albatross (unidentified, short-tailed [*Phoebastria albatrus*], Laysan [*P. immutabilis*], and black-footed [*P. nigripes*]) in the southeastern and north Bering Sea combined, an average of 46 albatross were taken per year from 2013 through 2022 (Table 2, Table 3, Figure 134). No black-footed albatross or short-tailed albatross were reported as taken in either region in 2023. The number of Laysan albatross taken in the southeastern Bering Sea in 2023 (34 birds) was similar compared to the 2013–2022 average of 30 birds. No Laysan albatross takes were reported in the north Bering Sea in 2023, similar to the 0 takes reported in 2022. This is below the 2013–2022 average of 5 Laysan albatross per year. There were no reported takes of short-tailed albatross in either the southeastern Bering Sea or north Bering Sea groundfish fisheries in 2023. The most recent short-tailed albatross take was observed in the 2020 on a single Pacific cod pot vessel in the southeastern Bering Sea.

Table 2: **Estimated** seabird bycatch in southeastern Bering Sea groundfish and halibut fisheries for all gear types, 2013 through 2023. Note that these numbers represent extrapolations from observed bycatch, not direct observations. See text for estimation methods.

Species Group	2013	2014	2015	2016	2017	2018	2019	2020	2021	2022	2023
Unidentified Albatross	0	12	0	0	0	0	0	0	0	0	0
Short-tailed Albatross	0	11	0	0	0	0	0	11	0	0	0
Laysan Albatross	8	13	12	12	18	148	13	7	23	45	34
Black-footed Albatross	0	6	0	0	0	0	0	0	0	63	0
Northern Fulmar	2,729	663	2,299	4,438	2,756	1,933	1,980	1,790	964	1,507	1,500
Shearwaters	196	115	340	2903	878	146	2469	243	677	491	721
Storm Petrels	0	0	0	0	0	0	0	0	3	0	0
Gull	406	562	907	557	320	364	141	167	106	663	135
Kittiwake	3	4	12	0	22	37	16	21	13	6	21
Murre	3	47	0	52	10	0	0	6	1	0	0
Puffin	0	0	0	7	0	0	0	0	0	0	0
Auklets	4	67	18	1	25	0	0	0	0	4	0
Other Alcid	0	0	0	0	0	6	6	0	0	0	0
Cormorant	0	0	3	0	0	0	0	0	0	0	0
Other	0	0	0	0	63	0	0	7	0	48	0
Unidentified	267	73	144	257	230	52	135	232	105	408	175
Grand Total	3,616	1,573	3,737	8,228	4,323	2,686	4,760	2,486	1,892	3,236	2,586

Table 3: **Estimated** seabird bycatch in northern Bering Sea groundfish and halibut fisheries for all gear types, 2013 through 2023. Note that these numbers represent extrapolations from observed bycatch, not direct observations. See text for estimation methods.

Species Group	2013	2014	2015	2016	2017	2018	2019	2020	2021	2022	2023
Unidentified Albatross	0	0	0	0	0	0	0	0	0	0	0
Short-tailed Albatross	0	0	0	0	0	0	0	0	0	0	0
Laysan Albatross	1	0	2	0	10	27	0	1	10	0	0
Black-footed Albatross	0	2	0	0	0	0	0	0	0	6	0
Northern Fulmar	4	13	34	615	760	875	672	302	40	263	99
Shearwaters	0	0	18	257	104	398	661	128	254	92	31
Storm Petrels	0	0	0	0	0	0	0	0	0	0	0
Gull	4	14	20	20	51	140	15	5	45	10	63
Kittiwake	0	0	0	5	0	0	2	3	0	18	0
Murre	0	0	0	0	0	0	0	0	7	0	0
Puffin	0	0	0	3	0	0	0	0	0	0	0
Auklets	0	0	0	0	0	0	0	0	0	0	0
Other Alcid	0	0	0	0	0	0	0	0	0	0	0
Cormorant	0	0	0	0	0	0	0	0	0	0	0
Other	0	0	0	0	0	0	0	0	0	0	0
Unidentified	1	0	0	25	22	25	50	133	60	15	2
Grand Total	11	29	73	925	948	1,465	1,399	571	415	403	175

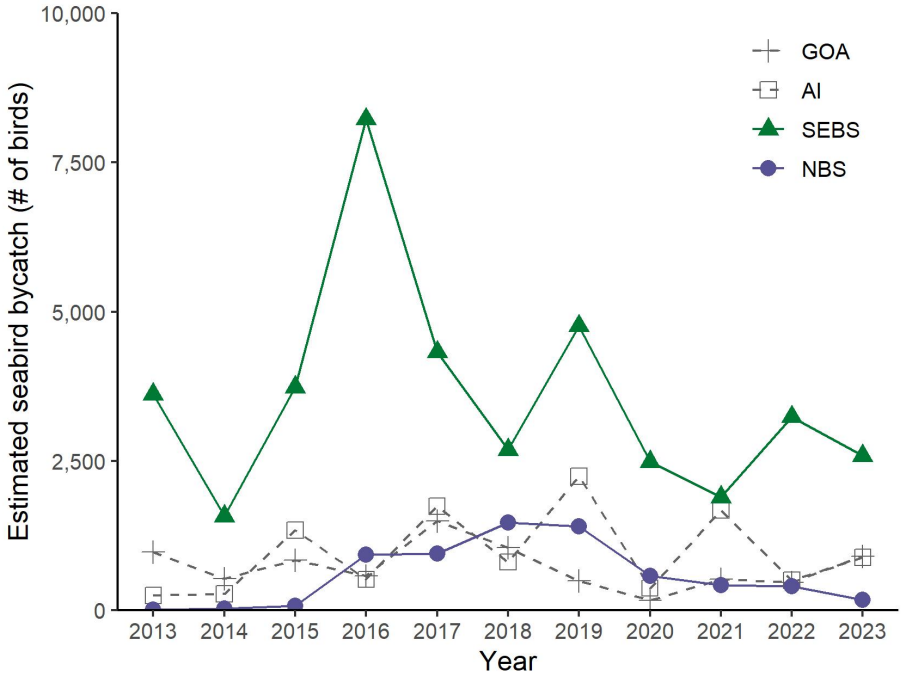

Figure 133: Total estimated seabird bycatch in Gulf of Alaska (GOA), Aleutian Islands (AI), southeastern Bering Sea (SEBS), and northern Bering Sea (NBS) groundfish and halibut fisheries, all gear types combined, 2013 through 2023.

Aside from the endangered short-tailed albatross, two species of eider are also listed under the U.S. Endangered Species Act. These are the threatened spectacled eider and the threatened Alaska-breeding population of Steller's eider. Two other populations of Steller's eider occur in waters off Alaska but only the Alaska-breeding population is listed under the U.S. Endangered Species Act (ESA). Prior to 2019, there had been no reported takes of either the spectacled eider or the Alaska-breeding population of Steller's eider by vessels operating in federal fisheries off Alaska. However, in October of 2019, twenty-two spectacled eider fatally collided with a demersal longline vessel in the northern Bering Sea (NMFS did not receive a report on this take until 2020). Then in March of 2020, a Steller's eider collided with another demersal longline vessel in the southeastern Bering Sea. These vessels were not fishing at the time of the bird strike mortality events. Since these birds were not taken by fishing gear, they are not included in the bycatch estimates provided in this report.

Because of the take of threatened spectacled and Steller's eider, NMFS reinitiated formal consultation under section 7 of the ESA with U.S. Fish and Wildlife Service (USFWS) to ensure that the BSAI and GOA groundfish fisheries are not likely to jeopardize the continued existence of the spectacled and Steller's eider or adversely modify their designated critical habitat. In March of 2021, the USFWS finalized their 2021 Biological Opinion (USFWS, 2021), which anticipated the take of up to 25 spectacled eider every 4 years and up to 3 Steller's eider from the Alaska-breeding population every 4 years in the BSAI and GOA FMP areas (either by demersal longline or trawl).

There have been zero takes of short-tailed albatross, spectacled eider, or Steller's eider in the groundfish fisheries or the commercial Pacific halibut fisheries in the southeastern or north Bering Sea in 2023. Seabird avoidance and mitigation measures remain in place; this includes the use of streamer lines as prescribed at 50 CFR 679.24(e) in hook-and-line fisheries.

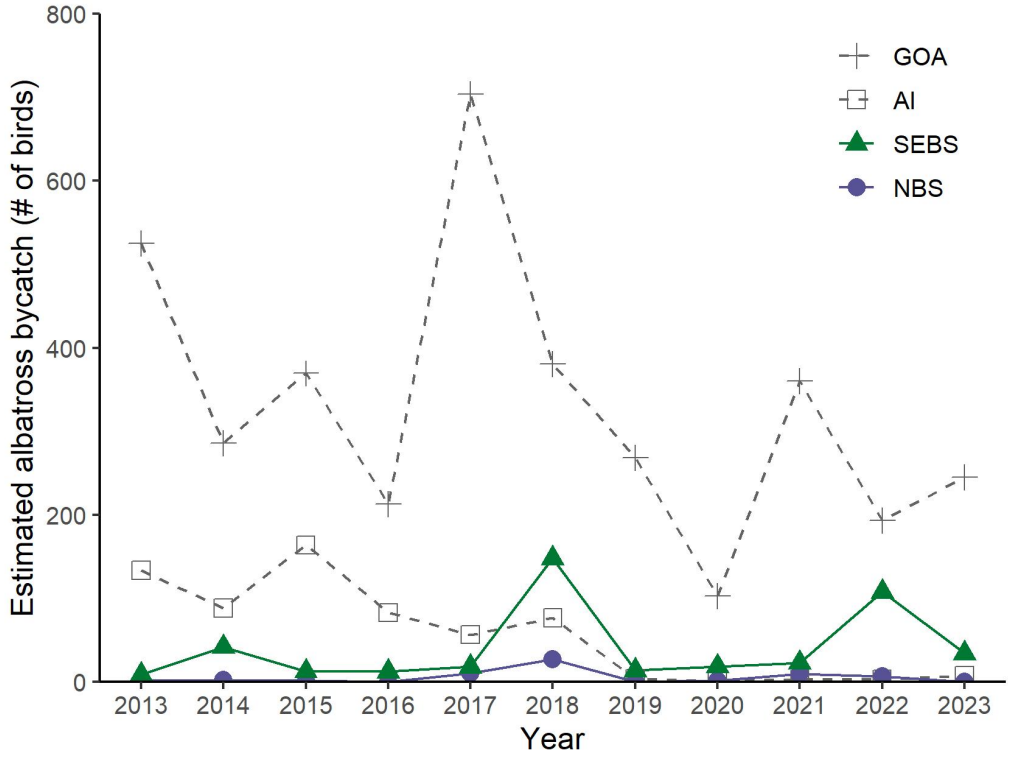

Figure 134: Total estimated albatross bycatch in Gulf of Alaska (GOA), Aleutian Islands (AI), southeastern Bering Sea (SEBS), and northern Bering Sea (NBS) groundfish and halibut fisheries, all gear types combined, 2013 through 2023.

Factors influencing observed trends: There are many factors that may influence annual variation in bycatch rates, including seabird distribution, population trends, prey supply, and fisheries activities.

Overall, total seabird bycatch in the eastern Bering Sea (north and southeastern regions combined) decreased in comparison to both 2022 and the 2013–2022 annual average. Bycatch patterns in these regions are largely driven by northern fulmar and shearwater bycatch.

In the southeastern Bering Sea, there is typically a very large level of northern fulmar takes. This is driven in part due to their tendencies to associate with fishing vessels for food, and by the proximity of fishing fleets in this area to their breeding colonies on the Pribilof Islands. Northern fulmars also forage on fish, cephalopods, and zooplankton, and their foraging distributions are often similar to that of black-legged kittiwakes (*Rissa tridactyla*; Mallory and Nettleship, 2020). In 2023, black-legged kittiwake eggs hatched earlier on average than in previous years, indicating good availability of prey early in the breeding season (Siddon, 2023). This could also indicate similarly positive natural foraging conditions for northern fulmars in the region, with the possibility of helping reduce the species's dependence on fishing vessels and thus helping to keep fulmar bycatch low relative to pre-2020 levels.

Shearwater bycatch increased in the southeastern Bering Sea in 2023, while decreasing in the northern Bering Sea. When both regions are combined into a single eastern Bering Sea unit, shearwater bycatch in the region was 27% higher than in 2022 and 29% higher than the 2013–2022 average. In the eastern Bering Sea, shearwater bycatch tends to be higher in odd years (with the exception of 2016), similar to patterns seen in the Aleutian Islands. In the Aleutian Islands, shearwater prey abundances and die-offs

have been correlated to pink salmon mediated trophic dynamics (Rojek et al., 2023). This suggests that there may also be a link between pink salmon abundances and the level of shearwater bycatch in the Aleutian Island region, as the birds may be more attracted to fishery sources of food in years of low natural prey. Such effects could also impact shearwater bycatch in the eastern Bering Sea region.

For the decrease in overall bycatch in the eastern Bering Sea, another factor to consider is the distribution of fishing effort. Factors such as the extent of the cold pool, socioeconomic conditions, and other factors may alter fishing distribution and effort in ways that could either increase or decrease seabird bycatch.

It is worth noting that standard observer sampling methods on trawl vessels do not account for additional mortalities from net entanglements, cable strikes, and other sources. Thus, the trawl estimates may be downward biased.

Implications: Estimated seabird bycatch in the Bering Sea federal fisheries off of Alaska in 2023 decreased from 2022, and was below the 2013–2022 average estimates for the southeastern and northern Bering Sea.

The first reported interactions between fishing vessels in the southeastern and northern Bering Sea groundfish fisheries in 2020 with threatened spectacled eider may be a direct result of ecological change in the southeastern Bering Sea. Even though no takes of ESA-listed seabirds occurred in federal fisheries in the eastern Bering Sea region in 2023, in recent years changes in ocean temperatures in the Bering Sea/Aleutian Islands region and the resulting ecological response of commercially valuable fish species, mainly Pacific cod, has led to an increase in the amount of fishing vessel traffic in areas near spectacled eider designated critical habitat. NMFS has observed a corresponding northward shift in fishing vessel activity and an increased harvest of Pacific cod, primarily in the northern areas of regulatory zones 514 and 524 from 2016 through 2020. In NMFS (2020) (the NMFS analysis completed for the 2021 Biological Opinion, USFWS, 2021), the authors note that compared to the number of fishing vessels present in the northern areas of the Bering Sea in 2015 (the baseline for that analysis), 2016 through 2019 show a substantial increase in the number of vessels, especially north of 61°N (as described in Section 7.9.2 of NMFS, 2020). How this fleet response to new ecological conditions will affect other species of seabirds remains to be seen.

Overall, it can be difficult to determine how seabird bycatch estimates and trends in some fisheries are linked to changes in ecosystem components because seabird mitigation gear is used in the longline fleet. There does appear to be a link between poor ocean conditions and the peak bycatch years, on a species-group basis. Fishermen have noted in some years that the birds appear starved and attack baited longline gear more aggressively. This probably indicates changes in food availability rather than distinct changes in how well the fleet employs mitigation gear. Additionally, many seabird species caught in groundfish and halibut fisheries in Alaska are wide-ranging and can fly hundreds of miles per day, resulting in less restricted foraging areas.

Fisheries bycatch can also affect seabird populations directly. In Alaska, bycatch of federally listed species is tightly regulated, and NOAA works in conjunction with outside agencies and partners to assess and manage the risk of bycatch to unlisted seabird species, including requiring seabird bycatch mitigation tools in hook-and-line groundfish and halibut fisheries.

Sustainability (for consumptive and non-consumptive uses)

Fish Stock Sustainability Index – Bering Sea and Aleutian Islands

Contributed by George A. Whitehouse
Cooperative Institute for Climate, Ocean, and Ecosystem Studies (CICOES), University of Washington, Seattle, WA
Contact: andy.whitehouse@noaa.gov
Last updated: August 2024

Description of indicator: The Fish Stock Sustainability Index (FSSI) is a performance measure for the sustainability of fish stocks selected for their importance to commercial and recreational fisheries[25]. The FSSI will increase as overfishing is ended and stocks rebuild to the level that provides maximum sustainable yield. The FSSI is calculated by awarding points for each stock based on the following rules:

1. Stock has known status determinations:
   (a) overfishing level is defined = 0.5
   (b) overfished biomass level is defined = 0.5
2. Fishing mortality rate is below the "overfishing" level defined for the stock = 1.0
3. Biomass is above the "overfished" level defined for the stock = 1.0
4. Biomass is at or above 80% of the biomass that produces maximum sustainable yield (B_{MSY}) = 1.0 (this point is in addition to the point awarded for being above the "overfished" level)

The maximum score for each stock is 4.

In the Alaska Region, there are 35 FSSI stocks and an overall FSSI of 140 would be achieved if every stock scored the maximum value, 4. Over time, the number of stocks included in the FSSI has changed as stocks have been added and removed from Fishery Management Plans (FMPs). To keep FSSI scores for Alaska comparable across years we report the FSSI as a percentage of the maximum possible score.

Additionally, there are 26 non-FSSI stocks in Alaska, three ecosystem component species complexes, and Pacific halibut which are managed under an international agreement. Two of the non-FSSI crab stocks are overfished but are not subject to overfishing. The Pribilof Islands blue king crab stock is in year ten of a rebuilding plan, and the Saint Matthews Island blue king crab stock is in year four of a 26-year rebuilding plan. None of the other non-FSSI stocks are known to be subject to overfishing, are overfished, or known to be approaching an overfished condition. For more information on non-FSSI stocks see the Status of U.S. Fisheries webpage[1].

[25] https://www.fisheries.noaa.gov/national/population-assessments/fishery-stock-status-updates

Status and trends: The overall Alaska FSSI generally trended upwards from 80% in 2006 to a high of 94% in 2018, then trended downward from 2018 to 88.2% in 2022 (Figure 135). It increased incrementally to 89% in 2023 and 90% in 2024.

As of June 30, 2024, no BSAI groundfish stock or stock complex is subject to overfishing, is known to be overfished, or known to be approaching an overfished condition (Table 4). The BSAI groundfish FSSI score is 59 out of a maximum possible 64. The AI Pacific cod stock and the walleye pollock Bogoslof stock both have FSSI scores of 1.5 due to not having known overfished status or known biomass relative to their overfished levels or to B_{MSY}. All other BSAI groundfish FSSI stocks received the maximum possible score of four points.

The BSAI king and tanner crab FSSI is 19 out of a possible 20. One point was deducted for the Bering Sea snow crab biomass being below the B/B_{MSY} threshold.

The overall BSAI FSSI score is 78 out of a maximum possible score of 84 (Table 4). The BSAI FSSI trended upward from 74% in 2006 to a peak of 95.5% in 2019. It dropped to 92.9% in 2020 and has generally been stable since then (Figure 136).

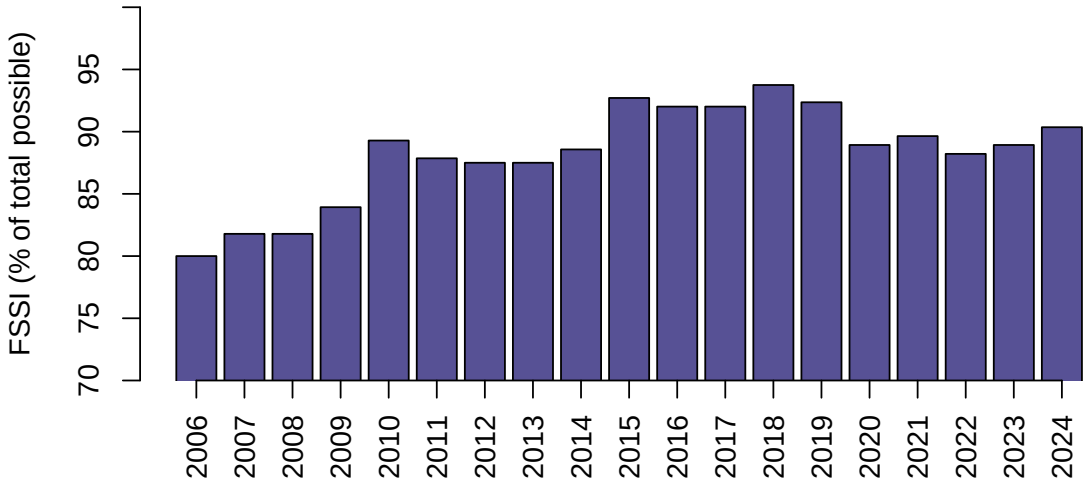

Figure 135: The trend in overall Alaska FSSI from 2006 through 2024, as a percentage of the maximum possible FSSI. The maximum possible FSSI was 140 from 2006 to 2014, 144 from 2015 to 2019, and 140 since 2020. All scores are reported through the second quarter (June) of each year, and are retrieved from the Status of U.S. Fisheries website: `https://www.fisheries.noaa.gov/national/population-assessments/fishery-stock-status-updates`.

Factors influencing observed trends: The overall trend in Alaska FSSI has been positive over much of the duration examined here (2006–2024). The recent improvement is due to Bristol Bay red king crab and Bering Sea snow crab contributing a two point increase to this year's FSSI.

Implications: The majority of Alaska groundfish and crab fisheries appear to be sustainably managed. None of the FSSI groundfish or crab stocks in the BSAI are subject to overfishing or known to be overfished.

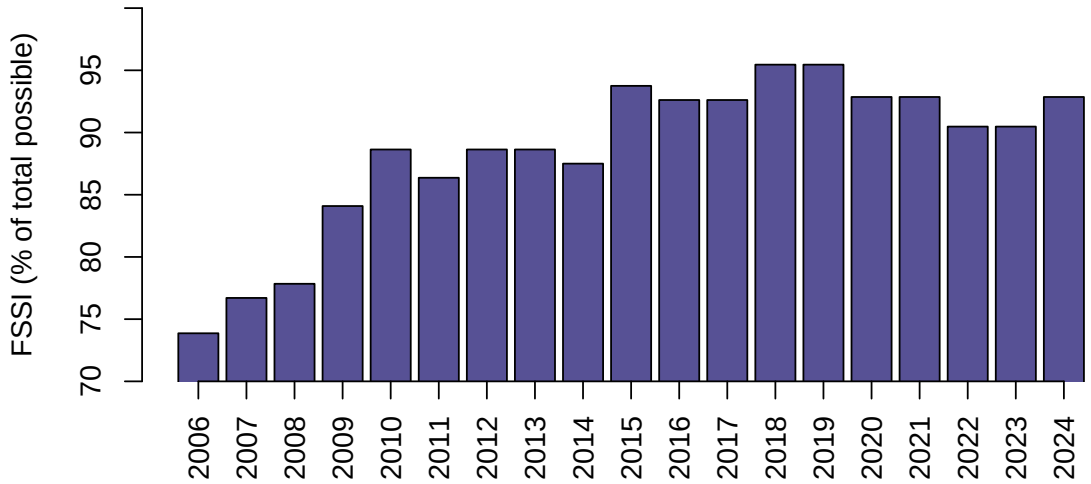

Figure 136: The trend in BSAI FSSI from 2006 through 2024 as a percentage of the maximum possible FSSI. All scores are reported through the second quarter (June) of each year, and are retrieved from the Status of U.S. Fisheries website: `https://www.fisheries.noaa.gov/national/population-assessments/fishery-stock-status-updates`.

Table 4: BSAI FSSI stocks under NPFMC jurisdiction updated through June 2024 adapted from the NOAA Fishery Stock Status Updates webpage: https://www.fisheries.noaa.gov/national/population-assessments/fishery-stock-status-updates. *See FSSI and Non-FSSI Stock Status Table on the Fishery Stock Status Updates webpage for definition of stocks, stock complexes, and notes on rebuilding.

Stock	Overfishing	Overfished	Approaching	Progress	B/Bmsy	FSSI Score
Golden king crab - Aleutian Islands*	No	No	No	NA	1.121, 0.918	4
Red king crab - Bristol Bay	No	No	No	NA	0.947	4
Red king crab - Norton Sound	No	No	No	NA	1.240	4
Snow crab - Bering Sea*	No	No - rebuilding	No	Year 1 of 6 year plan	0.593	3
Southern Tanner crab - Bering Sea	No	No	No	NA	2.039	4
BSAI Alaska plaice	No	No	No	NA	1.578	4
BSAI Atka mackerel	No	No	No	NA	1.164	4
BSAI Arrowtooth Flounder	No	No	No	NA	2.583	4
BSAI Kamchatka flounder	No	No	No	NA	1.504	4
BSAI Flathead Sole Complex*	No	No	No	NA	2.077	4
BSAI Rock Sole Complex*	No	No	No	NA	1.612	4
BSAI Skate Complex*	No	No	No	NA	2.065	4
BSAI Greenland halibut	No	No	No	NA	1.489	4
BSAI Northern rockfish	No	No	No	NA	2.095	4
BS Pacific cod	No	No	No	NA	1.075	4
AI Pacific cod	No	Unknown	Unknown	NA	not estimated	1.5
BSAI Pacific Ocean perch	No	No	No	NA	1.600	4
Walleye pollock - Aleutian Islands	No	No	No	NA	1.309	4
Walleye pollock - Bogoslof	No	Unknown	Unknown	NA	not estimated	1.5
Walleye pollock - Eastern Bering Sea	No	No	No	NA	1.373	4
BSAI Yellowfin sole	No	No	No	NA	1.699	4

References

Aagaard, K., T. J. Weingartner, S. L. Danielson, R. A. Woodgate, G. C. Johnson, and T. E. Whitledge. 2006. Some controls on flow and salinity in Bering Strait. Geophysical Research Letters **33**.

Adams, G. D., K. K. Holsman, S. J. Barbeaux, M. W. Dorn, J. N. Ianelli, I. Spies, I. J. Stewart, and A. E. Punt. 2022. An ensemble approach to understand predation mortality for groundfish in the Gulf of Alaska. Fisheries Research **251**:106303.

Anderson, D. M., T. J. Alpermann, A. D. Cembella, Y. Collos, E. Masseret, and M. Montresor. 2012. The globally distributed genus *Alexandrium*: multifaceted roles in marine ecosystems and impacts on human health. Harmful algae **14**:10–35.

Anderson, D. M., E. Fachon, R. S. Pickart, P. Lin, A. D. Fischer, M. L. Richlen, V. Uva, M. L. Brosnahan, L. McRaven, and F. Bahr. 2021. Evidence for massive and recurrent toxic blooms of *Alexandrium catenella* in the Alaskan Arctic. Proceedings of the National Academy of Sciences **118**.

Anderson, S. C., E. J. Ward, P. A. English, and L. A. Barnett. 2022. sdmTMB: an R package for fast, flexible, and user-friendly generalized linear mixed effects models with spatial and spatiotemporal random fields. BioRxiv page 2022.03. 24.485545 .

Andrews, A., M. Cook, E. Siddon, and A. Dimond. 2019. Prey quality provides a leading indicator of energetic content for age-0 walleye pollock. Report, North Pacific Fishery Management Council, 1007 W 3rd Ave, Suite 400, Anchorage, AK 99501.

Andrews, A. G., W. W. Strasburger, E. V. Farley, J. M. Murphy, and K. O. Coyle. 2015. Effects of warm and cold climate conditions on capelin (*Mallotus villosus*) and Pacific herring (*Clupea pallasii*) in the eastern Bering Sea. Deep Sea Research Part II: Topical Studies in Oceanography .

Andrews III, A. G., W. W. Strasburger, E. V. Farley Jr, J. M. Murphy, and K. O. Coyle. 2016. Effects of warm and cold climate conditions on capelin (*Mallotus villosus*) and Pacific herring (*Clupea pallasii*) in the eastern Bering Sea. Deep Sea Research Part II: Topical Studies in Oceanography **134**:235–246.

Aydin, K., and F. Mueter. 2007. The Bering Sea - a dynamic food web perspective. Deep Sea Research Part II: Topical Studies in Oceanography **54**:2501–2525.

Bacheler, N. M., L. Ciannelli, K. M. Bailey, and J. T. DUFFY-ANDERSON. 2010. Spatial and temporal patterns of walleye pollock (Theragra chalcogramma) spawning in the eastern Bering Sea inferred from egg and larval distributions. Fisheries Oceanography **19**:107–120.

Baetscher, D. S., M. R. Pochardt, P. D. Barry, and W. A. Larson. 2024. Tide impacts the dispersion of eDNA from nearshore net pens in a dynamic high-latitude marine environment. Environmental DNA **6**:e533.

Bailey, K. M. 1989. Interaction between the vertical distribution of juvenile walleye pollock Theragra chalcogramma in the eastern Bering Sea, and cannibalism. Mar. Ecol. Prog. Ser **53**:205–213.

Baker, M. 2023. Marine Ecosystems of the North Pacific Ocean 2009-2016: Region 14 (Northern Bering Sea), page 80 . North Pacific Marine Science Organization, Sidney, BC, Canada.

Baker, M. R., K. K. Kivva, M. N. Pisareva, J. T. Watson, and J. Selivanova. 2020. Shifts in the physical environment in the Pacific Arctic and implications for ecological timing and conditions. Deep Sea Research Part II: Topical Studies in Oceanography **177**:104802.

Barbeaux, S. J., K. Holsman, and S. Zador. 2020. Marine heatwave stress test of ecosystem-based fisheries management in the Gulf of Alaska Pacific Cod Fishery. Frontiers in Marine Science **7**:703.

Batten, S. D., G. T. Ruggerone, and I. Ortiz. 2018. Pink salmon induce a trophic cascade in plankton populations in the southern Bering Sea and around the Aleutian Islands. Fisheries Oceanography **27**:548–559.

Beamish, R. J., and C. Mahnken. 2001. A critical size and period hypothesis to explain natural regulation of salmon abundance and the linkage to climate and climate change. Progress in Oceanography **49**:423–437.

Berkeley, S. A., M. A. Hixon, R. J. Larson, and M. S. Love. 2004. Fisheries sustainability via protection of age structure and spatial distribution of fish populations. Fisheries **29**:23–32.

Bi, H., H. Yu, A. I. Pinchuk, and H. R. Harvey. 2015. Interannual summer variability in euphausiid populations on the eastern Bering Sea shelf during the recent cooling event (2008–2010). Deep Sea Research Part I: Oceanographic Research Papers **95**:12–19.

Blackwell, B. G., M. L. Brown, and D. W. Willis. 2000. Relative weight (Wr) status and current use in fisheries assessment and management. Reviews in fisheries Science **8**:1–44.

Blanchard, F., and J. Boucher. 2001. Temporal variability of total biomass in harvested communities of demersal fishes. Fisheries Research **49**:283–293.

Boldt, J. 2007. Ecosystem Considerations for 2008. Stock Assessment and Fishery Evaluation Report for the Groundfish Resources of the Bering Sea/Aleutian Islands and Gulf of Alaska. North Pacific Fishery Management Council, 605 W. 4th Ave., Suite 306, Anchorage, AK 99501.

Boldt, J. L., and L. J. Haldorson. 2004. Size and condition of wild and hatchery pink salmon juveniles in Prince William Sound, Alaska. Transactions of the American Fisheries Society **133**:173–184.

Bond, N. A., M. F. Cronin, H. Freeland, and N. Mantua. 2015. Causes and impacts of the 2014 warm anomaly in the NE Pacific. Geophysical Research Letters **42**:3414–3420.

Brodeur, R. D., T. W. Buckley, G. M. Lang, D. L. Draper, J. C. Buchanan, and R. E. Hibpshman. 2021. Demersal fish predators of gelatinous zooplankton in the Northeast Pacific Ocean. Marine Ecology Progress Series **658**:89–104.

Brodeur, R. D., M. B. Decker, L. Ciannelli, J. E. Purcell, N. A. Bond, P. J. Stabeno, E. Acuna, and G. L. Hunt. 2008. Rise and fall of jellyfish in the eastern Bering Sea in relation to climate regime shifts. Progress in Oceanography **77**:103–111.

Brodeur, R. D., R. L. Emmett, J. P. Fisher, E. Casillas, D. J. Teel, and T. W. Miller. 2004. Juvenile salmonid distribution, growth, condition, origin, and environmental and species associations in the Northern California Current. Fishery Bulletin **102**:25–46.

Buckley, T. W., I. Ortiz, S. Kotwicki, and K. Aydin. 2016. Summer diet composition of walleye pollock and predator–prey relationships with copepods and euphausiids in the eastern Bering Sea, 1987–2011. Deep Sea Research Part II: Topical Studies in Oceanography **134**:302–311.

Cahalan, J., J. Gasper, and J. Mondragon. 2014. Catch sampling and estimation in the Federal groundfish fisheries off Alaska, 2015 edition. Report, U.S. Dep. Commer., NOAA Tech. Memo. NMFS-AFSC-286, 46 p.

Cahalan, J., J. Mondragon, and J. Gasper. 2010. Catch sampling and estimation in the Federal groundfish fisheries off Alaska. Report, U.S. Dep. Commer., NOAA Tech. Memo. NMFS-AFSC-205, 42 p.

Ciannelli, L., and K. M. Bailey. 2005. Landscape dynamics and resulting species interactions: the cod-capelin system in the southeastern Bering Sea. Marine Ecology Progress Series **291**:227–236.

Ciannelli, L., R. Drodeur, and T. Buckley. 1998. Development and application of a bioenergetics model for juvenile walleye pollock. Journal of Fish Biology **52**:879–898.

Cline, T. J., J. Ohlberger, and D. E. Schindler. 2019. Effects of warming climate and competition in the ocean for life-histories of Pacific salmon. Nature Ecology Evolution **3**:935–942.

Coachman, L. 1986. Circulation, water masses, and fluxes on the southeastern Bering Sea shelf. Continental Shelf Research **5**:23–108.

Coiley-Kenner, P., T. Krieg, M. Chythlook, and G. Jennings. 2003. Wild resource harvests and uses by residents of Manokotak, Togiak, and Twin Hills, 1999/2000. Alaska Department of Fish and Game Division of Subsistence Technical Paper **No. 275**.

Collins, R. A., O. S. Wangensteen, E. J. O'Gorman, S. Mariani, D. W. Sims, and M. J. Genner. 2018. Persistence of environmental DNA in marine systems. Communications Biology **1**:185.

Cooper, D. W., and D. G. Nichol. 2016. Juvenile northern rock sole (Lepidopsetta polyxystra) spatial distribution and abundance patterns in the eastern Bering Sea: spatially dependent production linked to temperature. ICES Journal of Marine Science **73**:1138–1146.

Coyle, K. O., L. Eisner, F. J. Mueter, A. Pinchuk, M. Janout, K. Cieciel, E. Farley, and A. Andrews. 2011. Climate change in the southeastern Bering Sea: impacts on pollock stocks and implications for the Oscillating Control Hypothesis. Fisheries Oceanography **20**:139–156.

Coyle, K. O., and A. Pinchuk. 2002. The abundance and distribution of euphausiids and zero-age pollock on the inner shelf of the southeast Bering Sea near the Inner Front in 1997–1999. Deep Sea Research Part II: Topical Studies in Oceanography **49**:6009–6030.

Coyle, K. O., A. Pinchuk, L. Eisner, and J. M. Napp. 2008. Zooplankton species composition, abundance and biomass on the eastern Bering Sea shelf during summer: the potential role of water column stability and nutrients in structuring the zooplankton community. Deep-Sea Research Part II **55**:1755–1791.

Cunningham, C. J., P. A. Westley, and M. D. Adkison. 2018. Signals of large scale climate drivers, hatchery enhancement, and marine factors in Yukon River Chinook salmon survival revealed with a Bayesian life history model. Global Change Biology **24**:4399–4416.

Danielson, S., O. Ahkinga, C. Ashjian, E. Basyuk, L. Cooper, L. Eisner, E. Farley, K. Iken, J. Grebmeier, and L. Juranek. 2020. Manifestation and consequences of warming and altered heat fluxes over the Bering and Chukchi Sea continental shelves. Deep Sea Research Part II: Topical Studies in Oceanography **177**:104781.

De Robertis, A., D. R. McKelvey, and P. H. Ressler. 2010. Development and application of an empirical multifrequency method for backscatter classification. Canadian Journal of Fisheries and Aquatic Sciences **67**:1459–1474.

Decker, M. B., R. D. Brodeur, L. Ciannelli, L. L. Britt, N. A. Bond, B. P. DiFiore, and G. L. Hunt Jr. 2023. Cyclic variability of eastern Bering Sea jellyfish relates to regional physical conditions. Progress in Oceanography **210**:102923.

DeFilippo, L. B., J. T. Thorson, C. A. O'Leary, S. Kotwicki, J. Hoff, J. N. Ianelli, V. V. Kulik, and A. E. Punt. 2023. Characterizing dominant patterns of spatiotemporal variation for a transboundary groundfish assemblage. Fisheries Oceanography .

Donnellan, M. A., S.J. 2024. Run forecasts and harvest projections for 2024 Alaska salmon fisheries and review of the 2023 season. Report, Alaska Department of Fish and Game, Special Publication No. 24-09, Anchorage, AK.

Dorn, M. W., and S. G. Zador. 2020. A risk table to address concerns external to stock assessments when developing fisheries harvest recommendations. Ecosystem Health and Sustainability **6**:1813634.

Duffy-Anderson, J. T., P. J. Stabeno, E. C. Siddon, A. G. Andrews, D. W. Cooper, L. B. Eisner, E. V. Farley, C. E. Harpold, R. A. Heintz, and D. G. Kimmel. 2017. Return of warm conditions in the southeastern Bering Sea: Phytoplankton-Fish. PloS one **12**:e0178955.

Edullantes, B. 2019. ggplottimeseries: Visualisation of Decomposed Time Series with ggplot2. R package version **0.1.0**.

Eisner, L. B., J. C. Gann, C. Ladd, K. D. Cieciel, and C. W. Mordy. 2016. Late summer/early fall phytoplankton biomass (chlorophyll a) in the eastern Bering Sea: Spatial and temporal variations and factors affecting chlorophyll a concentrations. Deep Sea Research Part II: Topical Studies in Oceanography **134**:100–114.

Eisner, L. B., A. I. Pinchuk, D. G. Kimmel, K. L. Mier, C. E. Harpold, and E. C. Siddon. 2018. Seasonal, interannual, and spatial patterns of community composition over the eastern Bering Sea shelf in cold years. Part I: zooplankton. ICES Journal of Marine Science **75**:72–86.

Eisner, L. B., E. M. Yasumiishi, A. G. Andrews III, and C. A. O'Leary. 2020. Large copepods as leading indicators of walleye pollock recruitment in the southeastern Bering Sea: Sample-Based and spatio-temporal model (VAST) results. Fisheries Research **232**:105720.

Elison, T., P. Salomone, T. Sands, G. Buck, K. Sechrist, and D. Koster. 2018. 2017 Bristol Bay area annual management report. Report, Alaska Department of Fish and Game, Fishery Management Report No. 18-11.

Fall, J., C. Brown, N. Braem, L. Hutchinson-Scarbrough, D. Koster, T. Krieg, and A. Brenner. 2012. Subsistence harvests and uses in three Bering Sea communities, 2008: Akutan, Emmonak, and Togiak. ADFG Division of Subsistence, Technical Paper **No. 371**.

Farley, E., J. Moss, and R. Beamish. 2007. A Review of the critical size, critical period hypothesis for juvenile Pacific salmon. North Pacific Anadromous Fish Commission Bulletin **4**:311–317.

Farley, E. V., R. A. Heintz, A. G. Andrews, and T. P. Hurst. 2016. Size, diet, and condition of age-0 Pacific cod (*Gadus macrocephalus*) during warm and cool climate states in the eastern Bering Sea. Deep Sea Research Part II: Topical Studies in Oceanography **134**:247–254.

Farley, E. V., A. Starovoytov, S. Naydenko, R. Heintz, M. Trudel, C. Guthrie, L. Eisner, and J. R. Guyon. 2011. Implications of a warming eastern Bering Sea for Bristol Bay sockeye salmon. ICES Journal of Marine Science **68**:1138–1146.

Farley Jr, E., J. Murphy, M. Adkison, and L. Eisner. 2007. Juvenile sockeye salmon distribution, size, condition and diet during years with warm and cool spring sea temperatures along the eastern Bering Sea shelf. Journal of Fish Biology **71**:1145–1158.

Farley Jr, E. V., E. M. Yasumiishi, J. M. Murphy, W. Strasburger, F. Sewall, K. Howard, S. Garcia, and J. H. Moss. 2024. Critical periods in the marine life history of juvenile western Alaska chum salmon in a changing climate. Marine Ecology Progress Series **726**:149–160.

Feddern, M. L., R. Shaftel, E. R. Schoen, C. J. Cunningham, B. M. Connors, B. A. Staton, A. von Finster, Z. Liller, V. R. von Biela, and K. G. Howard. 2024. Body size and early marine conditions drive changes in Chinook salmon productivity across northern latitude ecosystems. Global Change Biology **30**:e17508.

Fetterer, F., K. Knowles, W. N. Meier, M. Savoie, and A. K. Windnagel. 2017. Sea Ice Index, Version 3. Regional Daily Data. Report, Boulder, Colorado USA. NSIDC: National Snow and Ice Data Center.

Frey, K. E., J. A. Maslanik, J. C. Kinney, and W. Maslowski. 2014. Recent variability in sea ice cover, age, and thickness in the Pacific Arctic region, pages 31–63 . Springer.

Froese, R. 2006. Cube law, condition factor and weight–length relationships: history, meta-analysis and recommendations. Journal of Applied Ichthyology **22**:241–253.

Gann, J. C., L. B. Eisner, S. Porter, J. T. Watson, K. D. Cieciel, C. W. Mordy, E. M. Yasumiishi, P. J. Stabeno, C. Ladd, R. A. Heintz, and E. V. Farley. 2016. Possible mechanism linking ocean conditions to low body weight and poor recruitment of age-0 walleye pollock (*Gadus chalcogrammus*) in the southeast Bering Sea during 2007. Deep Sea Research Part II: Topical Studies in Oceanography **134**:115–127.

Gillooly, J. F. 2000. Effect of body size and temperature on generation time in zooplankton. Journal of plankton research **22**:241–251.

Glover, D. M., W. J. Jenkins, and S. C. Doney. 2011. Modeling methods for marine science. Cambridge University Press.

Gold, Z., J. Sprague, D. J. Kushner, E. Zerecero Marin, and P. H. Barber. 2021. eDNA metabarcoding as a biomonitoring tool for marine protected areas. PLOS ONE **16**:e0238557.

Graham, C. J., T. M. Sutton, M. D. Adkison, M. V. McPhee, and P. J. Richards. 2019. Evaluation of growth, survival, and recruitment of Chinook salmon in southeast Alaska rivers. Transactions of the American Fisheries Society **148**:243–259.

Grüss, A., J. T. Thorson, C. C. Stawitz, J. C. Reum, S. K. Rohan, and C. L. Barnes. 2021. Synthesis of interannual variability in spatial demographic processes supports the strong influence of cold-pool extent on eastern Bering Sea walleye pollock (*Gadus chalcogrammus*). Progress in Oceanography **194**:102569.

Haberle, I., L. Bavčević, and T. Klanjscek. 2023. Fish condition as an indicator of stock status: Insights from condition index in a food-limiting environment. Fish and Fisheries .

Hare, C. E., K. Leblanc, G. R. DiTullio, R. M. Kudela, Y. Zhang, P. A. Lee, S. Riseman, and D. A. Hutchins. 2007. Consequences of increased temperature and CO2 for phytoplankton community structure in the Bering Sea. Marine Ecology Progress Series **352**:9–16.

Hare, S. R., N. J. Mantua, and R. C. Francis. 1999. Inverse production regimes: Alaska and west coast Pacific salmon. Fisheries **24**:6–14.

Harley, J. R., K. Lanphier, E. G. Kennedy, T. A. Leighfield, A. Bidlack, M. O. Gribble, and C. Whitehead. 2020. The Southeast Alaska Tribal Ocean Research (SEATOR) Partnership: Addressing Data Gaps in Harmful Algal Bloom Monitoring and Shellfish Safety in Southeast Alaska. Toxins **12**:407.

Harris, R. P., P. H. Wiebe, J. Lenz, H. R. Skjoldal, and M. Huntley. 2000. ICES Zooplankton Methodology Manual. Amsterdam, The Netherlands.

Heintz, R. A., E. C. Siddon, E. V. Farley Jr, and J. M. Napp. 2013. Correlation between recruitment and fall condition of age-0 pollock (*Theragra chalcogramma*) from the eastern Bering Sea under varying climate conditions. Deep Sea Research Part II: Topical Studies in Oceanography **94**:150–156.

Hendrix, A. M., K. A. Lefebvre, L. Quakenbush, A. Bryan, R. Stimmelmayr, G. Sheffield, G. Wisswaesser, M. L. Willis, E. K. Bowers, and P. Kendrick. 2021. Ice seals as sentinels for algal toxin presence in the Pacific Arctic and subarctic marine ecosystems. Marine Mammal Science .

Hennon, T., L. Barnett, N. Bond, M. Callahan, L. Divine, K. Kearney, E. Lemagie, A. Lestenkof, J. Overland, S. Rohan, K. Siwicke, R. Thoman, and M. Wang. 2023. Physical Environment Synthesis. *In*: Siddon, E. Ecosystem Status Report 2023: Eastern Bering Sea. Stock Assessment and Fishery Evaluation Report, North Pacific Fishery Management Council, 1007 West Third, Suite 400, Anchorage, Alaska 99501.

Hilborn, R., T. P. Quinn, D. E. Schindler, and D. E. Rogers. 2003. Biocomplexity and fisheries sustainability. Proceedings of the National Academy of Sciences of the United States of America **100**:6564–6568.

Hirst, A., and A. Bunker. 2003. Growth of marine planktonic copepods: global rates and patterns in relation to chlorophyll a, temperature, and body weight. Limnology and Oceanography **48**:1988–2010.

Holsman, K., A. Haynie, A. Hollowed, J. Reum, K. Aydin, A. Hermann, W. Cheng, A. Faig, J. Ianelli, and K. Kearney. 2020. Ecosystem-based fisheries management forestalls climate-driven collapse. Nature communications **11**:4579.

Holsman, K. K., and K. Aydin. 2015. Comparative methods for evaluating climate change impacts on the foraging ecology of Alaskan groundfish. Marine Ecology Progress Series **521**:217–235.

Holsman, K. K., K. Aydin, J. Sullivan, T. Hurst, and G. H. Kruse. 2019. Climate effects and bottom-up controls on growth and size-at-age of Pacific halibut (*Hippoglossus stenolepis*) in Alaska (USA). Fisheries Oceanography **28**:345–358.

Holsman, K. K., J. Ianelli, K. Aydin, A. E. Punt, and E. A. Moffitt. 2016. A comparison of fisheries biological reference points estimated from temperature-specific multi-species and single-species climate-enhanced stock assessment models. Deep Sea Research Part II: Topical Studies in Oceanography **134**:360–378.

Holsman, K. K., J. Ianelli, K. Shotwell, S. Barbeaux, K. Aydin, G. Adams, K. Kearney, A. Sulc, and S. Wassermann. 2024. Climate-enhanced multispecies stock assessment for walleye pollock, Pacific cod, and arrowtooth flounder in the eastern Bering Sea. Report, North Pacific Fisheries Management Council.

Hoondert, R. P., N. W. van den Brink, M. J. Van den Heuvel-Greve, A. J. Ragas, and A. Jan Hendriks. 2020. Implications of trophic variability for modeling biomagnification of POPs in marine food webs in the Svalbard archipelago. Environmental science technology **54**:4026–4035.

Howard, K. G., S. Garcia, J. Murphy, and T. Dann. 2019. Juvenile Chinook salmon abundance index and survey feasibility assessment in the northern Bering Sea, 2014–2016. Report, Alaska Department of Fish and Game, Fishery Data Series No. 19-04, Anchorage.

Howard, K. G., S. Garcia, J. Murphy, and T. Dann. 2020. Northeastern Bering Sea juvenile Chinook salmon survey, 2017 and Yukon River adult run forecasts, 2018–2020. Report, Alaska Department of Fish and Game, Fishery Data Series No. 20-08, Anchorage.

Howard, K. G., and V. von Biela. 2023. Adult spawners: A critical period for subarctic Chinook salmon in a changing climate. Global Change Biology **29**:1759–1773.

Hsieh, C.-H., C. S. Reiss, J. R. Hunter, J. R. Beddington, R. M. May, and G. Sugihara. 2006. Fishing elevates variability in the abundance of exploited species. Nature **443**:859–862.

Hunt, G. L., P. H. Ressler, G. A. Gibson, A. De Robertis, K. Aydin, M. F. Sigler, I. Ortiz, E. J. Lessard, B. C. Williams, and A. Pinchuk. 2016. Euphausiids in the eastern Bering Sea: A synthesis of recent studies of euphausiid production, consumption and population control. Deep Sea Research Part II: Topical Studies in Oceanography **134**:204–222.

Hunt, G. L., P. Stabeno, G. Walters, E. Sinclair, R. D. Brodeur, J. M. Napp, and N. A. Bond. 2002. Climate change and control of the southeastern Bering Sea pelagic ecosystem. Deep-Sea Research Part II-Topical Studies in Oceanography **49**:5821–5853.

Hunt, J., George L., K. O. Coyle, L. B. Eisner, E. V. Farley, R. A. Heintz, F. Mueter, J. M. Napp, J. E. Overland, P. H. Ressler, S. Salo, and P. J. Stabeno. 2011. Climate impacts on eastern Bering Sea foodwebs: a synthesis of new data and an assessment of the Oscillating Control Hypothesis. ICES Journal of Marine Science **68**:1230–1243.

Huntley, M. E., and M. D. Lopez. 1992. Temperature-dependent production of marine copepods: a global synthesis. The American Naturalist **140**:201–242.

Ianelli, J., K. K. Holsman, A. E. Punt, and K. Aydin. 2016. Multi-model inference for incorporating trophic and climate uncertainty into stock assessments. Deep Sea Research Part II: Topical Studies in Oceanography **134**:379–389.

Ianelli, J., T. Honkalehto, S. Wassermann, N. Lauffenburger, C. McGillard, and E. Siddon. 2023. Stock assessment for eastern Bering Sea walleye pollock. In Stock Assessment and Fishery Evaluation Report for the Groundfish Resources of the Bering Sea/Aleutian Islands. Report, North Pacific Fishery Management Council, Anchorage, AK.

Ianelli, J., T. Honkalehto, S. Wassermann, A. McCarthy, S. Steinessen, C. McGillard, and E. Siddon. 2024. Stock assessment for eastern Bering Sea walleye pollock. In Stock Assessment and Fishery Evaluation Report for the Groundfish Resources of the Bering Sea/Aleutian Islands. Report, North Pacific Fishery Management Council, Anchorage, AK.

Jerde, C. L. 2021. Can we manage fisheries with the inherent uncertainty from eDNA? Journal of Fish Biology **98**:341–353.

Jones, B., P. Crane, C. Larson, and M. Cunningham. 2021. Traditional Ecological Knowledge and Harvest Assessment of Dolly Varden and Other Nonsalmon Fish Utilized by Residents of the Togiak National Wildlife Refuge. Report, Alaska Department of Fish and Game, Division of Subsistence, Technical Paper No. 482, Anchorage, AK.

Jones, T., L. M. Divine, H. Renner, S. Knowles, K. A. Lefebvre, H. K. Burgess, C. Wright, and J. K. Parrish. 2019. Unusual mortality of Tufted puffins (*Fratercula cirrhata*) in the eastern Bering Sea. PloS one **14**:e0216532.

JTC. 2024. Joint Technical Committee of the Yukon River Panel: Yukon River salmon 2023 season summary and 2024 seasonal outlook. Alaska Department of Fish and Game, Division of Commercial Fisheries, Regional Information Report 24-01. Anchorage, AK. Report.

Jurado-Molina, J., P. A. Livingston, and J. N. Ianelli. 2005. Incorporating predation interactions in a statistical catch-at-age model for a predator-prey system in the eastern Bering Sea. Canadian Journal of Fisheries and Aquatic Sciences **62**:1865–1873.

Kaga, T., S. Sato, T. Azumaya, N. D. Davis, and M.-a. Fukuwaka. 2013. Lipid content of chum salmon Oncorhynchus keta affected by pink salmon O. gorbuscha abundance in the central Bering Sea. Marine Ecology Progress Series **478**:211–221.

Kalnay, E., M. Kananitcu, R. Kistler, W. Collins, and D. Deaven. 1996. The NCEP/NCAR 40-year reanalysis project. Bulletin of the American Meteorological Society **77**:437–471.

Kasmi, Y., T. Blancke, E. Eschbach, B. Möckel, L. Casas, M. Bernreuther, P. Nogueira, G. Delfs, S. Kadhim, T. Meißner, M. Rödiger, A. Eladdadi, C. Stransky, and R. Hanel. 2023. Atlantic cod (Gadus morhua) assessment approaches in the North and Baltic Sea: A comparison of environmental DNA analysis versus bottom trawl sampling. Frontiers in Marine Science **10**.

Kimmel, D. G., L. B. Eisner, and A. I. Pinchuk. 2023. The northern Bering Sea zooplankton community response to variability in sea ice: evidence from a series of warm and cold periods. Marine Ecology Progress Series **705**:21–42.

Kimmel, D. G., L. B. Eisner, M. T. Wilson, and J. T. Duffy-Anderson. 2018. Copepod dynamics across warm and cold periods in the eastern Bering Sea: Implications for walleye pollock (*Gadus chalcogrammus*) and the Oscillating Control Hypothesis. Fisheries Oceanography **27**:143–158.

Kiorboe, T., and M. Sabatini. 1995. Scaling of fecundity, growth and development in marine planktonic copepods. Marine ecology progress series. Oldendorf **120**:285–298.

Koenker, B. L., B. J. Laurel, L. A. Copeman, and L. Ciannelli. 2018. Effects of temperature and food availability on the survival and growth of larval Arctic cod (Boreogadus saida) and walleye pollock (Gadus chalcogrammus). ICES Journal of Marine Science **75**:2386–2402.

Koslow, J., S. Brault, J. Dugas, R. Fournier, and P. Hughes. 1985. Condition of larval cod (Gadus morhua) off southwest Nova Scotia in 1983 in relation to plankton abundance and temperature. Marine Biology **86**:113–121.

Kotwicki, S., and R. R. Lauth. 2013. Detecting temporal trends and environmentally-driven changes in the spatial distribution of bottom fishes and crabs on the eastern Bering Sea shelf. Deep Sea Research Part II: Topical Studies in Oceanography **94**:231–243.

Ladd, C., and P. J. Stabeno. 2012. Stratification on the Eastern Bering Sea shelf revisited. Deep Sea Research Part II: Topical Studies in Oceanography **65**:72–83.

Laurel, B. J., M. Spencer, P. Iseri, and L. A. Copeman. 2016. Temperature-dependent growth and behavior of juvenile Arctic cod (Boreogadus saida) and co-occurring North Pacific gadids. Polar Biology **39**:1127–1135.

Lebida, R. C., and D. C. Whitmore. 1985. Bering Sea herring aerial survey manual. Report, Alaska Department of Fish and Game, Division of Commercial Fisheries, Bristol Bay Data Report No. 85-2, Anchorage, AK.

Lefebvre, K. A., E. Fachon, E. K. Bowers, D. G. Kimmel, J. A. Snyder, R. Stimmelmayr, J. M. Grebmeier, S. Kibler, D. R. Hardison, and D. M. Anderson. 2022. Paralytic shellfish toxins in Alaskan Arctic food webs during the anomalously warm ocean conditions of 2019 and estimated toxin doses to Pacific walruses and bowhead whales. Harmful Algae **114**:102205.

Lefebvre, K. A., L. Quakenbush, E. Frame, K. B. Huntington, G. Sheffield, R. Stimmelmayr, A. Bryan, P. Kendrick, H. Ziel, and T. Goldstein. 2016. Prevalence of algal toxins in Alaskan marine mammals foraging in a changing arctic and subarctic environment. Harmful Algae **55**:13–24.

Levins, R. 1974. Discussion paper: the qualitative analysis of partially specified systems. Annals of the New York Academy of Sciences **231**:123–138.

Litzow, M. A., E. J. Fedewa, M. J. Malick, B. M. Connors, L. Eisner, D. G. Kimmel, T. Kristiansen, J. M. Nielsen, and E. R. Ryznar. 2024. Human-induced borealization leads to the collapse of Bering Sea snow crab. Nature Climate Change pages 1–4 .

Litzow, M. A., M. E. Hunsicker, N. A. Bond, B. J. Burke, C. J. Cunningham, J. L. Gosselin, E. L. Norton, E. J. Ward, and S. G. Zador. 2020*a*. The changing physical and ecological meanings of North Pacific Ocean climate indices. Proceedings of the National Academy of Sciences **117**:7665–7671.

Litzow, M. A., M. J. Malick, N. A. Bond, C. J. Cunningham, J. L. Gosselin, and E. J. Ward. 2020*b*. Quantifying a Novel Climate Through Changes in PDO-Climate and PDO-Salmon Relationships. Geophysical Research Letters **47**:e2020GL087972.

Livingston, P. A., K. Aydin, T. W. Buckley, G. M. Lang, M.-S. Yang, and B. S. Miller. 2017. Quantifying food web interactions in the North Pacific–a data-based approach. Environmental Biology of Fishes **100**:443–470.

Long, W. C., K. M. Swiney, and R. J. Foy. 2023. Direct, carryover, and maternal effects of ocean acidification on snow crab embryos and larvae. Plos one **18**:e0276360.

Long, W. C., K. M. Swiney, C. Harris, H. N. Page, and R. J. Foy. 2013. Effects of ocean acidification on juvenile red king crab (*Paralithodes camtschaticus*) and Tanner crab (*Chionoecetes bairdi*) growth, condition, calcification, and survival. PloS one **8**:e60959.

Maes, S. M., S. Desmet, R. Brys, K. Sys, T. Ruttink, S. Maes, K. Hostens, L. Vansteenbrugge, and S. Derycke. 2024. Detection and quantification of two commercial flatfishes (Solea solea and Pleuronectes platessa) in the North Sea using environmental DNA. Environmental DNA **6**:e426.

Maiello, G., L. Talarico, P. Carpentieri, F. De Angelis, S. Franceschini, L. R. Harper, E. F. Neave, O. Rickards, A. Sbrana, P. Shum, V. Veltre, S. Mariani, and T. Russo. 2022. Little samplers, big fleet: eDNA metabarcoding from commercial trawlers enhances ocean monitoring. Fisheries Research **249**:106259.

Malecha, P., and J. Heifetz. 2017. Long-term effects of bottom trawling on large sponges in the Gulf of Alaska. Continental shelf research **150**:18–26.

Mallory, S. A. H., M. L., and D. N. Nettleship. 2020. Northern Fulmar (Fulmarus glacialis), version 1.0. Birds of the World. Cornell Lab of Ornithology, Ithaca, NY, USA.

Mantua, N. J., S. R. Hare, Y. Zhang, J. M. Wallace, and R. C. Francis. 1997. A Pacific Interdecadal Climate Oscillation with Impacts on Salmon Production. Bulletin of the American Meteorological Society **78**:1069–1079.

Maritorena, S., O. H. F. d'Andon, A. Mangin, and D. A. Siegel. 2010. Merged satellite ocean color data products using a bio-optical model: Characteristics, benefits and issues. Remote Sensing of Environment **114**:1791–1804.

Markowitz, H., E. Dawson, C. Anderson, S. Rohan, E. Charriere, B. Prohaska, and D. Stevenson. 2023. Results of the 2022 Eastern and Northern Bering Sea Continental Shelf Bottom Trawl Survey of Groundfish and Invertebrate Fauna .

Martinson, E. C., H. H. Stokes, and D. L. Scarnecchia. 2012. Use of juvenile salmon growth and temperature change indices to predict groundfish post age-0 yr class strengths in the Gulf of Alaska and eastern Bering Sea. Fisheries Oceanography **21**:307–319.

McCarthy, A., T. Honkalehto, N. Lauffenburger, and A. De Robertis. 2020. Results of the acoustic-trawl survey of walleye pollock (*Gadus chalcogrammus*) on the US Bering Sea Shelf in June-August 2018 (DY1807) .

Monnahan, C., B. Ferriss, S. Shotwell, Z. Oyafuso, M. Levine, J. Thorson, L. Rogers, S. J., and J. Champagnat. 2024. Assessment of the Walleye Pollock Stock in the Gulf of Alaska. Report, North Pacific Fishery Management Council, 1007 W 3rd Ave, Suite 400, Anchorage, AK 99501.

Montero-Serra, I., C. Linares, D. F. Doak, J. Ledoux, and J. Garrabou. 2018. Strong linkages between depth, longevity and demographic stability across marine sessile species. Proceedings of the Royal Society B: Biological Sciences **285**:20172688.

Moss, J. H., D. A. Beauchamp, A. D. Cross, K. W. Myers, E. V. Farley Jr, J. M. Murphy, and J. H. Helle. 2005. Evidence for size-selective mortality after the first summer of ocean growth by pink salmon. Transactions of the American Fisheries Society **134**:1313–1322.

Mueter, F. J., and M. A. Litzow. 2008. Sea ice retreat alters the biogeography of the Bering Sea continental shelf. Ecological Applications **18**:309–320.

Murphy, J., S. Garcia, J. Dimond, J. Moss, F. Sewall, W. Strasburger, E. Lee, T. Dann, E. Labunski, T. Zeller, A. Gray, C. Waters, D. Jallen, D. Nicolls, R. Conlon, K. Cieciel, K. Howard, B. Harris, N. Wolf, and E. Farley. 2021. Northern Bering Sea surface trawl and ecosystem survey cruise report, 2019. Report, U.S. Dep. Commer., NOAA Tech. Memo. NMFS-AFSC-423, 124 p.

Murphy, J. M., K. G. Howard, J. C. Gann, K. C. Cieciel, W. D. Templin, and C. M. Guthrie. 2017. Juvenile Chinook Salmon abundance in the northern Bering Sea: Implications for future returns and fisheries in the Yukon River. Deep-Sea Research Part II-Topical Studies in Oceanography **135**:156–167.

Neuswanger, J. R., M. S. Wipfli, M. J. Evenson, N. F. Hughes, and A. E. Rosenberger. 2015. Low productivity of Chinook salmon strongly correlates with high summer stream discharge in two Alaskan rivers in the Yukon drainage. Canadian Journal of Fisheries and Aquatic Sciences **72**:1125–1137.

Nielsen, J. M., M. F. Sigler, L. B. Eisner, J. T. Watson, L. A. Rogers, S. W. Bell, N. Pelland, C. W. Mordy, W. Cheng, and K. Kivva. 2024. Spring phytoplankton bloom phenology during recent climate warming on the Bering Sea shelf. Progress in Oceanography **220**:103176.

NMFS. 2020. Programmatic biological assessment on the effects of the fishery management plans for the Gulf of Alaska and Bering Sea/Aleutian Islands groundfish fisheries and the State of Alaska parallel groundfish fisheries on the endangered short-tailed albatross (*Phoebastria albatrus*), the threatened Alaska-breeding population of Steller's eider (*Polysticta stelleri*), and the threatened spectacled eider (*Somateria fischeri*). Report, Juneau, Alaska, 97 p.

Ogonowski, M., E. Karlsson, A. Vasemägi, J. Sundin, P. Bohman, and G. Sundblad. 2023. Temperature moderates eDNA–biomass relationships in northern pike. Environmental DNA **5**:750–765.

Ohlberger, J., D. E. Schindler, R. J. Brown, J. M. Harding, M. D. Adkison, A. R. Munro, L. Horstmann, and J. Spaeder. 2020. The reproductive value of large females: consequences of shifts in demographic structure for population reproductive potential in Chinook salmon. Canadian Journal of Fisheries and Aquatic Sciences **77**:1292–1301.

Ohlberger, J., D. E. Schindler, E. J. Ward, T. E. Walsworth, and T. E. Essington. 2019. Resurgence of an apex marine predator and the decline in prey body size. Proceedings of the National Academy of Sciences **116**:26682–26689.

Oke, K. B., F. Mueter, and M. A. Litzow. 2022. Warming leads to opposite patterns in weight-at-age for young versus old age classes of Bering Sea walleye pollock. Canadian Journal of Fisheries and Aquatic Sciences **79**:1655–1666.

Ortiz, I., F. Weise, and A. Greig. 2012. Marine regions boundary data for the Bering Sea shelf and slope. UCAR/NCAR—Earth Observing Laboratory/Computing, Data, and Software Facility. Dataset. doi **10**:D6DF6P6C.

Oyafuso, Z. 2024. gapindex: Standard AFSC GAP Product Calculations. R package version 2.2.0, https://github.com/afsc-gap-products/gapindex .

Parsley, M. B., and C. S. Goldberg. 2024. Environmental RNA can distinguish life stages in amphibian populations. Molecular Ecology Resources **24**:e13857.

Paul, A., and J. Paul. 1999. Interannual and regional variations in body length, weight and energy content of age-0 Pacific herring from Prince William Sound, Alaska. Journal of fish biology **54**:996–1001.

Pauly, D., V. Christensen, J. Dalsgaard, R. Froese, and F. Torres. 1998. Fishing down marine food webs. Science **279**:860–863.

Perrette, M., A. Yool, G. Quartly, and E. E. Popova. 2011. Near-ubiquity of ice-edge blooms in the Arctic. Biogeosciences **8**:515–524.

Petitgas, P. 1993. Geostatistics for fish stock assessments: a review and an acoustic application. ICES Journal of Marine Science: Journal du Conseil **50**:285–298.

Pickart, R., G. Moore, T. Weingartner, S. Danielson, and K. Frey. 2013. Physical Drivers of the Chukchi, Beaufort, and Northern Bering Seas. Developing a Conceptual Model of the Arctic Marine Ecosystem **2**.

Pickart, R. S., M. A. Spall, G. W. Moore, T. J. Weingartner, R. A. Woodgate, K. Aagaard, and K. Shimada. 2011. Upwelling in the Alaskan Beaufort Sea: Atmospheric forcing and local versus non-local response. Progress in Oceanography **88**:78–100.

Pilcher, D. J., D. M. Naiman, J. N. Cross, A. J. Hermann, S. A. Siedlecki, G. A. Gibson, and J. T. Mathis. 2019. Modeled effect of coastal biogeochemical processes, climate variability, and ocean acidification on aragonite saturation state in the Bering Sea. Frontiers in Marine Science **5**:508.

Pinger, C., L. Copeman, M. Stowell, B. Cormack, C. Fugate, and M. Rogers. 2022. Rapid measurement of total lipids in zooplankton using the sulfo-phospho-vanillin reaction. Analytical Methods **14**:2665–2672.

Pinger, C., D. Porter, B. Cormack, C. Fugate, and M. Rogers. 2024. High-throughput determination of total lipids from North Pacific marine fishes via the sulfo-phospho-vanillin microplate assay. Limnology and Oceanography: Methods .

Preston, C., K. Yamahara, D. Pargett, C. Weinstock, J. Birch, B. Roman, S. Jensen, B. Connon, R. Jenkins, J. Ryan, and C. Scholin. 2024. Autonomous eDNA collection using an uncrewed surface vessel over a 4200-km transect of the eastern Pacific Ocean. Environmental DNA **6**:e468.

Punt, A. E., R. J. Foy, M. G. Dalton, W. C. Long, and K. M. Swiney. 2016. Effects of long-term exposure to ocean acidification conditions on future southern Tanner crab (*Chionoecetes bairdi*) fisheries management. ICES Journal of Marine Science **73**:849–864.

Purcell, J. E., and M. N. Arai. 2001. Interactions of pelagic cnidarians and ctenophores with fish: a review. Hydrobiologia **451**:27–44.

Ramírez-Amaro, S., M. Bassitta, A. Picornell, C. Ramon, and B. Terrasa. 2022. Environmental DNA: State-of-the-art of its application for fisheries assessment in marine environments. Frontiers in Marine Science **9**.

Rand, P. S., and G. T. Ruggerone. 2024. Biennial patterns in Alaskan sockeye salmon ocean growth are associated with pink salmon abundance in the Gulf of Alaska and the Bering Sea. ICES Journal of Marine Science **81**:701–709.

Ressler, P., A. De Robertis, and S. Kotwicki. 2014. The spatial distribution of euphausiids and walleye pollock in the eastern Bering Sea does not imply top-down control by predation. Marine Ecology Progress Series **503**:111–122.

Ressler, P. H., A. De Robertis, J. D. Warren, J. N. Smith, and S. Kotwicki. 2012. Developing an acoustic survey of euphausiids to understand trophic interactions in the Bering Sea ecosystem. Deep Sea Research Part II: Topical Studies in Oceanography **65–70**:184–195.

Reum, J. C., C. R. Kelble, C. J. Harvey, R. P. Wildermuth, N. Trifonova, S. M. Lucey, P. S. McDonald, and H. Townsend. 2021. Network approaches for formalizing conceptual models in ecosystem-based management. ICES Journal of Marine Science **78**:3674–3686.

Reum, J. C. P., P. S. McDonald, W. C. Long, K. K. Holsman, L. Divine, D. Armstrong, and J. Armstrong. 2020. Rapid assessment of management options for promoting stock rebuilding in data-poor species under climate change. Conservation Biology **34**:611–621.

Riaz, M., M. Kuemmerlen, C. Wittwer, B. Cocchiararo, I. Khaliq, M. Pfenninger, and C. Nowak. 2020. Combining environmental DNA and species distribution modeling to evaluate reintroduction success of a freshwater fish. Ecological Applications **30**:e02034.

Richardson, A., A. Walne, A. John, T. Jonas, J. Lindley, D. Sims, D. Stevens, and M. Witt. 2006. Using continuous plankton recorder data. Progress in Oceanography **68**:27–74.

Robinson, K. L., J. J. Ruzicka, M. B. Decker, R. Brodeur, F. Hernandez, J. Quiñones, E. Acha, S. Uye, H. Mianzan, and W. Graham. 2014. Jellyfish, forage fish, and the world's major fisheries. Oceanography **27**:104–115.

Rodgveller, C. J. 2019. The utility of length, age, liver condition, and body condition for predicting maturity and fecundity of female sablefish. Fisheries Research **216**:18–28.

Rodionov, S., and J. E. Overland. 2005. Application of a sequential regime shift detection method to the Bering Sea ecosystem. Ices Journal of Marine Science **62**:328–332.

Rodionov, S. N., N. A. Bond, and J. E. Overland. 2007. The Aleutian Low, storm tracks, and winter climate variability in the Bering Sea. Deep Sea Research Part II: Topical Studies in Oceanography **54**:2560–2577.

Rogers, L. A., and D. E. Schindler. 2011. Scale and the detection of climatic influences on the productivity of salmon populations. Global Change Biology **17**:2546–2558.

Rohan, S. 2024. esrindex: Abundance index products for Alaska ESRs. R package version 0.1.0, https://github.com/afsc-gap-products/esrindex .

Rohan, S., L. Barnett, and N. Charriere. 2022. Evaluating approaches to estimating mean temperatures and cold pool area from Alaska Fisheries Science Center bottom trawl surveys of the eastern Bering Sea .

Rojek, N., H. Renner, T. Jones, J. Lindsey, R. Kaler, K. Kuletz, I. Ortiz, and S. Zador. 2023. Integrated Seabird Information. Stock Assessment and Fishery Evaluation Report, North Pacific Fishery Management Council,1007 West 3rd Ave., Suite 400, Anchorage, AK 99501.

Rooper, C. N., P. Goddard, and R. Wilborn. 2019. Are fish associations with corals and sponges more than an affinity to structure? Evidence across two widely divergent ecosystems. Canadian Journal of Fisheries and Aquatic Sciences **76**:2184–2198.

Rooper, C. N., M. F. Sigler, P. Goddard, P. Malecha, R. Towler, K. Williams, R. Wilborn, and M. Zimmermann. 2016. Validation and improvement of species distribution models for structure-forming invertebrates in the eastern Bering Sea with an independent survey. Marine Ecology Progress Series **551**:117–130.

Rourke, M. L., A. M. Fowler, J. M. Hughes, M. K. Broadhurst, J. D. DiBattista, S. Fielder, J. Wilkes Walburn, and E. M. Furlan. 2022. Environmental DNA (eDNA) as a tool for assessing fish biomass: A review of approaches and future considerations for resource surveys. Environmental DNA **4**:9–33.

RTeam. 2023. R: A language and environment for statistical computing. R Foundation for Statistical Computing. http://www. R-project. org/., Vienna, Austria.

Ruggerone, G. T., B. A. Agler, B. M. Connors, E. V. Farley Jr, J. R. Irvine, L. I. Wilson, and E. M. Yasumiishi. 2016. Pink and sockeye salmon interactions at sea and their influence on forecast error of Bristol Bay sockeye salmon. North Pacific Anadromous Fish Commission Bulletin **6**:349–361.

Ruggerone, G. T., and J. L. Nielsen. 2004. Evidence for competitive dominance of pink salmon (*Oncorhynchus gorbuscha*) over other salmonids in the North Pacific Ocean. Reviews in Fish Biology and Fisheries **14**:371–390.

Ruggerone, G. T., A. M. Springer, G. B. van Vliet, B. Connors, J. R. Irvine, L. D. Shaul, M. R. Sloat, and W. I. Atlas. 2023. From diatoms to killer whales: impacts of pink salmon on North Pacific ecosystems. Marine Ecology Progress Series **719**:1–40.

Ruzicka, J., R. D. Brodeur, K. Cieciel, and M. B. Decker. 2020. Examining the ecological role of jellyfish in the Eastern Bering Sea. ICES Journal of Marine Science **77**:791–802.

Salter, I., M. Joensen, R. Kristiansen, P. Steingrund, and P. Vestergaard. 2019. Environmental DNA concentrations are correlated with regional biomass of Atlantic cod in oceanic waters. Communications Biology **2**:461.

Schindler, D. E., R. Hilborn, B. Chasco, C. P. Boatright, T. P. Quinn, L. A. Rogers, and M. S. Webster. 2010. Population diversity and the portfolio effect in an exploited species. Nature **465**:609–613.

Schindler, D. E., P. R. Leavitt, S. P. Johnson, and C. S. Brock. 2006. A 500-year context for the recent surge in sockeye salmon (*Oncorhynchus nerka*) abundance in the Alagnak River, Alaska. Canadian Journal of Fisheries and Aquatic Sciences **63**:1439–1444.

Seung, C. K., M. G. Dalton, A. E. Punt, D. Poljak, and R. Foy. 2015. Economic impacts of changes in an Alaska crab fishery from ocean acidification. Climate Change Economics **6**:1550017.

Shea, D., N. Frazer, K. Wadhawan, A. Bateman, S. Li, K. M. Miller, S. Short, and M. Krkošek. 2022. Environmental DNA dispersal from Atlantic salmon farms. Canadian Journal of Fisheries and Aquatic Sciences **79**:1377–1388.

Shelton, A. O., R. P. Kelly, J. L. O'Donnell, L. Park, P. Schwenke, C. Greene, R. A. Henderson, and E. M. Beamer. 2019. Environmental DNA provides quantitative estimates of a threatened salmon species. Biological Conservation **237**:383–391.

Shelton, A. O., A. Ramón-Laca, A. Wells, J. Clemons, D. Chu, B. E. Feist, R. P. Kelly, S. L. Parker-Stetter, R. Thomas, K. M. Nichols, and L. Park. 2022. Environmental DNA provides quantitative estimates of Pacific hake abundance and distribution in the open ocean. Proceedings of the Royal Society B: Biological Sciences **289**:20212613.

Shin, Y.-J., M.-J. Rochet, S. Jennings, J. G. Field, and H. Gislason. 2005. Using size-based indicators to evaluate the ecosystem effects of fishing. ICES Journal of marine Science **62**:384–396.

Shin, Y.-J., L. J. Shannon, A. Bundy, M. Coll, K. Aydin, N. Bez, J. L. Blanchard, M. d. F. Borges, I. Diallo, and E. Diaz. 2010. Using indicators for evaluating, comparing, and communicating the ecological status of exploited marine ecosystems. Part 2. Setting the scene. ICES Journal of Marine Science **67**:692–716.

Siddon, E. 2020. Ecosystem Status Report 2020: Eastern Bering Sea. Report, North Pacific Fishery Management Council, 1007 West Third, Suite 400, Anchorage, Alaska 99501.

Siddon, E. 2022. Ecosystem Status Report 2022: Eastern Bering Sea. Report, North Pacific Fishery Management Council, 1007 West Third, Suite 400, Anchorage, Alaska 99501.

Siddon, E. 2023. Ecosystem Status Report 2023: Eastern Bering Sea, Stock Assessment and Fishery Evaluation Report. Report, North Pacific Fishery Management Council, 1007 West 3rd Ave., Suite 400, Anchorage, AK 99501.

Siddon, E. C., R. A. Heintz, and F. J. Mueter. 2013. Conceptual model of energy allocation in walleye pollock (*Theragra chalcogramma*) from age-0 to age-1 in the southeastern Bering Sea. Deep Sea Research Part II: Topical Studies in Oceanography **94**:140–149.

Sigler, M. F., F. J. Mueter, B. A. Bluhm, M. S. Busby, E. D. Cokelet, S. L. Danielson, A. De Robertis, L. B. Eisner, E. V. Farley, and K. Iken. 2017. Late summer zoogeography of the northern Bering and Chukchi seas. Deep Sea Research Part II: Topical Studies in Oceanography **135**:168–189.

Sigler, M. F., P. J. Stabeno, L. B. Eisner, J. M. Napp, and F. J. Mueter. 2014. Spring and fall phytoplankton blooms in a productive subarctic ecosystem, the eastern Bering Sea, during 1995–2011. Deep Sea Research Part II: Topical Studies in Oceanography **109**:71–83.

Simonsen, K. A., P. H. Ressler, C. N. Rooper, and S. G. Zador. 2016. Spatio-temporal distribution of euphausiids: an important component to understanding ecosystem processes in the Gulf of Alaska and eastern Bering Sea. ICES Journal of Marine Science: Journal du Conseil page fsv272 .

Sinclair, E. H., L. S. Vlietstra, D. S. Johnson, T. K. Zeppelin, G. V. Byrd, A. M. Springer, R. R. Ream, and G. L. Hunt. 2008. Patterns in prey use among fur seals and seabirds in the Pribilof Islands. Deep-Sea Research Part II-Topical Studies in Oceanography **55**:1897–1918.

Smart, T., E. Siddon, and J. Duffy-Anderson. 2013. Vertical distributions of the early life stages of walleye pollock (Theragra chalcogramma) in the Southeastern Bering Sea. Deep Sea Research Part II: Topical Studies in Oceanography **94**:201–210.

Smith, J. N., P. H. Ressler, and J. D. Warren. 2013. A distorted wave Born approximation target strength model for Bering Sea euphausiids. ICES Journal of Marine Science: Journal du Conseil **70 (1)**:204–214.

Smith, S. L. 1991. Growth, development and distribution of the euphausiids *Thysanoessa raschi* (M. Sars) and *Thysanoessa inermis* (Krøyer) in the southeastern Bering Sea. Polar Research **10**:461–478.

Spear, A., and A. G. Andrews III. 2021. Vertical Distribution of Age-0 Pollock in the Southeastern Bering Sea. In Ecosystem Status Report 2021: Eastern Bering Sea. Report, North Pacific Fishery Management Council, 1007 W 3rd Ave, Suite 400, Anchorage, AK 99501.

Spear, A., A. G. Andrews III, J. Duffy-Anderson, T. Jarvis, D. Kimmel, and D. McKelvey. 2023. Changes in the vertical distribution of age-0 walleye pollock (Gadus chalcogrammus) during warm and cold years in the southeastern Bering Sea. Fisheries Oceanography **32**:177–195.

Spencer, P. D. 2008. Density-independent and density-dependent factors affecting temporal changes in spatial distributions of eastern Bering Sea flatfish. Fisheries Oceanography **17**:396–410.

Spencer, P. D., K. K. Holsman, S. Zador, N. A. Bond, F. J. Mueter, A. B. Hollowed, and J. N. Ianelli. 2016. Modelling spatially dependent predation mortality of eastern Bering Sea walleye pollock, and its implications for stock dynamics under future climate scenarios. ICES Journal of Marine Science **73**:1330–1342.

Springer, A. M., and G. B. van Vliet. 2014. Climate change, pink salmon, and the nexus between bottom-up and top-down forcing in the subarctic Pacific Ocean and Bering Sea. Proceedings of the National Academy of Sciences **111**:E1880–E1888.

Stabeno, P., J. Duffy-Anderson, L. Eisner, E. Farley, R. Heintz, and C. Mordy. 2017. Return of warm conditions in the southeastern Bering Sea: Physics to fluorescence. PloS one **12**:e0185464.

Stabeno, P. J., and S. W. Bell. 2019. Extreme conditions in the Bering Sea (2017–2018): record-breaking low sea-ice extent. Geophysical Research Letters **46**:8952–8959.

Stabeno, P. J., J. Farley, E. V., N. B. Kachel, S. Moore, C. W. Mordy, J. M. Napp, J. E. Overland, A. I. Pinchuk, and M. F. Sigler. 2012*a*. A comparison of the physics of the northern and southern shelves of the eastern Bering Sea and some implications for the ecosystem. Deep-Sea Research Part II-Topical Studies in Oceanography **65-70**:14–30.

Stabeno, P. J., N. B. Kachel, S. E. Moore, J. M. Napp, M. Sigler, A. Yamaguchi, and A. N. Zerbini. 2012*b*. Comparison of warm and cold years on the southeastern Bering Sea shelf and some implications for the ecosystem. Deep Sea Research Part II: Topical Studies in Oceanography **65**:31–45.

Stevenson, D. E., and R. R. Lauth. 2019. Bottom trawl surveys in the northern Bering Sea indicate recent shifts in the distribution of marine species. Polar Biology **42**:407–421.

Stoeckle, M. Y., J. Adolf, Z. Charlop-Powers, K. J. Dunton, G. Hinks, and S. M. VanMorter. 2020. Trawl and eDNA assessment of marine fish diversity, seasonality, and relative abundance in coastal New Jersey, USA . ICES Journal of Marine Science **78**:293–304.

Stone, R. P., H. Lehnert, and G. R. Hoff. 2019. Inventory of the eastern Bering Sea sponge fauna, geographic range extensions and description of Antho ridgwayi sp. nov. Zootaxa **4567**:zootaxa. 4567.2. 2–zootaxa. 4567.2. 2.

Stram, D. L., and J. N. Ianelli. 2015. Evaluating the efficacy of salmon bycatch measures using fishery-dependent data. ICES Journal of Marine Science **72**:1173–1180.

Sullivan, J., and L. Balstad. 2022. rema: A generalized framework to fit the random effects (RE) model, a state-space random walk model developed at the Alaska Fisheries Science Center (AFSC) for apportionment and biomass estimation of groundfish and crab stocks. R package version 1.2.0, https://github.com/afsc-assessments/rema .

Sullivan, J., C. Monnahan, P. Hulson, J. Ianelli, J. Thorson, and A. Havron. 2022. REMA: A consensus version of the random effects model for ABC apportionment and tier 4/5 assessments. Report, 605 W 4th Ave, Suite 306 Anchorage, AK 99501.

Swiney, K. M., W. C. Long, and R. J. Foy. 2017. Decreased pH and increased temperatures affect young-of-the-year red king crab (*Paralithodes camtschaticus*). ICES Journal of Marine Science **74**:1191–1200.

Theilacker, G. H., K. M. Bailey, M. F. Canino, and S. M. Porter. 1996. Variations in larval walleye pollock feeding and condition: a synthesis. Fisheries Oceanography **5**:112–123.

Thomsen, P. F., J. Kielgast, L. L. Iversen, P. R. Møller, M. Rasmussen, and E. Willerslev. 2012. Detection of a Diverse Marine Fish Fauna Using Environmental DNA from Seawater Samples. PLOS ONE **7**:e41732.

Thorson, J., M. Fossheim, F. Mueter, E. Olsen, R. Lauth, R. Primicerio, B. Husson, J. Marsh, A. Dolgov, and S. Zador. 2019. Comparison of near-bottom fish densities show rapid community and population shifts in Bering and Barents Seas. Arctic Report Card .

Thorson, J., and E. Siddon. 2023. Quantifying Linkages Among Report Card Indicators. Stock Assessment and Fishery Evaluation Report, North Pacific Fishery Management Council, 1007 West Third Ave, Suite 400, Anchorage, AK 99501.

Thorson, J. T. 2019*a*. Guidance for decisions using the Vector Autoregressive Spatio-Temporal (VAST) package in stock, ecosystem, habitat and climate assessments. Fisheries Research **210**:143–161.

Thorson, J. T. 2019*b*. Measuring the impact of oceanographic indices on species distribution shifts: The spatially varying effect of cold-pool extent in the eastern Bering Sea. Limnology and Oceanography **64**:2632–2645.

Thorson, J. T., A. G. Andrews III, T. E. Essington, and S. I. Large. 2024. Dynamic structural equation models synthesize ecosystem dynamics constrained by ecological mechanisms. Methods in Ecology and Evolution **15**:744–755.

Thorson, J. T., L. Ciannelli, and M. A. Litzow. 2020. Defining indices of ecosystem variability using biological samples of fish communities: A generalization of empirical orthogonal functions. Progress in Oceanography **181**:102244.

Thorson, J. T., and K. Kristensen. 2016. Implementing a generic method for bias correction in statistical models using random effects, with spatial and population dynamics examples. Fisheries Research **175**:66–74.

Thorson, J. T., A. O. Shelton, E. J. Ward, and H. J. Skaug. 2015. Geostatistical delta-generalized linear mixed models improve precision for estimated abundance indices for West Coast groundfishes. ICES Journal of Marine Science **72**:1297–1310.

Tobin, E. D., C. L. Wallace, C. Crumpton, G. Johnson, and G. L. Eckert. 2019. Environmental drivers of paralytic shellfish toxin producing *Alexandrium catenella* blooms in a fjord system of northern Southeast Alaska. Harmful algae **88**:101659.

Tojo, N., G. H. Kruse, and F. C. Funk. 2007. Migration dynamics of Pacific herring (*Clupea pallasii*) and response to spring environmental variability in the southeastern Bering Sea. Deep Sea Research Part II: Topical Studies in Oceanography **54**:2832–2848.

Trenberth, K., and J. W. Hurrell. 1994. Decadal atmosphere-ocean variations in the Pacific. Climate Dynamics **9**:303–319.

USFWS. 2021. Biological Opinion on the Proposed Modification of the EPA General Permit AKG524000 for Offshore Seafood Processors in Alaska and on the NMFS Groundfish Fishery for the Gulf of Alaska, Bering Sea, and Aleutians Islands. Anchorage, AK. Report, 80 p.

Vandersea, M. W., S. R. Kibler, P. A. Tester, K. Holderied, D. E. Hondolero, K. Powell, S. Baird, A. Doroff, D. Dugan, and R. W. Litaker. 2018. Environmental factors influencing the distribution and abundance of *Alexandrium catenella* in Kachemak bay and lower cook inlet, Alaska. Harmful algae **77**:81–92.

Vollenweider, J. J., R. A. Heintz, L. Schaufler, and R. Bradshaw. 2011. Seasonal cycles in whole-body proximate composition and energy content of forage fish vary with water depth. Marine biology **158**:413–427.

Wakabayashi, K. 1985. Methods of the US-Japan demersal trawl surveys. In: Bakkala, RG, Wakabayashi, K.(eds) Results of cooperative US-Japan groundfish investigations in the Bering Sea during May-August 1979. Int. North Pac. Fish. Mgmt. **12**:7–26.

Waldbusser, G. G., B. Hales, C. J. Langdon, B. A. Haley, P. Schrader, E. L. Brunner, M. W. Gray, C. A. Miller, and I. Gimenez. 2015. Saturation-state sensitivity of marine bivalve larvae to ocean acidification. Nature Climate Change **5**:273–280.

Wespestad, V., and D. Gunderson. 1991. Climatic induced variation in Eastern Bering Sea herring recruitment. Report, Proceedings of the International Herring Symposium, Anchorage, AK. Alaska Sea Grant.

Wilderbuer, T., W. Stockhausen, and N. Bond. 2013. Updated analysis of flatfish recruitment response to climate variability and ocean conditions in the Eastern Bering Sea. Deep Sea Research Part II: Topical Studies in Oceanography **94**:157–164.

Wilderbuer, T. K. 2017. Eastern Bering Sea Winter Spawning Flatfish Recruitment and Wind Forcing. Stock Assessment and Fishery Evaluation Report, North Pacific Fishery Management Council, 605 W 4th Ave, Suite 306, Anchorage, AK 99501.

Wilderbuer, T. K., A. B. Hollowed, W. J. Ingraham, P. D. Spencer, M. E. Conners, N. A. Bond, and G. E. Walters. 2002. Flatfish recruitment response to decadal climatic variability and ocean conditions in the eastern Bering Sea. Progress in Oceanography **55**:235–247.

Williams, E. H., and T. J. Quinn. 2000. Pacific herring, *Clupea pallasii*, recruitment in the Bering Sea and north-east Pacific Ocean, I: relationships among different populations. Fisheries Oceanography **9**:285–299.

Winemiller, K. O. 2005. Life history strategies, population regulation, and implications for fisheries management. Canadian Journal of Fisheries and Aquatic Sciences **62**:872–885.

Woodgate, R. A., T. J. Weingartner, and R. Lindsay. 2012. Observed increases in Bering Strait oceanic fluxes from the Pacific to the Arctic from 2001 to 2011 and their impacts on the Arctic Ocean water column. Geophysical Research Letters **39**.

Wooster, W. S., and A. B. Hollowed. 1995. Decadal-scale variations in the eastern subarctic Pacific: 1. Winter ocean conditions. Canadian Special Publication of Fisheries and Aquatic Sciences pages 81–85 .

Wuenschel, M. J., W. D. McElroy, K. Oliveira, and R. S. McBride. 2019. Measuring fish condition: an evaluation of new and old metrics for three species with contrasting life histories. Canadian Journal of Fisheries and Aquatic Sciences **76**:886–903.

Yasumiishi, E. M., A. Andrews, A. Dimond, J. Murphy, E. Farley, and E. Siddon. 2023. Trends in the biomass of forage fish species in the south- and northeastern Bering Sea during the late summer surface trawl survey, 2003-2023. Report, North Pacific Fishery Management Council, 605 W 4th Ave, Suite 306, Anchorage, AK 99501.

Yasumiishi, E. M., K. Cieciel, A. G. Andrews, J. Murphy, and J. A. Dimond. 2020. Climate-related changes in the biomass and distribution of small pelagic fishes in the eastern Bering Sea during late summer, 2002–2018. Deep Sea Research Part II: Topical Studies in Oceanography **181**:104907.

Yasumiishi, E. M., C. J. Cunningham, E. V. Farley Jr, L. B. Eisner, W. W. Strasburger, J. A. Dimond, and P. Irvin. 2024. Biological and environmental covariates of juvenile sockeye salmon distribution and abundance in the southeastern Bering Sea, 2002–2018. Ecology and Evolution **14**:e11195.

Yates, M. C., T. M. Wilcox, M. Y. Stoeckle, and D. D. Heath. 2023. Interspecific allometric scaling in eDNA production among northwestern Atlantic bony fishes reflects physiological allometric scaling. Environmental DNA **5**:1105–1115.

Appendix

History of the Ecosystem Status Reports

Since 1995, staff at the Alaska Fisheries Science Center have prepared a separate Ecosystem Status (formerly Considerations) Report within the annual Stock Assessment and Fishery Evaluation (SAFE) report. Each new Ecosystem Status Report provides updates and new information to supplement the original report. The original 1995 report presented a compendium of general information on the Gulf of Alaska, Bering Sea, and Aleutian Island ecosystems as well as a general discussion of ecosystem-based management. The 1996 edition provided additional information on biological features of the North Pacific, and highlighted the effects of bycatch and discards on the ecosystem. The 1997 edition provided a review of ecosystem-based management literature and ongoing ecosystem research, and provided supplemental information on seabirds and marine mammals. The 1998 edition provided information on the precautionary approach, essential fish habitat, effects of fishing gear on habitat, El Niño, local knowledge, and other ecosystem information. The 1999 edition again gave updates on new trends in ecosystem-based management, essential fish habitat, research on effects of fishing gear on seafloor habitat, marine protected areas, seabirds and marine mammals, oceanographic changes in 1997/98, and local knowledge.

In 1999, a proposal came forward to enhance the Ecosystem Status Report by including more information on indicators of ecosystem status and trends and more ecosystem-based management performance measures. The purpose of this enhancement was to accomplish several goals:

1. Track ecosystem-based management efforts and their efficacy
2. Track changes in the ecosystem that are not easily incorporated into single-species assessments
3. Bring results from ecosystem research efforts to the attention of stock assessment scientists and fishery managers
4. Provide a stronger link between ecosystem research and fishery management
5. Provide an assessment of the past, present, and future role of climate and humans in influencing ecosystem status and trends

Each year since 1999, the Ecosystem Status Reports have included some new contributions and will continue to evolve as new information becomes available. Evaluation of the meaning of observed changes should be in the context of how each indicator relates to a particular ecosystem component.

For example, particular oceanographic conditions, such as bottom temperature increases, might be favorable to some species but not for others. Evaluations should follow an analysis framework such as that provided in the draft Programmatic Groundfish Fishery Environmental Impact Statement that links indicators to particular effects on ecosystem components.

In 2002, stock assessment scientists began using indicators contained in this report to systematically assess ecosystem factors such as climate, predators, prey, and habitat that might affect a particular stock. Information regarding a particular fishery's catch, bycatch, and temporal/spatial distribution can be used to assess possible impacts of that fishery on the ecosystem. Indicators of concern can be highlighted within each assessment and can be used by the Groundfish Plan Teams and the Council to justify modification of allowable biological catch (ABC) recommendations or time/space allocations of catch.

We initiated a regional approach to the ESR in 2010 and presented a new ecosystem assessment for the eastern Bering Sea. In 2011, we followed the same approach and presented a new assessment for the Aleutian Islands based on a similar format to that of the eastern Bering Sea but with regional report cards for the western, central, and eastern Aleutian Islands. In 2012, we provided a preliminary ecosystem assessment on the Arctic. Our intent was to provide an overview of general Arctic ecosystem information that may form the basis for more comprehensive future Arctic ecosystem assessments. In 2015, we presented a new Gulf of Alaska report card and assessment, which was further divided into Western and Eastern Gulf of Alaska report cards beginning in 2016. This was also the year that the previous Alaska-wide ESR was split into four separate reports, one for the Gulf of Alaska, Aleutian Islands, eastern Bering Sea, and the Arctic[26].

The eastern Bering Sea and Aleutian Islands ecosystem assessments were based on additional refinements contributed by Ecosystem Synthesis Teams. For these assessments, the teams focused on a subset of broad, community-level indicators to determine the current state and likely future trends of ecosystem productivity in the EBS and ecosystem variability in the Aleutian Islands. The teams also selected indicators that reflect trends in non-fishery apex predators and maintaining a sustainable species mix in the harvest as well as changes to catch diversity and variability. Indicators for the Gulf of Alaska report card and assessment were also selected by a team of experts, via an online survey first, then refined in an in-person workshop.

Originally, contributors to the Ecosystem Status Reports were asked to provide a description of their contributed indicator, summarize the historical trends and current status of the indicator, and identify potential factors causing those trends. Beginning in 2009, contributors were also asked to describe why the indicator is important to groundfish fishery management and implications of indicator trends. In particular, contributors were asked to briefly address implications or impacts of the observed trends on the ecosystem or ecosystem components, what the trends mean and why are they important, and how the information can be used to inform groundfish management decisions. Answers to these types of questions will help provide a "heads-up" for developing management responses and research priorities.

In 2018, a risk table framework was developed for individual stock assessments as a means of documenting concerns external to the stock assessment model, but relevant to setting the Acceptable Biological Catch (ABC) value for the current year. These concerns could be categorized as those reflecting the assessment model, the population dynamics of the stock, and environmental and ecosystem concerns—including those based on information from Ecosystem Status Reports. In the past, concerns used to justify an ABC below the maximum estimated by the assessment model were documented in an ad-hoc

[26]The Arctic report is under development

manner in the stock assessment report or in the minutes of the Groundfish Plan Teams or Scientific and Statistical Committee (SSC) reviews. With the risk table, formal consideration of concerns—including ecosystem—are documented and ranked, and the stock assessment author presents a recommendation for the maximum ABC as specified by the stock assessment model or a lower value. The recommended ABC (whether at maximum or lower) from the lead stock assessment author is subsequently reviewed and adjusted or accepted by the Groundfish Plan Team and the Scientific and Statistical Committee. Five risk tables were completed in 2018 as a test case. After review, the Council requested risk tables to be included in all full stock assessments in 2019. The SSC also requested a fourth category of concern to be added to the risk tables. The fishery performance category serves to represent any concerns related to the recommended ABC that can be inferred from commercial fisheries performance. Importantly, these concerns refer to indications of stock status, not economic performance.

In Briefs were started in 2018 for the Eastern Bering Sea, 2019 for the Gulf of Alaska, and 2020 for the Aleutian Islands. These more public-friendly succinct versions of the full ESRs have since been produced annually in tandem with the ESRs.

In 2019, risk tables were completed for all full assessments. Ecosystem scientists collaborated with stock assessment scientists to use the Ecosystem Status Reports to help inform the ecosystem concerns in the risk tables. Some ecosystem information can also be used to inform concerns related to the population dynamics of the stock. Initially, there were 4 levels of concern from no concern to extreme. In 2023 (and revised in 2024), based on a recommendation from the SSC, the levels of risk were reduced to 3: Level 1 (Normal), Level 2 (Increased concern), and Level 3 (Extreme concern). For stock assessments which include an Ecosystem and Socioeconomic Profile (ESP), the ESP is also used to inform the ecosystem risk column as well as the population dynamics and fisheries performance columns.

ESPs were initiated in 2017 (sablefish) and ESR editors began working closely with ESP teams in 2019 (starting with GOA walleye pollock). These complimentary annual status reports inform groundfish management and alignment in research that feeds these reports increases efficiency and collaboration between ecosystem and stock assessment scientists.

This report represents much of the first three steps in Alaska's IEA: defining ecosystem goals, developing indicators, and assessing the ecosystems (Figure 137). The primary stakeholders in this case are the North Pacific Fishery Management Council. Research and development of risk analyses and management strategies is ongoing and will be referenced or included as possible.

It was requested that contributors to the Ecosystem Status Reports provide actual time series data or make them available electronically. The Ecosystem Status Reports and data for many of the time series presented within are available online at: `https://alaskaesr.psmfc.org`. These reports and data are also available through the NOAA-wide IEA website at: `https://www.integratedecosystemassessment.noaa.gov/regions/alaska`.

Past reports and all groundfish stock assessments are available at: `https://www.fisheries.noaa.gov/alaska/population-assessments/north-pacific-groundfish-stock-assessment-and-fishery-evaluation`.

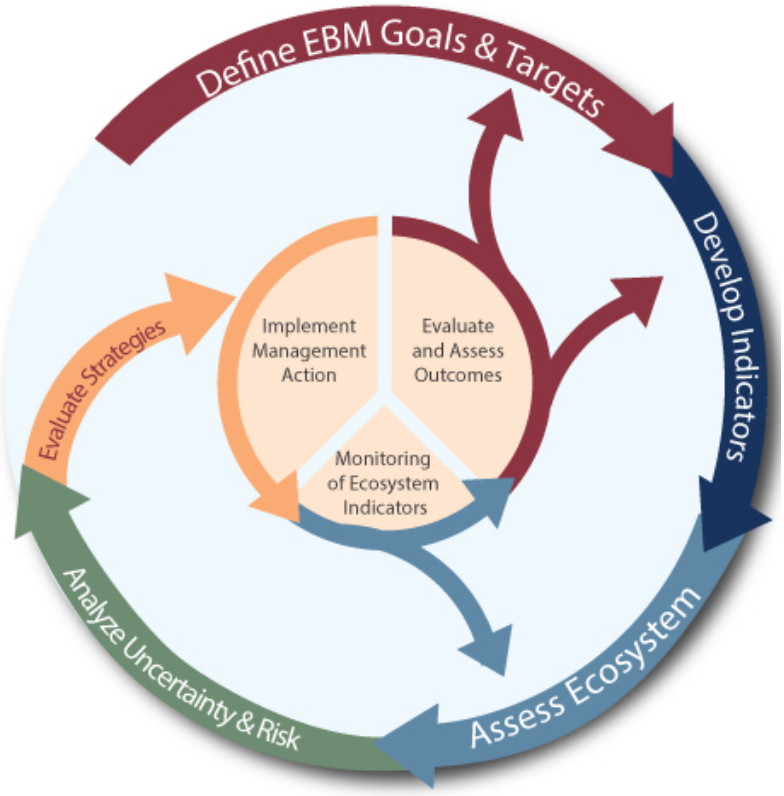

Figure 137: The IEA (integrated ecosystem assessment) process.

Responses to SSC Comments From December 2023

December 2023 SSC Final Report to the NPFMC
C3 BSAI and C4 GOA Ecosystem Status Reports
The SSC received presentations from Elizabeth Siddon (NOAA-AFSC) for the eastern Bering Sea (EBS), Ivonne Ortiz (University of Washington) for the Aleutian Islands (AI), and Bridget Ferriss (NOAA-AFSC) for the Gulf of Alaska (GOA). Christopher Tran (Aleut Community of St. Paul Island) and Terese Vicente (Kuskokwim River Inter-Tribal Fish Commission) provided public testimony on the EBS ESR. There was no public testimony for the AI or GOA ESRs. The SSC thanks the ESR authors for their continued progress in collecting a large number of indicators and summarizing this information to better understand the status of marine ecosystems that support federally managed fisheries off Alaska. The SSC appreciated the structure of the reports, especially the consolidated information provided in the Report Card, Ecosystem Assessment, Noteworthy Topics, and Indicator Summary sections. The SSC acknowledges the continued value of the graphics in each report and separate "In Briefs" that visually translate how information is incorporated into Council processes and informs broader audiences.

Thank you. We want to acknowledge the effort and thank all those involved in collecting, analyzing, interpreting, and communicating the observations included in these reports.

The SSC finds no major ecosystem concerns from 2023, but items that are noteworthy include low productivity in the Bering Sea, continued warm conditions in the western Aleutian Islands, mixed recovery from recent heatwaves in the GOA, and potential effects of El Niño in 2024.

General Comments Applicable to all three ESRs
The SSC thanks the authors for their responses to SSC comments and continued efforts to further integrate and synthesize indicators in ways that are most relevant to understanding potential effects on managed stocks.
There appear to be different seasonal warming patterns among the ESR regions with winter warming more prominent in the EBS, winter and summer in the AI, and summer in the GOA. This will affect recruitment of different groundfish species, depending on seasonality of early life stages, and is another aspect by which to sustain efforts in addressing prior comments from the SSC regarding how different species might respond to changing temperatures. The SSC appreciates the inclusion of case studies in this year's document addressing life stage phenology and temperature thresholds, and encourages continued efforts along these lines.

The ESR editors agree these case studies of phenology and temperature can be useful and will continue to explore their integration into ESRs when applicable and when resources are available.

The SSC suggests more focus on multi-year patterns and whether they are similar to other periods during the time series. This moves us beyond comparing the current year to previous years. The SSC recommends these comparisons are independent of warm or cold stanzas so that there is no a priori *determination and to account for possible changes in climate-biology relationships.*

The eastern Bering Sea Ecosystem Assessment addresses the ecosystem response (both SEBS and NBS) to the shift from interannual variability (prior to 2000) to the recent prolonged warm period to the return to average thermal conditions since ∼2021.

The SSC recommends considering options for identifying step changes in times series that might indicate a new "baseline" or "regime" for that indicator. These efforts might also be relevant for time series beyond the ESRs. The SSC recognizes the sensitivity of referring to regime changes and management implications, however it is important to be vigilant of step changes in metrics and how to adapt to them.

The EBS ESR includes a borealization index that addresses changes in ecosystem state relative to the shifts in marine community composition. The GOA ESR will include an updated ecosystem state analysis based on Ferriss et al. (submitted) in 2025.

Several recent publications note that the position of the Aleutian Low affects climate in the Bering Sea. All three ESRs share the North Pacific Index contribution which reflects the strength of the Aleutian Low. Whereas current atmospheric pressure anomaly maps in ESRs show the average position of the Aleutian Low graphically, its mean position cannot be compared to previous years. The SSC recommends that ESR authors evaluate ways to present a time series of the position of the Aleutian Low for this contribution.

In 2024, the ESRs include a new contribution this year from Jim Overland and Muyin Wang that describes the strength and position of the Aleutian Low Pressure System. Likewise, the ESR editors worked with Emily Lemagie, NOAA-PMEL, to include new graphics of climate conditions that represent the Aleutian Low climatology and current year.

The SSC appreciates the one to five month lead forecasts of expected El Niño effects in Alaska. Given that as of November 9, 2023, the NOAA National Center for Environmental Prediction suggests a 35% chance of a historically strong El Niño this winter, the SSC encourages continued monitoring of El Niño development and potential ecosystem affects, especially in the GOA.

The ESR editors monitored the El Niño event through the winter of 2023/2024, including via satellite-derived SSTs and observations from NOAA's winter acoustic-trawl survey in Shelikof Strait. Most notably, impacts of the El Niño event were presented at the Spring Preview of Ecosystem and Economic Conditions (PEEC) workshop. By that time (May 2024) the ENSO index had already transitioned from a positive (El Niño) to a neutral value, and the impacts of the El Niño in AK appeared more moderate than predicted. If the impacts had been more extreme, the ESR editors were prepared to discuss developing impacts with the Council at their June or October meeting (if requested).

The SSC notes that the ESR process has matured over several decades to effectively use ecosystem trends to inform annual specifications and encourages the use of trans-disciplinary approaches for linking ESR and ESPs to stock assessments in the future. The GOA pollock assessment was suggested as a potential case study, particularly in contrasting differences in the strength of 2018 vs. 2019 year classes.

A research model is presented in the Gulf of Alaska walleye pollock assessment Appendix 1E (Monnahan et al., 2024) that explores incorporating environmental data into the GOA pollock stock assessment. This model embeds a dynamic structural equation model (DSEM) into the assessment, and uses complex causal relationships among eight environmental indicators (sourced from the GOA ESR and GOA pollock ESP) to explain recruitment variation. Preliminary results are encouraging, with strong statistical evidence that this approach can substantially reduce unexplained recruitment variation and improve short-term projections like those used for management.

The SSC further discussed the process of selecting and refining indicators to minimize redundancy and ensure key information is included.

The ESR editors continues to refine the process of minimizing redundancy while ensuring a holistic perspective based on spatially- and temporally-restricted data sets. Some redundancy is intentionally retained in the process to ensure data are available in alternating years when NOAA surveys are not conducted (even years for GOA and odd years for AI). In addition, Ferriss et al. (submitted) conducted a dynamic factor analyses on a subset of ESR time-series to identify those that produce a common trend over time, informing the potential reduction of redundancy.

The SSC supports the process where indicators are brought forward by authors and integrated into Council documents to inform NS1, NS2, NS4 and NS8 issues where appropriate. Additionally, the SSC suggests that workshops (see General Assessment Comments) or modeling could be used as part of the process to help identify indicators. It was promising to see some socioeconomic indicators in the Aleutian Islands ESR (school enrollment) and the SSC encourages ESR authors to collaborate with other social scientists about other potential indicators.

The ESR editors continue to be a part of broader discussions on the identification of effective social and economic indicators and the most appropriate tools with which to communicate them to the Council (i.e., ESRs, ESPs, Economic SAFE, ACEPO).

The SSC notes that many satellite-derived chlorophyll-a time series have a declining trend. To be certain these reflect real, in situ *conditions, the SSC recommends that ESR authors work with contributors of these metrics to identify what calibration efforts have occurred, what additional calibrations might be needed, and how interpretation of the satellite time series might be affected.*

The ESR editors reached out to the satellite-derived chlorophyll-a contributors for a response:

"We thank the SSC for this comment. Contributors have continued to cross-validate globcolour satellite chla data from globcolour that is used in the annual ESRs with both single sensor data (e.g., VIIRS) and another combined product (i.e., OC-CCI). While contributors have done similar cross-product comparisons in the past - these were prior to 2023. In 2024, new cross-product comparisons showed relatively larger discrepancies among products than those from previous years. Consequently, contributors have paused contributions of satellite-derived chla trends to this year's ESRs until they have confidently resolved what is causing these discrepancies. They noted all combined (multi satellite sensor) chla products that are currently available are from external sources. Unfortunately that limits the ability to directly apply calibrations and corrections to the satellite data products."

Public testimony encouraged development of ways to uptake ESR information into decision making and highlighted the traditional knowledge contribution regarding the chum salmon life cycle in the Yukon and Kuskokwim Rivers and the importance of this information to EBFM.

BSAI Ecosystem Status Reports

Eastern Bering Sea

While some physical oceanographic metrics including sea ice extent and water temperatures have shifted back to near average condition in 2023, biological metrics have lagged in their return to levels typical

of cooler conditions.
The recent warm stanza has been positive for some year classes of pollock, sablefish, Togiak herring, Bristol Bay sockeye salmon, and the multivariate seabird breeding index. Conditions have also been more favorable in the north, including improved juvenile salmon condition, adult pollock condition, and the auklet breeding population on St. Lawrence Island, which is very high after nearly empty colonies the last few years. This warm stanza, however, has been negative for ice and cold pool extent that only in the past two years has increased to the long-term mean. There have been declining trends in chlorophyll-a concentration, large zooplankton, pelagic and benthic forage fishes, reduced abundance of several crab stocks, and runs of multiple species of Western Alaska salmon. Given these and other metrics showing contrasting trends, the SSC concurs with the ESR author that ecologically, the EBS remains in a transitional state in 2023.
The SSC notes that walleye pollock provide a good potential case study for studying mechanisms of contrasting patterns of low body condition for adult and juvenile age classes during the current warm period, yet having a particularly strong year class in 2018 that remains unexplained.

The EBS ESR Ecosystem Assessment brings together a few hypotheses for the strong 2018 year class and continued increase in pollock biomass over the EBS shelf. Combined with the EBS potentially entering a new era of prolonged warm periods, with average being the new cool, the EBS ESR editor concurs that further exploration into drivers of pollock dynamics is warranted.

Projections for the EBS in 2024 suggest that even with El Niño, anticipated conditions should not be extreme relative to the past 20–30 years and that sea ice should extend south of 60°N latitude and as far south as Bristol Bay along the coast. However, the retreat of the sea ice is expected to occur earlier than average in the spring of 2024.

The NMME projections from last year (August 2023) predicted a near-normal SST environment in the Bering Sea for the period of November 2023 to April 2024. This was largely borne out by observations. However, the retreat of sea ice did not occur early in spring 2024. Sea ice persisted in spring, with 2024 having the highest May ice extent since 2013.

The SSC supports the use of Dynamic Structural Equation Modeling as a promising new tool to help identify ecological mechanisms and drivers of change. The SSC agrees with incrementally moving forward with increasing complexity. The SSC notes that currently interactions are unidirectional and suggests adding interactions in the model that allow two-way interactions or feedback loops. The SSC also recommends using species-specific case studies and notes that the goal of these models is to explore correlations among variables; however, the current ESR indicators used in this pilot effort were specifically chosen to be independent.

Please see the contribution "Forage Fish Dynamics in the Eastern Bering Sea" on p. 115.

Responses to Crab Plan Team Comments from September 2024

Climate Overview
The CPT minutes summarize the Climate Overview presentation. No recommendations were made.

Ecosystem Status Report - Bering Sea
The CPT minutes summarize the EBS ESR presentation. No recommendations were made.

Responses to Joint Groundfish Plan Team Comments from September 2024

ESR climate update
There was discussion about deep water incursion onto the shelf that brings water that is cold, low-oxygen, high salinity and low pH. Additional discussion focused on terminology to describe marine heatwaves in the Aleutians, including: 1. how are "moderate," "severe," and "extreme" defined (the proportion of time spent between the long term mean and various percentiles of temperature), 2. how should "baseline" be defined, while acknowledging that changes are variable among areas, depending on data availability, and 3. When do we stop calling a heatwave a heatwave instead of a temperature shift? One minor suggestion was to align the colors of years among slides to facilitate easier comparison of different environmental variables in the same year.

The ESR editors appreciate the discussion and will continue to refine how we present these terms and our use of baselines.

Responses to SSC Comments from October 2024

Ecosystem Status Report Preview
The SSC appreciates the authors and contributors providing near real-time data that are within months to days of collection. This is only possible because of the dedication of the ESR team, the rapport they have fostered with data contributors, and the value placed on this information by all involved in the Council process.
The Bering Sea cold pool is broadly defined as bottom temperatures $<2^{o}$; however, there were references to other cold pool temperatures with respect to juvenile snow crab in the ESP. The Groundfish Assessment Program calculates cold pool temperature proportions at $1^{o}C$ intervals between $2^{o}C$ and $-2^{o}C$. The SSC recommends evaluating whether there is a benefit to quantifying specific temperature ranges within the broad definition of the cold pool when assessing conditions for different size-classes or species of crabs. The SSC also requests that when physical data from a model output (e.g., ROMS) are first used that comparisons with available in situ data be provided (spatially if relevant) to assess potential biases.

Some research efforts are underway to examine specific temperature ranges within the broad definition of the cold pool for different species, specifically through Species Distribution Models (SDMs). Skill analysis of the Bering10K model survey-replicated temperature raster relative to the observational raster has been completed and the paper is in review. We will bring forward a summary of that analysis during the December SSC 2024 EBS ESR presentation.

The SSC appreciates the ESR team's continued efforts to explore new ways to visualize data, make data available and discoverable, and consolidate data in more integrated ways. For example, the new wind, ice, and temperature integrated maps of the Alaska-wide climate overview are particularly informative.

Thank you. We appreciate the opportunity to participate in your October meeting.

Description of the SEBS Report Card Indicators

1. The North Pacific Index (NPI) winter average (Nov-Mar): The NPI index (Trenberth and Hurrell, 1994) was selected as the single most appropriate index for characterizing the climate forcing of the Bering Sea. The NPI is a measure of the strength of the Aleutian Low, specifically the area-weighted sea level pressure (SLP) for the region of 30°N to 65°N, 160°E to 140°W. Above (below) average winter (November–March) NPI values imply a weak (strong) Aleutian Low and generally calmer (stormier) conditions.

The advantages of the NPI include its systematic relationship to the primary causes of climate variability in the Northern Hemisphere, especially the El Niño-Southern Oscillation (ENSO) phenomenon, and to a lesser extent the Arctic Oscillation (AO). It may also respond to North Pacific SST and high-latitude snow and ice cover anomalies, but it is difficult to separate cause and effect.

The NPI also has some drawbacks: (1) it is relevant mostly to the atmospheric forcing in winter, (2) it relates mainly to the strength of the Aleutian Low rather than its position, which has also been shown to be important to the seasonal weather of the Bering Sea (Rodionov et al., 2007; see Figure 15), and (3) it is more appropriate for the North Pacific basin as a whole than for a specific region (i.e., Bering Sea shelf).

Implications: For the Bering Sea, the strength of the Aleutian Low relates to wintertime temperatures, with a deeper low (negative SLP anomalies) associated with a greater preponderance of maritime air masses and hence warmer conditions.

Contact: Muyin Wang
Muyin.Wang@noaa.gov

2. Bering Sea ice extent: Annual sea ice extent for the southeastern Bering Sea was calculated using National Snow and Ice Data Center (NSIDC) daily sea ice concentration data at a 25 km resolution with a 0.15 concentration threshold. Monthly sea ice extent values were first computed from the daily data for each region, defined by marine ecosystem management boundaries, and then averaged to obtain the annual sea ice extent. The Python code used to compute the extent is available at `github.com/polarwatch/alaska-seaice`. *Implications:* Seasonal sea-ice coverage impacts, for example, the extent of the cold pool, bloom strength and timing, and bottom-up productivity.

Contact: Sunny Bak-Hospital
sun.bak-hospital@noaa.gov

3. Cold pool extent: Area of the cold pool in the eastern Bering Sea (EBS) shelf bottom trawl survey area (including strata 82 and 90) from 1982–2024. The cold pool is defined as the area of the EBS continental shelf with bottom temperature <2°C, in square kilometers (km^2). *Implications:* The cold pool has a strong influence on the thermal stratification and influences the spatial structure of the demersal community (Spencer, 2008; Kotwicki and Lauth, 2013; Thorson et al., 2020), trophic structure of the eastern Bering Sea food web (Mueter and Litzow, 2008; Spencer et al., 2016), and demographic processes of fish populations (Grüss et al., 2021).

Contact: Sean Rohan and Lewis Barnett
Sean.Rohan@noaa.gov and Lewis.Barnett@noaa.gov

4. Proportion of open water blooms: The timing of ice retreat[27] and bloom peak was used to estimate bloom type over the southeastern Bering Sea shelf (<60°N). Bloom type differentiates between open-water blooms (i.e., ice retreat occurred $\geq$21 days prior to bloom peak) and ice-associated blooms (i.e., ice retreat occurred $<$21 days prior to bloom peak) for each year (Perrette et al., 2011). Timing of sea-ice retreat was determined as the date when ice coverage remained below 15% based on the 15-day running mean of the daily sea-ice fraction data. Bloom peak timing was estimated using standardized merged ocean color satellite data of 8-day satellite chlorophyll-a (chl-a, μg/L) at a 4 km-resolution from The Hermes GlobColour website[28] covering the years 1998–2024. *Implications:* Bloom type provides a metric of the bloom dynamics related to sea ice; increased ice-associated blooms tend to correlate positively with higher abundances of large zooplankton and have been suggested to favor pollock recruitment (Hunt et al., 2011).

Contact: Jens Nielsen
Jens.Nielsen@noaa.gov

5. Large copepod abundance: Large copepods (predominantly *Calanus* spp.) are quantified from 505 μm mesh, 60 cm bongo net samples taken during the fall (Aug/Sept) 70 m isobath survey over the southeastern Bering Sea shelf. Detailed information on sampled taxa is provided after in-lab processing protocols have been conducted (1 year post survey). The current year value is an estimate of relative abundance derived from an at-sea Rapid Zooplankton Assessment (RZA). RZA abundance estimates may not closely match historical estimates of abundance as methods differ between laboratory processing and ship-board RZA. *Implications:* Large copepods are an important prey and trophic link between primary production and fish, marine mammals, and seabirds.

Contact: David Kimmel
David.Kimmel@noaa.gov

[27] `https://coastwatch.pfeg.noaa.gov/erddap/griddap/NOAA_DHW.html`
[28] `http://hermes.acri.fr/`, Maritorena et al., 2010

6. Euphausiid biomass: In the absence of direct measurements of secondary production in the eastern Bering Sea, we rely on estimates of biomass. We use an estimate of euphausiid biomass as determined by acoustic backscatter and midwater trawl data collected during biennial pollock surveys. Since the previous update to this index, euphausiid backscatter observations from the 2020 acoustic-only Saildrone uncrewed surface vehicle survey as well as the 2024 acoustic-trawl survey of pollock were added to the time series. *Implications:* The data presented here suggest that euphausiid prey availability is below average in 2024. Euphausiids form a key, large group of macrozooplankton that function as intermediaries in the trophic transfer from primary production to living marine resources (commercial fisheries and protected species). Understanding the mechanisms that control secondary production is an obvious goal toward building better ecosystem syntheses.

Contact: Mike Levine
Mike.Levine@noaa.gov

7. Pelagic forage fish biomass: This index represents the relative biomass of small fishes captured in the BASIS surface trawl (upper 25 m) survey in the southeastern Bering Sea during late summer. Primary fish caught and included in the forage fish species aggregate are age-0 pollock, age-0 Pacific cod, capelin, Pacific herring, juvenile Chinook, sockeye, chum, pink, and coho salmon, rainbow smelt, and saffron cod. Due to changes in survey station locations and timing across years, a Vector Autoregressive Spatio-Temporal model with day of year as a catchability covariate was used. *Implications:* When this index is higher (lower), it indicates there may be more (less) food available to upper trophic predators (e.g., fish, seabirds, and mammals).

Contact: Ellen Yasumiishi
Ellen.Yasumiishi@noaa.gov

8., 9., 10., 11. Description of the fish and invertebrate guilds: We present four guilds to indicate the status and trends for fish and invertebrates in the eastern Bering Sea: motile epifauna, benthic foragers, pelagic foragers, and apex predators. Each is described in detail below. The full guild analysis involved aggregating all eastern Bering Sea species included in a food web model (Aydin and Mueter, 2007) into 18 guilds by trophic role, habitat, and physiological status (Table 5). For the four guilds included here, time trends of biomass are presented for 1982–2024. Foraging guild biomass is based on catch data from the NMFS-AFSC annual summer bottom trawl survey of the EBS shelf ($<$200 m), modified by an Ecopath-estimated catchability coefficient that takes into account the minimum biomass required to support predator consumption (see Appendix 1 in (Boldt, 2007) for complete details). This survey index is specific to the standard bottom trawl survey area in the southeastern Bering Sea (does not include strata 82 and 90) and does not include the northern Bering Sea. The foraging guild biomass is weighted by strata area (km^2) which has resulted in a minor shift in the biomass values from reporting in previous years but the trends and patterns remain the same. Also, we no longer include species that lack time series and were previously represented by a constant biomass equal to the mid-1990s mass balance level estimated in (Aydin and Mueter, 2007).

Contact: Kerim Aydin or George A. Whitehouse
Kerim.Aydin@noaa.gov or Andy.Whitehouse@noaa.gov

Table 5: Composition of foraging guilds in the eastern Bering Sea.

Motile Epifauna	Benthic Foragers	Pelagic Foragers	Apex Predators
Eelpouts	Yellowfin sole	W. pollock	P. cod
Octopuses	Flathead sole	P. herring	Arrowtooth
Tanner crab	N. rock sole	Atka mackerel	Kamchatka fl.
King crab	Alaska plaice	Misc. fish shallow	Greenland turbot
Snow crab	Dover sole	Salmon returning	P. halibut
Sea stars	Rex sole	Capelin	Alaska skate
Brittle stars	Misc. flatfish	Eulachon	Other skates
Other echinoderms	Greenlings	Sandlance	Sablefish
Snails	Other sculpins	Other pelagic smelts	Large sculpins
Hermit crabs		Other managed forage	
Misc. crabs		Scyphozoid jellies	

8. Motile epifauna (fish and benthic invertebrates): This guild includes both commercial and non-commercial crabs, sea stars, snails, octopuses, other mobile benthic invertebrates, and eelpouts. There are ten commercial crab stocks in the current Fishery Management Plan for Bering Sea/Aleutian Islands King and Tanner Crabs; we include seven on the eastern Bering Sea shelf: two red king crab *Paralithodes camtschaticus* (Bristol Bay, Pribilof Islands), two blue king crab *P. platypus* (Pribilof District and St. Matthew Island), one golden king crab *Lithodes aequispinus* (Pribilof Islands), and two Tanner crab stocks (southern Tanner crab *Chionoecetes bairdi* and snow crab *C. opilio*). The three dominant species comprising the eelpout group are marbled eelpout (*Lycodes raridens*), wattled eelpout (*L. palearis*), and shortfin eelpout (*L. brevipes*). The composition of seastars in shelf trawl catches is dominated by the purple-orange seastar (*Asterias amurensis*), which is found primarily in the inner/middle shelf regions, and the common mud star (*Ctenodiscus crispatus*), which is primarily an inhabitant of the outer shelf. *Implications:* Trends in the biomass of motile epifauna indicate benthic productivity and/or predation pressure, although individual species and/or taxa may reflect shorter or longer time scales of integrated impacts of bottom-up or top-down control.

9. Benthic foragers (fish only): The species which comprise the benthic foragers group are the Bering Sea shelf flatfish species, greenlings, and small sculpins. *Implications:* Trends in the biomass of benthic foragers indirectly indicate availability of infauna (i.e., prey of these species).

10. Pelagic foragers (fish and Scyphozoid jellies only): This guild includes adult and juvenile walleye pollock (*Gadus chalcogrammus*), other forage fish such as Pacific herring (*Clupea pallasi*), capelin (*Mallotus villosus*), eulachon (*Thaleichthys pacificus*), and sandlance, salmon, Atka mackerel (*Pleurogrammus monopterygius*), and scyphozoid jellies. *Implications:* Trends in the biomass of pelagic foragers largely track walleye pollock which is an important component of the Bering Sea ecosystem, both as forage and as a predator.

11. Apex predators (shelf fish only): This guild includes Pacific cod (*Gadus macrocephalus*), arrowtooth flounder, Kamchatka flounder (*Atheresthes evermanni*), Pacific halibut (*Hippoglossus stenolepis*), Greenland turbot (*Reinhardtius hippoglossoides*), sablefish (*Anoplopoma fimbria*), Alaska skate, and large sculpins. *Implications:* Trends in the biomass of apex predators indicate relative predation pressure on zooplankton and juvenile fishes within the ecosystem.

12. Multivariate seabird breeding index: This index represents the dominant trend among 17 reproductive seabird data sets from the Pribilof Islands that include diving and surface-foraging seabirds. The trend of the leading principal component (PC1) explains 51% of the variance among the data sets and represents all seabird hatch timing and the reproductive success of murres and cormorants, defined as loadings $>|0.2|$. *Implications:* Above-average index values reflect high reproductive success and/or early breeding (assumed to be mediated through food supply) and indicate better than average recruitment of year classes that seabirds feed on (e.g., age-0 pollock), or better than average supply of forage fish that commercially-fished species feed on (e.g.,capelin eaten by both seabirds and Pacific cod).

Contact: Stephani Zador
Stephani.Zador@noaa.gov

13. Borealization index: To measure the progression of borealization, this index analyzes nine time series that reflect the difference between Arctic and boreal conditions in the southeastern Bering Sea between 1972 and 2024. To create an overall index of borealization from the individual time series we used Dynamic Factor Analysis (DFA), a state-space approach for identifying shared variability across multiple time series. The DFA model identified a single shared trend that combines negative loadings for time series associated with Arctic conditions, and positive loadings for time series associated with boreal conditions. *Implications:* This index reflects the transition from an Arctic physical state supporting a cold-adapted species assemblage to a subarctic (boreal) physical state supporting a warm-adapted assemblage.

Contact: Mike Litzow
Mike Litzow@noaa.gov

Description of the NBS Report Card Indicators

1. The North Pacific Index (NPI) winter average (Nov-Mar): Please see 'Description of the SEBS Report Card indicators' (p. 261).

Contact: Muyin Wang
Muyin.Wang@noaa.gov

2. Bering Sea ice extent: Annual sea ice extent for the northern Bering Sea was calculated using NSIDC daily sea ice concentration data. Please see 'Description of the SEBS Report Card indicators' (p. 261) for more information.

Contact: Sunny Bak-Hospital
sun.bak-hospital@noaa.gov

3. Cold pool extent: Area of the cold pool in the northern Bering Sea (NBS) shelf bottom trawl survey area (strata 70, 71, and 81) from 2010, 2017, 2019, and 2021–2023. Please see 'Description of the SEBS Report Card indicators' (p. 261) for more information.

Contact: Sean Rohan and Lewis Barnett
Sean.Rohan@noaa.gov and Lewis.Barnett@noaa.gov

4. Proportion of open water blooms: The timing of ice retreat[29] and bloom peak was used to estimate bloom type over the northern Bering Sea shelf (>60°N). Please see 'Description of the SEBS Report Card indicators' (p. 261) for more information.

Contact: Jens Nielsen
Jens.Nielsen@noaa.gov

5. Large copepod abundance: Large copepods (predominantly *Calanus* spp.) are quantified from 505 μm mesh, 60 cm bongo net samples taken during the fall (Aug/Sept) surface trawl survey over the northern Bering Sea shelf. Please see 'Description of the SEBS Report Card indicators' (p. 261) for more information.

Contact: David Kimmel
David.Kimmel@noaa.gov

[29] `https://coastwatch.pfeg.noaa.gov/erddap/griddap/NOAA_DHW.html`

6. Pelagic forage fish biomass: This index represents the relative biomass of small fishes captured in the surface trawl (upper 25 m) survey in the northern Bering Sea during late summer. Please see 'Description of the SEBS Report Card indicators' (p. 261) for more information.

Contact: Ellen Yasumiishi
Ellen.Yasumiishi@noaa.gov

7. Juvenile snow crab: The estimated biomass (metric tons) of juvenile snow crab sampled during the northern Bering Sea bottom trawl survey (strata 70, 71, and 81) in 2010, 2017–2019, and 2021–2023. *Implications:* Trends in the biomass of juvenile snow crab, an important component of the benthic community, reflect broad scale benthic production and indicate the strength of crab recruitment as these crabs mature and likely move south into the eastern Bering Sea.

Contact: Shannon Hennessey
shannon.hennessey@noaa.gov

8. Yellowfin sole: The estimated biomass index (metric tons) of yellowfin sole sampled during the northern Bering Sea bottom trawl survey (strata 70, 71, and 81) in 2010, 2017, 2019, and 2021–2023. *Implications:* Trends in the biomass of yellowfin sole indicate relative predation pressure on small infaunal prey (e.g., polychaete worms, bivalves, small crustaceans).

Contact: Sean Rohan
sean.rohan@noaa.gov

9. Walleye pollock: The estimated biomass index (metric tons) of walleye pollock sampled during the northern Bering Sea bottom trawl survey (strata 70, 71, and 81) in 2010, 2017, 2019, and 2021–2023. *Implications:* Trends in the biomass of walleye pollock indirectly indicate relative predation pressure on zooplankton and forage fish.

Contact: Sean Rohan
sean.rohan@noaa.gov

10. Pacific cod: The estimated biomass index (metric tons) of Pacific cod sampled during the northern Bering Sea bottom trawl survey (strata 70, 71, and 81) in 2010, 2017, 2019, and 2021–2023. *Implications:* Trends in the biomass of Pacific cod, a generalist apex predator, indicate relative predation pressure on forage fish and crab within the ecosystem.

Contact: Sean Rohan
sean.rohan@noaa.gov

Methods Description for the Report Card Plots

For each plot, the mean (green dashed line) and ±1 standard deviation (SD; green solid lines) are shown as calculated for the entire time series. Time periods for which the time series was outside of this ±1 SD range are shown in yellow (for high values) and blue (for low values).

The shaded green window shows the most recent 5 years prior to the date of the current report. The symbols on the right side of the graph are all calculated from data inside this 5-year moving window (maximum of 5 data points). The first symbol represents the "2019–2023 Mean" as follows: '+ or -' if the recent mean is outside of the ±1 SD long-term range, '.' if the recent mean is within this long-term range, or 'x' if there are fewer than 2 data points in the moving window. The symbol choice does not take into account statistical significance of the difference between the recent mean and long-term range. The second symbol represents the "2019–2023 Trend" as follows: if the magnitude of the linear slope of the recent trend is greater than 1 SD/time window (a linear trend of >1 SD in 5 years), then a directional arrow is shown in the direction of the trend (up or down), if the change is <1 SD in 5 years, then a double horizontal arrow is shown, or 'x' if there are fewer than 3 data points in the moving window. Again, the statistical significance of the recent trend is not taken into account in the plotting.

The intention of the figure is to flag ecosystem features and the magnitude of fluctuations within a generalized "fisheries management" time frame (i.e., trends that, if continued linearly, would go from the mean to ±1 SD from the mean within 5 years or less) for further consideration, rather than serving as a full statistical analysis of recent patterns.